NATIONAL CENTER FOR EARTHQUAKE ENGINEERING RESEARCH

State University of New York at Buffalo

# Experimental Verification of a Number of Structural System Identification Algorithms

by

R. G. Ghanem, H. Gavin and M. Shinozuka

Department of Civil Engineering and Operations Research
Princeton University
Princeton, New Jersey 08544

Technical Report NCEER-91-0024

September 18, 1991

This research was conducted at Princeton University and was partially supported by the National Science Foundation under Grant No. ECE 86-07591.

# NOTICE

50272-101

| REPORT DOCUMENTATION PAGE | 1. REPORT NO. NCEER-91-0024 | 2. | 3. PB92-176577 |
|---|---|---|---|

**4. Title and Subtitle**
Experimental Verification of a Number of Structural System Identification Algorithms

**5. Report Date**
September 18, 1991

**6.**

**7. Author(s)**
R.G. Ghanem, H. Gavin and M. Shinozuka

**8. Performing Organization Rept. No.**

**9. Performing Organization Name and Address**
Department of Civil Engineering and Operations Research
Princeton University
Princeton, New Jersey 08544

**10. Project/Task/Work Unit No.**

**11. Contract(C) or Grant(G) No.**
(C) 90-1102
ECE 86-07591
(G)

**12. Sponsoring Organization Name and Address**
National Center for Earthquake Engineering Research
State University of New York at Buffalo
Red Jacket Quadrangle
Buffalo, N.Y. 14261

**13. Type of Report & Period Covered**
Technical Report

**14.**

**15. Supplementary Notes**
This research was conducted at Princeton University and was partially supported by the National Science Foundation under Grant No. ECE 86-07591

**16. Abstract (Limit: 200 words)**
The investigation examines the application of four system identification techniques to problems of earthquake engineering. A number of techniques for structural system identification has been developed which successfully identify properties of linearized and time-invariant equivalent structural systems. In this paper, a number of structural identification algorithms are reviewed and applied to the identification of structural systems subjected to earthquake excitations. The algorithms are applied to experimental data obtained in controlled laboratory conditions. The data pertains to the acceleration records from two building models subjected to various loading conditions. The performance of the various identification algorithms is critically assessed and guidelines are obtained regarding their suitability to various engineering applications.

**17. Document Analysis a. Descriptors**

b. Identifiers/Open-Ended Terms

EARTHQUAKE ENGINEERING. SYSTEM IDENTIFICATION TECHNIQUES.
STRUCTURAL SYSTEMS. RECURSIVE INSTRUMENTAL VARIABLE METHOD.
EXPERIMENTAL VERIFICATION. STRUCTURAL IDENTIFICATION ALGORITHMS.
EXTENDED KALMAN FILTERS. MAXIMUM LIKELIHOOD ESTIMATES.
BUILDING MODELS. RECURSIVE LEAST SQUARES METHOD.

c. COSATI Field/Group

| 18. Availability Statement | 19. Security Class (This Report) | 21. No. of Pages |
|---|---|---|
| Release Unlimited | Unclassified | [redacted] |
| | 20. Security Class (This Page) | 22. Price |
| | Unclassified | |

(See ANSI-Z39.18) See Instructions on Reverse OPTIONAL FORM 272 (4-77) (Formerly NTIS-35)

# Experimental Verification of a Number of Structural System Identification Algorithms

by

R.G. Ghanem[1], H. Gavin[2] and M. Shinozuka[3]

September 18, 1991

Technical Report NCEER-91-0024

NCEER Project Number 90-1102

NSF Master Contract Number ECE 86-07591

1 Visiting Assistant Professor, Department of Civil Engineering, State University of New York at Buffalo
2 Research Assistant, Department of Civil Engineering, University of Michigan; former Graduate Student, Department of Civil Engineering, Princeton University
3 Sollenberger Professor of Civil Engineering, Department of Civil Engineering, Princeton University

NATIONAL CENTER FOR EARTHQUAKE ENGINEERING RESEARCH
State University of New York at Buffalo
Red Jacket Quadrangle, Buffalo, NY 14261

## PREFACE

The National Center for Earthquake Engineering Research (NCEER) is devoted to the expansion and dissemination of knowledge about earthquakes, the improvement of earthquake-resistant design, and the implementation of seismic hazard mitigation procedures to minimize loss of lives and property. The emphasis is on structures and lifelines that are found in zones of moderate to high seismicity throughout the United States.

NCEER's research is being carried out in an integrated and coordinated manner following a structured program. The current research program comprises four main areas:

- Existing and New Structures
- Secondary and Protective Systems
- Lifeline Systems
- Disaster Research and Planning

This technical report pertains to Program 1, Existing and New Structures, and more specifically to reliability analysis and risk assessment.

The long term goal of research in Existing and New Structures is to develop seismic hazard mitigation procedures through rational probabilistic risk assessment for damage or collapse of structures, mainly existing buildings, in regions of moderate to high seismicity. This work relies on improved definitions of seismicity and site response, experimental and analytical evaluations of systems response, and more accurate assessment of risk factors. This technology will be incorporated in expert systems tools and improved code formats for existing and new structures. Methods of retrofit will also be developed. When this work is completed, it should be possible to characterize and quantify societal impact of seismic risk in various geographical regions and large municipalities. Toward this goal, the program has been divided into five components, as shown in the figure below:

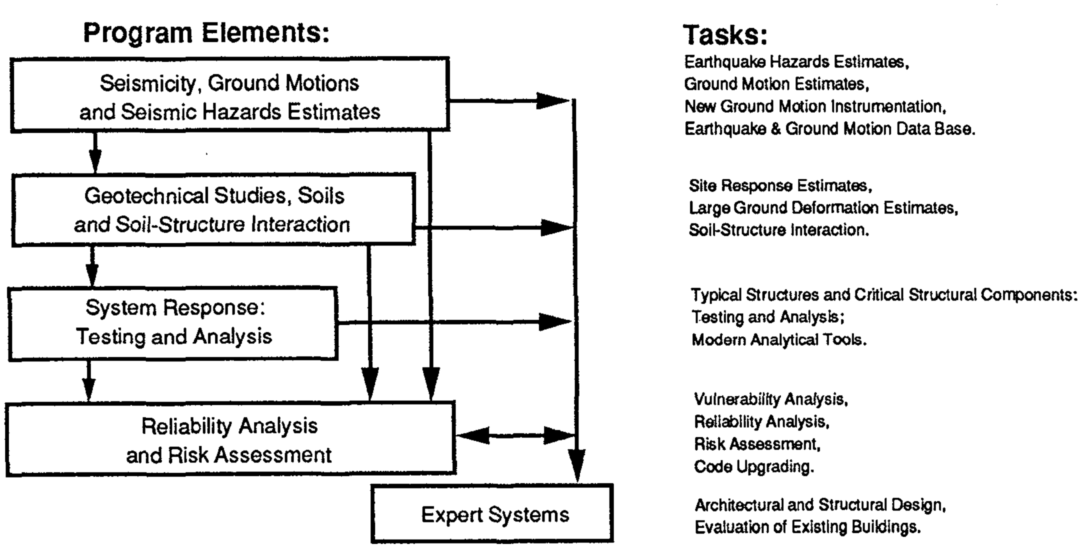

Reliability analysis and risk assessment research constitutes one of the important areas of Existing and New Structures. Current research addresses, among others, the following issues:

1. Code issues - Development of a probabilistic procedure to determine load and resistance factors. Load Resistance Factor Design (LRFD) includes the investigation of wind vs. seismic issues, and of estimating design seismic loads for areas of moderate to high seismicity.
2. Response modification factors - Evaluation of RMFs for buildings and bridges which combine the effect of shear and bending.
3. Seismic damage - Development of damage estimation procedures which include a global and local damage index, and damage control by design; and development of computer codes for identification of the degree of building damage and automated damage-based design procedures.
4. Seismic reliability analysis of building structures - Development of procedures to evaluate the seismic safety of buildings which includes limit states corresponding to serviceability and collapse.
5. Retrofit procedures and restoration strategies.
6. Risk assessment and societal impact.

Research projects concerned with reliability analysis and risk assessment are carried out to provide practical tools for engineers to assess seismic risk to structures for the ultimate purpose of mitigating societal impact.

*This study presents the results from implementing a number of system identification algorithms to experimental data. The experiments were carried out under controlled laboratory conditions. The data set consisted of acceleration records measured at various floor levels of multistory buildings. Each of these records was analyzed using four different system identification techniques. This procedure helped emphasize the importance of accelerogram placement on obtaining useful measurements. The sensitivity of each of the system identification algorithms to accelerogram placement was also investigated.*

*The four system identification techniques used were the extended Kalman filter, the maximum likelihood estimation, the recursive least squares and the recursive instrumental variable. The program EXKAL2 implemented the extended Kalman filter, and program LINEARID was used for the maximum likelihood estimation. Two variants of the recursive least squares, recommended in the literature by various investigators, were also implemented. The first one provides for an exponential phasing out of old data, while the second one discards old data in batches using a moving window of varying size. Furthermore, a variant of the recursive instrumental variable technique which resulted in an improved instrumental variable series was implemented. A comparative study of the performance and the accuracy of these techniques was also carried out. In addition, the program MUMOID was used to identify model parameters from the measured data. This program implements a maximum likelihood algorithm with a moving window to track time variation of system parameters. Finally, a method based on curve-fitting a rational polynomial to the frequency response function allowed a comparison of the above techniques to one of the most widely used methods.*

## Abstract

The investigation reported herein looks into the application of a number of system identification techniques to problems of earthquake engineering.

A number of techniques for structural system identification have been developed over the past few years. Many of these techniques have been successful at identifying properties of linearized and time-invariant equivalent structural systems. Most of these techniques were verified using mathematical models simulated on the computer.

In this paper, a number of structural identification algorithms are reviewed and applied to the identification of structural systems subjected to earthquake excitations. The algorithms are applied to experimental data obtained in controlled laboratory conditions. The data pertains to the acceleration records from two building models subjected to various loading conditions. The performance of the various identification algorithms is critically assessed and guidelines are obtained regarding their suitability to various engineering applications.

# Contents





**Preceding page blank**

# List of Illustrations

# List of Tables

# Section 1

# Introduction

Recent years have witnessed a resurgence in research activity in connection with structural system identification. The bibliography at the end of the report is a representative cross-section of the various research thrusts in this context, as well as in adjacent fields having a close connection to structural dynamics. This flurry of activity can be intimately related to the trend for increased availability and capability of computational facilities. Indeed, the enhancement in computing resources has made it possible both to acquire and analyse large data bases as well as to develop sophisticated computational models of physical systems. The effect of these developments on structural engineering research continues to be substantial. Specifically, in relation to earthquake engineering, where a large number of data sets consisting of measured acceleration records are available, the effect has been the developments of a number of algorithms to enhance the quality and quantity of information extracted from these records. The trend in structural system identification has been to couple these algorithms with computer simulation models for structural systems. This practice has helped both in verifying the system identification algorithms by applying them to simulated structures with preset parameters and also in calibrating computer models for real structures by identifying their parameters from field measurements. As useful as this procedure has been, it should be viewed with caution to the extent that computer models are at best an approximation of real structures. Even the most sophisticated such models are likely to be put to a hard test when subjected to such harsh and unpredictable environmental conditions as exist during an earthquake. This is mainly due to the fact that the continual damage sustained by a structure during an earthquake causes a degradation in the performance of the structure which is usually not tractable even with the most sophisticated structural analysis computer programs. In addition to emphasizing the need for structural identification techniques that provide for time varying parameters, this fact underlines the need to verify, experimentally, both the identification algorithms and the structural analysis computer programs.

In two previous reports, a number of system identification algorithms were developed in the context of structural dynamics (Yun and Shinozuka, 1990; Maruyama et.al 1989). These algorithms included a number of off-line techniques such as the ordinary least squares method, the instrumental variable method, the maximum likelihood method, and the extended Kalman filter method. These methods were incorporated into two system identification computer programs, LINEARID and EXKAL2. Two on-line techniques are developed for the present study, namely the recursive least squares and the recursive instrumental variable methods. Two variations on the recursive least squares are also implemented, as is a variation on the instrumental variable method. The choice of the above methods was based on an extensive review and analysis of the literature pertaining to system identification with the main criteria being accuracy and adaptability to the context of structural dynamics.

It is the purpose of this study to present the results from implementing a number of these system identification algorithms to experimental data. The experiments reported herein were carried out under controlled laboratory conditions.

The data set from each of the experiments consisted of acceleration records measured at various floor levels of multistory buildings. Each of these records was analysed using four different system identification techniques. This procedure helped emphasize the importance of accelerogram placement on obtaining useful measurements. The sensitivity of each of the system identification algorithms to accelerogram placement was also investigated.

The four system identification techniques which were used in this study consisted of the extended Kalman filter, the maximum likelihood estimation, the recursive least squares and the recursive instrumental variable. The program EXKAL2 implemented the extended Kalman filter, and program LINEARID was used for the maximum likelihood estimation. Two variants of the recursive least squares, recommended in the literature by various investigators, were also implemented. The first one provides for an exponential phasing out of old data, while the second one discards old data in batches using a moving window of varying size. Furthermore, a variant of the recursive instrumental variable technique which resulted in an improved instrumental variable series was implemented. A comparative study of the performance and the accuracy of these techniques was also carried out. In addition to the above techniques, the program MUMOID (DiPasquale and Cakmak 1987), was also used to identify model parameters from the measured data. This program implements a maximum likelihood algorithm with a moving window to track time variation of system parameters. Finally, a method based on curve-fitting a rational polynomial to the frequency response function allowed a comparison of the above techniques to one of the most widely used methods.

It should be noted that the methods indicated above, and which were implemented in this study, are not the only available methods for estimating the parameters of a structural system. Other methods include the weighted least squares (Isserman, 1974; Goodwin and Payne, 1977), the recursive maximum likelihood technique (Kashyap, 1970; Saridis, 1974). Recently, variations on the recursive maximum likelihood algorithm were implemented in the context of earthquake engineering (Lee, 1990; Lee and Yun, 1991; Yun et.al, 1991), and were used to identify a multi-input multi-output (MIMO) system.

# Section 2

# Mathematical Model for the Structural System

A generic mathematical model suitable for most physical systems can be represented by the following equation

$$\mathcal{L}\left[\mathbf{u}(t)\right] \; = \; \mathbf{f}(t) \;, \tag{2.1}$$

where $\mathbf{f}(t)$ is an input to the system which generates a corresponding output $\mathbf{u}(t)$, and $\mathcal{L}\left[.\right]$ denotes the functional relationship between the input and the output. The ultimate purpose of any system identification technique is to determine an algorithm which can be used to forecast the response of the system under consideration to any given input. In other words, it should provide a mean of evaluating the functional $\mathcal{L}\left[.\right]$. Such a task can be accomplished in a number of ways, all of which provide, by necessity, only approximations to $\mathcal{L}\left[.\right]$. The suitability of one or the other of these alternatives must be judged in relation to the purpose to which the mathematical model will be utilized. For example, if equation (2.1) is to be used in conjunction with an open loop control algorithm, then a finite difference model for this equation is called for. Indeed, in most such control strategies, it is a certain norm of the response which is to be monitored and the underlying mechanics can usually be treated as a black box operator. On the other hand, if a system identification process is needed to calibrate a structural design program, then a differential equation model is more appropriate for equation (2.1) since most such design aids are themselves based on the differential equation governing the mechanics of the structural system. Yet another purpose for system identification may be the assessment of the damage inflicted on a structure by some outside agent. Depending on the form of the particular damage index utilized in the process, one or the other of the possible formulations will be more suitable. In the remainder of this section, a discussion is presented of these two modeling strategies, namely differential equation models and difference equation models. Relationships establishing transformations between them are also developed.

The class of structures that fall within the scope of the present investigation can be adequately modeled by the following $N$-dimensional system of equations which describes the motion of the structure,

$$\mathbf{M}\ddot{\mathbf{u}} \; + \; \mathbf{C}\dot{\mathbf{u}} \; + \; \mathbf{K}\mathbf{u} \; + \; \mathbf{g}\left[\mathbf{u},\dot{\mathbf{u}}\right] \; = \; \mathbf{f}(t) \;. \tag{2.2}$$

Here, $\mathbf{M}$ denotes the inertia matrix associated with the structure, $\mathbf{C}$ denotes the corresponding viscous damping matrix and $\mathbf{K}$ the stiffness matrix. Furthermore, the vector

$\mathbf{f}(t)$ denotes the externally applied forces, and $\mathbf{g}[\mathbf{u}, \dot{\mathbf{u}}]$ is a vector whose components are nonlinear functions of the structural displacement $\mathbf{u}$ and its first derivative $\dot{\mathbf{u}}$. The matrix form in which equation (2.2) is cast is usually derived from a partial differential equation of the continuum through a discretization procedure such as the Finite Element Method or the Boundary Element Method. Implicit in this discrete form is the assumption that only $N$ degrees of freedom of the structure are significant in the pursuant analysis. For certain applications, it is more expedient to rewrite equation (2.2) using a state space representation, resulting in the following equation

$$\mathbf{A}\dot{\mathbf{z}} = \mathbf{h}[\mathbf{z}] \ , \tag{2.3}$$

where,

$$\mathbf{z} = \left\{ \begin{array}{c} \mathbf{u} \\ \dot{\mathbf{u}} \end{array} \right\} . \tag{2.4}$$

The functional $\mathbf{g}[.]$ can provide for anticipated nonlinear behavior of the physical system.

In most instances, equation (2.2) provides merely an approximation to the behavior of the real structure. The level of this approximation being a function of, among others, the adequacy of the discretization process, the appropriateness of the functional $\mathbf{g}[.]$ at modeling the nonlinear behavior of the system, as well as other uncertainties related to the mechanics of the system. In some cases, it may be appropriate to account for the uncertainty of the model expressed in equation (1) by adding a term to the equation which represents an effective mathematical modeling noise, leading to the equation,

$$\mathbf{M}\ddot{\mathbf{u}} + \mathbf{C}\dot{\mathbf{u}} + \mathbf{K}\mathbf{u} + \mathbf{g}[\mathbf{u}, \dot{\mathbf{u}}] = \mathbf{f}(t) + \omega(t) \ . \tag{2.5}$$

Obviously, the term $\omega(t)$ in the above equation can also be used to model an additive noise to the excitation process $\mathbf{f}(t)$. In this case, the noise may be attributed to unmeasured environmental factors. The most useful form for this noise process has proven to be a zero-mean stationary Gaussian white noise.

For the purpose of structural identification, measurement devices are placed at certain locations throughout the structure. Their number, denoted herein by $M$, is usually less than the number $N$ of degrees of freedom of the structure. This is due to both the expense associated with additional measurements, as well as to the fact that theoretically, each measured record contains enough information to permit the identification of all the unknown parameters. Measurement noise is usually associated with the measurement process, leading to the following observation equation which relates the observation vector at the $i^{th}$ observation time interval to the response vector at that instant,

$$\mathbf{y}_i = \mathbf{H}\ddot{\mathbf{u}}_i + \mathbf{e}_i \ . \tag{2.6}$$

In the above equation, $\mathbf{H}$ is a matrix which reflects the location of the measurement devices in relation to the structural nodes, and the associated amplification or attenuation factors, and $\mathbf{e}_i$ is a vector denoting the measurement noise and is usually assumed to be a zero-mean Gaussian white noise. The term $\ddot{\mathbf{u}}$ in equation (2.6) reflects the fact that in typical earthquake engineering applications, it is the accelerations that are usually monitored. Also, the discrete form of the equation is commensurate with the form of data retrieval and storage used in practical applications. A continuous form of the observation equation can be used in the theoretical development. It would not, however, correspond to a realistic situation.

The structural system identification problem can then be stated as follows: to infer about the parameters of the model used to represent the system using noise corrupted observations of the response and its associated input.

Alternatively, the identification problem can be cast completely in terms of the observed input and output, without any reference to the underlying mechanics or the associated differential equation. This approach provides an algorithm which permits forecasts of the response of the structure that are compatible, in some sense, with measured past input and output. A general form of this model is obtained by making the $i^{th}$ observation of the response a function of $k$ previous observations of the output, $l$ previous observations of the input, the current input observation and also a function of $m$ previous observations of the prediction error $\mathbf{e}$. This can be expressed by the equation

$$\mathbf{y}_i \;=\; \mathcal{Y}_i\left(\mathbf{y}_{i-1},\ldots,\mathbf{y}_{i-k},\mathbf{f}_i,\ldots,\mathbf{f}_{i-l},\mathbf{e}_{i-1},\ldots,\mathbf{e}_{i-m}\right) \;. \tag{2.7}$$

In the above equation, the subscript $i$ on the functional $\mathcal{Y}_i$ provides for time variation in the structure of the model. The inclusion of the prediction error in the argument list of the functional $\mathcal{Y}_i$ allows the prediction algorithm to learn from its previous errors. Equation (2.7) describes what has recently come to be known as state-dependent models (Priestley, 1980). This class of models is fairly general in that a minimum number of restrictions is imposed on the form of the functional $\mathcal{Y}_i$. The finite memory assumption implicit in this equation is not a severe restriction and can be made to fit most physically realizable situations. As a special case of this model, the bilinear and the threshold autoregressive models can be obtained. Also, for the special case where $\mathcal{Y}_i$ is a linear functional of its arguments, the autoregressive (AR) or autoregressive moving average (ARMA) models are obtained, depending on which coefficients in the model are zero. A class of models referred to as the prediction error models is obtained for the special case where equation (7) can be rewritten as (Goodwin and Payne, 1977)

$$\mathbf{y}_i \;=\; \mathcal{Y}_i\left(\mathbf{y}_{i-1},\ldots,\mathbf{y}_{i-k},\mathbf{f}_i,\ldots,\mathbf{f}_{i-l}\right) \;+\; \mathbf{e}_i \;. \tag{2.8}$$

Obviously, the more complicated the form of the functional $\mathcal{Y}_i$, the more sophisticated the model is, but also the more specialized and less robust it is. In the important case of a linear functional relationship, equation (2.7) can be conveniently rewritten as

$$\mathbf{y}_i \;=\; \boldsymbol{\theta}_i^T\, \mathbf{x}_i \;+\; \mathbf{e}_i \tag{2.9}$$

where $\boldsymbol{\theta}_i$ is a matrix of the coefficients in the linear expansion, and

$$\mathbf{x}_i \;=\; [\;\mathbf{y}_{i-1},\ldots,\mathbf{y}_{i-k},\mathbf{f}_i,\ldots,\mathbf{f}_{i-l}\;] \;. \tag{2.10}$$

Equation (2.6) involves the output of the system which has to be replaced by its estimated, or predicted, values, hence the error term appearing in that equation is also referred to as a prediction error. Since equations (2.2) and (2.7) are mathematical expressions of the same physical problem, an equivalence, in some sense, should be anticipated between them. Depending on the dimension of the observation space, this equivalence can take one of many forms. Also, the extent of the desired equivalence is problem dependent and is usually limited to the equivalence of the predicted output of a linearized version of these equations. One of the most prevalent approaches for establishing this equivalence consists of integrating a linearized version of equation (2.2), and expressing the response at the end of a time interval $i$ as a linear combination of the response at the end of the two previous time intervals. Accordingly, the following difference equation is obtained

$$\mathbf{u}_i = \mathbf{A}_1\mathbf{u}_{i-1} + \mathbf{A}_2\mathbf{u}_{i-2} + \mathbf{B}_1\mathbf{f}_{i-1} + \mathbf{B}_2\mathbf{f}_{i-2} + \boldsymbol{\omega}_i , \tag{2.11}$$

where $\boldsymbol{\omega}_i$ denotes a discrete white noise process. Note that since the above equation is obtained by integrating the equation of motion, it involves prediction for all the degrees of freedom of the system, which must therefore be observable. Once the coefficients in equation (2.11) have been evaluated, the difference equation is identified with a special form of equation (2.7), and a correspondence is established between these coefficients and the physical coefficients appearing in equation (2.2). In most practical situations, however, a limited number of degrees of freedom is monitored, as described by equation (2.6), and the above procedure for establishing an equivalence between the two equations breaks down since each of the equations contains a different amount of information. Another approach for achieving this purpose is obtained by noting that each measured record contains, to a greater or lesser extent, information about all the structural parameters of interest. Therefore, by matching the spectral density of the response of a linearized version of equation (2.2), with that of an appropriate linear difference equation model, a system of equations is obtained from which a correspondence is then established between this difference equation and the differential equation model. Thus the difference equation associated with a scalar observable can be written as

$$\sum_{k=0}^{2N} a_k y_{i-k} + \sum_{k=0}^{2N} b_k f_{i-k} = 0 . \tag{2.12}$$

The transfer function associated with equation (11) is given by the equation

$$\mathcal{H}(z) = \frac{\left|\sum_{k=0}^{2N} b_k z^k\right|^2}{\left|\sum_{k=0}^{2N} a_k z^k\right|^2} . \tag{2.13}$$

Since the denominator in the above equation is a polynomial of order $2N$, it possesses $2N$ roots, which appear in complex conjugate pairs. These can be matched with the $N$ roots associated with the spectral density function of the response to the linearized version of equation (2.2). The validity of this procedure depends on the peaks in the spectral density of the excitation not coinciding with the poles of the transfer function. This will insure that the rational polynomial in equation (2.13) is irreducible, and therefore that no system pole is hidden by a dominant frequency of the excitation. Denoting the $j^{th}$ pole of $\mathcal{H}(z)$ with positive imaginary part by $z_j$, this procedure leads to the equation

$$z_j = e^{\left(-\xi_j\omega_j + i\omega_j\sqrt{1-\xi_j^2}\right)\Delta t} \tag{2.14}$$

where $\xi_j$ and $\omega_j$ denote the percent of critical damping and the natural frequency, respectively, associated with the $j^{th}$ mode of vibration of the structure, and $i = \sqrt{-1}$. After some algebraic manipulations, the following relationships are obtained

$$\omega_j = \frac{\sqrt{\lambda_j^2 + \delta_j^2}}{\Delta t}$$
$$\xi_j = \frac{\delta}{\sqrt{\lambda_j^2 + \delta_j^2}} \tag{2.15}$$

where $\Delta t$ denotes the sampling rate, and

$$\lambda_j = -\tfrac{i}{2}\ln\frac{z_j}{z_j^*} = \text{Arg}\,[z_j]$$
$$\delta_j = -\tfrac{1}{2}\ln z_j z_j^* = -\tfrac{1}{2}\ln|z_j|^2 \tag{2.16}$$

Thus, from a knowledge of the coefficients in the difference equation (2.12), the modal parameters of an equivalent linear system can be recovered. Note that by allowing the coefficients to be a function of the observation step, evolution in time of the modal parameters can be monitored. Also note that if the vector form of equation (2.12) is used, then the order of the expansion has to be reduced until the total number of unidentified parameters is adequate for a one-to-one correspondence with the modal parameters to be established. This is in essence what is expressed in equation (2.11), where the dimension of the observation space is equal to $N$, thus restricting the order of the regression to two.

Note that equation (2.14) involves the implicit assumption that the motion of the structural system is governed by a linear differential equation. Therefore, although equation (2.12) may be an accurate representation of the input-output functional relationship of the structure, the correspondence established in equation (2.15) is only valid to the extent that the assumption of a linear differential equation with proportional damping, is adequate. Specifically, it is noted that for $z_j$ real, a value of 100% is obtained for the corresponding critical damping ratio $\xi_j$. This eventuality should be viewed as a mathematical instability with respect to deviations from the postulated linear model. This phenomena can be physically explained by the nonlinear behavior of the structure which results in coupling between the various modes, thus putting into question the validity of the modal damping assumption (Nayfeh, 1985 ; Balachandran et.al, 1990, 1991; Anderson, 1991). It is reminded, however, that this instability does not carry over to the difference equation model, as it is solely based on the observed data, and is a good predictor model to within the specified optimality criterion. Furthermore it is noted that, according to equations (2.15) and (2.16), whenever $z_j$ lies outside of the unit circle, the resulting damping has a negative value. Again, this instability is not associated with a physical phenomena. In these cases, the root in question was reflected back inside the unit circle according to the equation

$$z_j = \frac{z_j}{|z_j|^2} \,. \tag{2.17}$$

This procedure has the merit of preserving the value of $\lambda_j$ in equation (2.16), and therefore reducing the corresponding variation in the estimated natural frequencies.

Of all the system identification techniques implemented in this study, only the extended Kalman filter deals directly with the differential equation model of the structural system. It also provides for the nonlinear behavior of the structure. All the other techniques start by identifying a linear prediction model as in equation (2.12), from which the modal parameters are subsequently obtained.

# Section 3

# The Identification Algorithms

## 3.1 Extended Kalman Filter

The extended Kalman filter algorithm is derived from the state space form of the differential equation of motion, as provided by equation (2.3). The algorithm has been extensively used in the literature in relation to a large number of applications, both its theoretical development and its convergence properties are well established (Kalman, 1960; Kalman and Bucy, 1961; Jazwinski, 1970; Yun and Shinozuka, 1980; Shinozuka, Yun, and Imai, 1982; Meinhold and Singpurwalla, 1983; Brown, 1983; Hoshiya and Saito, 1983; Sorenson, 1982, 1985; Ruymgaart and Soong, 1985; Soong, 1986; Hoshiya, 1987; Imai et.al, 1988; Maruyama et.al, 1989; Bao, 1989). It is based on considering an extended state vector which includes, in addition to the response vector and its derivative, all the parameters to be identified. Starting from an initial guess, this extended state space is recursively updated as new observations are made available. The update is based on the Kalman filter formalism. The extended Kalman filter algorithm is summarized in this section. It has been coded in program EXKAL2 to estimate parameters for linear multi-degree-of-freedom systems and hysteretic single-degree-of-freedom systems (Maruyama, Yun, Hoshiya, and Shinozuka, 1989).

$$\hat{\mathbf{z}}_{k+1|k} = \hat{\mathbf{z}}_{k|k} + \int_{t_k}^{t_{k+1}} \mathrm{h}\left[\hat{\mathbf{z}}_{t|k}\right] dt \tag{3.1}$$

$$\mathbf{P}_{k+1|k} = \boldsymbol{\Phi}_{k+1|k}\, \mathbf{P}_{k|k}\, \boldsymbol{\Phi}^{T}_{k+1|k} + \mathbf{Q}_{k+1} \tag{3.2}$$

The term $\boldsymbol{\Phi}_{k+1|k}$ is the state transition matrix which relates the state at time instant $k$ to the state at time instant $k+1$. The state transition matrix implements the finite difference mathematical model for the system dynamics. Hence, it is a function of the motion parameters as well as the physical parameters, and is linearized at each time step. In the analyses performed herein, the state transition matrix is obtained by integrating the equations of motion using the linear acceleration method. Since the accuracy of the the linear acceleration method is dependent upon the size of the time step of integration, the execution of the extended Kalman filter requires a smaller sampling interval than many other parameter estimation methods. The state transition matrix can be obtained approximately as

$$\boldsymbol{\Phi}_{k+1|k} = \mathbf{I} + \Delta t \left[ \frac{d\mathbf{h}\left[\hat{\mathbf{z}}_{t|k}\right]}{d\left[\hat{\mathbf{z}}_{t|k}\right]} \right] \tag{3.3}$$

The filtered state $\hat{\mathbf{z}}_{k+1|k+1}$ and its error covariance matrix $\mathbf{P}_{k+1|k+1}$ can be estimated as

$$\hat{\mathbf{z}}_{k+1|k+1} = \hat{\mathbf{z}}_{k+1|k} + \mathbf{K}_{k+1} \left[ \mathbf{y}_{k+1} - \mathbf{H}\mathbf{z}_{k+1|k} \right] \tag{3.4}$$

$$\mathbf{P}_{k+1|k+1} = [\, \mathbf{I} - \mathbf{K}_{k+1}\, \mathbf{M}_{k+1} \,]\; \mathbf{P}_{k+1|k}\; [\, \mathbf{I} - \mathbf{K}_{k+1}\, \mathbf{M}_{k+1} \,]^T + \mathbf{K}_{k+1}\mathbf{R}_{k+1}\mathbf{K}_{k+1}^T\,. \tag{3.5}$$

In the above equations, $\mathbf{K}_{k+1}$ is the Kalman gain matrix which is defined as

$$\mathbf{K}_{k+1} = \mathbf{P}_{k+1|k}\mathbf{M}_{k+1}^T \left[ \mathbf{M}_{k+1}\mathbf{P}_{k+1|k}\mathbf{M}_{k+1}^T + \mathbf{R}_{k+1} \right]^{-1} \tag{3.6}$$

and $\mathbf{M_k}$ is a matrix whose $j^{th}$ row is given by the following equation

$$\mathbf{M}_k = \left[ \frac{\partial \mathbf{H}(\mathbf{z})}{\partial \mathbf{z}_j} \right]_{\mathbf{z}_k = \hat{z}_{k|k}} \tag{3.7}$$

In all of the above equations, the subscript $_{k+1|k}$ denotes a quantity evaluated at instant $k+1$ based on observation at instant $k$. The algorithm is started with an initial guess for the parameters and the error covariance matrix. The convergence of the algorithm as well as the final values are known to depend, to a great extent, on this inital guess.

## 3.2 Recursive Least Squares

The recursive least squares method consists of updating a least squares fit to the available data, as more data is made available. The corresponding algorithm can be summarized by the following equations (Jazwinski, 1970),

$$\hat{\boldsymbol{\theta}}_{k+1} = \hat{\boldsymbol{\theta}}_k + \mathbf{K}_{k+1} \left[ y_{k+1} - \mathbf{x}_{k+1}^T \hat{\boldsymbol{\theta}}_k \right] \tag{3.8}$$

$$\mathbf{x}_{k+1}^T = [\, -y_k \;\cdots\; -y_{k-l}\; f_{k+1}\; f_k \;\cdots\; f_{k-l} \,] \tag{3.9}$$

$$\hat{\boldsymbol{\theta}}_k^T = [\, a_k \;\cdots\; a_{k-l}\; b_{k+1}\; b_k \;\cdots\; b_{k-l} \,] \tag{3.10}$$

$$\mathbf{K}_{k+1} = \frac{\mathbf{P}_k \mathbf{x}_{k+1}}{1 + \mathbf{x}_{k+1}^T \mathbf{P}_k \mathbf{x}_{k+1}} \tag{3.11}$$

$$\mathbf{P}_{k+1} = \left[ \mathbf{I} - \mathbf{P}_k \frac{\mathbf{x}_{k+1}\mathbf{x}_{k+1}^T}{1 + \mathbf{x}_{k+1}^T \mathbf{P}_k \mathbf{x}_{k+1}} \right] \mathbf{P}_k\,. \tag{3.12}$$

In these equations, $\mathbf{x}_{k+1}$ represents a vector of the data available at the observation instant $k+1$, $\hat{\boldsymbol{\theta}}_k$ denotes a vector of the estimated linear regression coefficients with respect to $\mathbf{x}_{k+1}$, and $y_{k+1}$ denotes the newest output observation obtained at instant $k+1$. Furthermore, $f_k$ denotes an observation of the input at instant $k$. The recursive least squares algorithm is equivalent to the off-line least squares. It has the merit, however, of requiring the storage of only a small portion of the data at any one time. In all the subsequent implementation of this algorithm, a zero initial guess for the regression coefficients, and a diagonal matrix with large elements (1000) for the matrix $\mathbf{P}$ were used.

### 3.2.1 Recursive Least Squares with Exponential Memory

It can be shown that the estimates obtained using a least squares algorithm tend to be biased unless the prediction errors are uncorrelated, which is seldom the case. The bias is generally associated with the propagation of the initial error in the estimates. The effect of this error can be substantially reduced by implementing a process whereby less weight is given to older data. An exponential weighting function has been successfully implemented to this end in a number of investigations. This technique is mathematically based on minimizing the following loss function (Goodwin and Payne, 1977),

$$S_k(\boldsymbol{\theta}_k) \;=\; \alpha S_{k-1}(\boldsymbol{\theta}_k) \;+\; \left(y_k - \mathbf{x}_k^T \boldsymbol{\theta}_k\right)^2 , \tag{3.13}$$

where the second term represents the error associated with the current observation, and $0 < \alpha < 1$. It can be shown that the cost function given by the above equation is equivalent to the cost function given by the equation

$$S_k(\boldsymbol{\theta}) \;=\; \sum_{i=1}^{k} \left(y_i - \mathbf{x}_{i+1}^T \boldsymbol{\theta}\right) \alpha^{k-i} . \tag{3.14}$$

The prediction equation remains the same as above and is given by

$$\hat{\boldsymbol{\theta}}_{k+1} \;=\; \hat{\boldsymbol{\theta}}_k \;+\; \mathbf{K}_{k+1} \left[\, \mathbf{y}_{k+1} - \mathbf{x}_{k+1}^T \hat{\boldsymbol{\theta}}_k \,\right] . \tag{3.15}$$

The gain matrix, however, is now given by the equation

$$\mathbf{K}_{k+1} \;=\; \frac{\mathbf{P}_k \mathbf{x}_{k+1}}{\alpha + \mathbf{x}_{k+1}^T \mathbf{P}_k \mathbf{x}_{k+1}} , \tag{3.16}$$

and the recursion for matrix $\mathbf{P}$ is given by

$$\mathbf{P}_{k+1} \;=\; \frac{1}{\alpha} \left[\, \mathbf{I} - \mathbf{P}_k \frac{\mathbf{x}_{k+1} \mathbf{x}_{k+1}^T}{\alpha + \mathbf{x}_{k+1}^T \mathbf{P}_k \mathbf{x}_{k+1}} \,\right] \mathbf{P}_k . \tag{3.17}$$

Values of $\alpha$ of 0.99 have been recommended in the literature. In the course of the present research, values of $\alpha$ ranging from 0.7 to 0.99 were implemented.

### 3.2.2 Recursive Least Squares with Rectangular Window

Another modification of the least squares technique features a moving rectangular window which effectively discards prior data in batches. In its original form, the rectangular window algorithm requires the storage of all the data inside the current bandwidth of the window. In situations where the sampling rate is very high, this procedure may be limited by memory requirements. An alternative procedure, requiring the storage only of the information at the beginning of the window can be derived. Thus, assuming a window bandwidth of $N$ observations, the prediction algorithm is given by the equations (Goodwin and Payne, 1977),

$$\hat{\boldsymbol{\theta}}_{k+N+1|k} \;=\; \hat{\boldsymbol{\theta}}_{k+N|k} \;+\; \mathbf{K}_{k+N+1|k} \left[\, \mathbf{y}_k - \mathbf{x}_k^T \hat{\boldsymbol{\theta}}_{k+N|k} \,\right] . \tag{3.18}$$

$$\mathbf{K}_{k+N+1|k} \;=\; \frac{\mathbf{P}_{k+N|k} \mathbf{x}_k}{1 + \mathbf{x}_k^T \mathbf{P}_{k+N|k} \mathbf{x}_k} , \tag{3.19}$$

$$\mathbf{P}_{k+N+1|k} = \left[ \mathbf{I} - \mathbf{P}_{k+N|k} \frac{\mathbf{x}_k \mathbf{x}_k^T}{1 + \mathbf{x}_k^T \mathbf{P}_{k+N|k} \mathbf{x}_k} \right] \mathbf{P}_{k+N|k} \; . \tag{3.20}$$

In the above equations, the subscript ${}_{k+N|k}$ denotes the estimate of a quantity based on observation between $k$ and $k + N$. When the size of the window has reached $2N$, the first $N$ observations are discarded according to the equation

$$\hat{\boldsymbol{\theta}}_{k+2N|k+N+1} = \mathbf{P}_{k+2N|k+N+1} \left[ \mathbf{P}^{-1}_{k+2N|k+1} \hat{\boldsymbol{\theta}}_{k+2N+1|k} - \mathbf{P}^{-1}_{k+N+1|k} \hat{\boldsymbol{\theta}}_{k+N+1|k} \right] \tag{3.21}$$

$$\mathbf{P}^{-1}_{k+2N+1|k+N} = \mathbf{P}^{-1}_{k+2N+1|k} - \mathbf{P}^{-1}_{k+N+1|k} \; . \tag{3.22}$$

By limiting the information from past observations, both the exponential window and the rectangular window algorithms tend to eliminate the effect of the initial guess on subsequent estimates.

## 3.3 Recursive Instrumental Variable

The least squares criterion for system identification can be viewed as a minimization of the following norm of the prediction error

$$||e|| = \int \epsilon^2 dt \; . \tag{3.23}$$

A useful generalization of this concept is to view the above integral as a weighted residual. It is then apparent that a more flexible criterion for computing the coefficients of the hypothesized model is obtained by using the following norm of the error

$$||e|| = \int e.f dt \; , \tag{3.24}$$

where now $f$ is a function which can be customized to suit a particular application. In the above, continuous time was utilized only to emphasize the connection with the method of weighted residuals widely known in engineering mechanics. A formulation for discrete time problems is readily established by interpreting the above integrals as inner products and rewriting equation (23) as

$$||e|| = \; <e, f> \; , \tag{3.25}$$

where $< \, , >$ denotes a suitable inner products and $e$ and $f$ denote either functions or discrete series. In the system identification literature, the procedure described above has been referred to as the template function method (Eykhoff, 1982). The Instrumental variable method is obtained as a special case of the template function method. Specifically, the weighting series is so chosen as to be minimally correlated with the error, while having a large correlation with the output of the system, uncorrupted by the measurement errors. It can be shown that this choice of template function has a number of desirable effects on the statistical properties of the estimates. This is not to imply that it is a trivial matter to identify a weighting function or series having the properties of an instrumental variable. Other weighting techniques have also been used in the literature (Beck and Jennings, 1980; Werner et.al, 1987).

### 3.3.1 Non-Filtered Instrumental Variables

The series given by the vector

$$\mathbf{v}_k^T = [\ f_{k-L-l} \cdots f_{k-L}\ f_{k-l} \cdots f_k\ ] \qquad (3.26)$$

has been suggested as an instrumental variable series (Young, 1984). This series consists of two observation blocks of the input separated by a lag of $L$ observations. Assuming the input to be uncorrelated with the observation noise, the above series obviously satisfies one of the requirements for an instrumental variable. Furthermore, the lag parameter $L$ can be so adjusted as to achieve maximum correlation with the output series corresponding to the system response. In this investigation, the parameter $L$ was chosen in such a way that the two observation blocks were adjacent and non-overlapping. The resulting recursion algorithm is quite similar to the one derived for the recursive least squares, and is given by the following equations

$$\hat{\boldsymbol{\theta}}_{k+1} = \hat{\boldsymbol{\theta}}_k + \mathbf{K}_{k+1}\left[\ \mathbf{y}_{k+1} - \mathbf{x}_{k+1}^T\hat{\boldsymbol{\theta}}_k\ \right] , \qquad (3.27)$$

where

$$\mathbf{K}_{k+1} = \frac{\mathbf{P}_k\mathbf{x}_{k+1}}{1+\mathbf{x}_{k+1}^T\mathbf{P}_k\mathbf{v}_{k+1}} , \qquad (3.28)$$

and

$$\mathbf{P}_{k+1} = \left[\ \mathbf{I} - \mathbf{P}_k\frac{\mathbf{x}_{k+1}\mathbf{x}_{k+1}^T}{1+\mathbf{x}_{k+1}^T\mathbf{P}_k\mathbf{v}_{k+1}}\ \right]\mathbf{P}_k . \qquad (3.29)$$

It is important to note that although the recursive least squares can be shown to yield identical results to the non-recursive least-squares, the same is not true for the recursive instrumental variable algorithm.

### 3.3.2 Filtered Instrumental Variables

A more general implementation of the Instrumental variable technique can be achieved by an instrumental variable series having the following form

$$\mathbf{v}_k^T = [\ h_k \cdots h_{k-l}\ f_k \cdots f_{k-l}\ ] , \qquad (3.30)$$

where $h_k$ is a series so chosen as to maximize the correlation with the output of the system while minimizing the correlation with the measurement noise. One way to achieve this goal is to chose $\{h_k\}$ as the output of an auxiliary system which is a good approximation to the real system. In this case, $h_k$ is given by the following recursive equation

$$h_k = \boldsymbol{\beta}_k^T\mathbf{v}_k , \qquad (3.31)$$

where $\boldsymbol{\beta}_k$ denotes the parameters of the auxiliary system. In this investigation, they are obtained from the estimated system parameters through the following algorithm (Isserman et.al, 1974),

$$\boldsymbol{\beta}_{k+1} = (1-\gamma)\boldsymbol{\beta}_k + \gamma\boldsymbol{\theta}_{k+1} . \qquad (3.32)$$

Note that for $\gamma$ equal to 1, the auxiliary system coincides with the real, noise-corrupted, system. Values of $\gamma$ between 0.03 and 0.1 have been suggested in the literature. In addition to this range of values, values between 0.1 and 1 are also implemented in order to provide a comprehensive assessment of the sensitivity of the algorithm, in the context of earthquake engineering, to variations in $\gamma$.

# Section 4

# The Experiments

Two sets of experiments provided acceleration time histories for the verification of the above parameter estimation algorithms. The experiments involved a three story steel building model and a five story reinforced concrete model. In all the experiments, accelerometers measured the structural response at floor levels. Digital band-pass filters conditioned the acceleration time histories after digital data acquisition. Filtering the low frequency components is especially important in time-domain analyses since experimental acceleration bias errors are physically meaningless in structural vibrations.

## 4.1 Three Story Building Model

The miniature three story building model has flexible steel walls and rigid aluminum floors. The walls are welded to a rigid steel base and are connected to the aluminum floors via a moment resisting clamp connection. The walls are 5in. tall, 2in. wide, and 0.036in. deep. The floors are 0.5in. deep, 6in. long, and 4in. wide. A schematic of the model is depicted in Figure (4.1). Each floor weighs 1.157 lb. and the stiffness of the inter-story wall system is 3.32 lb/in. for each inter-story stiffness. The relative flexibility of the floors with respect to the walls can be adequately approximated using a shear beam model.

### 4.1.1 Set-up Description

The test on the three story building model was carried out at the Department of Civil Engineering and Operations Research at Princeton University. The model was rigidly fixed to a horizontal shaking table. An elcetro-dynamic long stroke shaker actuated the table. Its acceleration was controlled via a proportional gain analog feedback loop such that the base shear of the structure would not influence the table's motion. A 12-bit digital to analog converter output pre-recorded time histories of wide-band random data and the El Centro 1940 N-S accelerogram to the feed-back control network. A function generator output swept sinusoidal data. The feed-back control network mixed the command input and the response measured by a force-balance accelerometer on the shaker's armature, low-pass filtered the mixed signal, and sent it to the shaker's power amplifier. A two channel oscilloscope monitored the command input and the feed-back acceleration signals to confirm that the shaker motion was tracking the command input and that feed-back instabilities would not develop. Piezo-electric accelerometers on the shaker's armature and on each of the floor levels measured horizontal accelerations. A 12-bit multiplexing analog to digital converter recorded the acceleration records at 1000 samples per second and stored

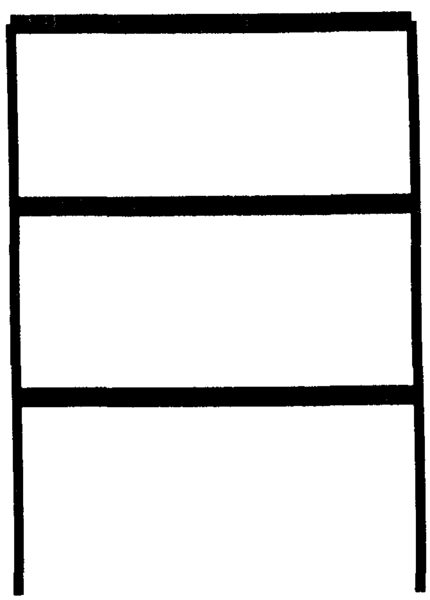

Figure 4.1: Three Story Steel Building Model Subjected to Base Excitation.

**Figure 4.1**

| Approximate Analytical Results | |
|---|---|
| Mode | Frequency (Hz) |
| 1 | 7.476 |
| 2 | 21.212 |
| 3 | 31.000 |

Table 4-I: **Modal Parameters of the Three Story Building Model Using Eigenvalue Analysis.**

them directly on the hard disk of a networked workstation. Three data sets were obtained corresponding to El Centro, swept sine, and a white noise input excitations. A 1024 point Kaiser FIR band-pass filter was utilized to eliminate spurious frequencies below 0.5Hz. and above 50Hz.. The filtered time histories were then used in the parameter estimation algorithms. Figures (4.2)-(4.4) show the time histories of the input records and of the measured accelerations at the various floors. The associated spectral densities are shown in Figure (4.5)-(4.7). These were obtained by fitting an autoregressive model to the observed data. Figure (4.8) shows the transfer function corresponding to the Kaiser filter used in processing the measured data.

### 4.1.2 Dynamic Properties

An eigenvalue analysis of the three degree of freedom shear building model resulted in approximate analytical modal data. Each aluminum floor weighed 1.173 lb. The four steel columns were 1 inch wide, 0.035 inches deep, and 5 inches long. The first story height, however, was 5.25 inches. In the discrete formulation of the problem, one-third of the adjacent column mass was lumped to the floor mass and the mass matrix was diagonal. The stiffness matrix was assembled assuming rigid floors. Estimates of the natural frequencies obtained from solving the associated eigenvalue problem are shown in Table (4.1).

## 4.2 Five Story Building Model

Acceleration records from a recent large scale test of a five story reinforced concrete frame structure were obtained from the Ketter Laboratory of the State University of New York at Buffalo. A schematic of the building model is shown in Figure (4.9).

### 4.2.1 Set-up Description

The shaking table at SUNY-Buffalo incorporates multi axis control via hydraulic actuators. Hence, rocking motion of the table caused by the over-turning moment of the structure could be controlled. The Ketter Laboratory uses piezo-resistive accelerometers in large scale structural vibration measurements since piezo-resistive accelerometers have steady state and low frequency response. The two sets of horizontal floor level accelerations obtained from the Ketter Laboratory correspond to excitation in the form of the El-Centro 1940 NS earthquake, and white noise excitation. The records were filtered so as to eliminate very low and very high spurious frequencies. Figures (4.10) and (4.11) show the time series

## Measurements with El-Centro Input

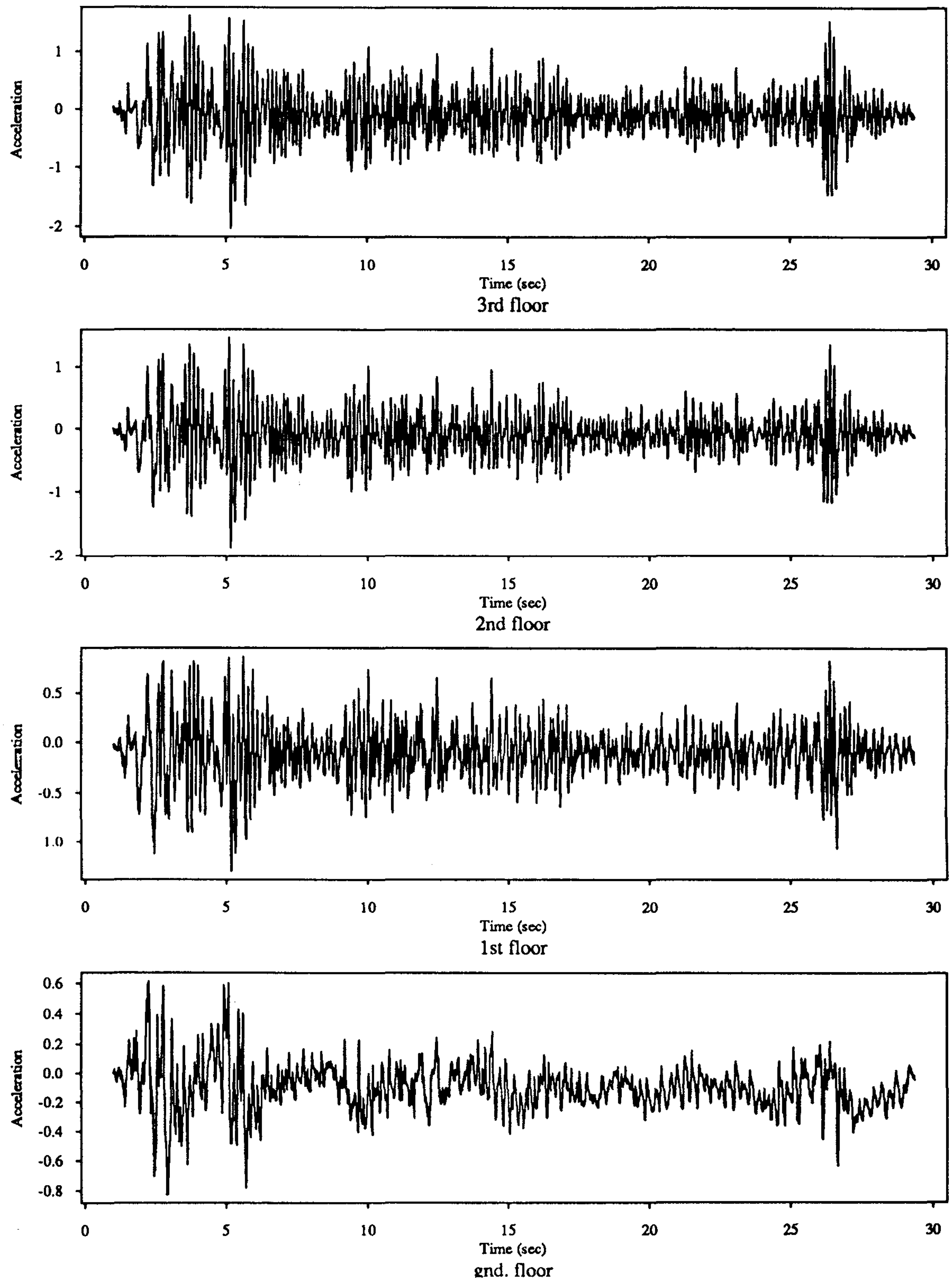


**Figure 4.2**

Measurements with Sine-Sweep Input

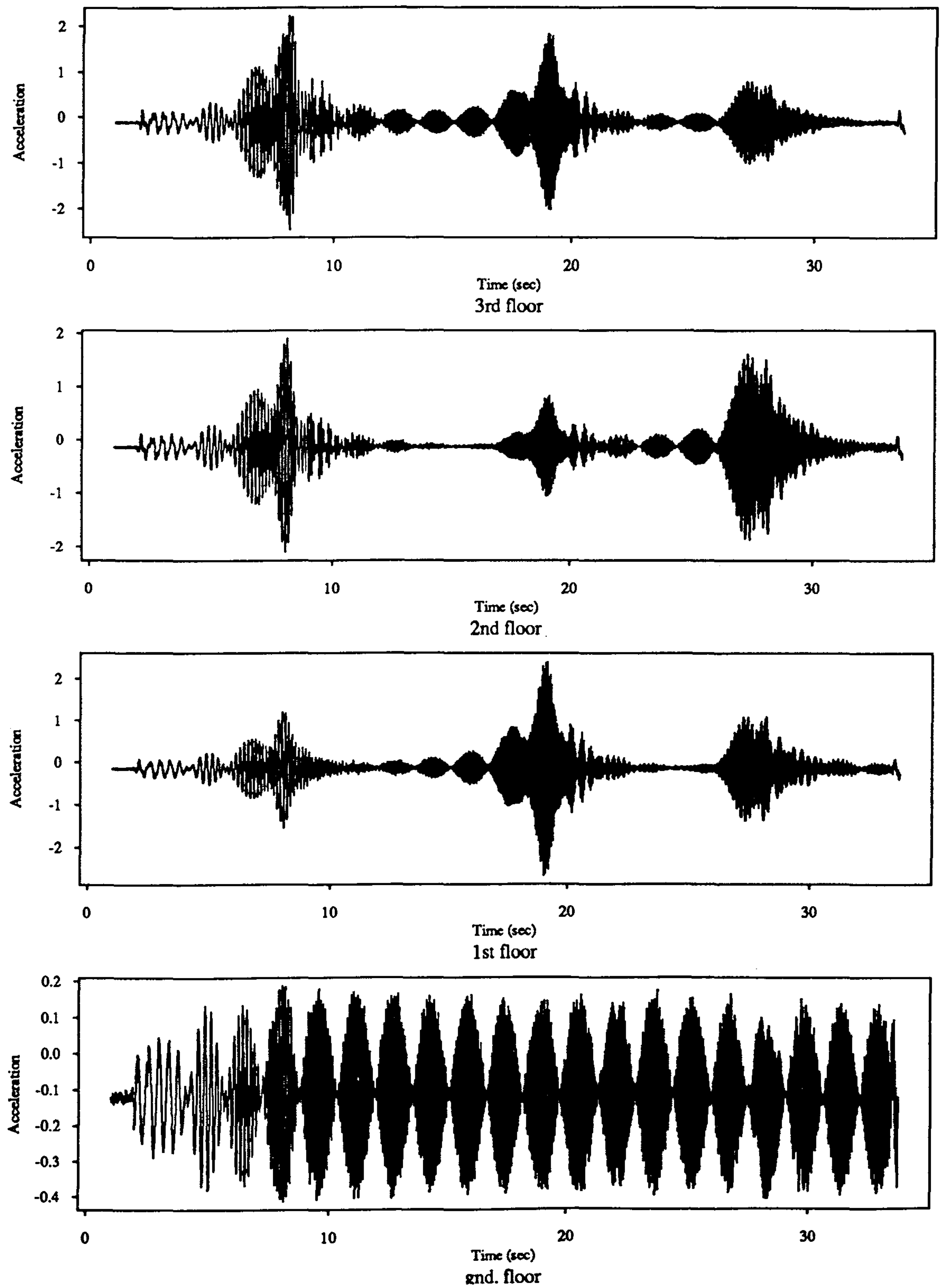


Figure 4.3

## Measurements with White-Noise Input

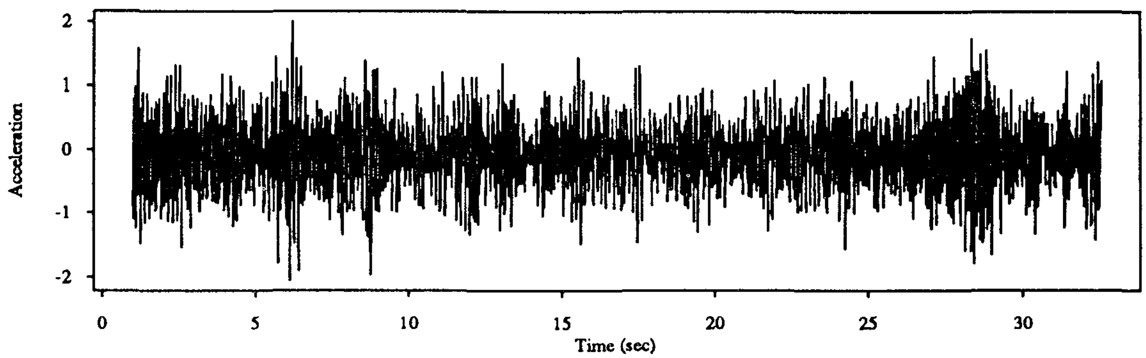


3rd floor

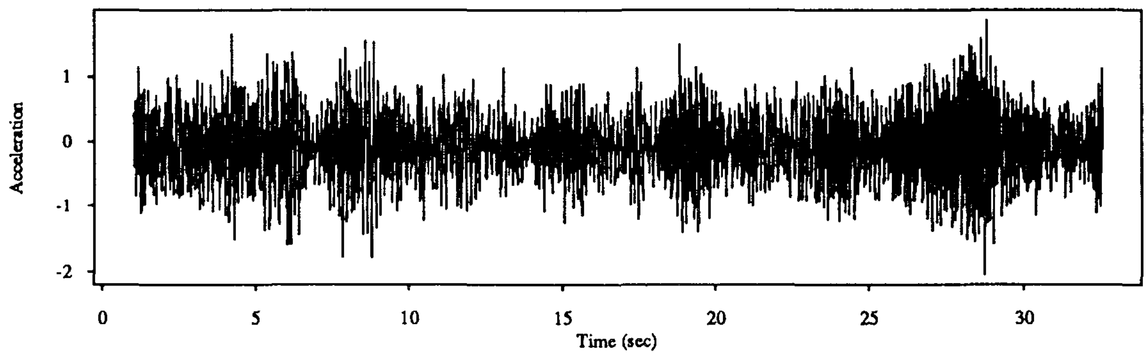


2nd floor

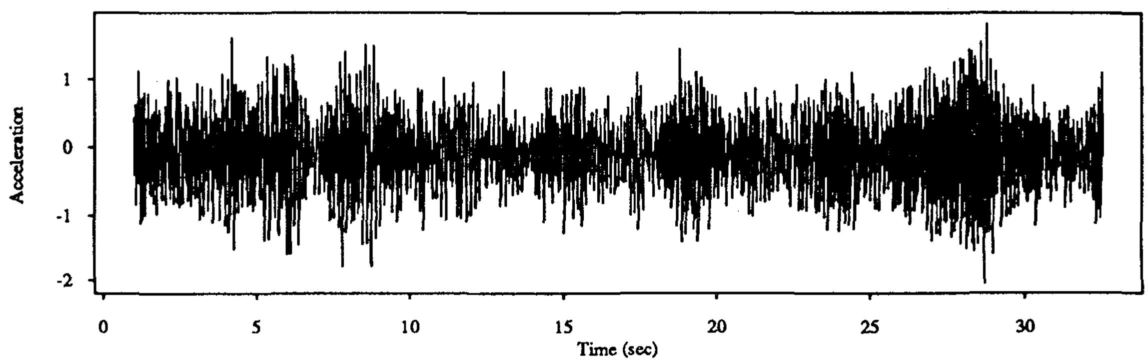


1st floor

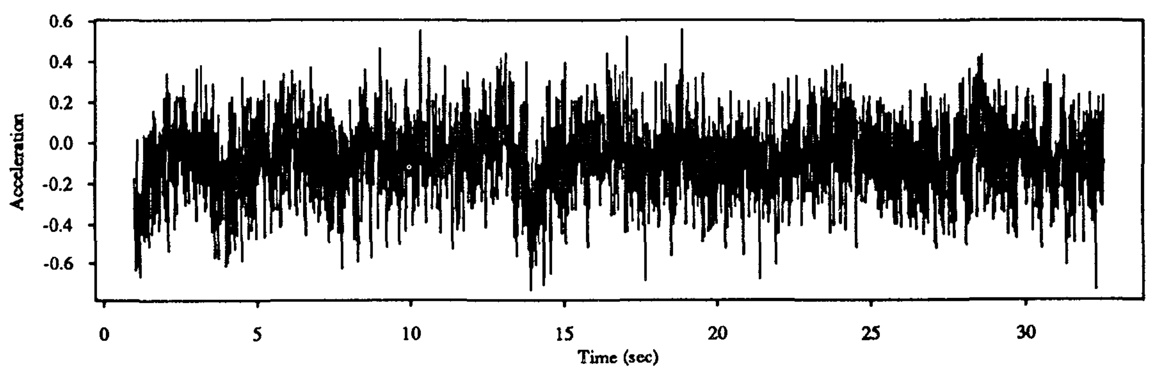


gnd. floor

Figure 4.4

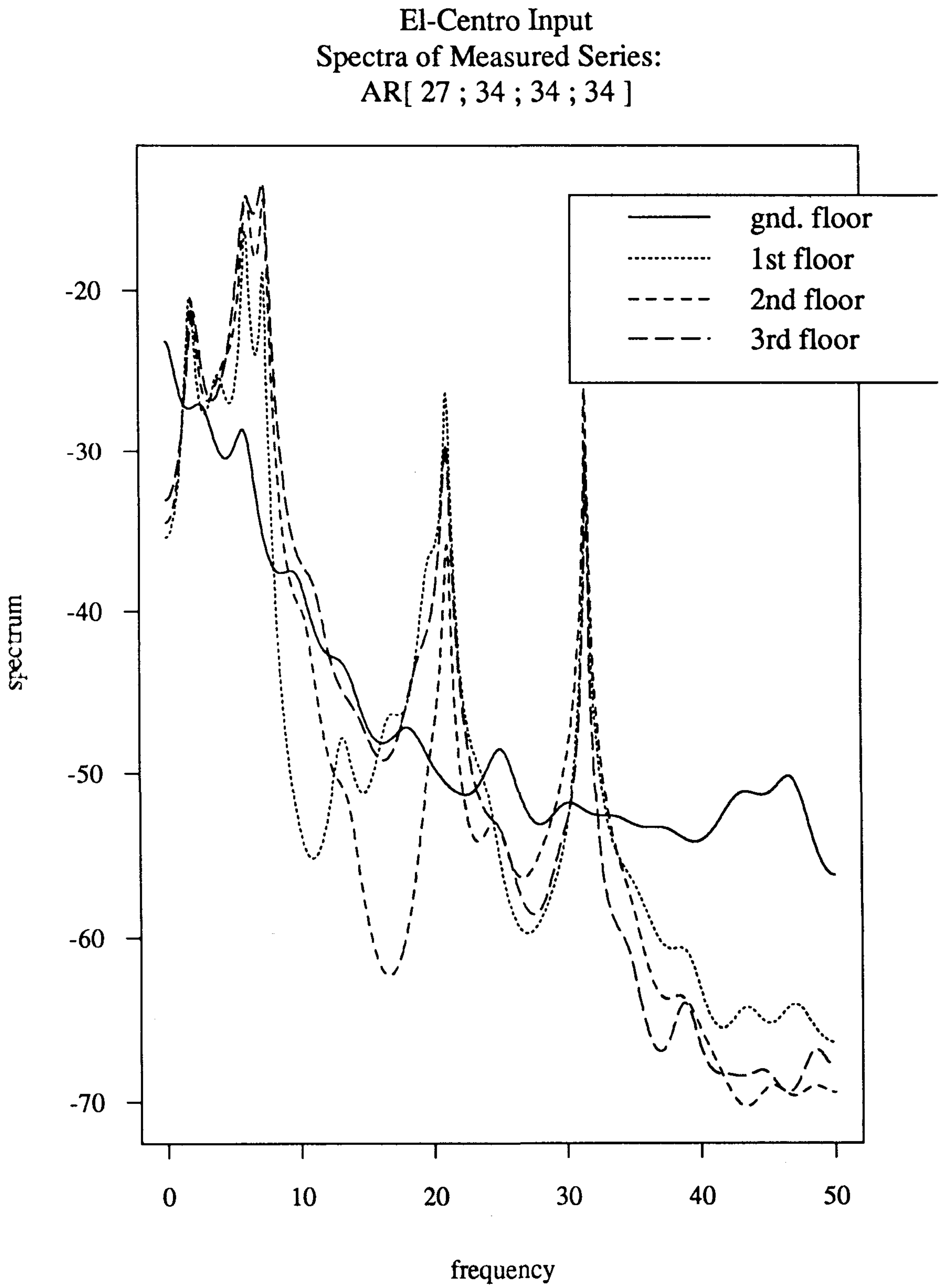
El-Centro Input
Spectra of Measured Series:
AR[ 27 ; 34 ; 34 ; 34 ]
gnd. floor
1st floor
2nd floor
3rd floor
spectrum
-20
-30
-40
-50
-60
-70
0
10
20
30
40
50
frequency

**Figure 4.5**

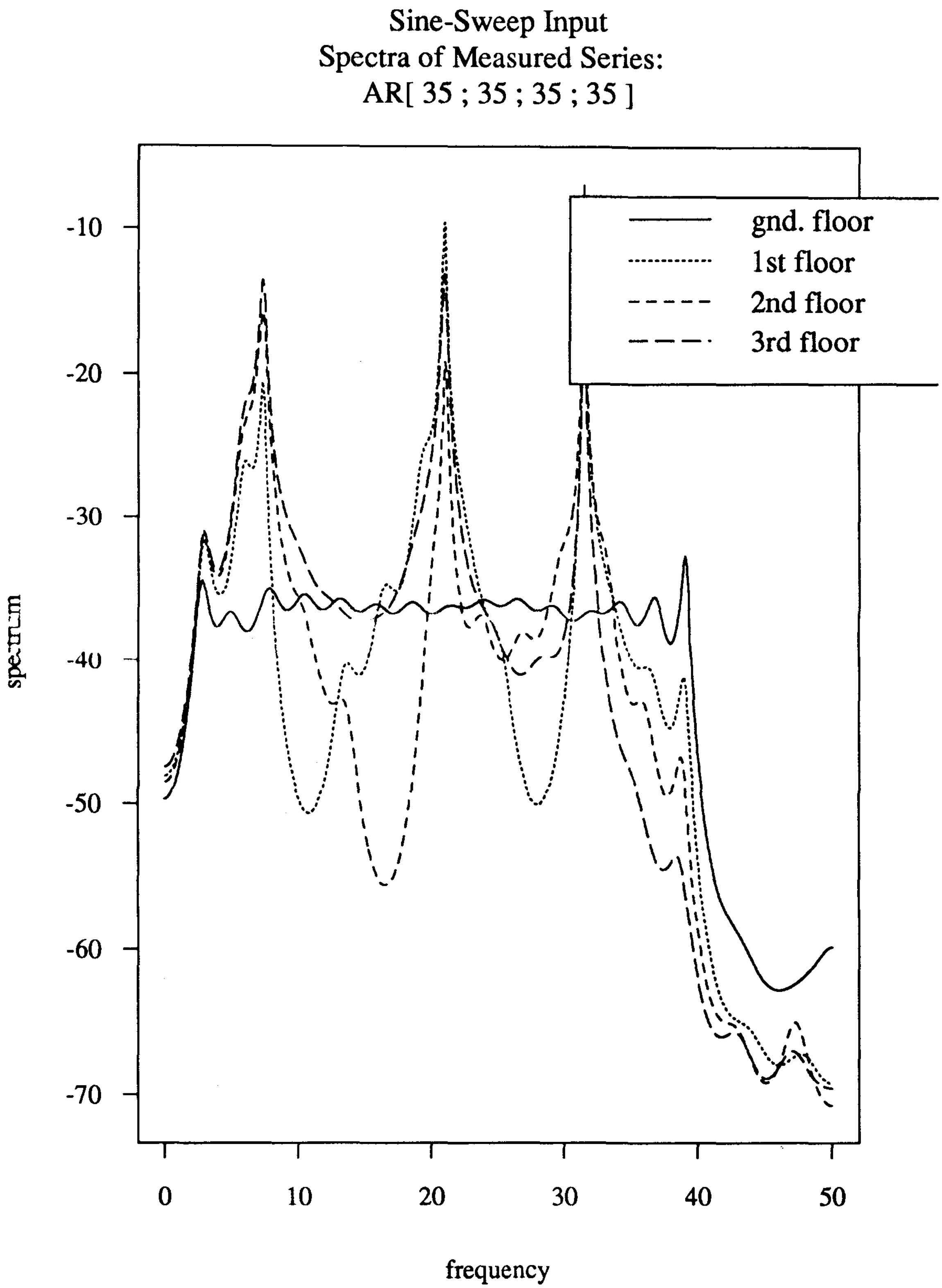
Sine-Sweep Input
Spectra of Measured Series:
AR[ 35 ; 35 ; 35 ; 35 ]
gnd. floor
1st floor
2nd floor
3rd floor
-10
-20
-30
-40
-50
-60
-70
0
10
20
30
40
50
frequency

Figure 4.6

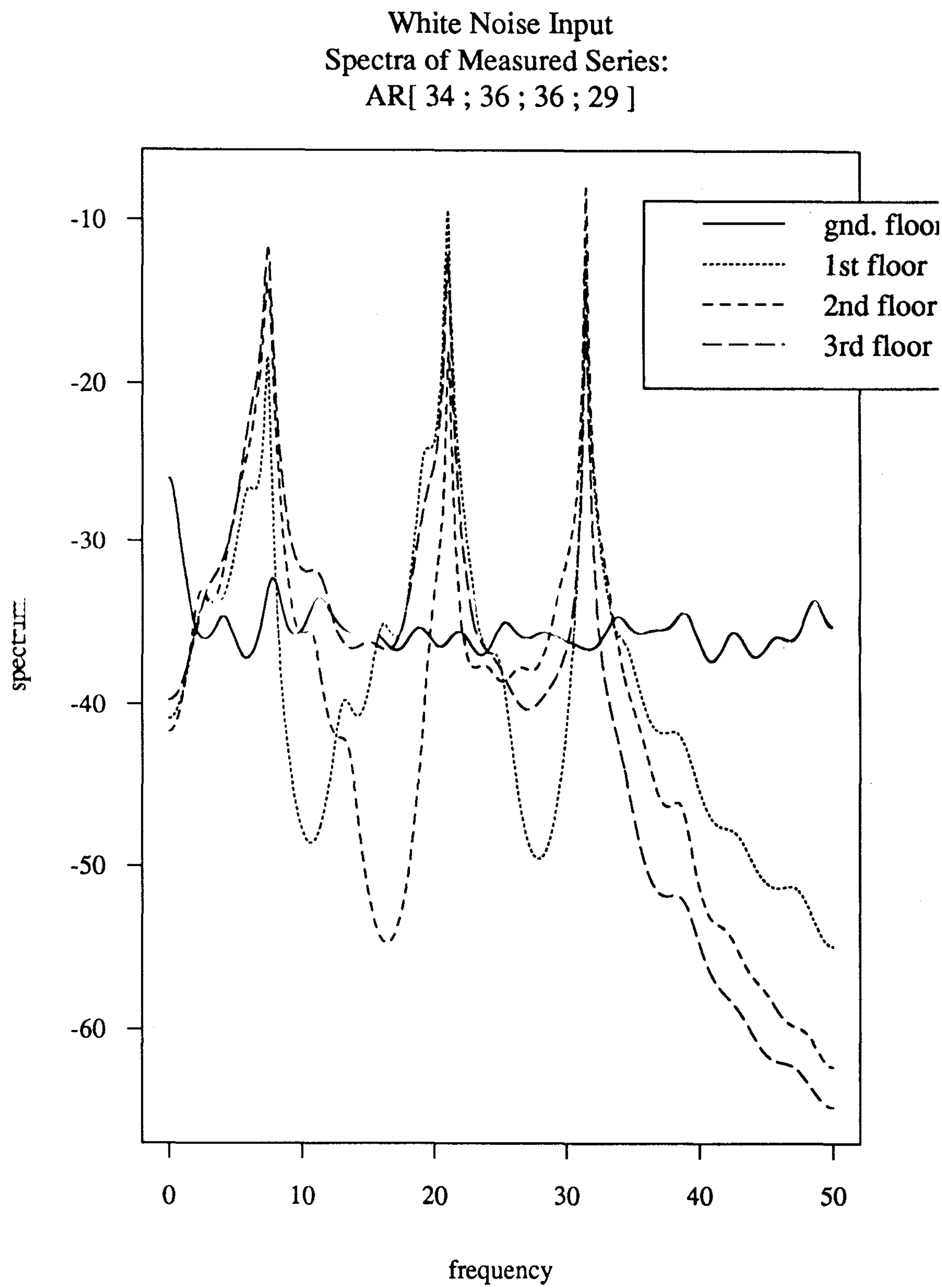
White Noise Input
Spectra of Measured Series:
AR[ 34 ; 36 ; 36 ; 29 ]
gnd. floor
1st floor
2nd floor
3rd floor
-10
-20
-30
-40
-50
-60
spectrum
0
10
20
30
40
50
frequency

**Figure 4.7**

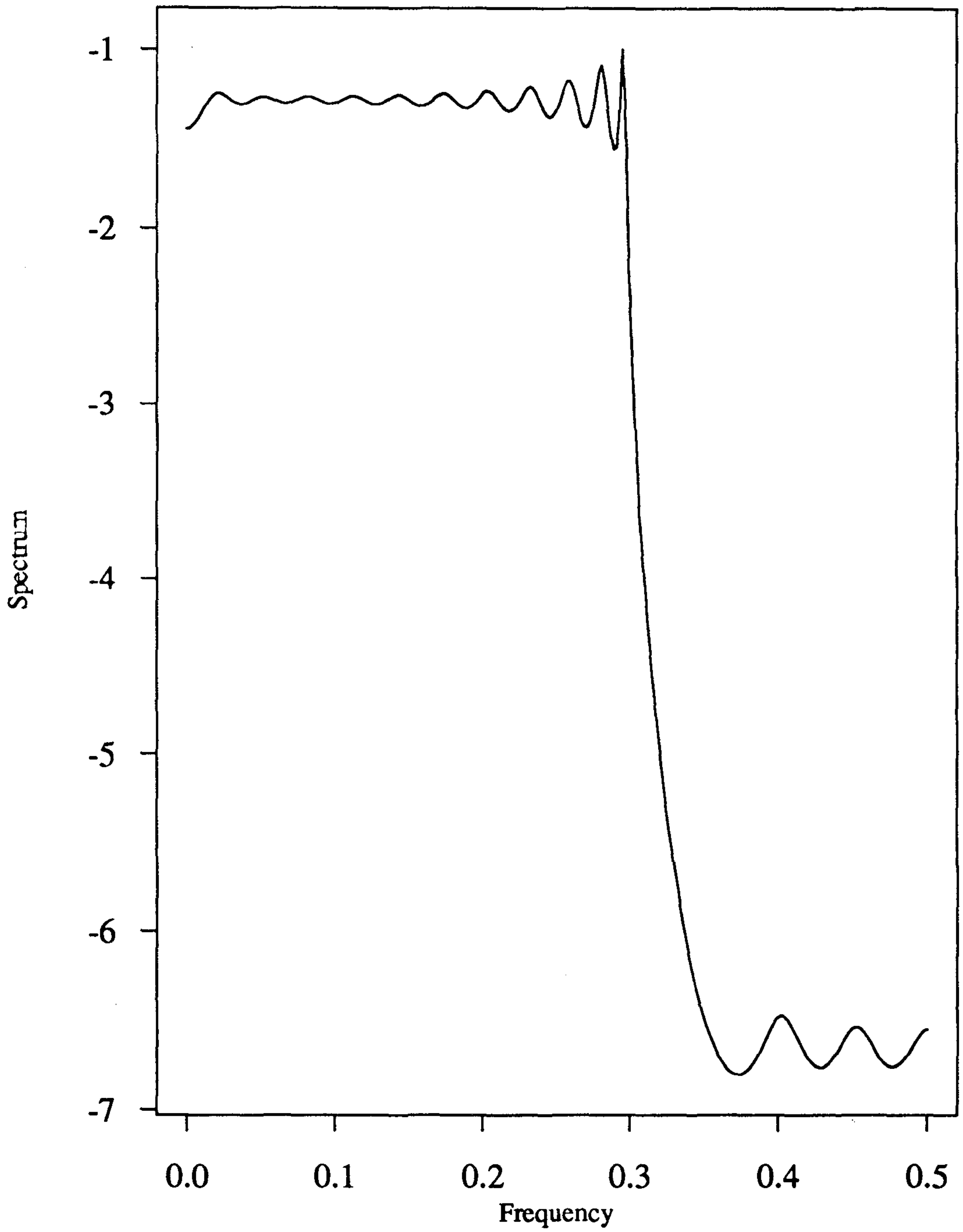


Spectrum of the Kaiser Filter
AR(27), Using Yule-Walker

Figure 4.8

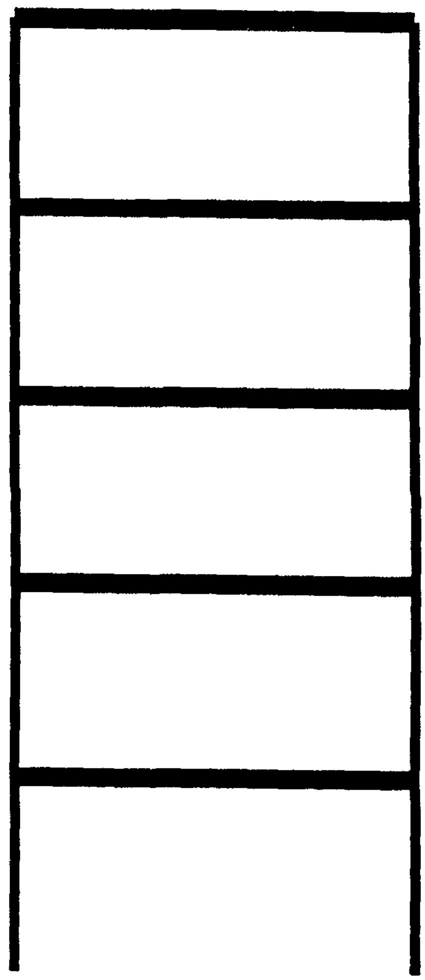

Figure 4.9: Five Story Reinforced Concrete Building Model Subjected to Base Excitation.

**Figure 4.9**

## Measurements with El-Centro Input

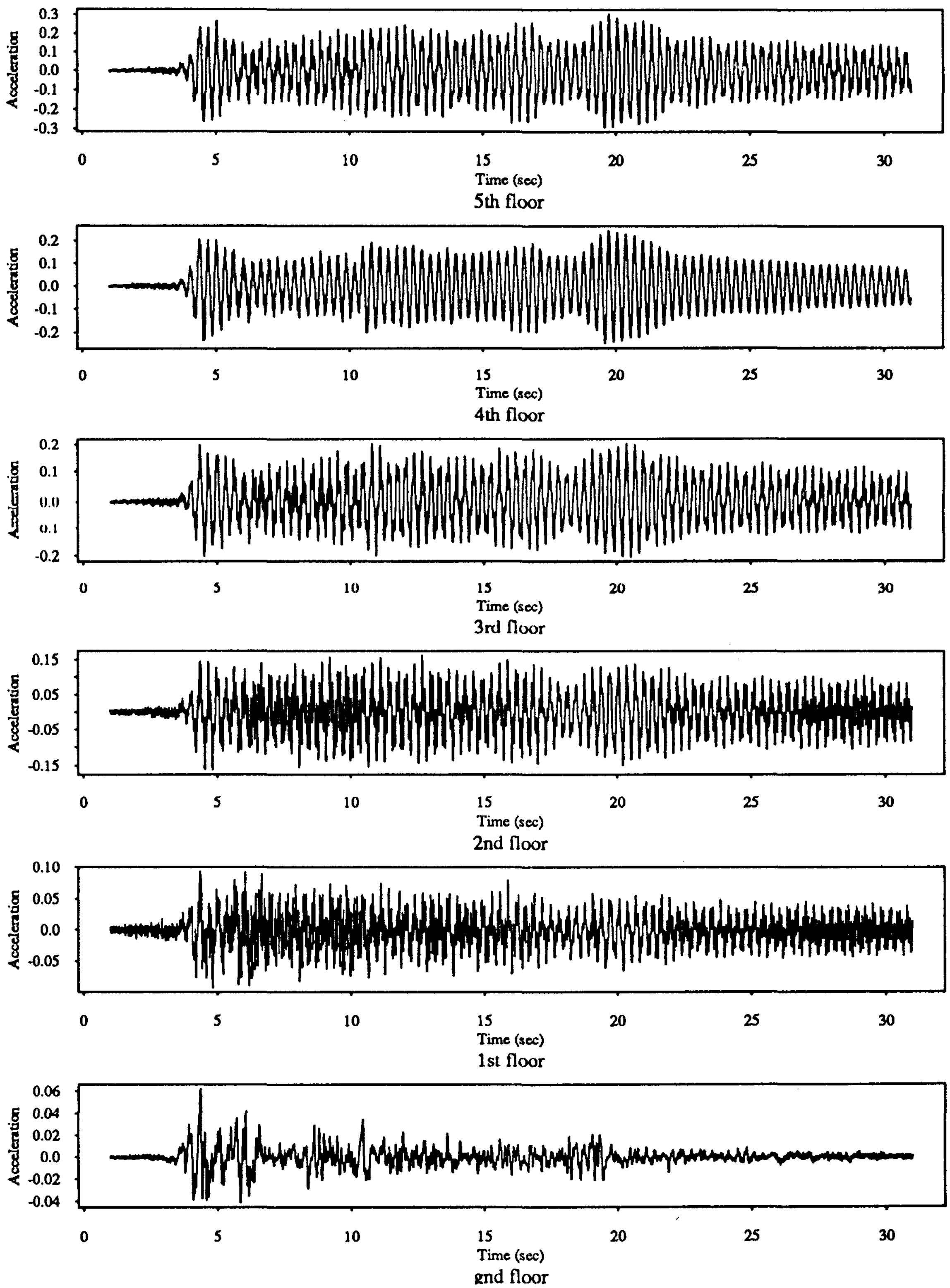


**Figure 4.10**

Measurements with White Noise Input

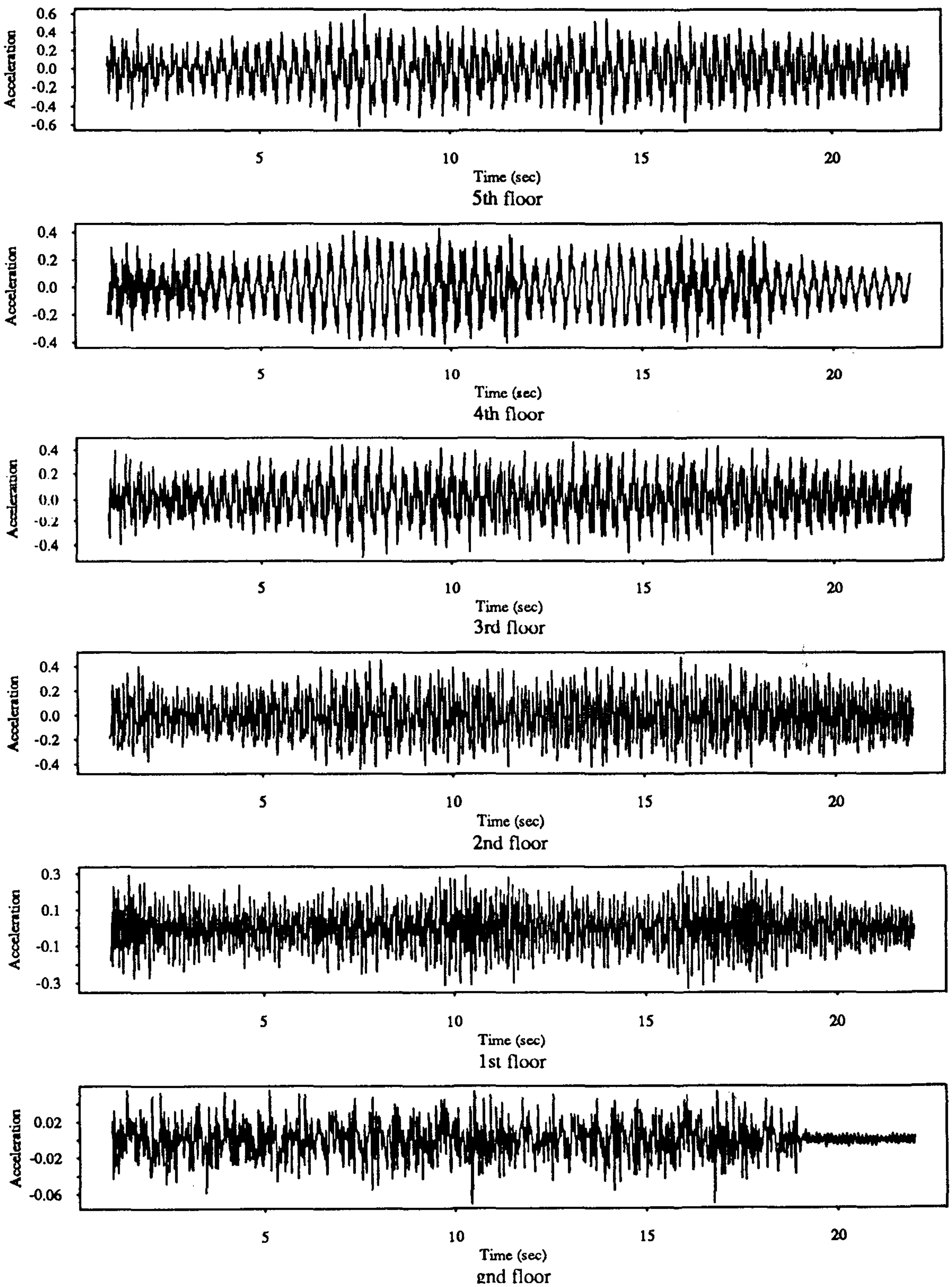


**Figure 4.11**

| | 1st Floor | 2nd Floor | 3rd Floor | 4th Floor | 5th Floor |
|---|---|---|---|---|---|
| Stiffness $lb/in$ | 32284 | 12362 | 11382 | 11314 | 12824 |
| Mass $lb-s^2/in$ | 3.29 | 3.29 | 3.29 | 3.29 | 3.39 |

Table 4-II: **Physical Properties of the Five-Story Building Model Tested at SUNY at Buffalo.**

corresponding to the input motions and the measured output motions while Figures (4.12)-(4.13) show the corresponding spectral densities.

### 4.2.2 Dynamic Properties

Table (4.2) presents the values of the individual floor stiffnesses and masses estimated from measuring the physical dimensions of the various structural components. Based on this data, and assuming a shear-type building model, the stiffness and mass matrices were evaluated and found to be as follows,

$$\mathbf{M} = \begin{bmatrix} 6.58 & 0 & 0 & 0 & 0 \\ 0 & 6.58 & 0 & 0 & 0 \\ 0 & 0 & 6.58 & 0 & 0 \\ 0 & 0 & 0 & 6.58 & 0 \\ 0 & 0 & 0 & 0 & 3.29 \end{bmatrix}, \tag{4.1}$$

$$\mathbf{K} = \begin{bmatrix} 44646 & -12362 & 0 & 0 & 0 \\ -12362 & 23744 & -11382 & 0 & 0 \\ 0 & -11382 & 22696 & -11314 & 0 \\ 0 & 0 & -11314 & 24138 & -12824 \\ 0 & 0 & 0 & -12824 & 12824 \end{bmatrix}. \tag{4.2}$$

A rough approximation to the eigenvalues and eigenfunctions of the structure can be obtained by solving the following generalized eigenvalue problem associated with an undamped model of the structure,

$$\mathbf{K}\phi = \omega^2\mathbf{M}\phi . \tag{4.3}$$

In the above equation, $\omega$ denotes the natural frequency of the structure, and $\phi$ denotes the associated natural mode. The modal parameters estimated based on this approach are shown in Table (4.3). Note that the procedure outlined above does not take into account any dissipative mechanism in the structure, and therefore, the resulting estimates have to be viewed with caution.

| Approximate Analytical Results | |
| --- | --- |
| Mode | Frequency (Hz) |
| 1 | 2.42 |
| 2 | 6.92 |
| 3 | 10.64 |
| 4 | 13.27 |
| 5 | 14.11 |

Table 4-III: **Modal Parameters of the Five Story Building Model Using Eigenvalue Analysis.**

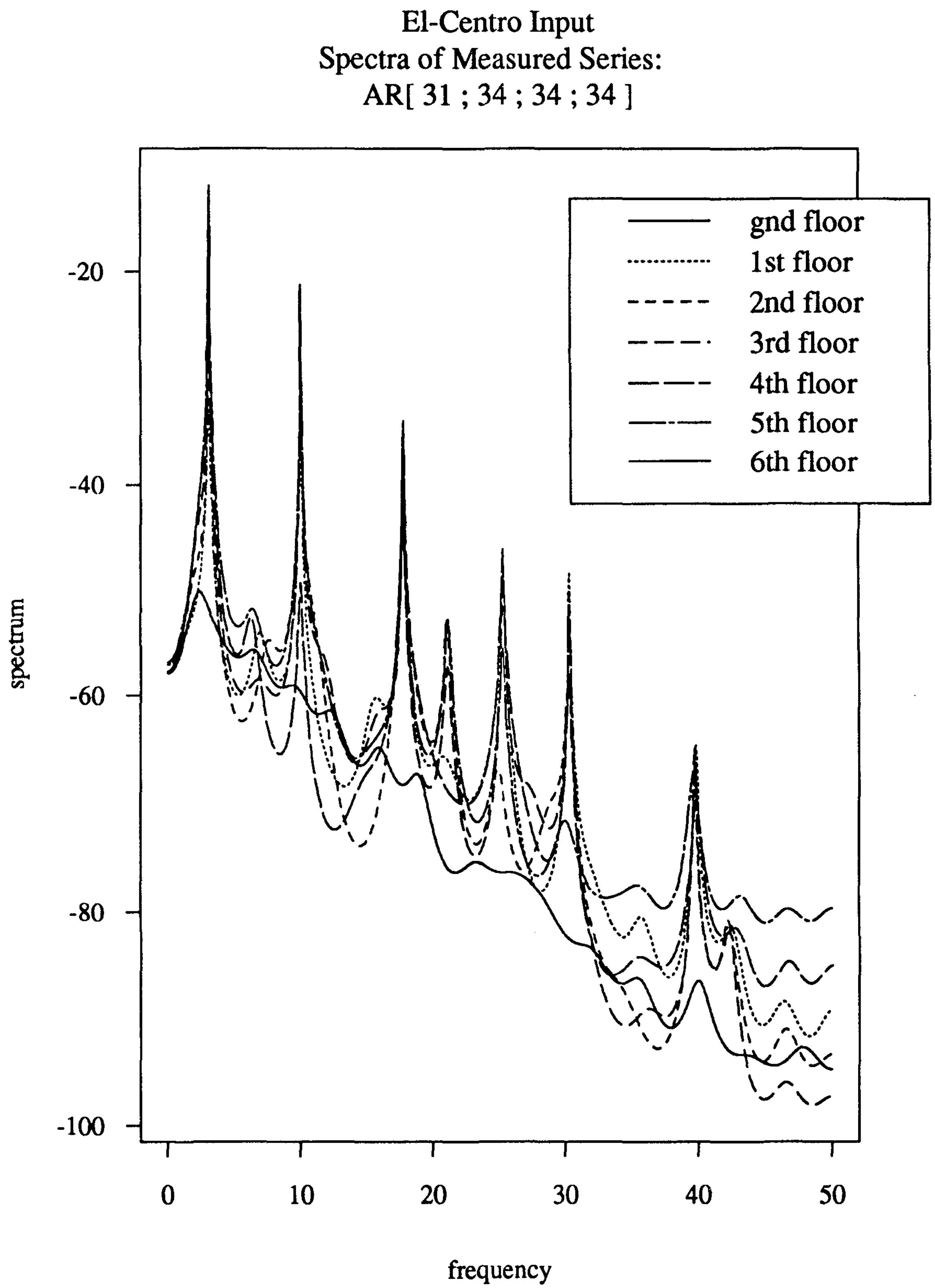
El-Centro Input
Spectra of Measured Series:
AR[ 31 ; 34 ; 34 ; 34 ]
gnd floor
1st floor
2nd floor
3rd floor
4th floor
5th floor
6th floor
-20
-40
-60
-80
-100
spectrum
0
10
20
30
40
50
frequency

Figure 4.12

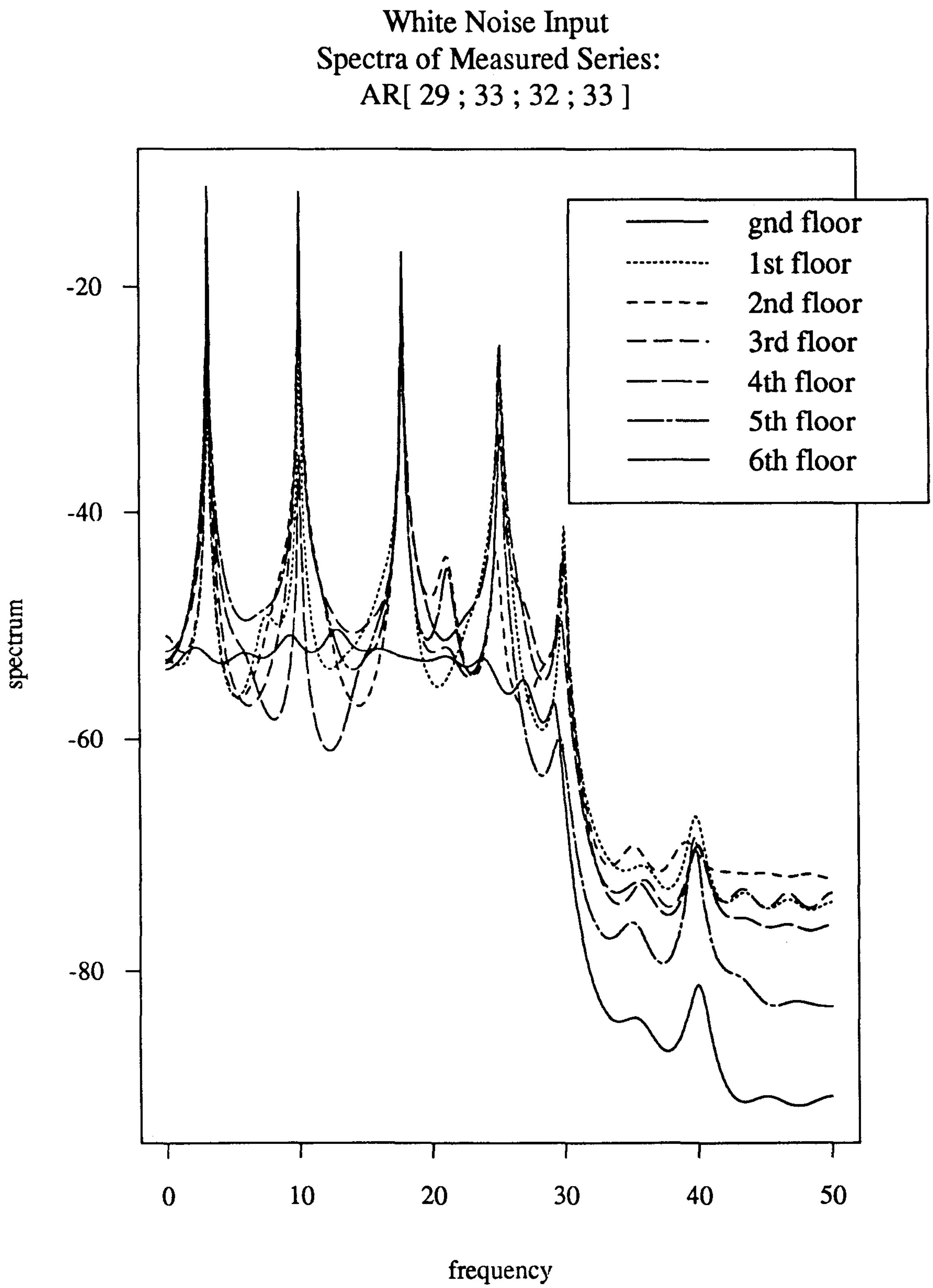
White Noise Input
Spectra of Measured Series:
AR[ 29 ; 33 ; 32 ; 33 ]
gnd floor
1st floor
2nd floor
3rd floor
4th floor
5th floor
6th floor
-20
-40
-60
-80
spectrum
0
10
20
30
40
50
frequency

**Figure 4.13**

# Section 5

# The Results

Except for the extended Kalman filter, all the parameter estimation techniques described in section 3 involve two stages. In a first stage, the parameters of a linear prediction model are computed. These represent the regression coefficients of each new observation on previous observations. In the second stage, these coefficients are used to obtain approximations to the modal parameters of a linear differential equation model of the structure. Again it is emphasized that this second stage involves assumptions that cannot necessarily be inferred from the measured data. Since the results associated with either section can be useful in their own right, they are presented in two separate sections. The first section features an analysis of the coefficients associated with the various prediction models that are implemented. Their behavior is numerically analysed. The second section concerns the modal parameters, specifically the natural frequencies and damping ratios of the structures analysed. However, since the programs LINEARID and MUMOID do not provide, as part of their standard output, results pertaining to the coefficients of the linear prediction model, only results featuring the modal estimates are shown in relation to these two programs.

## 5.1 Parameters of the Prediction Model

Each of the recursive estimation algorithms described in section 3 was implemented using each of the data sets obtained from the experiments. Each of the algorithms were run in turn on combinations of two measured records. The first one was the acceleration measured at the base of the structure, while the second one consisted of the acceleration at one of the floor levels. This way, the system parameters of the three-story model was identified using three different sets of data, while those of the five-story structure were identified using five sets. For the purpose of identifying a linearized model of the structure, only the autoregressive part of the prediction model is needed. In this section, therefore, only these coefficients are presented.

### 5.1.1 Recursive Least Squares Algorithms

The recursive least squares algorithm was implemented on the data as described above. Furthermore, the modified least squares algorithms as described in section 3 were also implemented. These consist of the exponential window and the rectangular oscillating window. In order to provide a comprehensive analysis of the effects of these windows on earthquake engineering data, a parametric study was carried out by varying the parameter controlling the exponential decay in the exponential window and that controlling the width of the rectangular window.

The results for the five-story building model associated with the unmodified recursive least squares are shown in Figures (5.1)-(5.10). Figures (5.1)-(5.5) show the evolution of the estimated parameters corresponding to the El-Centro input motion as more observations were being processed. Figures (5.6)-(5.10) show the corresponding results for the white-noise input motion. It is noted that some of the coefficients have not reached a steady state value by the end of the measurement period. The extent of the ensuing error can only be assessed by investigating the capability of the resulting model at predicting the behavior of the system. This capability can in turn be related to the behavior of the poles of the transfer function of the model. Figure (5.11)-(5.20) show the wandering of these zeros in the complex plane as more data is processed. It is noted that in all the cases studied, a steady state condition was reached before the end of the measurement period. This fact indicates that the observed variation in the coefficients of the linear prediction model are not detrimental to the identification process. Figures (5.21)-(5.29) show the coefficients corresponding to the three-story building model. Note the good convergence achieved by the coefficients associated with the white noise input. This observation cannot, however, be extended to the case of the five-story building model.

The exponential window algorithm was implemented on the above data. Values of the parameter $\alpha$ equal to 0.7, 0.8, 0.9, and 0.99 were tried. Only the case corresponding to a value of $\alpha$ of 0.99 resulted in meaningful estimates. Other values of $\alpha$ resulted in estimated parameters that exhibited very large and frequent variations, and will therefore be omitted from the present discussion. Figures (5.39)-(5.48) show the new values of the coefficients of the prediction model. Note that although the coefficients have reached what seems to be a steady state, they exhibit fluctuations that seem to be more critical to the behavior of the poles of the transfer function than was the steady change in the values of the parameters observed for $\alpha$ equal to 1. The location of the poles corresponding to this case is shown in Figures (5.49)-(5.58). The results corresponding to the three-story model are shown in Figures (5.59)-(5.67) for the coefficients and in Figures (5.68)-(5.76) for the pole location. Note the wandering of the poles in the complex plane, even towards the end of the observation period. An important observation can be made concerning the results associated with the exponential window. Specifically, it is noted that the effect on the first few observations is a desirable smoothing of the estimates, which deteriorates for later observations. With that in mind, a variant of the algorithm was implemented whereby the exponential window was used only for a fraction of the observations. In this case, one fourth of the data at the beginning of each record was processed through an exponential window with a value for the parameter $\alpha$ equal to 0.99. The effect of this procedure on the stability of the estimates was quite significant. As can be seen in Figures (5.77)-(5.86) associated with the five story building model, the coefficients have reached a stable value well before the end of the measurement period. Unlike the standard exponential window, however, the location of the poles of the system is fixed in the complex plane, at a quite early stage in the estimation process. These are shown in Figures (5.87)-(5.96). Similar results were obtained for the three story building model and are shown in Figures (5.97)-(5.105) for the coefficients, and Figures (5.106)-(5.114) for the pole location.

As mentioned earlier, the rectangular window algorithm was also implemented on the available data. Values for the width of the window ranging from 100 to 1000 observations were tried. At the sampling rate of 100Hz., these correspond to a range of window widths between 1sec and 10sec. It was observed that everytime a block of old data was discarded, the behavior of the subsequent estimates was disrupted over a number of observations. This fact sets a limit on the usable window width. The results obtained using this technique, for all the values of the window width used, were generally poor. Although encouraging results were obtained in applications to other fields, this technique cannot be recommended for earthquake engineering applications. It is noted at this point that the program MUMOID (DiPasquale and Cakmak, 1987), developed at Princeton University, implements a moving window technique for tracking time dependent system parameters. That program, however, relies on a maximum likelihood algorithm for estimating the parameters of the system. It is known that maximum likelihood estimates are better behaved than least squares estimates, and that program can be expected to yield better results than the algorithm presented herein. However, estimation using maximum likelihood algorithms is very computer intensive and cannot be geared towards on-line implementation. Furthermore, numerical experimentation with the MUMOID program, reported below, have shown that the results of the estimation algorithm are very sensitive to the window width utilized, and also that convergence problems were frequent for all the cases tested.

### 5.1.2 Recursive Instrumental Variable Algorithms

The recursive instrumental variable algorithms described in section 3 where implemented in a fashion similar to that described above for the recursive least squares algorithms. The first algorithm involved an unfiltered instrumental variable series. The coefficients of the linear prediction model identified in this fashion exhibited a pronounced transient behavior which was indicative of either a nonlinear relationship between the input and output series, or a deficient instrumental variable series which was incapable of identifying the parameters of the model. Results pertaining to these coefficients, and associated with the five-story building model, are displayed in Figures (5.115)-(5.124). A look at the pole location associated with these coefficients Figures(5.125)-(5.134), however, indicates that the model is not consistently stable. Similar behavior was observed in connection with the three-story building model. The corresponding results are shown in Figures (5.135)-(5.152).

The use of a filtered instrumental variable series in the identification algorithm resulted in a substantial improvement in the behavior of the coefficients. The algorithm was described in section 3 and consists of using as the instrumental variable series the series corresponding to the input motion after passing it through an auxiliary filter so that it approximates the real output of the system, uncorrupted by measurement noise. A parametric study was performed by varying the value of the parameter $\gamma$ in the auxiliary filter. Results from this analysis pertaining to the five story model are shown in Figures (5.153)-(5.164) for the coefficients, and in Figures (5.165)-(5.176) for the pole location. Similar results pertaining to the three-story building model are shown in Figures (5.177)-(5.182) and (5.183)-(5.188), respectively. A clear observation from this analysis related to the sensitivity of the estimation process to values of $\gamma$. Indeed, for certain combinations involving a specific value of $\gamma$ and a set of measured records, the estimation process diverged. For other such combinations, the estimated parameters of the prediction model reached their stationary values at an early stage in the estimation process. Also, it was observed that the suitable value of $\gamma$ was not the same for a given input motion. It depended both on the particular input motion used as well as on the particular floor level from which the measurements were obtained. Based on these observations, this parameter estimation technique does not seem fit for on-line identification, since it requires pre-tuning the auxiliary filter to the given data. However, in an off-line context, the results obtained using this technique feature a number of desirable properties, including stability of the coefficients and of the poles location in the complex plane.

## 5.2 Modal Parameters

As discussed in section 3, the coefficients in a linear prediction model can be associated with the parameters of an equivalent linear differential equation. These parameters can be related to such modal quantities as the natural frequencies and the damping ratios of the structure. In this section, these equivalent modal quantities are obtained which are associated with the coefficients presented in the previous section. Furthermore, a frequency domain analysis of the measured data was performed to provide a close approximation to the average modal quantities throughout the measuring period.

### 5.2.1 Rational Orthogonal Polynomial Curve-fit Estimation

Implementation of an established modal analysis parameter estimation routine resulted in the initial values for the extended Kalman filter estimation. Frequency response functions were calculated using averaged auto-power spectra, $G_{yy}$,$G_{xx}$, and cross power spectra, $G_{yx}$, of the response accelerations with respect to the ground accelerations. The $H_v$ estimator of the frequency response function minimizes noise effects on the excitation and the response simultaneously, and results in a frequency response function that is not as biased as traditional H1 or H2 estimators.

$$\mathcal{H}_v = \left(\frac{G_{yx}}{|G_{yx}|}\right)\sqrt{\frac{G_{yy}}{G_{xx}}} \tag{5.1}$$

where $G_{yy}$ is the auto power spectrum of the response acceleration, $G_{xx}$ is the auto power spectrum of the excitation, and $G_{yx}$ is the cross power spectrum of the response with respect to the excitation (Vold, Crowley, and Rocklin, 1984; Rocklin, Crowley, and Vold, 1985). Frequency response functions for seismically excited structures can be computed using absolute accelerations directly by subtracting 1 from the real part of the frequency response function as computed in the above equation (Vigneron and Soucy, 1986). By fitting rational orthogonal polynomials to measured frequency response functions the poles can be extracted from the denominator polynomial and the residues can be calculated from the analytic curve fit transfer function and the previously computed poles. The use of orthogonal polynomials improves the numerical conditioning of the polynomial coefficient computation. Once coefficients for the orthogonal polynomials have been found, the corresponding power polynomial coefficients can be calculated. (Forsythe, 1957; Richardson and Formenti, 1982, 1985; Shih, Tsuei, Allemang, and Brown, 1988; Vold, 1990). The denominator polynomial coefficients are fit globally to an ensemble of transfer functions from an entire structure, using a singular value decomposition. Complex residues are calculated for each transfer function individually (Richardson and Formenti, 1985; Adcock and Potter, 1985; Allemang, 1983; Ewins, 1984). Modal amplitudes are computed as the norm of the complex residue and phases are computed as the phase of the complex residue. The frequency domain method allows for a step-by-step validation of intermediate results and provides a

| El Centro | | | | | |
|---|---|---|---|---|---|
| Mode | Frequency (Hz) | Damping Ratio (%) | 1st Floor | 2nd Floor | 3rd Floor |
| 1 | 6.88 | 0.692 | 8.35 | 14.7 | 17.7 |
| | | | -5.15 | -5.20 | -5.36 |
| 2 | 20.78 | 0.451 | 2.14 | 0.693 | -1.67 |
| | | | -0.904 | 2.82 | 176. |
| 3 | 31.5 | 0.176 | 0.376 | -0.505 | 0.290 |
| | | | 5.96 | -178. | 10.9 |

Table 5-I: **Identification of the Three Story Building Model From El-Centro Input; Rational Orthogonal Polynomial Curve-fit.**

goodness-of-fit parameter. The relative speed with which it computes modal parameters makes it well suited for establishing initial guesses to the extended Kalman filter and other computationally intensive parameter estimation methods. The rational orthogonal polynomial method is implemented in many modal analysis packages used for the analysis of both mechanical, aerospace, and civil structures, (Flesch and Kernbichler, 1988; Ho and Aktan, 1989; Lang, 1990), and thus, was chosen to provide a set of base-line parameters. Since time dependent behavior cannot be captured in a frequency domain analysis, the results obtained from this approach should be viewed with caution. Specifically, they cannot track changes in the modal parameters associated with structural deterioration. In addition, the rational orthogonal polynomial method encounters difficulties if the frequency resolution of the estimated frequency response function is too coarse. A coarse frequency interval results in degeneration of the orthogonality condition of the polynomial basis functions. Since the frequency resolution is inversely proportional to the length of the FFT, short data records, such as earthquake response records, are subject to this difficulty. Figures (5.189-5.197) illustrate frequency response functions and the rational orthogonal polynomial curvefit for the 3 story building model. These figures illustrate the exceptional accuracy of this frequency domain method when applied to lengthy data obtained from structures with little or no nonlinear behavior. Tables (5.3) and (5.4) summarize the parameters identified using the rational orthogonal polynomial method. The third, fourth and fifth columns show the estimated modal amplitudes and phase angles for each floor. The phase angles are shown below the corresponding amplitude.

In the experiments for the three story model, data was recorded over a large number of vibrational periods and with a high resolution in the time domain. The ensuing curve-fit matched the transfer functions and the phases of the residues were consistently within 10 degrees of 0 or 180.

The measurements obtained from the five story model in the Ketter laboratory featured relatively a coarse resolution in the time domain, which resulted in the observed poor performance of the curve-fitting procedure in the frequency domain. The phase angles digressed considerably from 0 or 180 degrees. Phase angles that do not equal 0 or 180 degrees imply the presence of complex modes resulting from non-proportional damping distributions (Lang, 1989). However, the poor curve-fits illustrated in Figures (5.198)-(5.207) call into question any conclusions regarding the parameters associated with these curve-fits. Since the short-lived, nonlinear, transient response of earthquake records com-

| White Noise | | | | | |
|---|---|---|---|---|---|
| Mode | Frequency (Hz) | Damping Ratio (%) | 1st Floor | 2nd Floor | 3rd Floor |
| 1 | 6.87 | 0.839 | 10.4 | 18.4 | 22.1 |
| | | | -0.898 | -0.797 | -0.957 |
| 2 | 20.7 | 0.476 | 2.35 | 0.764 | -1.82 |
| | | | 1.34 | 4.47 | 179. |
| 3 | 31.4 | 0.322 | 0.412 | -0.579 | 0.317 |
| | | | 3.74 | 178. | 7.89 |

Table 5-II: **Identification of the Three Story Building Model From White Noise Input; Rational Orthogonal Polynomial Curve-fit.**

| Sine Sweep | | | | | |
|---|---|---|---|---|---|
| Mode | Frequency (Hz) | Damping Ratio (%) | 1st Floor | 2nd Floor | 3rd Floor |
| 1 | 6.90 | 0.699 | 10.5 | 18.6 | 22.3 |
| | | | -7.28 | -7.23 | -7.41 |
| 2 | 20.8 | 0.471 | 2.28 | 0.758 | -1.76 |
| | | | 0.948 | 3.95 | 178. |
| 3 | 31.6 | 0.391 | 0.414 | -0.538 | 0.334 |
| | | | 1.85 | 174. | 7.07 |

Table 5-III: **Identification of the Three Story Building Model From Sine Sweep Input; Rational Orthogonal Polynomial Curve-fit.**

plicates frequency response function estimation, curve-fitting these functions with a model that assumes linear elastic behavior results in parameters that should be regarded with caution. Although modern modal analysis methods exhibit excellent results for structures tested for arbitrarily long periods, they have difficulty in estimating parameters from earthquake records. Indeed, modal analysis tests usually last several minutes, resulting in very large vibration data-bases and very fine frequency resolution. Also, response levels are continuously monitored to prevent non-linear behavior. The results shown in Figures (5.198)-(5.207) indicate that other methods are required in order to estimate the time-dependent parameters of structures responding to strong ground motions.

### 5.2.2 Recursive Least Squares Estimation

As mentioned earlier, the equivalent modal parameters of the system are directly related to the poles of the linear prediction model. Results pertaining to these poles were discussed in the previous section. Specifically, it was pointed out that the wandering in the complex plane of the poles is associated with unstable estimates which have not converged to their true values. It was also pointed out in section 3 that for values of the poles outside the unit circle, there corresponds negative damping, and therefore those poles were reflected back into the unit circle. Furthermore, for those poles lying on the real line, a value for the critical damping ratio equal to 1 is obtained. In general it seems that the damping values

| El Centro | | | | | | | |
|---|---|---|---|---|---|---|---|
| Mode | Frequency (Hz) | Damping Ratio (%) | 1st Floor | 2nd Floor | 3rd Floor | 4th Floor | 5th Floor |
| 1 | 3.18 | 1.35 | 8.75 | 29.2 | 49.0 | 64.2 | 73.4 |
| | | | 21.5 | 20.2 | 19.6 | 19.2 | 19.0 |
| 2 | 10.1 | 0.146 | 0.761 | 1.65 | 1.21 | -0.617 | -2.07 |
| | | | 110. | 109. | 99.7 | -26.8 | -54.5 |
| 3 | 18.0 | 0.245 | 1.02 | 1.17 | -0.667 | -0.896 | 1.01 |
| | | | -98.3 | -102. | 106. | 98.8 | -106. |
| 4 | 25.1 | 0.036 | 0.840 | 0.415 | -0.986 | 0.724 | -0.700 |
| | | | 6.02 | -178. | -178. | 13.5 | -179. |
| 5 | 30.3 | 0.020 | 0.633 | -0.483 | 0.535 | -0.191 | 0.185 |
| | | | 6.97 | -169. | 8.23 | -160. | -2.27 |

Table 5-IV: **Identification of the Five Story Building Model From El Centro Input; Rational Orthogonal Polynomial Curve-fit.**

are more sensitive to the poles location in the complex plane than the natural frequency values. Given also that the notion of modal damping is itself an artificial device, it should be anticipated that the identification of this quantity is intimately related to the extent to which this device is a good approximation of the real physical behavior of the structure. In light of the above, it is noted that although the modal quantities may be in error, in most cases this error reflects the poor correspondence between the modal description of the physical system and its real behavior.

Figures (5.208)-(5.217) show the estimated natural frequencies and damping ratios obtained from the five-story building model corresponding to measured data from the various floors, and using the unmodified recursive least squares algorithm. It is noted that, in most cases, after large initial fluctuations, the estimates stabilize. In some of the cases, however, a monotonic trend is observed even at the end of the estimation period, suggesting that the estimates have not yet reached their final values. This behavior may be attributed to a strong bias associated with the estimates. Yet in other cases, large fluctuations can be observed throughout the estimation period. These fluctuations seem to be, in most cases, between the values corresponding to two or three different frequencies. In this context, it is observed that whenever a given frequency estimator jumps to another frequency, one of the other estimators starts tracking the frequency lost by the first estimator. Therefore, the estimators seem to fluctuate at the same time, in the same direction. It is also observed that in none of the cases was the highest frequency correctly identified, and that at any given instant, two estimators seem to track the same frequency. A remedy to this problem was attempted by increasing the dimension of the system, by trying to identify more natural frequencies than the number of floors present. The same problem seemed to occur in this case, with the new estimator tracking one of the frequencies already being tracked by another estimator, and the highest frequency going unoticed. This fact may be attributed to the much smaller contribution to the total motion coming from the fifth mode. This can be observed by the much smaller fifth spectral peak in the power spectral densities associated with the measurements. It is also observed that poor frequency estimates are associated with poor damping ratio estimates. As to the effect of the input motion on the estimates, it is noted that the effect is minimal in this case, and similar behavior of

| White Noise | | | | | | | |
|---|---|---|---|---|---|---|---|
| Mode | Frequency (Hz) | Damping Ratio (%) | 1st Floor | 2nd Floor | 3rd Floor | 4th Floor | 5th Floor |
| 1 | 3.17 | 1.318 | 12.7 | 39.7 | 65.5 | 85.2 | 97.18 |
| | | | -11.5 | -13.3 | -13.8 | -14.0 | -14.2 |
| 2 | 10.0 | 0.010 | 1.09 | 2.84 | 2.73 | 0.540 | -1.64 |
| | | | -24.9 | -28.7 | -31.3 | -58.7 | 162. |
| 3 | 17.7 | 0.198 | 1.12 | 1.27 | -0.941 | -1.15 | 1.09 |
| | | | 32.0 | 24.4 | -125.8 | -134. | 26.8 |
| 4 | 25.2 | 0.192 | 0.957 | -0.254 | -0.589 | 1.16 | -0.324 |
| | | | -31.6 | -126. | -179.6 | -39.4 | -164. |
| 5 | 30.4 | 0.168 | 0.518 | -0.354 | 0.601 | -0.208 | 0.294 |
| | | | -38.6 | -172. | -50.9 | -122.7 | -62.6 |

Table 5-V: **Identification of the Five Story Building Model From White Noise Input; Rational Orthogonal Polynomial Curve-fit.**

the estimates is observed for both the El-Centro input motion and the white noise input motion. Results corresponding to the three-story building model are shown in Figures (5.218)-(5.226). Similar observations can be made with regards to these records, except for the effect of the input motion. Indeed, it seems that the results associated with the white-noise input reach their steady values at a much earlier stage than the estimates associated with the other inputs. Also, the estimates associates with the sine-sweep input do not seem to do as well as either of the other two inputs.

Figures (5.227)-(5.245) show the results corresponding to the least squares estimation using an exponential window. Except for few cases, these estimates are not well-behaved, and are in general poorer than the results without a the exponential window. The same algorithm was implemented with values of the parameters $\alpha$ equal to 0.7, 0.8, 0.9, 0.99, 0.995 and 0.997. The results shown here correspond to a value of $\alpha$ equal to 0.99, since this value was recommended in the literature and since the results, although not erratic, help to emphasize the better behavior of the non-windowed algorithm.

The processing of only an initial block of the data through the exponential window had a substantial positive effect on the results. As can be seen in Figures (5.246)-(5.264). The fluctuations have disappeared from all the estimates, except for the sine-sweep excitation in the three-story building model. Also, the monotic trend in the estimates has been reduced substantially, thus indicating that the bias associated with the least squares estimation technique has been substantially reduced. The problem of identifying the highest frequency in the five story building model still persists, though. As mentioned above, this is attributed to its small contribution to the overall motion. Variation of the starting point in the estimation algorithm is one way to tackle this problem, but it was deemed at odds with the purpose of the algorithm, namely to provide a robust identification scheme which would still provide good estimates under incomplete information about the system.

### 5.2.3 Recursive Instrumental Variable Estimation

The same general comments made in relation to the recursive least squares estimation technique are still valid in this case. Figures (5.284)-(5.302) show the corresponding figures for the five-story model and the three-story model. The results are not consistent. The estimated modal quantities vary widely between well behaved and widely fluctuating. The method, in this form, cannot form the basis for a reliable system identification technique.

By filtering the instrumental variable series as indicated in section 3, substantial improvement can be achieved. Figures (5.264)-(5.288) show the results corresponding to this case. The well behaved results obtained with this technique bely the difficulty of its implementation. Specifically, only certain values of the parameter $\gamma$ were found to yield converging estimates for a given record. However, as can be observed, when such a value was found, the estimates exhibited a pronounced improvement over the previous implementation of the instrumental variable algorithm.

### 5.2.4 Maximum Likelihood Estimation

**LINEARID**

Two programs were used in obtaining the results in this section. These are respectively, LINEARID and MUMOID. LINEARID is a program that implements parameter identification algorithms for multi-output systems. The program provides, in addition to the maximum likelihood technique, for least squares estimation and instrumental variable estimation. However, only results pertaining to the maximum likelihood estimation capability of the program are reported herein. LINEARID requires as many input records as the number of degrees of freedom to be identified. Therefore, only a single run was required on each of the two building models investigated. The output from the program consists of estimates of the matrices $\mathbf{M}^{-1}\mathbf{K}$, $\mathbf{M}^{-1}\mathbf{C}$, and $\mathbf{M}^{-1}\mathbf{F}$, where $\mathbf{M}$, $\mathbf{K}$, $\mathbf{C}$, and $\mathbf{F}$ denote respectively, the mass matrix, the stiffness matrix, the damping matrix, and the load vector associated with the system being analysed. The mass matrices associated with both the three-story model and the five-story model were given in section 4. These mass matrices, however, represent the masses lumped at the nodes of the structure, and do not necessarily coincide with the real mass matrix of the structure. This fact can be expected to cause unsymmetric and full matrices to be associated with LINEARID. Indeed, the resulting matrices associated with the three-story model excited by a white noise input were found to be equal to

$$\mathbf{M}^{-1}\mathbf{K} = \begin{bmatrix} 21930 & -11650 & 1056 \\ -12300 & 23920 & -12990 \\ 953.5 & -13060 & 12390 \end{bmatrix}, \tag{5.2}$$

$$\mathbf{M}^{-1}\mathbf{C} = \begin{bmatrix} 2.802 & 2.193 & 2.229 \\ -0.4784 & 0.3337 & -1.307 \\ 0.5817 & 0.3494 & 1.389 \end{bmatrix}. \tag{5.3}$$

The results for the three-story model corresponding to the El-Centro input motion were found to be

$$\mathbf{M}^{-1}\mathbf{K} = \begin{bmatrix} 8222 & -11460 & 3297 \\ -12140 & 25740 & -13890 \\ 995.8 & -11290 & 10780 \end{bmatrix}, \tag{5.4}$$

$$\mathbf{M}^{-1}\mathbf{C} = \begin{bmatrix} 0.07 & 4..317 & -7.291 \\ 3.452 & 3.476 & -1.149 \\ 0.6698 & 1.234 & 0.423 \end{bmatrix}. \tag{5.5}$$

| El Centro Input Motion | | |
|---|---|---|
| Input Record | Natural Frequency Hz. | Damping Ratio (%) |
| First Floor | 12.87 | 0.18 |
| Second Floor | 14.91 | 0.17 |
| Third Floor | 5.02 | 0.44 |

Table 5-VI: **Estimated Modal Parameters for the Three-Story Building Model using LINEARID in Single Input Mode**

| Sine Sweep Input Motion | | |
|---|---|---|
| Input Record | Natural Frequency Hz. | Damping Ratio (%) |
| First Floor | 14.72 | 0.02 |
| Second Floor | 6.37 | 0.17 |
| Third Floor | 5.79 | 0.21 |

Table 5-VII: **Estimated Modal Parameters for the Three-Story Building Model using LINEARID in Single Input Mode**

Note the wide discrepancy in the results, indicating a poor performance of the program for the given data. Moreover, the program failed to converge in the case of the five-story building model. Furthermore, the results obtained from this estimation procedure are not compatible with the results obtained from the other techniques used in the investigation. Specifically, the stiffness matrix cannot be directly related to the natural frequencies of the system, nor can the damping matrix be related to the modal damping ratios. However, the structure of the resulting matrices indicate the extent of cross-modal correlation and can therefore be used as an indication of the significance of an uncoupled modal analysis of the system. In addition to the above results, LINEARID was utilized to identify the dominant mode of the system present in each of the floor accelerations. Thus, the program was implemented in a single-input single-output mode, using the ground motion as input, and one of the floor accelerations as output. This was done for each of the floor accelerations, and for both the three-story model and the five-story model. In this case, the results from LINEARID were interpreted as representing the square of the natural frequencies, $\omega_i^2$ and the damping quantity $2\xi_i\omega_i$, respectively. Accordingly, the modal parameters could be calculated from the output of the program. The results associated with the three-story building model are shown in Tables (5.6)-(5.8) for various input motions, while those corresponding to the five-story model are shown in Tables (5.9) and (5.10). The results in this case are much more consistent than those obtained in the multi-output mode. It is observed that the results from the estimation algorithm are in the range of the two lowest natural frequencies of the structure. It is also obvious that the dominant frequency in a given measured record depends to a great extent on both the particular input motion and the particular floor level on which the measurements were obtained.

| White Noise Input Motion | | |
|---|---|---|
| Input Record | Natural Frequency Hz. | Damping Ratio (%) |
| First Floor | 1.94 | 1.36 |
| Second Floor | 17.27 | 0.10 |
| Third Floor | 17.23 | 0.10 |

Table 5-VIII: **Estimated Modal Parameters for the Three-Story Building Model using LINEARID in Single Input Mode**

| El Centro Input Motion | | |
|---|---|---|
| Input Record | Natural Frequency Hz. | Damping Ratio (%) |
| First Floor | 5.31 | 0.45 |
| Second Floor | 5.46 | 0.39 |
| Third Floor | 6.43 | 0.27 |
| Fourth Floor | 7.57 | 0.05 |
| Fifth Floor | 7.56 | 0.12 |

Table 5-IX: **Estimated Modal Parameters for the Five-Story Building Model using LINEARID in Single Input Mode**

| White Noise Input Motion | | |
|---|---|---|
| Input Record | Natural Frequency Hz. | Damping Ratio (%) |
| First Floor | 16.61 | 0.14 |
| Second Floor | 15.56 | 0.30 |
| Third Floor | 16.59 | 0.148 |
| Fourth Floor | 16.74 | 0.09 |
| Fifth Floor | 16.59 | 0.15 |

Table 5-X: **Estimated Modal Parameters for the Five-Story Building Model using LINEARID in Single Input Mode**

| White Noise Input Motion: Output at Fifth Floor | | | |
|---|---|---|---|
| Mode No. | Damping Factor (%) | Natural Frequency Hz. | Participation Factor |
| 1 | -0.0122 | 3.025 | 0.17 |
| 2 | 0.000742 | 10.19 | 0.20 |
| 3 | -0.0964 | 18.62 | 0.20 |
| 4 | 0.0440 | 28.01 | -2.90 |
| 5 | 0.0515 | 30.08 | 3.33 |

Table 5-XI: **Estimated Modal Parameters for the Five-Story Building Model using MUMOID and a 1sec segment of the data.**

### MUMOID

The program MUMOID was originally developed to incorporate system identification of structural systems into a damage assessment context. For the purpose of this study, only the system identification part was analysed. The algorithm consists of tracking variations in the parameters of the system using a moving rectangular window and performing the identification task using the data in the window and a maximum likelihood algorithm. The main issue in the implementation of the formalism underlying MUMOID, is the choice of a window size. A very small window size would be desirable for the purpose of tracking fine or sudden changes in the parameters of the system. However if the window is too small, then problems are encountered with the estimation algorithm which may fail to converge to stable estimates using the little information available in a narrow window. Various window values for the window width were tried, varying from two times the fundamental period of the structure to much larger values. In none of the cases was the program able to sweep through the whole data. That, is the program would fail at a certain window location. However, for those locations where the program was successful at identifying the natural frequencies corresponding to the structure, excellent results were obtained. In that case, even the highest natural frequency was successfully identified. Tables (5.11) and (5.12) shows the results obtained from applying MUMOID to the data associated with the five-story building model. It is immediately observed that the effect of the input motion on the estimated parameters is negligible, so is the effect of the floor level from which the measurements are taken. This is partially due to the fact that MUMOID provides for the processing of the prediction errors associated with the identified system. This processing insures that these errors are uncorrelated. However, such a processing does add to the complexity of the algorithm and prohibits its on-line implementation. As was observed with the recursive techniques presented above, even with no processing of the errors, or minimal processing, good estimation of the behavior of the system can be obtained.

## 5.2.5 Extended Kalman Filter Estimation

Results from the rational orthogonal polynomial curvefit were used as initial parameter values for estimation via EXKAL2. The parameters estimated from the three story building model are very consistent and correspond closely to the values obtained from the rational orthogonal polynomial curve-fit. The following tables show how the parameter estimation process depends on the excitation type. Within each test, frequency and damping estimates

| El-Centro Input Motion; Output at First Floor | | | |
|---|---|---|---|
| Mode No. | Damping Factor (%) | Natural Frequency Hz. | Participation Factor |
| 1 | -0.119 | 3.02 | -1.1 |
| 2 | 0.0395 | 10.1 | 0.38 |
| 3 | 0.565 | 18.6 | 3.1 |
| 4 | 0.306 | 28.0 | -1.8 |
| 5 | 0.0102 | 30.0 | 0.38 |

Table 5-XII: **Estimated Modal Parameters for the Five-Story Building Model using MUMOID and a 1sec segment of the data.**

are very consistent, however, the frequency and damping parameter estimates vary between tests. Large initial covariances allowed the parameters to deviate from their initial values before converging on the values reported in the tables below. Values in the columns labeled 'Participation Factor' are actually the product of the modal participation factor and the mass-normalized mode shape. This reflects both the mode's participation in the over-all response to the particular excitation and the actual mode-shape. In the preceding tables fields with a – indicate that EXKAL2 could not identify the corresponding quantity. In some cases values for a were repeated and in other cases the values were clearly in error. EXKAL2 consistently experienced difficulty in estimating the 2nd mode using data from the third floor. This illustrates the importance of sensor location for parameter estimation.

Unlike the frequency domain curve-fit, EXKAL2 does not estimate the frequencies and damping ratios in a global manner even though they are global parameters. Nevertheless, the estimated frequencies are within 0.1% of each other. The damping ratio estimations vary slightly more, however, damping ratios are, in general, more difficult to estimate. And very small damping does not play a significant role in a structure's overall performance.

Considering EXKAL2's reliance upon the linear acceleration method for estimation of dynamic properties, it fared remarkably well when applied to the data from the five story building model. In these tests the sample rate was only three times the highest natural frequency. The accuracy of the linear acceleration method deteriorates rapidly as the number of points per sinusoidal oscillation decreases. In fact, sample rates of at least five times the highest response frequency are recommended for numerical integration. Errors associated with the numerical integration of the fourth and fifth modes may have prevented accurate estimation of those modes using data from floors in which those modes do not contribute strongly to the overall response. In some cases, (the 1st and 4th floors of the white noise excitation case) the slow sample rate resulted in meaningless parameters for all floors or failure of the program to converge at all. These results are not reported. Nevertheless, the fourth and fifth modes were identified from the 1st and 2nd floors of the El Centro excitation case. Also, lower modes could be identified in a consistent fashion using data from any of the floors. The following tables summarize the modal parameters as estimated by EXKAL2 for the five story building model.

EXKAL2 obtained consistent results for the first 4 modes of the five story building undergoing El Centro excitation. However, the data files from the white noise case proved to be more challenging. This may have been due to a time step which was too large with respect to the highest natural frequency in the response. Ideally, the time step should

| El Centro; 1st Floor | | | |
|---|---|---|---|
| Mode | Frequency (Hz) | Damping Ratio | Participation Factor |
| 1 | 6.8 | 0.805 | 0.580 |
| 2 | 20.8 | 0.537 | 0.295 |
| 3 | 31.7 | 0.112 | 0.056 |

| El Centro; 2nd Floor | | | |
|---|---|---|---|
| Mode | Frequency (Hz) | Damping Ratio | Participation Factor |
| 1 | 6.89 | 0.810 | 1.02 |
| 2 | 20.8 | 0.520 | 0.0942 |
| 3 | 31.7 | 0.115 | -0.0798 |

| El Centro; 3rd Floor | | | |
|---|---|---|---|
| Mode | Frequency (Hz) | Damping Ratio | Participation Factor |
| 1 | 6.90 | 0.763 | 1.23 |
| 2 | 20.8 | 0.551 | -0.220 |
| 3 | 31.7 | 0.334 | 0.0412 |

Table 5-XIII: **Identification of the Three Story Building Model From El-Centro Input; Extended Kalman Filter Algorithm.**

be one-twentieth of the lowest period for EXKAL2 to accurately implement the linear acceleration method.

| White Noise; 1st Floor | | | |
|---|---|---|---|
| Mode | Frequency (Hz) | Damping Ratio | Participation Factor |
| 1 | 6.91 | 0.865 | 0.594 |
| 2 | 20.8 | 0.510 | 0.380 |
| 3 | 31.6 | 0.303 | 0.0953 |

| White Noise; 2nd Floor | | | |
|---|---|---|---|
| Mode | Frequency (Hz) | Damping Ratio | Participation Factor |
| 1 | 6.91 | 0.839 | 1.04 |
| 2 | 20.8 | 0.475 | 0.124 |
| 3 | 31.6 | 0.265 | -0.130 |

| White Noise; 3rd Floor | | | |
|---|---|---|---|
| Mode | Frequency (Hz) | Damping Ratio | Participation Factor |
| 1 | 6.91 | 0.870 | 1.34 |
| 2 | | 0.269 | -0.484 |
| 3 | 31.6 | 0.360 | 0.0784 |

Table 5-XIV: **Identification of the Three Story Building Model From a White Noise Input; Extended Kalman Filter Algorithm.**

| Sine Sweep; 1st Floor | | | |
|---|---|---|---|
| Mode | Frequency (Hz) | Damping Ratio | Participation Factor |
| 1 | 6.92 | 0.766 | 0.598 |
| 2 | 20.8 | 0.395 | 0.363 |
| 3 | 31.7 | 0.320 | 0.0999 |

| Sine Sweep; 2nd Floor | | | |
|---|---|---|---|
| Mode | Frequency (Hz) | Damping Ratio | Participation Factor |
| 1 | 6.92 | 0.756 | 1.04 |
| 2 | 20.6 | 0.386 | 0.117 |
| 3 | 31.7 | 0.318 | -0.140 |

| Sine Sweep; 3rd Floor | | | |
|---|---|---|---|
| Mode | Frequency (Hz) | Damping Ratio | Participation Factor |
| 1 | 6.92 | 0.757 | 1.32 |
| 2 | - | 9.84 | -0.486 |
| 3 | 31.7 | 0.330 | 0.0761 |

Table 5-XV: **Identification of the Three Story Building Model From a Sine Sweep Input; Extended Kalman Filter Algorithm.**

| El Centro; 1st Floor | | | |
|---|---|---|---|
| Mode | Frequency (Hz) | Damping Ratio | Participation Factor |
| 1 | 3.17 | 0.375 | 0.176 |
| 2 | 10.2 | 0.059 | 0.202 |
| 3 | 18.7 | 0.129 | 0.233 |
| 4 | 28.1 | 4.88 | -2.93 |
| 5 | 30.1 | 5.81 | 1.54 |

| El Centro; 2nd Floor | | | |
|---|---|---|---|
| Mode | Frequency (Hz) | Damping Ratio | Participation Factor |
| 1 | 3.17 | 0.377 | 0.546 |
| 2 | 10.2 | 0.0480 | 0.471 |
| 3 | 18.6 | 0.600 | 0.0906 |
| 4 | 25.6 | 2.08 | 0.0104 |
| 5 | 30.3 | 2.70 | 0.0259 |

| El Centro; 3rd Floor | | | |
|---|---|---|---|
| Mode | Frequency (Hz) | Damping Ratio | Participation Factor |
| 1 | 3.17 | 0.382 | 0.902 |
| 2 | 10.2 | 0.058 | 0.375 |
| 3 | 18.7 | 0.160 | -0.236 |
| 4 | - | - | - |
| 5 | - | - | - |

| El Centro; 4th Floor | | | |
|---|---|---|---|
| Mode | Frequency (Hz) | Damping Ratio | Participation Factor |
| 1 | 3.17 | 0.382 | 1.16 |
| 2 | 10.2 | 0.036 | -0.0347 |
| 3 | 18.7 | 0.125 | -0.255 |
| 4 | 28.1 | 0.946 | 0.279 |
| 5 | - | - | - |

| El Centro; 5th Floor | | | |
|---|---|---|---|
| Mode | Frequency (Hz) | Damping Ratio | Participation Factor |
| 1 | 3.17 | 0.380 | 1.32 |
| 2 | 10.2 | 0.055 | -0.425 |
| 3 | 18.7 | 0.680 | 0.586 |
| 4 | 25.9 | 10.2 | -0.0406 |
| 5 | - | - | - |

Table 5-XVI: **Identification of the Five Story Building Model From El-Centro Input; Extended Kalman Filter Algorithm.**

| White Noise; 2nd Floor | | | |
|---|---|---|---|
| Mode | Frequency (Hz) | Damping Ratio | Participation Factor |
| 1 | 3.17 | 0.719 | 0.637 |
| 2 | 10.2 | 0.086 | 0.575 |
| 3 | 18.7 | 0.229 | 0.275 |
| 4 | 27.8 | 0.116 | -0.0334 |
| 5 | - | - | - |

| White Noise; 3rd Floor | | | |
|---|---|---|---|
| Mode | Frequency (Hz) | Damping Ratio | Participation Factor |
| 1 | 3.17 | 0.719 | 1.04 |
| 2 | 10.3 | 0.084 | 0.446 |
| 3 | 18.8 | 0.224 | -0.225 |
| 4 | 27.8 | 0.087 | -0.193 |
| 5 | - | - | - |

| White Noise; 5th Floor | | | |
|---|---|---|---|
| Mode | Frequency (Hz) | Damping Ratio | Participation Factor |
| 1 | 3.18 | 0.776 | 1.708 |
| 2 | 10.3 | 0.093 | -0.515 |
| 3 | 18.7 | 0.204 | 0.229 |
| 4 | 27.8 | 0.107 | -0.107 |
| b5 | - | - | - |

Table 5-XVII: **Identification of the Five Story Building Model From White Noise Input; Extended Kalman Filter Algorithm.**

# Section 6

# Conclusions

This report presented the results from the final phase of a research effort whose aim was a comprehensive treatment of system identification techniques in earthquake engineering applications. It was the intention of this phase of the research to assess, experimentally, the accuracy and validity of the techniques developed in the earlier phases of the investigation.

The emphasis placed throughout the investigation on time domain techniques for system identification is justified by the desire to monitor the evolution in time of the identified parameters. This capability has the potential of permitting the synthesis of more meaningful damage assessment indices, as well as enhancing the reliability of adaptive schemes that may be used for on-line control of structural systems.

The experiments reported in this research involved models of buildings subjected to a number of different loading conditions, and whose motion was monitored at all floor levels. A number of system identification algorithms were used to obtain estimates of the parameters in a mathematical model describing the motion of the structure. At issue in this process were both the suitability of this mathematical model, as well as the validity of the identification algorithm itself. In addition to analyzing these two factors, results were presented that demonstrated the importance of monitoring the motion at different floor levels. Indeed, for different input motions, different measurements corresponding to different floor levels were best suited for the identification task. This observation emphasizes the importance of the location of the measuring device for monitoring the response of a structure. One of the main conclusions of this study was to stress the importance of robustness and simplicity in the identification algorithms. As observed from the results, the more sophisticated algorithms yielded better results, on some of the measurements, failing to converge, however, for the remaining ones. These algorithms were also quite sensitive to the initial guess regarding the unknown parameters. Such a behavior, although not quite serious in an off-line setting, and when experts are implementing the algorithms, can be detrimental in an on-line environment or with users of lesser expertise. The algorithms based on the least squares estimation, on the other hand, proved to be more versatile in that they always yielded results, the significance of which is intimately related to the concept of least squares interpolation. Variations on the basic least squares algorithm proved helpful in improving the statistical properties of these estimates. Specifically, giving less weight to the data in the early stages of the estimation process helped in eliminating the bias in the estimates. This can be explained by the fact that the early stages are corrupted by the error in the initial guess which tends to propagate unless properly damped out.

The issue of a suitable identification algorithm is compounded with the issue of deciding on an adequate mathematical model for the structure. This issue comes into play when

| Identification Techniques | Required Expertise | Numerical Convergence | On-Line Potential | Initial Guess | Reliability of Results |
|---|---|---|---|---|---|
| Maximum Likelihood | substantial | sometimes | low | close | good |
| Extended Kalman Filter | substantial | sometimes | low | close | good |
| Recursive Least Squares | minimal | always | high | anywhere | medium |
| Recursive Least Squares with Exponential Window | minimal | always | high | anywhere | good |
| Recursive Instrumental Variable | medium | always | high | anywhere | medium |
| Recursive Instrumental Variable with Filter | substantial | sometimes | high | anywhere | medium |

Table 6-I: **Comparison of System Identification Algorithms**

deriving an equivalence between the parameters of the linear prediction model and a set of physical parameters such as modal quantities. Whereas a linear prediction model has a definite interpretation as a linear relationship between the input and output measurements, a differential equation model based on modal superposition involves further assumptions that are likely not to hold under earthquake-type excitations. As a consequence of this, although the linear prediction model can be used to forecast the behavior of the structure with a well understood optimization criterion, the same does not hold for the differential equation model. Therefore, depending on the context in which the identification algorithm is being used, it may be more consistent to use the linear prediction model.

Table (6.1) summarizes the recommendations from this study while highlighting the issues that were deemed important in assessing the worthiness of each of the identification algorithms.

As mentioned in the introduction to this study, a system identification program is seldom an end product by itself. It is generally implemented as part of a broader strategy for the control or damage assessment of structural systems. From this perspective, it is believed that future research in the field of system identification should emphasize the implementation of simple and reliable identification algorithms, which are already widely available, into the final context in which they will be used. It is also believed that concepts from expert systems and neural networks have the potential of efficiently managing the large amount of information associated with on-line diagnostics and monitoring. In this way, complex strategies for decision making and control can be implemented that make the most out of the information extraction capabilities of whatever identification algorithm is used.

# Section 7

# References


[1] Adcock, J. and Potter, R., "A Frequency Domain Curve Fitting Algorithm with Improved Accuracy," *3rd International Modal Analysis Conference*, Orlando, FL. 1985.

[2] Agbabian, M.S., Masri, S.F., Miller, R.K., and Caughey, T.K., "System identification approach to detection of structural changes," *ASCE, Journal of Engineering Mechanics*, Vol. 117, No. 2, pp. 370-390, 1991.

[3] Akaike, H., "A new look at the statistical model identification," *IEEE Transactions on Automatic Control*, Vol. AC-19, No. 6, pp. 716-723, December, 1974.

[4] Allemang, R.J., "Experimental modal analysis," pp. 1-29, in *Modal Testing and Model Refinement*, AMD Vol. 59, Edited by David F.H. Chu, ASME, 1983.

[5] Anderson, T.J., Balachandran, B., and Nayfeh, A.H., "Investigation of multi-mode interactions in a continuous structure," $62^{nd}$ *Shock and Vibration Symposium*, Springfield VA, 29-31 October 1991.

[6] Anifantis, N., Rizzs, P. and Dimarogonas, A. "Identification of cracks on beams by vibration analysis," *Mechanical Signature Analysis, Machinery Vibration, Flow-Induced Vibration and Acoustic Noise Analysis*, Edited by Braun S., Lu, K.H., Au Yang, M.K. and Ungar, E.E., pp. 189-197, 1987.

[7] Astrom, K.J., "Maximum likelihood and prediction error methods," *Automatica*, Vol. 16, pp. 551-574, 1980.

[8] Balachandran, B., and Nayfeh, A.H., "Nonlinear motions of beam-mass structures," *Nonlinear Dynamics*, Vol. 2, pp. 39-61, 1990.

[9] Balachandran, B., Anderson, T.J., and Nayfeh, A.H., "Detection of nonlinear interactions in structures," $62^{nd}$ *Shock and Vibration Symposium*, Springfield VA, 29-31 October 1991.

[10] Balachandran, B., and Nayfeh, A.H., "Observations of modal interactions in resonantly forced beam-mass structures," *Nonlinear Dynamics*, Vol. 2, pp. 77-117, 1991.

[11] Bartlett, M.S., "On the theoretical specification and sampling properties of autocorrelated time-series," *Journal of the Royal Statistical Society*, Supplement 8, No. 1, pp. 27-41, 1946.

[12] Bao, Z-W. "Parameter Identification of Structural Models by Means of the Extended Kalman Filter." *7th International Modal Analysis Conference*, 1989.

[13] Beck, J.L., "Structural identification using linear models and earthquake records," *Earthquake Engineering and Structural Dynamics*, Vol. 8, pp. 145-160, 1980.

[14] Bottiger, F. and Panik, F. "Identification of physical parameters of road vehicles," *IFAC Identification and System Parameter Estimation Conference*, pp. 835-840, 1982.

[15] Braun, S. Editor *Mechanical Signature Analysis: Theory and Applications*, Academic Press, 1986.

[16] Brockett, R. W., "Volterra series and geometric control theory," *Automatica* Vol. 12, pp. 167-176, 1976. .XP

[17] Brown, R.G. *Introduction to Random Signal Analysis and Kalman Filtering*, New York: John Wiley and Sons, 1983.

[18] Cakmak, A., and Sherif, R.I., "Parametric time series models for earthquake strong ground motions and their relationship to site parameters," pp. 581-588, *Proceedings of the Eighth World Conference on Earthquake Engineering*, San Francisco, CA 1984.

[19] Cawley, P. and Ray, R. "A comparison of the natural frequency changes produced by cracks and slots," *Mechanical Signature Analysis, Machinery Vibration, Flow-Induced Vibration and Acoustic Noise Analysis*, Edited by Braun S., Lu, K.H., Au Yang, M.K. and Ungar, E.E., pp. 63-68, 1987.

[20] Cowan, C.F.N. and Adams P.F. "Non-linear system modelling: concept and application," *Proceedings of the ICASSP*, pp. 45.6.1-45.6.4, 1984.

[21] Cox, H., "On the estimation of state variables and parameters for noisy dynamic systems," *IEEE Transactions on Automatic Control*, Vol. AC-9, pp. 5-12, January 1964.

[22] Davies, P. and Hammond, J.K. "A comparison of Fourier and parametric methods for structural system identification," *Transactions of the ASME*, pp. 40-48, Vol. 106, January 1984.

[23] Dickinson, B.W. "Estimation theory and signal processing," *IFAC Identification and System Parameter Estimation*, pp. 91-92, 1982.

[24] DiPasquale, E., and Cakmak, A.S., *Detection and Assessment of Seismic Structural Damage*, Technical Report NCEER-87-0015, National Center for Earthquake Engineering Research, Buffalo, NY 1987.

[25] DiPasquale, E., and Cakmak, A.S., *Identification of the Serviceability Limit State and Direction of Seismic Structural Damage*, Technical Report NCEER-88-0022, National Center for Earthquake Engineering Research, Buffalo, NY 1988.

[26] Dobbs, M.W. and Riley, W.F., "System Identification of Large-Scale Structures," SAE Paper 811050, 1981.

[27] Douglas, B.M. and Reid, W.H., "Dynamic Tests and System Identification of Bridges," *ASCE, Journal of the Structural Division*, Vol. 108, No. ST10, October 1982.

[28] Emel, E. and Kannatey-Asibu Jr., E. "Tool failure monitoring in turning by pattern recognition analysis of AE signals," *ASME, Journal of Engineering for Industry*, Vol. 110, pp. 137-145, 1988.

[29] Evans, R.J., Xianya, X., Zhang, C., and Soh, Y.C., "Algorithms for discrete-time adaptive control of rapidly time-varying systems," pp. 251-282 in *Control and Dynamic Systems: Advances in Theory and Applications; Volume 29, Part 2*. Edited by C.T. Leondes, Academic Press, San Diego, 1988.

[30] Ewins, D.J., *Modal Testing: Theory and Practice*, Letchworth, Hertfordshire, England: Research Studies Press, 1984.

[31] Eykhoff, P. "On the coherence among the multitude of system identification methods," *IFAC System Identification and System Parameter Estimation*, pp. 31-42, 1982.

[32] Fassois, S.D., and Lee, J.E., "Suboptimum maximum likelihood identification of ARMAX processes," *ASME, Journal of Dynamic Systems, Measurement, and Control*, Vol. 112, pp. 586-595, 1990.

[33] Feder, Meir and Weinstein, Ehud, "On the finite maximum entropy extrapolation," *Proceedings of the IEEE*, Vol. 72, No. 11, pp. 1660-1662, November, 1984.

[34] Finn, G., "Expert systems for dynamic analysis interpretation," pp. 641-653, *Computing in Civil Engineering, Proceedings of the Fourth Conference*, Edited by W. Tracy Lenocker, 1986.

[35] Flesch, R.G. and Kernbichler, K., "A Dynamic Method for the Safety Inspection of Large Prestressed Bridges," *International NSF Workshop on Nondestructive Evaluation for Performance of Civil Structures* Edited by Agbabian, M.S. and Masri, S.F., UCLA, 1988.

[36] Forsythe, G.E., "Generation and Use of Orthogonal Polynomials for Data-Fitting with a Digital Computer," J. Soc. Indust. Appl. Mathematics, Vol. 5, No. 2, June 1957.

[37] Gaby, James E. and Hayes, Monson H. "Artificial intelligence applied to spectrum estimation," *Proceedings of the ICASSP*, pp. 13.5.1-13.5.4, 1984.

[38] Gersch, W., and Luo, S., "Discrete time series synthesis of randomly excited structural system response," *The Journal of the Acoustical Society of America*, Vol. 51, No. 1, pp. 402-408, 1972.

[39] Gersch, W., Nielsen, N.N., and Akaike, H., "Maximum likelihood estimation of structural parameters from random vibration data," *Journal of Sound and Vibration*, Vol. 31, No. 2, pp. 295-308, 1973.

[40] Gersch, W., and Liu, R.S-Z., "Time series methods for the synthesis of random vibration systems," *ASME, Journal of Applied Mechanics*, pp. 159-165, March 1976.

[41] Gertler, J., and Banyasz, C., "A recursive (on-line) maximum likelihood identification method," *IEEE Transactions on Automatic Control*, Vol. AC-19, No. 6, December 1974.

[42] Goodwin, G.C. and Payne, R.L., *Dynamic System Identification: Experiment Design and Data Analysis*, Academic Press, New York, San Francisco, London, 1977.

[43] Greblicki, W. "Nonparametric system identification by orthogonal series," *Problems of Control and Information Theory*, Vol.8, No. 1, pp. 67-73, 1979.

[44] Hac, Aleksander and Spanos Pol, "Time domain structural parameters identification," *Dynamics of Structures, Proceedings of the Sessions at Structures Congress 1987*, Edited by Jose M. Roesset, pp. 841-858, 1987.

[45] Haggan, V. and Ozaki, T., "Modelling nonlinear random vibrations using an amplitude-dependent autoregrassive time series model," *Biometrika*, Vol. 68, No. 1, pp. 189-196, 1981.

[46] Hamming, R.W., *Digital Filters, 3rd ed.*, Prentice Hall, Englewood Cliffs, NJ, 1989.

[47] Hart, G.C., and Yao, J.T.P., "System identification in structural dynamics," *ASCE, Journal of Engineering Mechanics*, Vol. 103, No. EM6, pp. 1089-1104, 1977.

[48] Hassenzagel, R. and Ziegler, F., "Elasto-Plastic Random Vibrations of Two-Story Frames - Experimental Results," Austrian Engineer and Architect, No. 134, pp. 407-410, 1989.

[49] Haykin, S. Editor, *Nonlinear Methods of Spectral Analysis*, Springer-Verlag, Berlin, Heidelberg, New York, 1979.

[50] Hespel, C., and Jacob, G., "Approximation of nonlinear systems by bilinear ones," pp. 511-520, in *Algebraic and Geometric Methods in Nonlinear Control Theory*,, Edited by M. Fliess and M. Hazewinkel, Reidel Publishing Company, 1986.

[51] Hjelmstad, K.D., Wood, S.L., and Clark, S., *Parameter Estimation in Complex Linear Structures*, Civil Engineering Studies, Structural Research Series No. 557, UILU-ENG-90-2015, University of Illinois, Urbana, Il, 1990.

[52] Ho, I-K., and Aktan, A.E., *Linearized Identification of Buildings with Cores for Seismic Vulnerability Assessment*, Technical Report NCEER-89-0041, National Center for Earthquake Engineering Research, Buffalo, NY 1989.

[53] Hoshiya, M., and Saito, E., "Structural identification by extended Kalman filter," *ASCE, Journal of Engineering Mechanics*, Vol. 110, No. 12, pp. 1757-1770, 1983.

[54] Hoshiya, M. "Application of the Extended Kalman Filter-WGI Method in Dynamic System Identification," Y.K. Lin Anniversary Memoirs, 1987.

[55] Hsia, T.C. *System Identification: Least Squares Methods*, Lexington Books, Lexington, MA, 1977.

[56] Hu, Yu Hen and Abdallah. Ali Hussein, "Knowledge-based adaptive signal processing," *Proceedings of the ICASSP*, pp. 43.5.1-43.5.4, 1987.

[57] Hung, J.C. and Miller, J.S., "On-Line Identification of Random Parameters in Two Parallel Systems," *Identification and System Parameter Estimation*, North-Holland Publishing Co. 1978.

[58] Imai, H., Yun, C-B., Maruyama, O., and Shinozuka, M., *Fundamentals of System Identification in Structural Dynamics*, Technical Report NCEER-89-0008, National Center for Earthquake Engineering Research, Buffalo, NY 1989.

[59] Imregun, M., and VIsser, W.J., "A review of model updating techniques," *The Shock and Vibration Digest.*, pp. 9-20.

[60] Isermann, R., Baur, U., Bamberger, W., Kneppo, P., and Siebert H., "Comparison of six on-line identification and parameter estimation methods," *Automatica,* Vol. 10, pp. 81-103, 1974.

[61] Iserman, R., "Process fault detection based on modeling and estimation methods," *Proceedings of the 6supth IFAC Symposium*, pp. 7-30, 1982.

[62] Iwan, W.D. and Cifuentes, A.O., "A Model for system identification of degrading structures," *Earthquake Engineering and Structural Dynamics,* Vol. 14, pp. 877-890, 1986.

[63] Jazwinski, A.H., *Stochastic Processes and Filtering Theory*, Academic Press, New York and London, 1970.

[64] Jazwinski, A.H., "Adaptive sequential estimation with applications," *Automatica,* Vol. 10, pp.203-207, 1974.

[65] Kallenbach, R., "Identification methods for vehicle system dynamics," *Vehicle System Dynamics*, Vol. 16, pp. 107-127, 1987.

[66] Kalman, R.E., "A New Approach to Linear Filtering and Prediction Problems," *ASME Journal of Basic Engineering* March, 1960.

[67] Kalman, R.E. and Bucy, R.S., "New Results in Linear Filtering and Prediction Theory," *ASME Journal of Basic Engineering* March, 1961.

[68] Kalra, Prem Kumar "Development of an expert system for fault diagnosis in HVDC systems using spectral approach," *Applications of Artificial Intelligence in Engineering Problems*, Edited by D. Sriram and R. Adey, pp. 1193-1198, 1986.

[69] Kashyap, R.L., "Maximum likelihood identification of stochastic linear systems," *IEEE Transactions on Automatic Control,* Vol. AC-15, No. 1, pp. 25-34, 1970.

[70] Kim, K.J., Eman, K.F. and Wu, S.M. "Identification of natural frequencies and damping ratios of machine tool structures by the dynamic data system approach," *Int. J. Mach. Tool Des. Res.,* Vol. 24, No. 3, pp. 161-169, 1984.

[71] Kimbrough, S., "Bilinear modelling and regulation of variable component suspension." pp. 235-255 in *Symposium on Simulation and Control of Ground Vehicles and Transportation Systems*, AMD-Vol. 80, DSC-Vol. 2, Edited by L. Segel, J.Y. Wong, E.H. Law, and D. Hrovat, 1986.

[72] Kozin, F., and Natke, H.G., "System identification techniques," *Structural Safety*, Vol. 3, pp. 269-316, 1986.

[73] Krishnabrahmam, V., Iyengar, K.R.S. and Kalyani, K. "Expert system for signature analysis," *Def. Sci. J.*, Vol. 37, No. 4, pp. 495-505, October, 1987.

[74] Kumamaru, K., Inoue, K., Nishimura, Y., Ono, T. and Kumamaru, T. "A hierarchical diagnosis for failure detection of dynamical systems," *IFAC Identification and System Parameter Estimation*, pp. 597-602, 1982.

[75] Kuroda, Y., Uchida, H. and Ohmasa, Y., "Multivariate arma modeling with spline functions for reactor noise," *Progress in Nuclear Energy*, Vol. 15, pp. 849-852, 1985.

[76] Lang, G.F., "Demystifying Complex Modes," *Sound and Vibration Magazine*, January, 1989.

[77] Lang, G.F., "PC Based Modal Analysis Comes of Age," *Sound and Vibration Magazine*, January, 1990.

[78] Larimore, W.E., "A survey of some recent developments in system parameter identification," *Proceedings of the 6supth IFAC Conference*, pp. 1107-1112, 1982.

[79] Lee, C.-G., *Parameter Estimations of Structural Dynamic Systems Using Sequential Prediction Error Method*, Ph.D. Thesis, Department of Civil Engineering, Korea Advanced Institute of Science and Technology, November 1990.

[80] Lee, C.-G., and Yun, C.-B., "Parameter Estimations of Structural Dynamic Systems," *Computers and Structures*, In press.

[81] Lee, C.K., *Optimal Estimation, Identification, and Control*, Research Monograph No. 28, The M.I.T. Press, Cambridge, MA, 1964.

[82] LePage, Richard, "Interactive software package for digital signal processing," *Proceedings of the ICASSP*, pp. 43.8.1-43.8.4, 1987.

[83] Lin, C.C., Soong, T.T., and Natke, H.G., "Real-time system identification of degrading structures," *ASCE, Journal of Engineering Mechanics*, Vol. 116, No. 10, pp. 2258-2274, October 1990.

[84] Ljung, L., Morf, M., and Falconer, D., "Fast calculation of gain matrices for recursive estimation schemes," *International Journal of Control*, Vol. 27, NO. 1, pp. 1-19, 1978.

[85] Ljung, L., "Asymptotic behavios of the extended Kalman filter as a parameter estimator for linear systems," *IEEE Transactions on Automatic Control*, Vol. AC-24, No. 1, pp. 36-50, February 1979.

[86] Ljung, L., "Identification Methods," *IFAC Identification and System Parameter Estimation*, pp. 57-64, 1982.

[87] Ljung, L., "Estimation of parameters in dynamical systems," pp.189-211, in *Handbook of Statistics*, Edited by E.J. Hannan, P.R. Krishnaiah, and M.M. Rao, Elsevier Science Publisher, 1985.

[88] Ljung, L., "Frequency and time domain methods in system identification," *Modelling, Identification and Robust Control*, Edited by C.I. Byrnes and A. Lindquist, pp. 615-624, 1986.

[89] Luk, Y.W., and Mitchell, L.D., "System identification via modal analysis," pp. 31-49, in *Modal Testing and Model Refinement*, AMD Vol. 59, Edited by David F.H. Chu, ASME, 1983.

[90] Lyon, R.H., "Progressive phase trends in multi-degree-of-freedom systems," *Journal of the Acoustical Society of America*, Vol. 73, No. 4, pp. 1223-1228, April 1983.

[91] Lyon, R.H. and DeJong, R.G., "Design of a high level diagnostic system," *Journal of Vibration, Acoustics, Stress and Reliability in Design*, Vol. 106, pp. 17-21, January 1984.

[92] Mansour, David, "Efficient nonlinear system identification," *Proceedings of the ICASSP*, pp. 45.3.1-45.3.4, 1984.

[93] Maruyama, O., Yun, C-B., Hoshiya, M., and Shinozuka, M., *Program EXKAL2 for Identification of Structural Dynamic Systems*, Technical Report NCEER-89-0014, National Center for Earthquake Engineering Research, Buffalo, NY, 1989.

[94] McElroy, J.W. and Scheibel, J.R. "On-line diagnostic monitoring," *InTech*, pp. 29-32, December 1987.

[95] Meinhold, R.J., and Singpurwalla, N.D., "Understanding the Kalman filter," *The American Statistician*, Vol. 37, No. 2, pp. 123-127, 1983.

[96] Mita, Tsutomu, "Optimal digital feedback control systems counting computation time of control laws," *IEEE Transactions on Automatic Control*, Vol. AC-30, No. 6, pp. 542-458, June 1985.

[97] Mottershead, J.E. and Stanway, R. "Identification of structural vibration parameters by using a frequency domain filter," *Journal of Sound and Vibration*, Vol. 109, No. 3, pp. 495-506, 1986.

[98] Nayfeh, A.H., "Parametric identification of nonlinear dynamic systems," *Computers and Structures*, Vol. 20, No. 1-3, pp. 487-493, 1985.

[99] Noguchi, H., Terui, I. and Usushiyama, Y., "A sensitivity analysis using frequency response function," pp. 980-986, *Proceedings of the Sixth International Modal Analysis Conference*, Kissimmee, Fla., 1988.

[100] Ogawa, H., Fu, K.S. and Yao, J.T.P "An expert system for structural damage assessment, *Pattern Recognition Letters*, Vol. 2, pp. 427-432, December, 1984.

[101] Ozaki, T., "Non-linear threshold autoregressive models for non-linear random vibrations," *Journal of Applied Probability*, Vol. 18, pp. 443-451, 1981.

[102] Ozaki, T., "The statistical analysis of perturbed limit cycle processes using nonlinear time series models," *Journal of Time Series Analysis,* Vol. 3, No. 1, pp. 29-41, 1982.

[103] Oppenheim, Alan V. and Lim, Jae S. "The importance of phase in signals," *Proceedings of the IEEE,* Vol. 69, No. 5, pp. 529-541, May, 1981.

[104] Pappa, R., and Juang, J-N., "Galileo spacecraft modal identification using an eigensystem realization algorithm," *The Journal of Astronautical Sciences,* Vol. 33, No. 1, pp. 15-33, 1985.

[105] Pau, L.F. "An adaptive signal classification procedure. Application to aircraft engine condition monitoring," *Pattern Recognition,* Vol. 9, pp. 121-130, 1977.

[106] Pau, L.F. "Failure detection processes by an expert system and hybrid pattern recognition," *Pattern Recognition Letters,* Vol. 2, pp. 419-425, December, 1984.

[107] Pau, L.F. "Survey of expert systems for fault detection, test generation and maintenance," *Expert Systems,* Vol. 3, No. 2, pp. 100-111, 1986.

[108] Pau, L.F. "Applications of pattern recognition in failure diagnosis and quality control," *Handbook of Statistics,* Edited by P.R. Krishnaiah and C.R. Rao, pp. 281-311, 1988.

[109] Priestley, M.B., "State-dependent models: a general approach to non-linear time series analysis," *Journal of Time Series Analysis,* Vol. 1, No. 1, pp. 47-71, 1980.

[110] Qiao, S., "Fast adaptive RLS algorithm: a generalized inverse unification," *SPIE Vol. 975, Advanced Algorithms and Architectures for Signal Processing III,* 1988.

[111] Reason, John "Continuous vibration monitoring moves into diagnostics," *Power,* pp. 47-51, January, 1987.

[112] Richardson, M.H. and Kniskern, J., "Identifying Modes of Large Structures from Multiple Input and Response Measurements," SAE Paper 760875. 1976.

[113] Richardson, M.H., "Modal Analysis Using Digital Test Systems," *1st International Modal Analysis Conference,* Orlando, FL, 1982.

[114] Richardson, M.H. and Formenti, D.L., "Parameter Estimation from Frequency Response Measurements Using Rational Fraction Polynomials," *1st International Modal Analysis Conference,* Orlando, FL, 1982.

[115] Richardson, M.H. and Formenti, D.L., "Global Curve-Fitting of Frequency Response Measurements Using the Rational Fraction Polynomial Method," *3rd International Modal Analysis Conference,* Orlando, FL, 1985

[116] Rocklin, G.T., Crowley, J., and Vold, H., "A Comparison of H1, H2, and Hv Frequency Response Functions," *3rd International Modal Analysis Conference,* Orlando FL, 1985.

[117] Romberg, T.M., Cassar, A.G. and Harris, R.W., "A comparison of traditional Fourier and maximum entropy spectral methods for vibration analysis," *Transactions of the ASME,* Vol. 106, pp. 36-39, January, 1984.

[118] Ruymgaart, P.A. and Soong, T.T., *Mathematics of Kalman-Bucy Filtering*, Springer-Verlag, Berlin, Heidelberg, New York, Tokyo, 1985.

[119] Sabnis, G.M., Harris, H.G., White, R.N., and Mirza, M.S., *Structural Modeling and Experimental Techniques*, Prentice-Hall, Englewood Cliffs, NJ, 1983.

[120] Salter, J.P., "Advances in numerology," *Shock and Vibration Digest*, pp. 3-8, 1991.

[121] Salter, R.G., "Maintenance management through diagnosis," *Rand Corporation Report, P-5867*, June, 1977.

[122] Saridis, G.N., "Comparison of six on-line identification algorithms.," *Automatica*, Vol. 10, pp. 69-79, 1974.

[123] Shih, C.Y., Tsuei, Y.G., Allemang, R.J., and Brown, D.L., "A Frequency Domain Global Parameter Estimation Method for Multiple Reference Frequency Response Measurements," *Journal of Mechanical Systems and Signal Processing*, Issue 2(4) 1988.

[124] Shinozuka, M., Yun, C-B., and Imai, H., "Identification of linear structural dynamic systems," *ASCE, Journal of Engineering Mechanics Division*, Vol. 108, No. EM6, pp. 1371-1390, 1982.

[125] Smith, M.T. "Practical guidelines for establishing a successful predictive maintenance program," *Mechanical Signature Analysis, Machinery Vibration, Flow-Induced Vibration and Acoustic Noise Analysis*, Edited by Braun S., Lu, K.H., Au Yang, M.K. and Ungar, E.E., pp. 115-122, 1987.

[126] Song, T.L., and Speyer, J.L., "The modified gain extended Kalman filter and parameter identification in linear systems," *Automatica*, Vol. 22, pp. 59-75, 1986.

[127] Sorenson, H.W. "Parameter and state estimation: introduction and interrelation," *IFAC Identification and System Parameter Estimation*, pp. 85-87, 1982.

[128] Sorenson, H.W. ed., *Kalman Filtering: Theory and Application*, IEEE Press, New York, 1985.

[129] Strejc, V., "Least squares parameter estimation," *Automatica*, Vol. 16, pp. 535-550, 1980.

[130] Subba Rao, T. and Tong, H., "Linear time-dependent systems," *IEEE Transactions on Automatic Control*, Vol. AC-19, No. 6, pp. 735-737, December 1974.

[131] Subba Rao, T., "On the theory of bilinear time series models," *Journal of the Royal Statistical Society*, Series B., Vol. 43, No. 2, pp. 244-255, 1981.

[132] Sunder, Shyam S., Grewatz, Stuart E. and Ting, Seng Kiong "Modal identification using spectral moments," *Structural Safety*, Vol. 3, pp. 1-11, 1985.

[133] Thangaraj, A. and Wright, P.K. "Computer-assisted prediction of drill-failure using in-process measurements of thrust force," *Transactions of the ASME*, Vol. 110, pp. 192-200, May, 1988.

[134] Thavaneswaran, A., and Abraham, B., "Estimation for non-linear time series models using estimating equations," *Journal of Times Series Analysis,* Vol. 9, No. 1, pp. 99-108, 1988.

[135] Thiel Jr., C.C. and Boissonnade, A.C. "System identification and information processing in seismic vulnerability analysis of structures," *Applications of Artificial Intelligence in Engineering Problems,* Edited by D. Sriram and R. Adey, pp. 277-286, 1986.

[136] Toki, K., Sato, T., and Kiyono, J., "Identification of structural parameters and input ground motion from response time histories," *Structural Engineering and Earthquake Engineering,* Vol. 6, NO. 2, pp. 413-421, October 1989.

[137] Udwadia, F.E., and Sharma, D.K., "On the identification of continuous vibrating systems modelled by hyperbolic partial differential equations," *Quarterly of Applied Mathematics,* Vol. 42, No. 4, pp. 411-424, January 1985.

[138] Udwadia, F.E., "Some uniqueness results related to soil and building structural identification," *SIAM Journal of Applied Mathematics,* Vol. 45, No. 4, pp. 674-685, August 1985.

[139] Udwadia, F.E., "Some results on the optimal spacing of measurement in the identification of structural systems," *Quarterly of Applied Mathematics,* Vol. 43, No. 3, pp. 263-274, October 1985.

[140] Udwadia, F.E., "Uniqueness in the identification of a bending beam modeled by finite elements," *SIAM Journal of Applied Mathematics,* Vol. 48, No. 6, pp. 1350-1360, December 1988.

[141] Upadhyaya, B.R. and Skorska, M. "A modular approach for the diagnostic analysis of dynamic systems using time series models," *IFAC Identification and System Parameter Estimation,* pp. 591-596, 1982.

[142] Ursin, B., "Asymptotic convergence properties of the extended Kalman filter using filtered state estimates," *IEEE Transactions on Automatic Control,* Vol. AC-25, No. 6, pp. 1207-1211, December 1980.

[143] Van der Auweraer, H. and Leuridian, J., "Multiple Input Orthogonal Polynomiial Parameter Estimation," *Journal of Mathematical Systems and Signal Processing,* Vol. 1, No. 3, 1987.

[144] Van Karsen, C. and Allemang, R., "Averaging for Improved Frequency Response Functions," *Sound and Vibration Magazine,* August, 1984.

[145] Vigneron, F.R. and Soucy, Y., "Driven Base Tests for Modal Parameter Estimation," AIAA Paper 86-0870, 1986.

[146] Vold, H., Crowley, J., and Rocklin, G.T., "New Ways of Estimating Frequency Response Functions," *Sound and Vibration Magazine,* November, 1984.

[147] Vold, H., "Numerically Robust Frequency Domain Modal Parameter Estimation," *Sound and Vibration Magazine,* January, 1990.

[148] Wang, M.L., Yang, S.Y. and Chang, R.Y., "Application of generalized orthogonal polynomials to parameter estimation of time-invariant and bilinear systems," *ASME, Journal of Dynamic Systems, Measurement, and Control*, Vol. 109, pp. 7-13, March 1987.

[149] Werner, S.D., "Seismic response evaluation of meloland road overpass using 1979 imperial valley earthquake records," *Earthquake Engineering and Structural Dynamics*, Vol. 15, pp. 249-274, 1987.

[150] Westerlund, T., and Tysso, A., "Remarks on "Asymptotic behavior of the extended Kalman filter as a parameter estimator for linear systems"," *IEEE Transactions on Automatic Control*, Vol. AC-25, No. 5, pp. 1011-1012, October 1980.

[151] Williams, Hywel J., *Transfer Function Techniques and Fault Location*, Research Studies Press Ltd., 1985.

[152] Willsky, Alan S., "A survey of design methods for failure detection in dynamic systems," *Automatica*, Vol. 12, pp. 601-611, 1976.

[153] Young, P., *Recursive Estimation and Time-Series Analysis: An Introduction*, Springer-Verlag, Berlin, Heidelberg, New York, Tokyo, 1984.

[154] Young, P., "Recursive identification, estimation, and control," pp. 213-255, in *Handbook of Statistics*, Edited bye E.J. Hannan, P.R. Krishnaiah, and M.M. Rao, Elsevier Science Publisher, 1985.

[155] Yang, J.N., Long, F.X., and Wong, D., "Optimal control of nonlinear structures," *ASME, Journal of Applied Mechanics*, Vol. 110, pp. 931-938, 1988.

[156] Yun, C-B., and Shinozuka, M., "Identification of nonlinear structural dynamic systems," *Journal of Structural Mechanics*, Vol. 8, No. 2, pp. 187-203, 1980.

[157] Yun, C-B., and Shinozuka, M., *Program LINEARID for Identification of Linear Structural Systems*, Technical Report NCEER-90-0011, National Center for Earthquake Engineering Research, Buffalo, NY, 1990.

[158] Yun, C.-B., Lee, C.-G., and Cho, H.-N., "Identification of structural dynamic systems by sequential prediction error method," *Proceedings of the First International Conference on Computational Stochastic Mechanics*, Corfu, Greece, August 1991.

Recursive Least Squares Estimation
Five Story Building Model; Elcentro Input
1st Floor alpha=1.

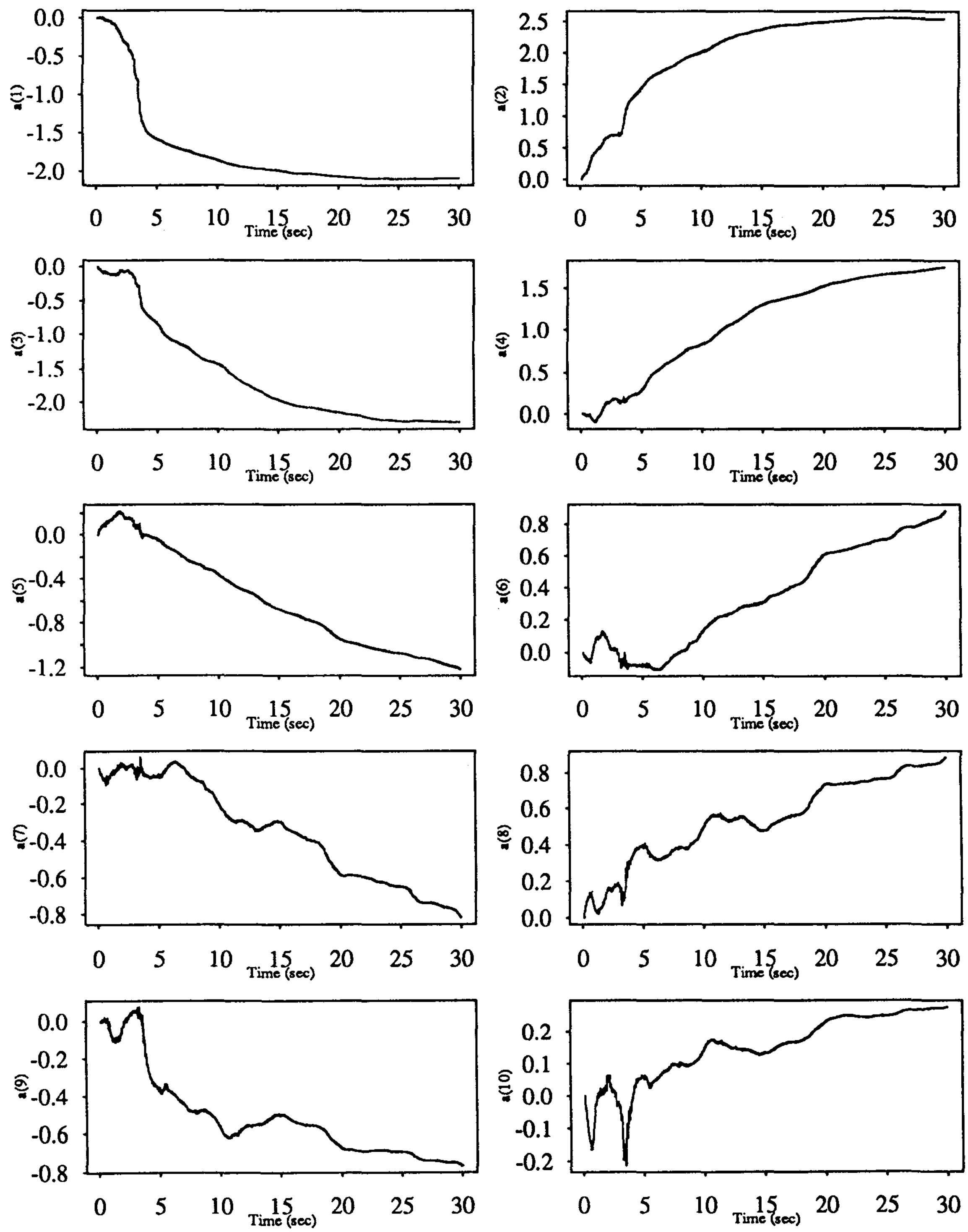


Figure 5.1

Recursive Least Squares Estimation
Five Story Building Model; Elcentro Input
2nd Floor alpha=1.

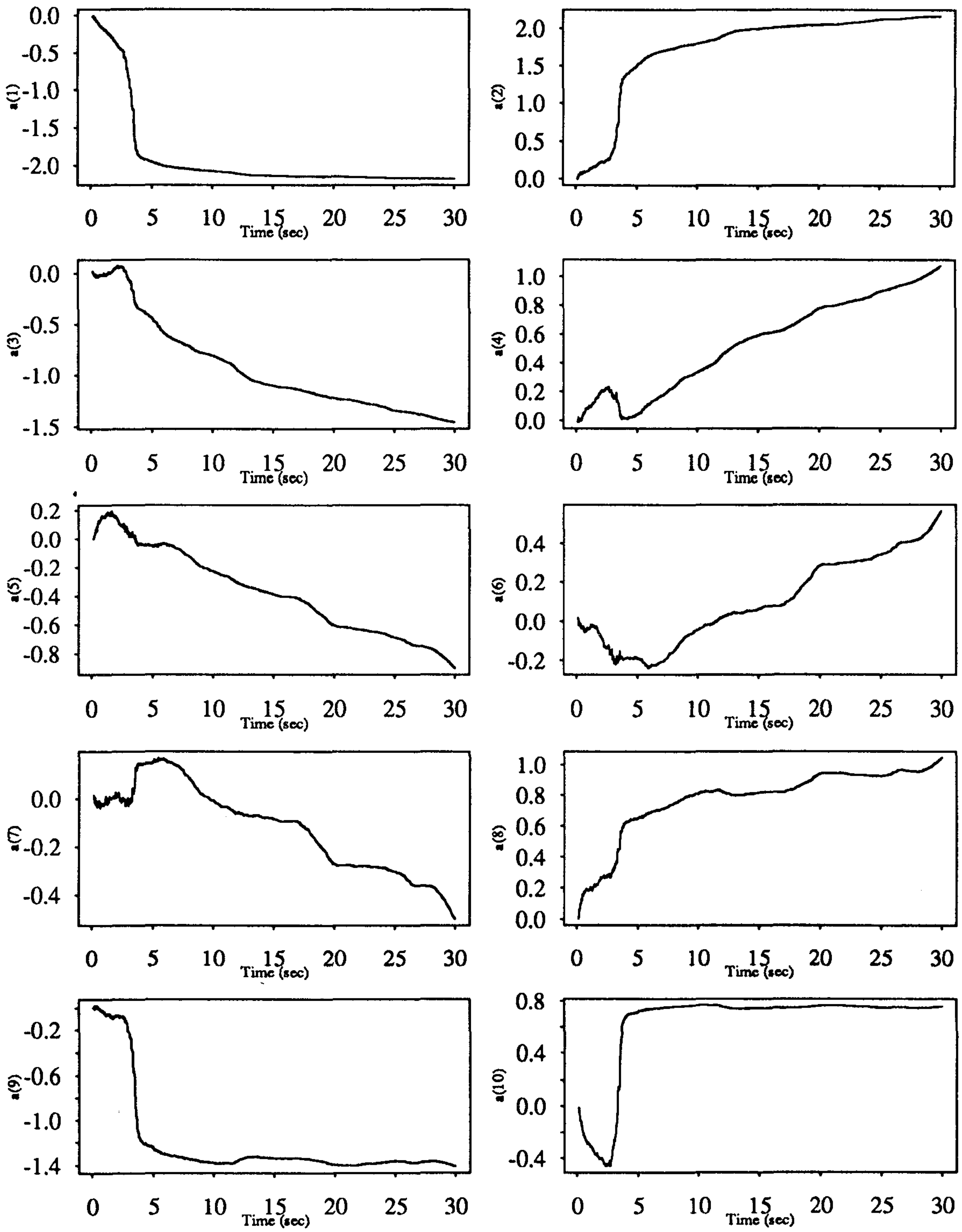


**Figure 5.2**

Recursive Least Squares Estimation
Five Story Building Model; Elcentro Input
3rd Floor alpha=1.

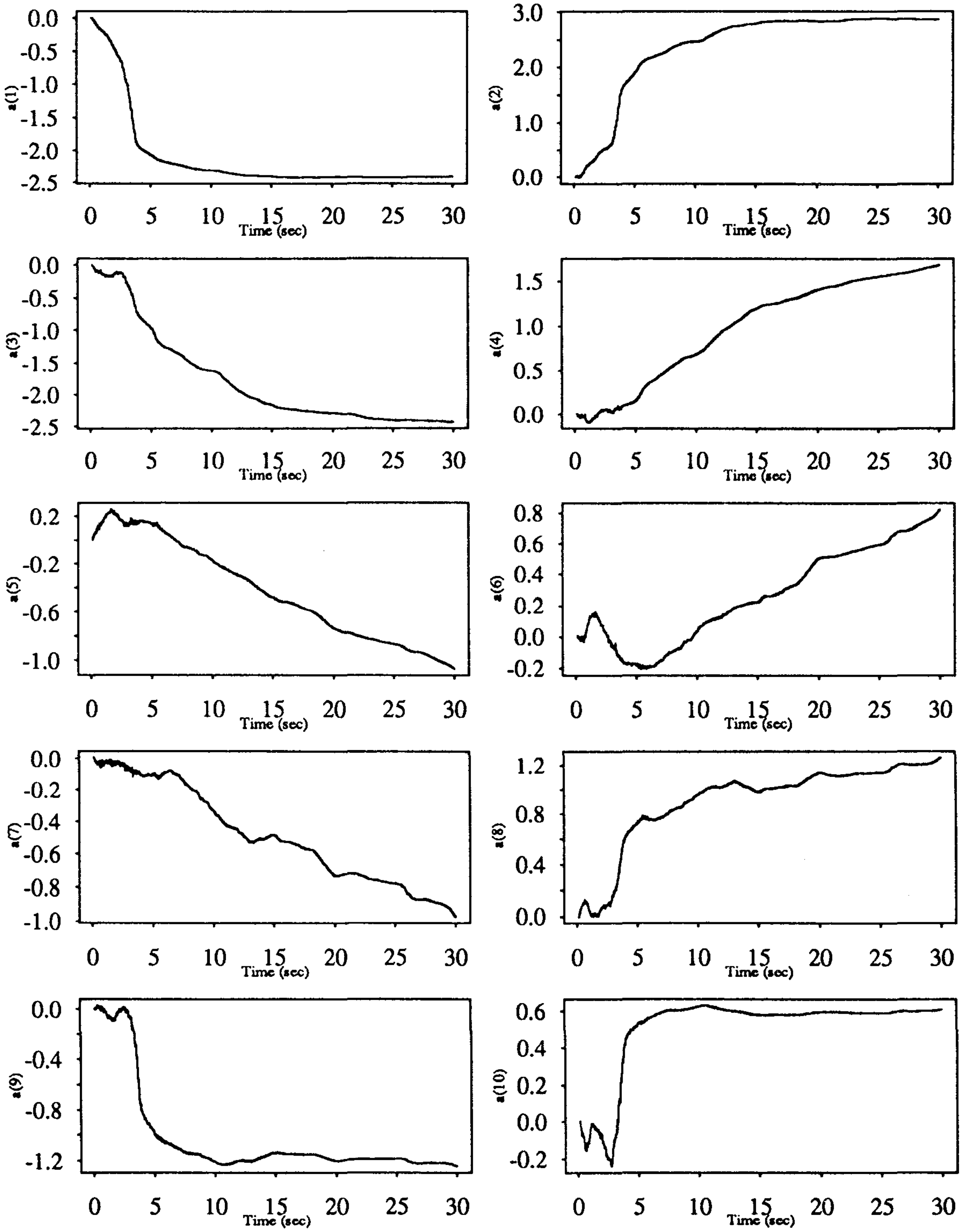


**Figure 5.3**

Recursive Least Squares Estimation
Five Story Building Model; Elcentro Input
4th Floor alpha=1.

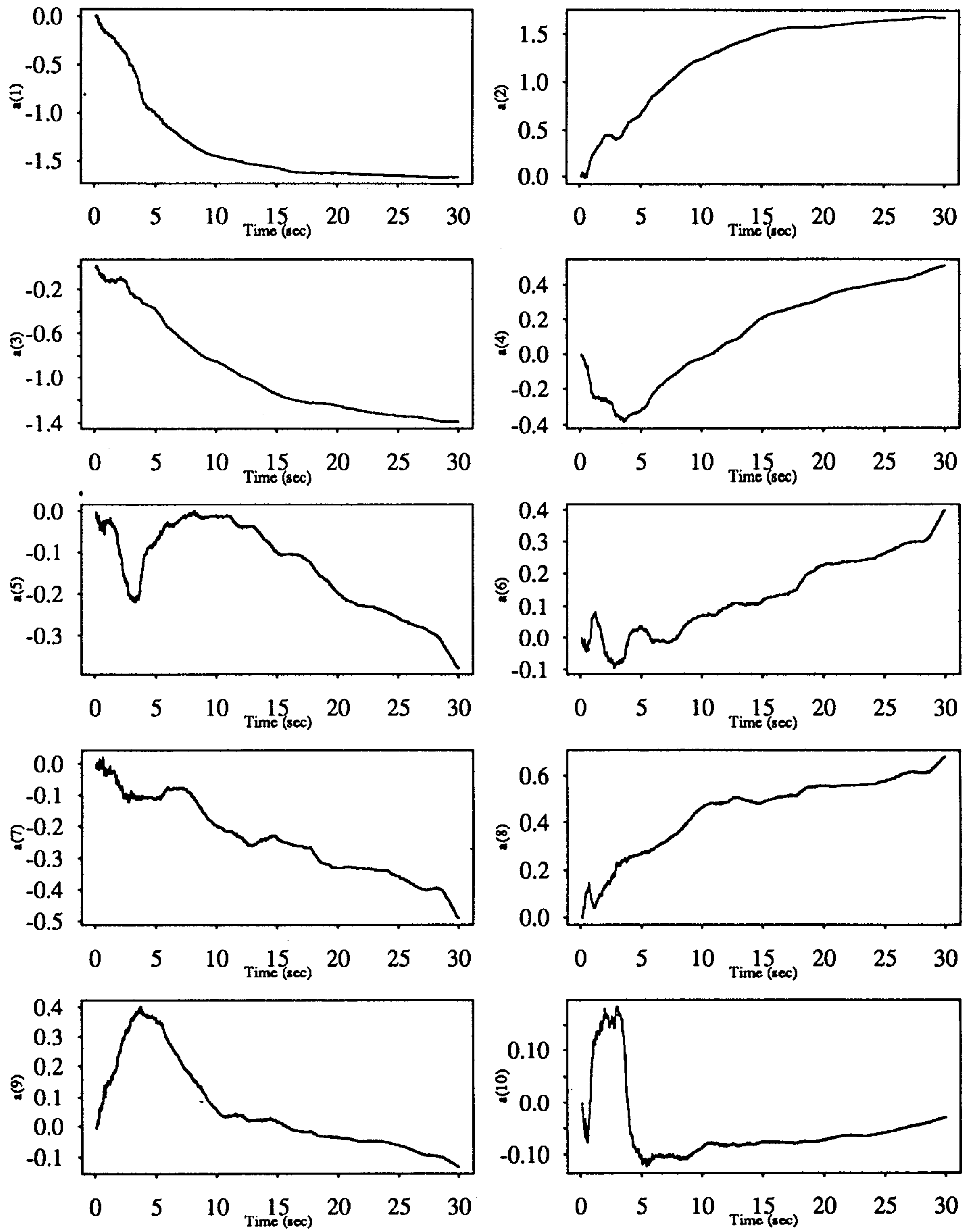


Figure 5.4

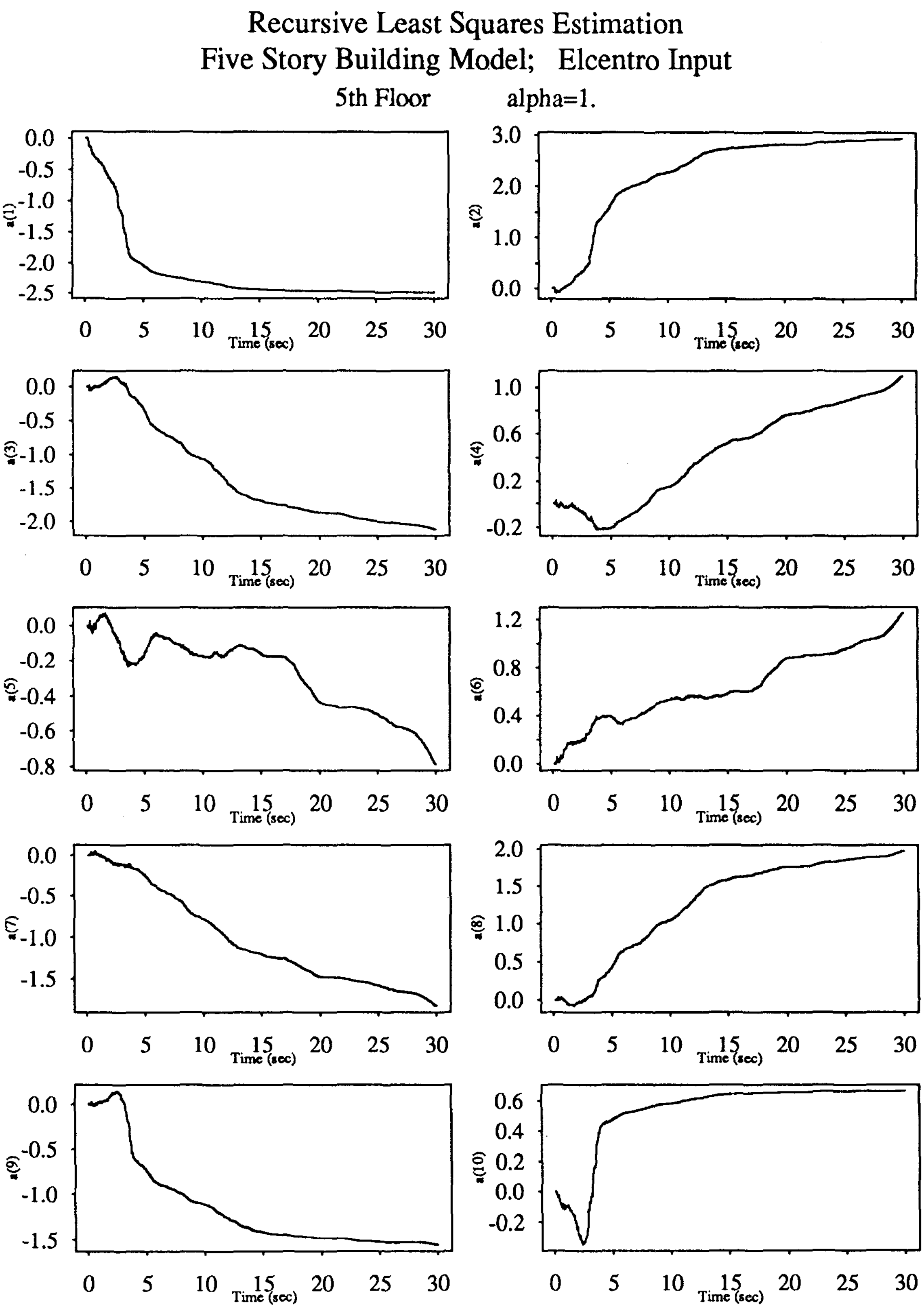
Recursive Least Squares Estimation
Five Story Building Model; Elcentro Input
5th Floor alpha=1.
a(1)
a(2)
a(3)
a(4)
a(5)
a(6)
a(7)
a(8)
a(9)
a(10)
Time (sec)

Figure 5.5

# Recursive Least Squares Estimation
## Five Story Building Model; White Noise Input

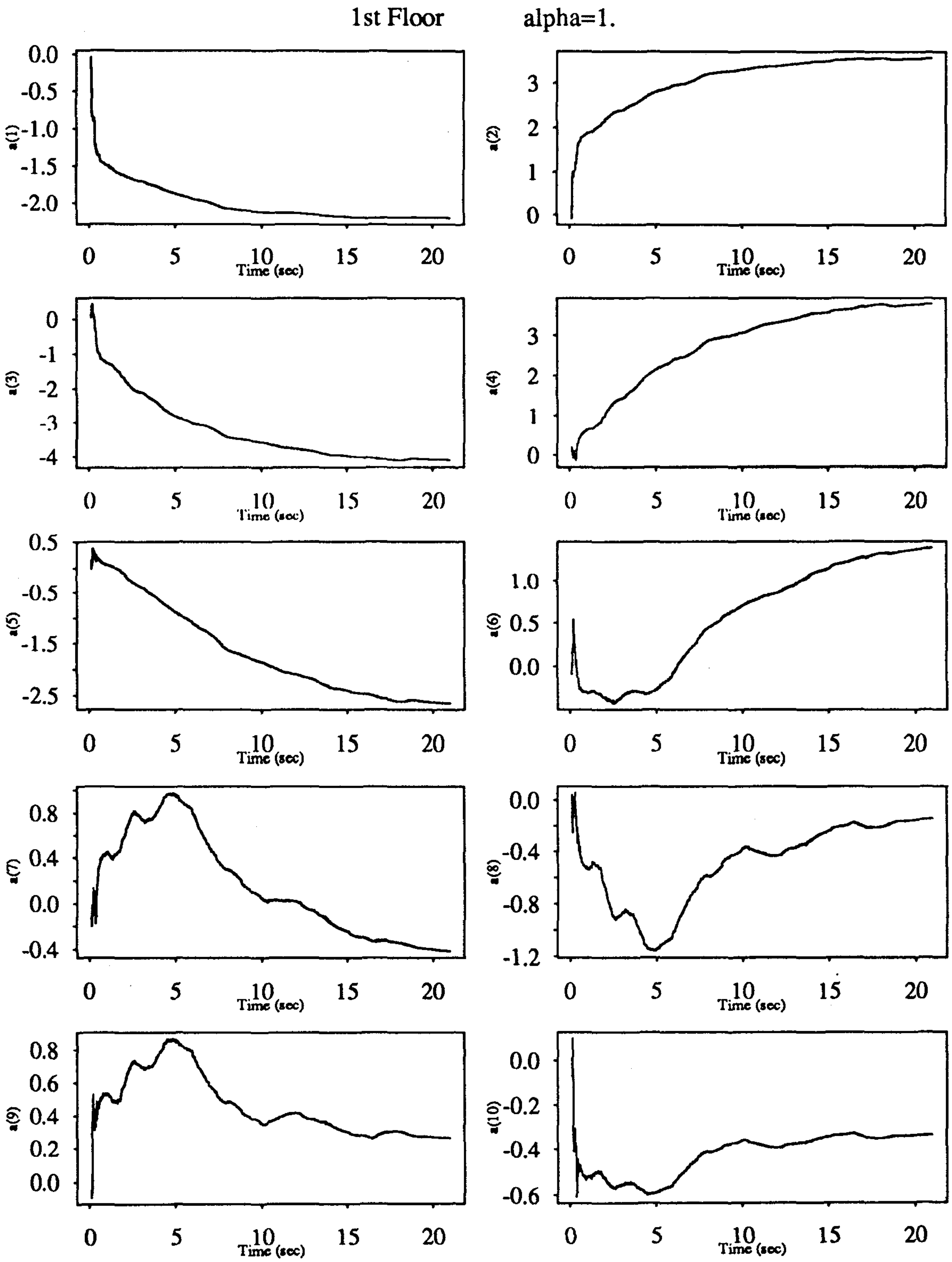


Figure 5.6

Recursive Least Squares Estimation
Five Story Building Model; White Noise Input
2nd Floor alpha=1.

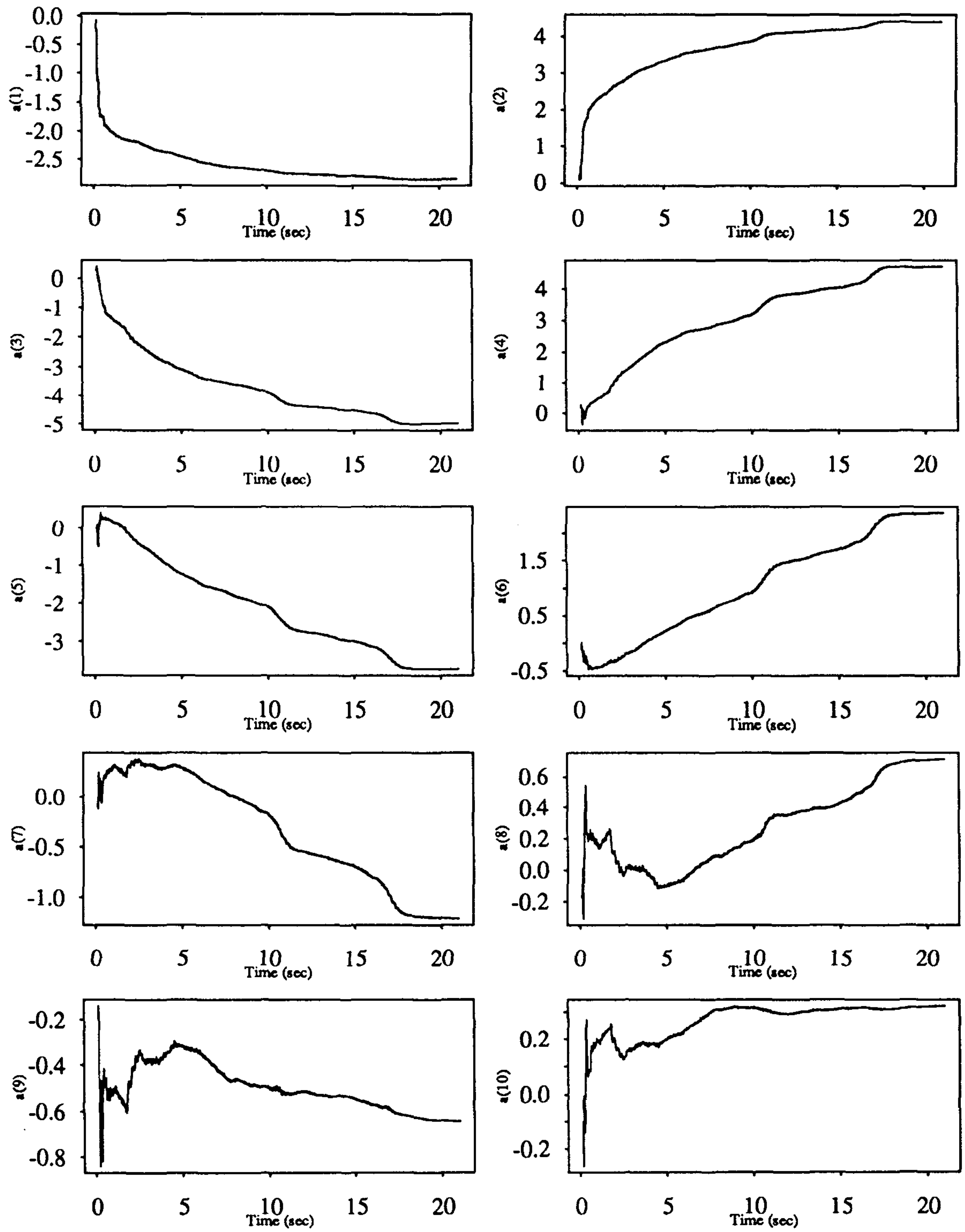


Figure 5.7

## Recursive Least Squares Estimation
## Five Story Building Model; White Noise Input

3rd Floor alpha=1.

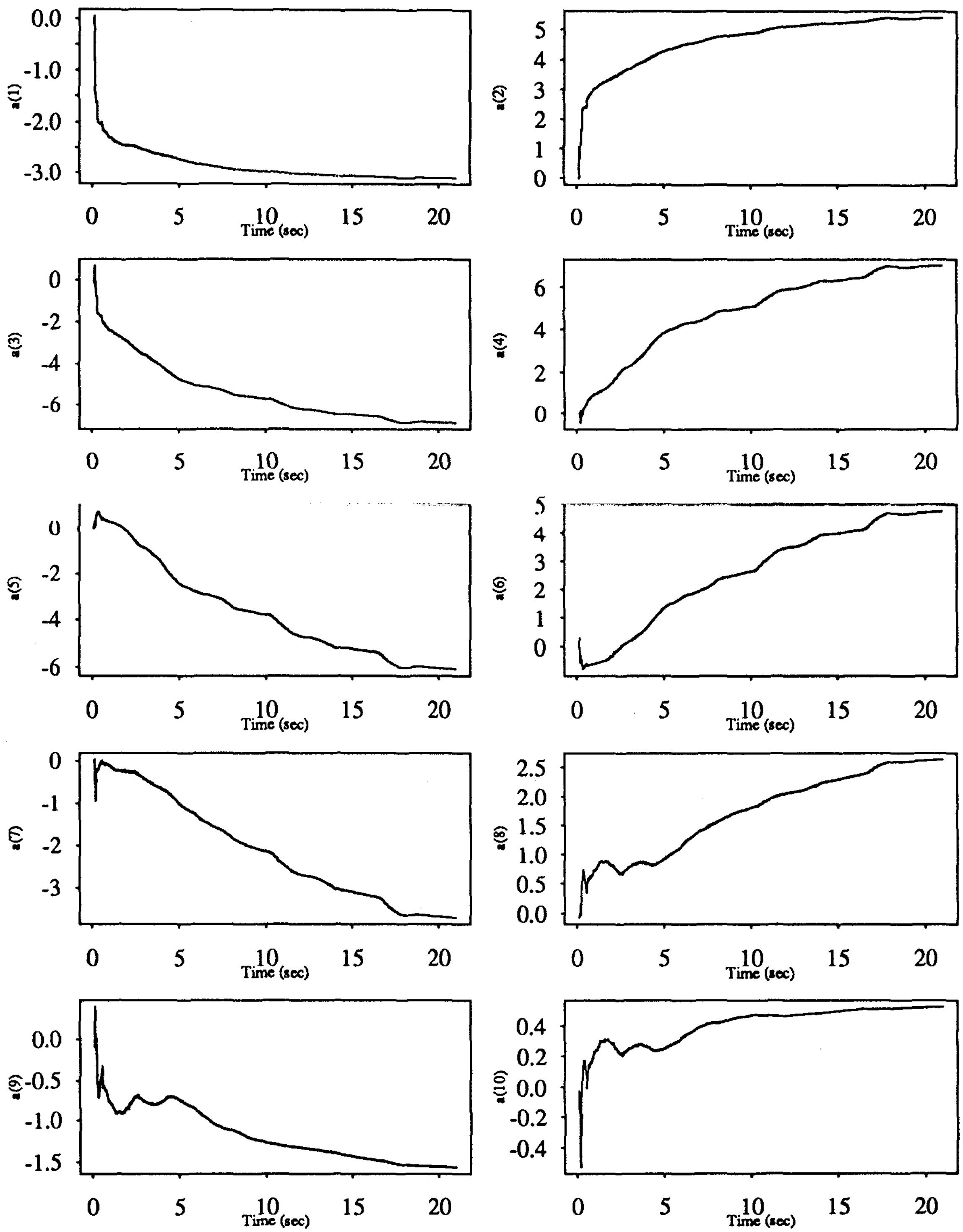


Figure 5.8

Recursive Least Squares Estimation
Five Story Building Model; White Noise Input
4th Floor alpha=1.

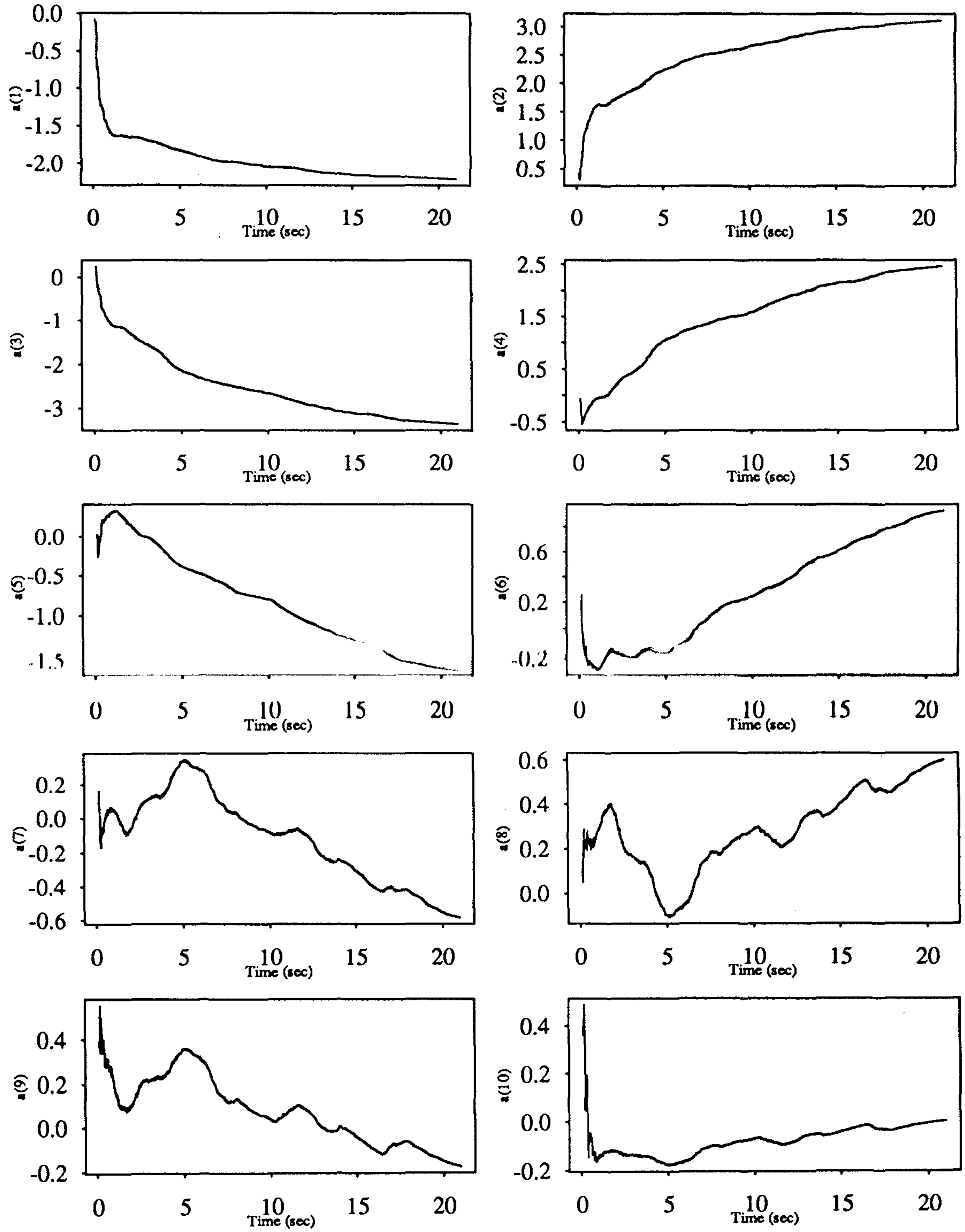


Figure 5.9

## Recursive Least Squares Estimation
## Five Story Building Model; White Noise Input

5th Floor alpha=1.

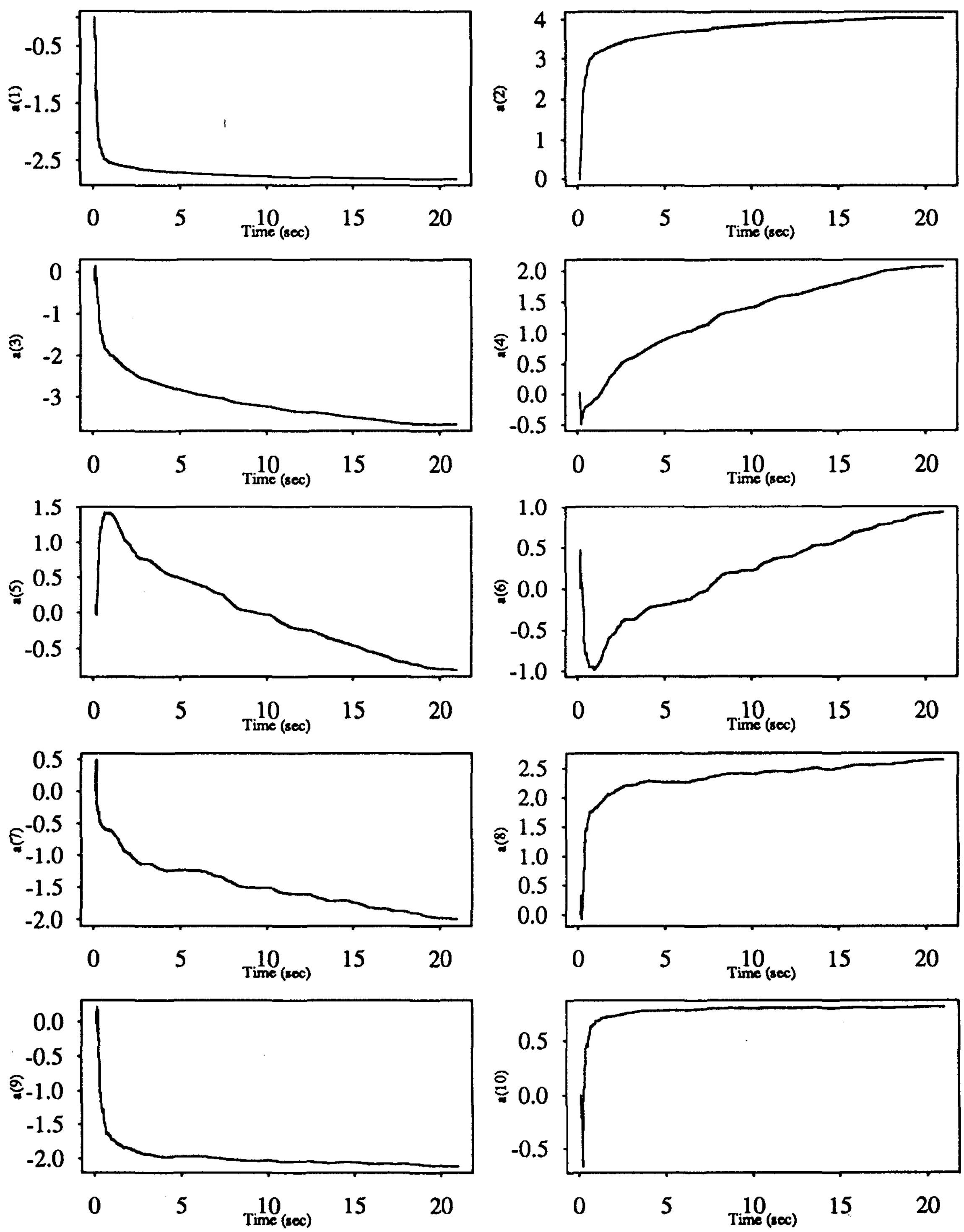


Figure 5.10

Recursive Least Squares Estimation
Five Story Building Model; Elcentro Input
1st Floor alpha=1.

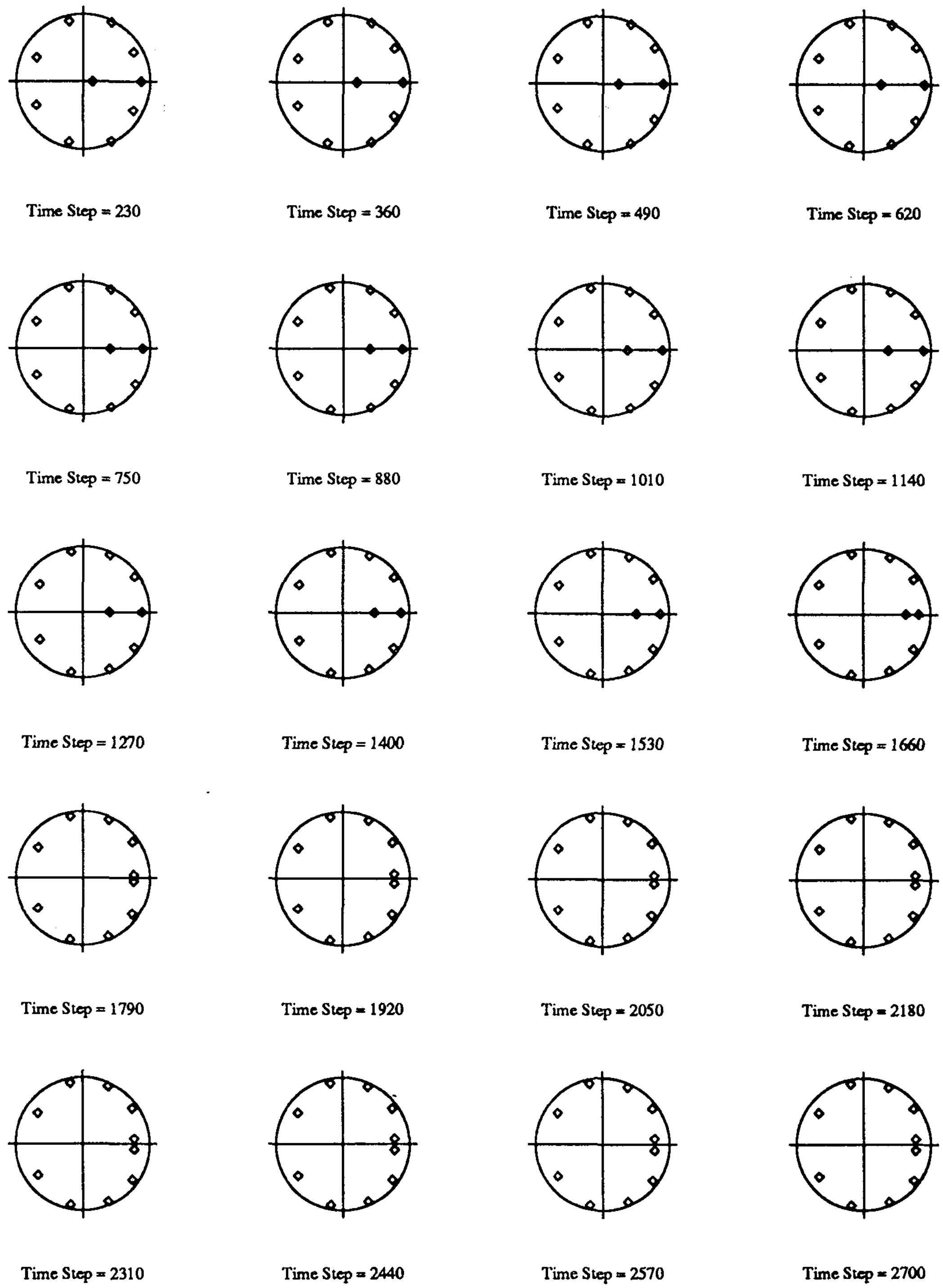


Figure 5.11

Recursive Least Squares Estimation
Five Story Building Model; Elcentro Input
2nd Floor alpha=1.

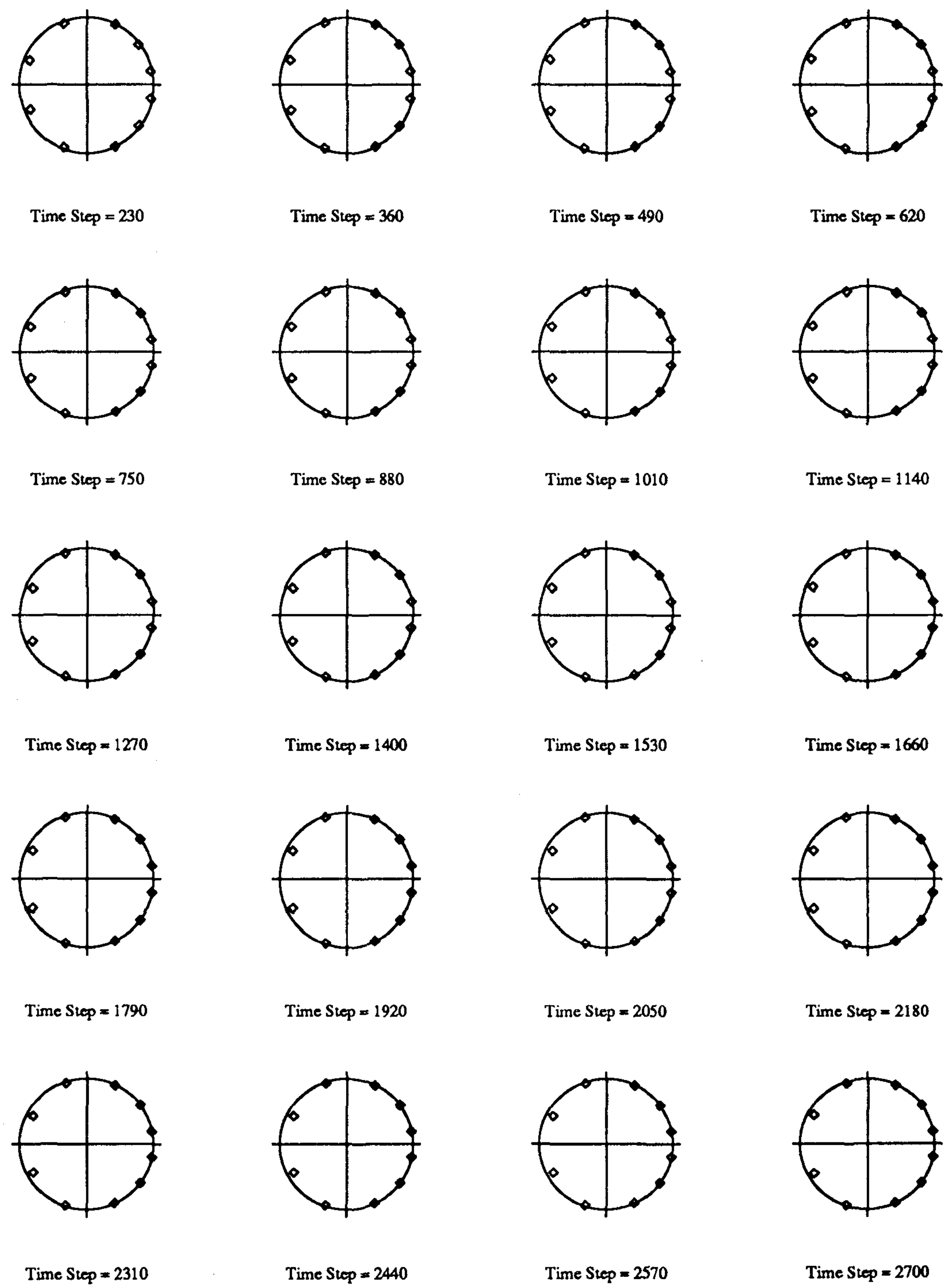


Figure 5.12

Recursive Least Squares Estimation
Five Story Building Model; Elcentro Input
3rd Floor alpha=1.

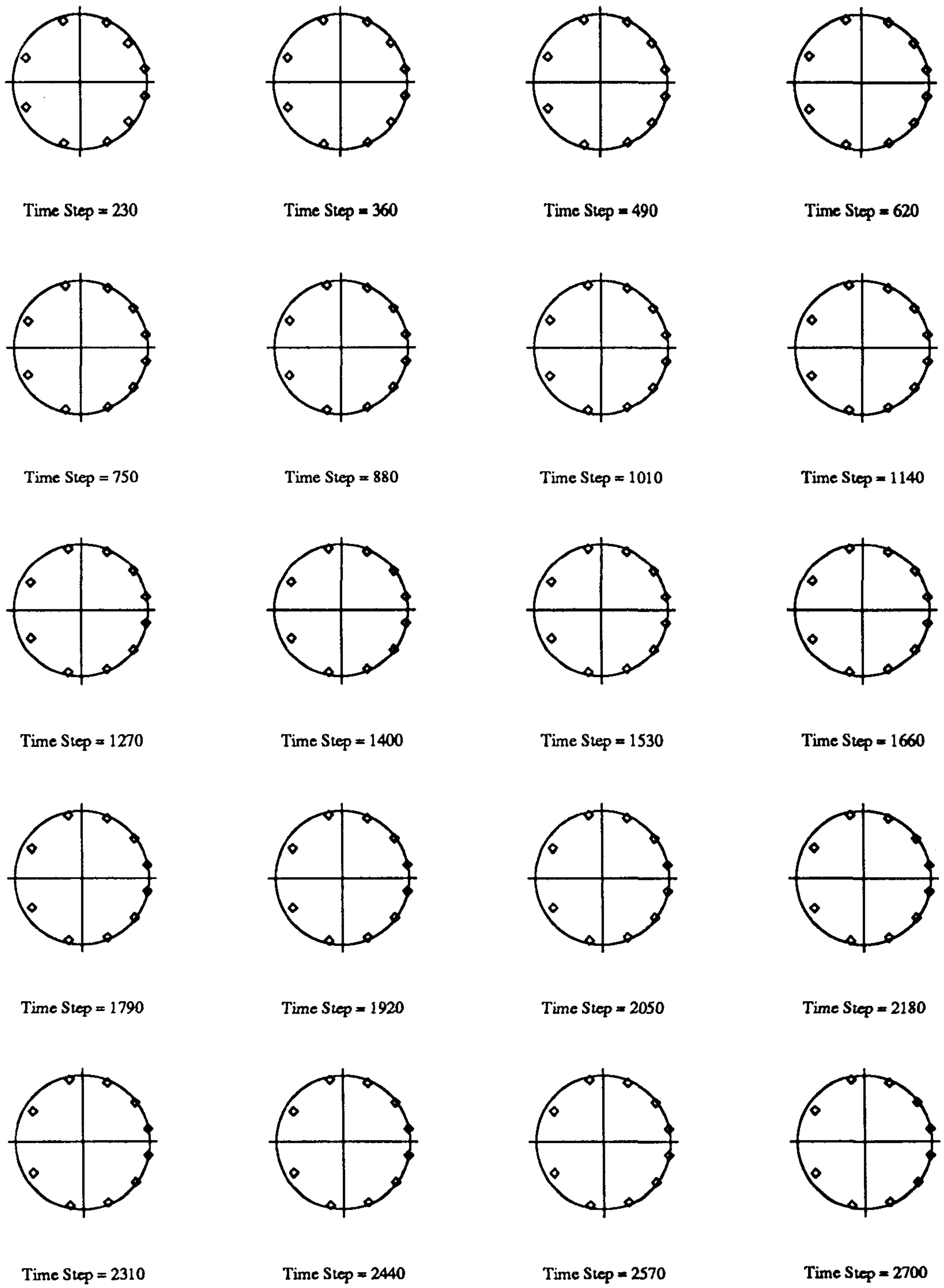


Figure 5.13

Recursive Least Squares Estimation
Five Story Building Model; Elcentro Input
4th Floor alpha=1.

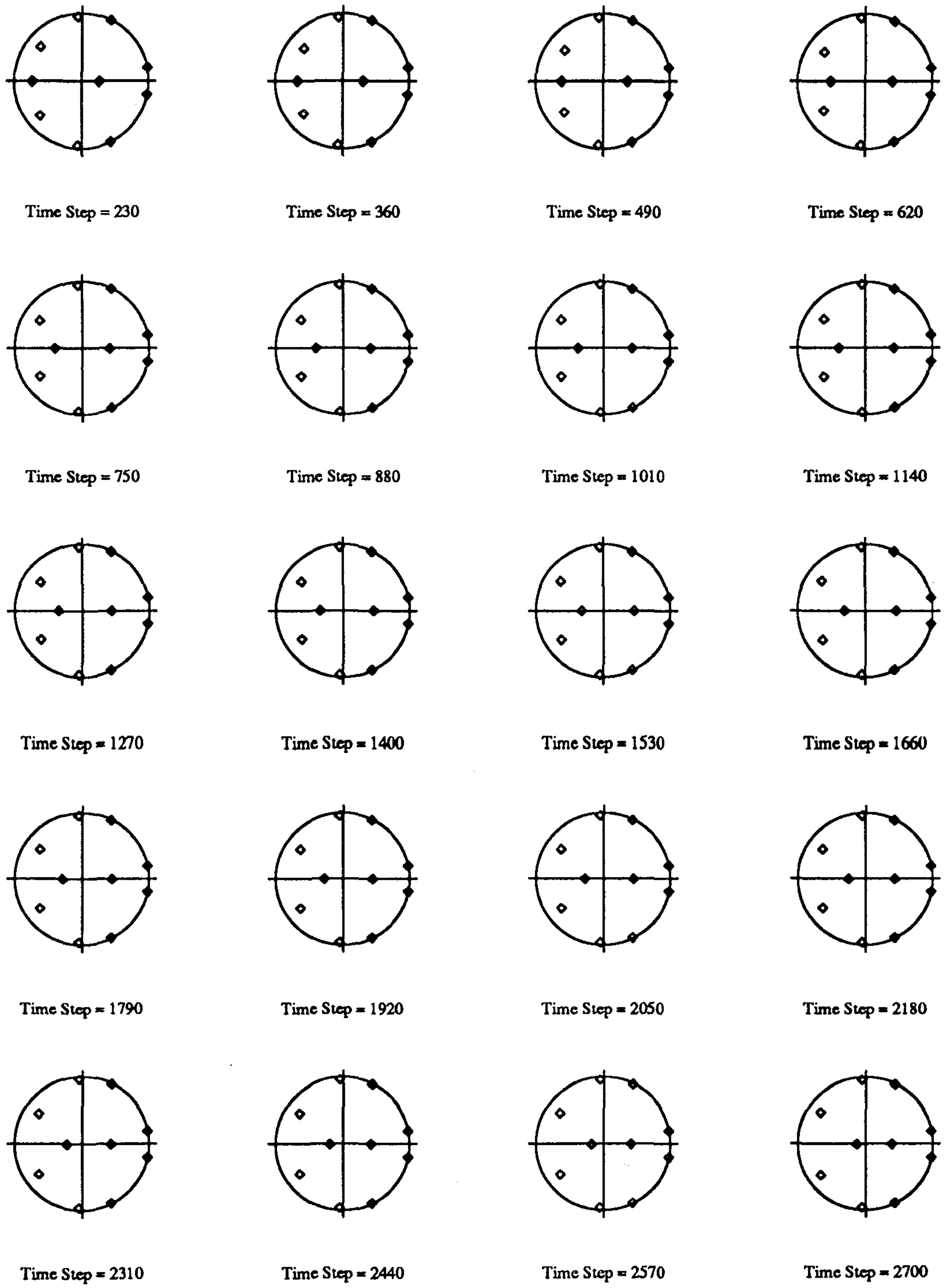


Figure 5.14

## Recursive Least Squares Estimation
## Five Story Building Model; Elcentro Input
5th Floor alpha=1.

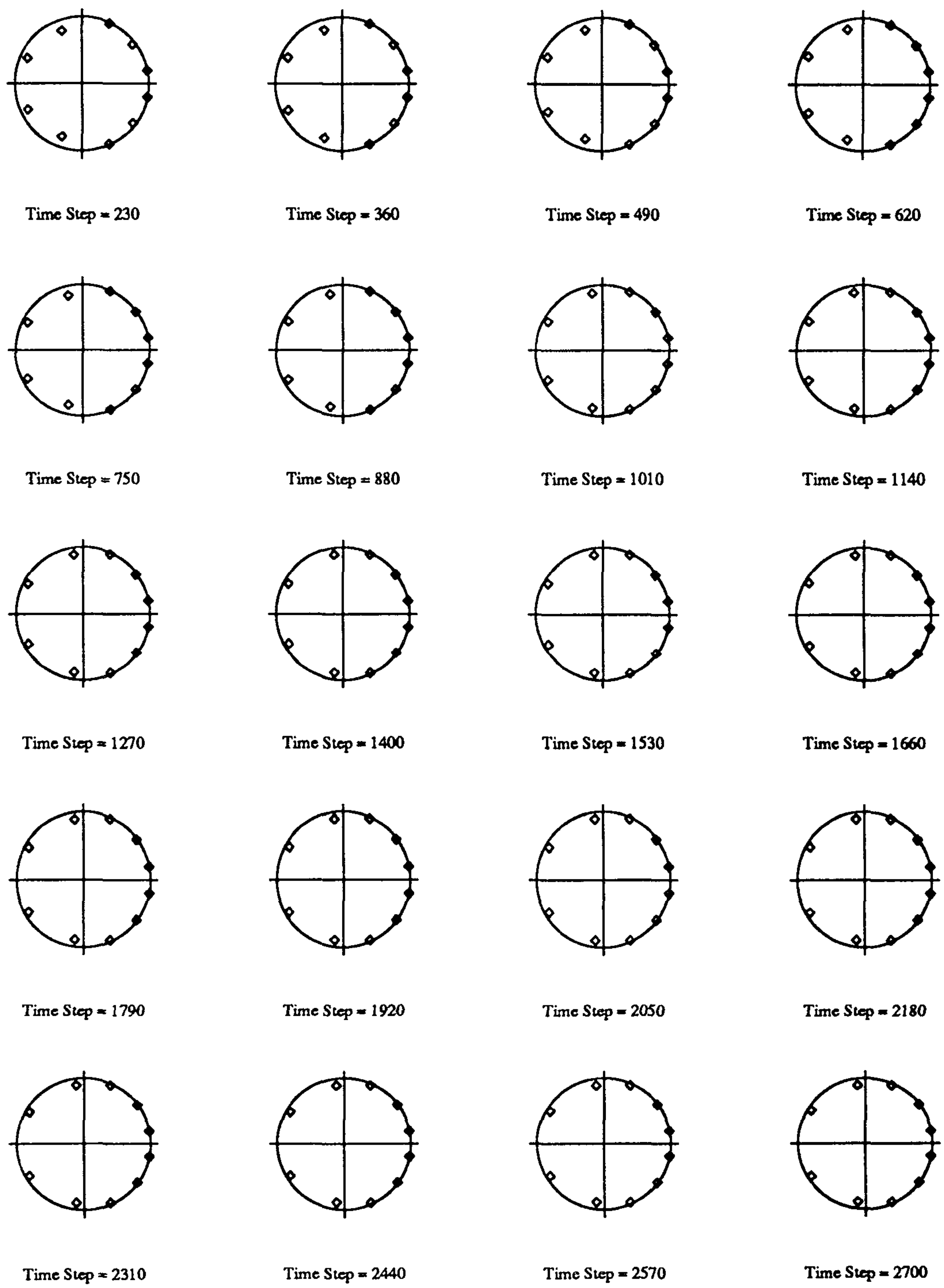


Figure 5.15

## Recursive Least Squares Estimation
## Five Story Building Model; White Noise Input
### 1st Floor alpha=1.

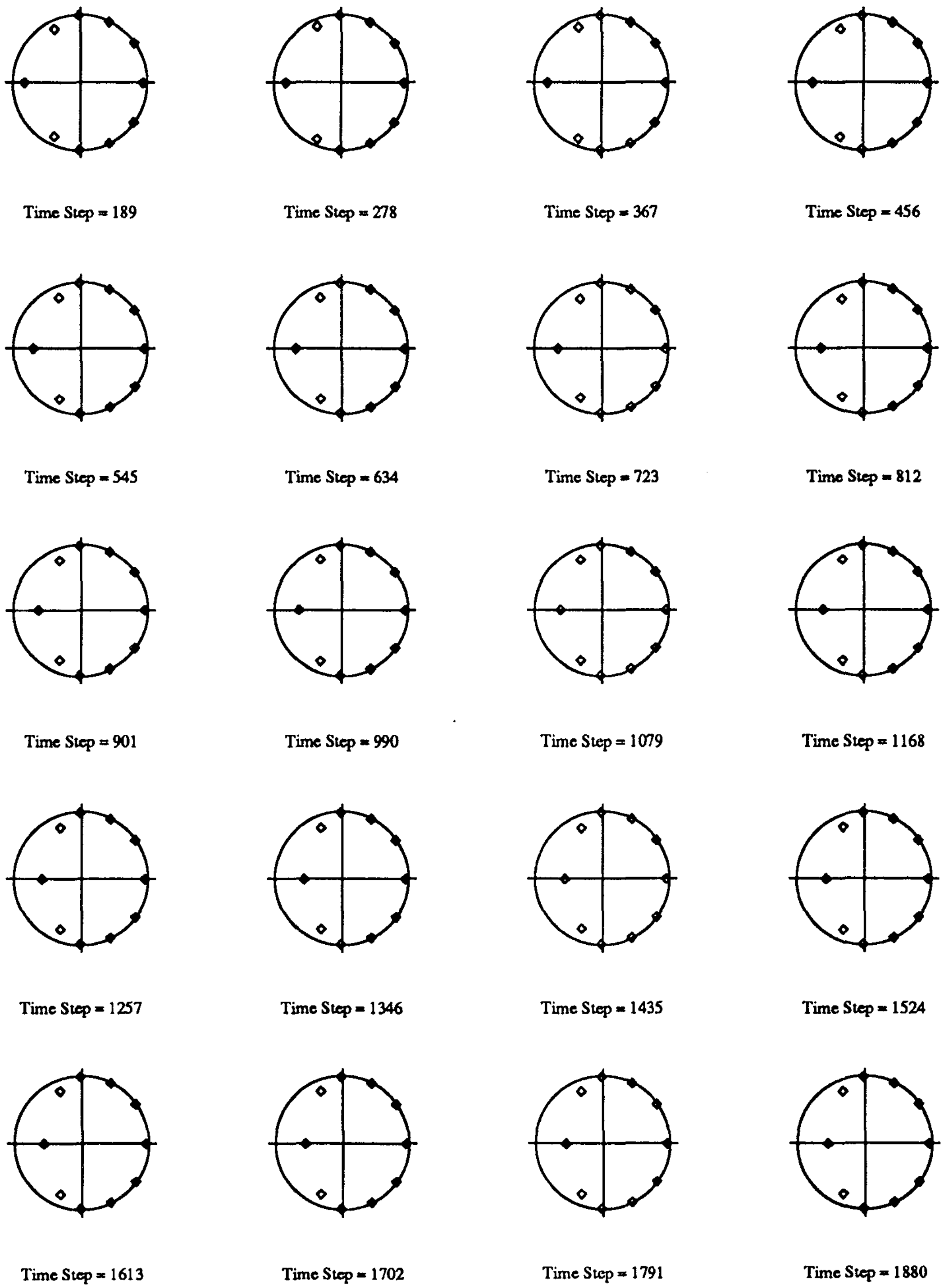


Figure 5.16

## Recursive Least Squares Estimation
## Five Story Building Model; White Noise Input

2nd Floor alpha=1.

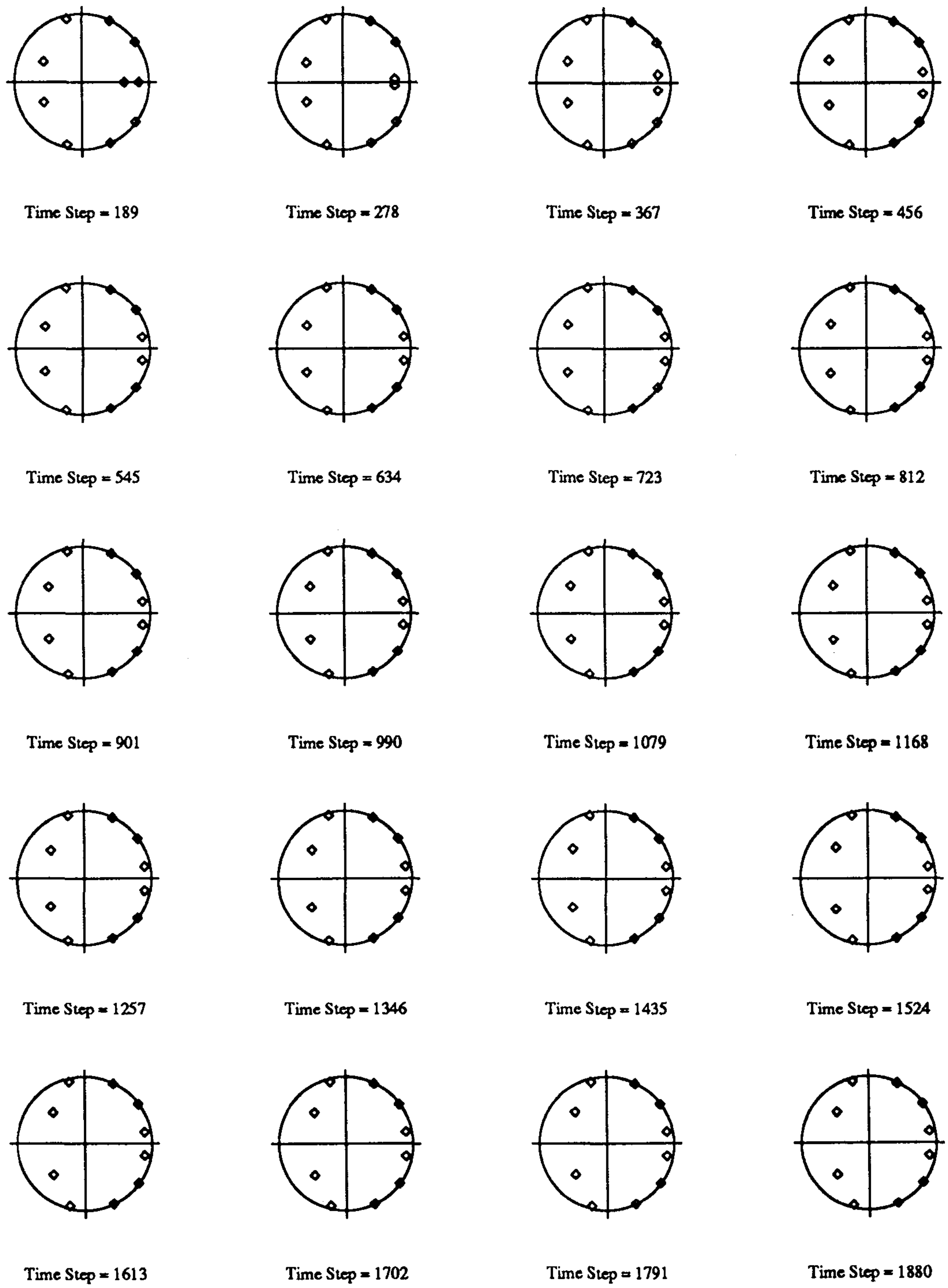


Figure 5.17

Recursive Least Squares Estimation
Five Story Building Model; White Noise Input
3rd Floor alpha=1.

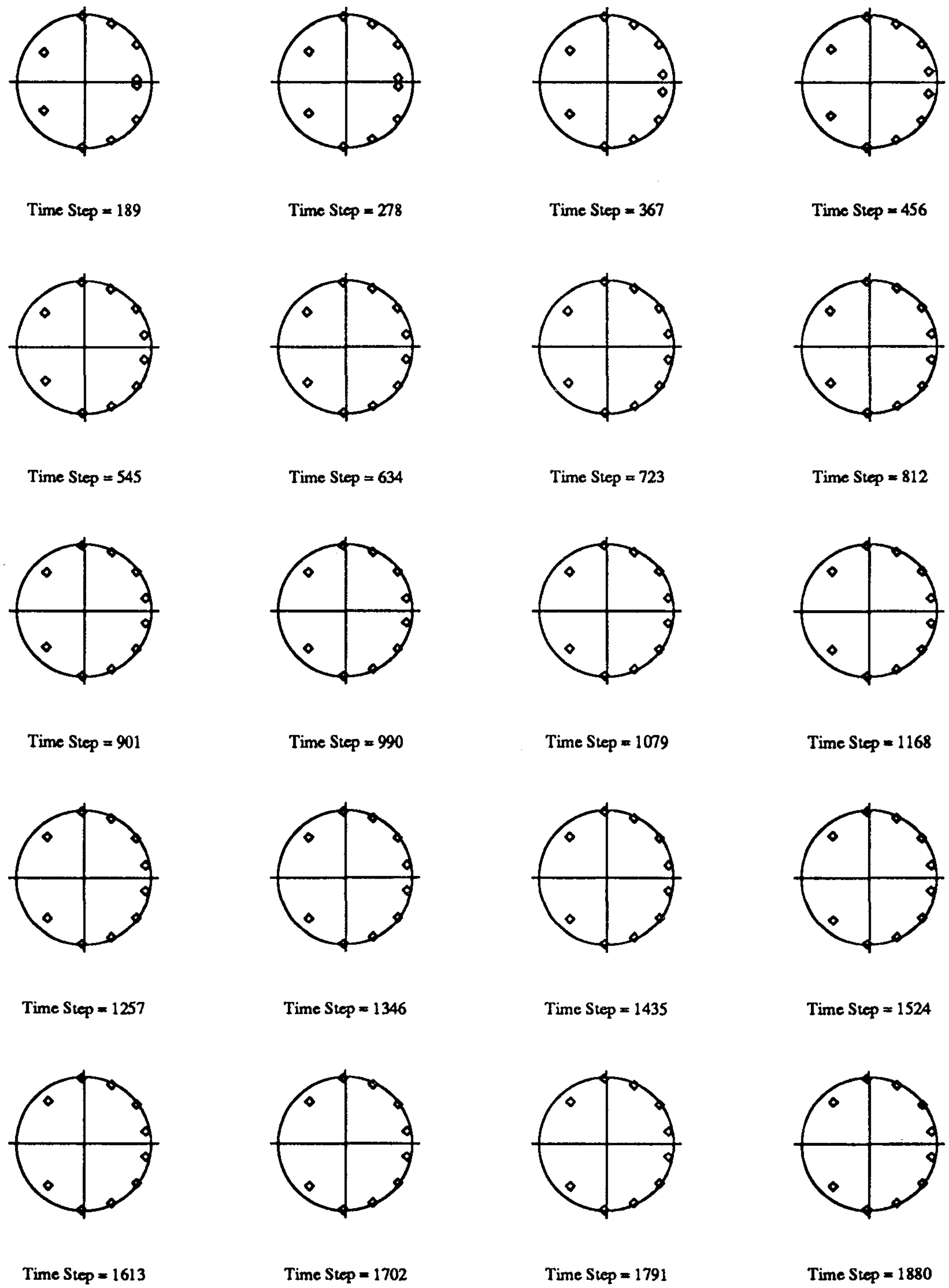


Figure 5.18

## Recursive Least Squares Estimation
## Five Story Building Model; White Noise Input
### 4th Floor alpha=1.

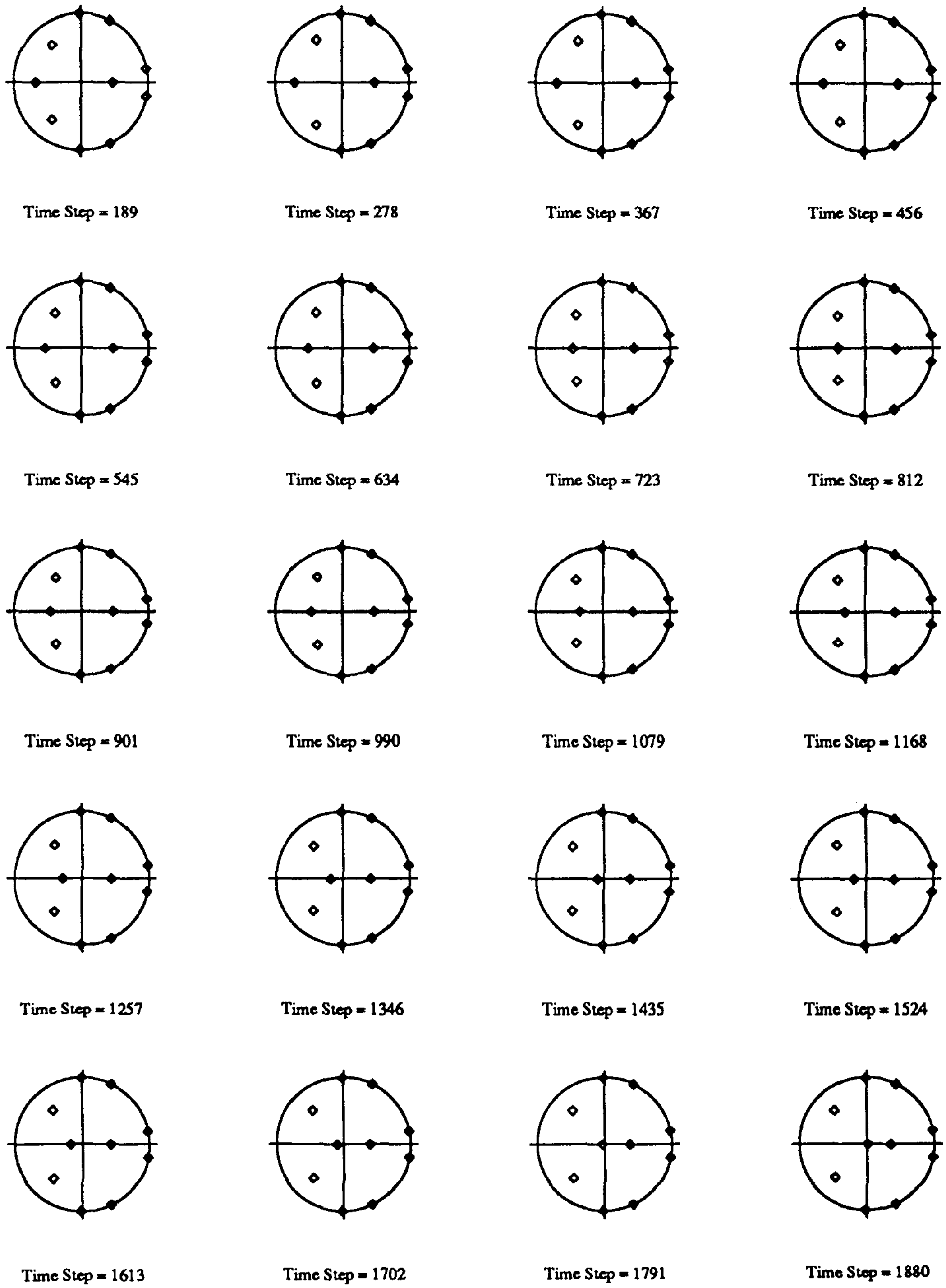


Figure 5.19

# Recursive Least Squares Estimation
## Five Story Building Model; White Noise Input
5th Floor alpha=1.

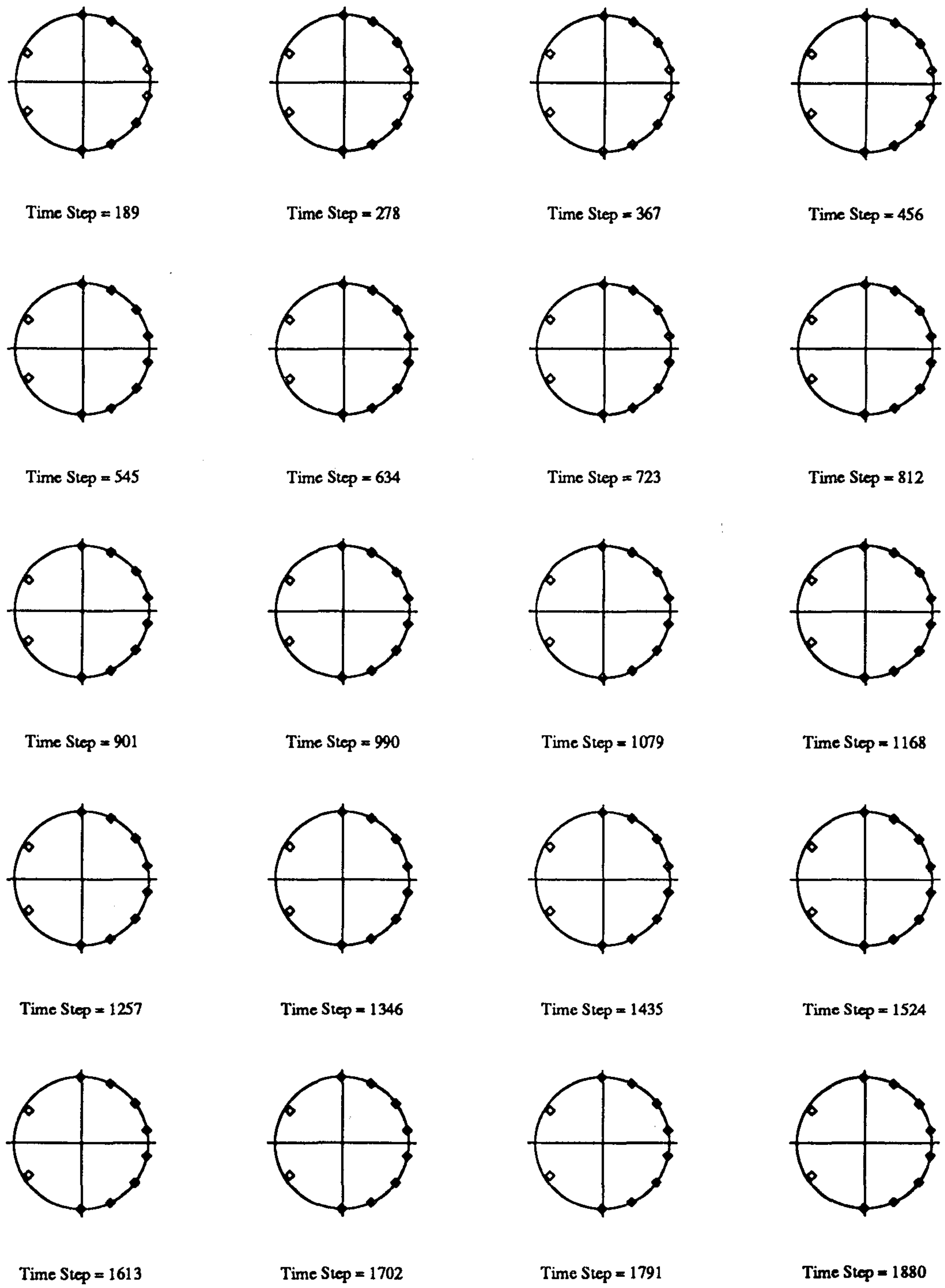


Figure 5.20

Recursive Least Squares Estimation
Three Story Building Model; El-Centro Input
1st Floor alpha=1.

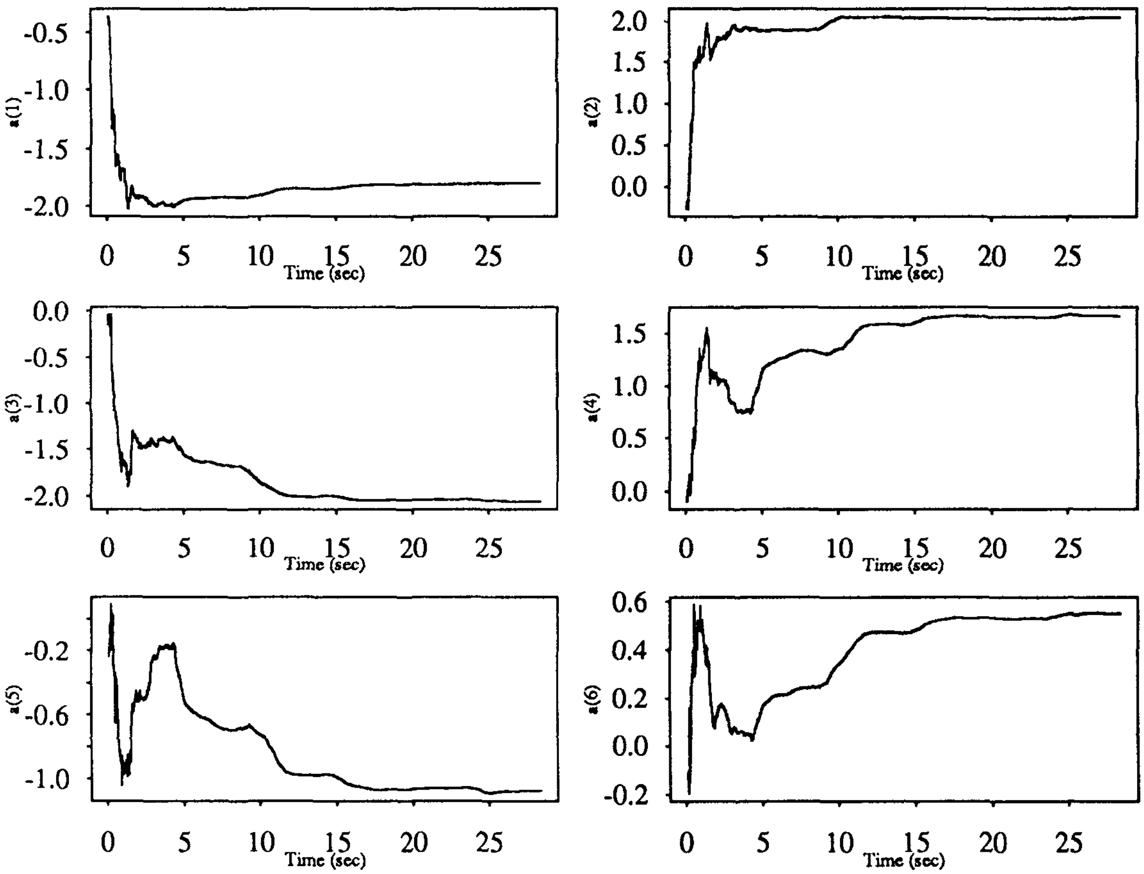


Figure 5.21

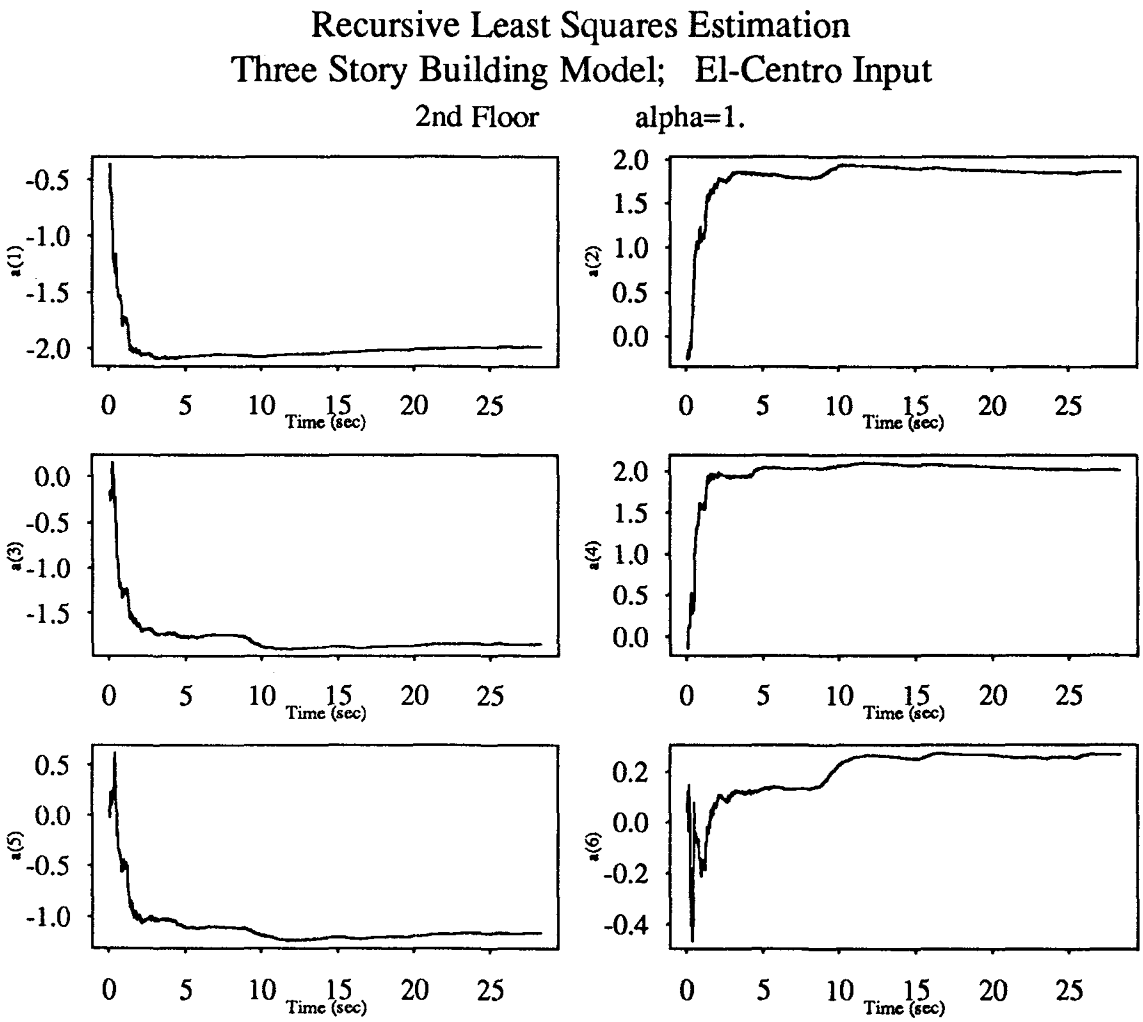

Recursive Least Squares Estimation
Three Story Building Model; El-Centro Input
2nd Floor
alpha=1.
a(1)
a(2)
a(3)
a(4)
a(5)
a(6)
Time (sec)
-0.5
-1.0
-1.5
-2.0
2.0
1.5
1.0
0.5
0.0
-0.2
-0.4
0.2
0
5
10
15
20
25


Figure 5.22

Recursive Least Squares Estimation
Three Story Building Model; El-Centro Input
3rd Floor alpha=1.

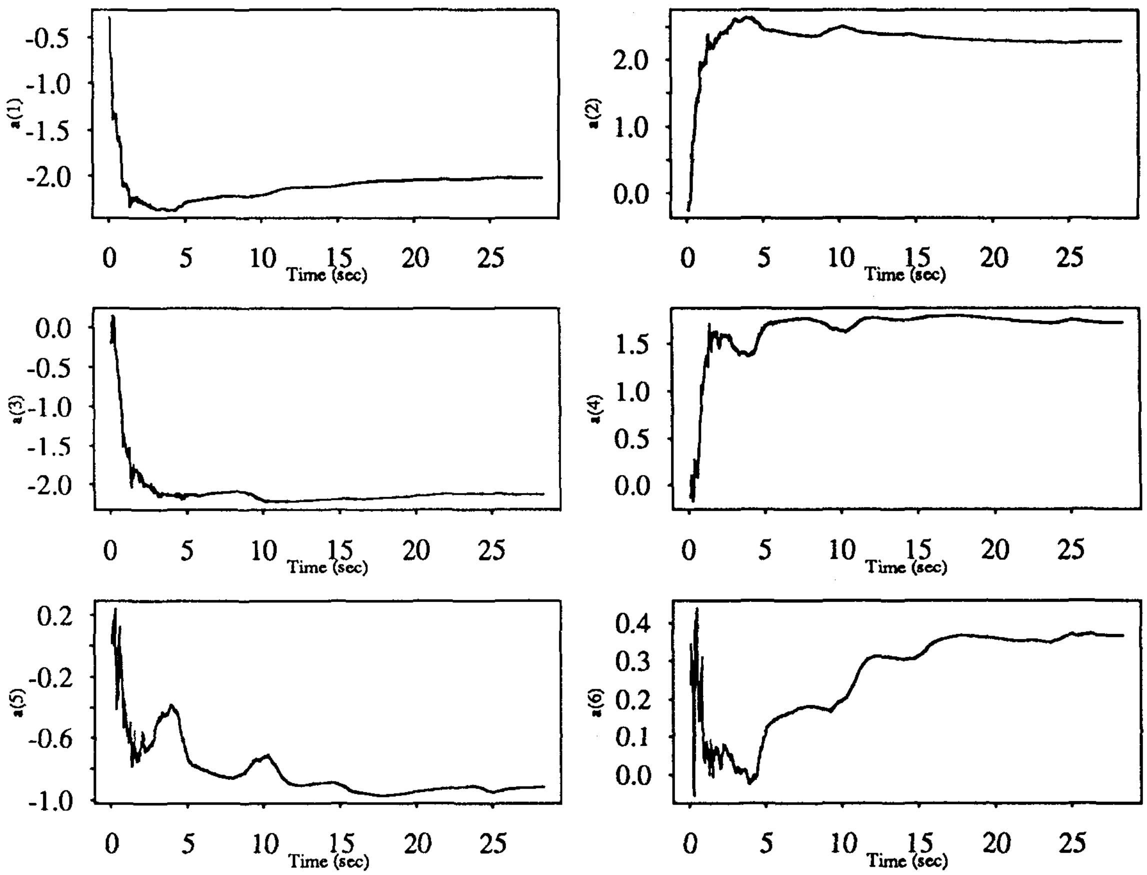


Figure 5.23

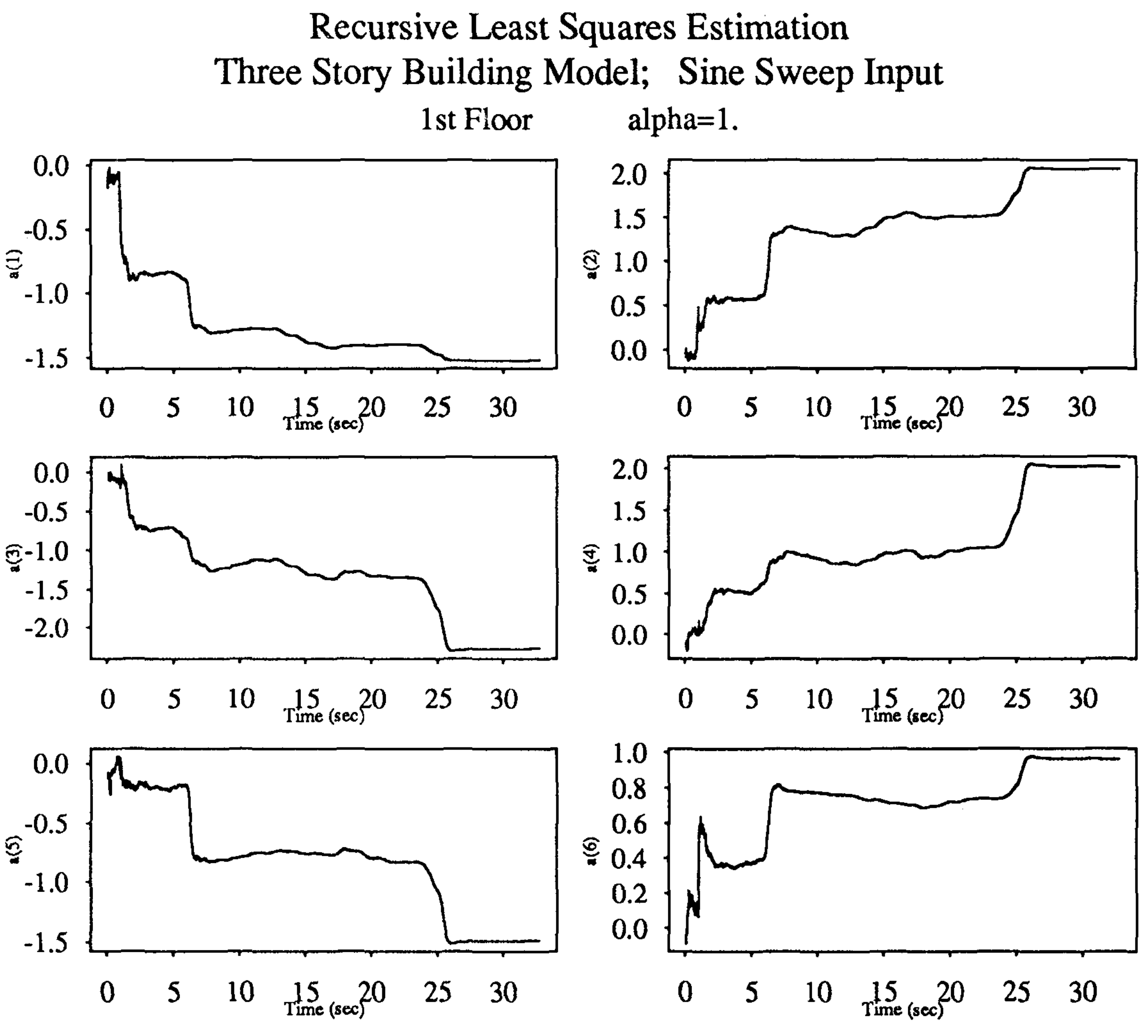
Recursive Least Squares Estimation
Three Story Building Model; Sine Sweep Input
1st Floor alpha=1.
a(1)
a(2)
a(3)
a(4)
a(5)
a(6)
Time (sec)

Figure 5.24

Recursive Least Squares Estimation
Three Story Building Model; Sine Sweep Input
2nd Floor alpha=1.

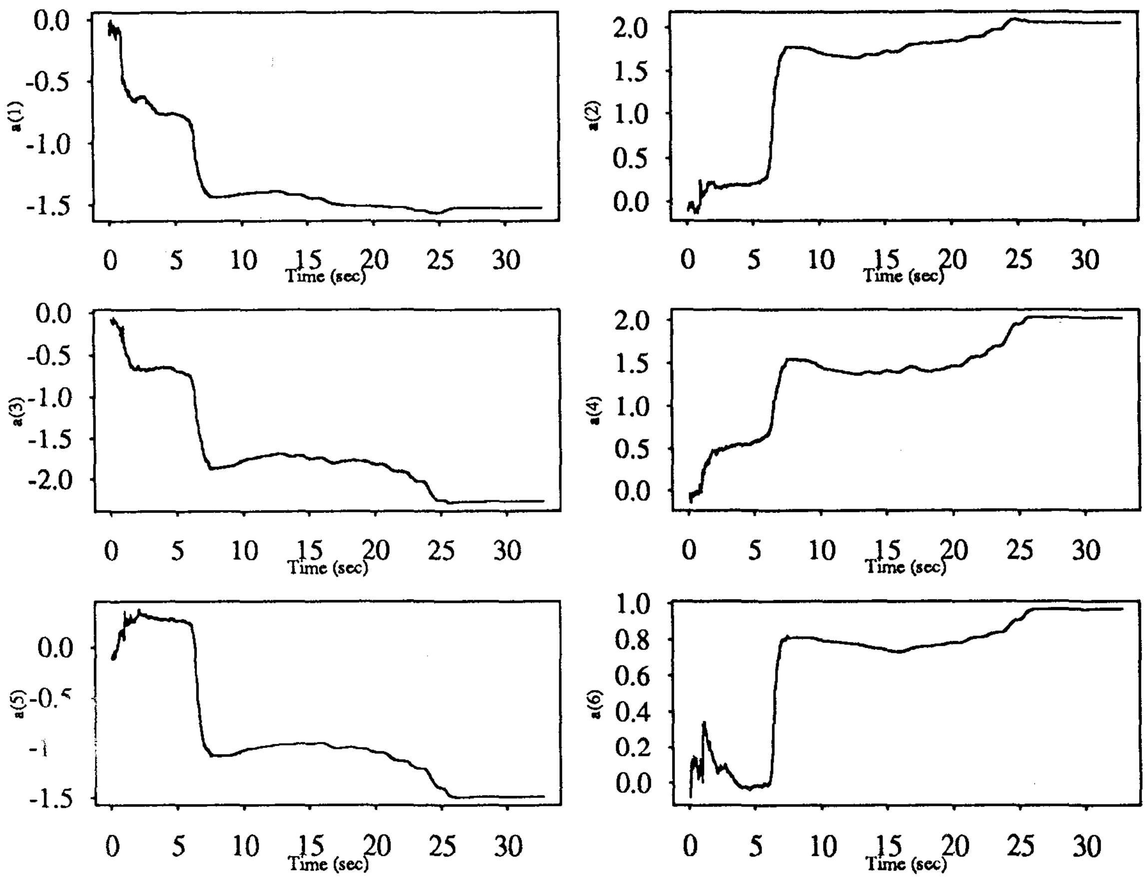


Figure 5.25

## Recursive Least Squares Estimation
## Three Story Building Model; Sine Sweep Input

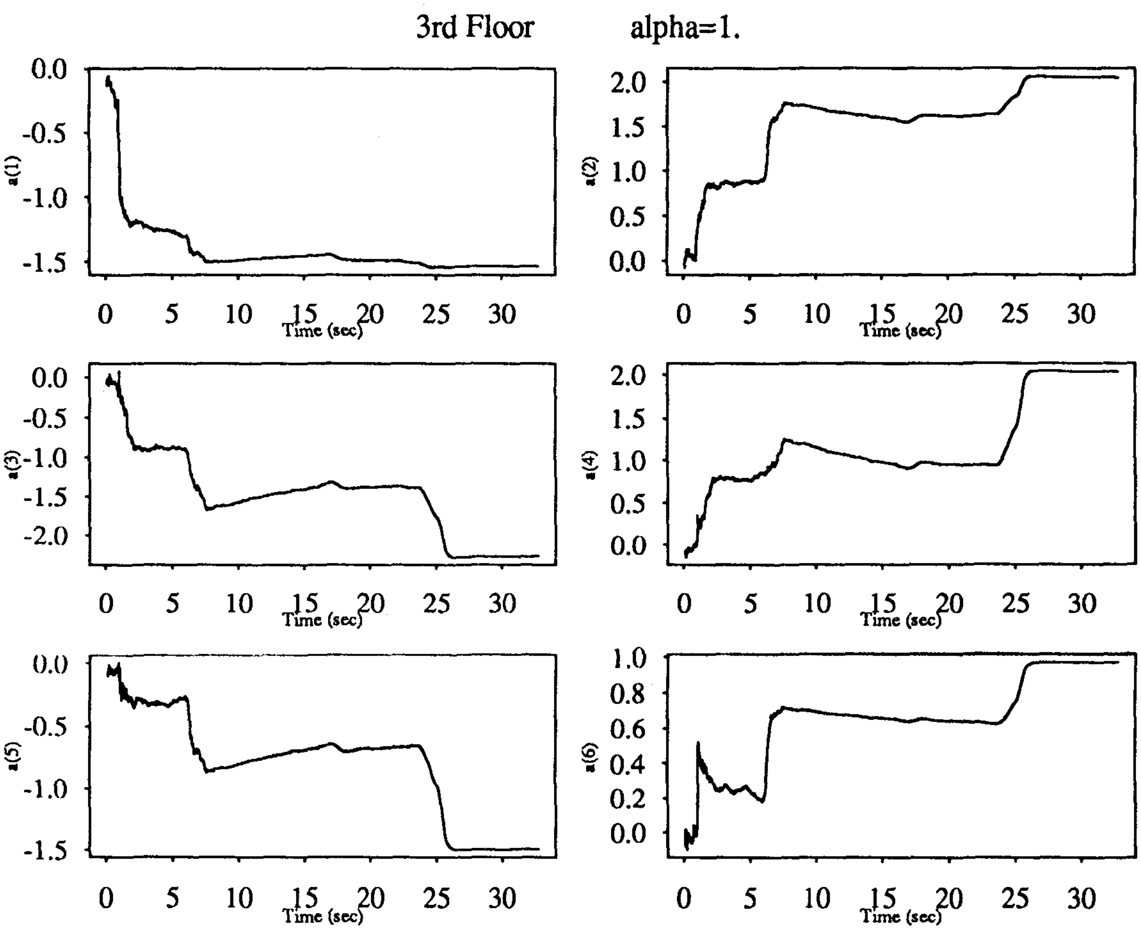


Figure 5.26

Recursive Least Squares Estimation
Three Story Building Model; White Noise Input
1st Floor alpha=1.

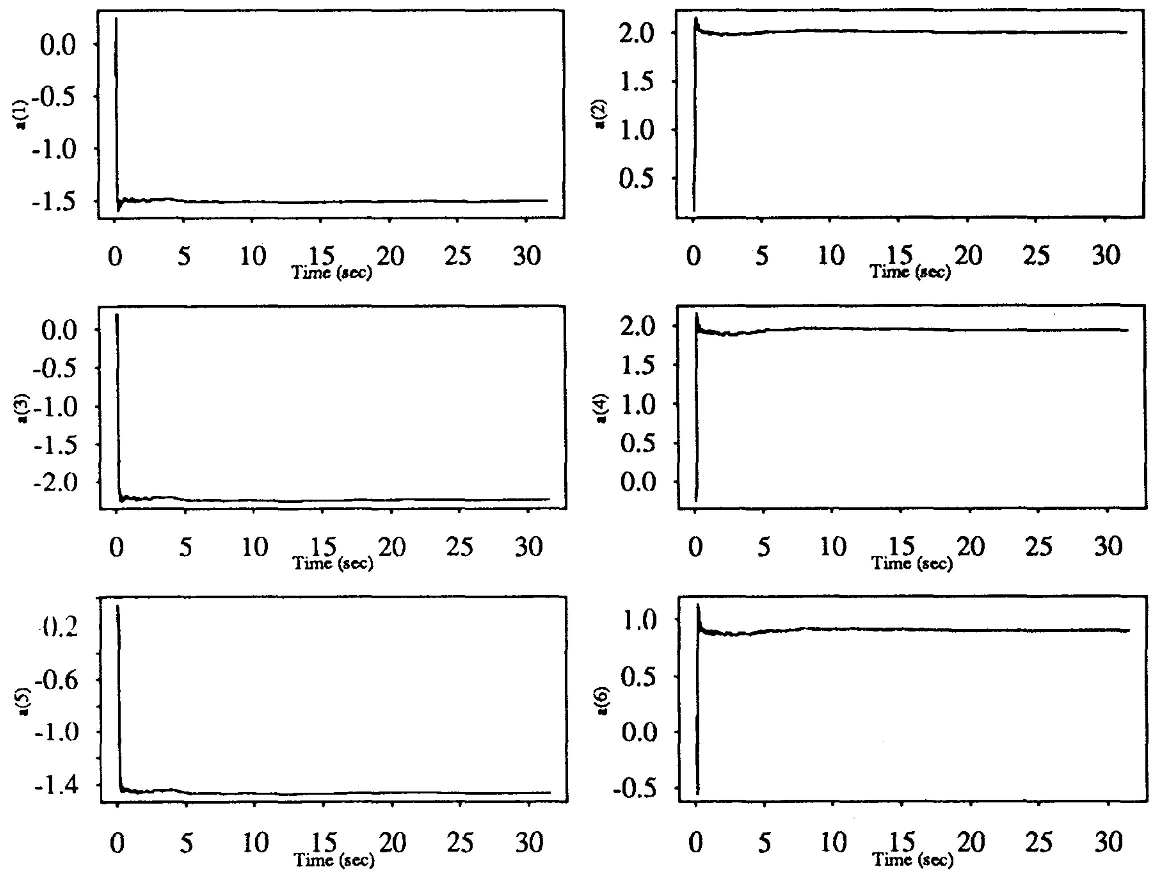


Figure 5.27

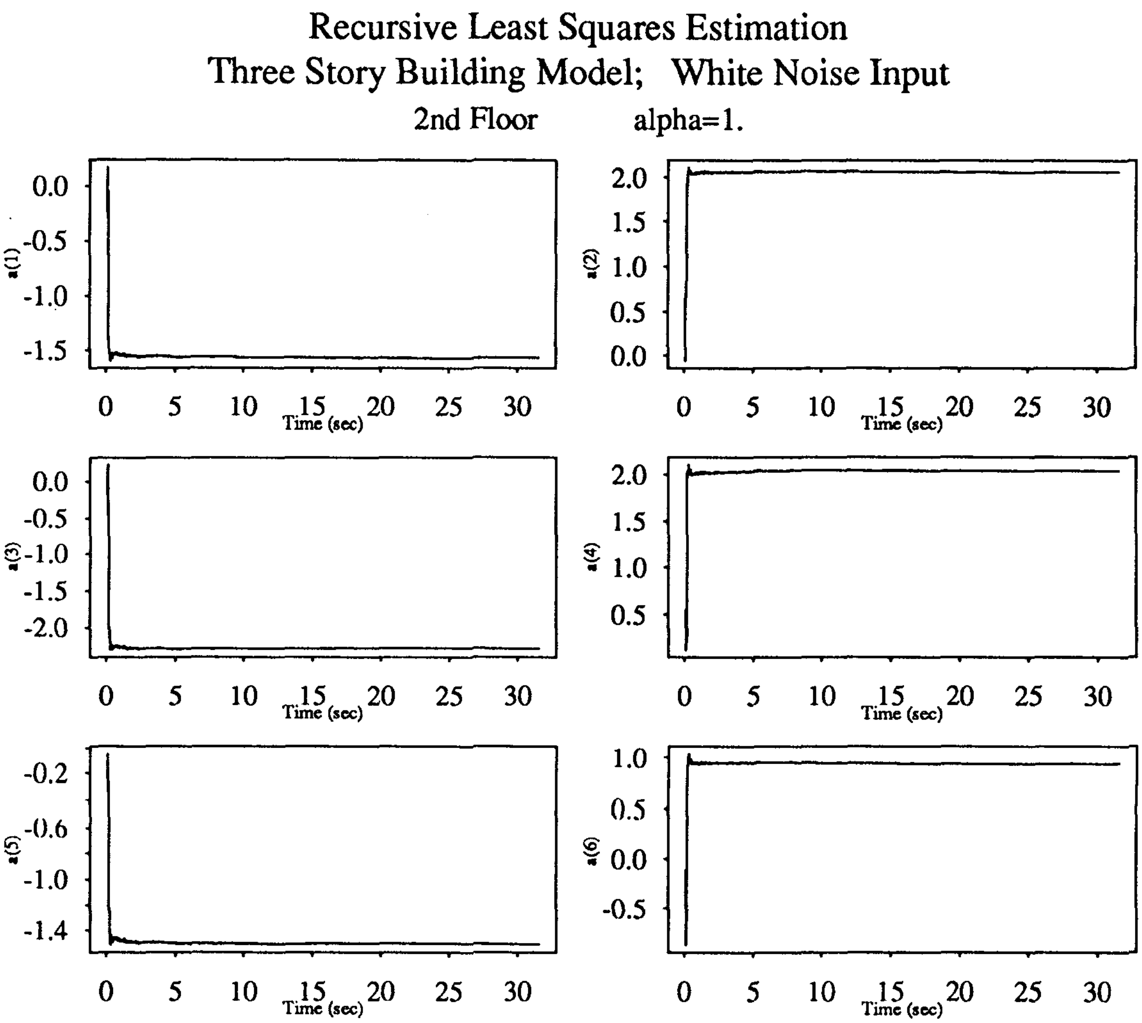
Recursive Least Squares Estimation
Three Story Building Model; White Noise Input
2nd Floor alpha=1.
a(1)
a(2)
a(3)
a(4)
a(5)
a(6)
Time (sec)

Figure 5.28

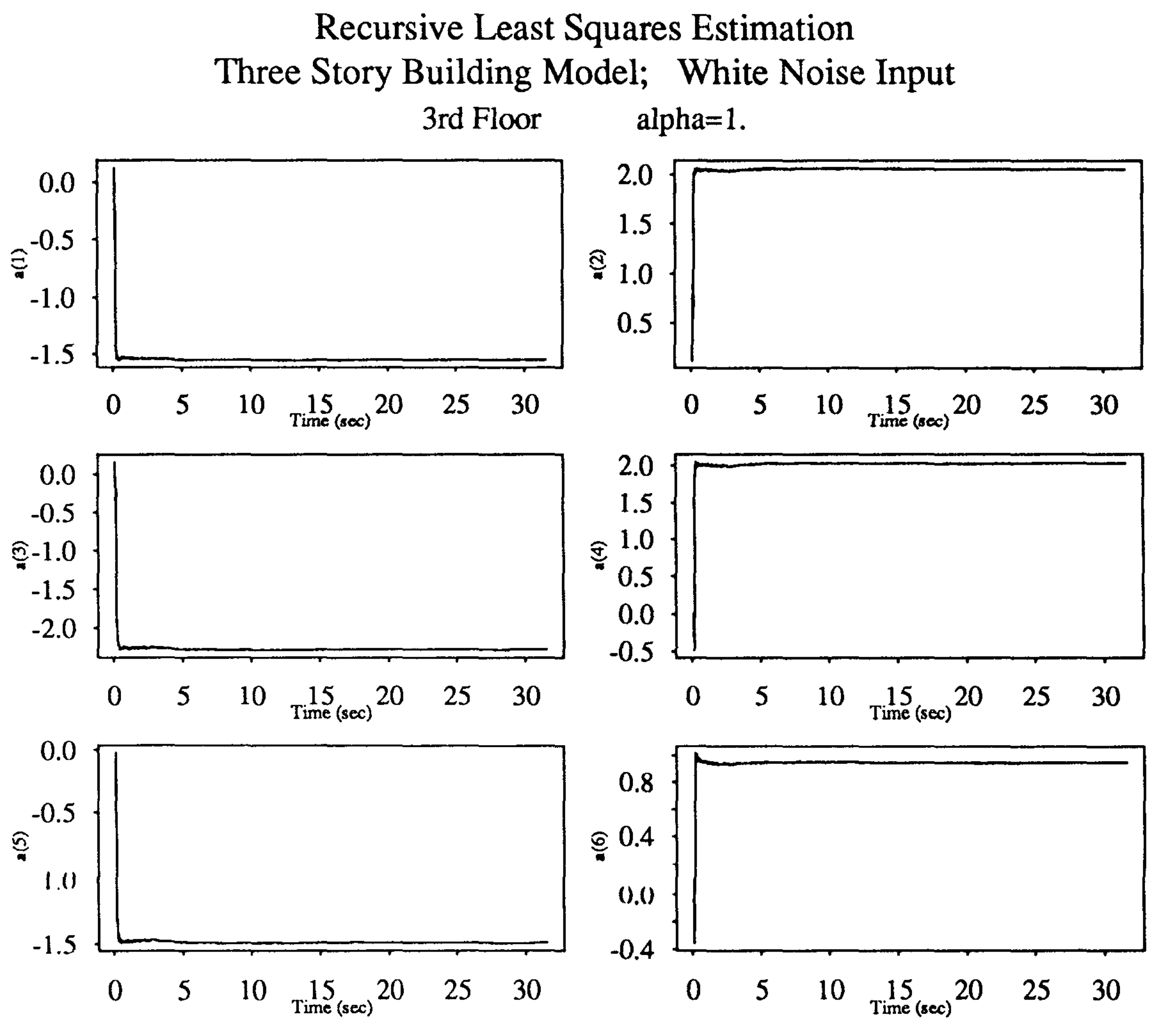
Recursive Least Squares Estimation
Three Story Building Model; White Noise Input
3rd Floor alpha=1.
a(1)
0.0
-0.5
-1.0
-1.5
a(2)
2.0
1.5
1.0
0.5
a(3)
0.0
-0.5
-1.0
-1.5
-2.0
a(4)
2.0
1.5
1.0
0.5
0.0
-0.5
a(5)
0.0
-0.5
-1.0
-1.5
a(6)
0.8
0.4
0.0
-0.4
0 5 10 15 20 25 30
Time (sec)

Figure 5.29

Recursive Least Squares Estimation
Three Story Building Model; El-Centro Input
1st Floor alpha=1.

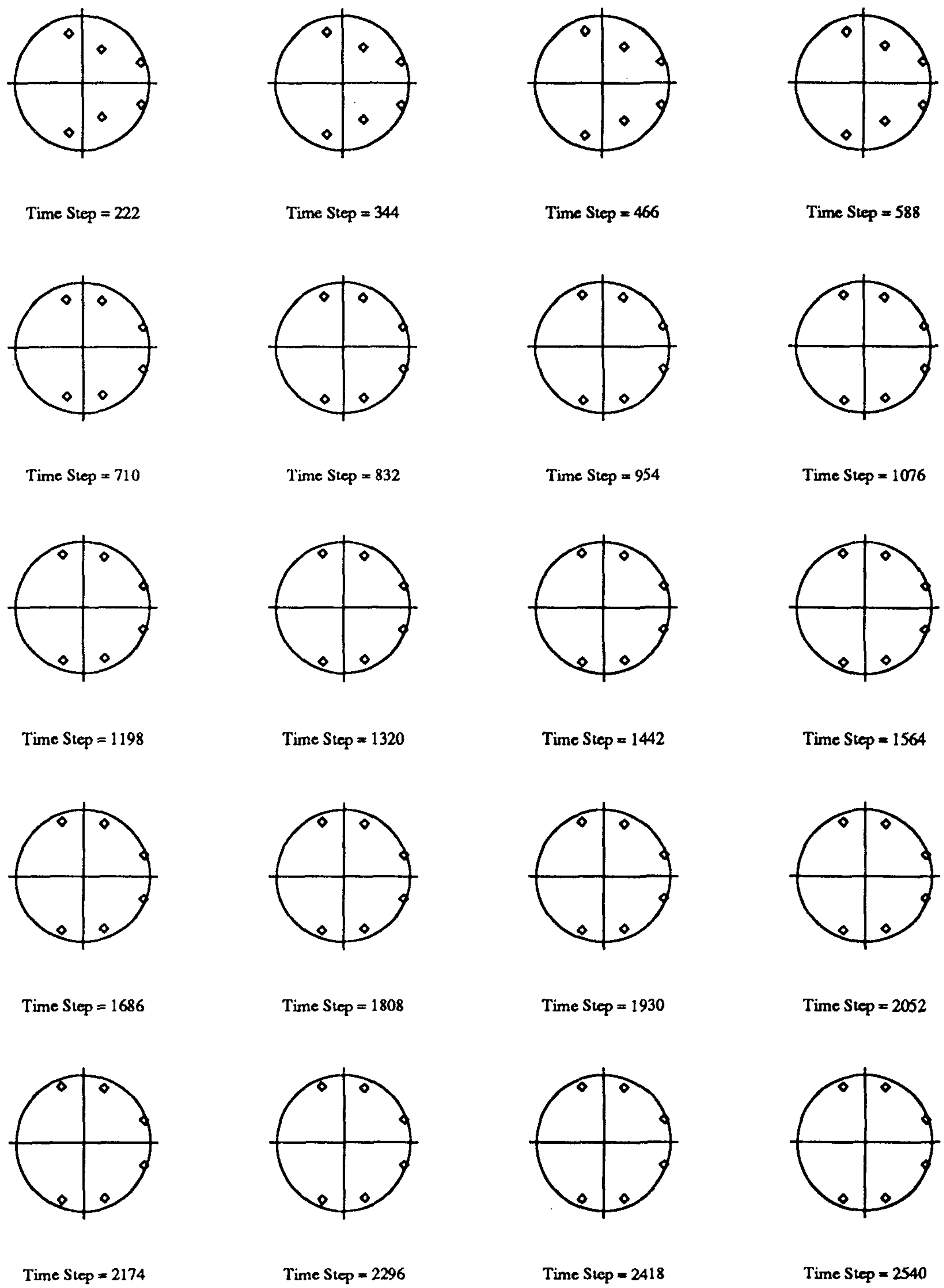


Figure 5.30

# Recursive Least Squares Estimation
## Three Story Building Model; El-Centro Input
2nd Floor alpha=1.

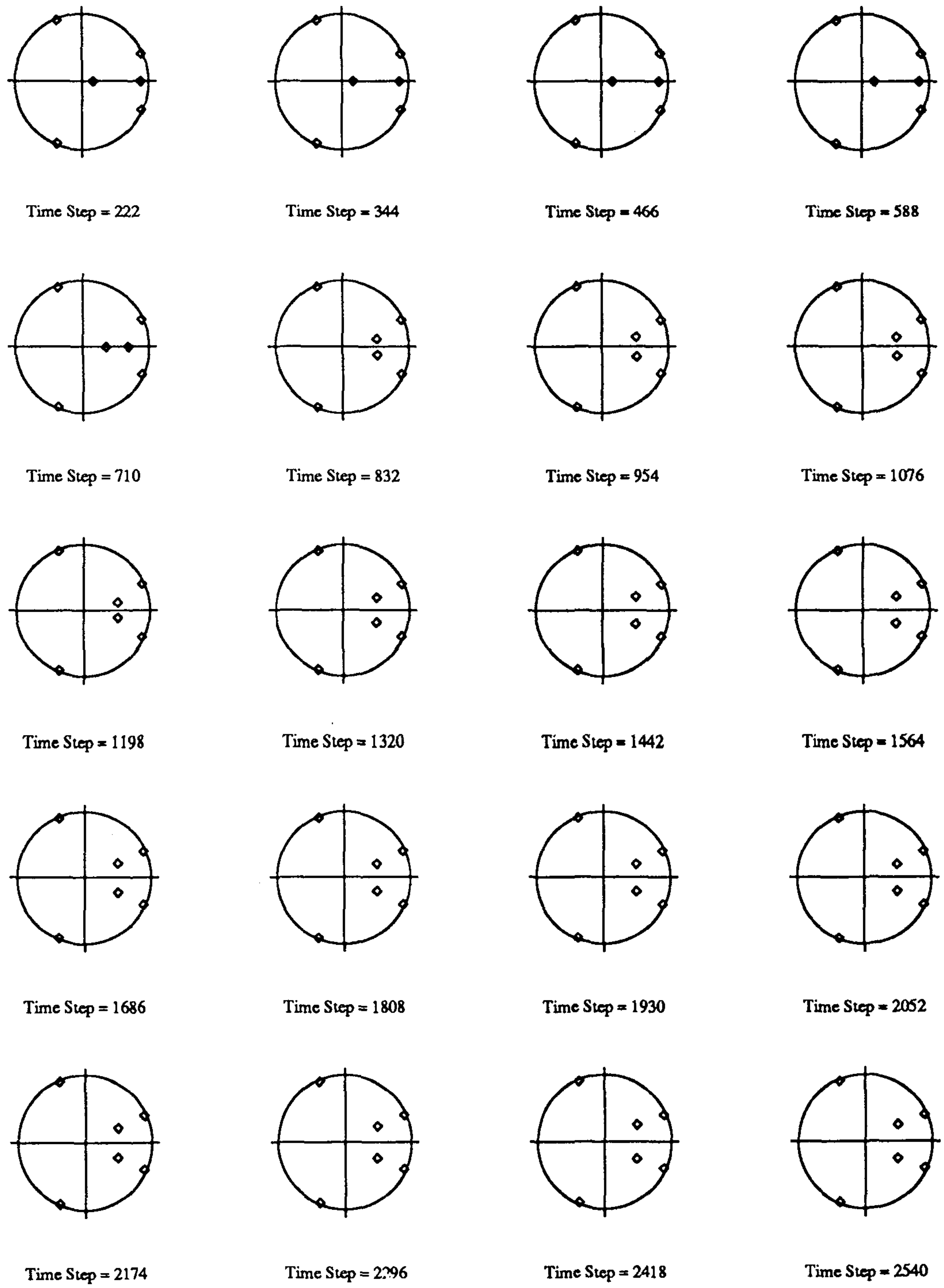


Figure 5.31

## Recursive Least Squares Estimation
## Three Story Building Model; El-Centro Input
3rd Floor alpha=1.

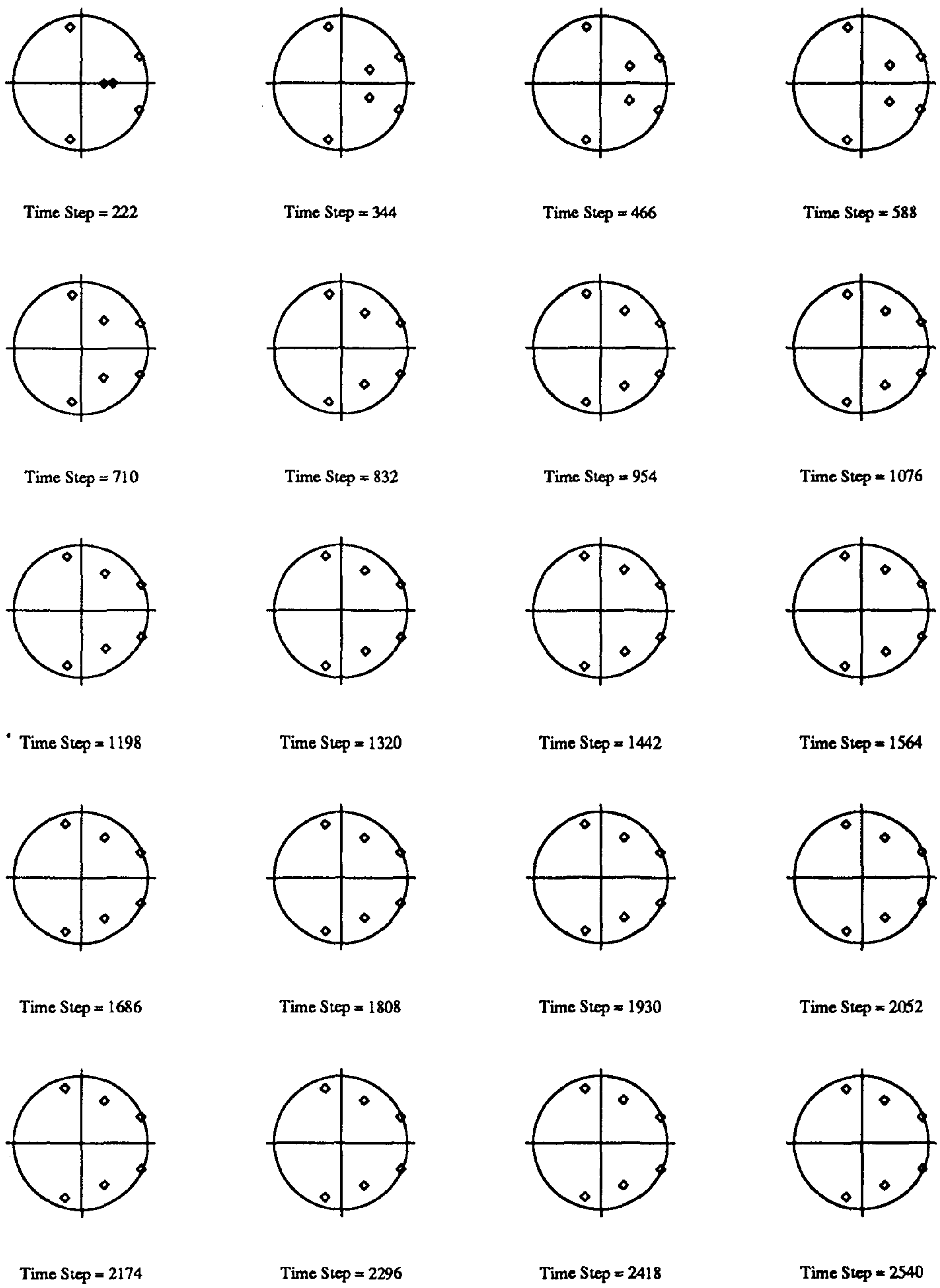


Figure 5.32

## Recursive Least Squares Estimation
## Three Story Building Model; Sine Sweep Input

1st Floor alpha=1.

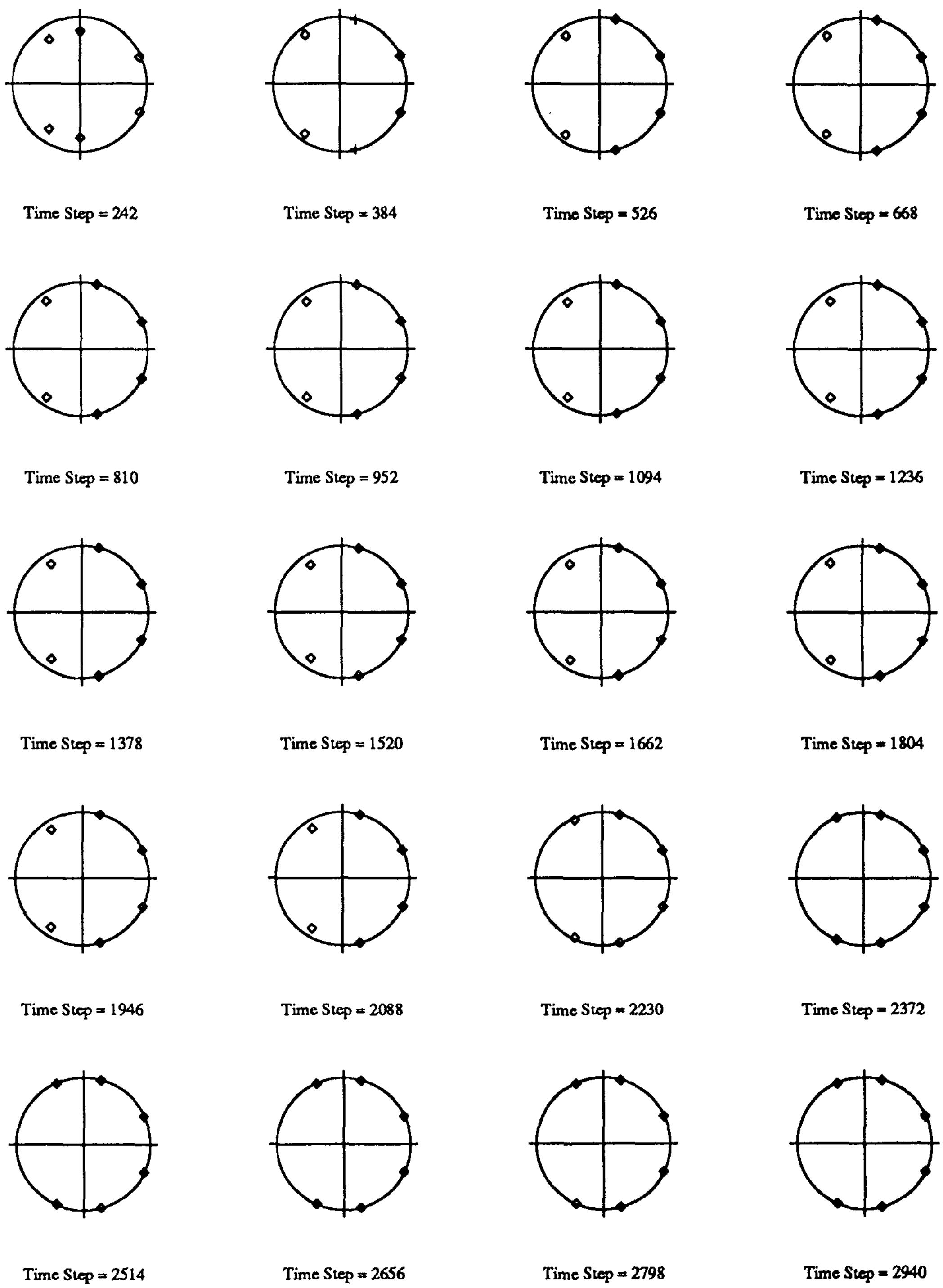


**Figure 5.33**

Recursive Least Squares Estimation
Three Story Building Model; Sine Sweep Input
2nd Floor alpha=1.

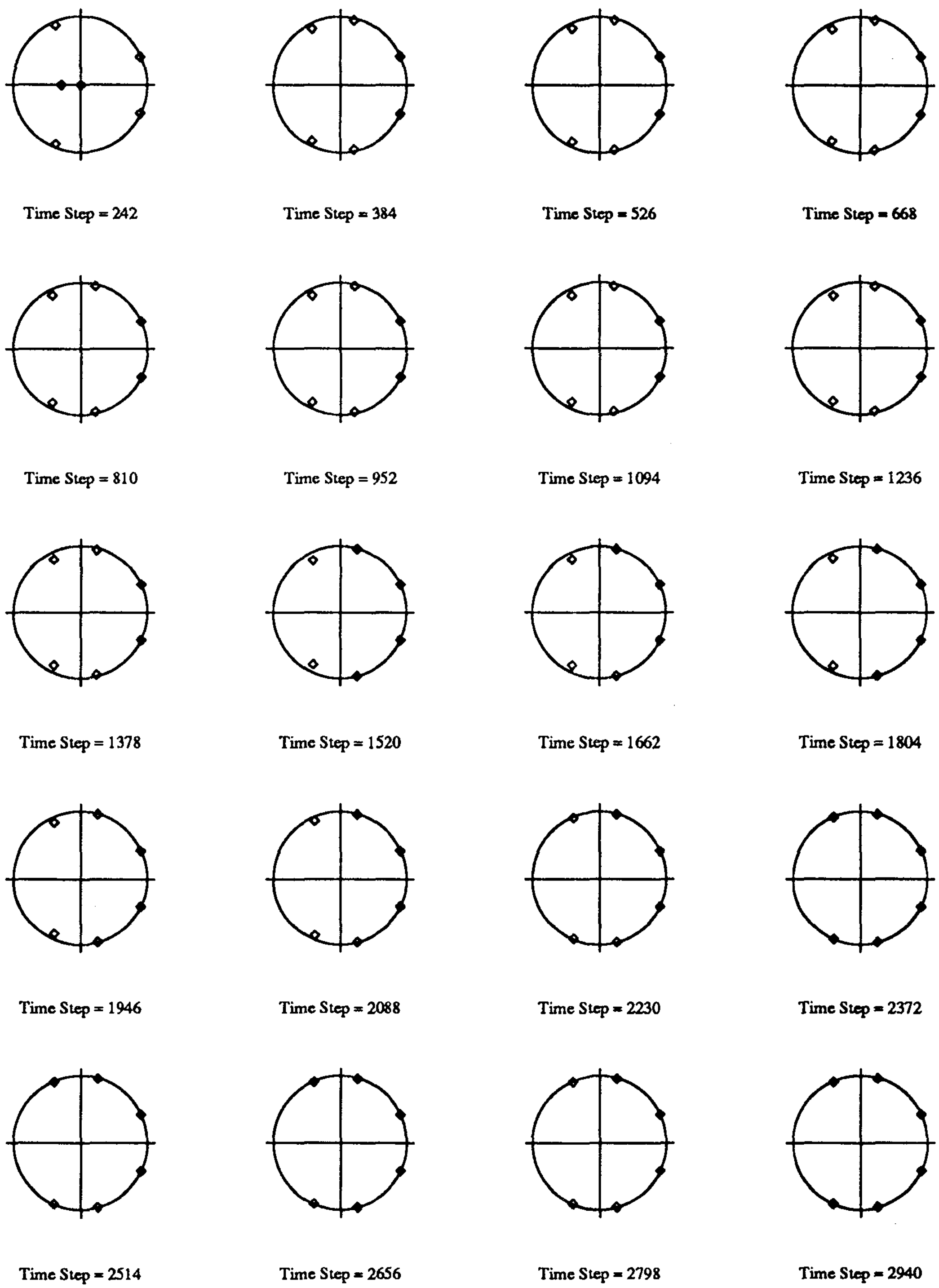


**Figure 5.34**

Recursive Least Squares Estimation
Three Story Building Model; Sine Sweep Input
3rd Floor alpha=1.

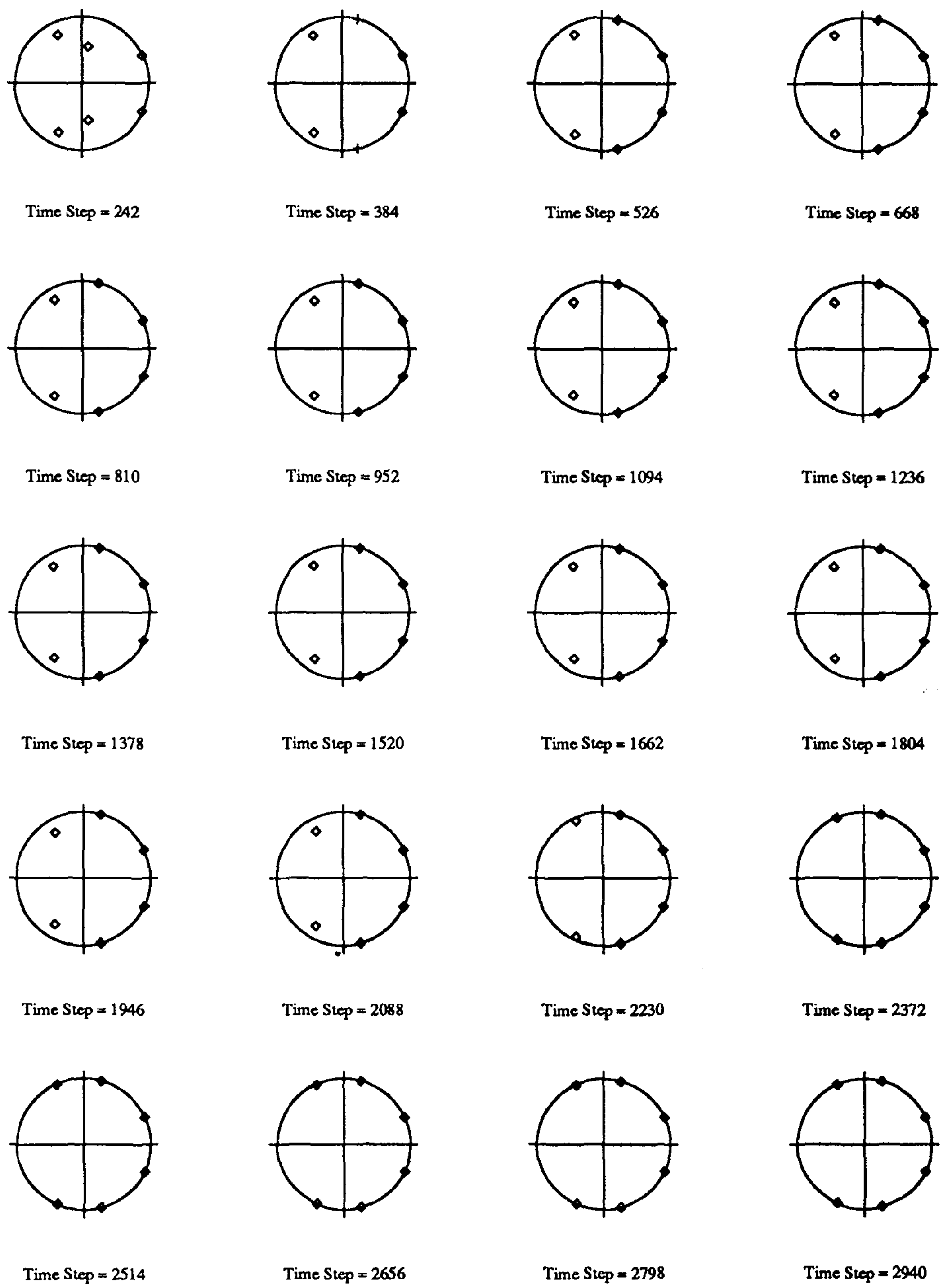


Figure 5.35

Recursive Least Squares Estimation
Three Story Building Model; White Noise Input
1st Floor alpha=1.

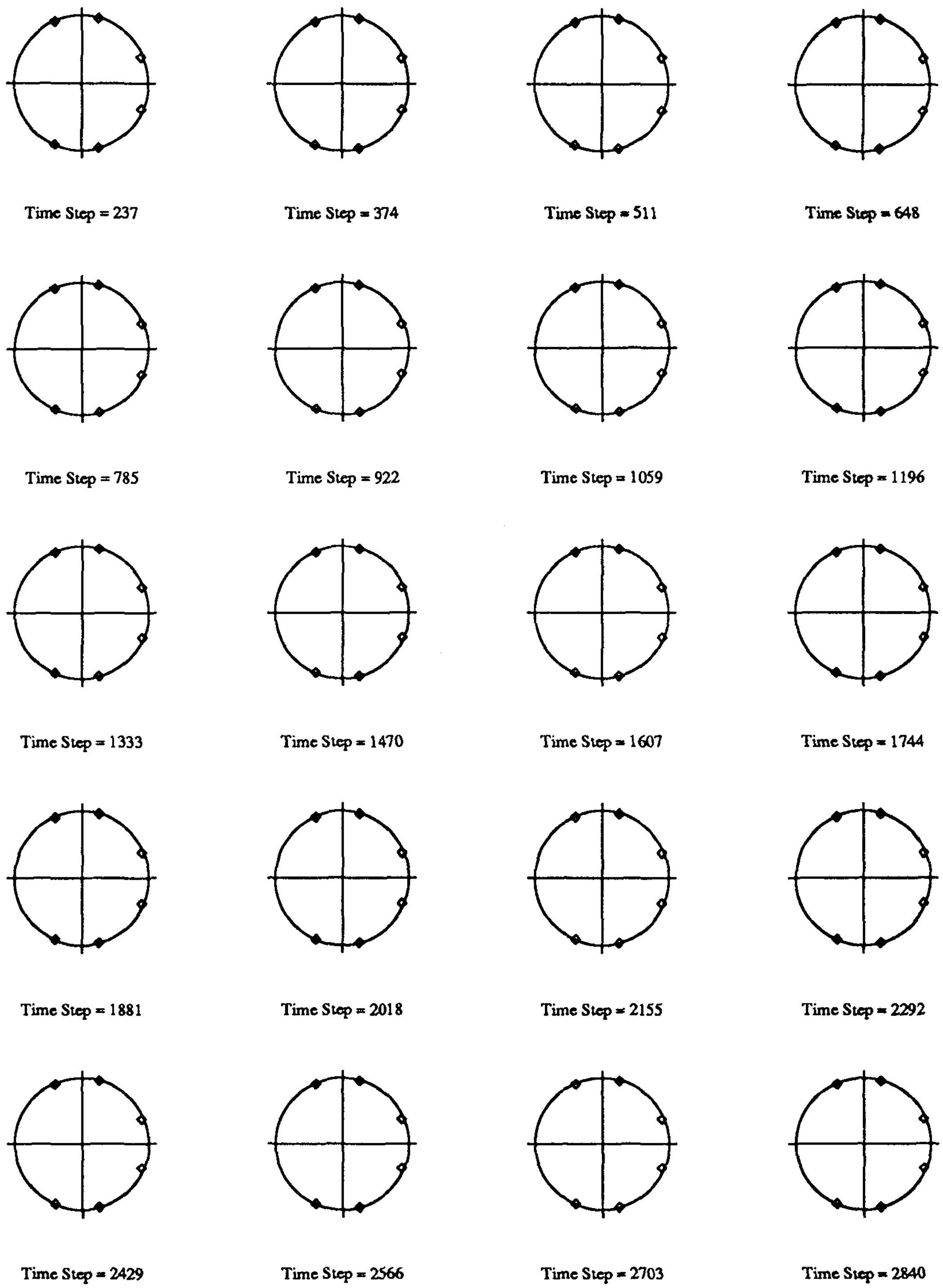


**Figure 5.36**

## Recursive Least Squares Estimation
## Three Story Building Model; White Noise Input
2nd Floor alpha=1.

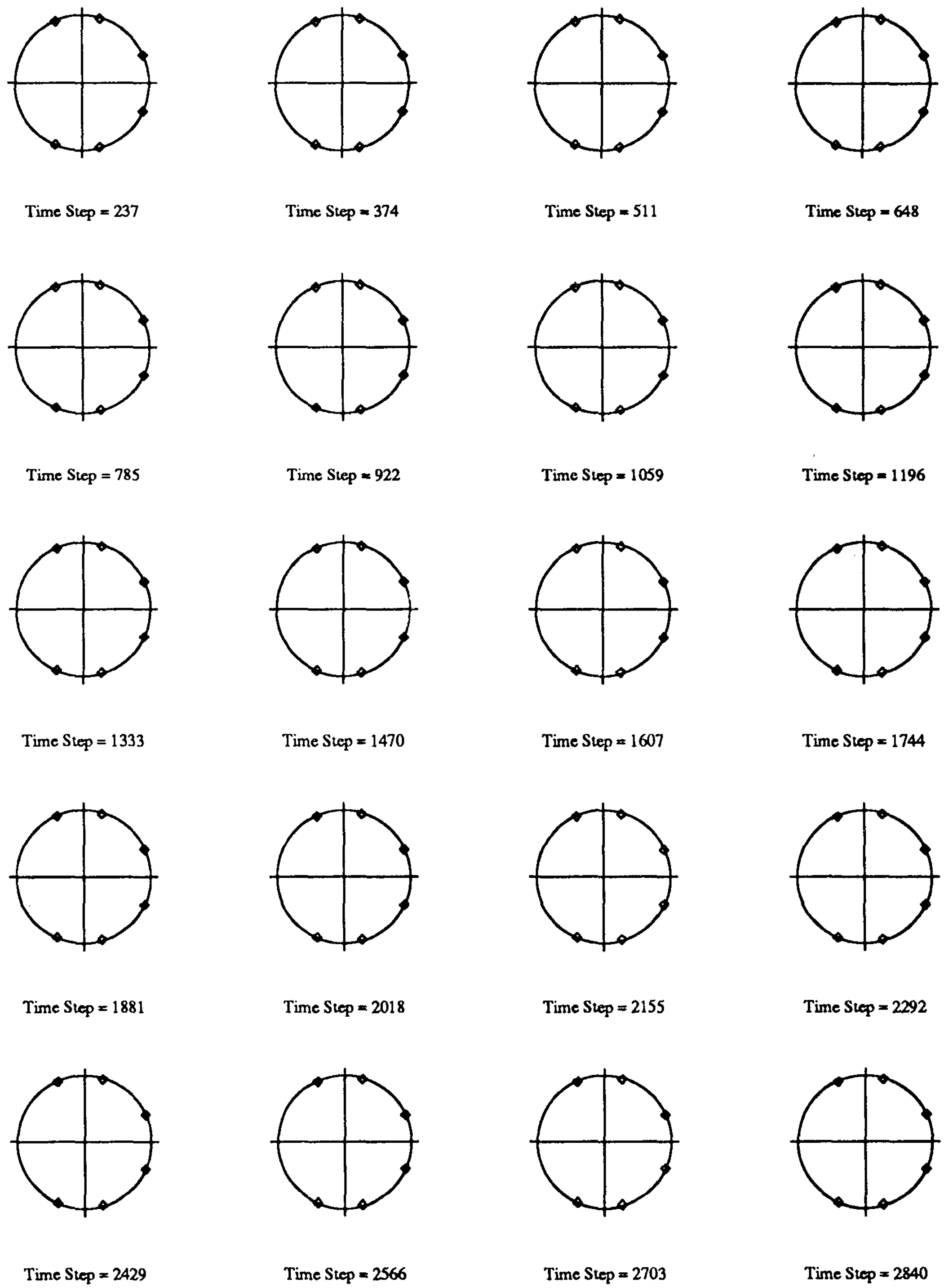


Figure 5.37

Recursive Least Squares Estimation
Three Story Building Model; White Noise Input
3rd Floor alpha=1.

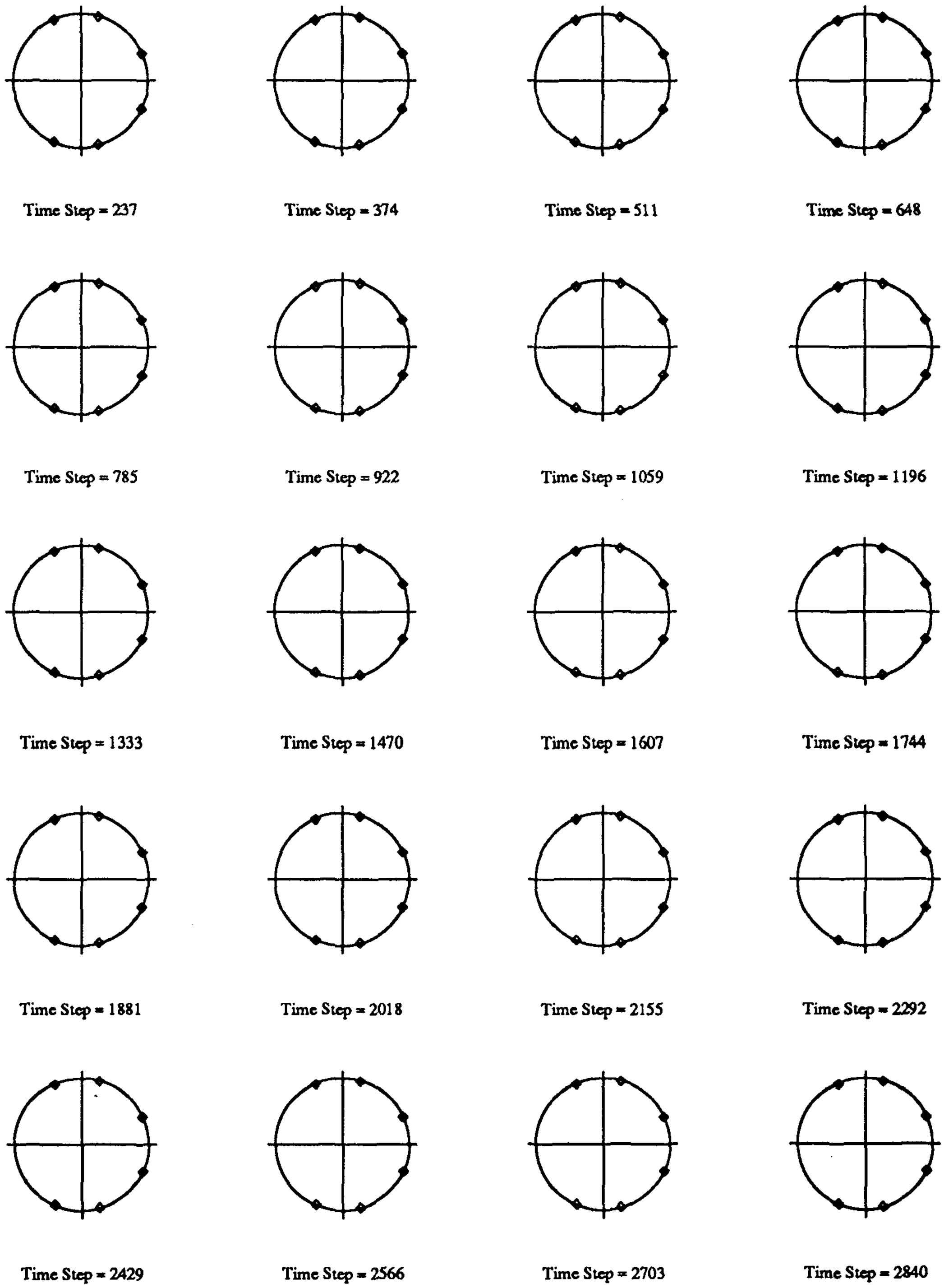


Figure 5.38

Recursive Least Squares Estimation
Five Story Building Model;  El-Centro Input
1st Floor          alpha=0.99

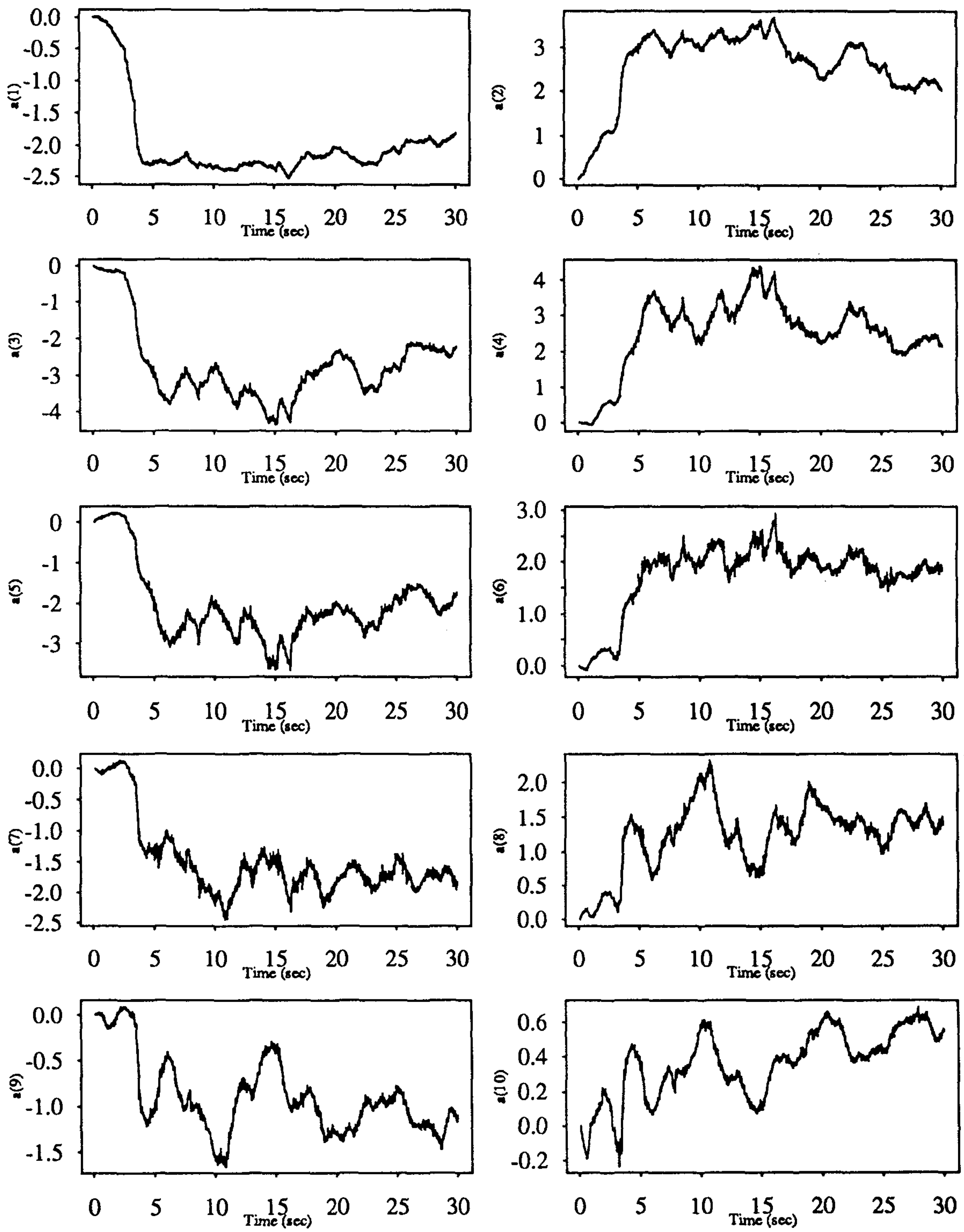


Figure 5.39

Recursive Least Squares Estimation
Five Story Building Model; El-Centro Input
2nd Floor alpha=0.99

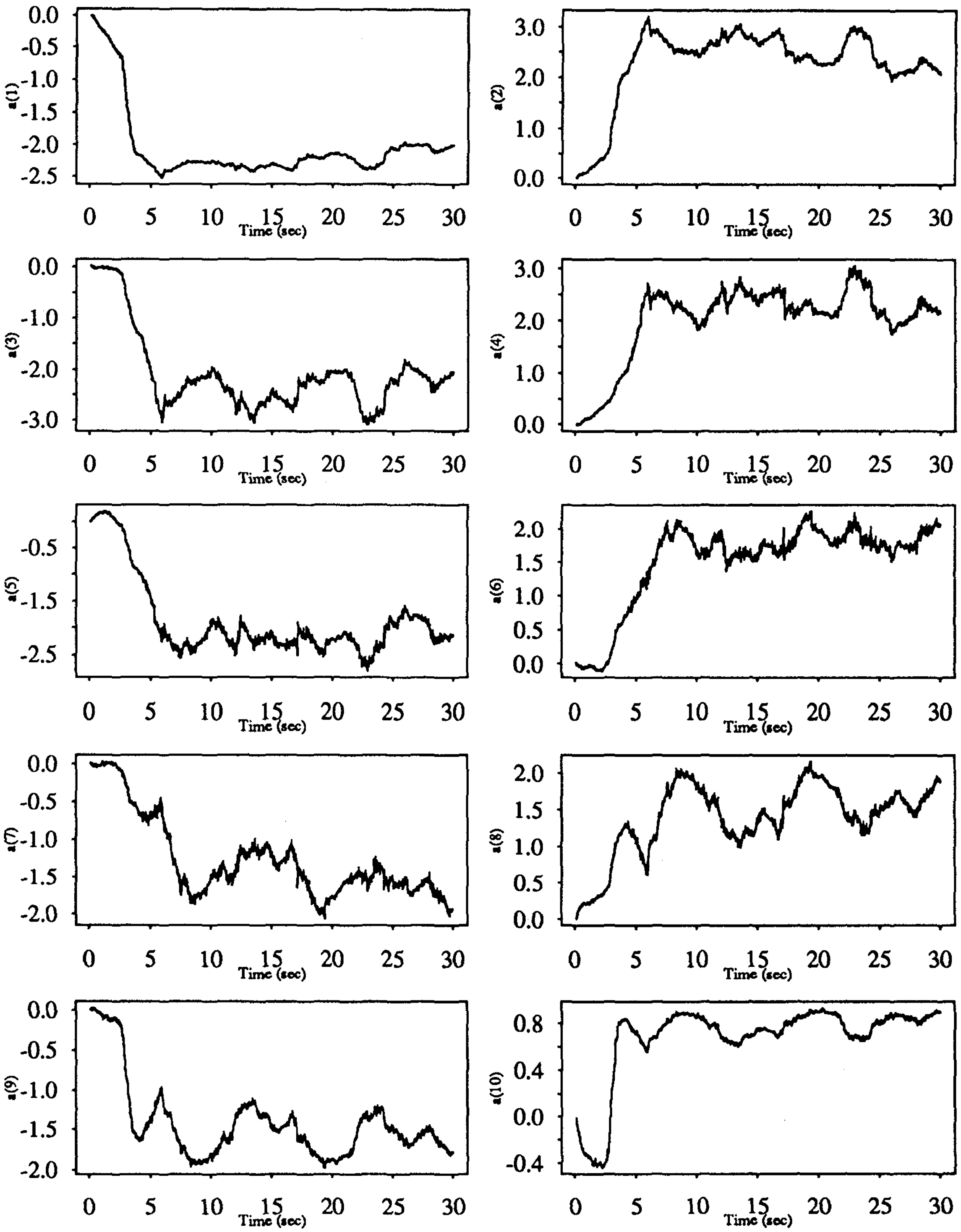


Figure 5.40

Recursive Least Squares Estimation
Five Story Building Model; El-Centro Input
3rd Floor alpha=0.99

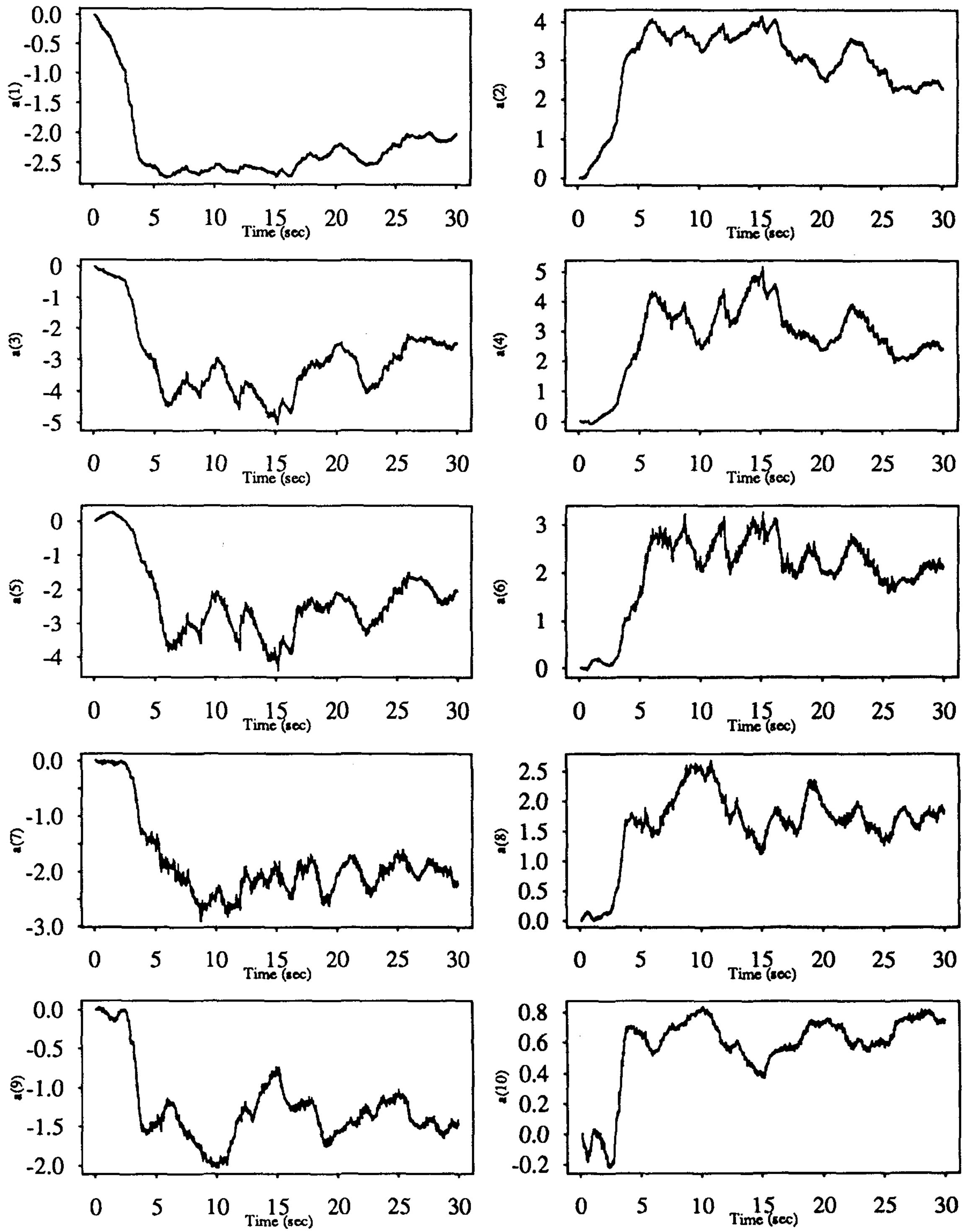


**Figure 5.41**

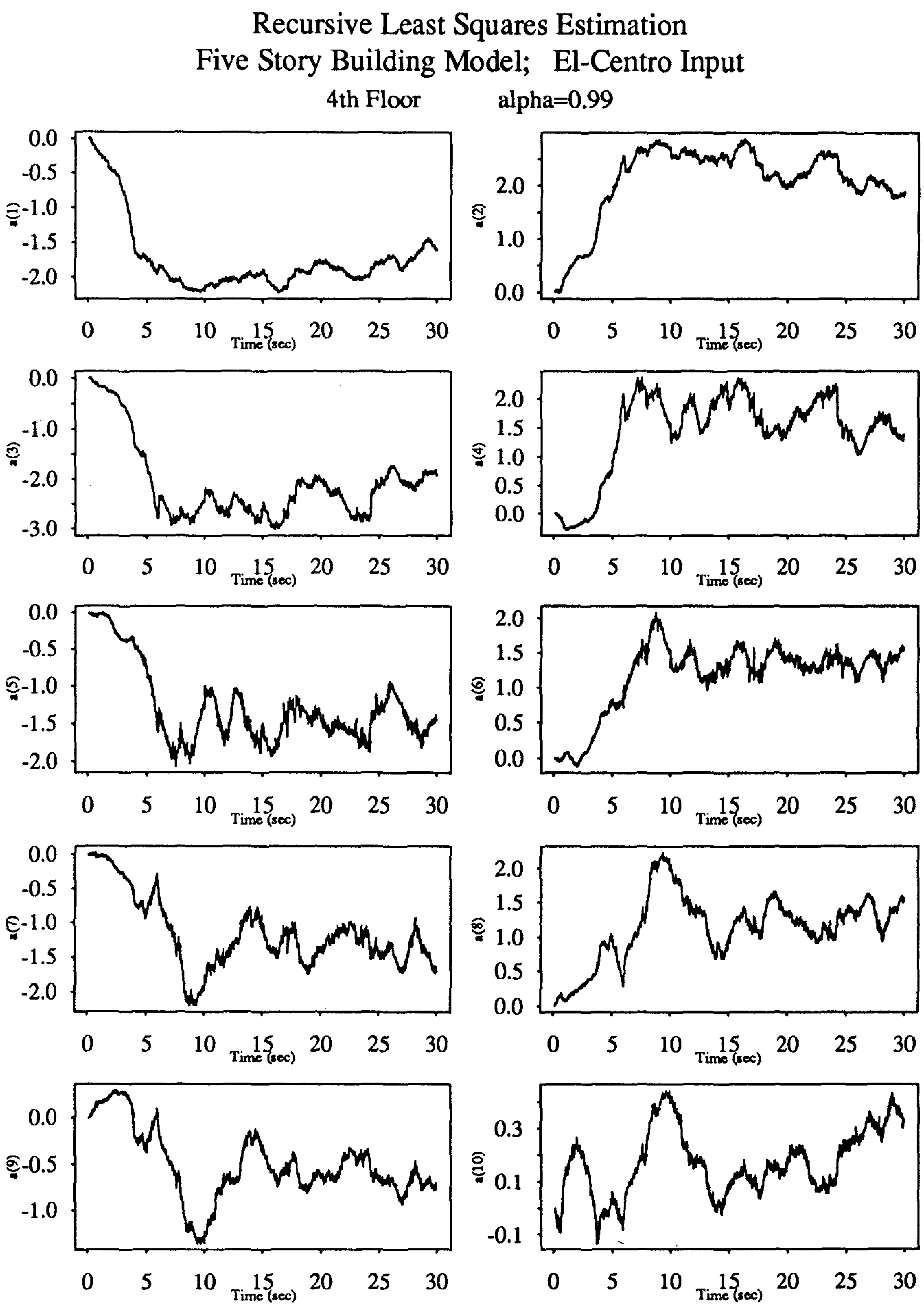
Recursive Least Squares Estimation
Five Story Building Model; El-Centro Input
4th Floor alpha=0.99
a(1)
a(2)
a(3)
a(4)
a(5)
a(6)
a(7)
a(8)
a(9)
a(10)
Time (sec)
0 5 10 15 20 25 30

Figure 5.42

# Recursive Least Squares Estimation
## Five Story Building Model; El-Centro Input
5th Floor alpha=0.99

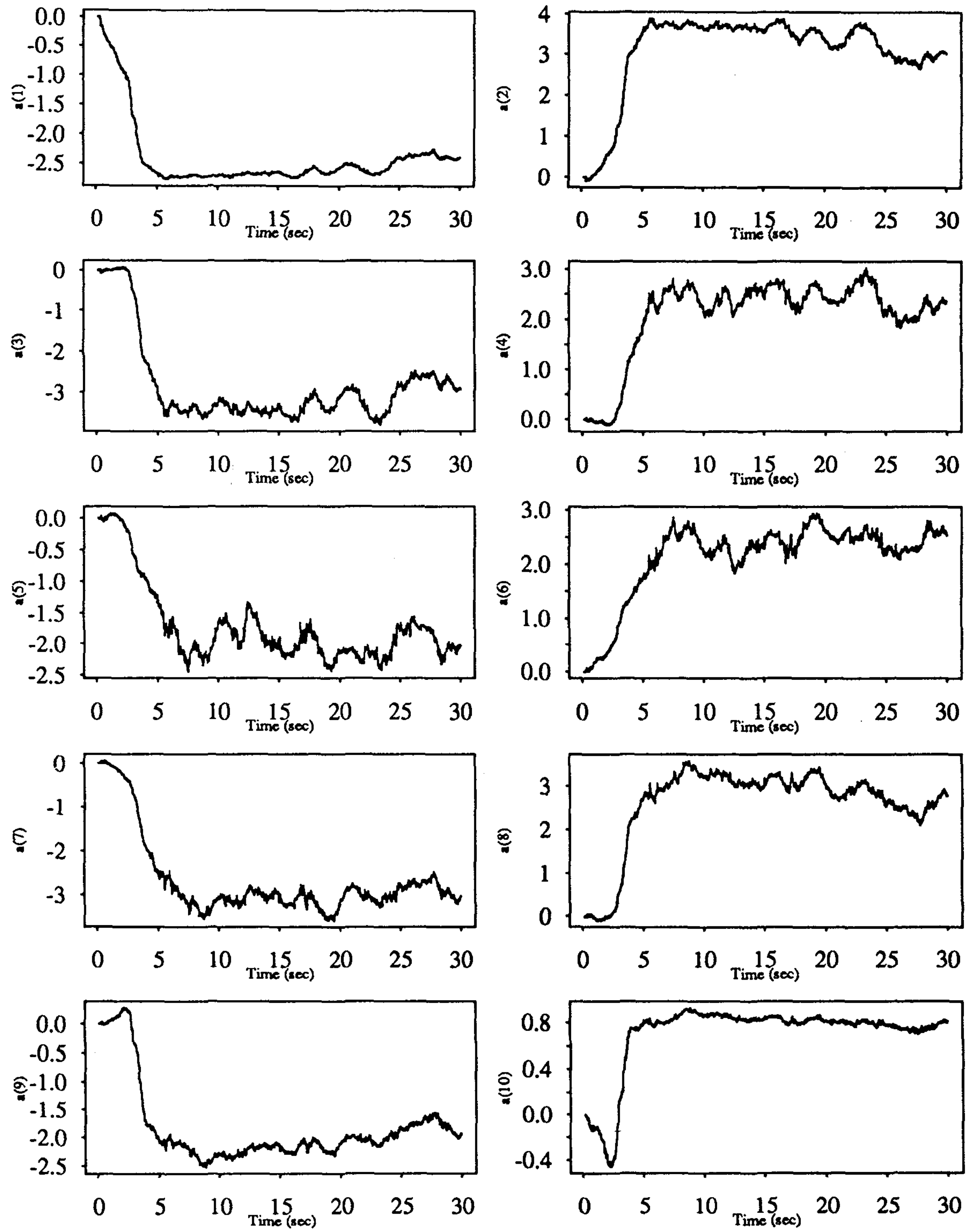


Figure 5.43

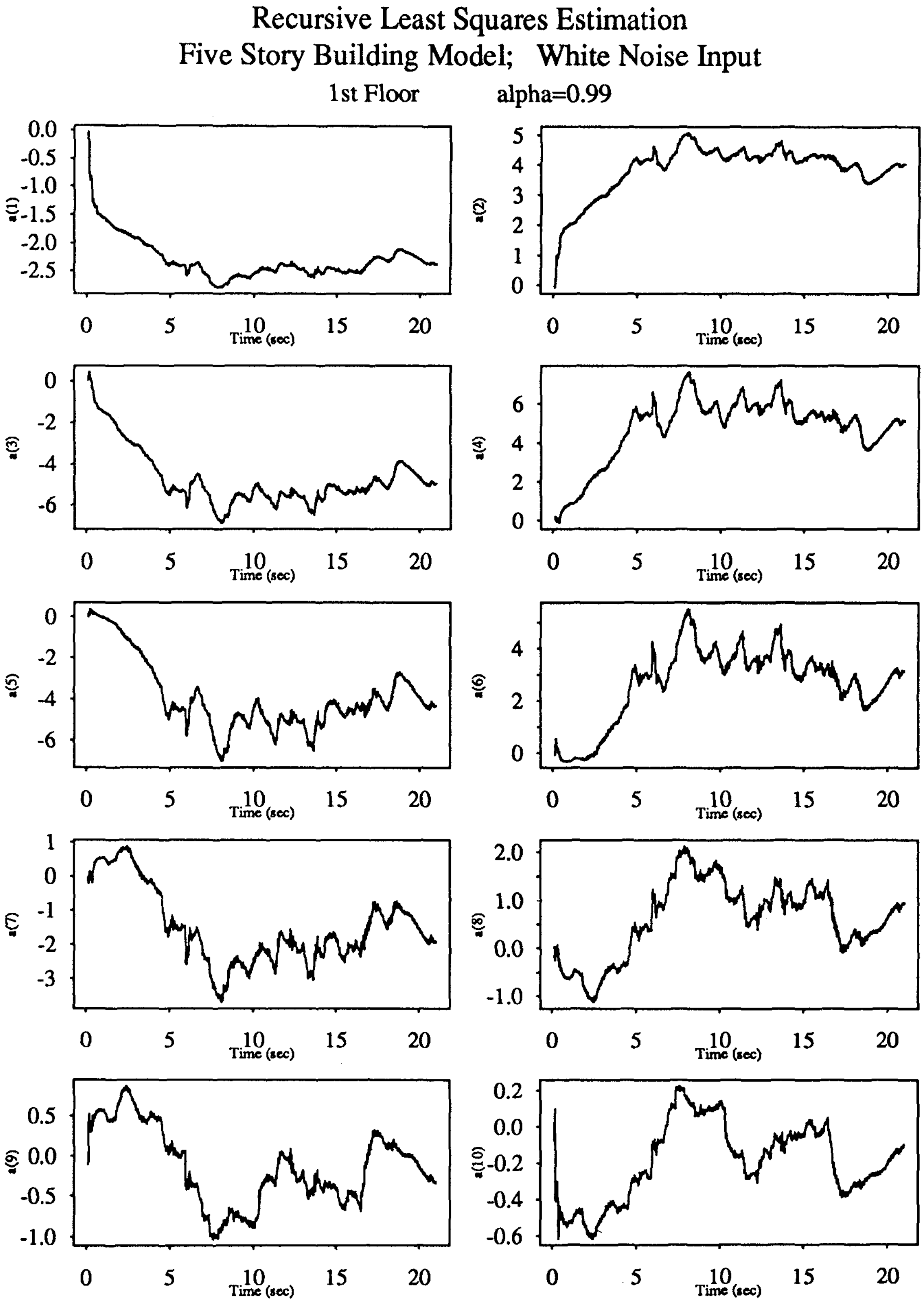
Recursive Least Squares Estimation
Five Story Building Model; White Noise Input
1st Floor
alpha=0.99
a(1)
a(2)
a(3)
a(4)
a(5)
a(6)
a(7)
a(8)
a(9)
a(10)
Time (sec)

Figure 5.44

Recursive Least Squares Estimation
Five Story Building Model; White Noise Input
2nd Floor alpha=0.99

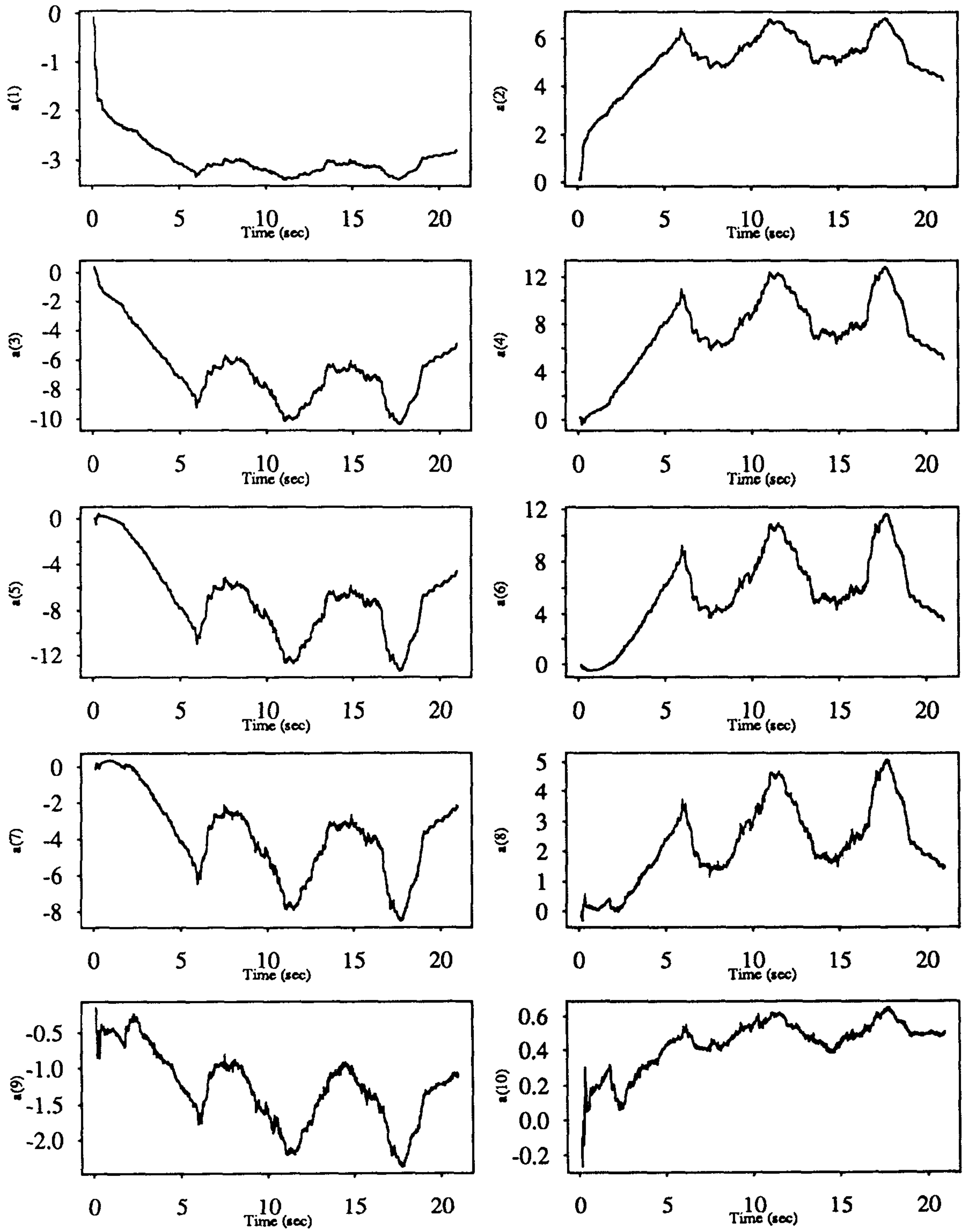


Figure 5.45

# Recursive Least Squares Estimation
## Five Story Building Model; White Noise Input

3rd Floor alpha=0.99

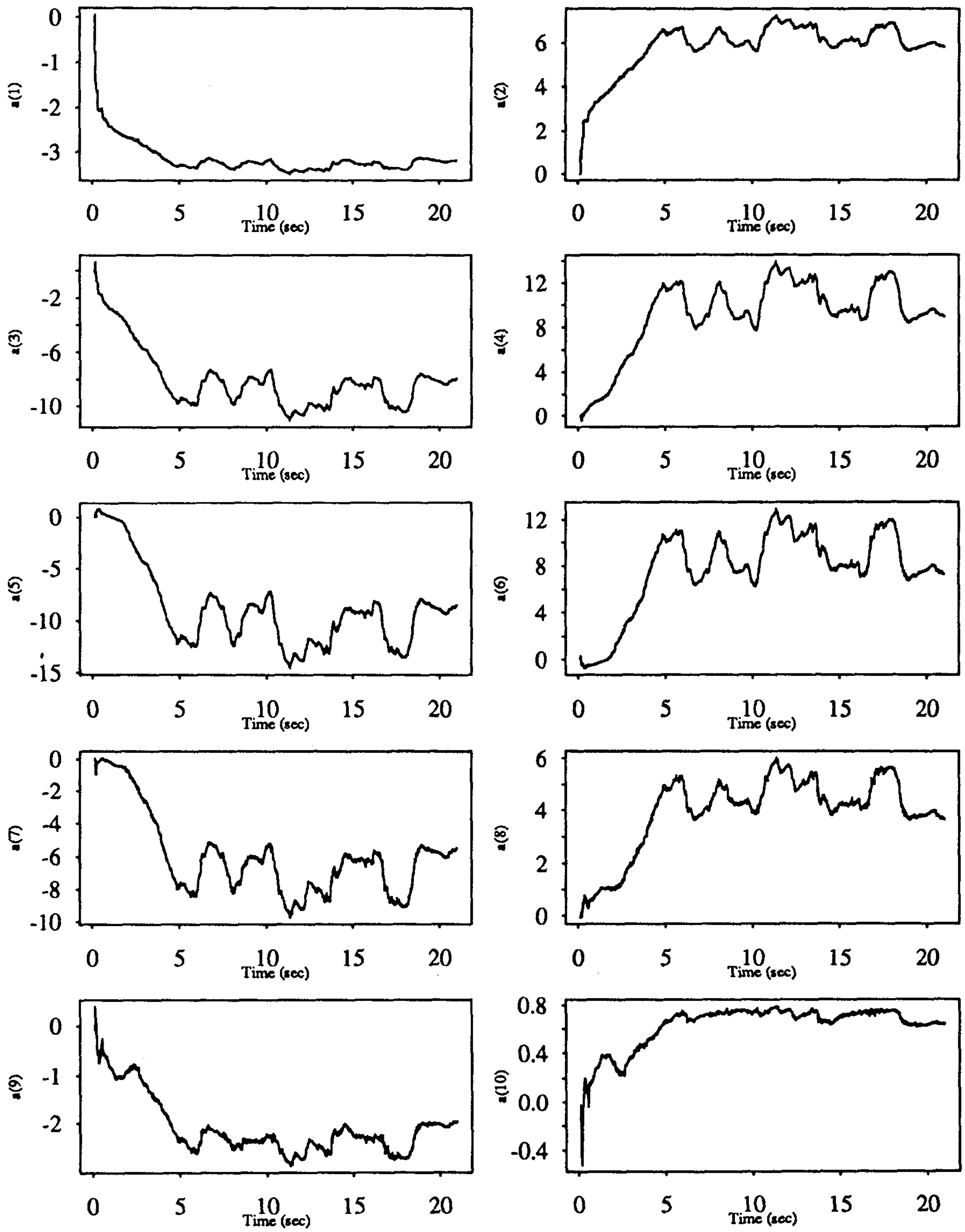


Figure 5.46

Recursive Least Squares Estimation
Five Story Building Model; White Noise Input
4th Floor alpha=0.99

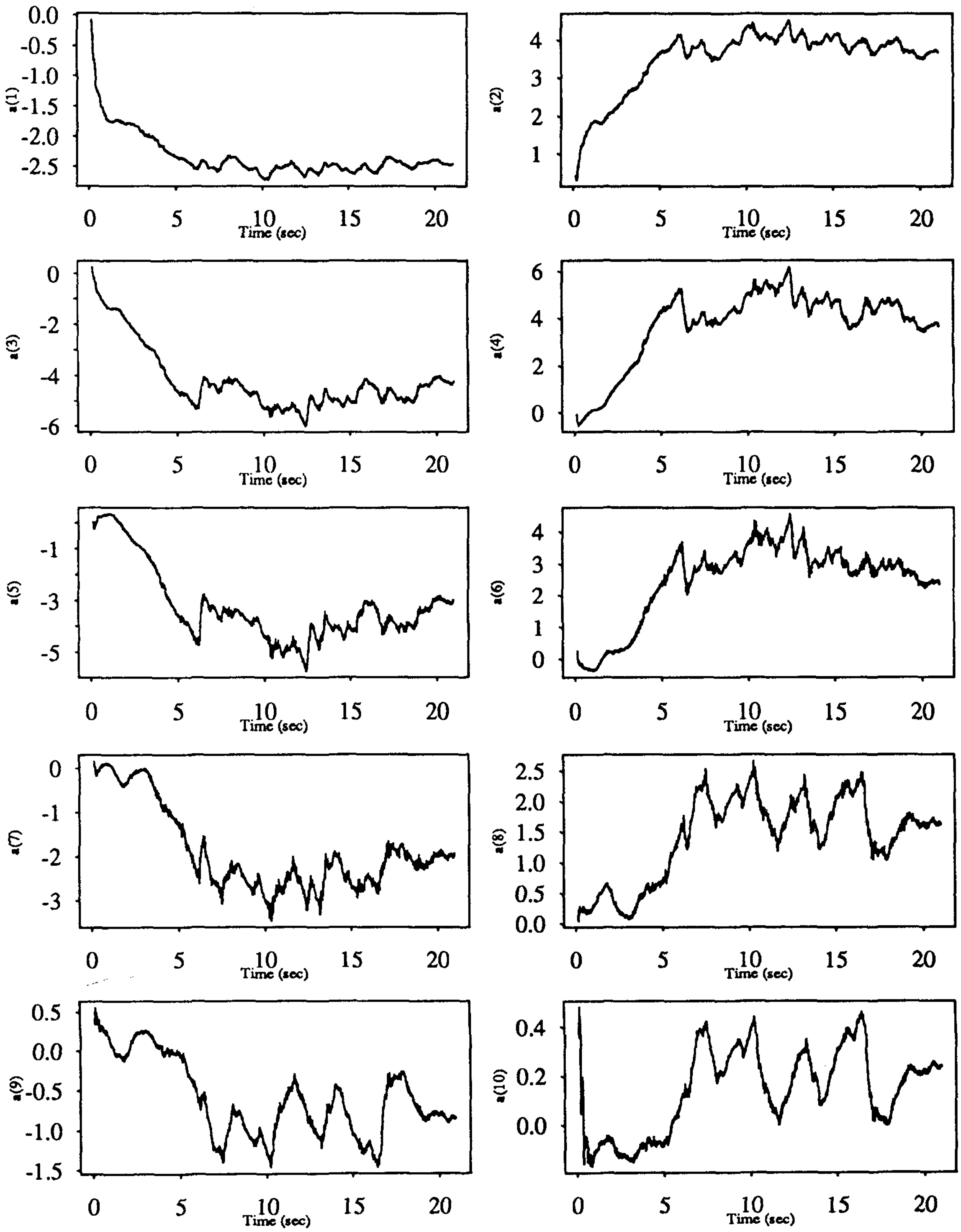


Figure 5.47

Recursive Least Squares Estimation
Five Story Building Model; White Noise Input
5th Floor alpha=0.99

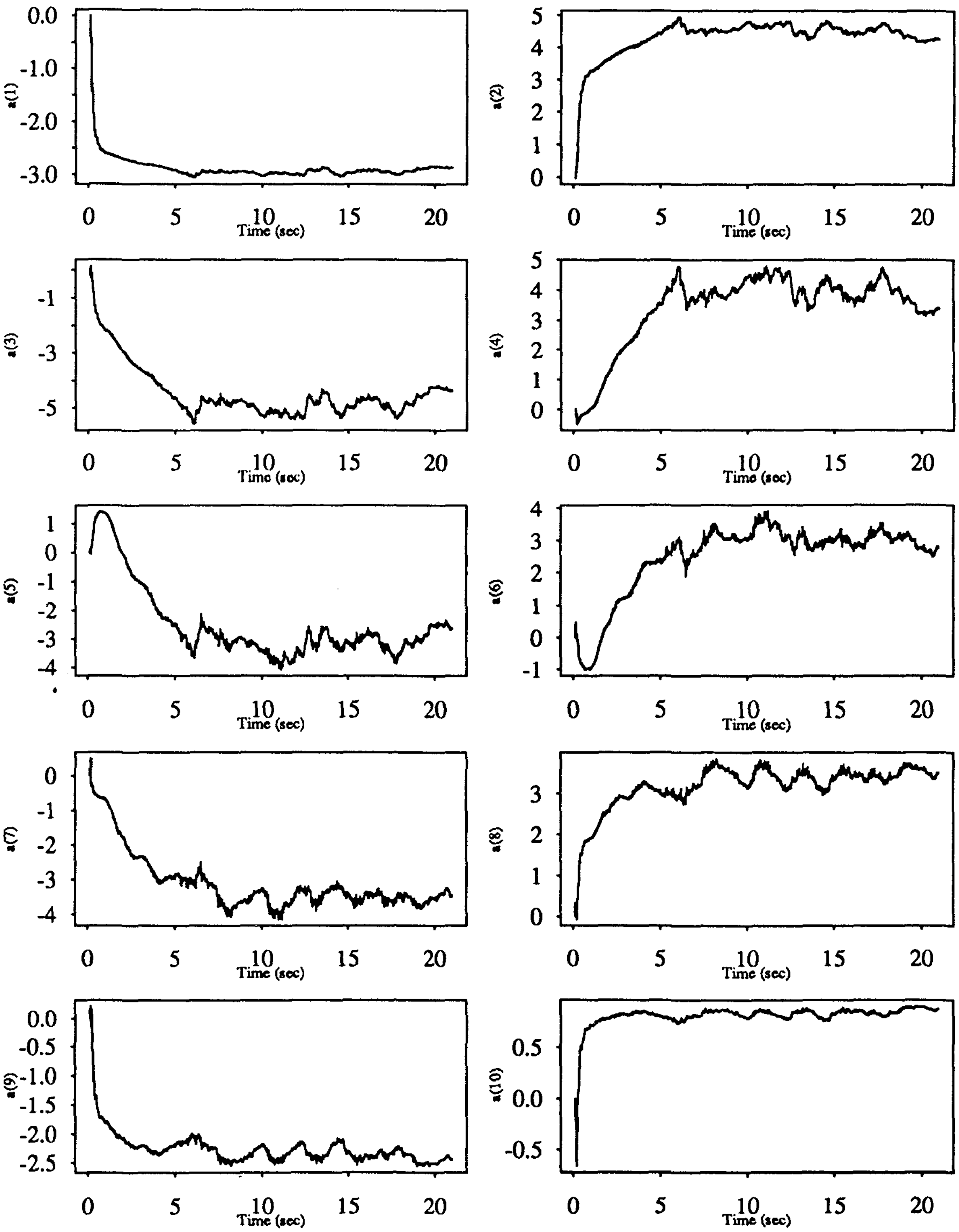


**Figure 5.48**

## Recursive Least Squares Estimation
## Five Story Building Model; El-Centro Input

1st Floor alpha=0.99

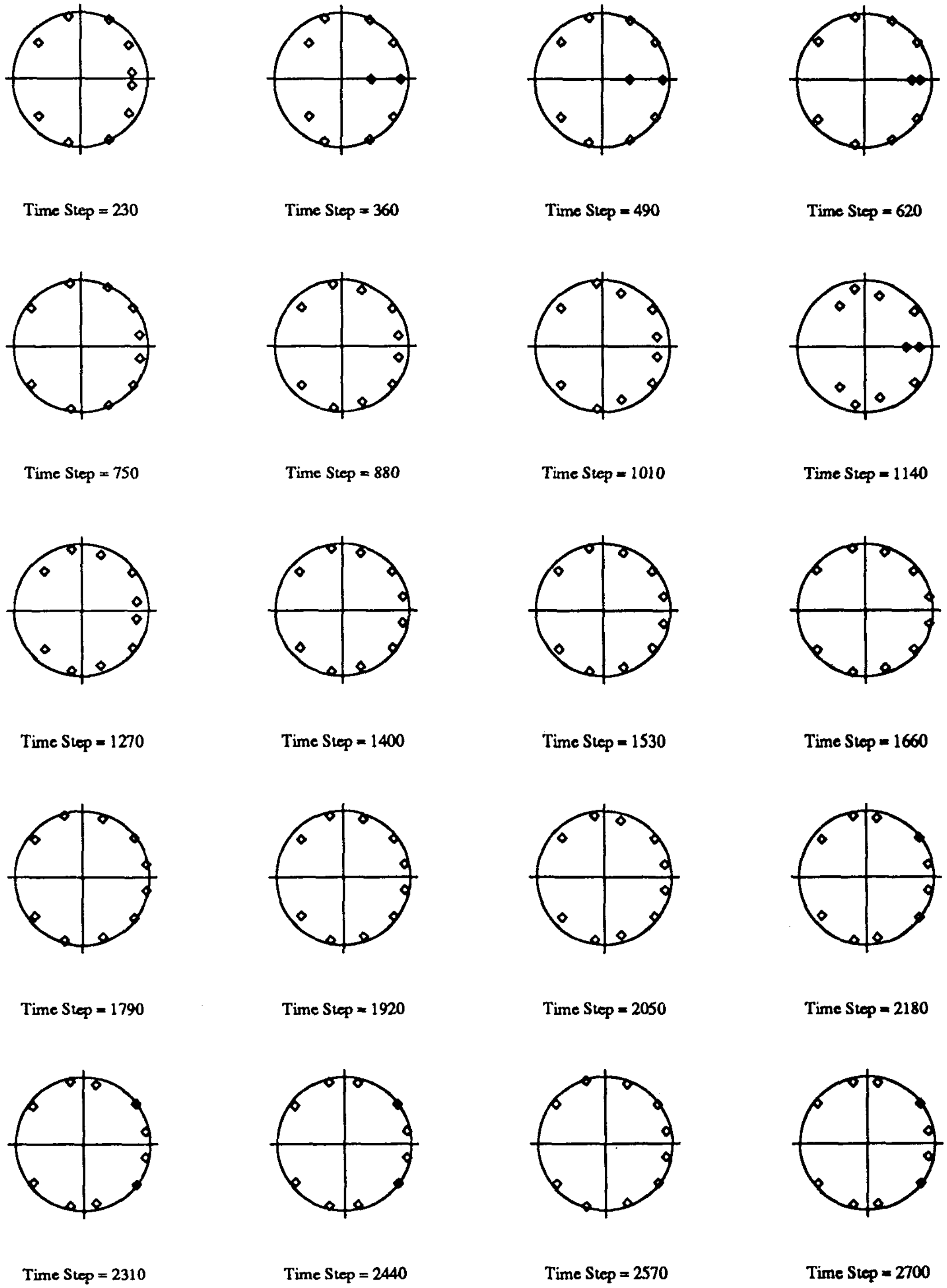


Figure 5.49

Recursive Least Squares Estimation
Five Story Building Model; El-Centro Input
2nd Floor alpha=0.99

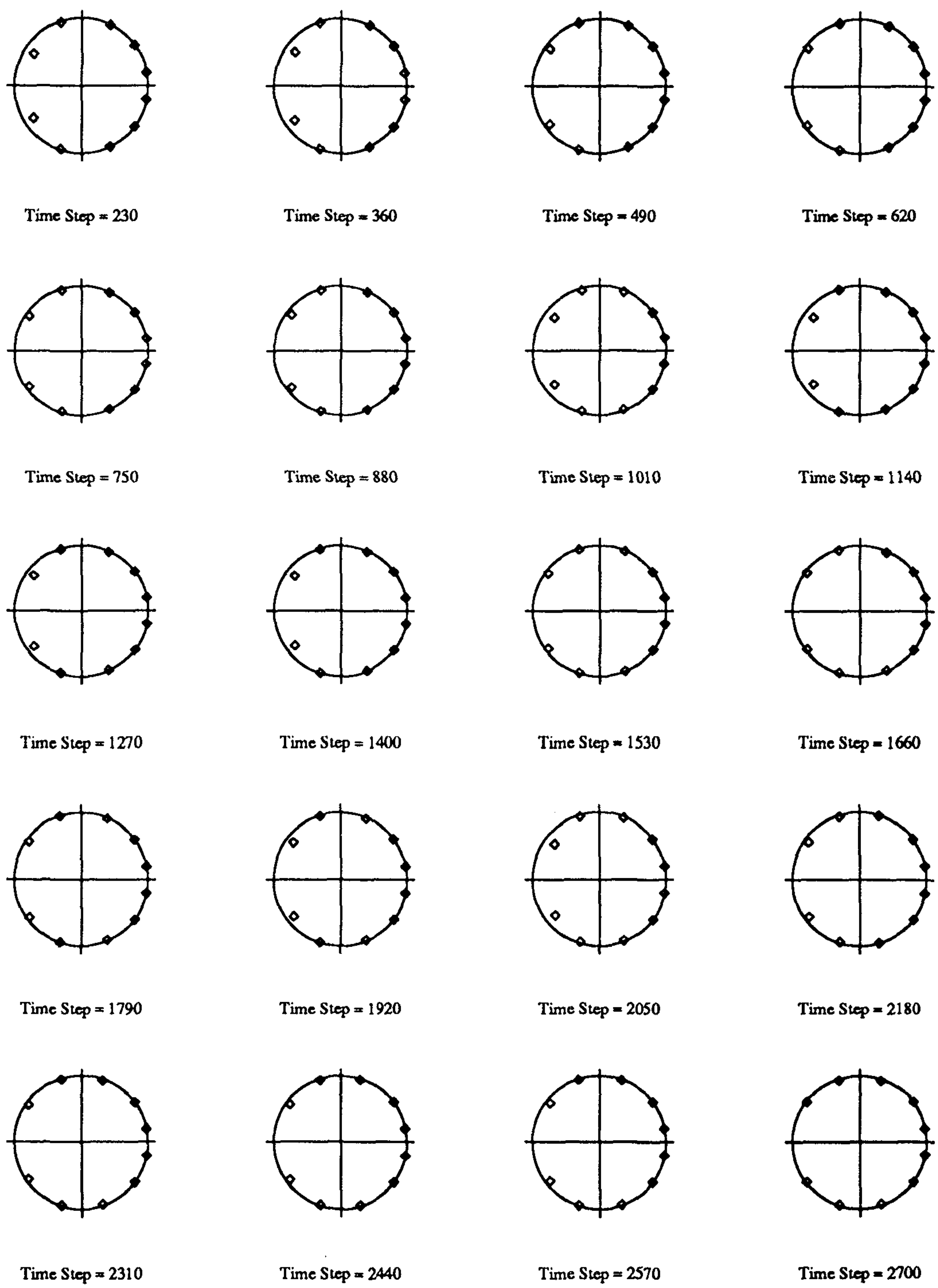


Figure 5.50

# Recursive Least Squares Estimation
## Five Story Building Model; El-Centro Input
3rd Floor alpha=0.99

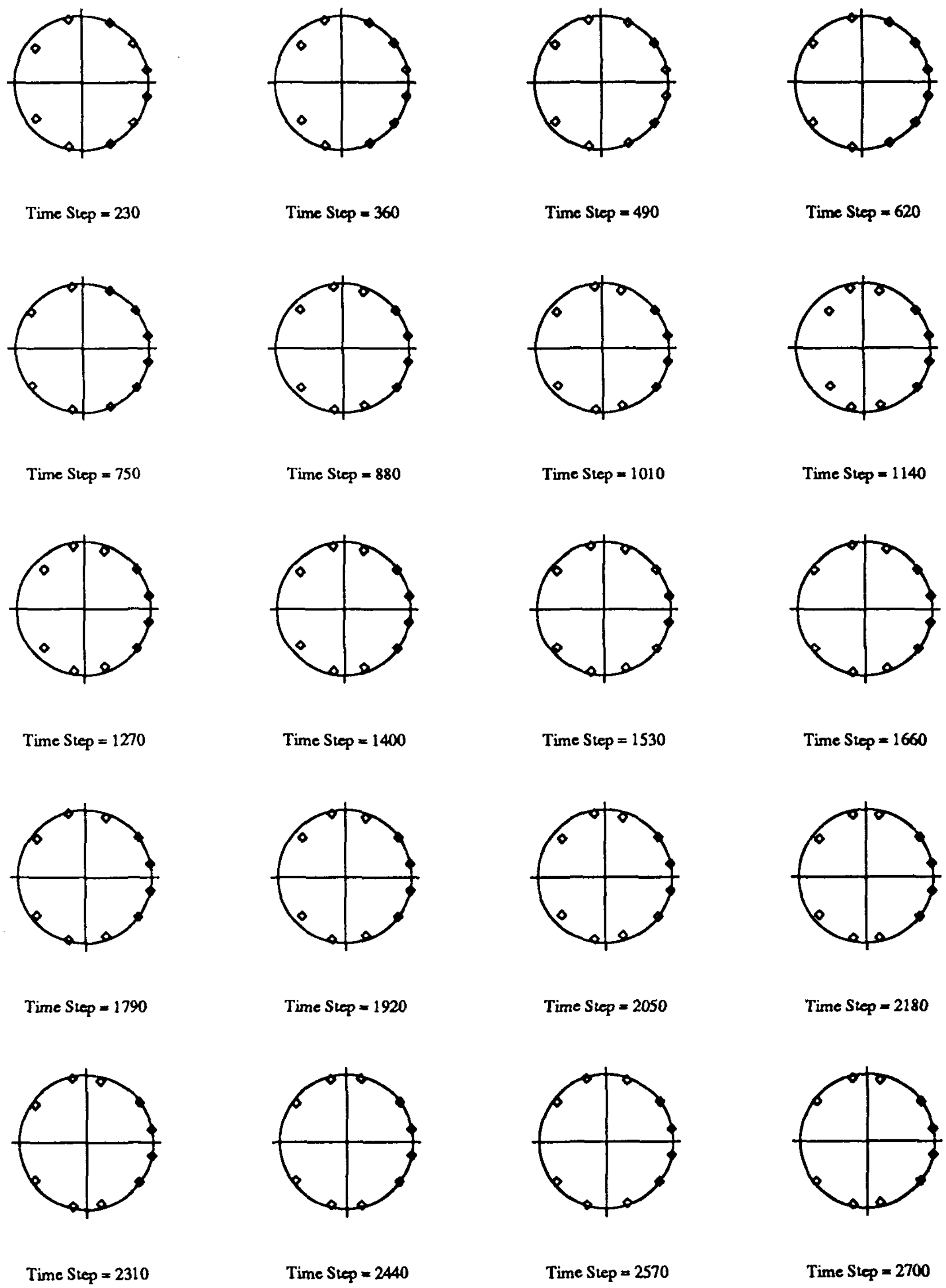


Figure 5.51

Recursive Least Squares Estimation
Five Story Building Model; El-Centro Input
4th Floor alpha=0.99

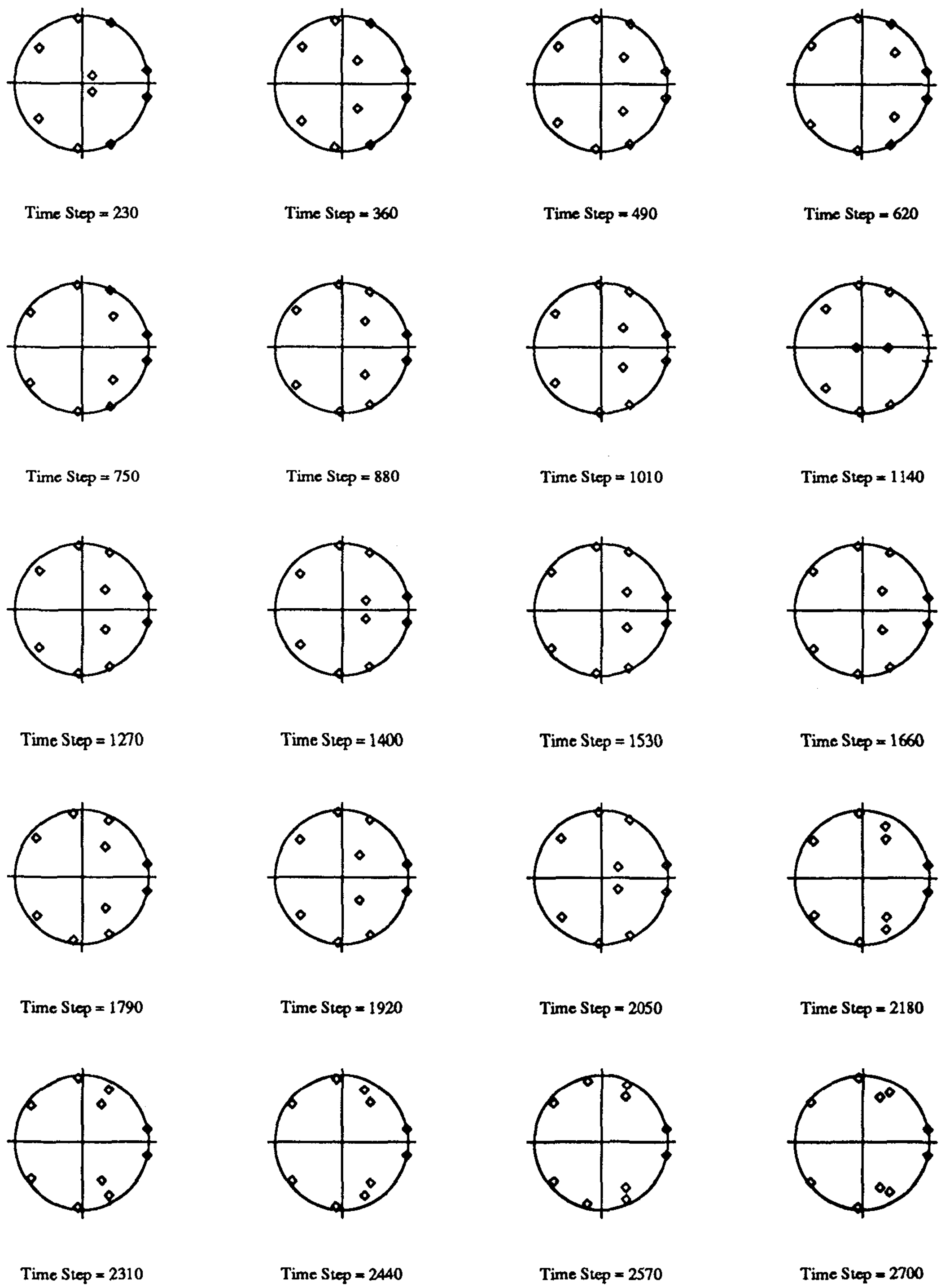


Figure 5.52

Recursive Least Squares Estimation
Five Story Building Model; El-Centro Input
5th Floor alpha=0.99

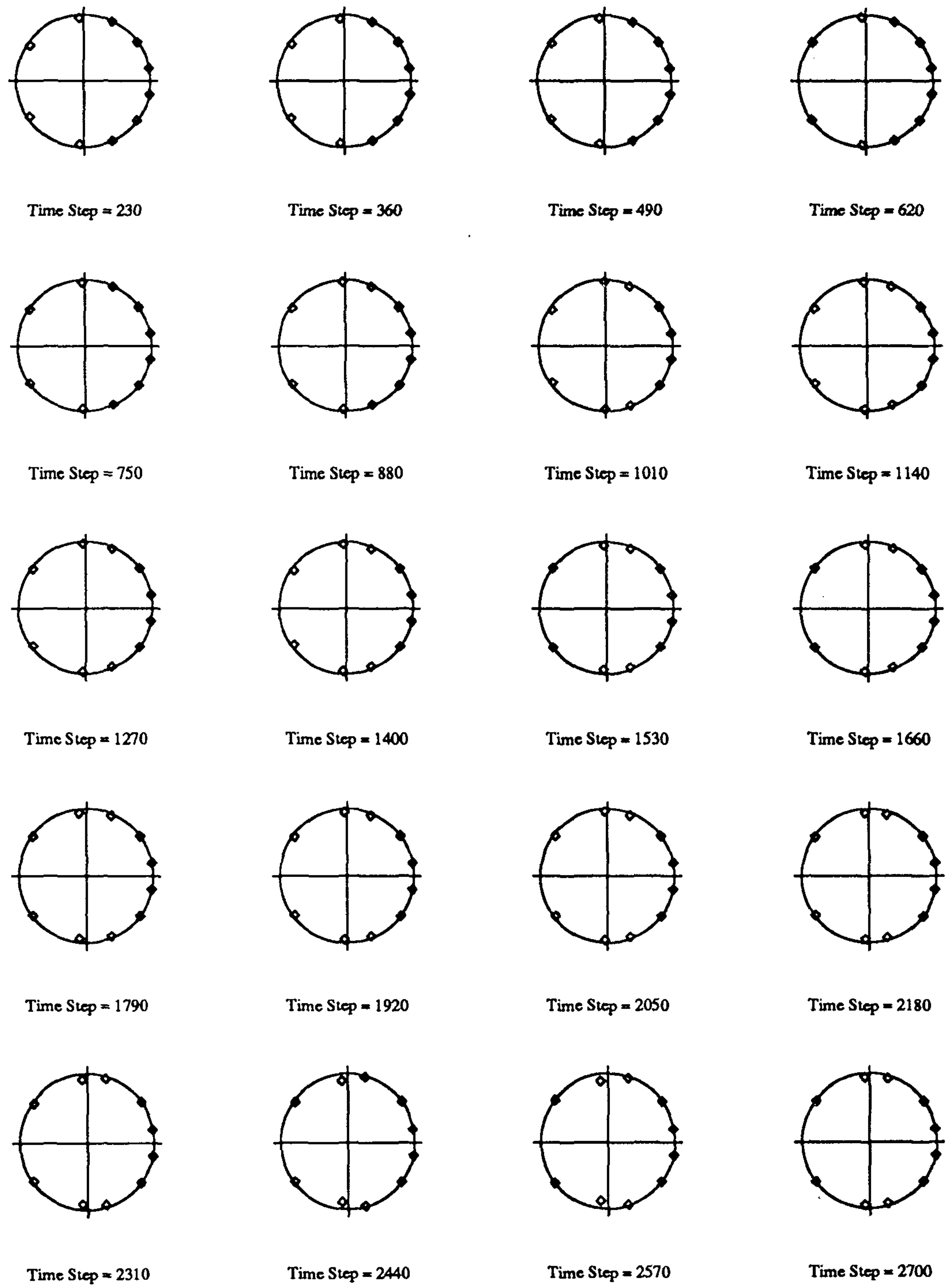


Figure 5.53

Recursive Least Squares Estimation

Five Story Building Model; White Noise Input

1st Floor alpha=0.99

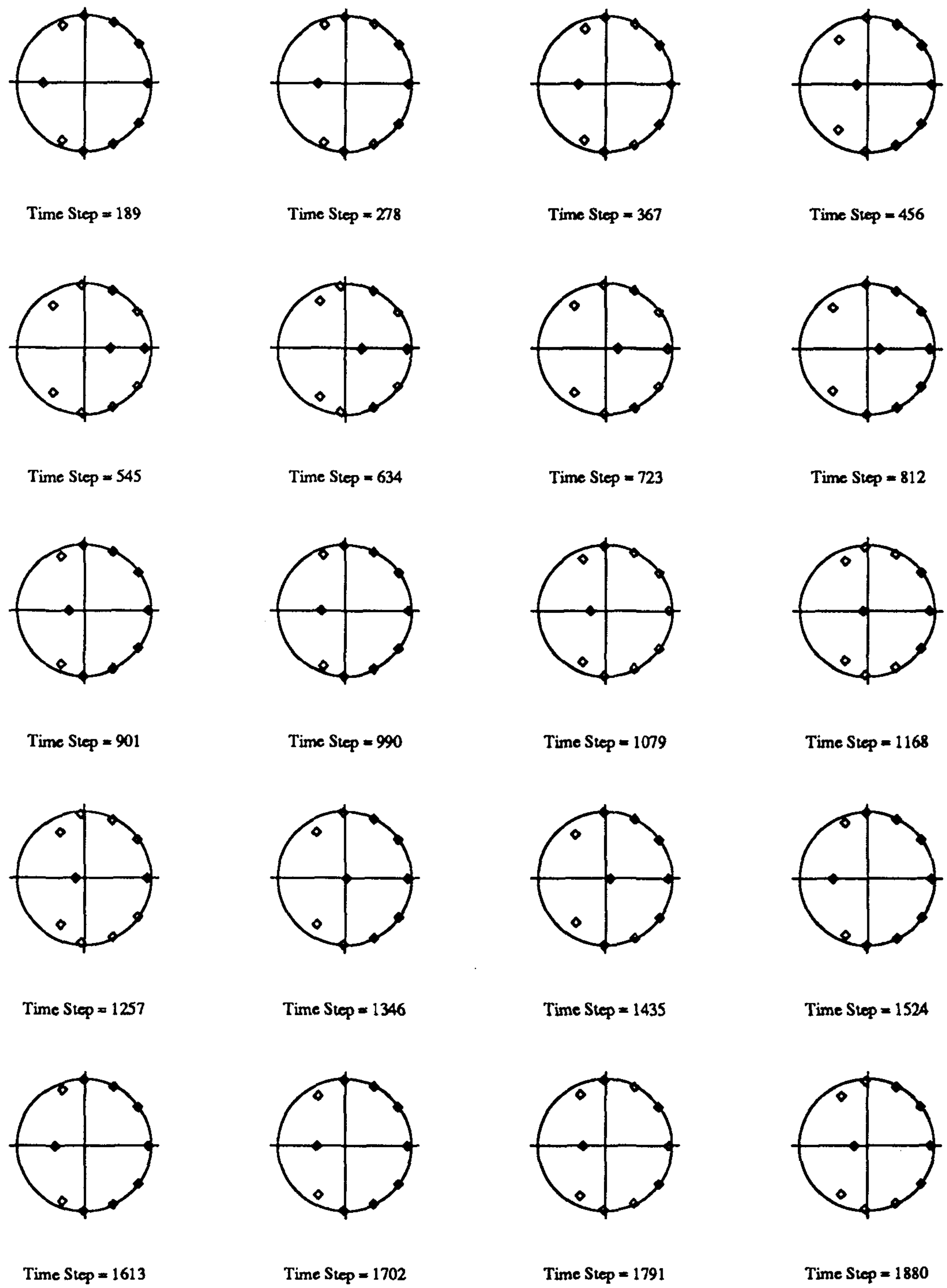


Figure 5.54

Recursive Least Squares Estimation
Five Story Building Model; White Noise Input
2nd Floor alpha=0.99

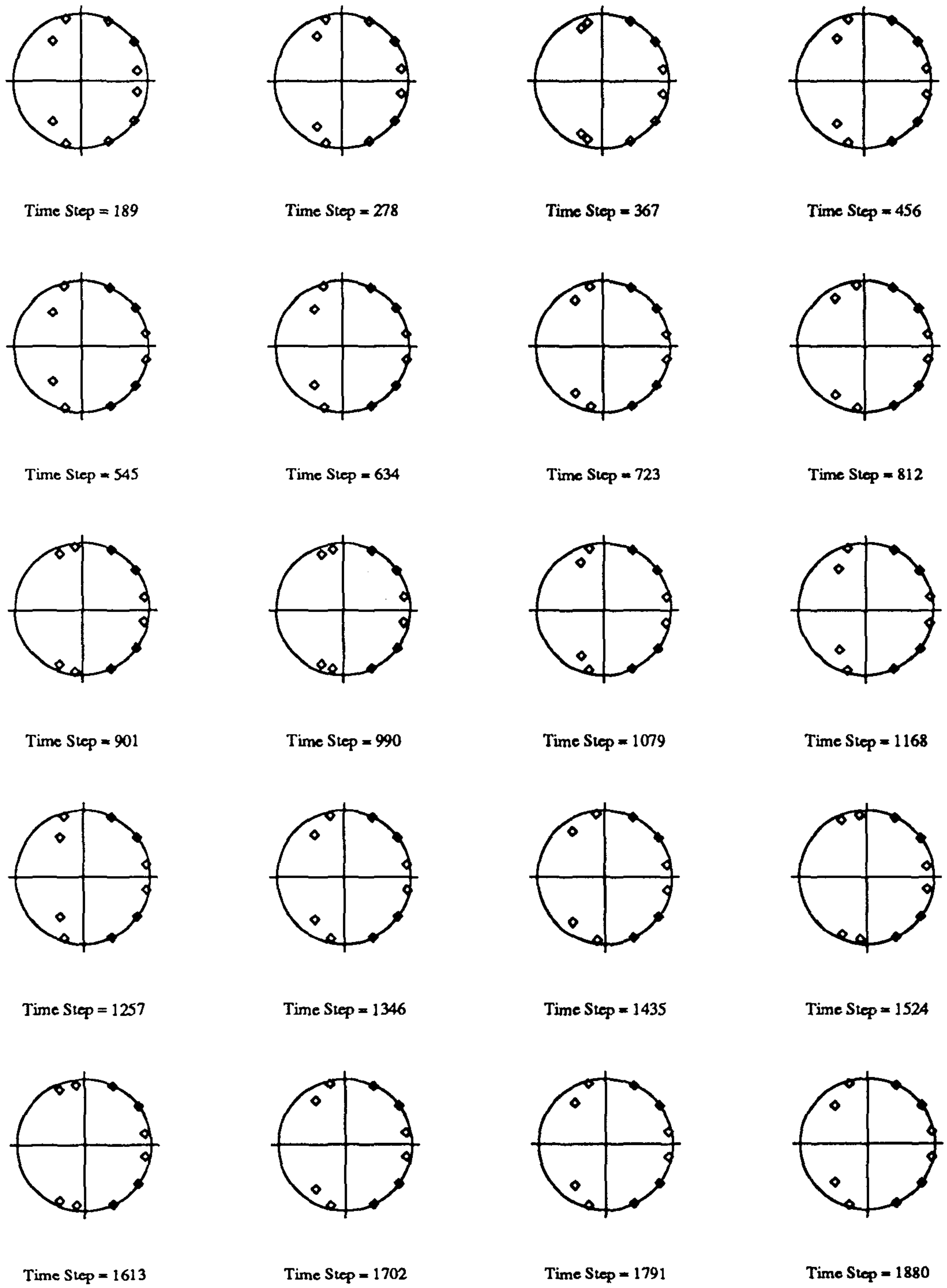


Figure 5.55

## Recursive Least Squares Estimation
## Five Story Building Model; White Noise Input
3rd Floor alpha=0.99

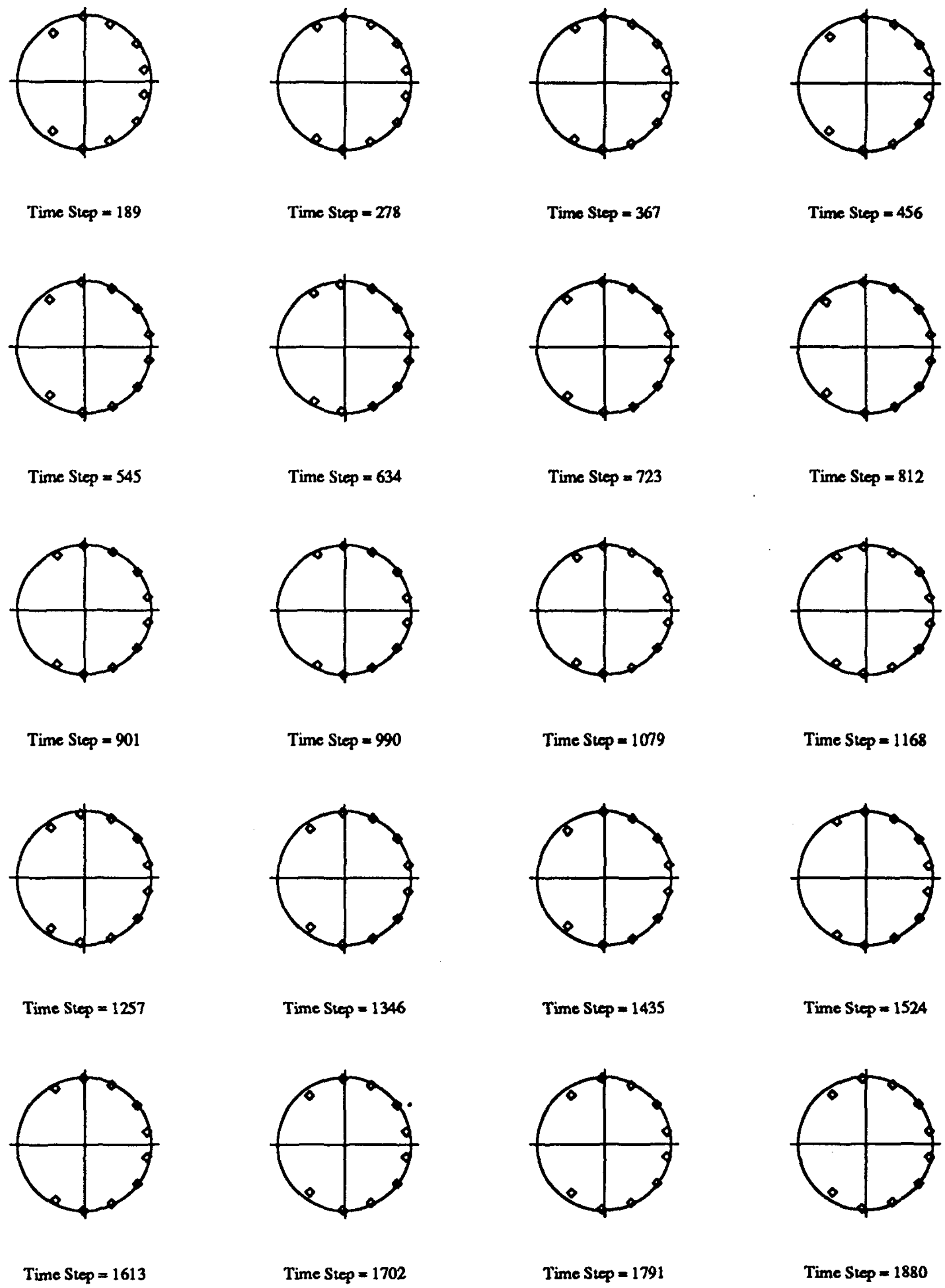


Figure 5.56

## Recursive Least Squares Estimation
## Five Story Building Model; White Noise Input
### 4th Floor alpha=0.99

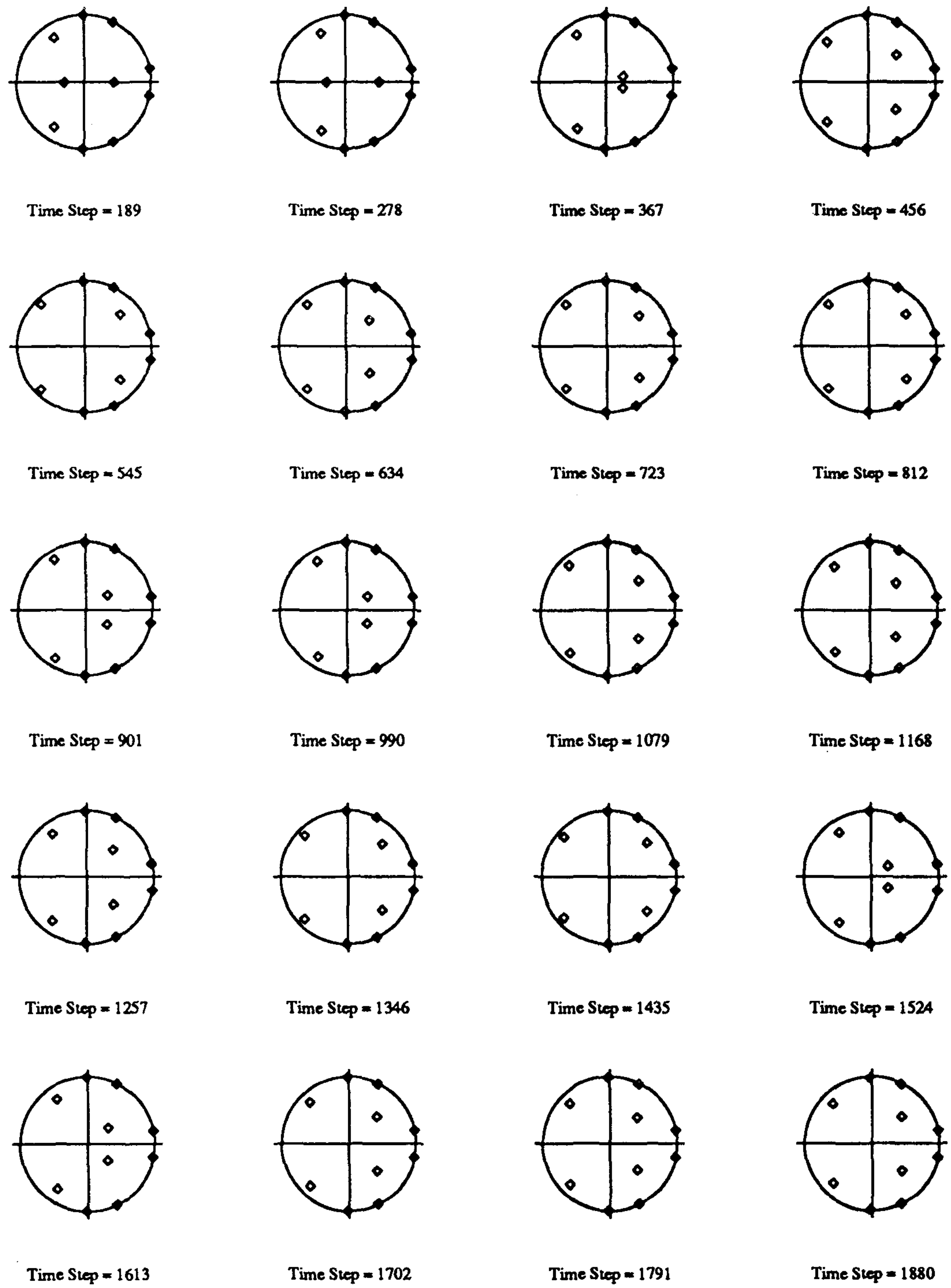


Figure 5.57

## Recursive Least Squares Estimation
## Five Story Building Model; White Noise Input

5th Floor alpha=0.99

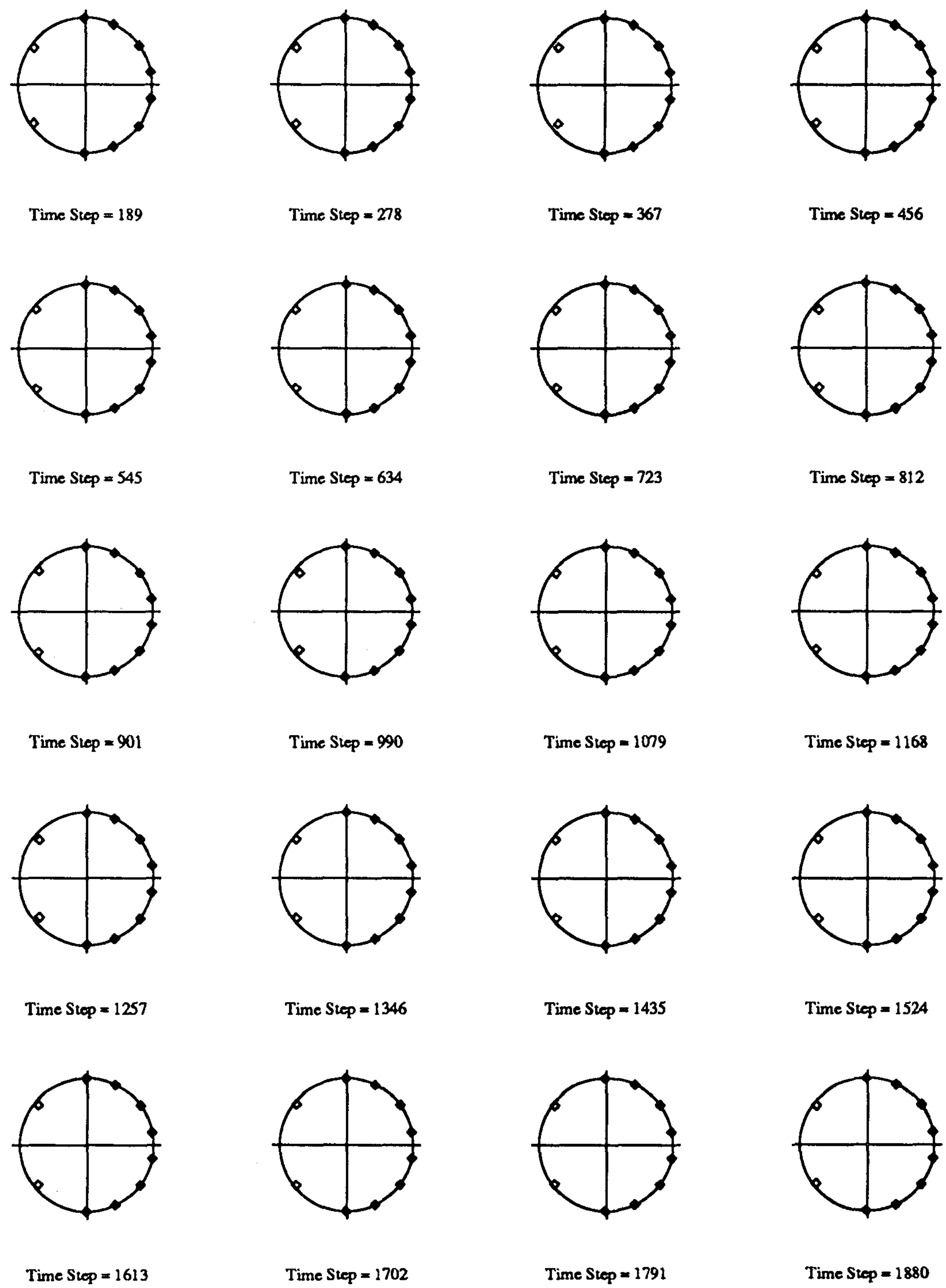


Figure 5.58

Recursive Least Squares Estimation
Three Story Building Model; El-Centro Input
1st Floor alpha=0.99

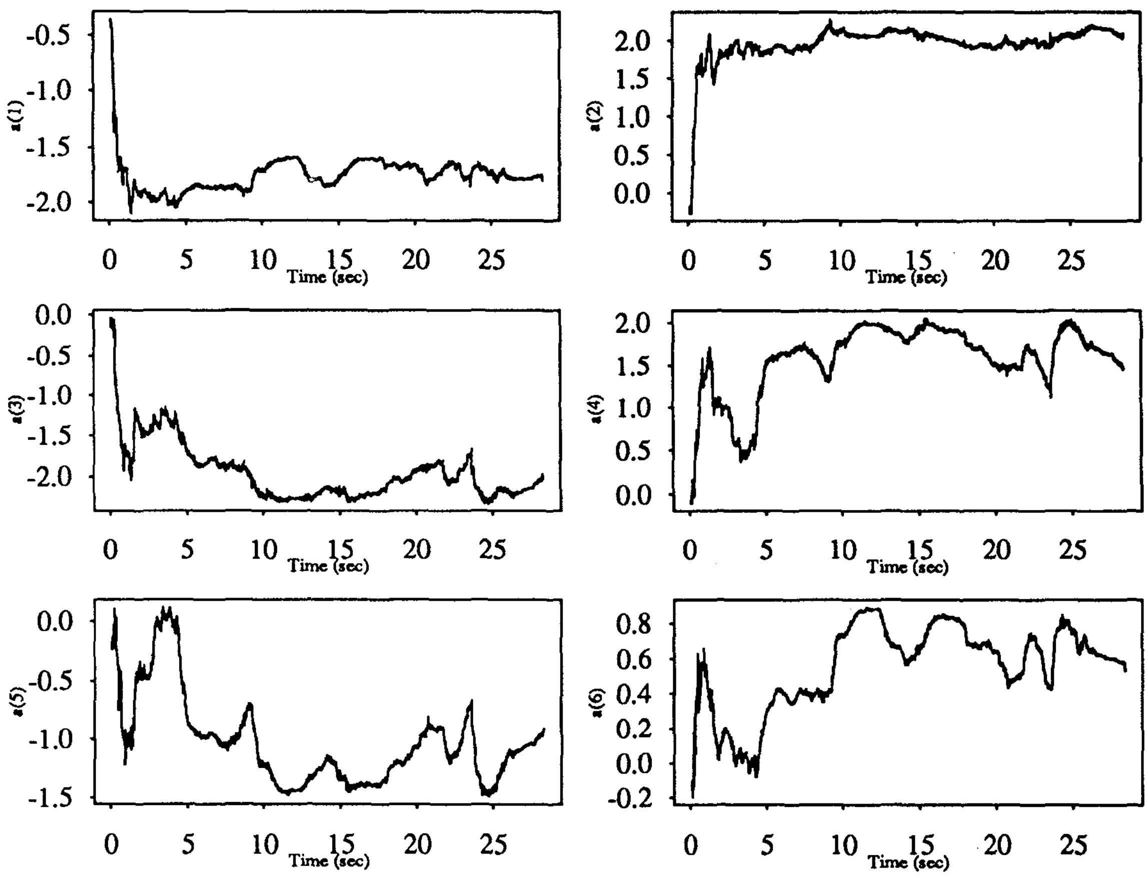


Figure 5.59

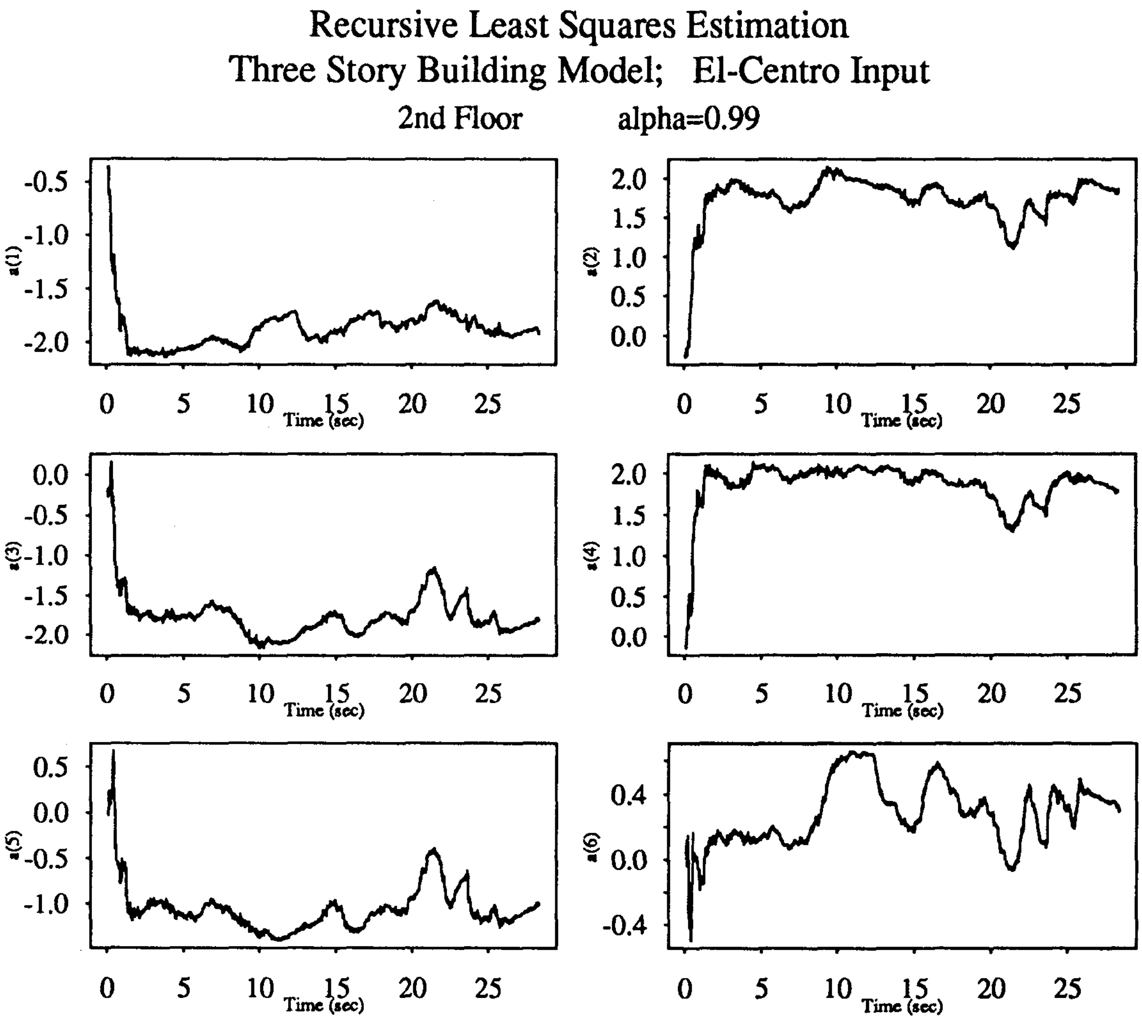
Recursive Least Squares Estimation
Three Story Building Model; El-Centro Input
2nd Floor alpha=0.99
a(1)
a(2)
a(3)
a(4)
a(5)
a(6)
Time (sec)

Figure 5.60

Recursive Least Squares Estimation
Three Story Building Model; El-Centro Input
3rd Floor alpha=0.99

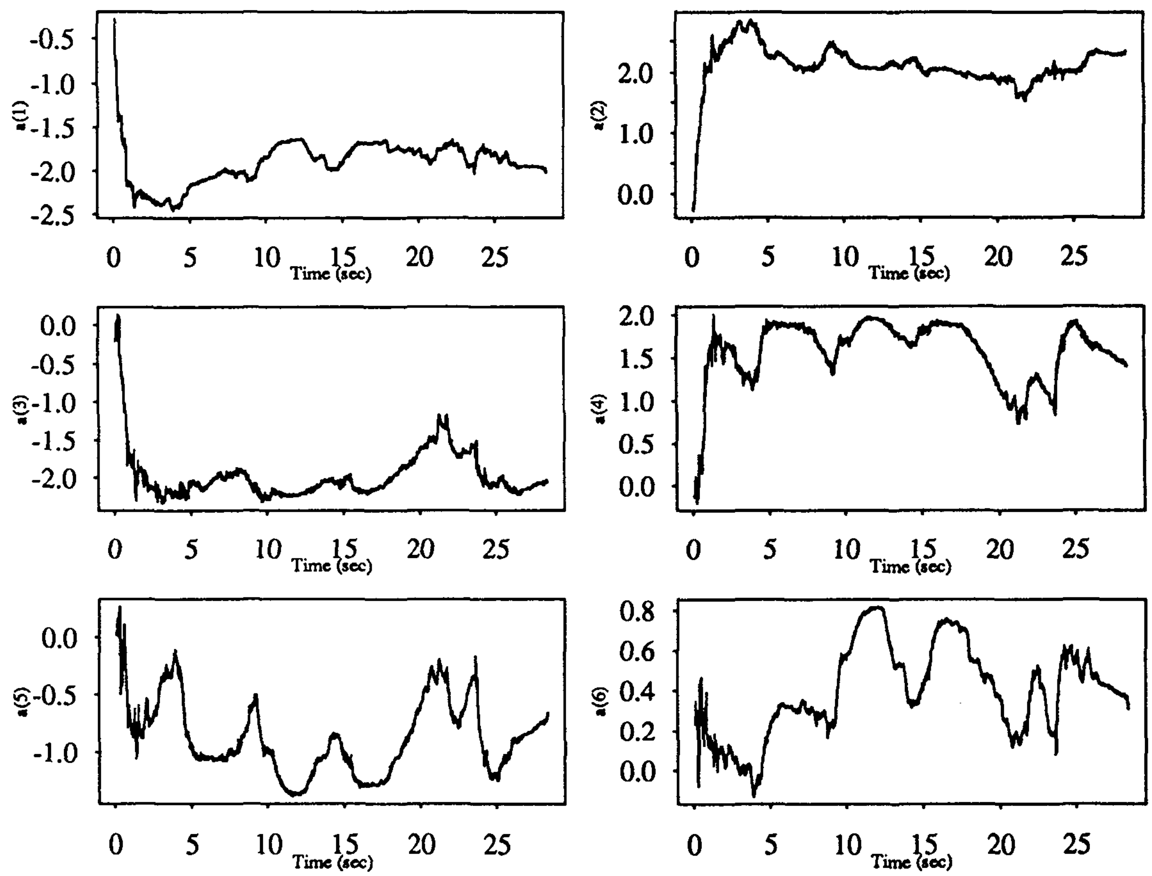


Figure 5.61

Recursive Least Squares Estimation
Three Story Building Model; Sine Sweep Input
1st Floor alpha=0.99

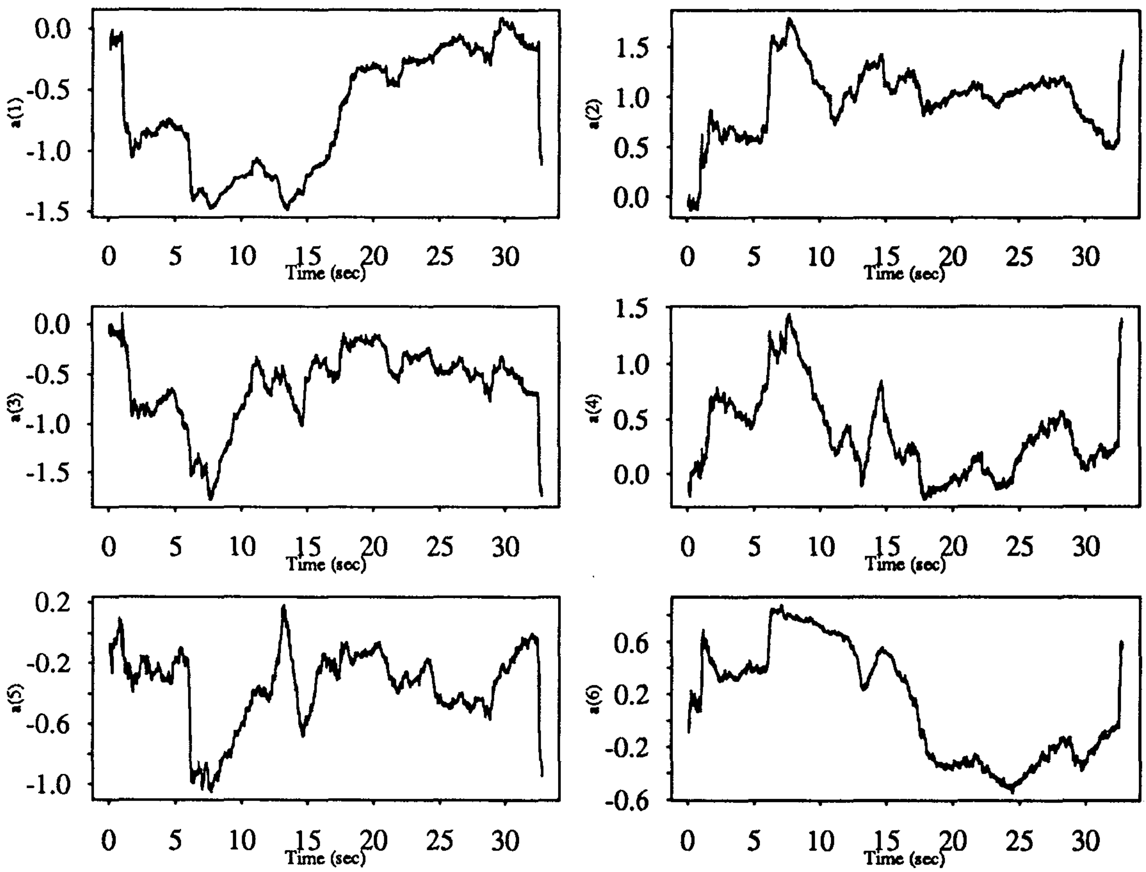


Figure 5.62

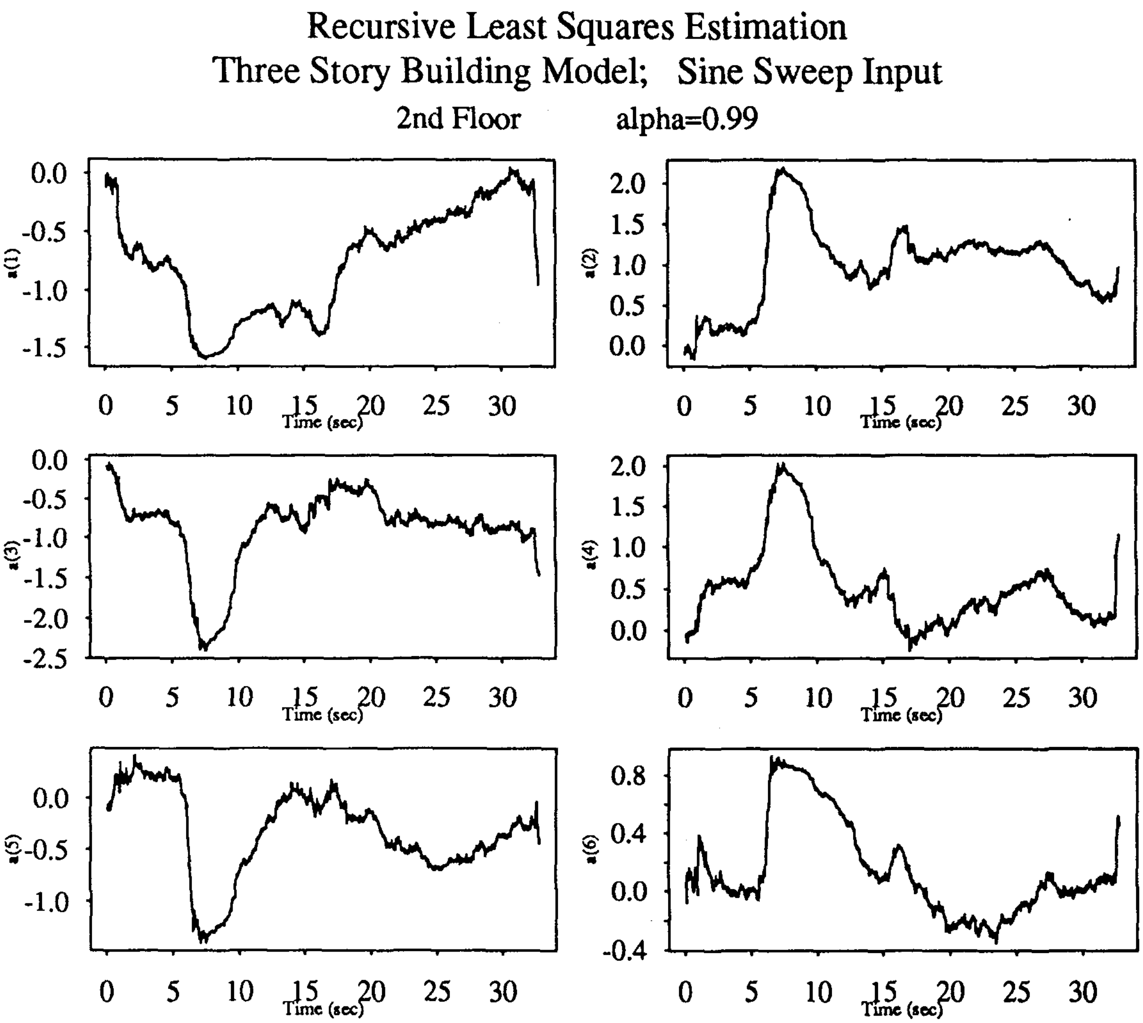
Recursive Least Squares Estimation
Three Story Building Model; Sine Sweep Input
2nd Floor alpha=0.99
a(1)
a(2)
a(3)
a(4)
a(5)
a(6)
Time (sec)

Figure 5.63

# Recursive Least Squares Estimation
## Three Story Building Model; Sine Sweep Input
3rd Floor alpha=0.99

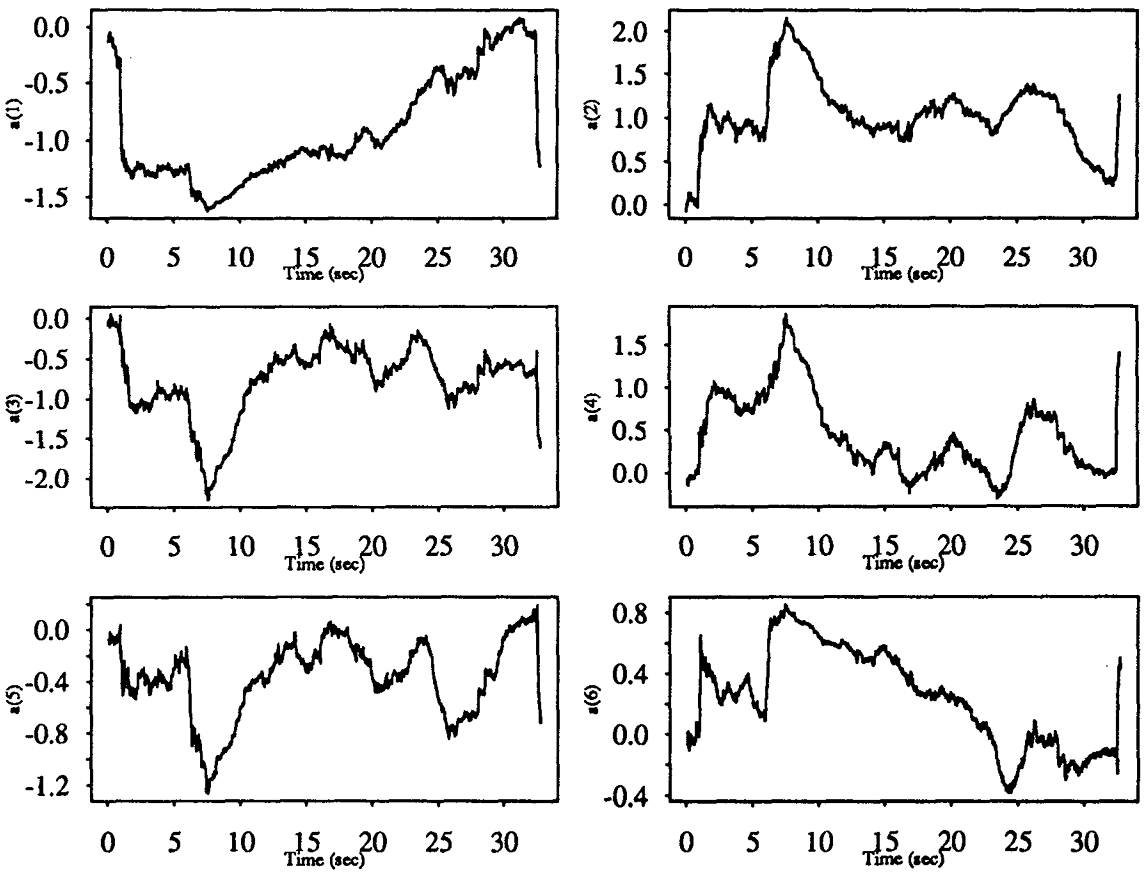


Figure 5.64

Recursive Least Squares Estimation
Three Story Building Model; White Noise Input
1st Floor alpha=0.99

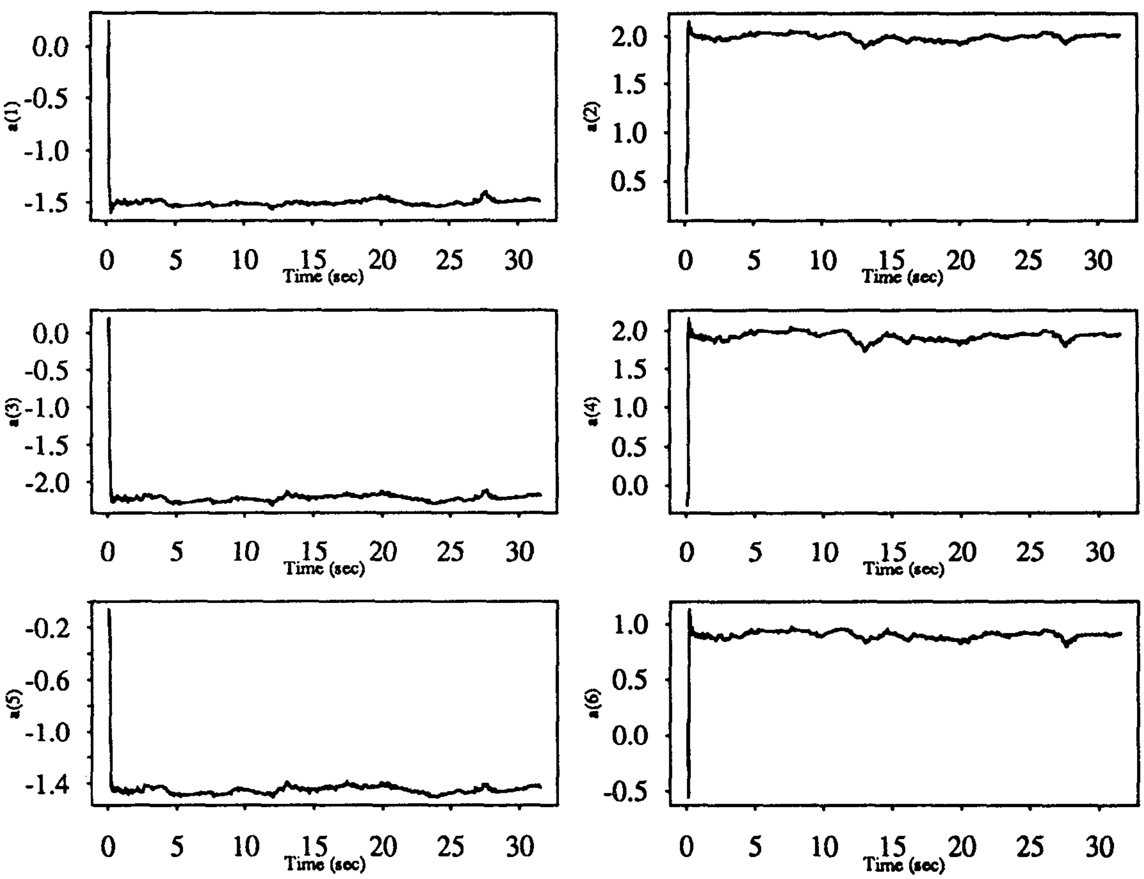


Figure 5.65

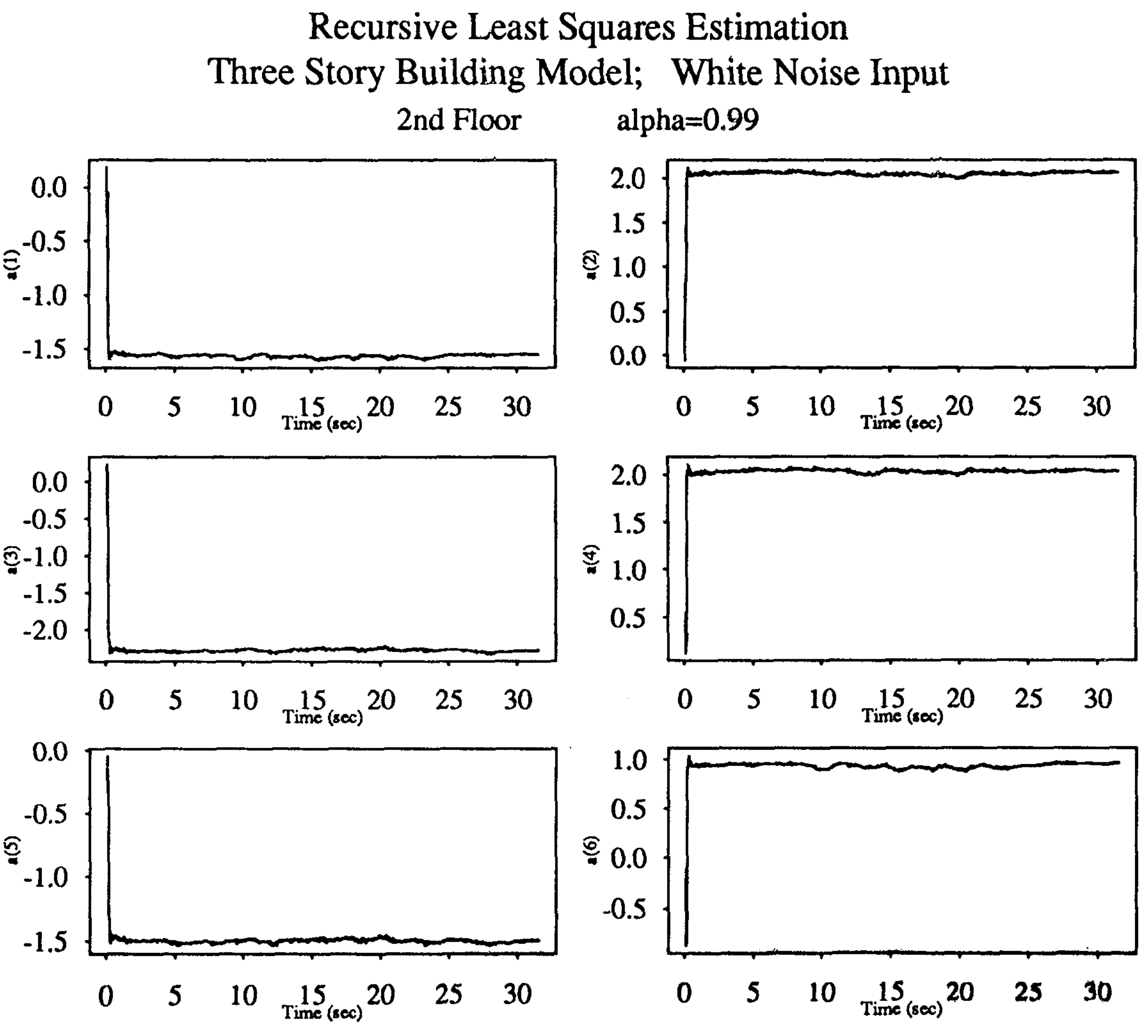
Recursive Least Squares Estimation
Three Story Building Model; White Noise Input
2nd Floor
alpha=0.99
a(1)
a(2)
a(3)
a(4)
a(5)
a(6)
Time (sec)

Figure 5.66

Recursive Least Squares Estimation
Three Story Building Model; White Noise Input
3rd Floor alpha=0.99

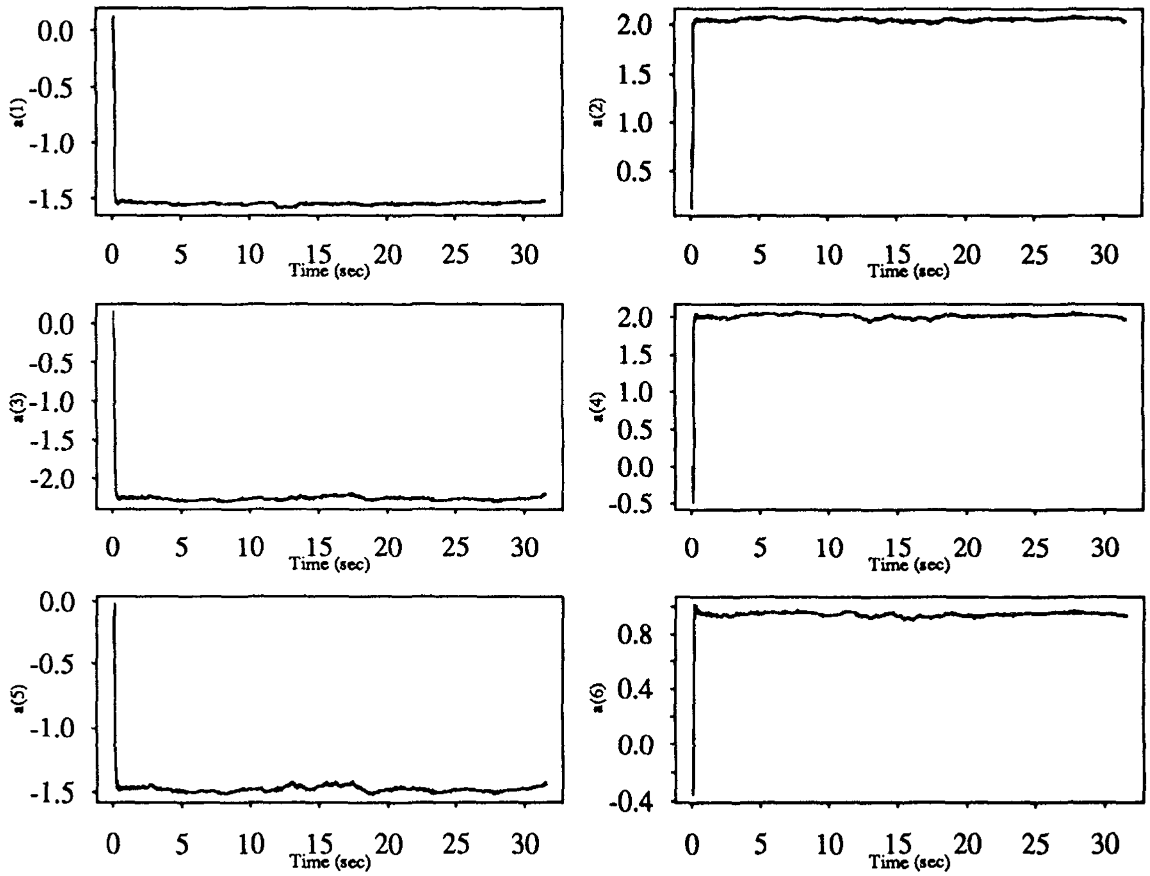


Figure 5.67

Recursive Least Squares Estimation
Three Story Building Model;   El-Centro Input
1st Floor          alpha=0.99

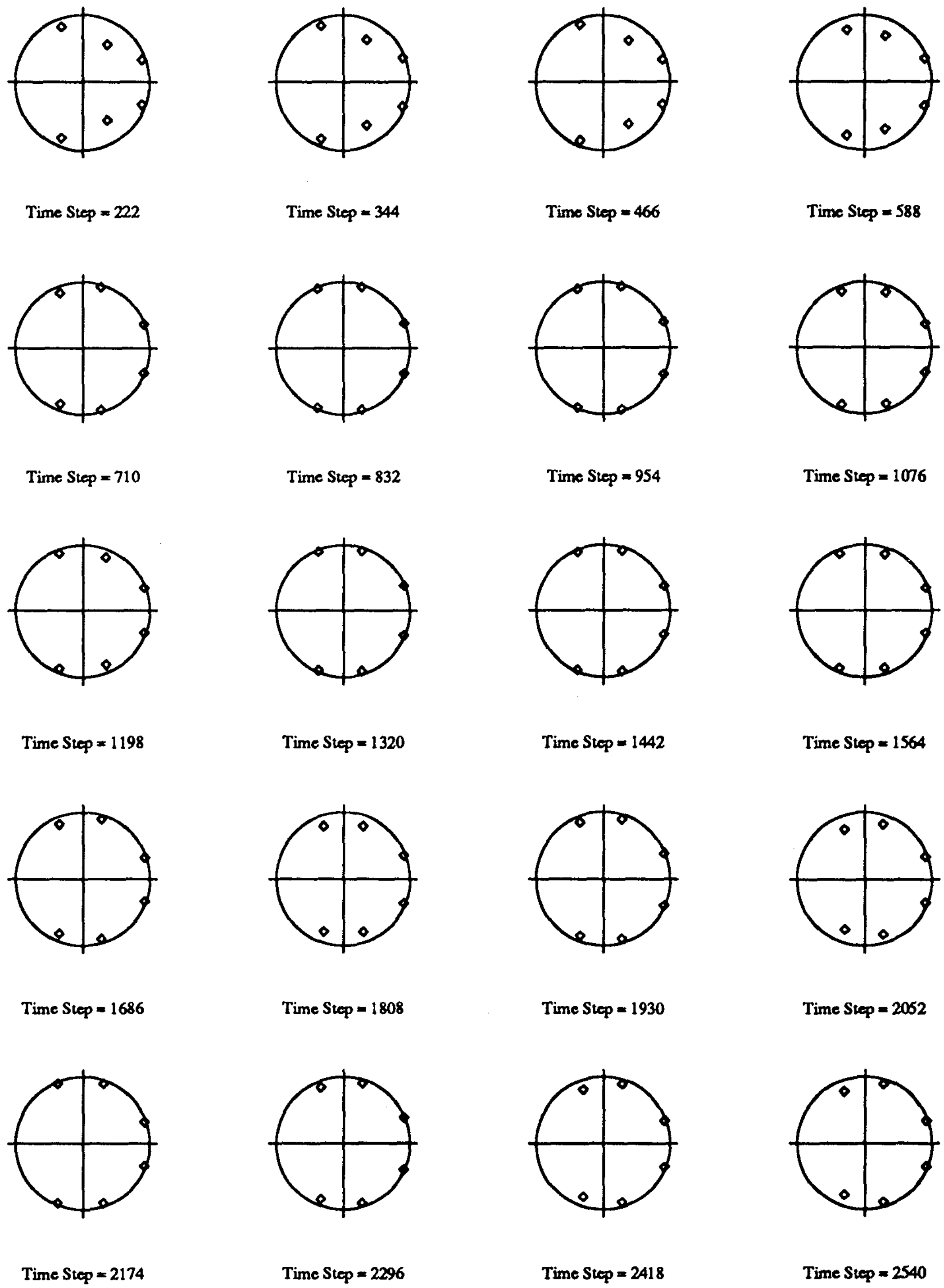


**Figure 5.68**

## Recursive Least Squares Estimation
## Three Story Building Model; El-Centro Input
2nd Floor alpha=0.99

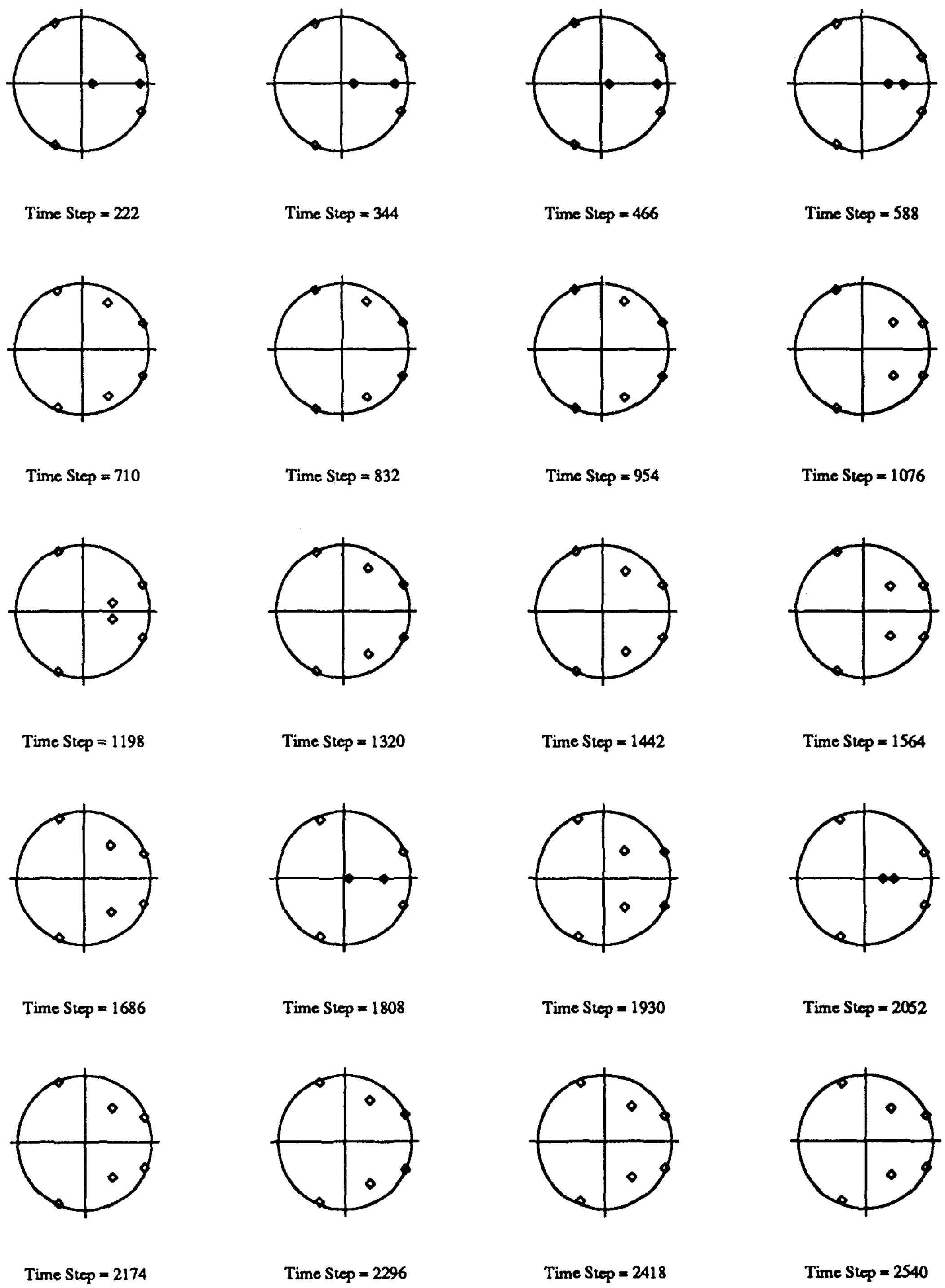


Figure 5.69

Recursive Least Squares Estimation

Three Story Building Model; El-Centro Input

3rd Floor alpha=0.99

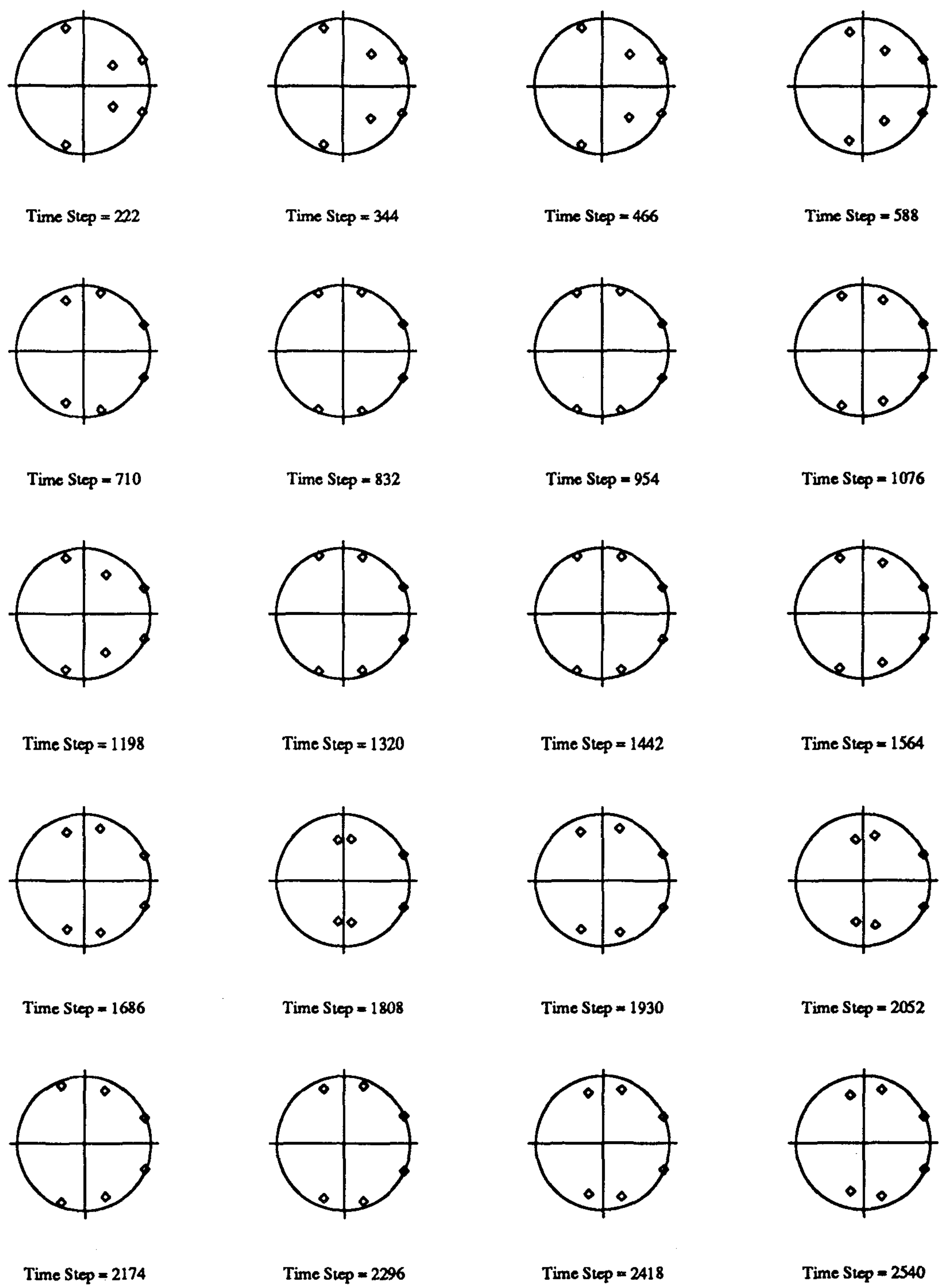


Figure 5.70

Recursive Least Squares Estimation
Three Story Building Model; Sine Sweep Input
1st Floor alpha=0.99

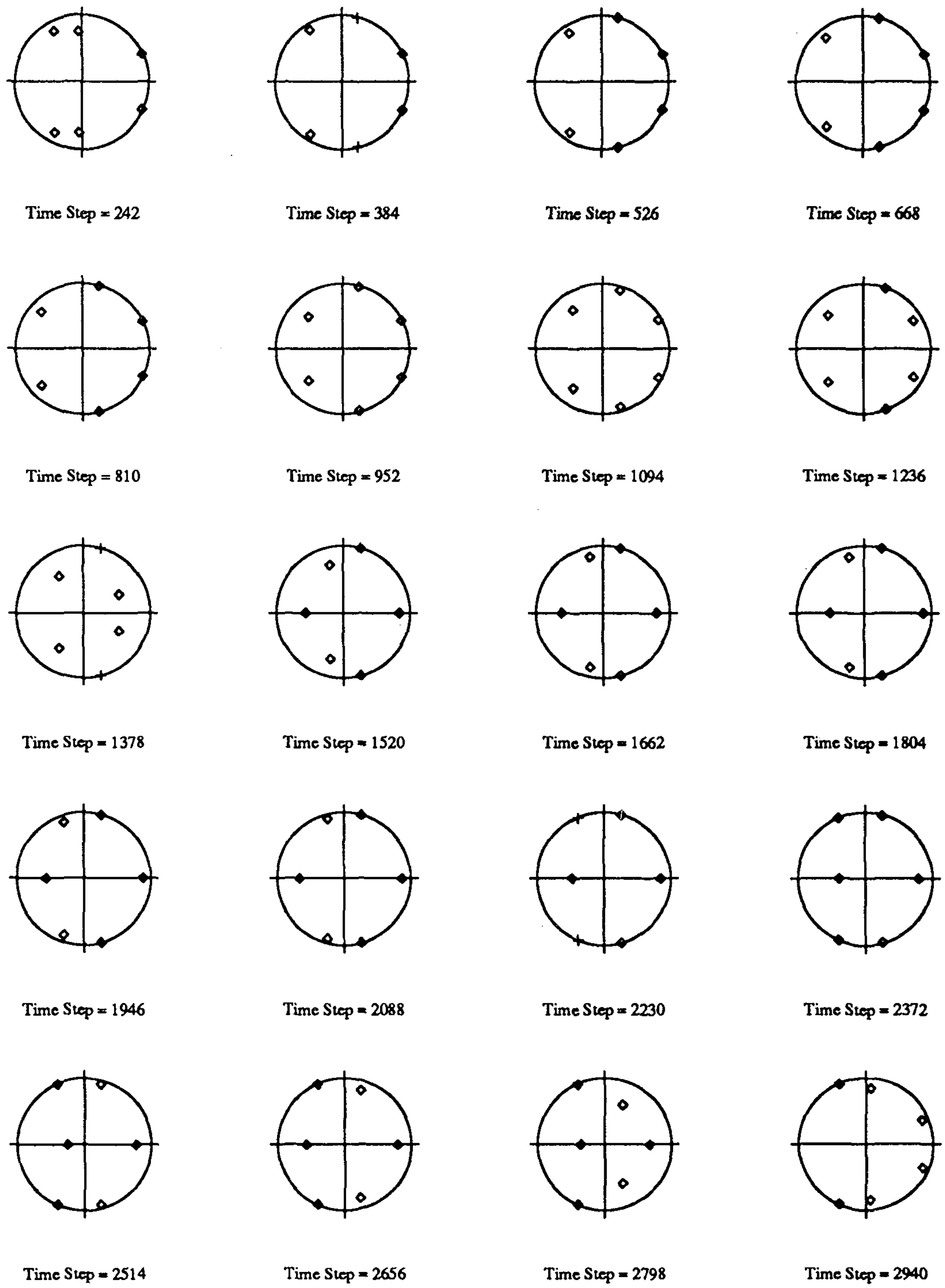


Figure 5.71

## Recursive Least Squares Estimation
## Three Story Building Model; Sine Sweep Input
2nd Floor alpha=0.99

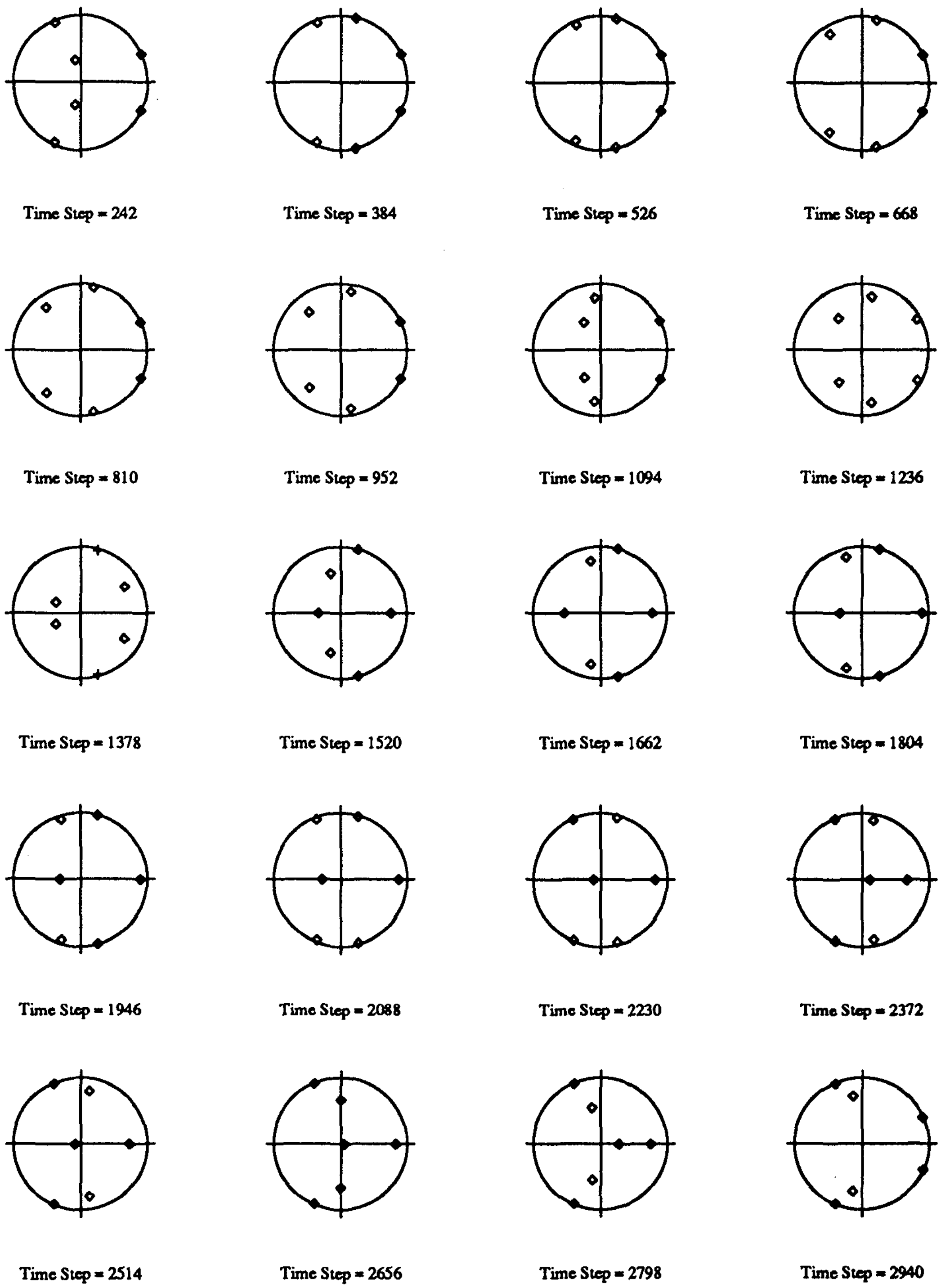


Figure 5.72

# Recursive Least Squares Estimation
## Three Story Building Model; Sine Sweep Input
### 3rd Floor alpha=0.99

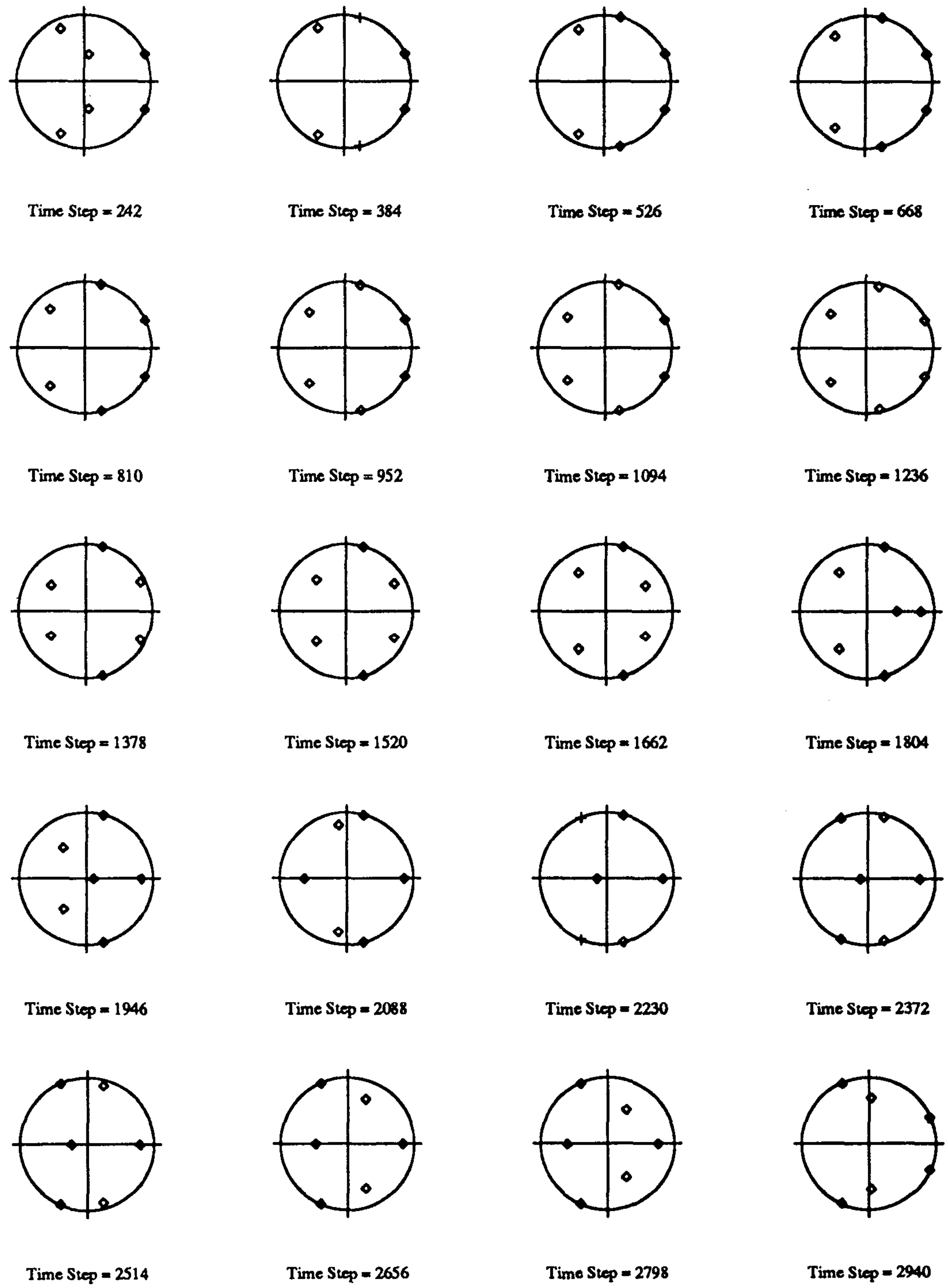


Figure 5.73

Recursive Least Squares Estimation
Three Story Building Model; White Noise Input
1st Floor alpha=0.99

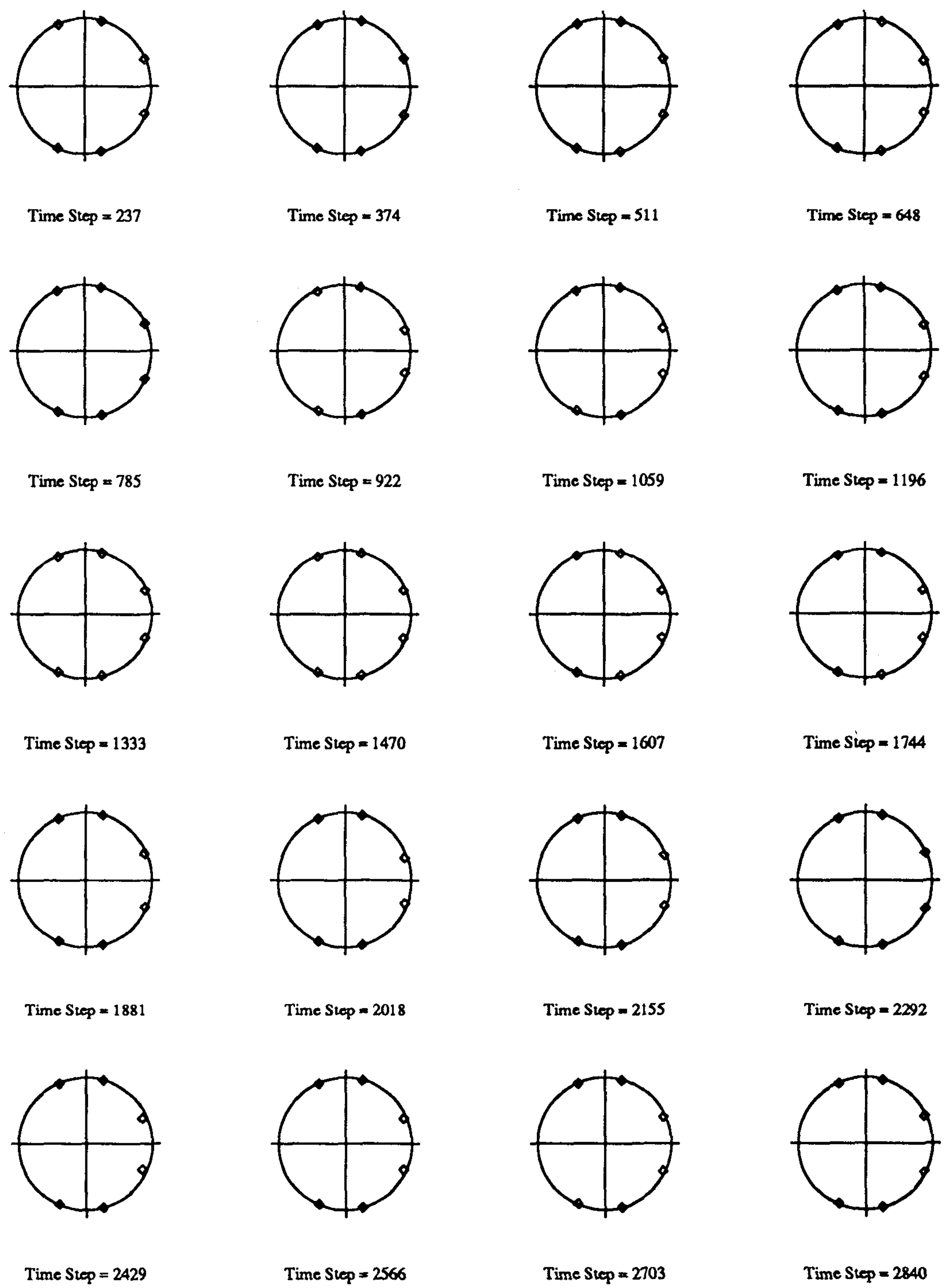


Figure 5.74

## Recursive Least Squares Estimation
## Three Story Building Model; White Noise Input
### 2nd Floor alpha=0.99

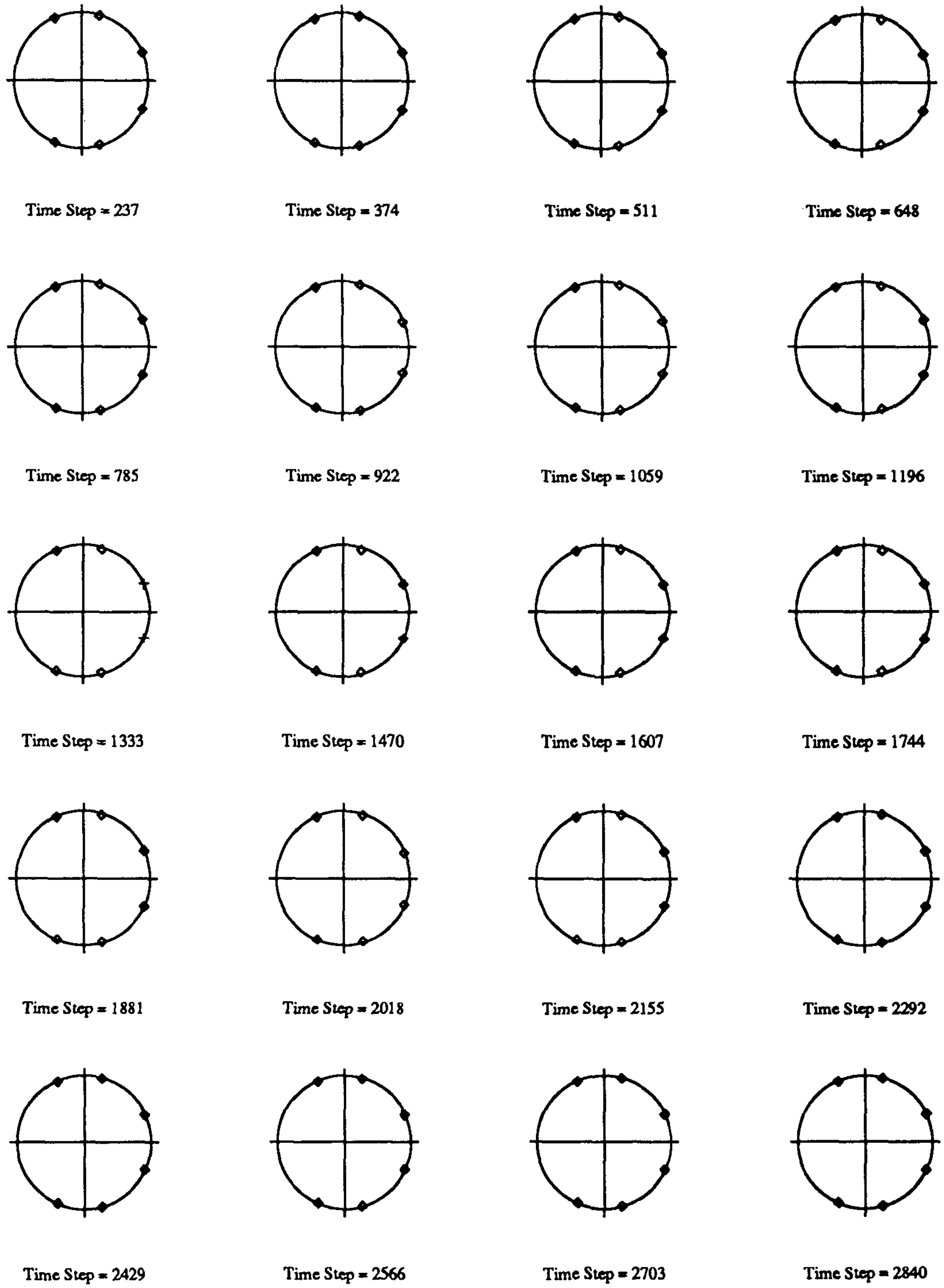


Figure 5.75

# Recursive Least Squares Estimation
## Three Story Building Model; White Noise Input
### 3rd Floor alpha=0.99

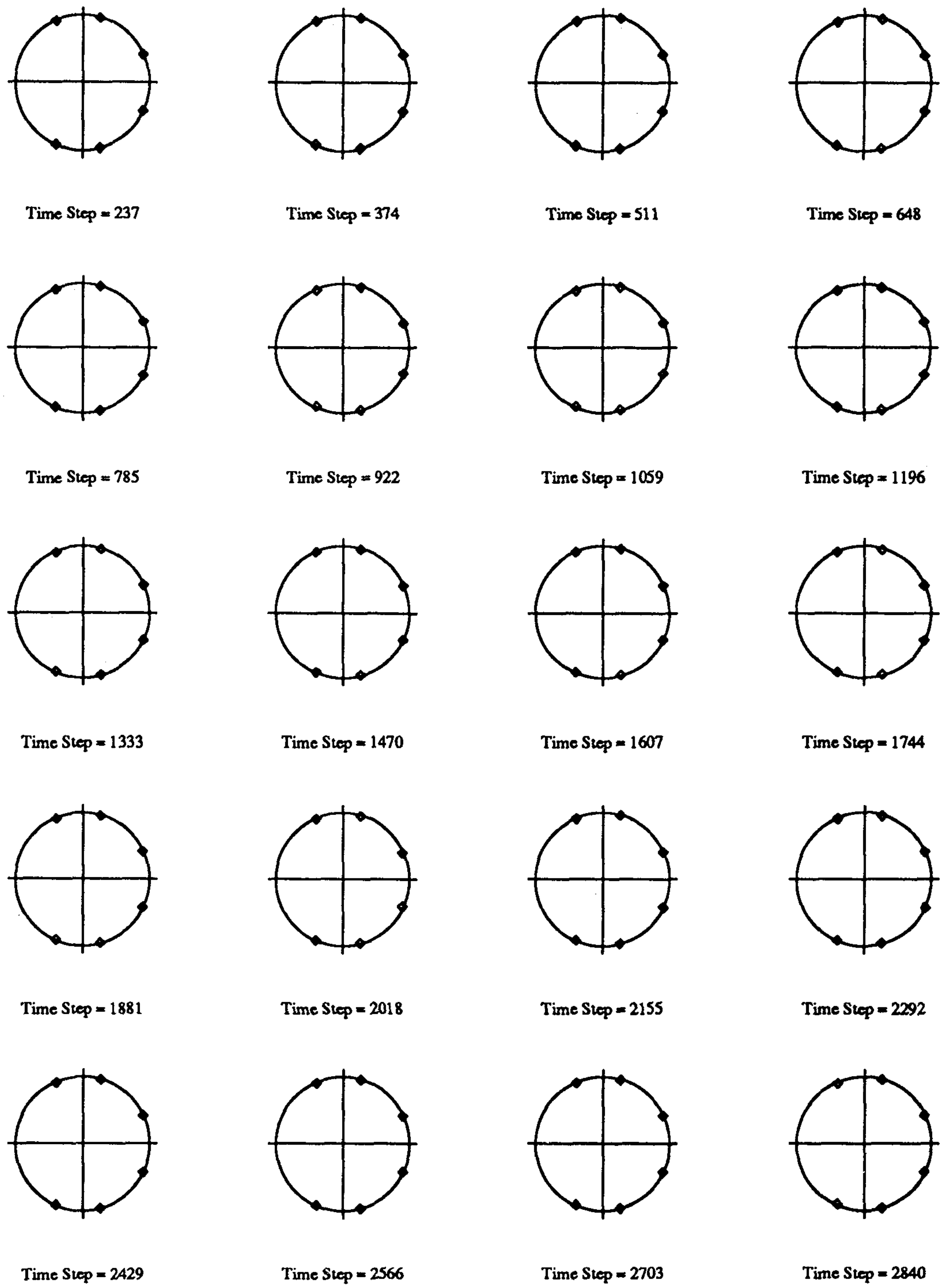


Figure 5.76

Recursive Least Squares Estimation
Five Story Building Model; El-Centro Input
1st Floor variable alpha=0.99

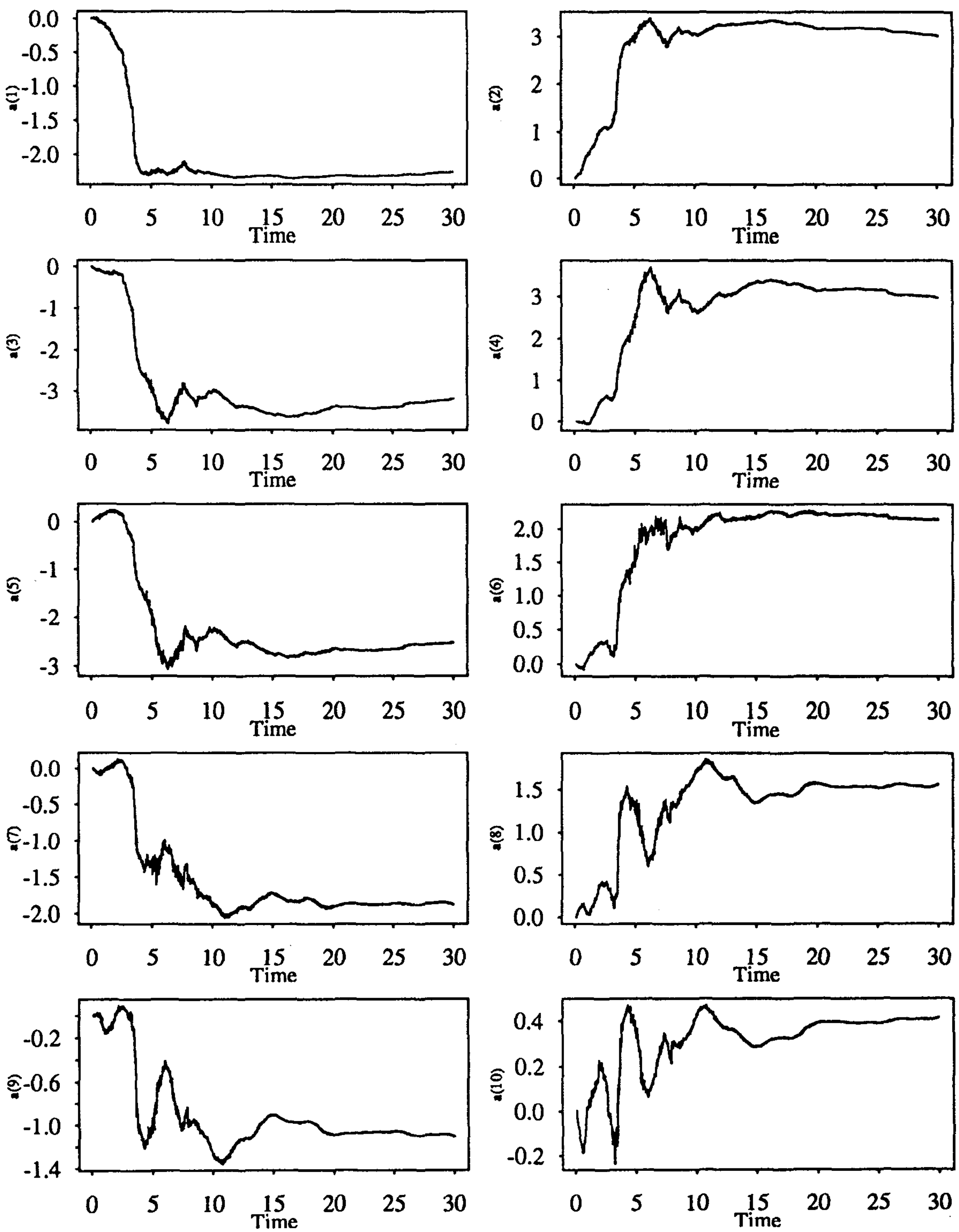


Figure 5.77

## Recursive Least Squares Estimation
## Five Story Building Model; El-Centro Input
### 2nd Floor variable alpha=0.99

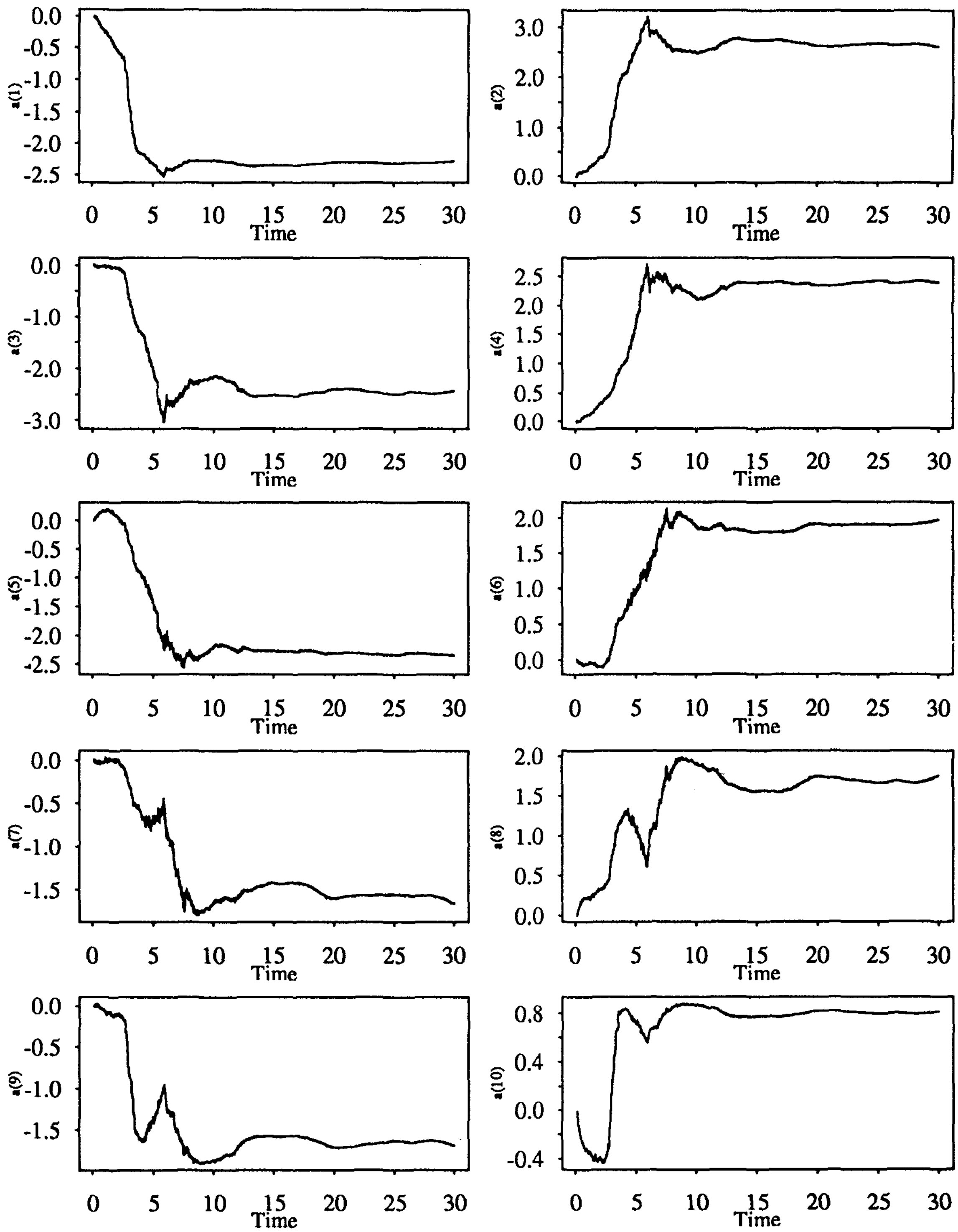


Figure 5.78

Recursive Least Squares Estimation
Five Story Building Model; El-Centro Input
3rd Floor variable alpha=0.99

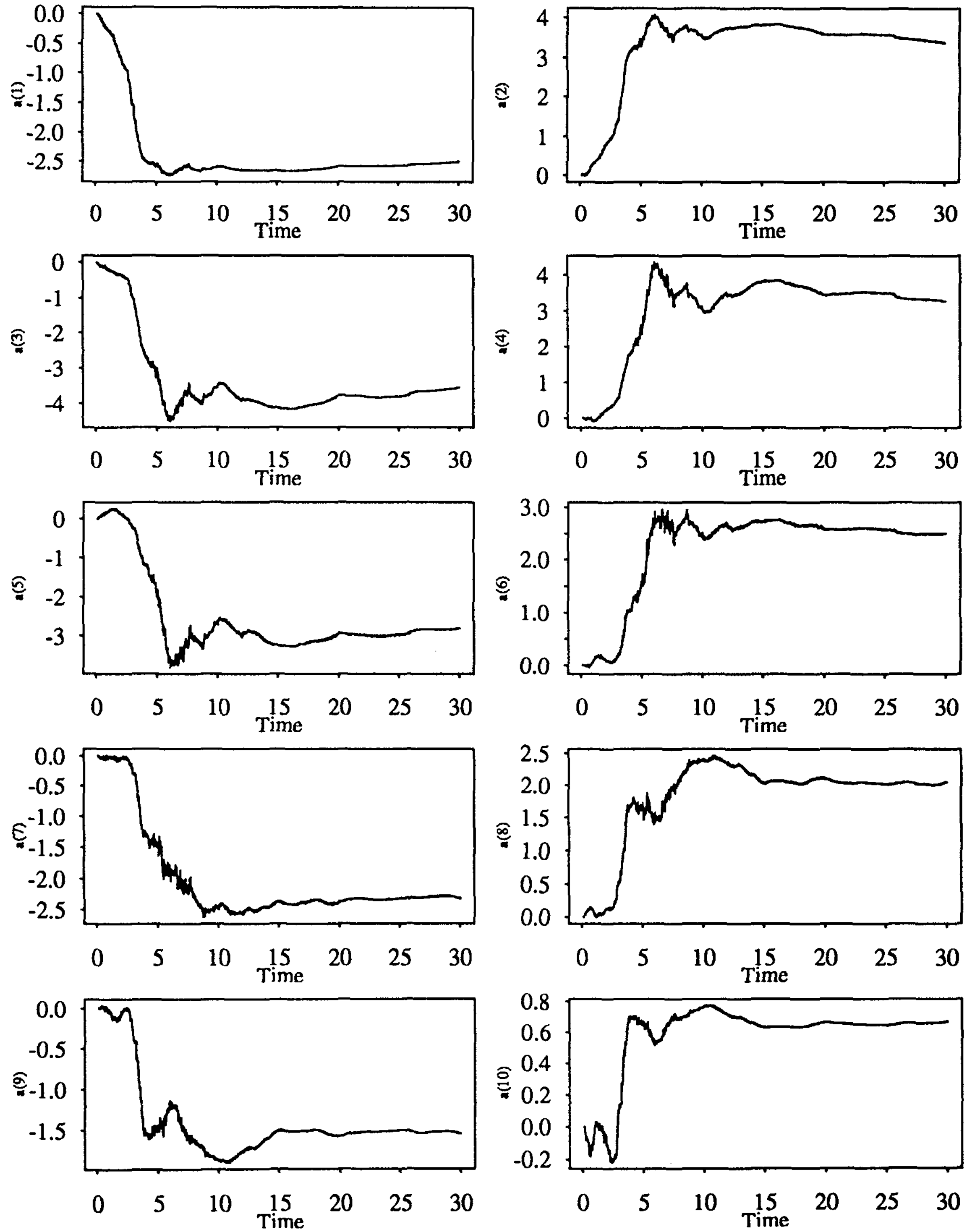


Figure 5.79

Recursive Least Squares Estimation
Five Story Building Model; El-Centro Input
4th Floor variable alpha=0.99

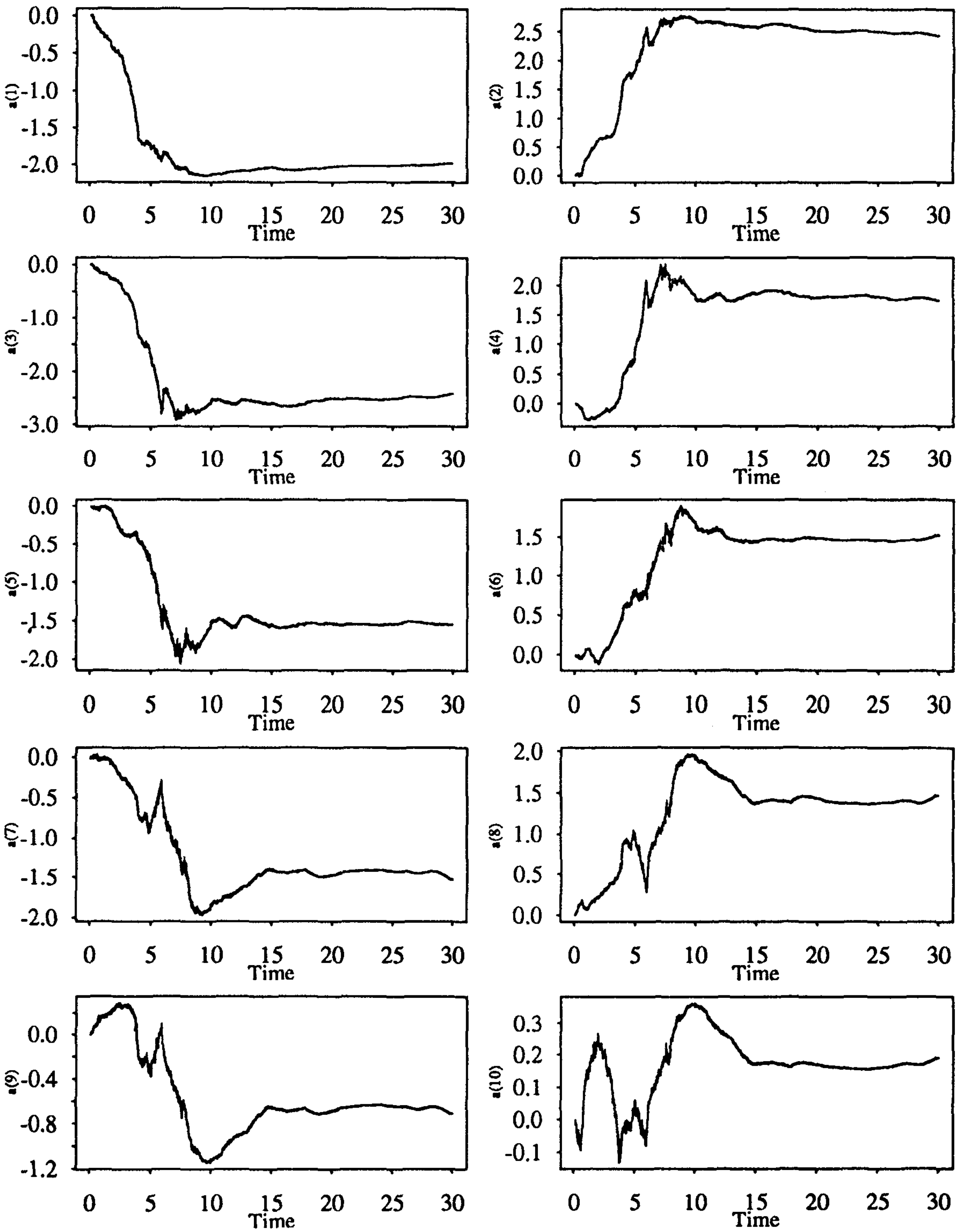


Figure 5.80

Recursive Least Squares Estimation
Five Story Building Model; El-Centro Input
5th Floor variable alpha=0.99

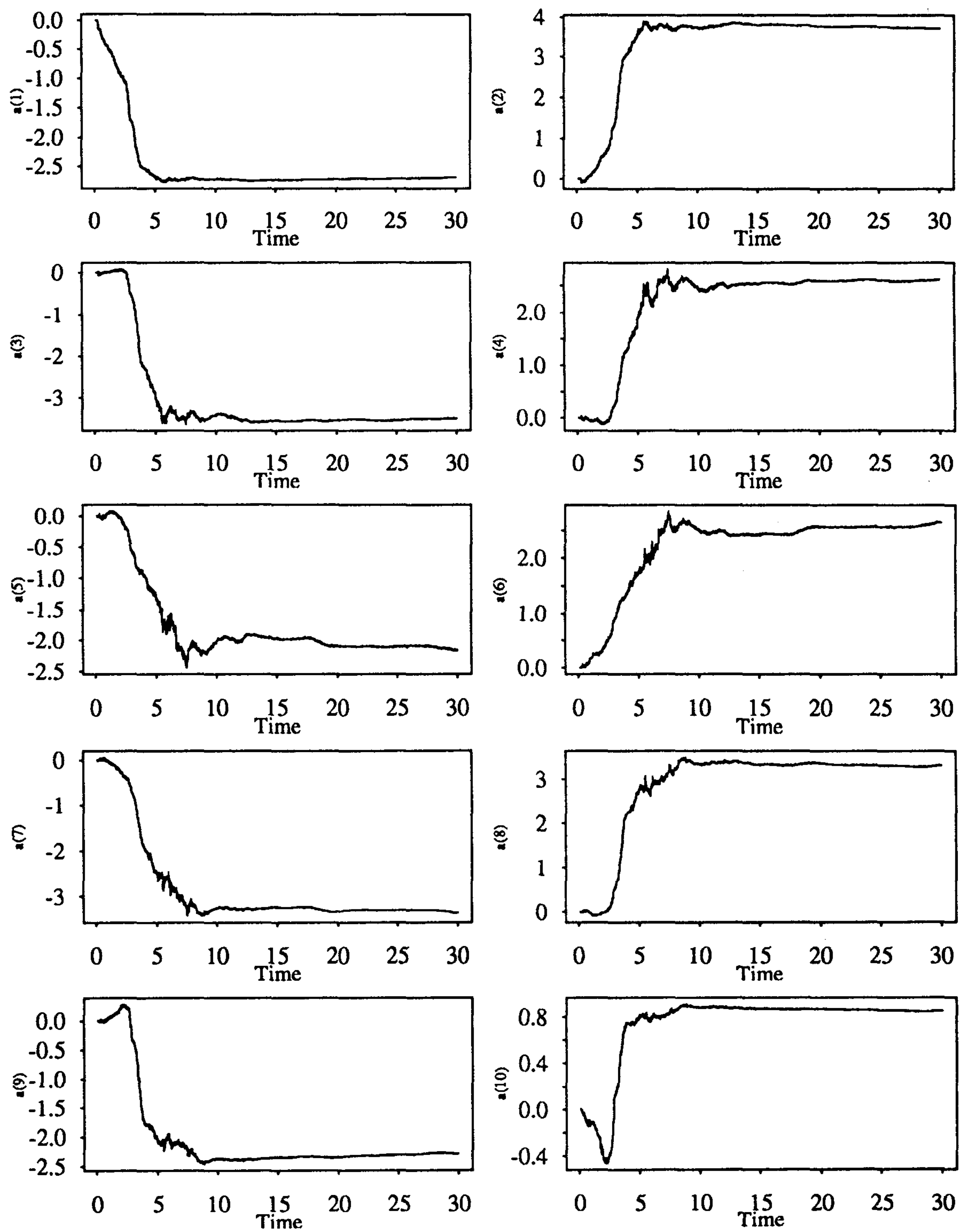


Figure 5.81

## Recursive Least Squares Estimation
## Five Story Building Model; White Noise Input

1st Floor variable alpha=0.99

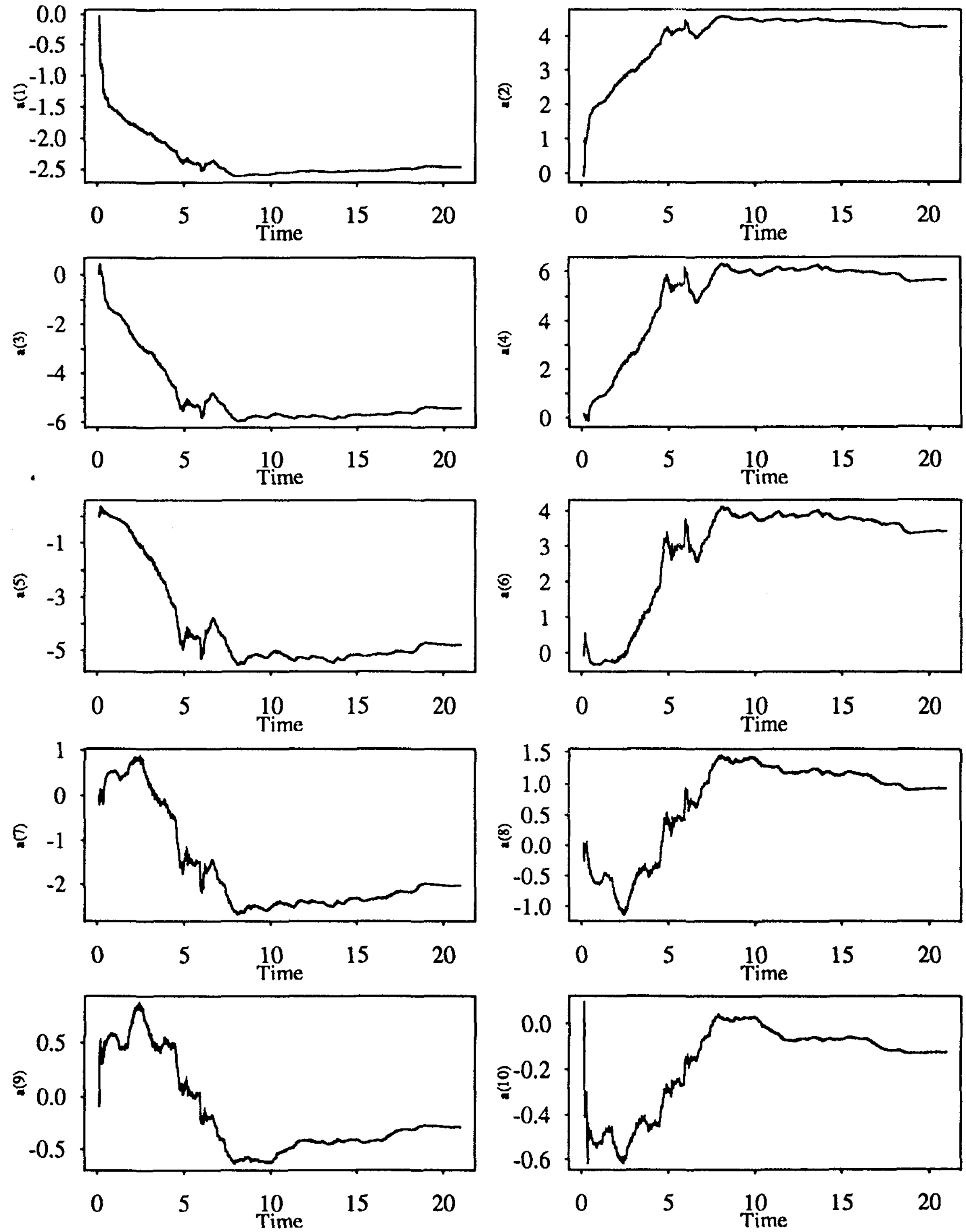


**Figure 5.82**

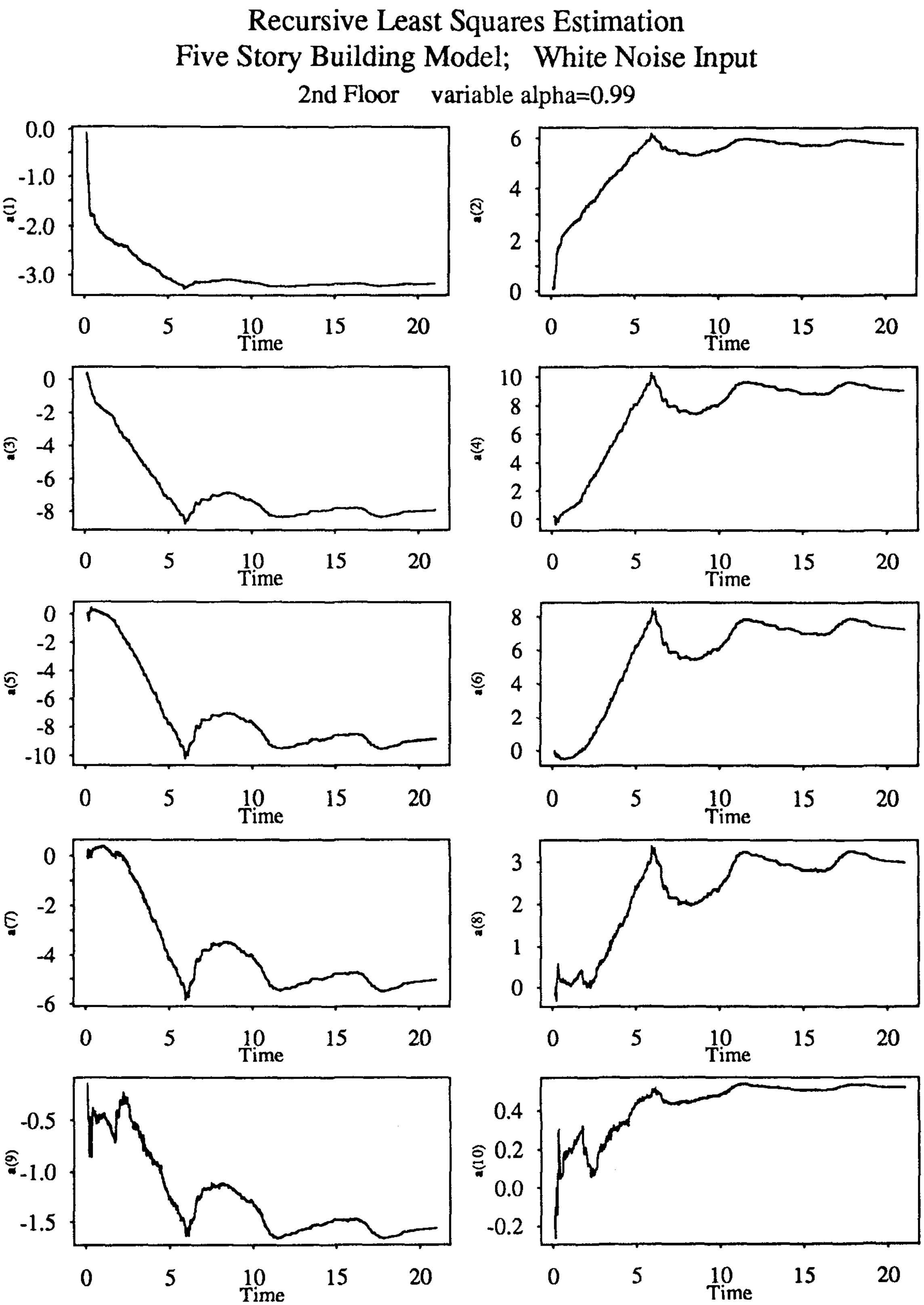
Recursive Least Squares Estimation
Five Story Building Model; White Noise Input
2nd Floor variable alpha=0.99
a(1)
a(2)
a(3)
a(4)
a(5)
a(6)
a(7)
a(8)
a(9)
a(10)
Time
0.0
-1.0
-2.0
-3.0
0
2
4
6
8
10
-2
-4
-6
-8
-10
1
3
-0.5
-1.0
-1.5
0.4
0.2
0.0
-0.2
5
15
20

Figure 5.83

## Recursive Least Squares Estimation
## Five Story Building Model; White Noise Input
3rd Floor variable alpha=0.99

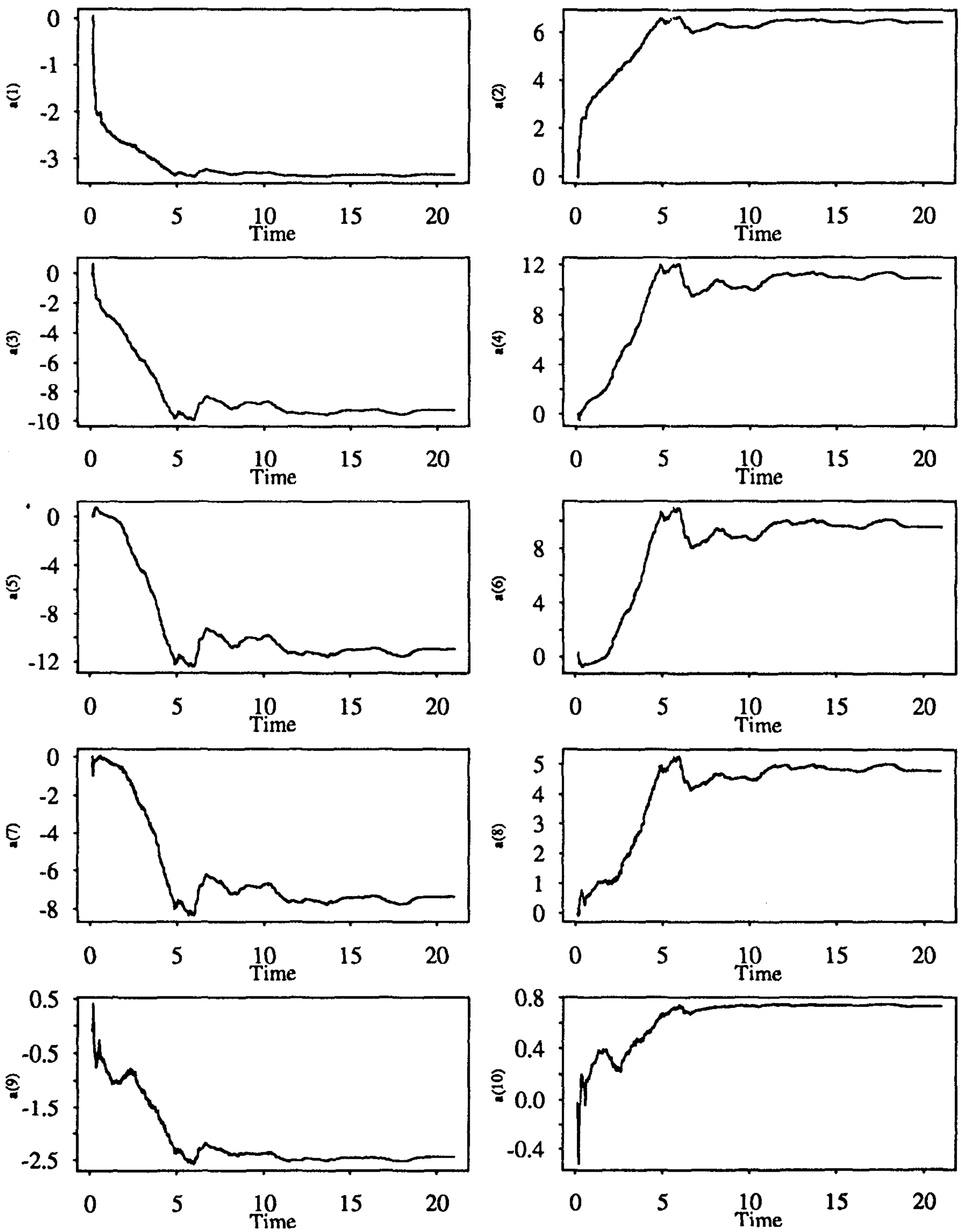


Figure 5.84

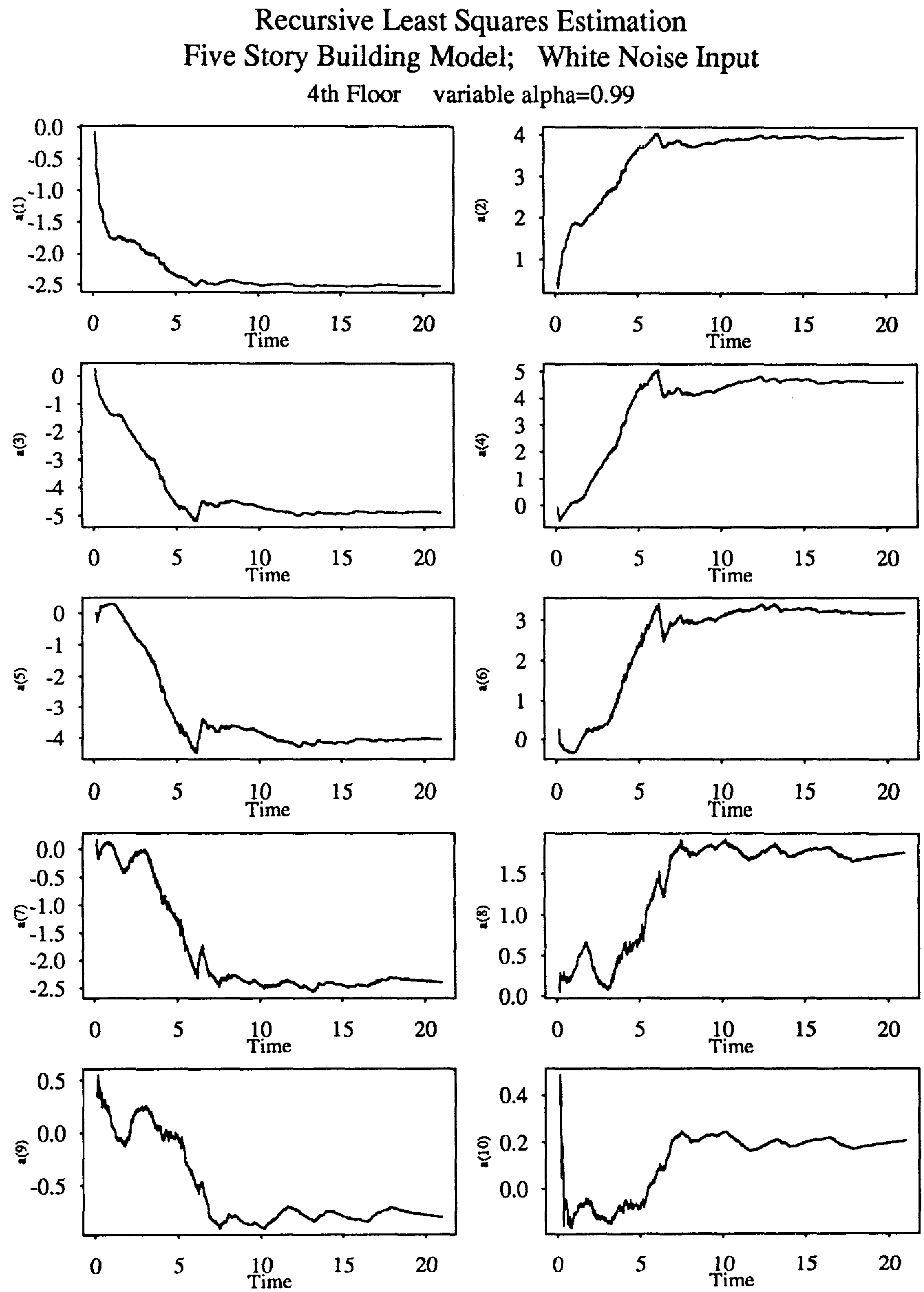
Recursive Least Squares Estimation
Five Story Building Model; White Noise Input
4th Floor variable alpha=0.99
a(1)
a(2)
a(3)
a(4)
a(5)
a(6)
a(7)
a(8)
a(9)
a(10)
Time

Figure 5.85

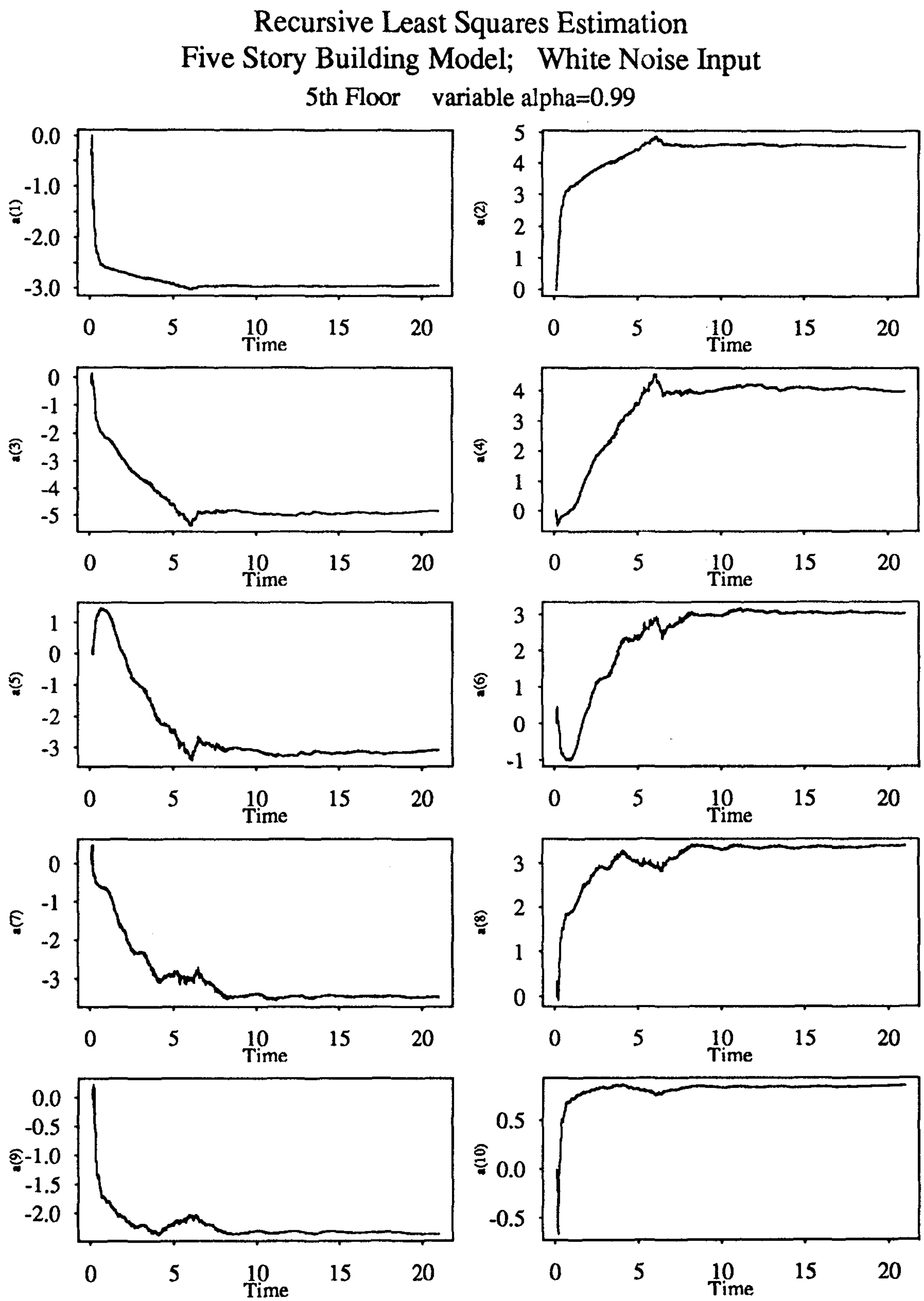
Recursive Least Squares Estimation
Five Story Building Model; White Noise Input
5th Floor variable alpha=0.99
a(1)
a(2)
a(3)
a(4)
a(5)
a(6)
a(7)
a(8)
a(9)
a(10)
Time

Figure 5.86

## Recursive Least Squares Estimation
## Five Story Building Model; El-Centro Input
1st Floor variable alpha=0.99

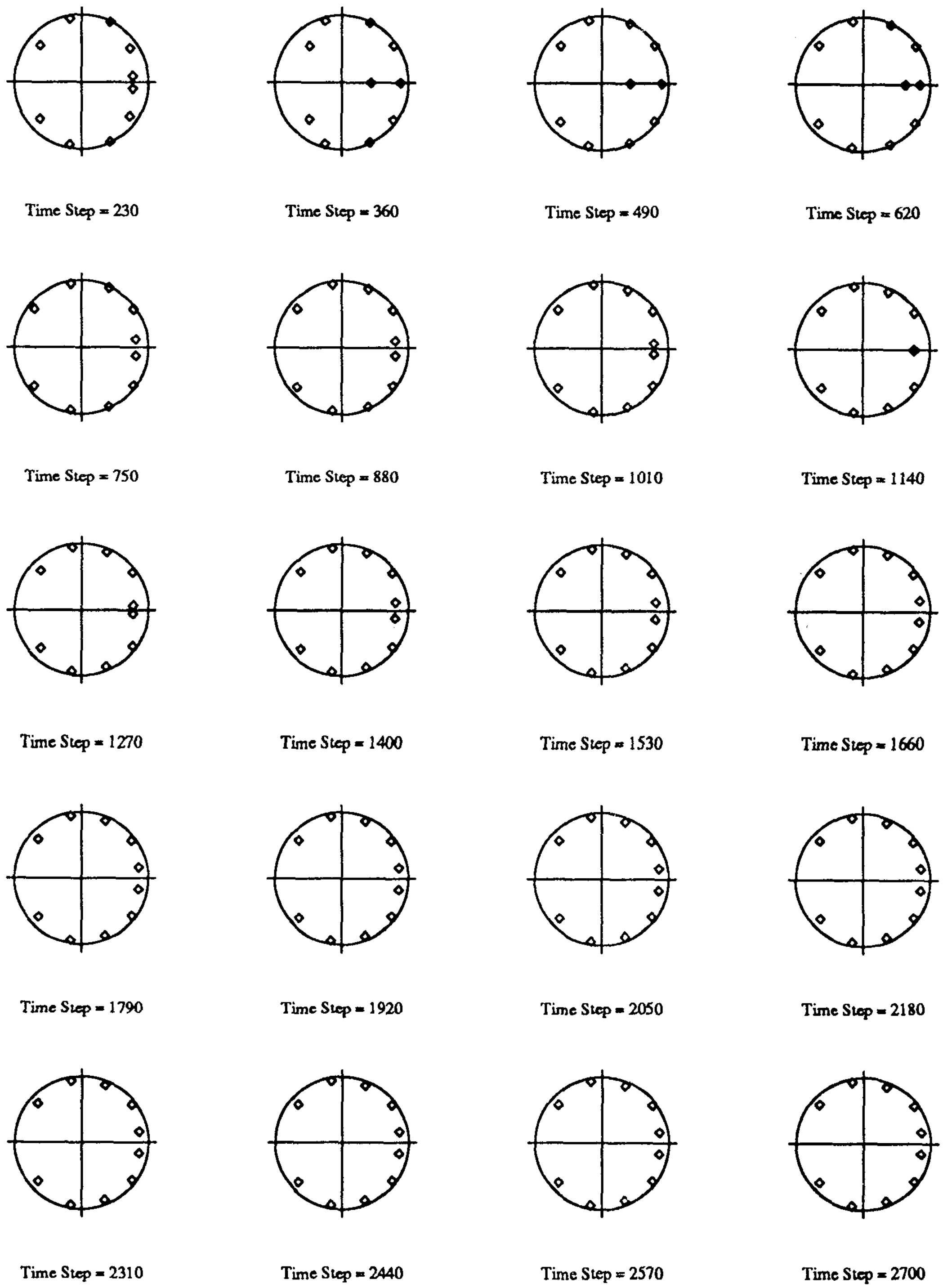


Figure 5.87

## Recursive Least Squares Estimation
## Five Story Building Model; El-Centro Input
### 2nd Floor variable alpha=0.99

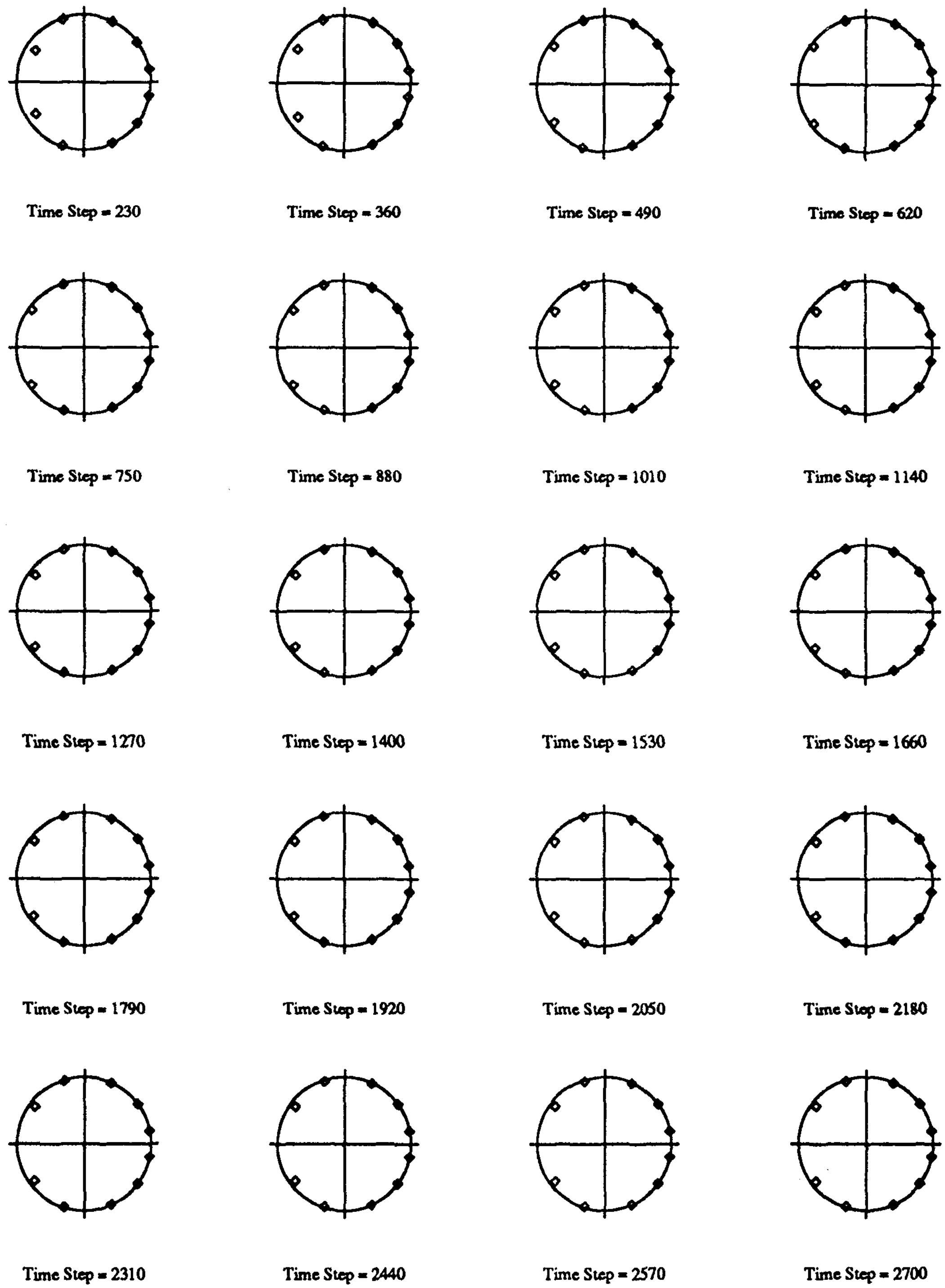


Figure 5.88

## Recursive Least Squares Estimation
## Five Story Building Model; El-Centro Input
### 3rd Floor variable alpha=0.99

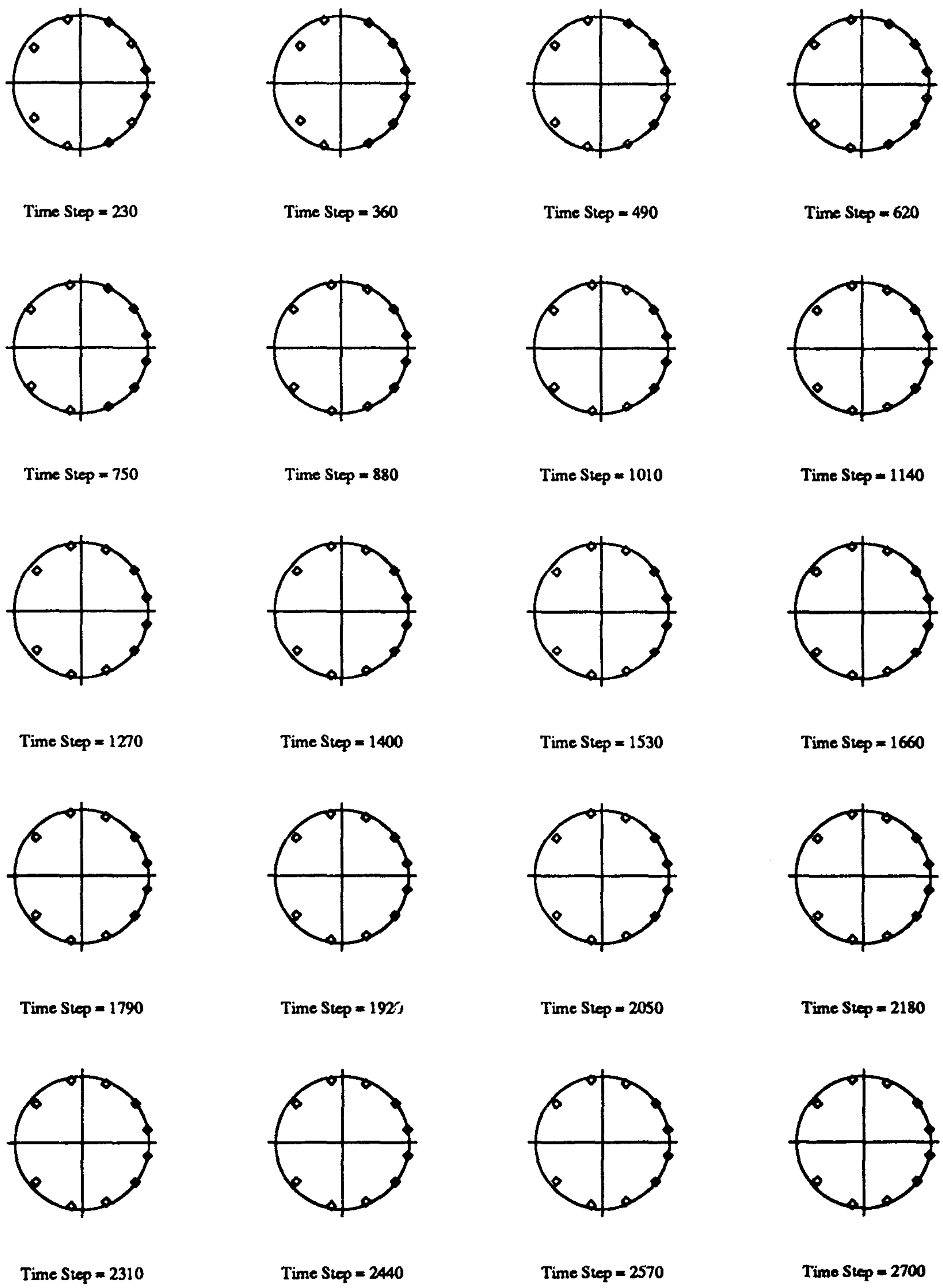


Figure 5.89

Recursive Least Squares Estimation
Five Story Building Model; El-Centro Input
4th Floor variable alpha=0.99

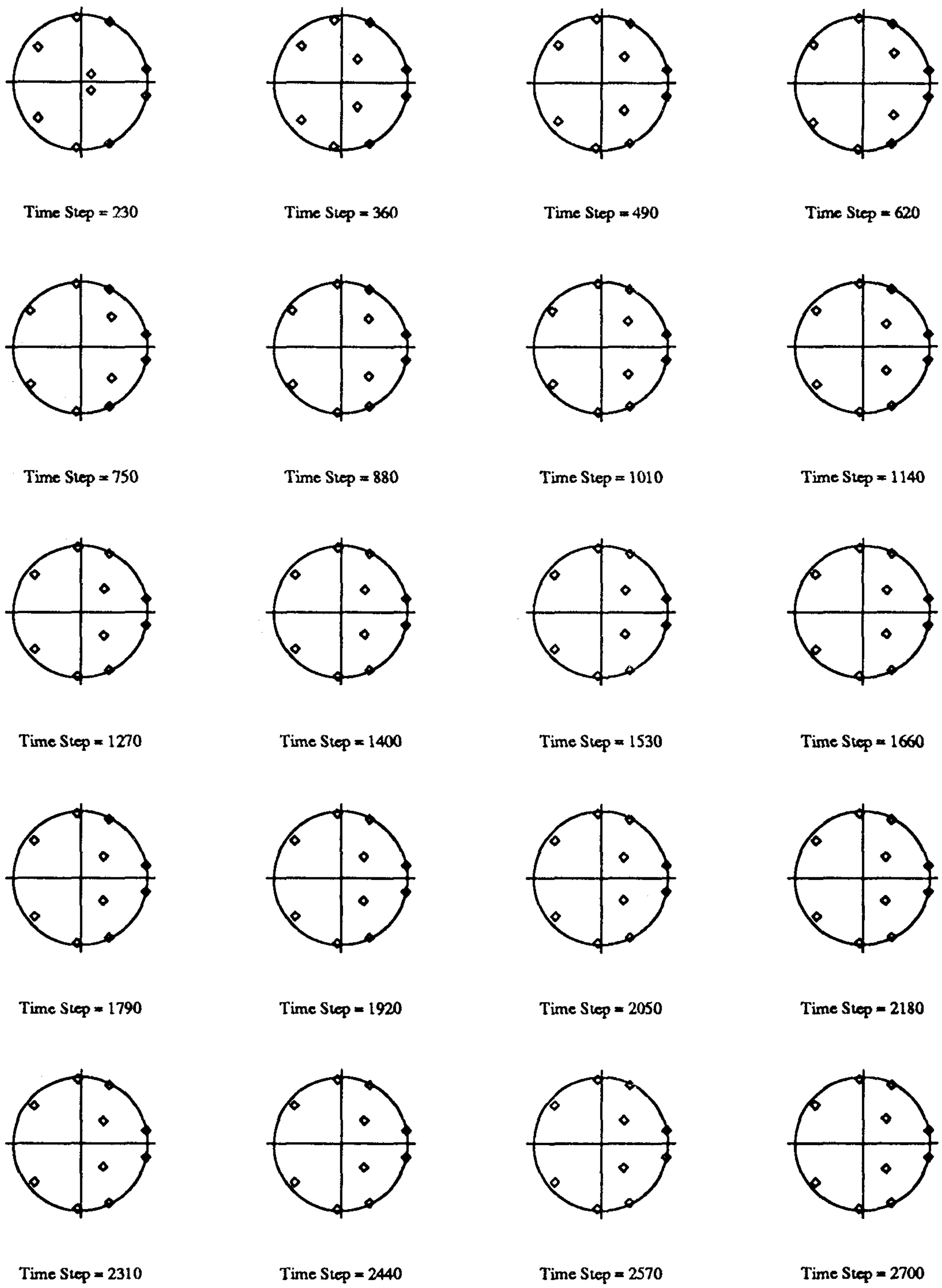


Figure 5.90

## Recursive Least Squares Estimation
## Five Story Building Model; El-Centro Input
### 5th Floor variable alpha=0.99

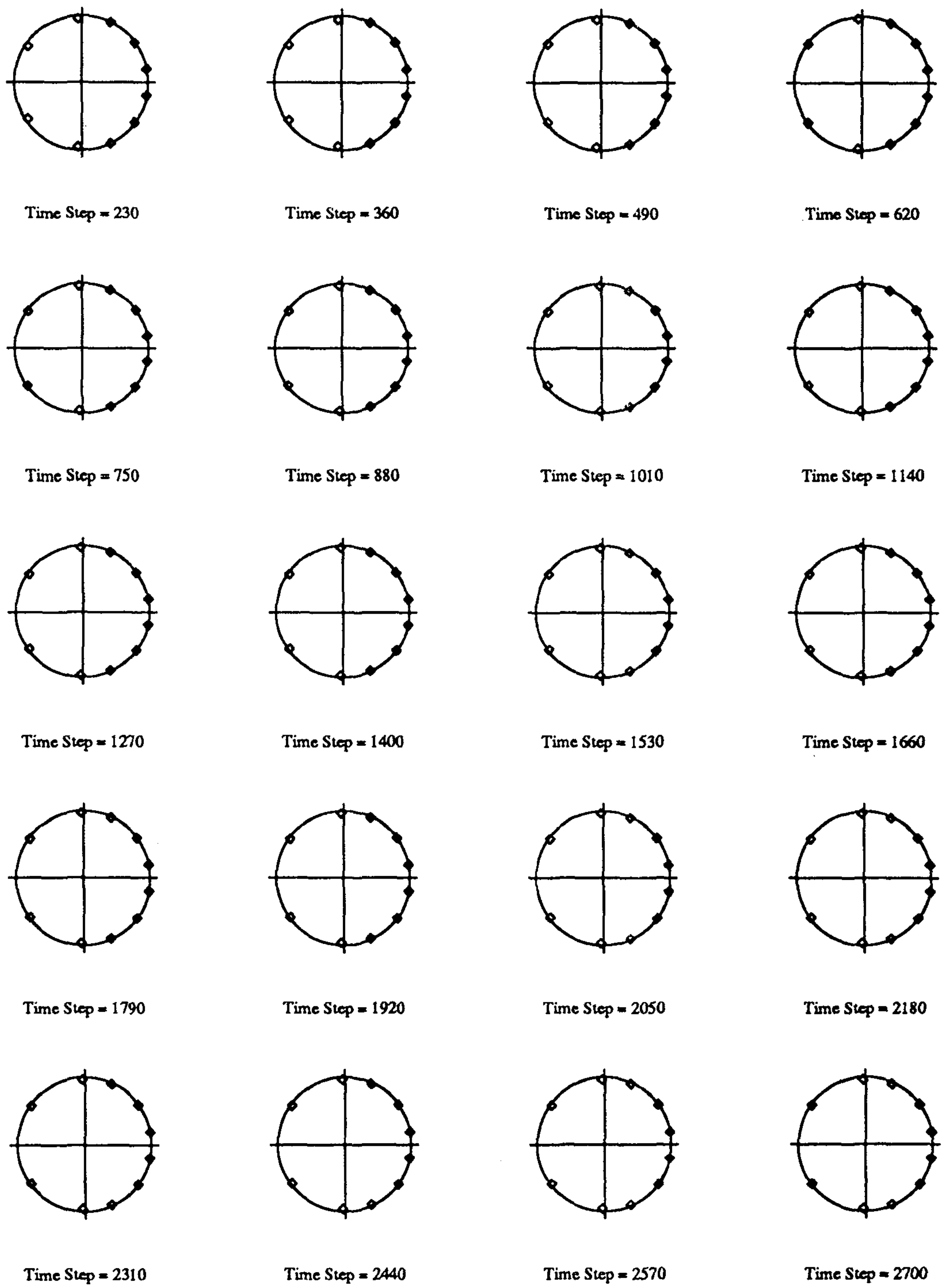


Figure 5.91

## Recursive Least Squares Estimation
## Five Story Building Model; White Noise Input
### 1st Floor variable alpha=0.99

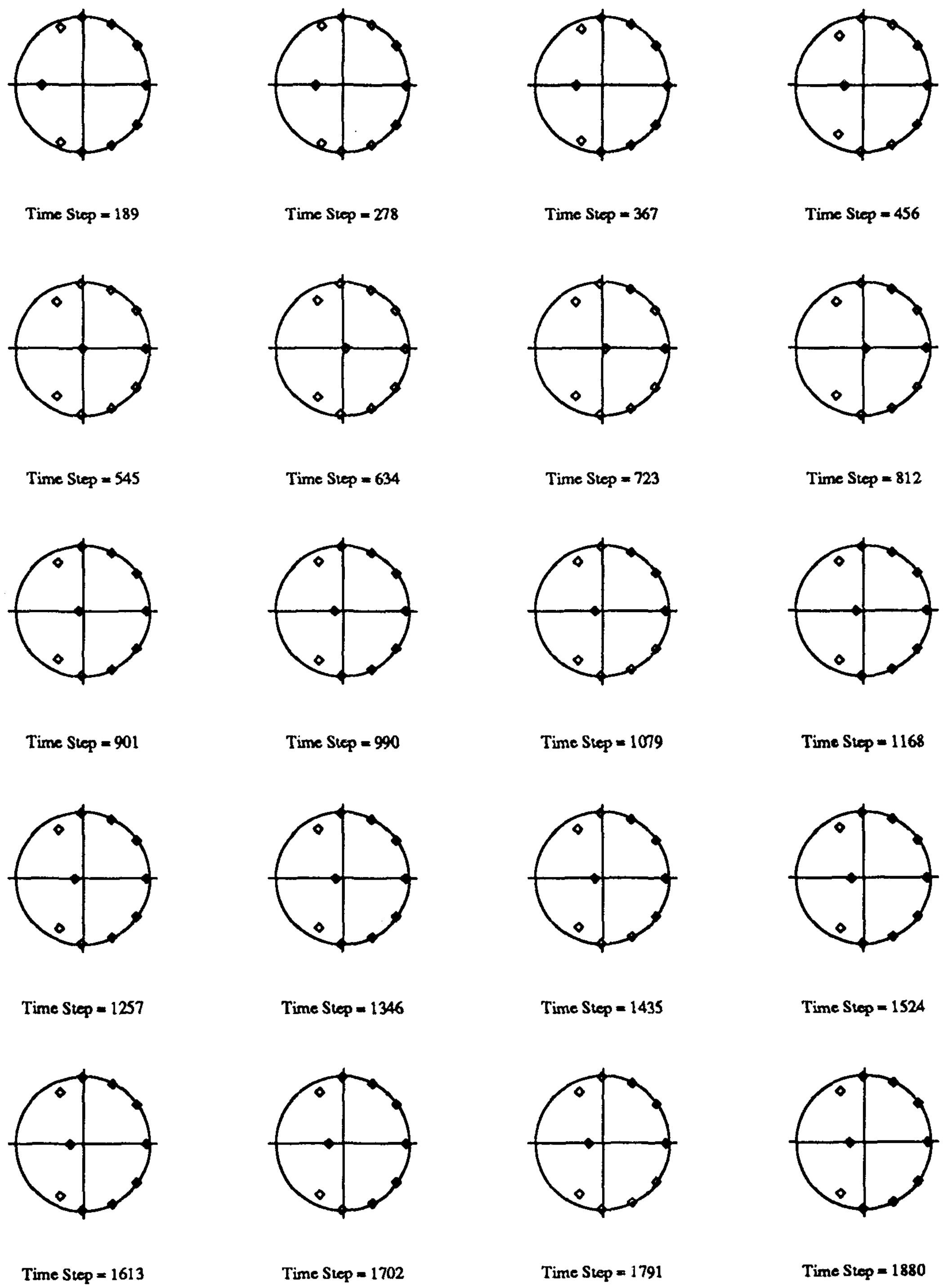


Figure 5.92

Recursive Least Squares Estimation
Five Story Building Model; White Noise Input
2nd Floor variable alpha=0.99

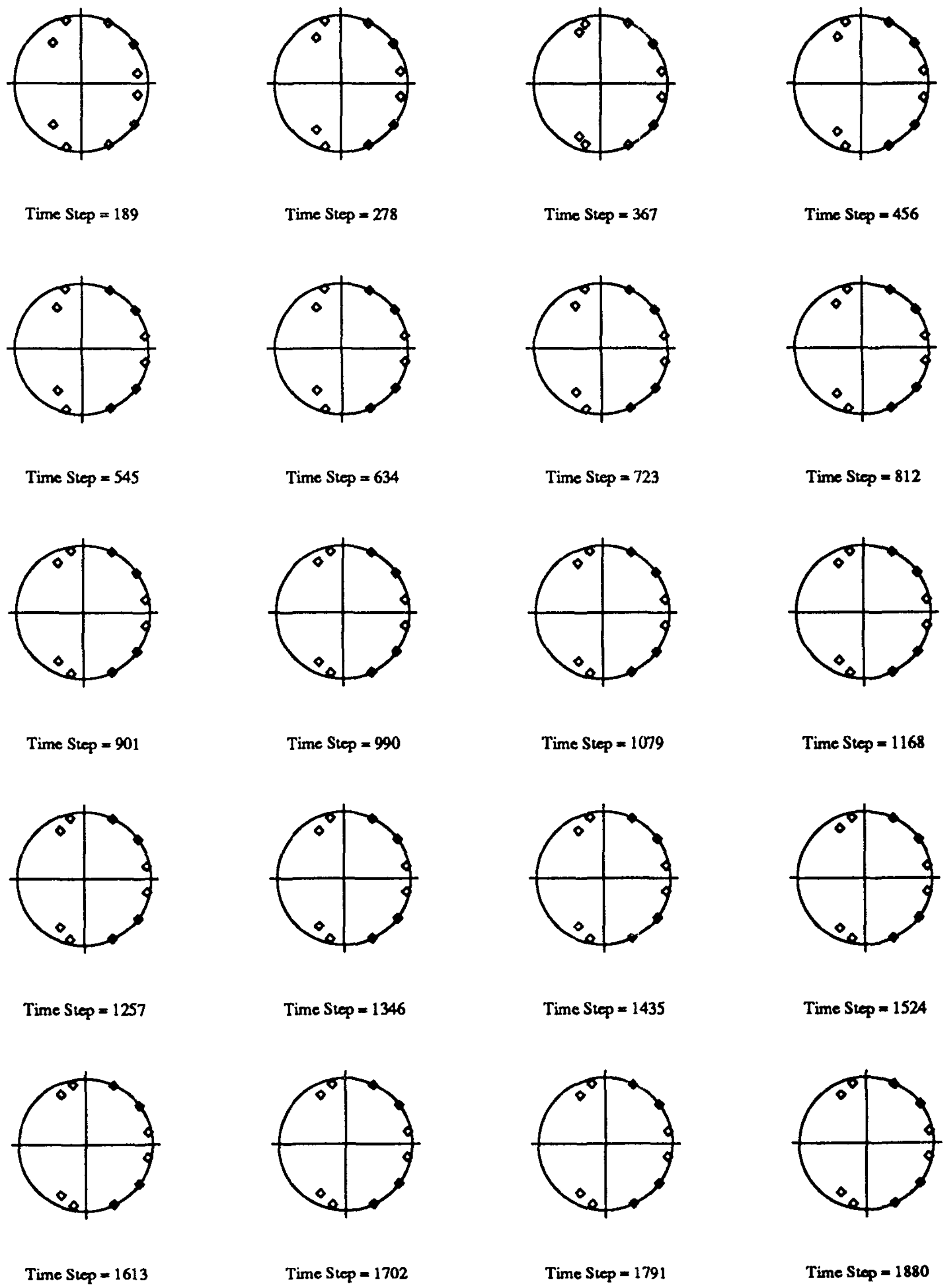


Figure 5.93

## Recursive Least Squares Estimation
## Five Story Building Model; White Noise Input
### 3rd Floor variable alpha=0.99

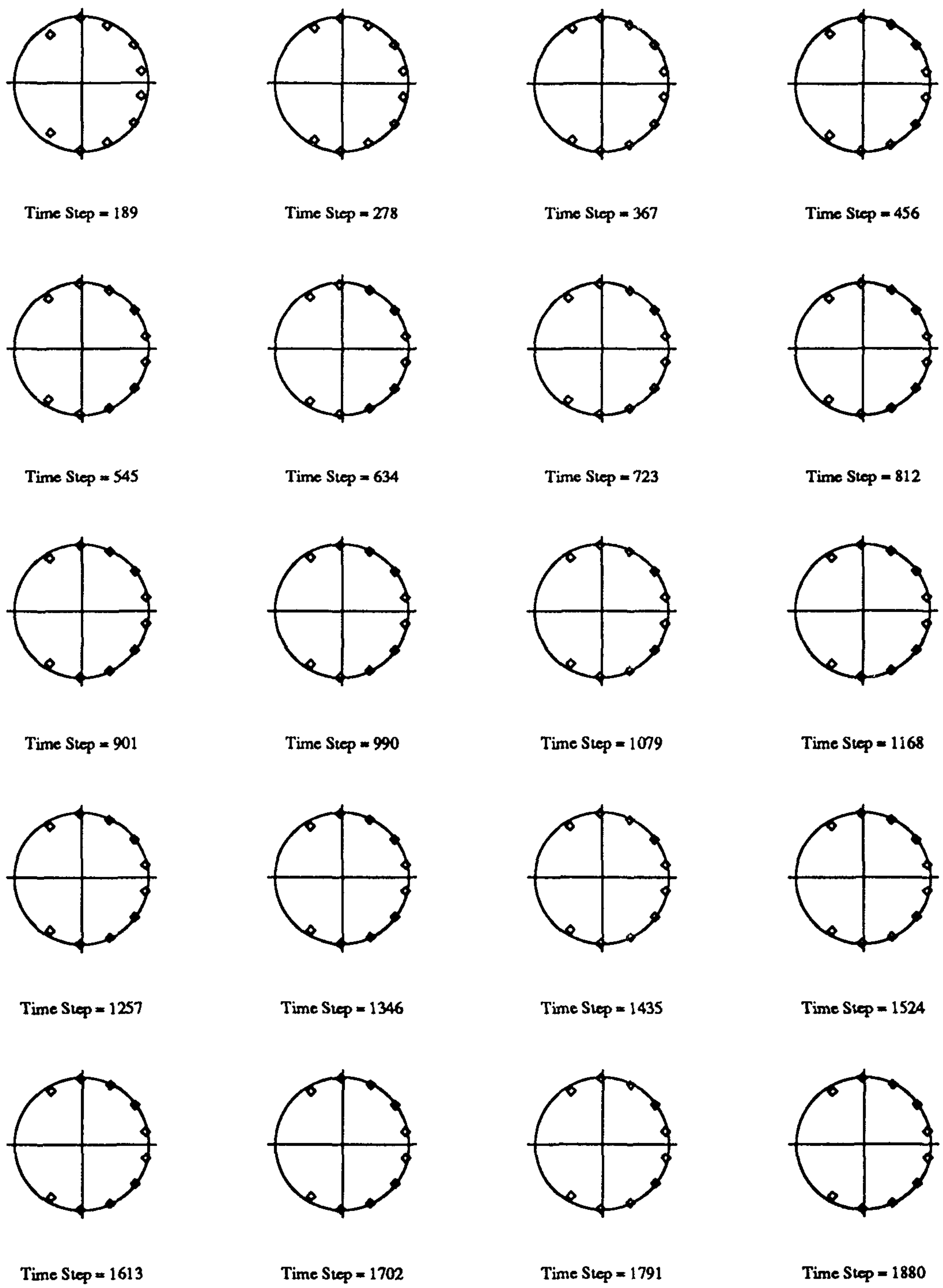


Figure 5.94

## Recursive Least Squares Estimation
## Five Story Building Model; White Noise Input
### 4th Floor variable alpha=0.99

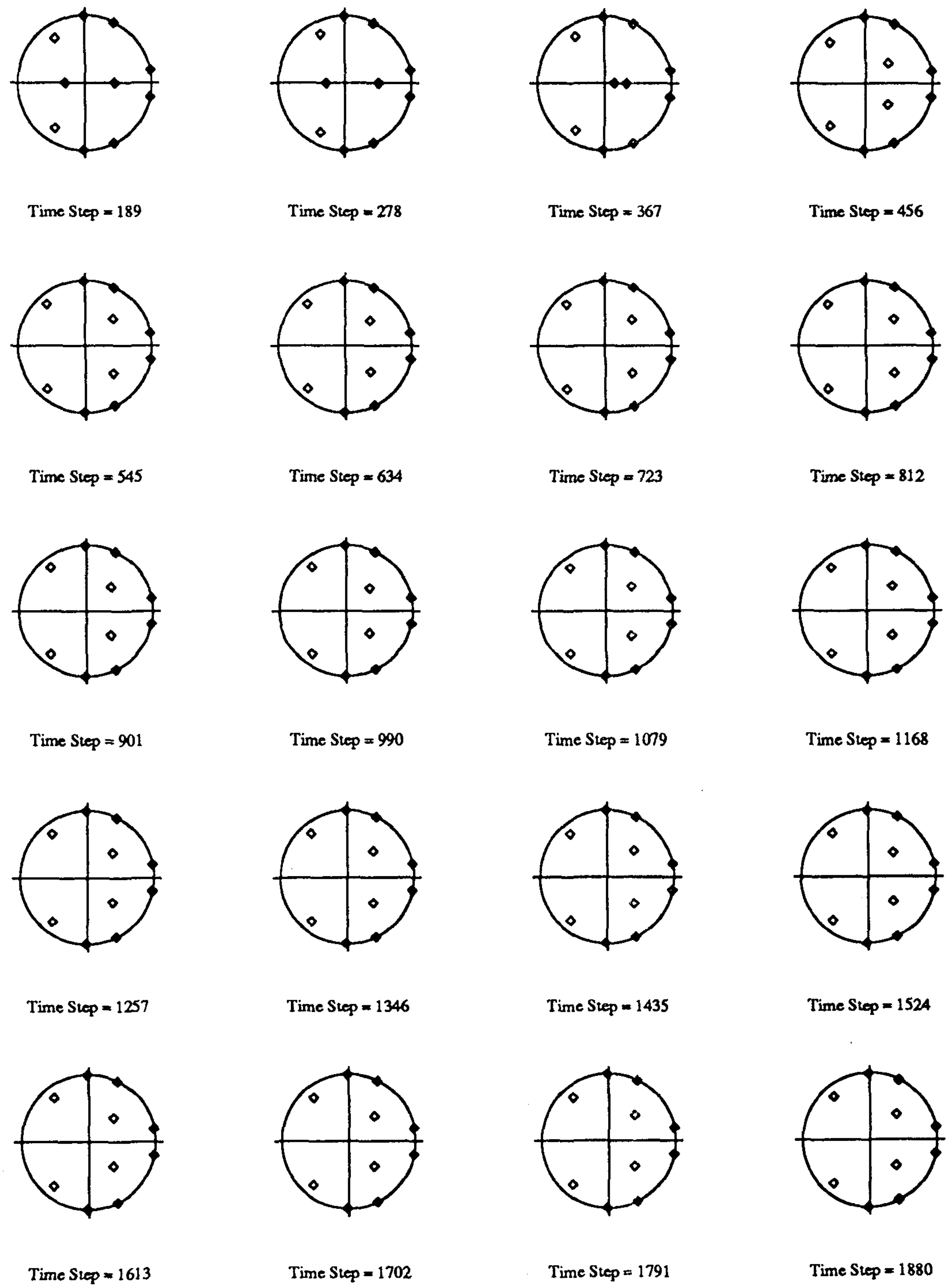


Figure 5.95

# Recursive Least Squares Estimation
## Five Story Building Model; White Noise Input
### 5th Floor variable alpha=0.99

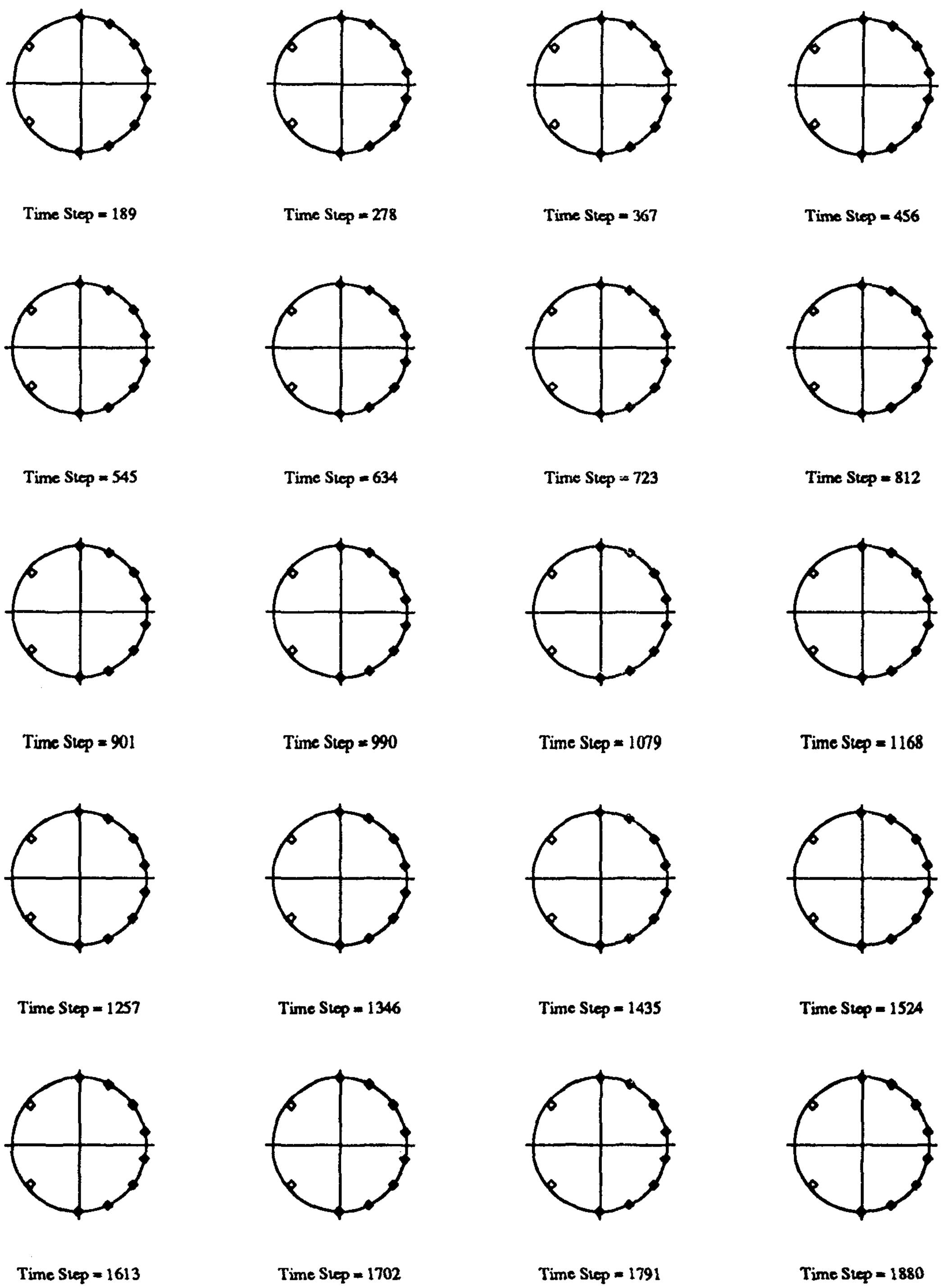


Figure 5.96

Recursive Least Squares Estimation
Three Story Building Model; El-Centro Input
1st Floor variable alpha=0.99

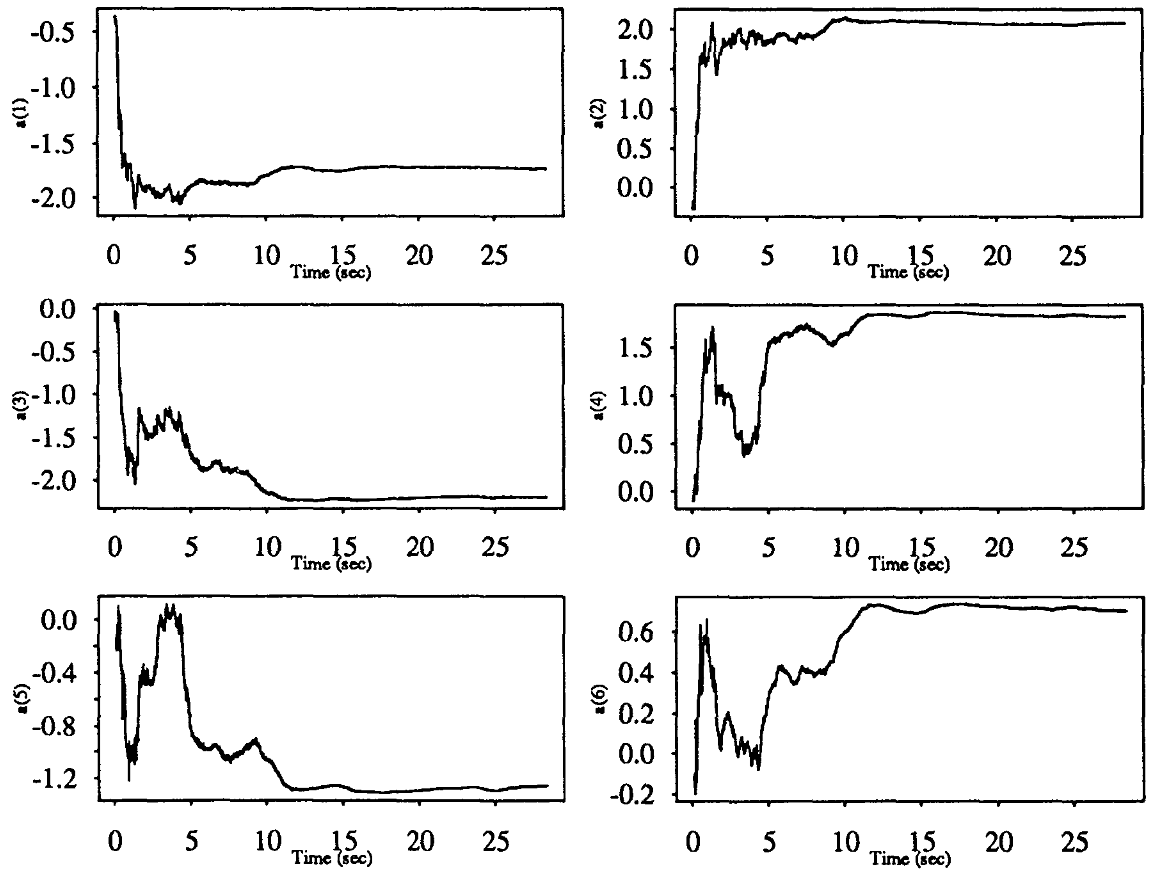


**Figure 5.97**

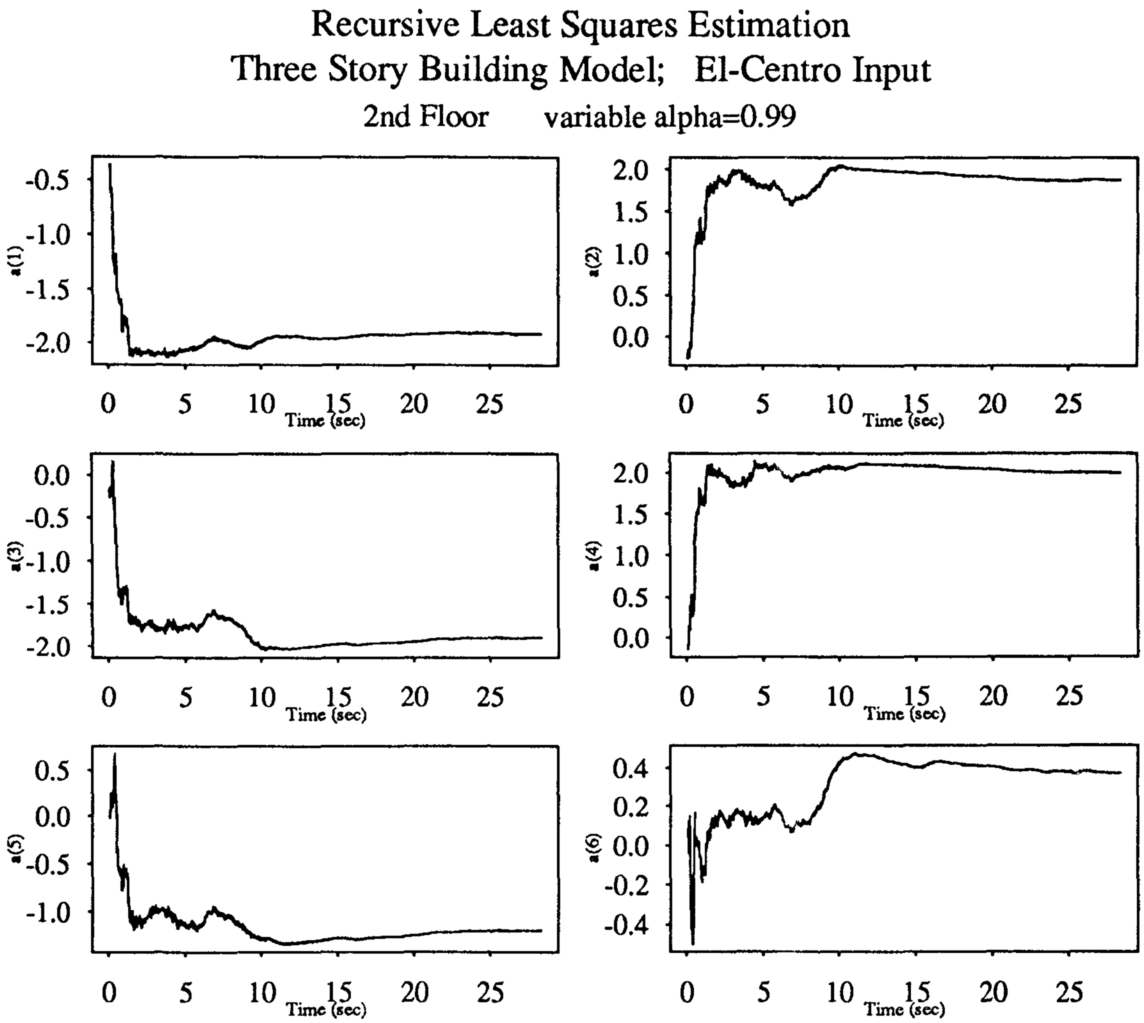
Recursive Least Squares Estimation
Three Story Building Model; El-Centro Input
2nd Floor variable alpha=0.99
a(1)
a(2)
a(3)
a(4)
a(5)
a(6)
Time (sec)

Figure 5.98

Recursive Least Squares Estimation
Three Story Building Model; El-Centro Input
3rd Floor variable alpha=0.99

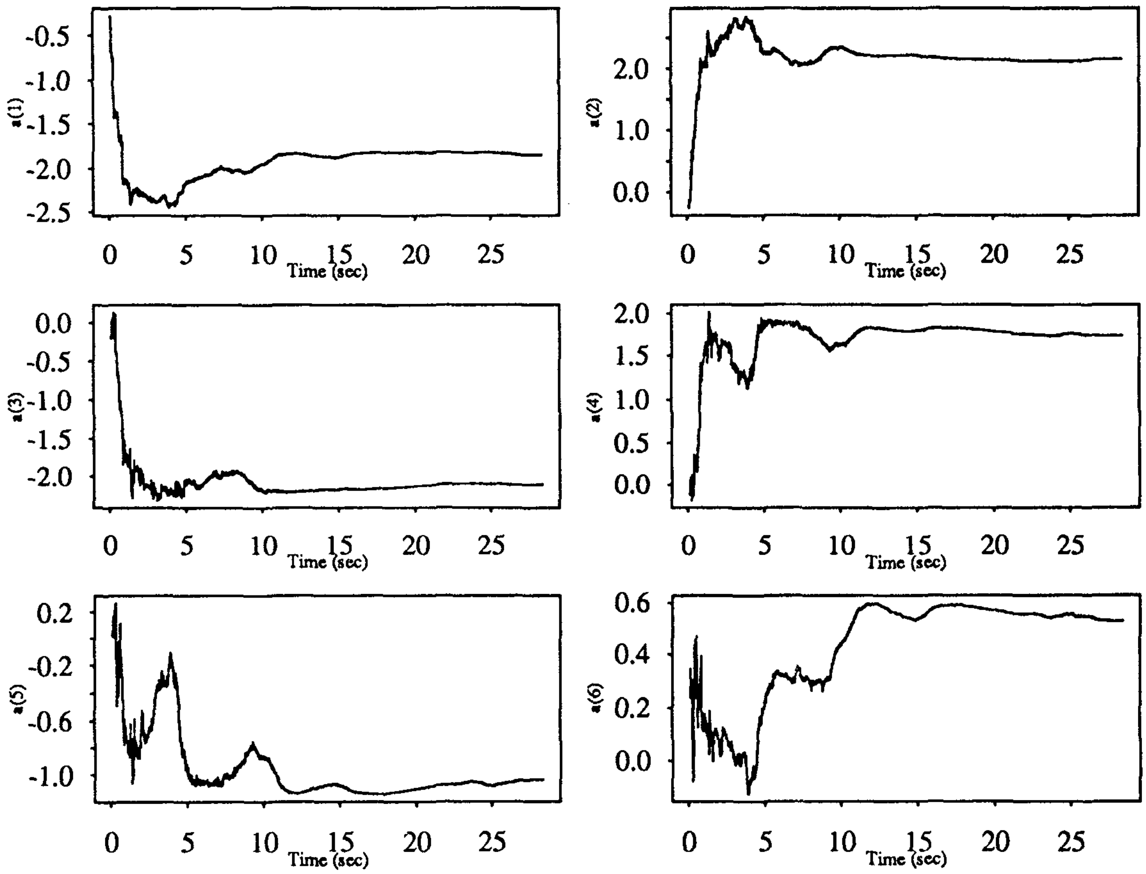


Figure 5.99

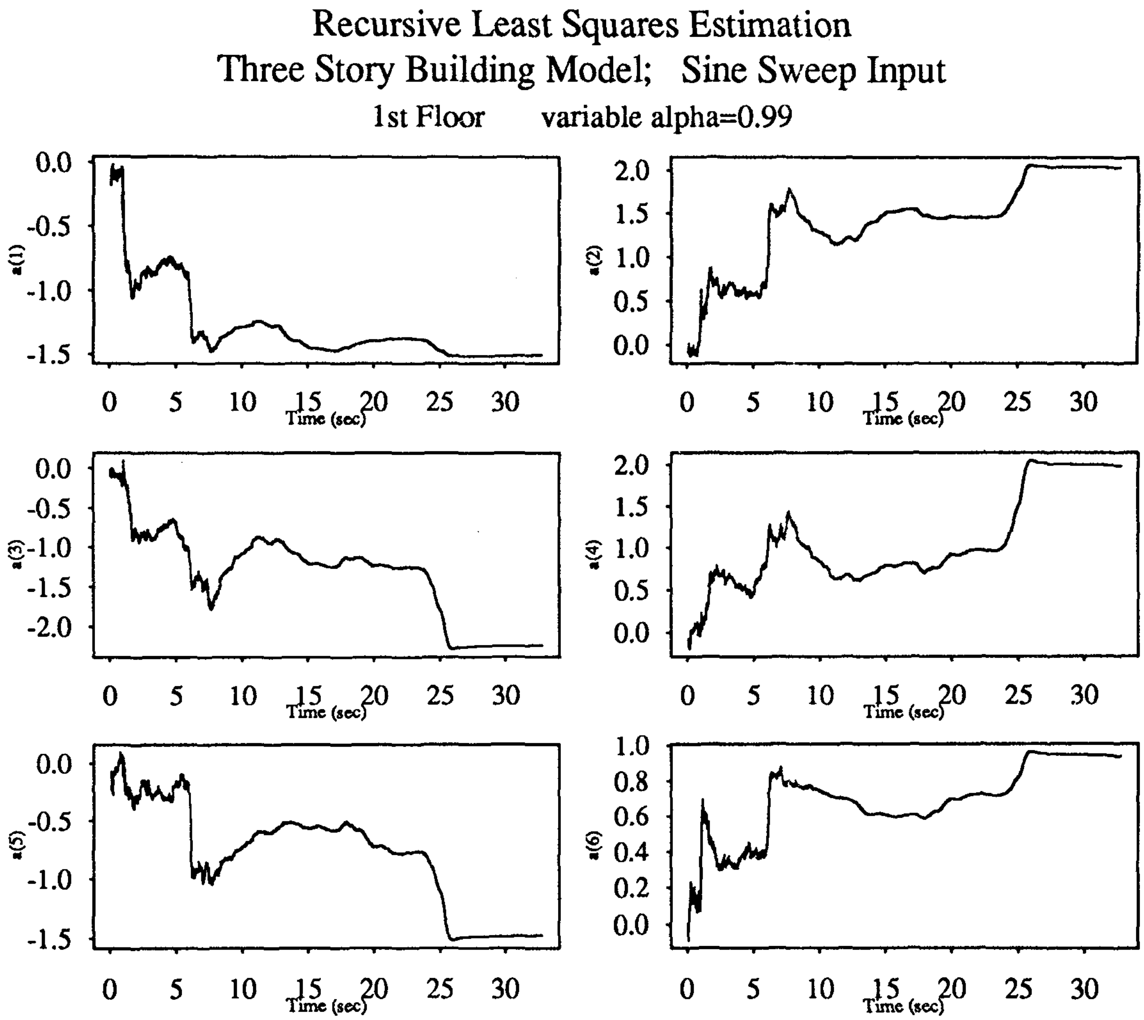

Recursive Least Squares Estimation
Three Story Building Model; Sine Sweep Input
1st Floor variable alpha=0.99
a(1)
a(2)
a(3)
a(4)
a(5)
a(6)
Time (sec)


Figure 5.100

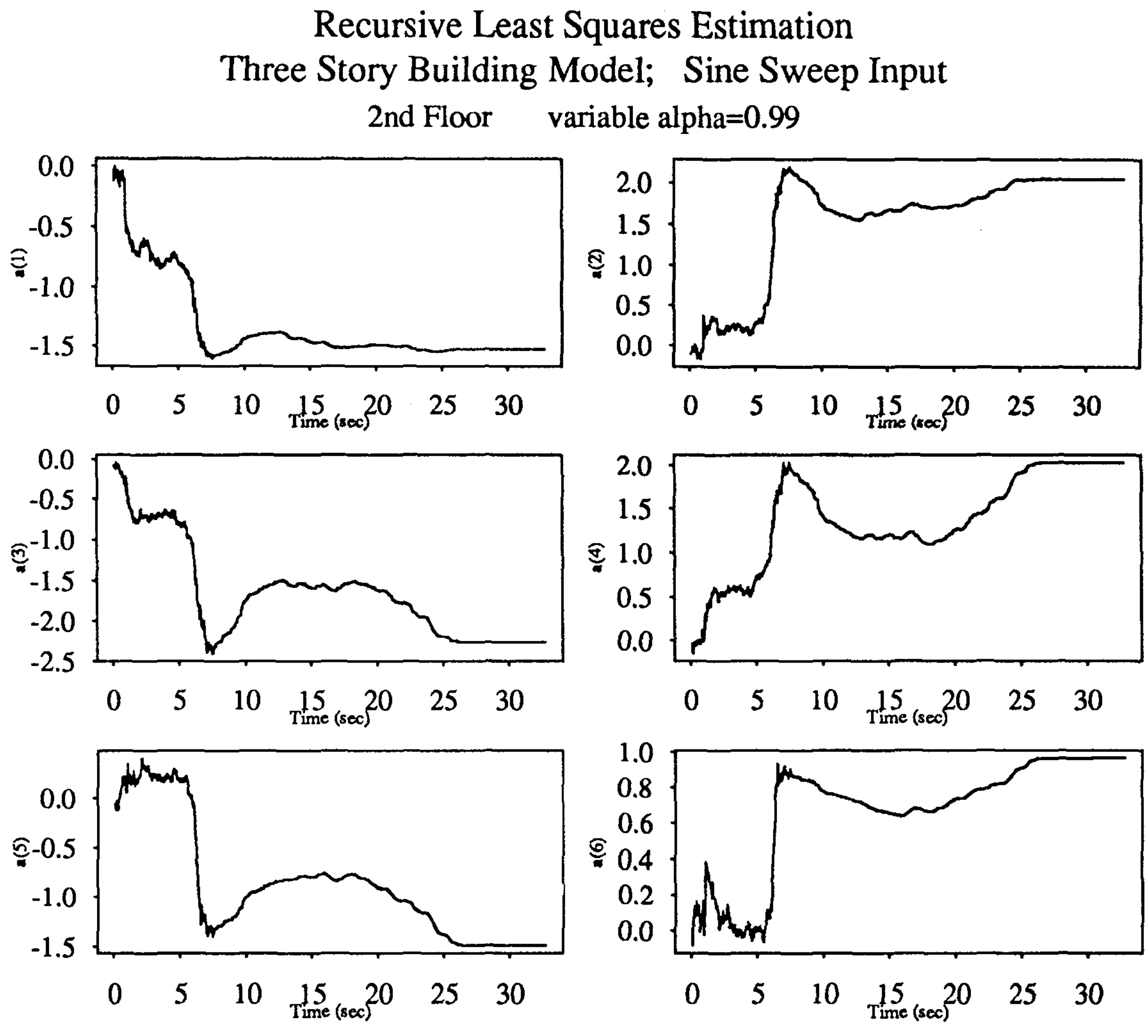

Recursive Least Squares Estimation
Three Story Building Model; Sine Sweep Input
2nd Floor variable alpha=0.99
a(1)
a(2)
a(3)
a(4)
a(5)
a(6)
Time (sec)


**Figure 5.101**

Recursive Least Squares Estimation
Three Story Building Model; Sine Sweep Input
3rd Floor variable alpha=0.99

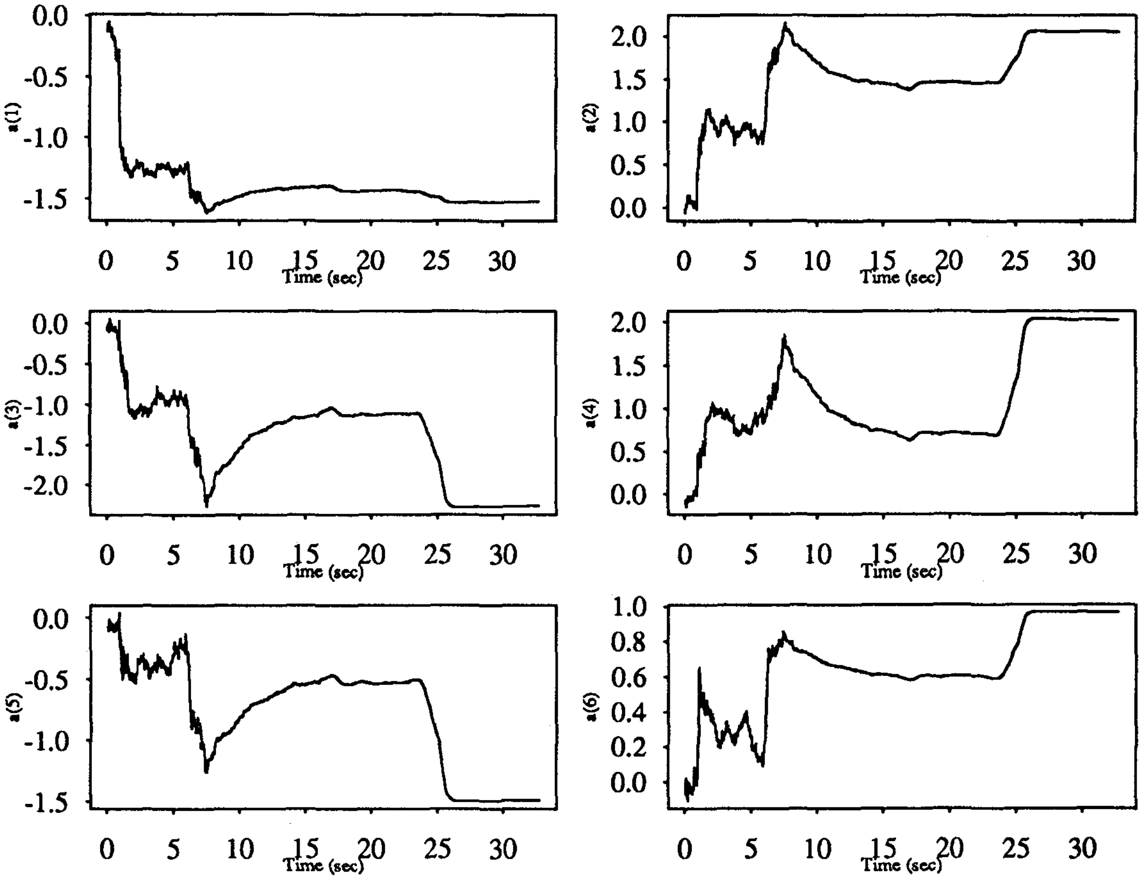


**Figure 5.102**

Recursive Least Squares Estimation
Three Story Building Model; White Noise Input
1st Floor variable alpha=0.99

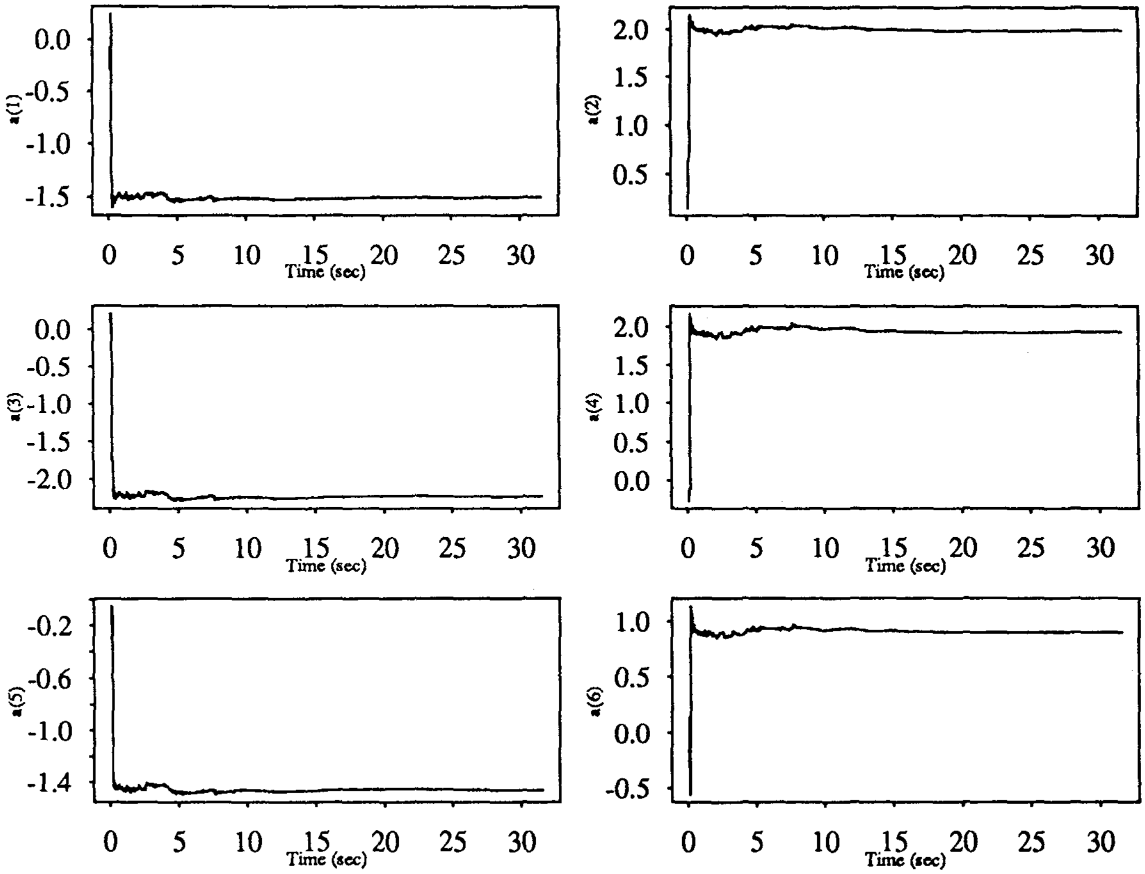


Figure 5.103

Recursive Least Squares Estimation
Three Story Building Model; White Noise Input
2nd Floor variable alpha=0.99

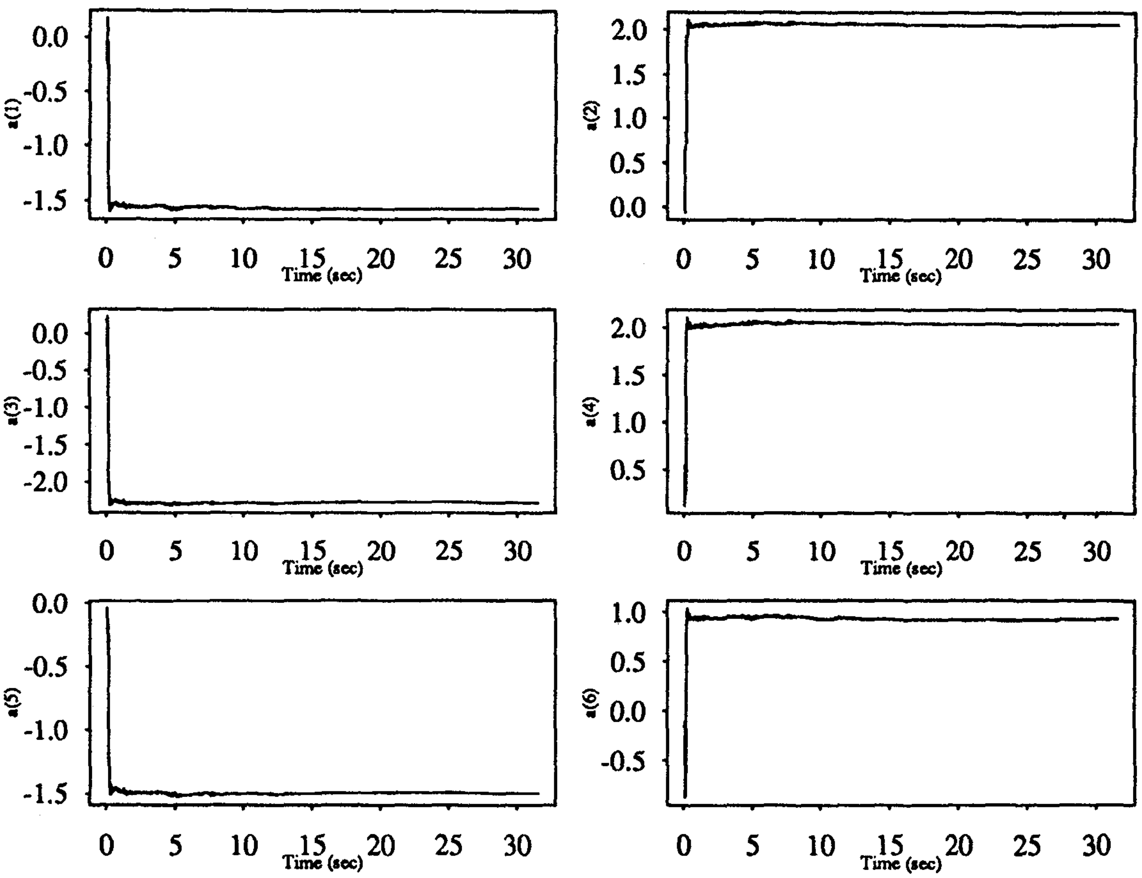


**Figure 5.104**

Recursive Least Squares Estimation
Three Story Building Model; White Noise Input
3rd Floor variable alpha=0.99

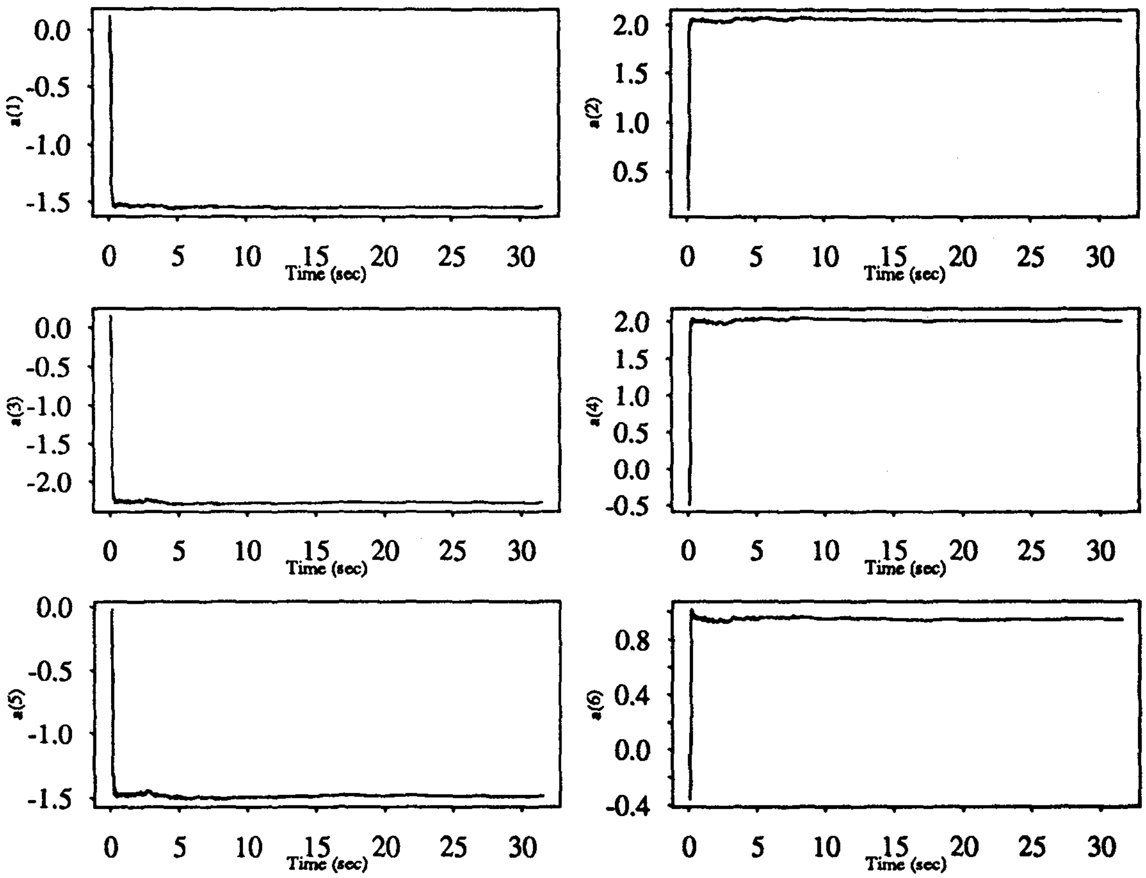


Figure 5.105

## Recursive Least Squares Estimation
## Three Story Building Model; El-Centro Input
1st Floor variable alpha=0.99

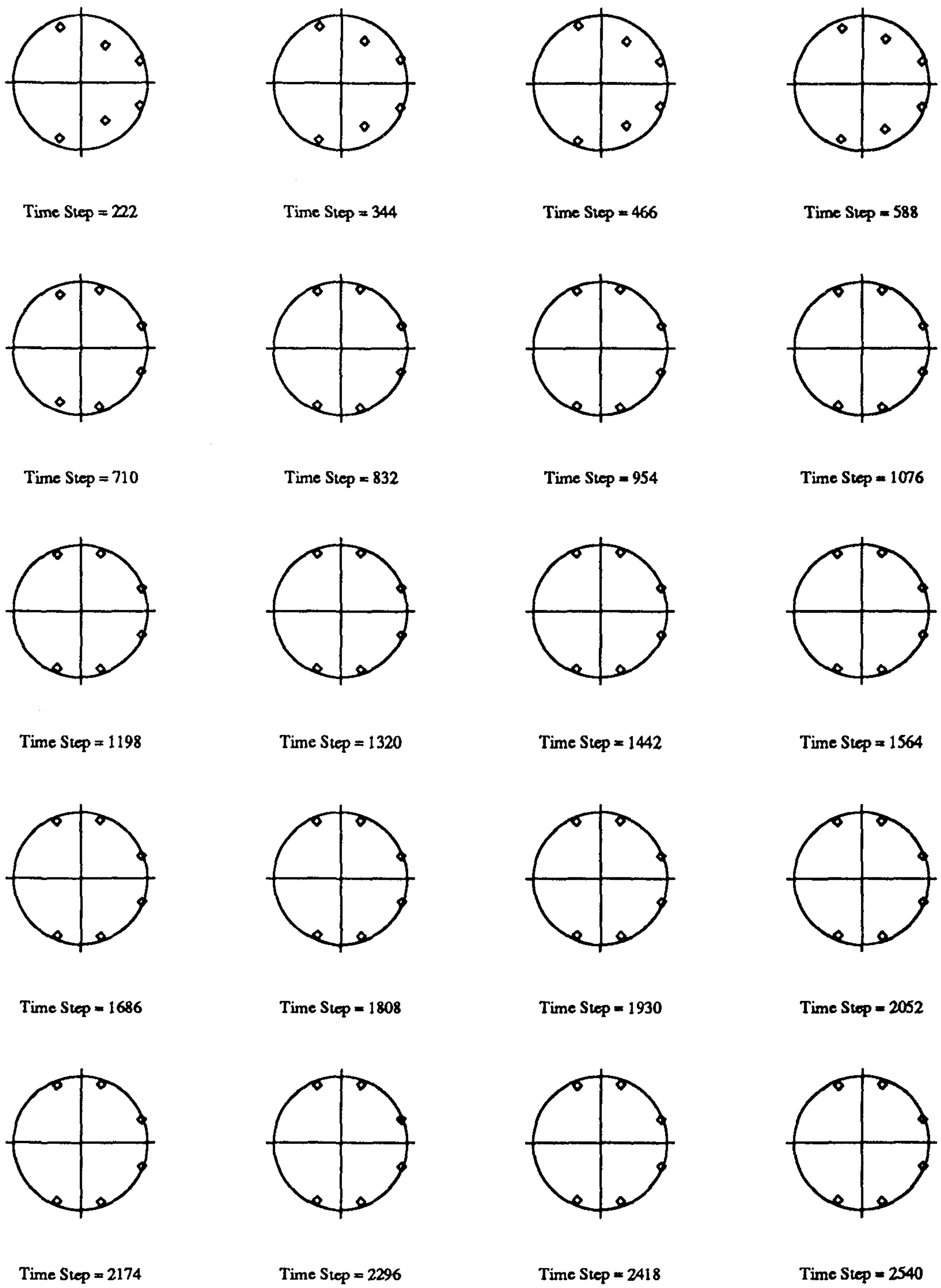


**Figure 5.106**

## Recursive Least Squares Estimation
## Three Story Building Model; El-Centro Input
### 2nd Floor variable alpha=0.99

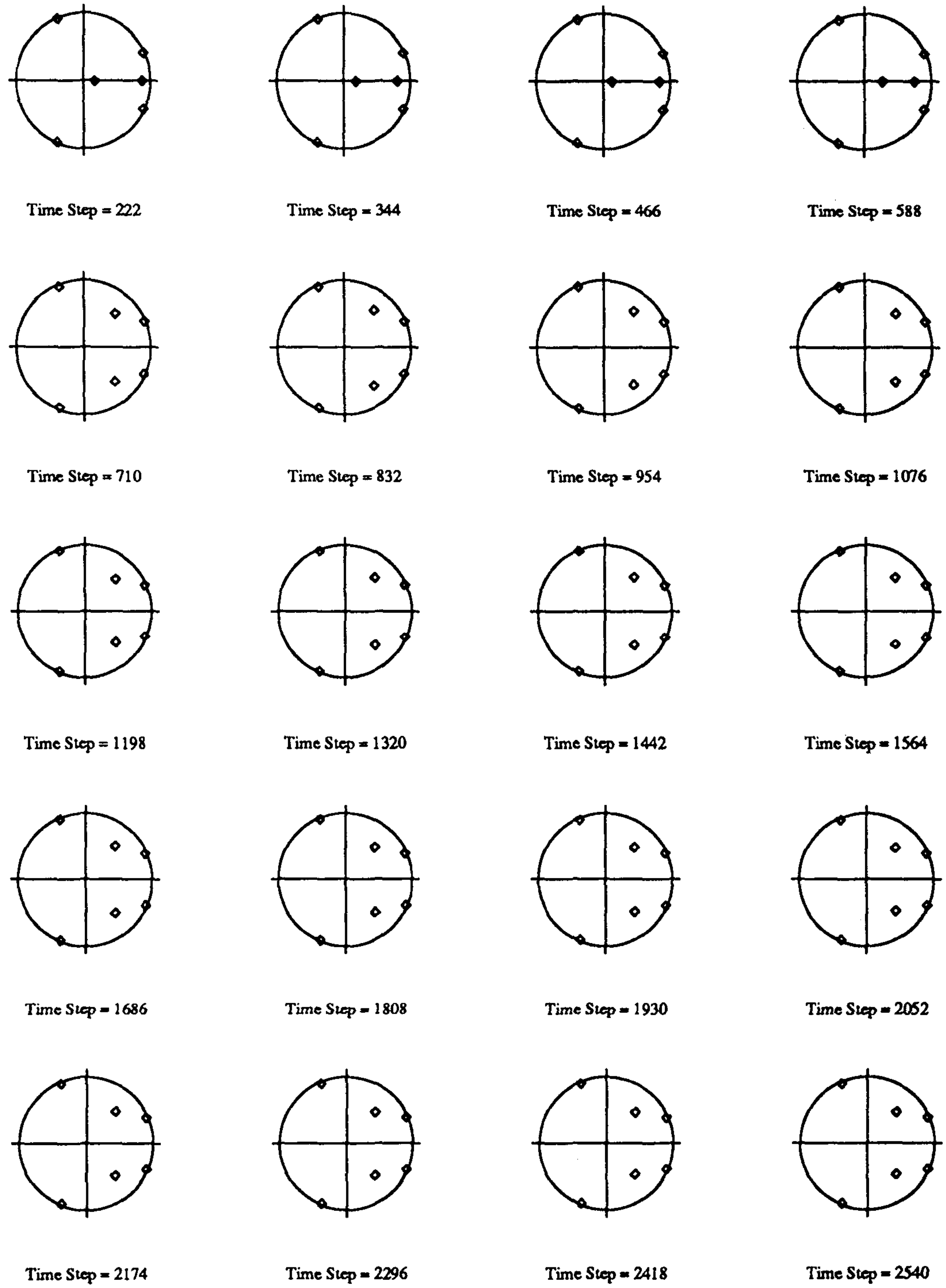


Figure 5.107

Recursive Least Squares Estimation
Three Story Building Model; El-Centro Input
3rd Floor variable alpha=0.99

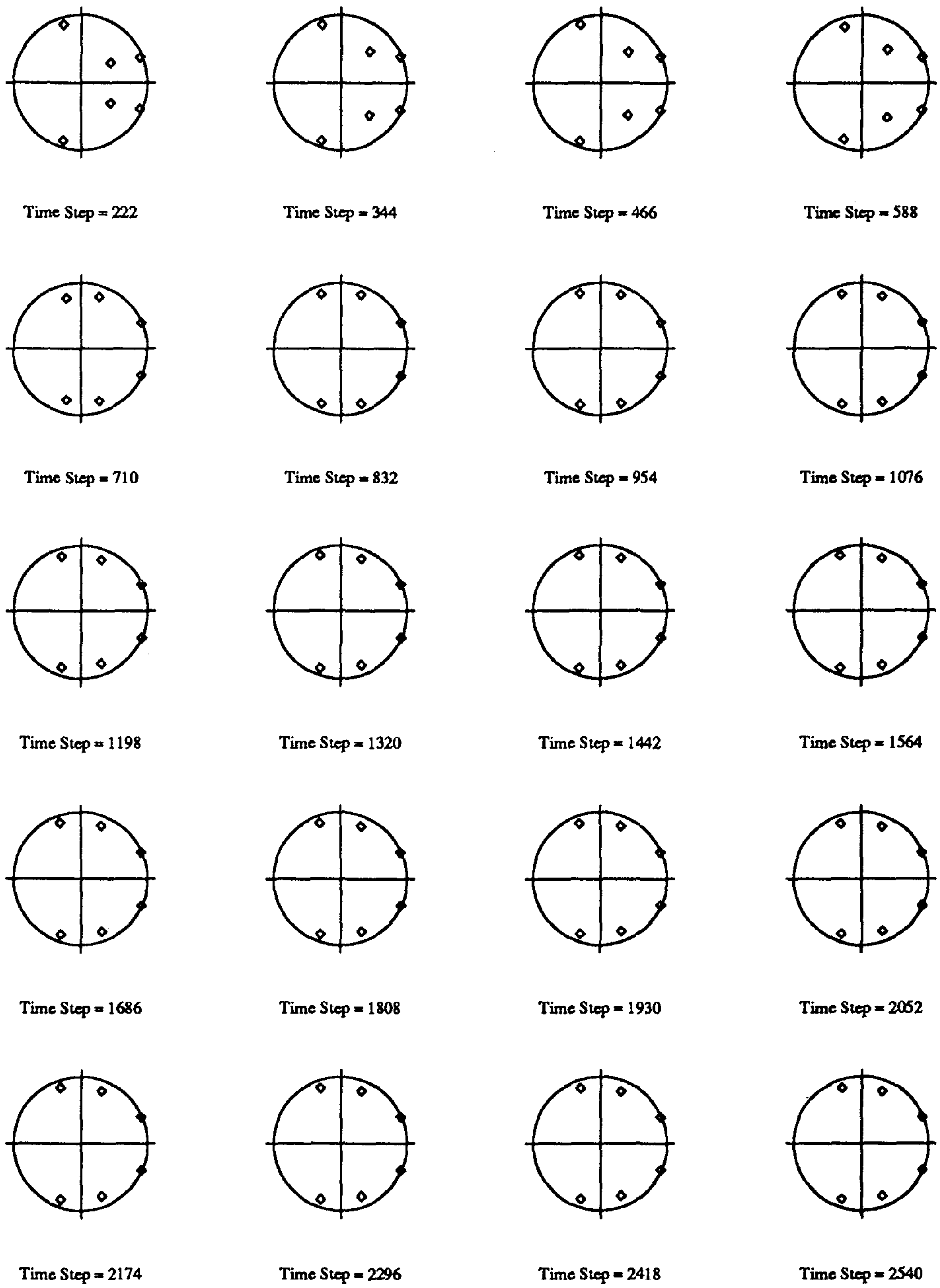


Figure 5.108

# Recursive Least Squares Estimation

## Three Story Building Model;  Sine Sweep Input

1st Floor    variable alpha=0.99

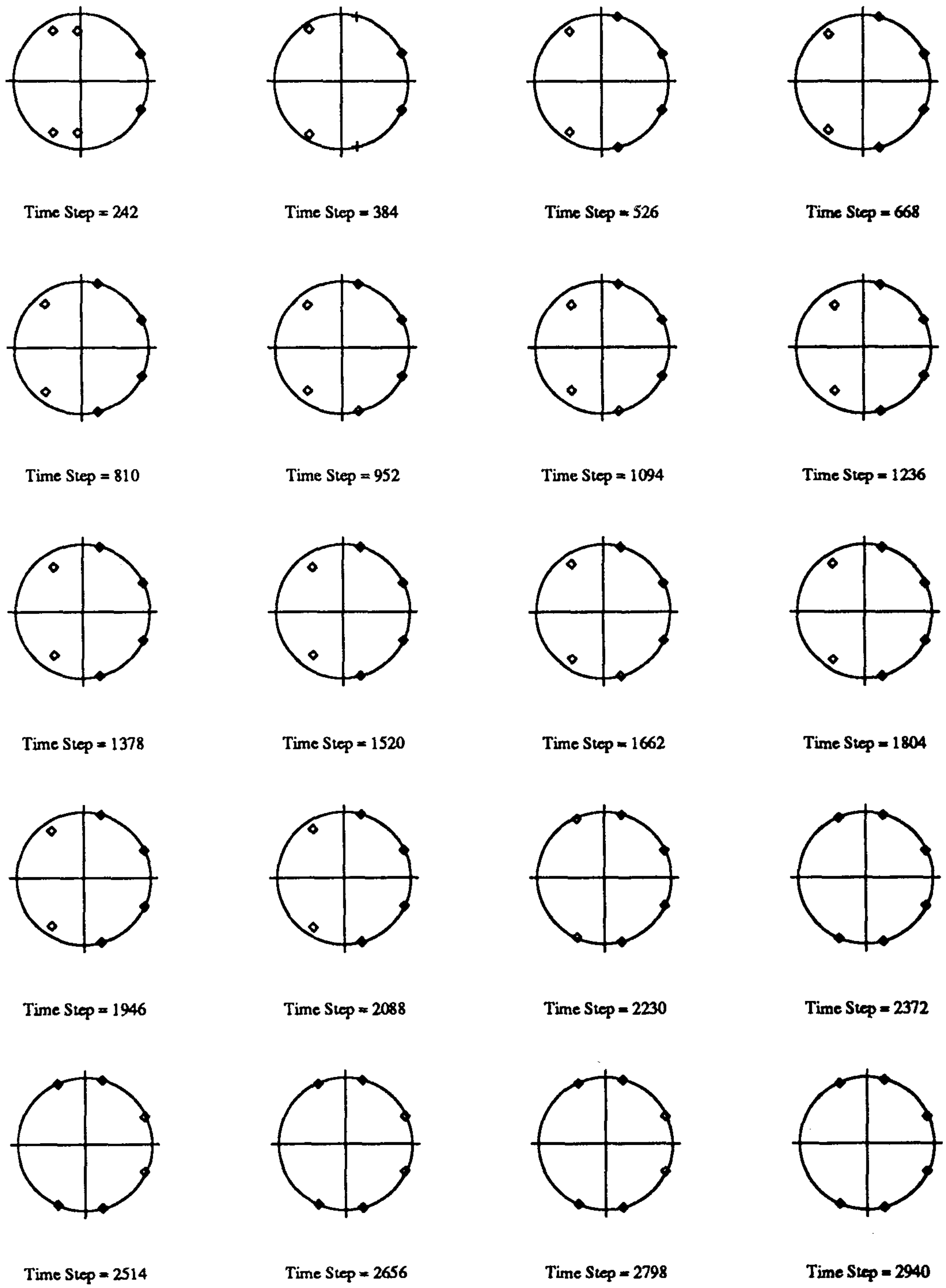


**Figure 5.109**

## Recursive Least Squares Estimation
## Three Story Building Model; Sine Sweep Input

2nd Floor variable alpha=0.99

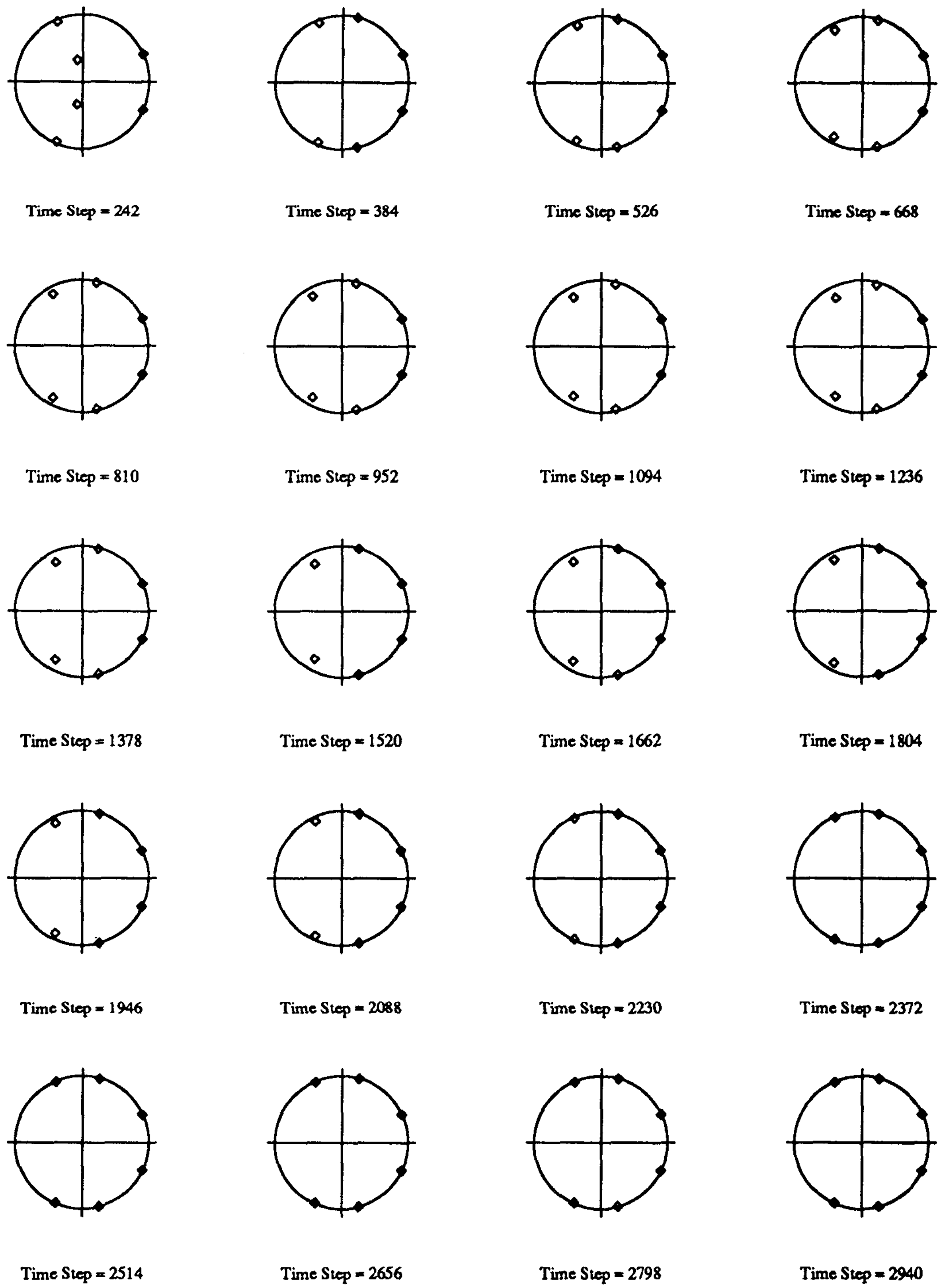


Figure 5.110

Recursive Least Squares Estimation
Three Story Building Model; Sine Sweep Input
3rd Floor variable alpha=0.99

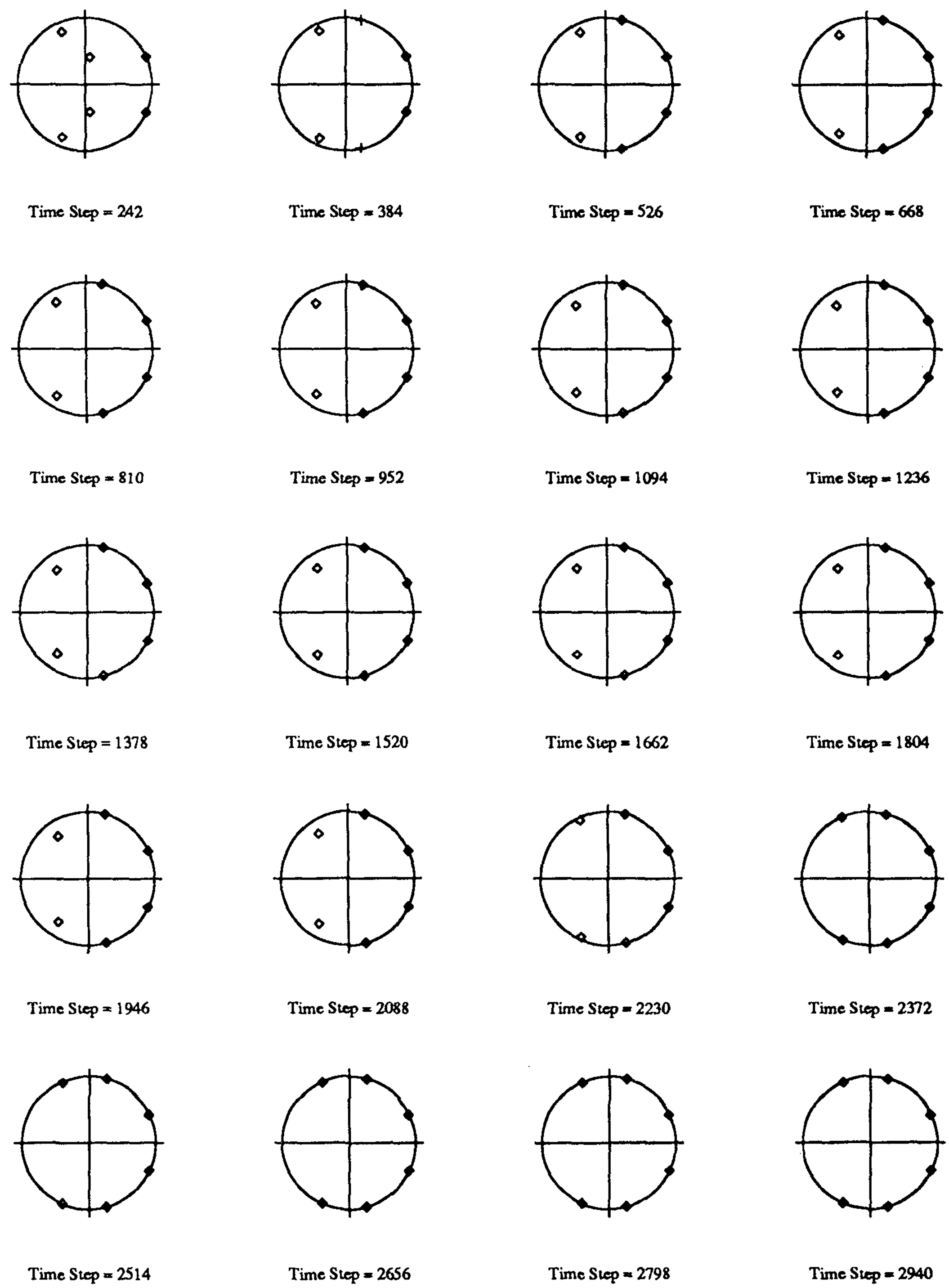


Figure 5.111

Recursive Least Squares Estimation
Three Story Building Model; White Noise Input
1st Floor variable alpha=0.99

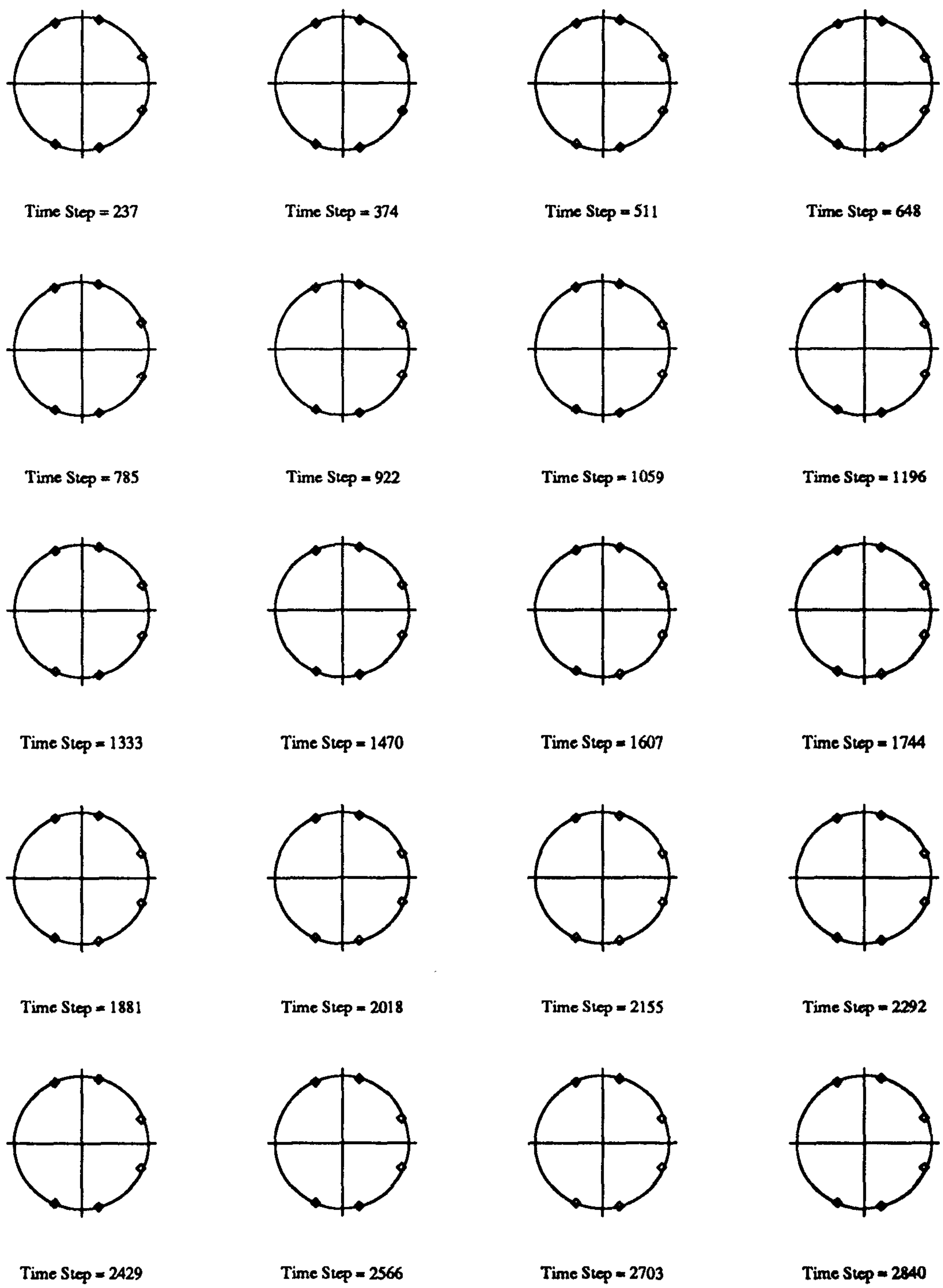


Figure 5.112

## Recursive Least Squares Estimation
## Three Story Building Model; White Noise Input
### 2nd Floor variable alpha=0.99

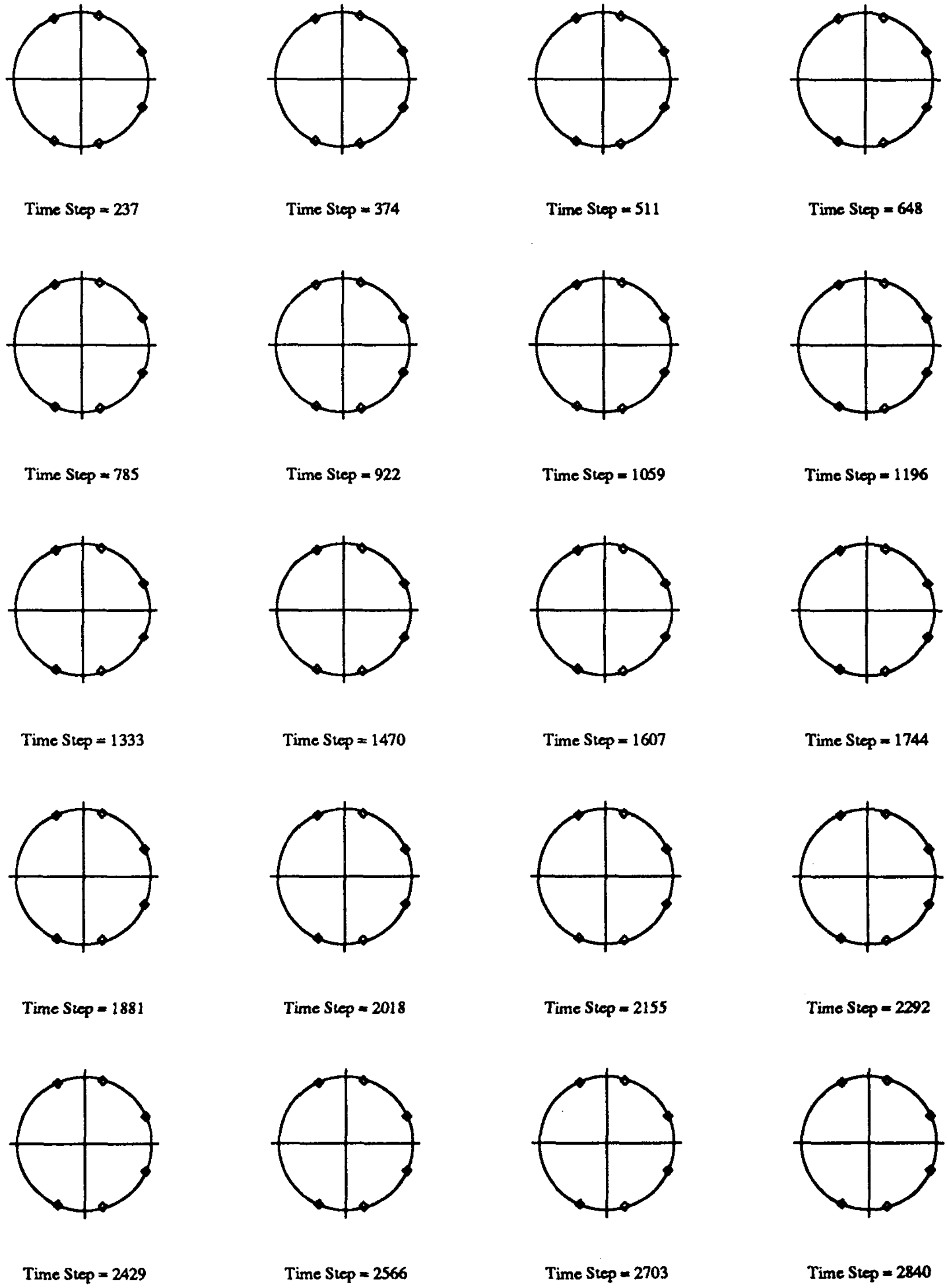


**Figure 5.113**

## Recursive Least Squares Estimation
## Three Story Building Model; White Noise Input
### 3rd Floor variable alpha=0.99

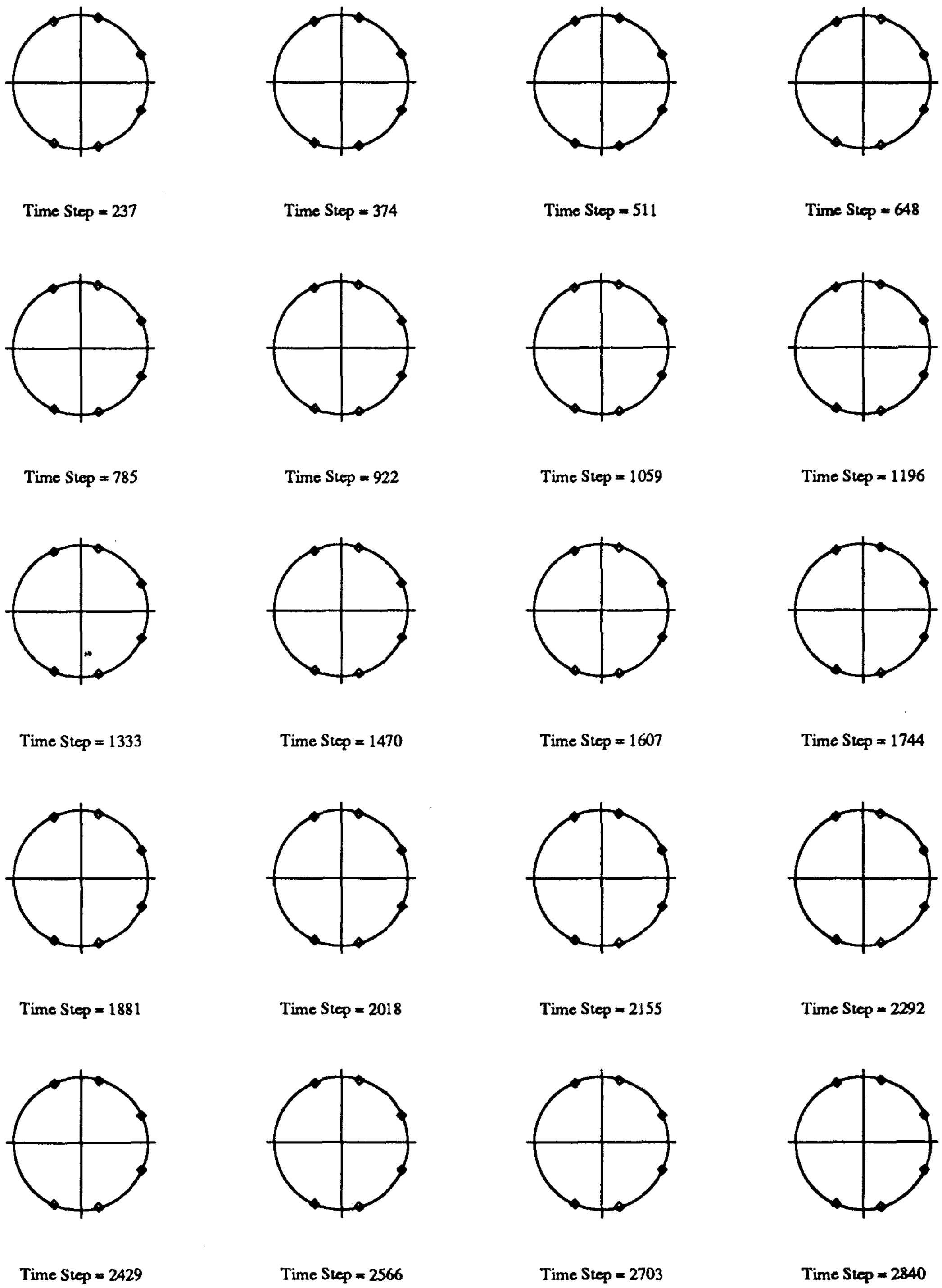


Figure 5.114

Recursive Instrumental Variable Estimation
Five Story Building Model;   El-Centro Input
1st Floor

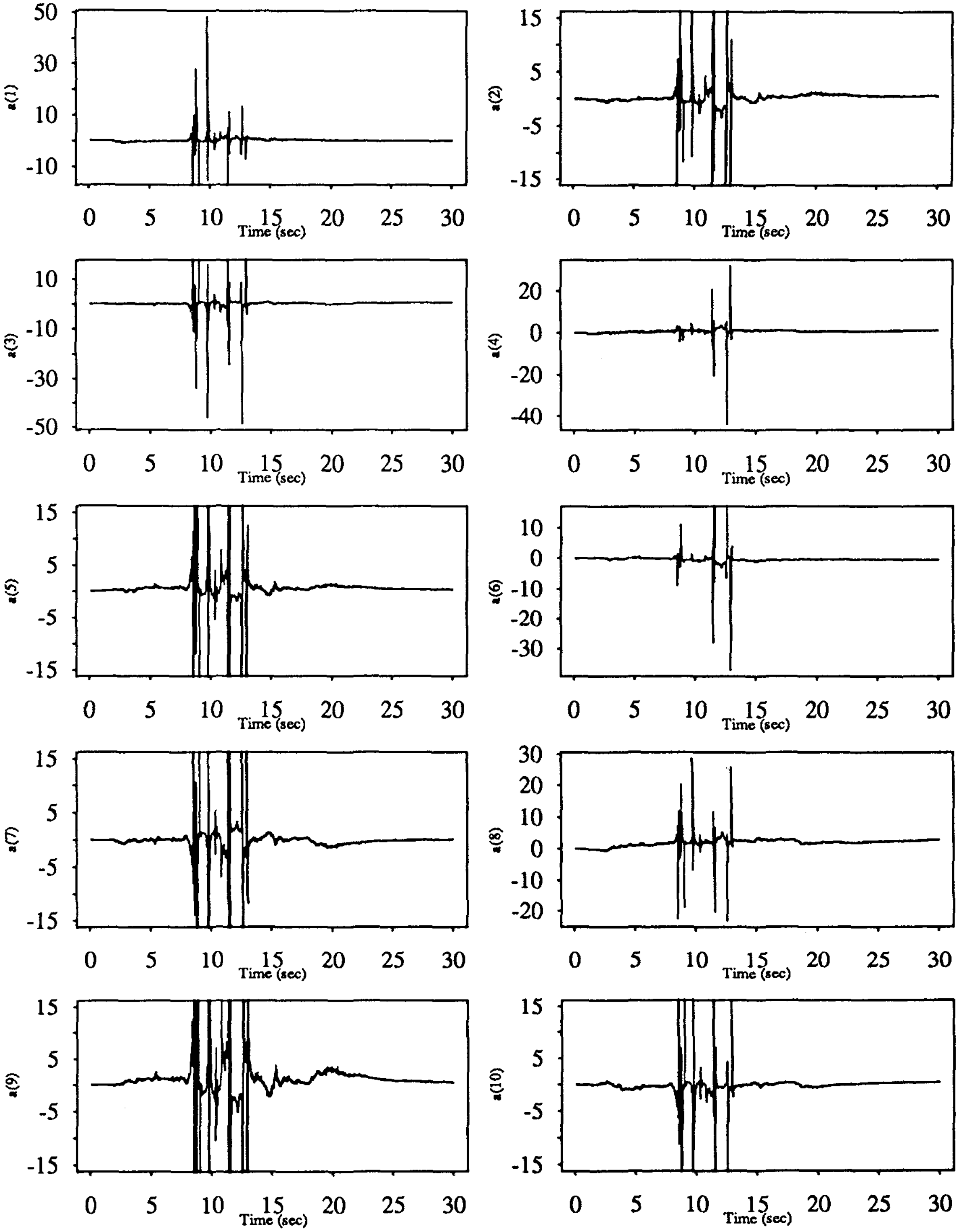


Figure 5.115

Recursive Instrumental Variable Estimation
Five Story Building Model; El-Centro Input
2nd Floor

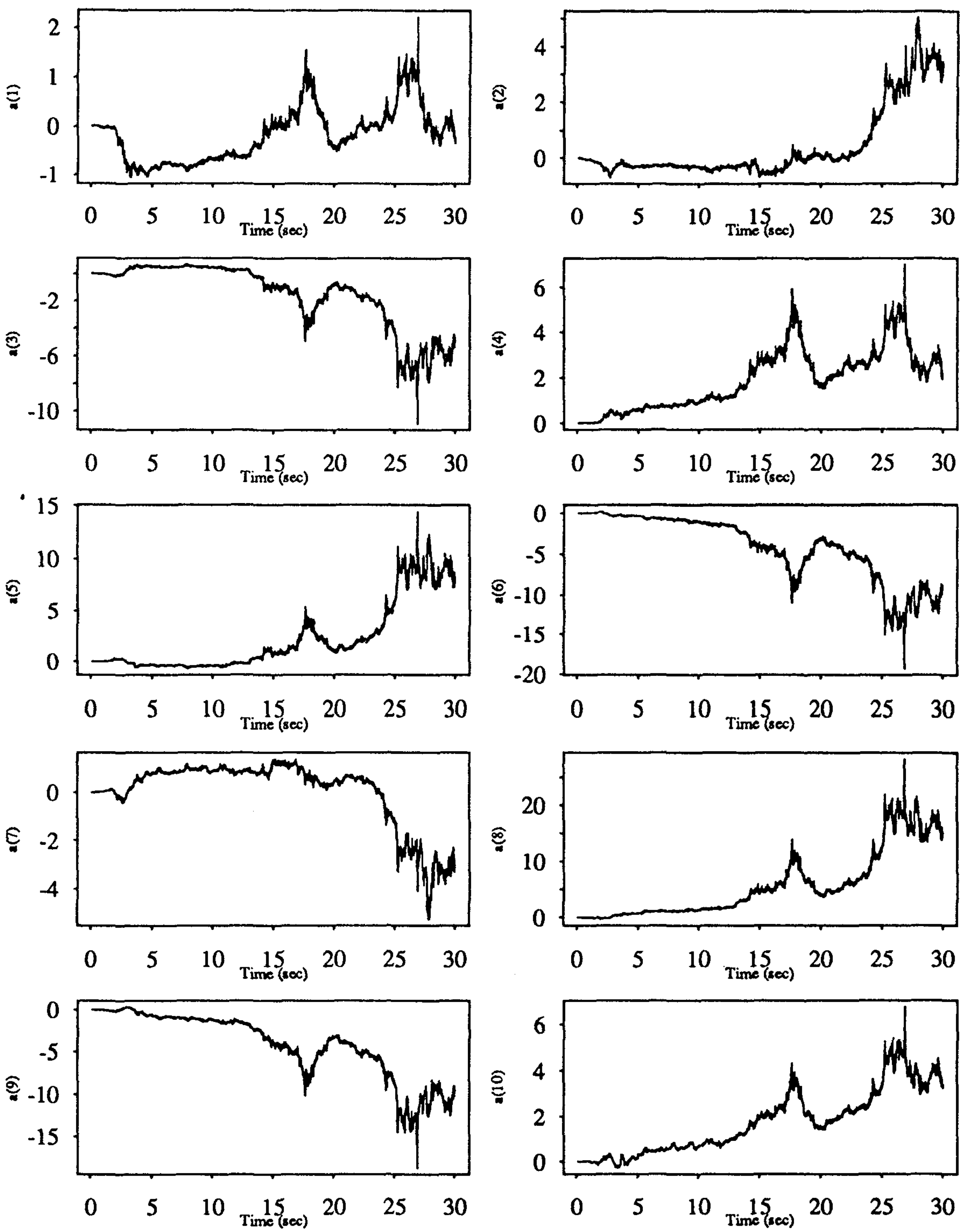


Figure 5.116

## Recursive Instrumental Variable Estimation
## Five Story Building Model; El-Centro Input

3rd Floor

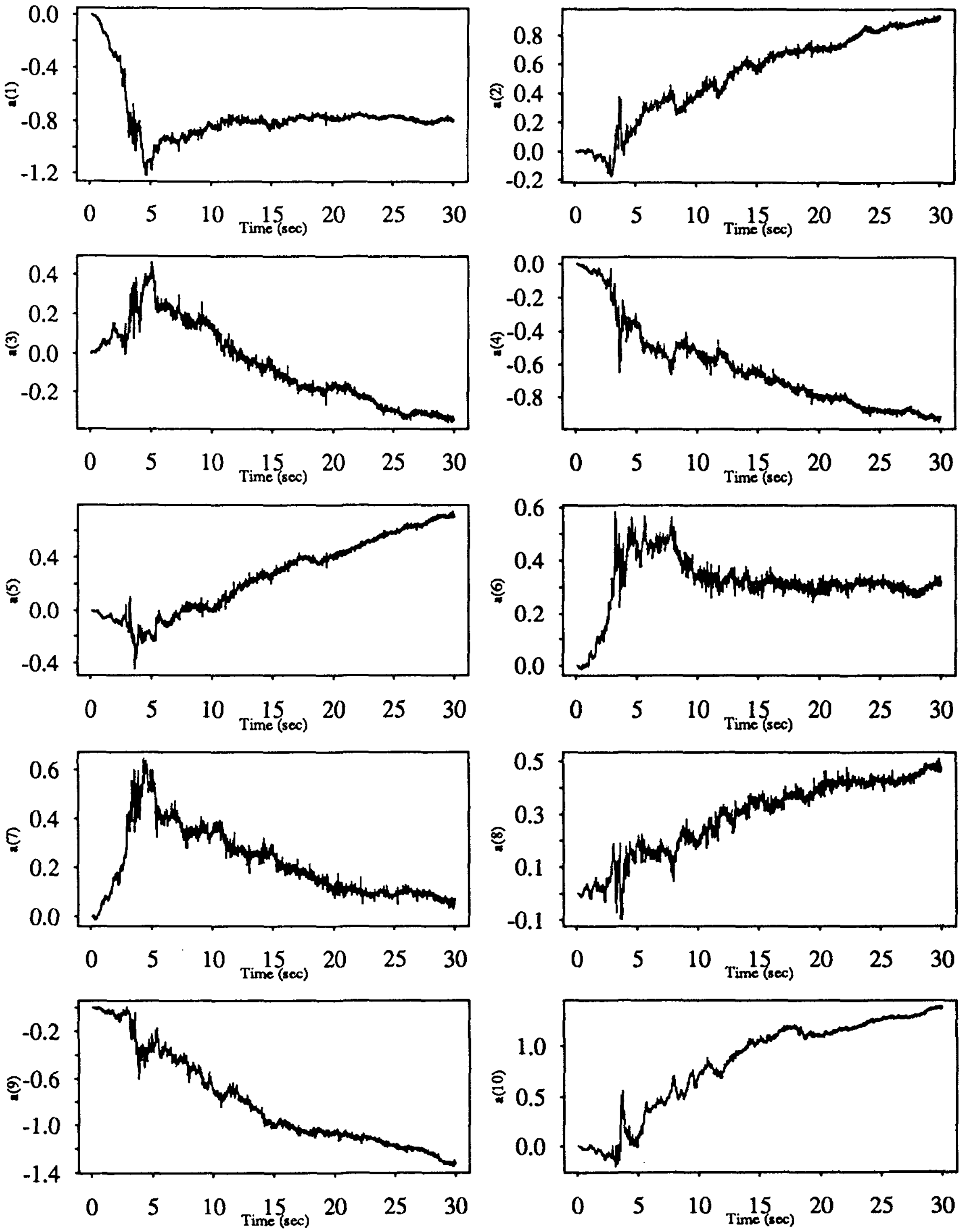


Figure 5.117

## Recursive Instrumental Variable Estimation
## Five Story Building Model; El-Centro Input

4th Floor

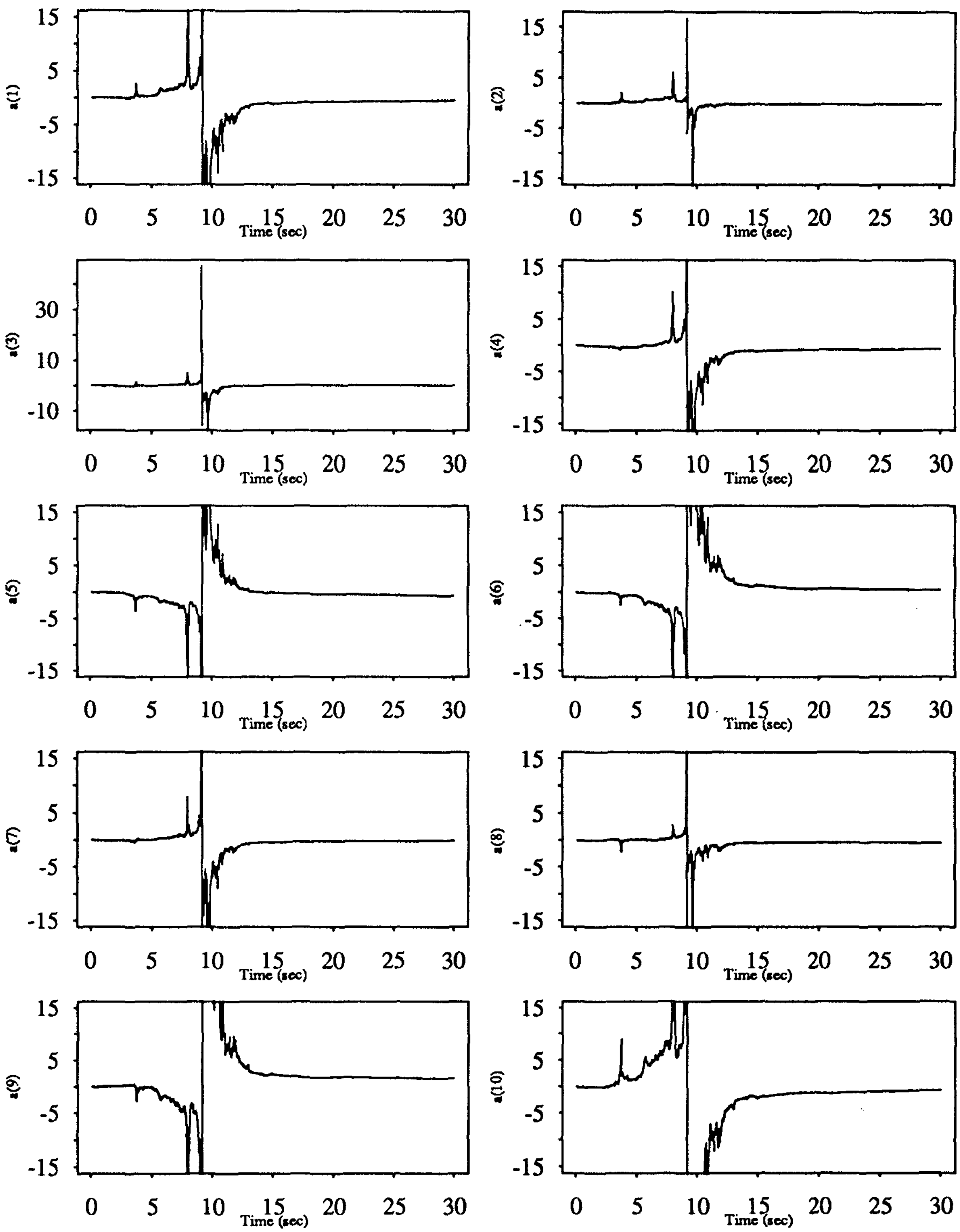


**Figure 5.118**

Recursive Instrumental Variable Estimation
Five Story Building Model; El-Centro Input
5th Floor

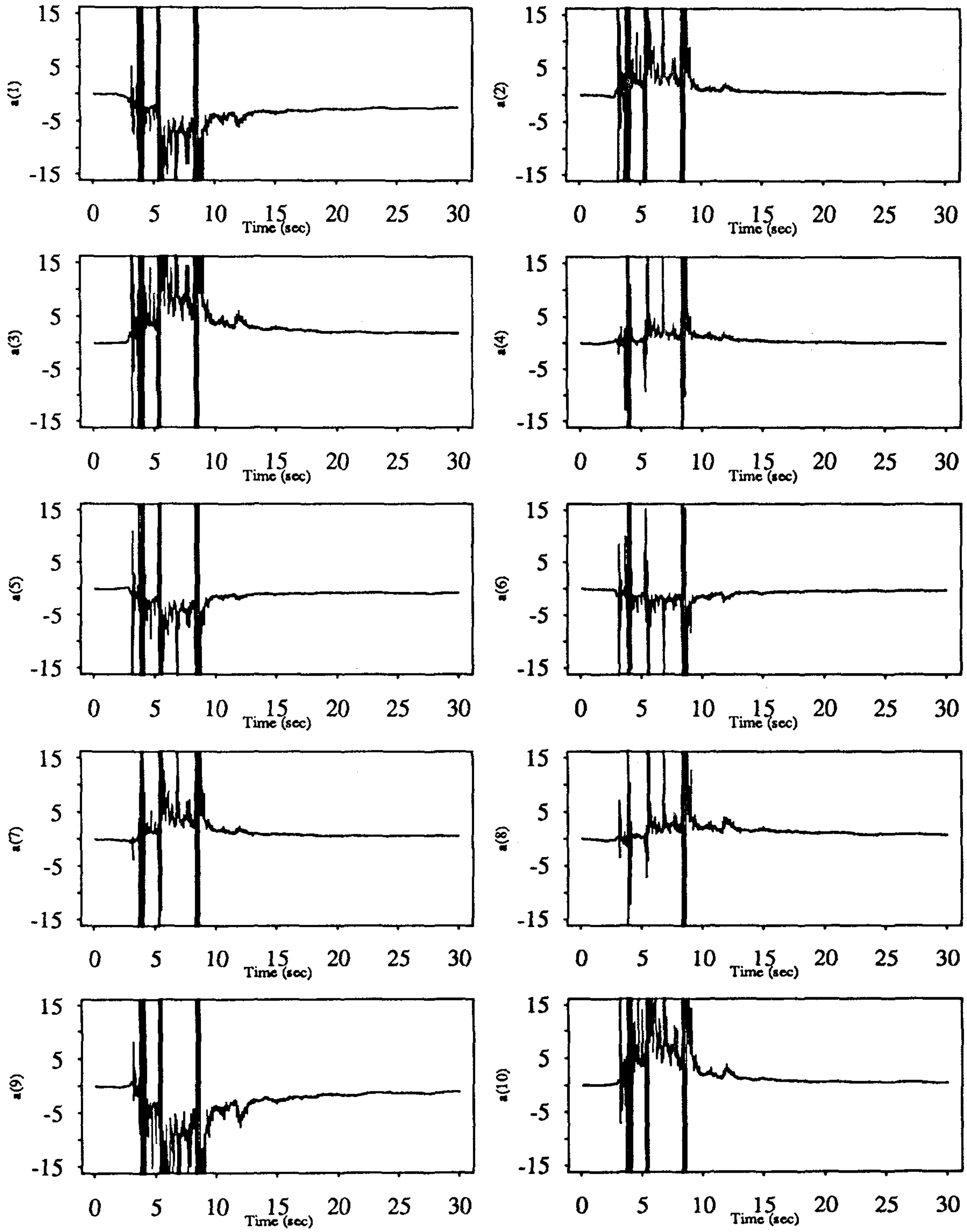


Figure 5.119

## Recursive Instrumental Variable Estimation
## Five Story Building Model; White Noise Input

1st Floor

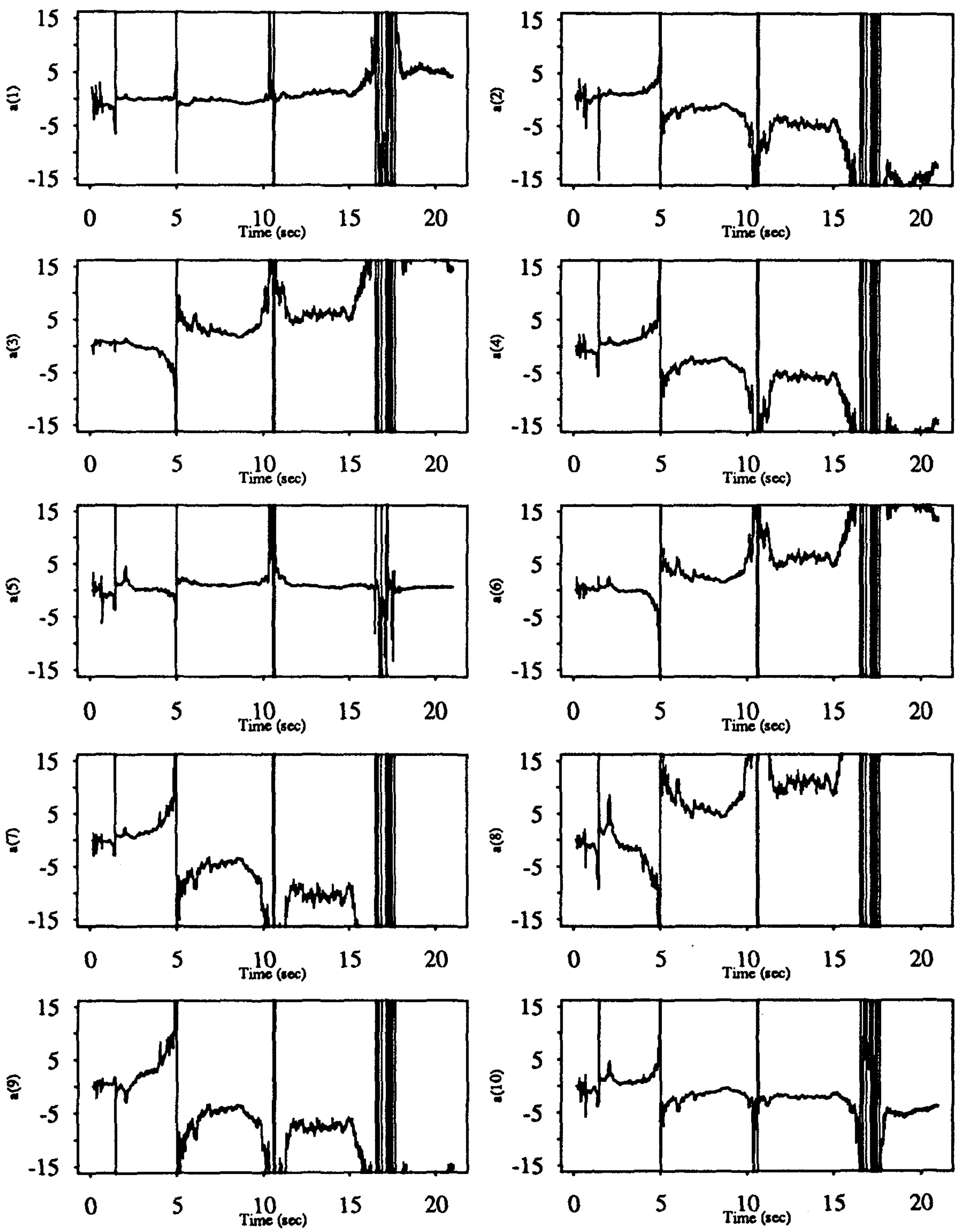


Figure 5.120

Recursive Instrumental Variable Estimation
Five Story Building Model; White Noise Input

2nd Floor

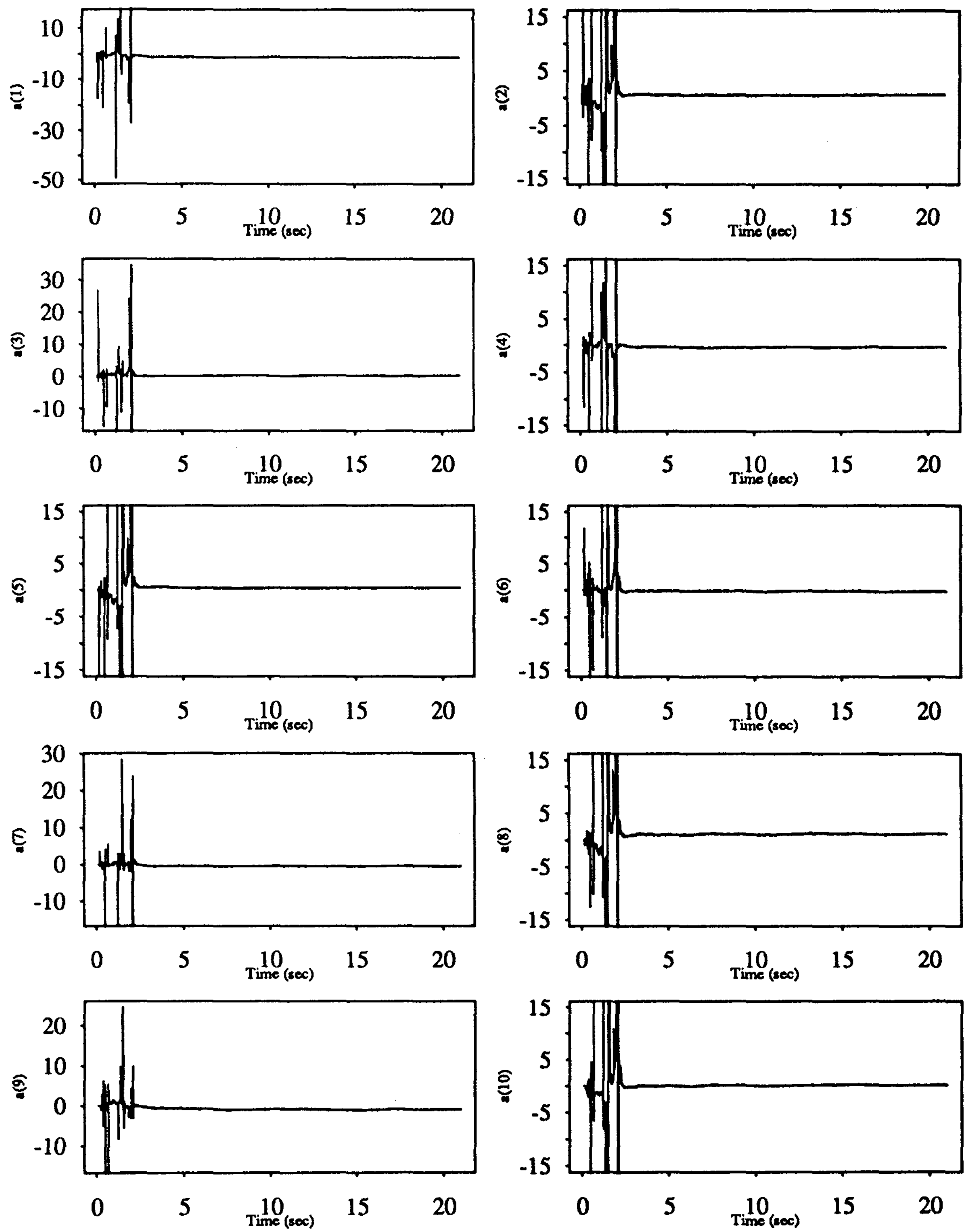


**Figure 5.121**

Recursive Instrumental Variable Estimation
Five Story Building Model; White Noise Input
3rd Floor

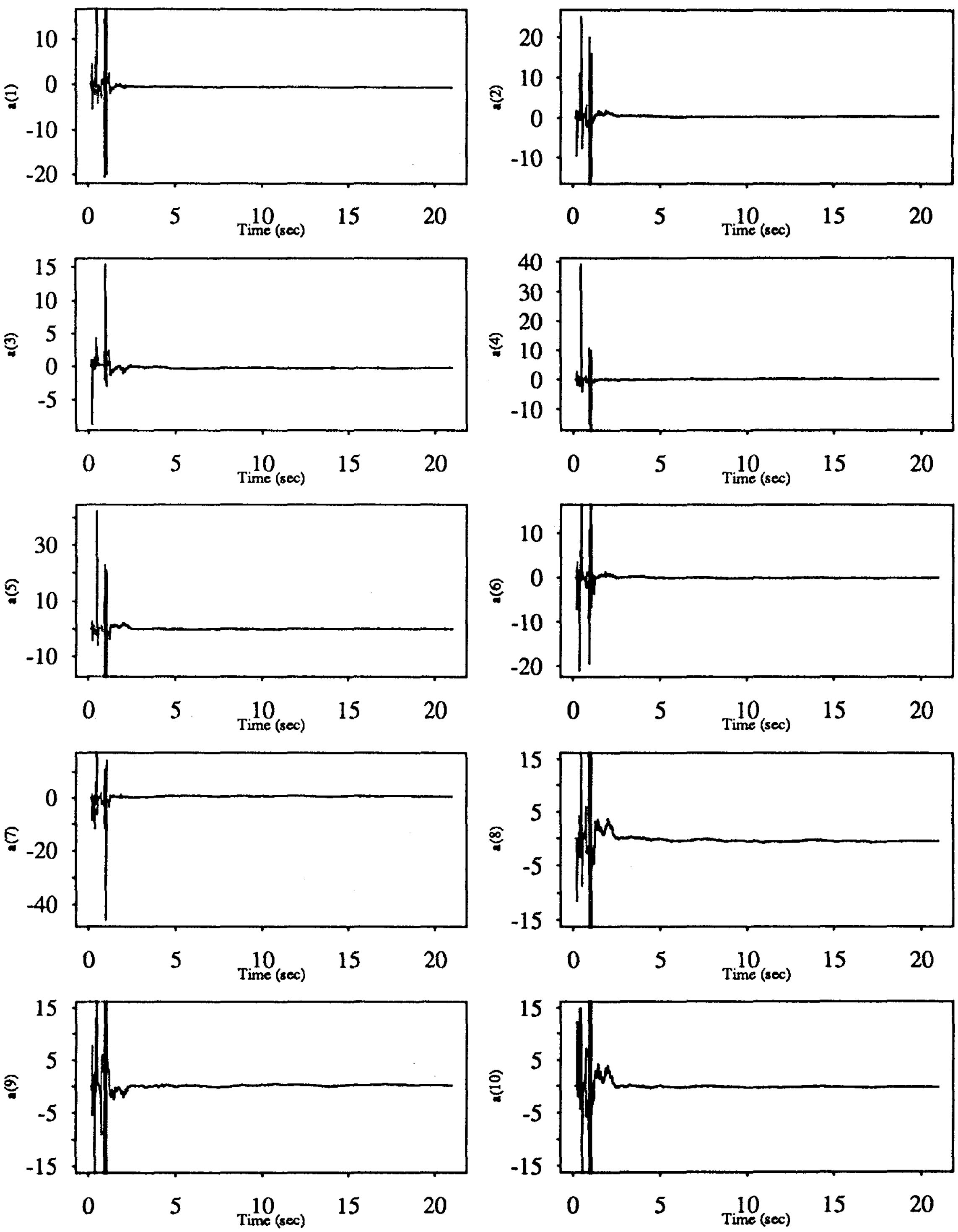


Figure 5.122

Recursive Instrumental Variable Estimation
Five Story Building Model; White Noise Input

4th Floor

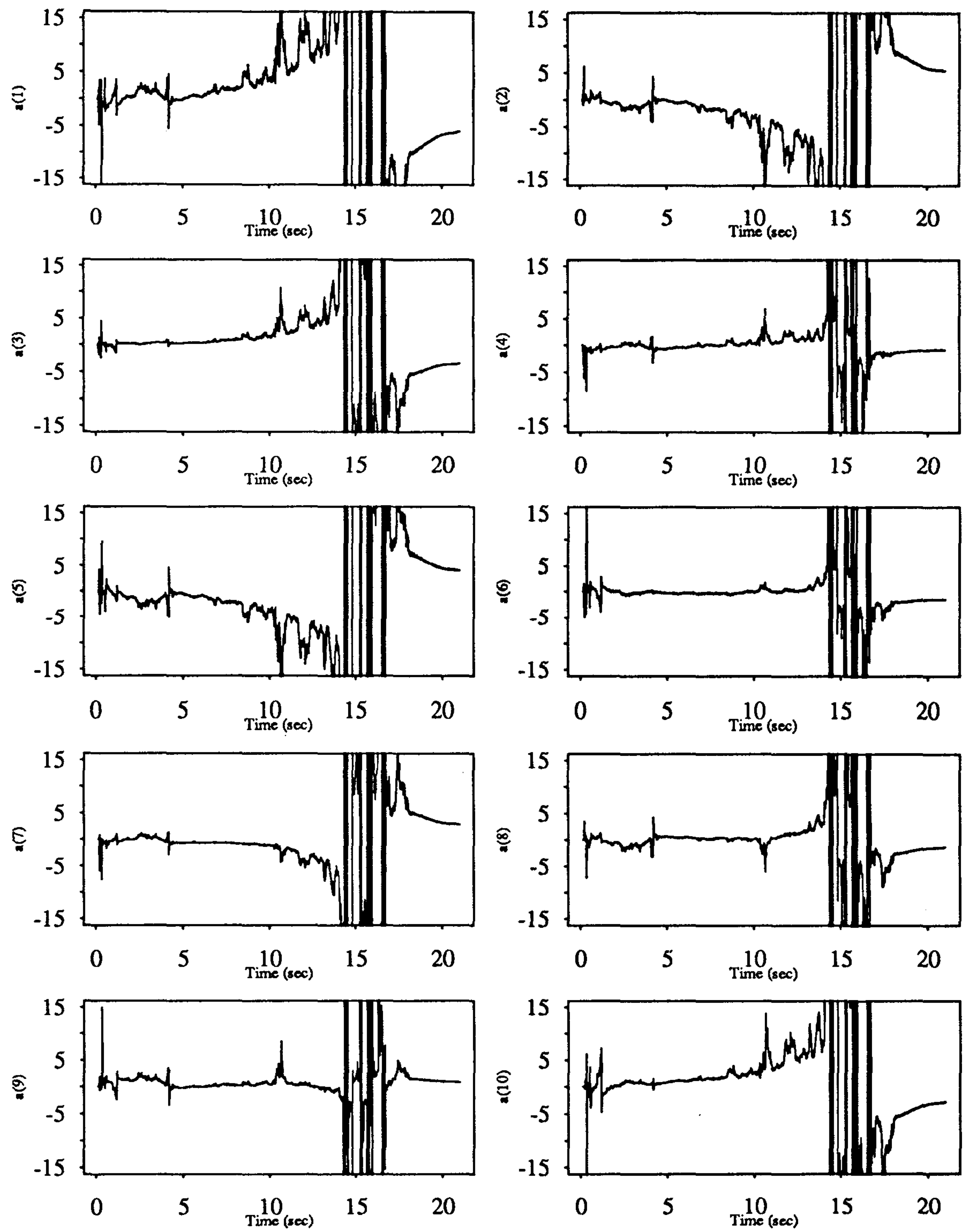


Figure 5.123

## Recursive Instrumental Variable Estimation
## Five Story Building Model; White Noise Input
### 5th Floor

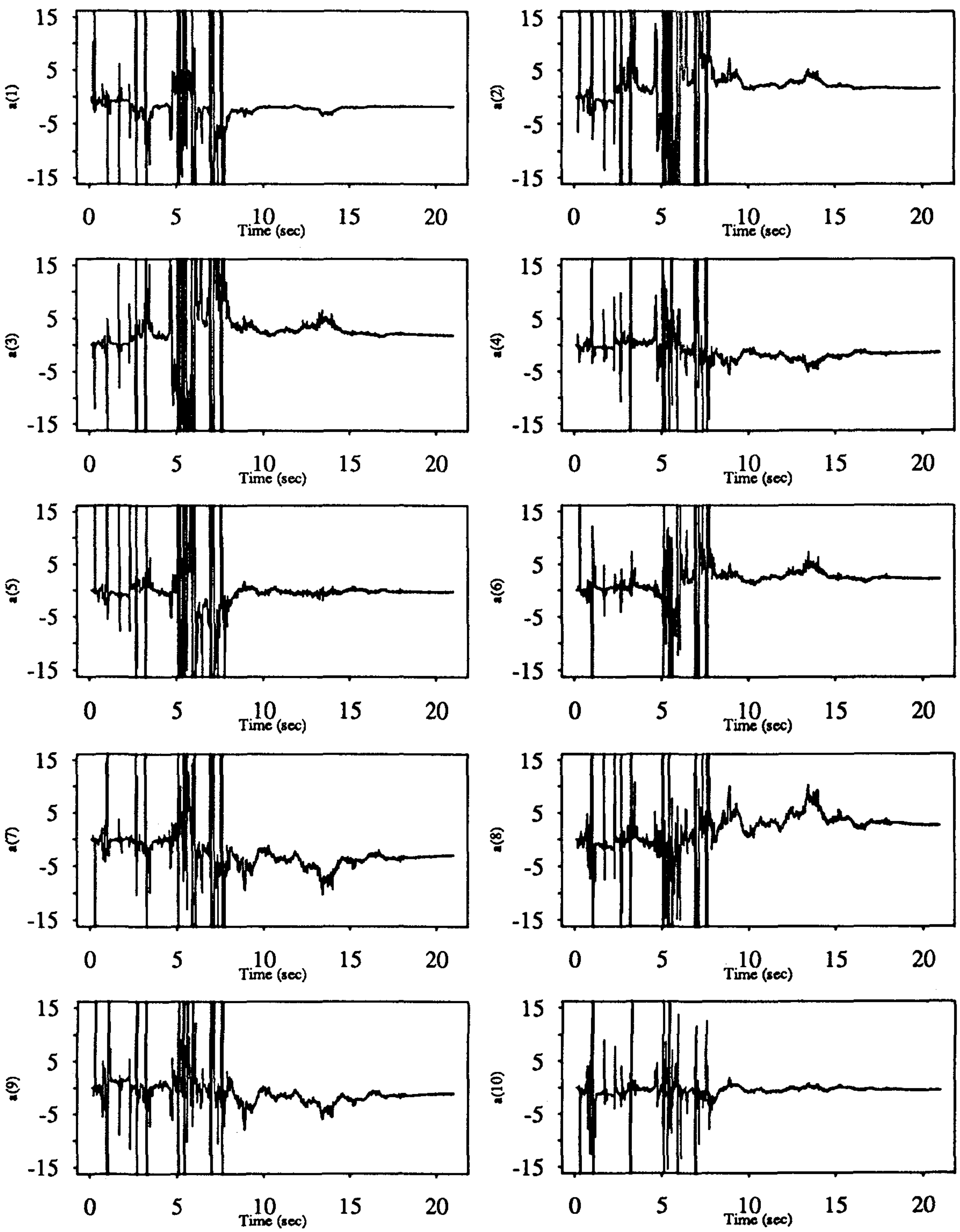


Figure 5.124

## Recursive Instrumental Variable Estimation
## Five Story Building Model;  El-Centro Input
### 1st Floor

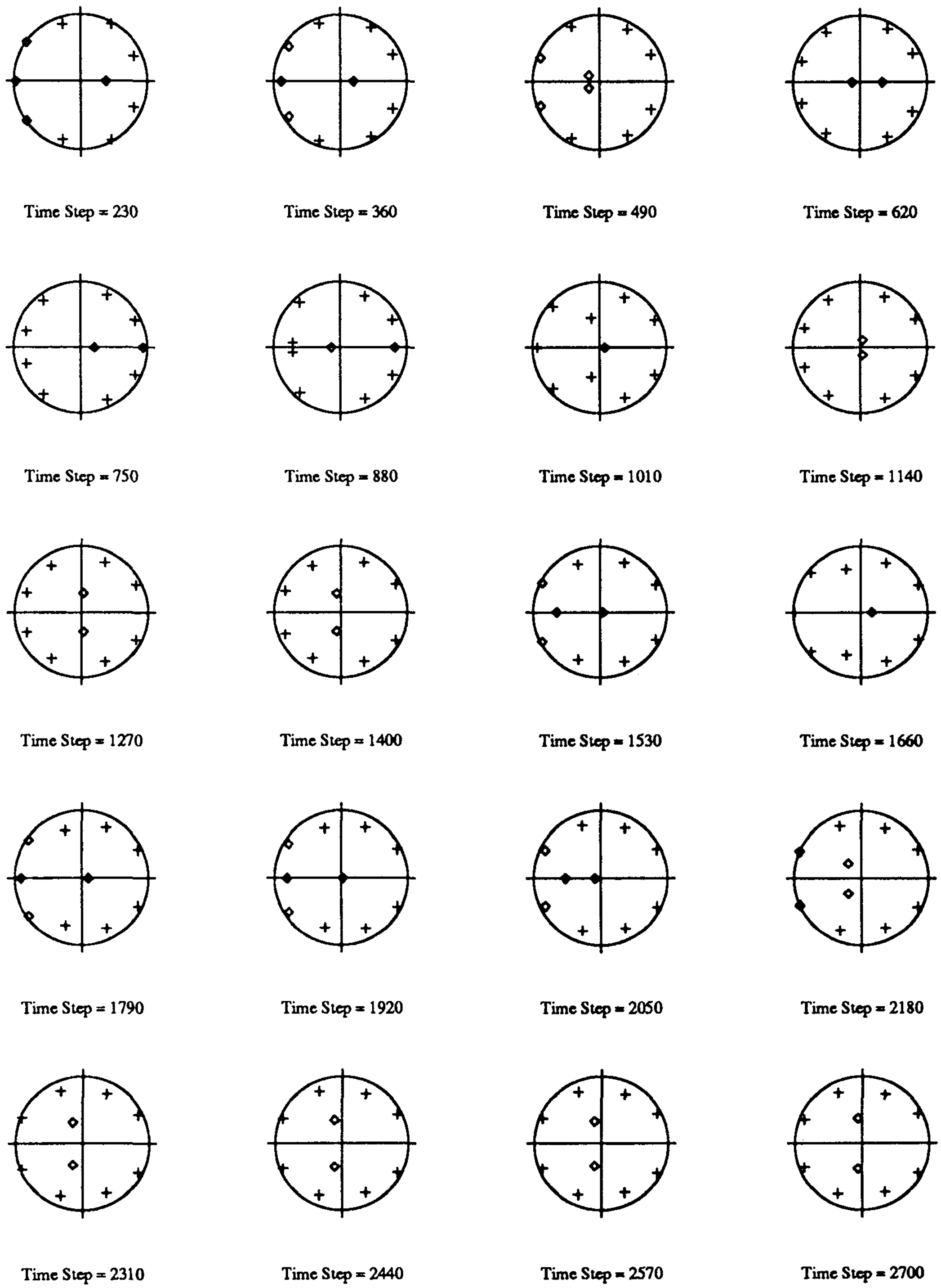


**Figure 5.125**

# Recursive Instrumental Variable Estimation
## Five Story Building Model; El-Centro Input
### 2nd Floor

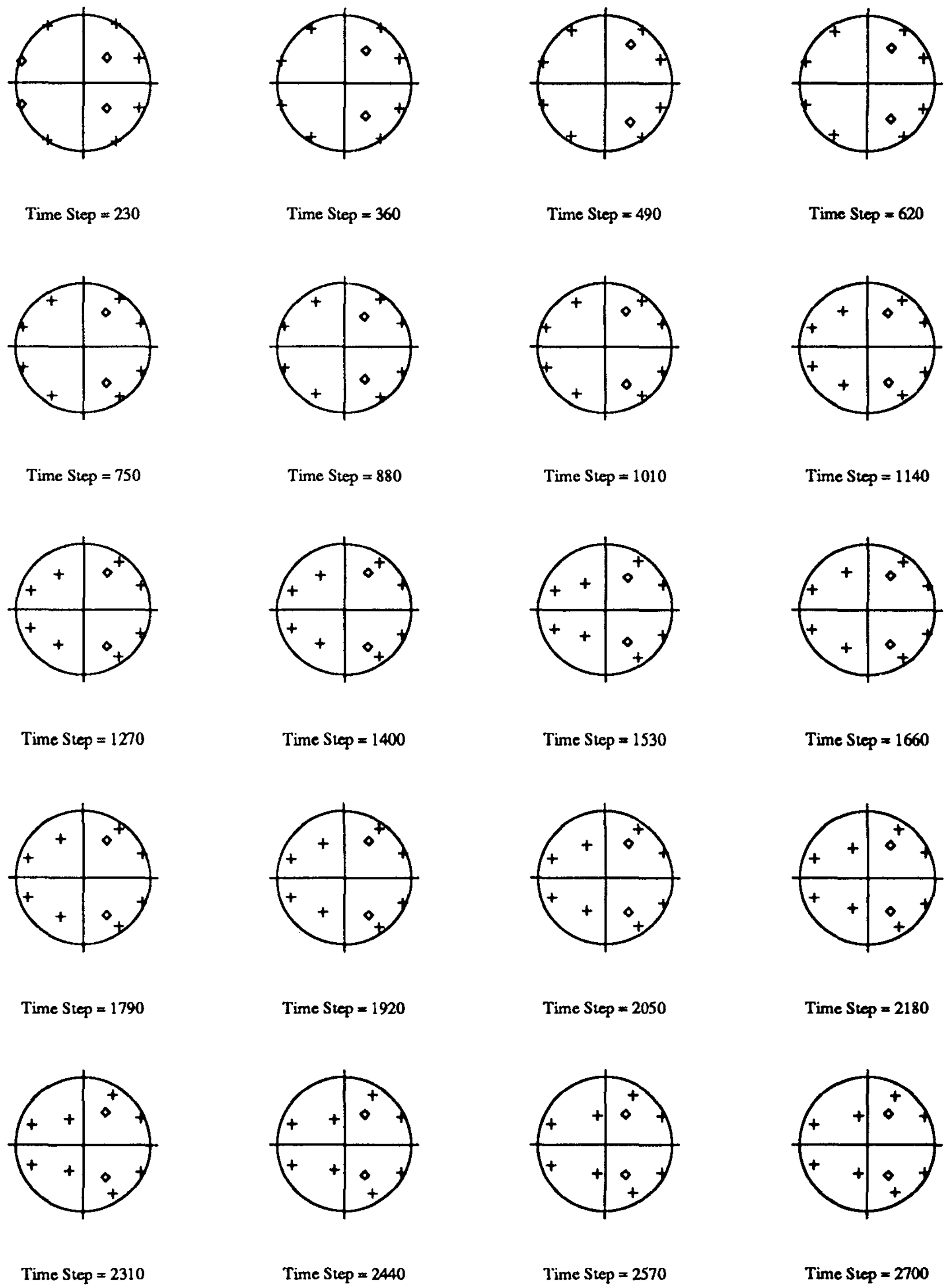


**Figure 5.126**

# Recursive Instrumental Variable Estimation
## Five Story Building Model; El-Centro Input
### 3rd Floor

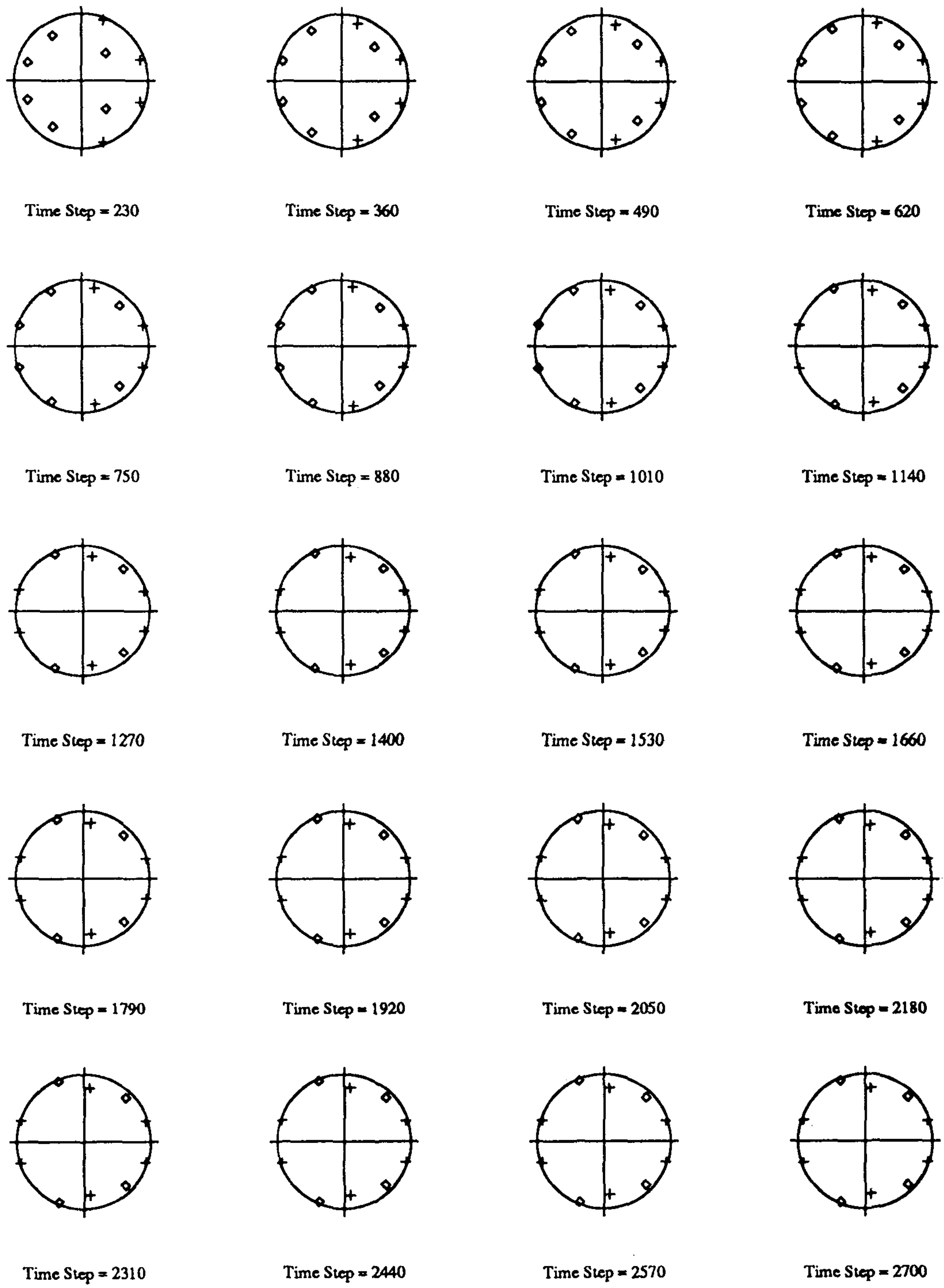


Figure 5.127

## Recursive Instrumental Variable Estimation
## Five Story Building Model; El-Centro Input
### 4th Floor

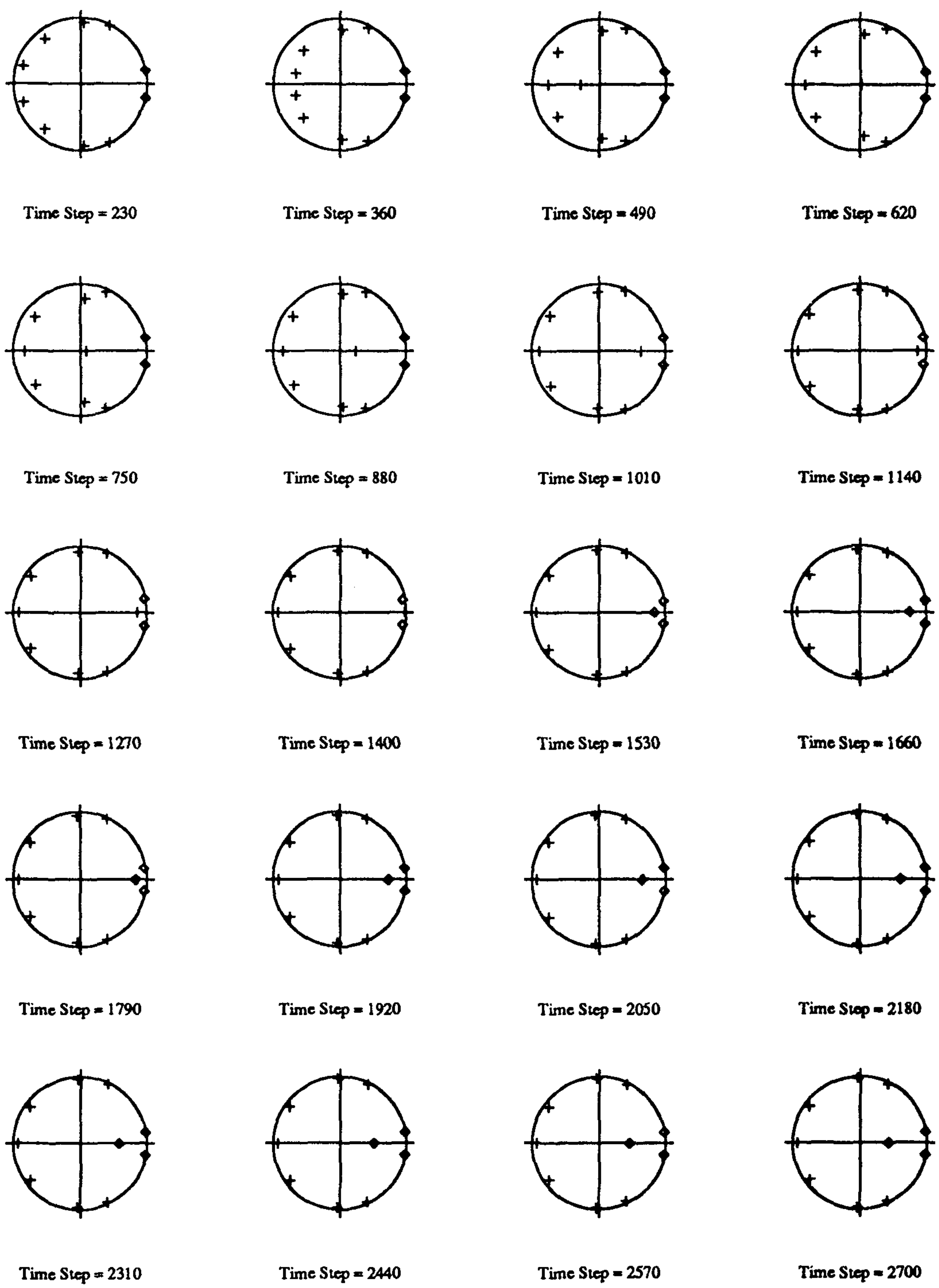


Figure 5.128

# Recursive Instrumental Variable Estimation
## Five Story Building Model;   El-Centro Input
### 5th Floor

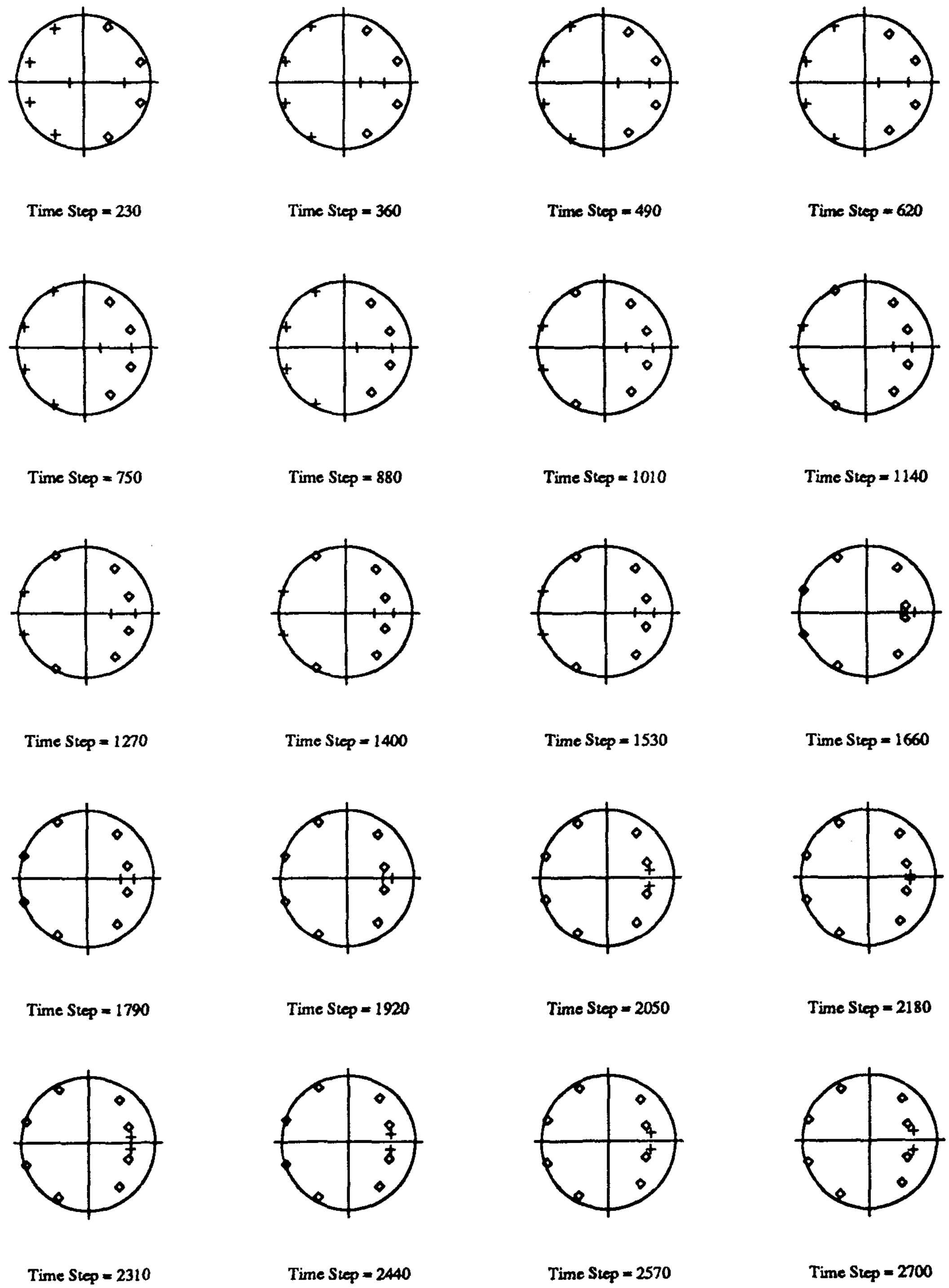


Figure 5.129

## Recursive Instrumental Variable Estimation
## Five Story Building Model; White Noise Input
### 1st Floor

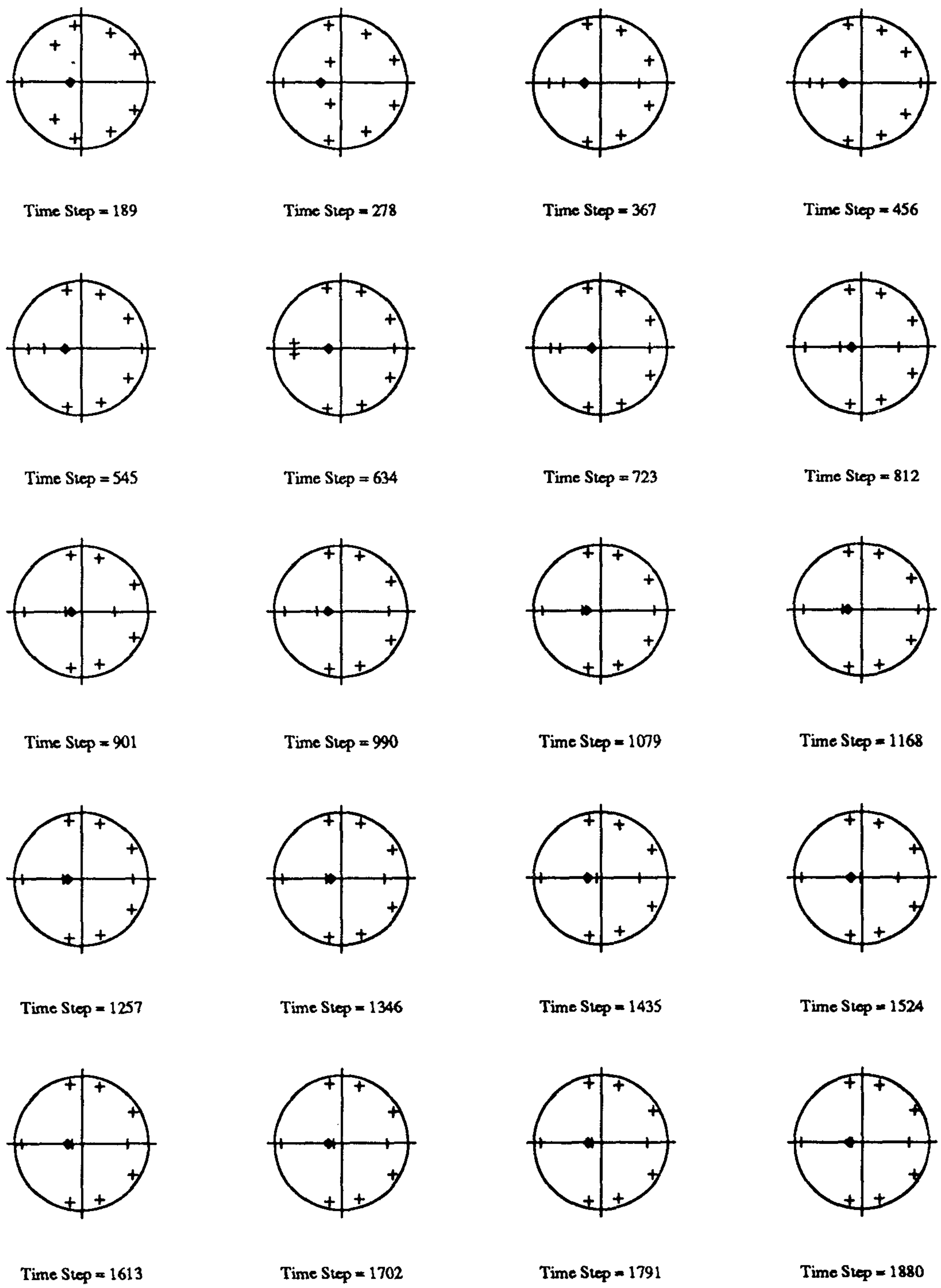


Figure 5.130

# Recursive Instrumental Variable Estimation
## Five Story Building Model; White Noise Input
### 2nd Floor

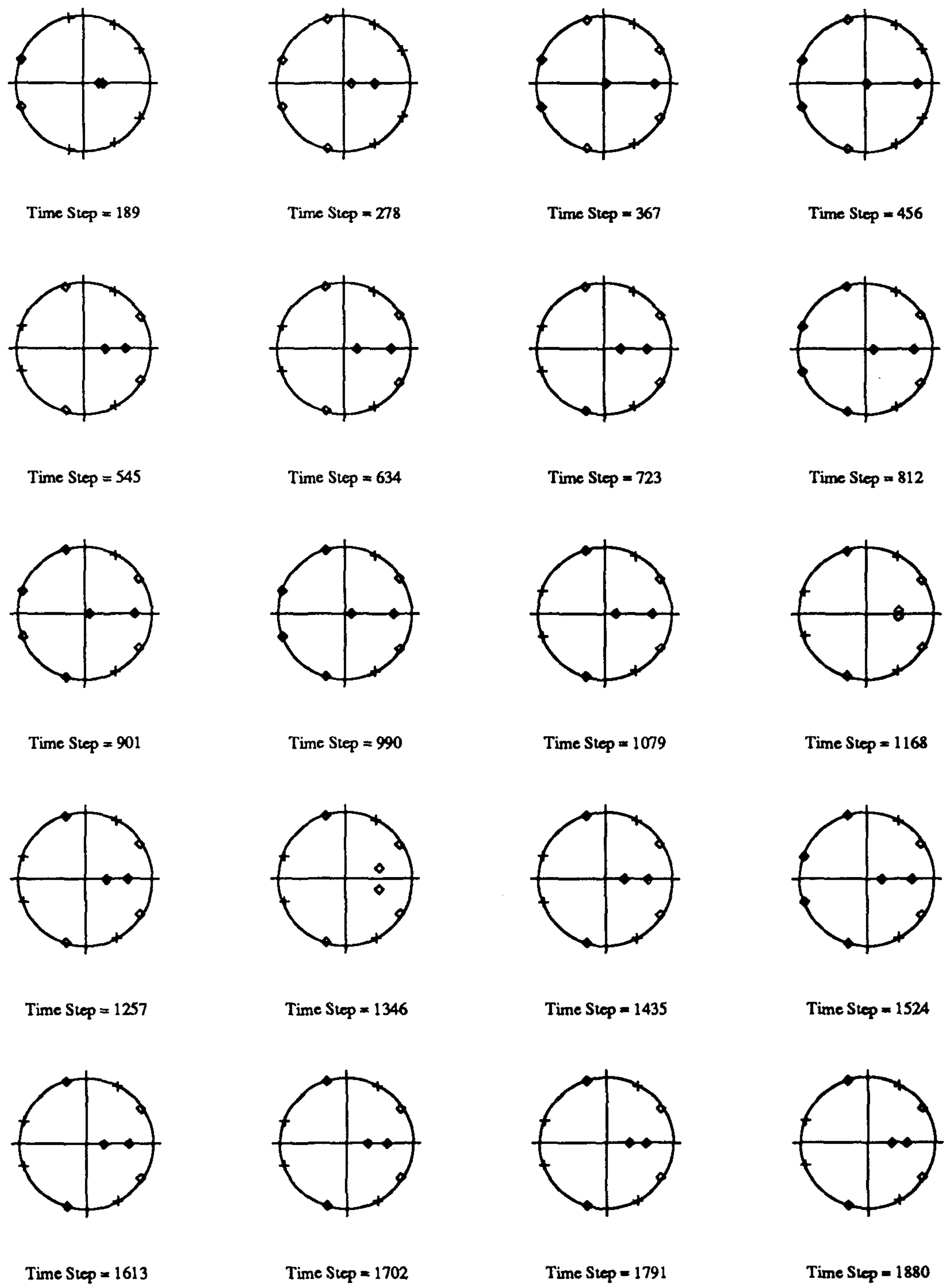


Figure 5.131

Recursive Instrumental Variable Estimation
Five Story Building Model; White Noise Input
3rd Floor

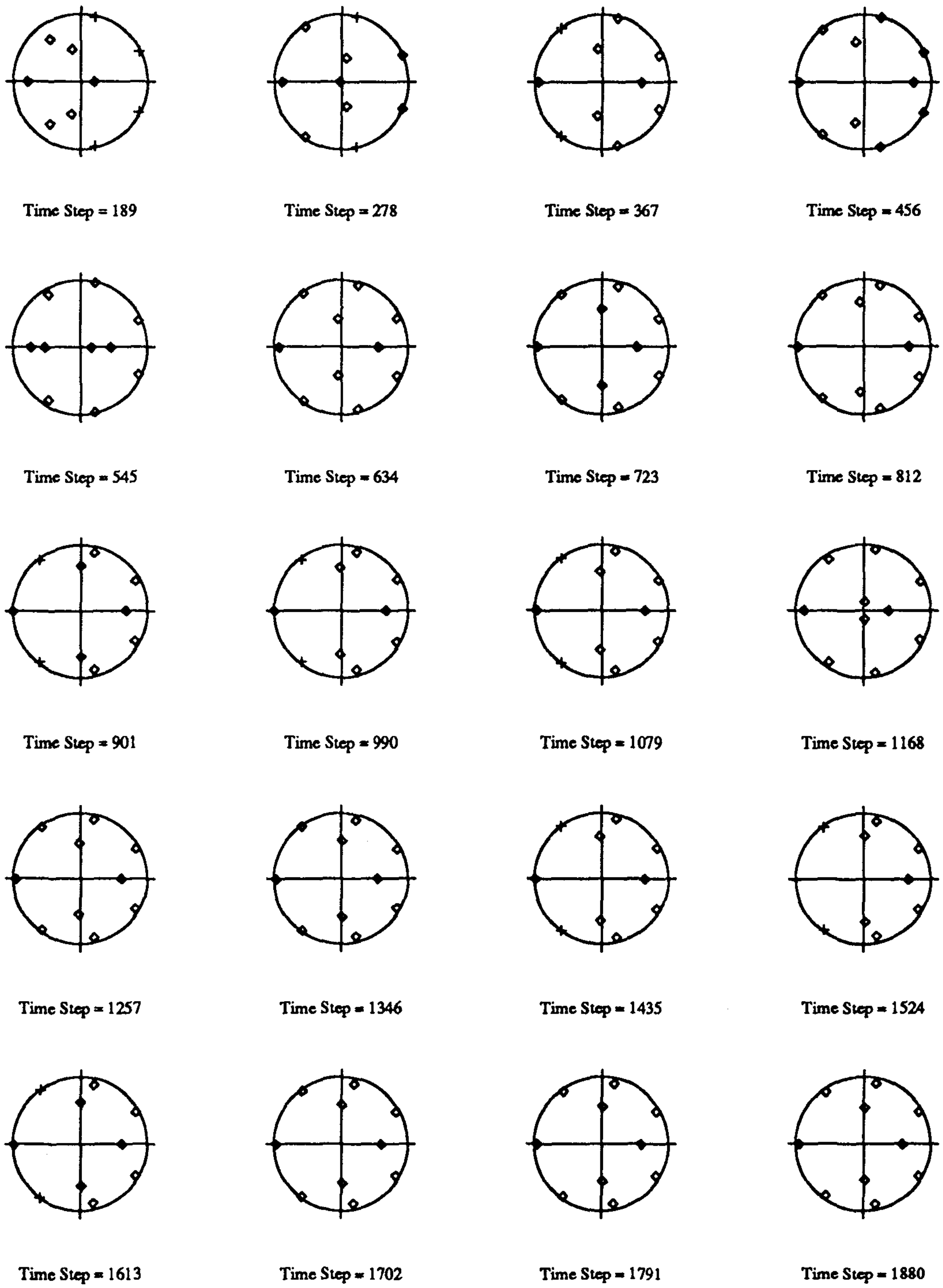


Figure 5.132

## Recursive Instrumental Variable Estimation
## Five Story Building Model; White Noise Input
### 4th Floor

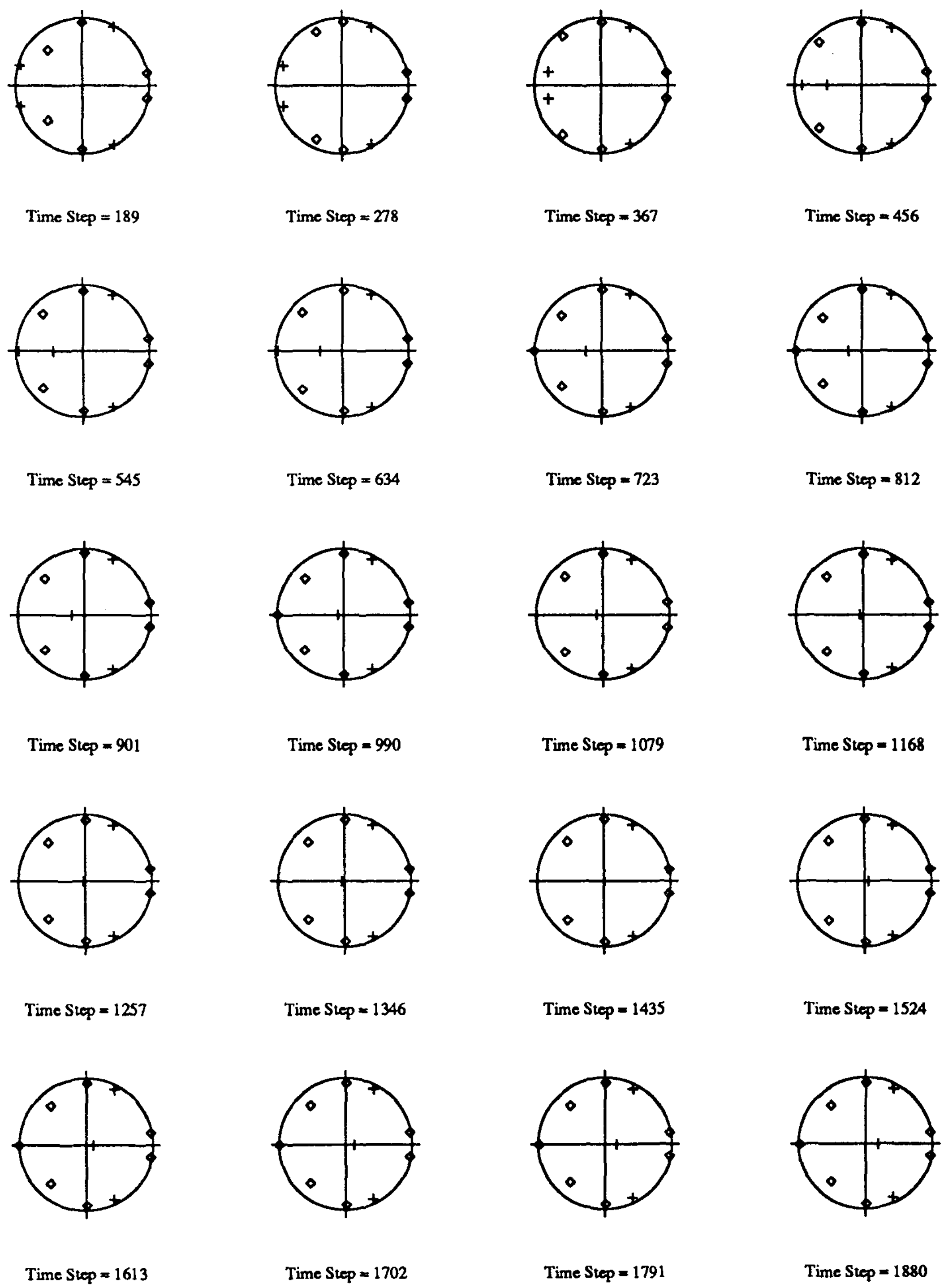


Figure 5.133

## Recursive Instrumental Variable Estimation
## Five Story Building Model; White Noise Input
### 5th Floor

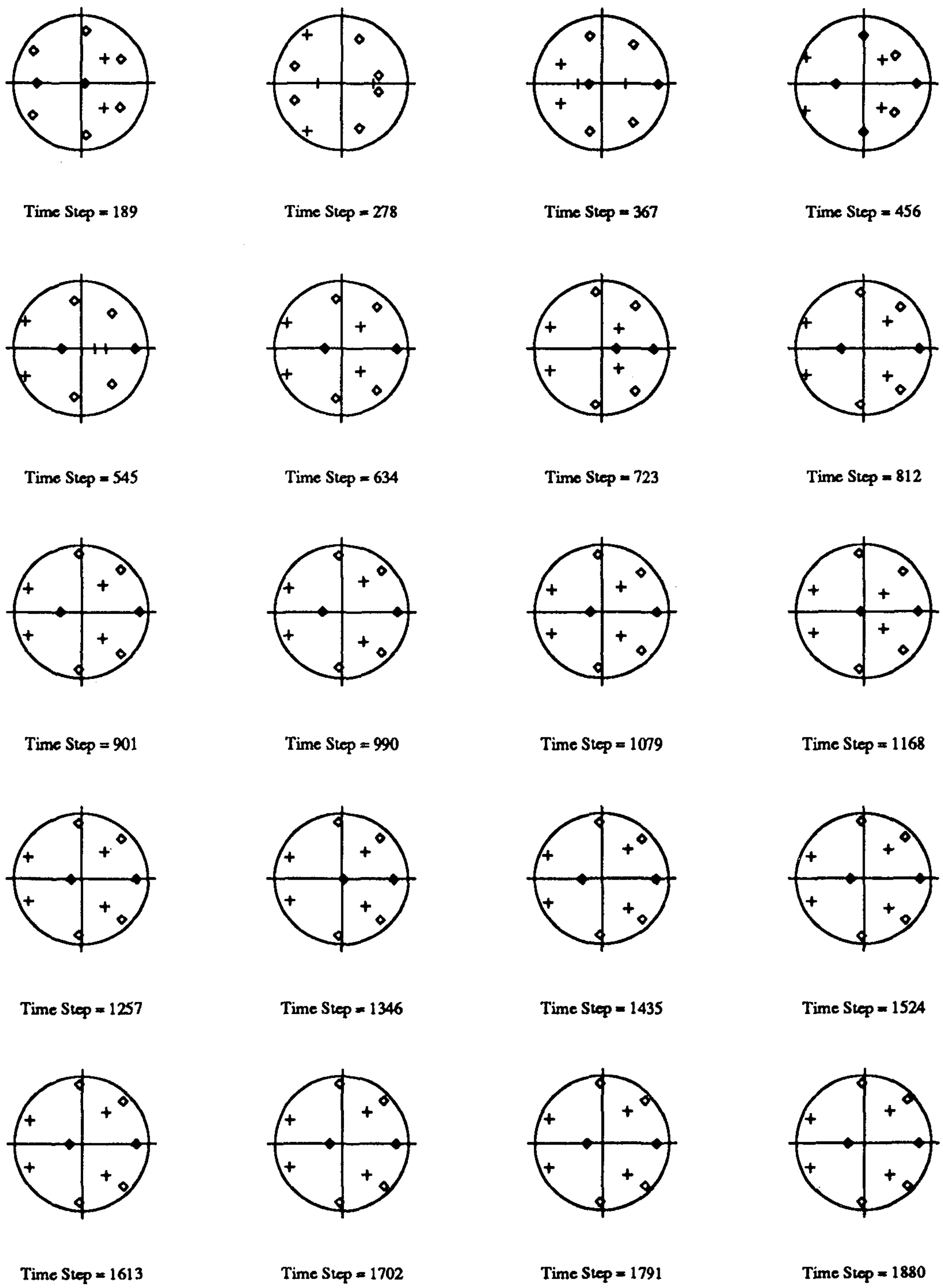


Figure 5.134

Recursive Instrumental Variable Estimation
Three Story Building Model; El-Centro Input
1st Floor

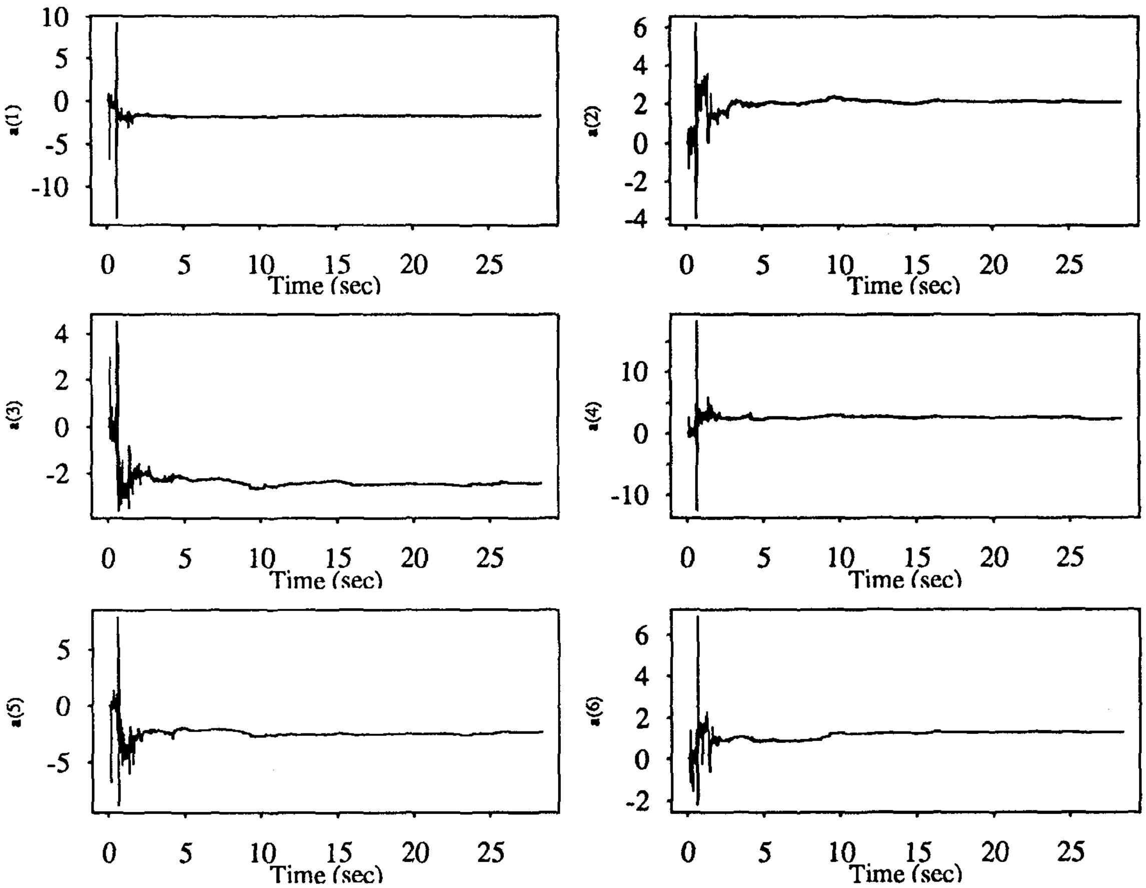


Figure 5.135

Recursive Instrumental Variable Estimation
Three Story Building Model;  El-Centro Input
2nd Floor

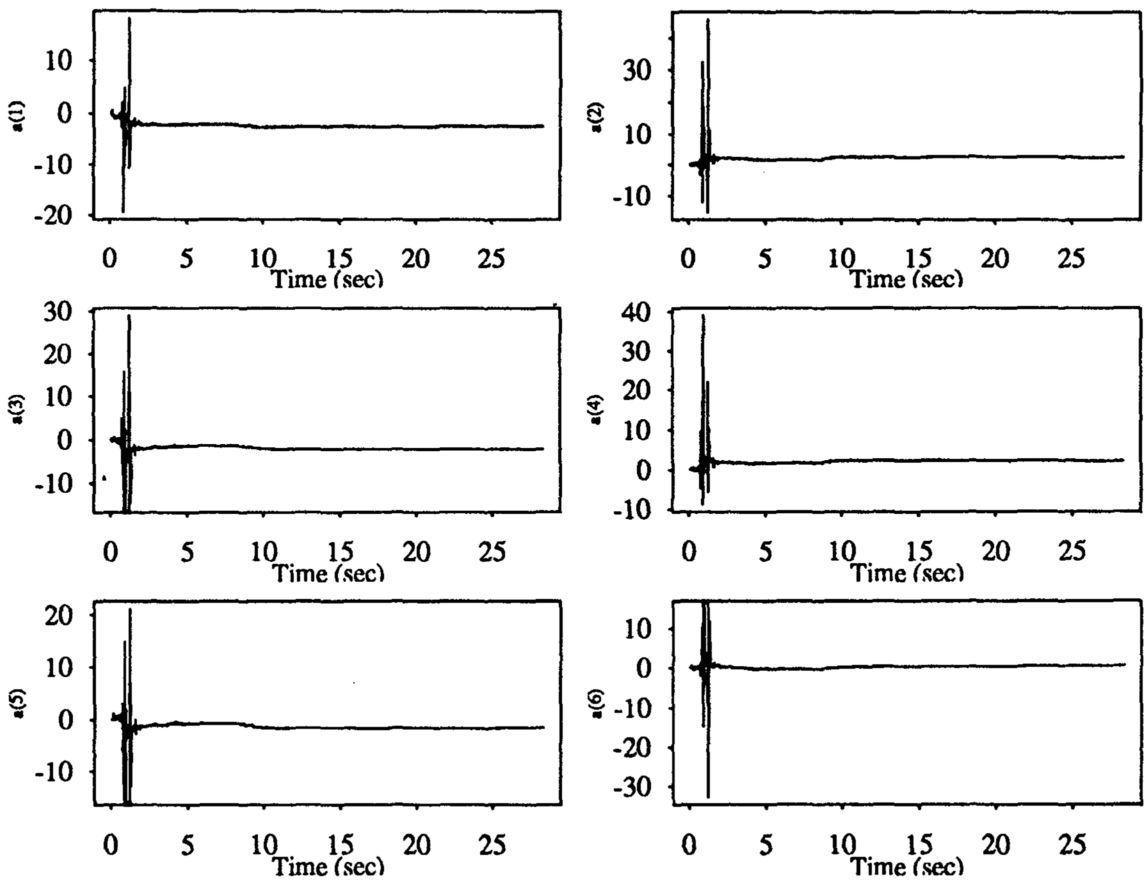


**Figure 5.136**

Recursive Instrumental Variable Estimation
Three Story Building Model; El-Centro Input
3rd Floor

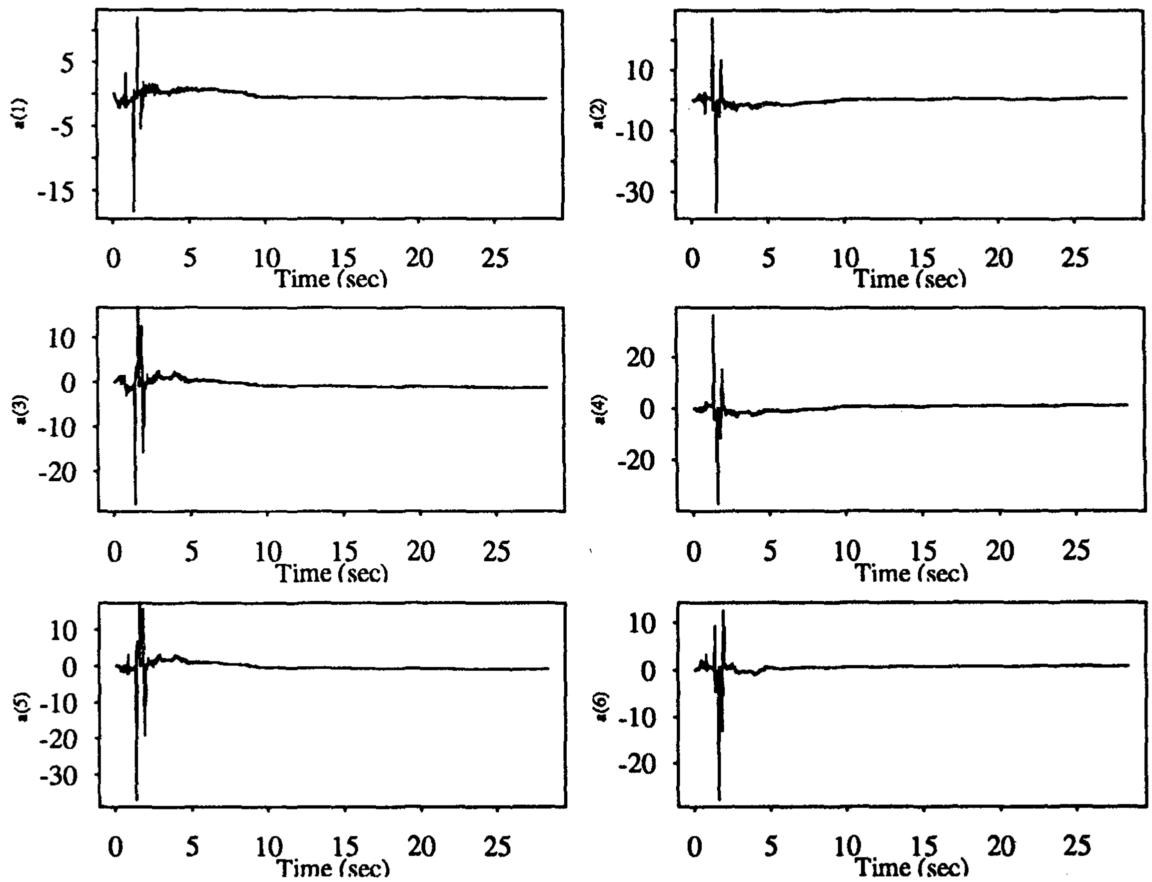


Figure 5.137

Recursive Instrumental Variable Estimation
Three Story Building Model; Sine Sweep Input
1st Floor

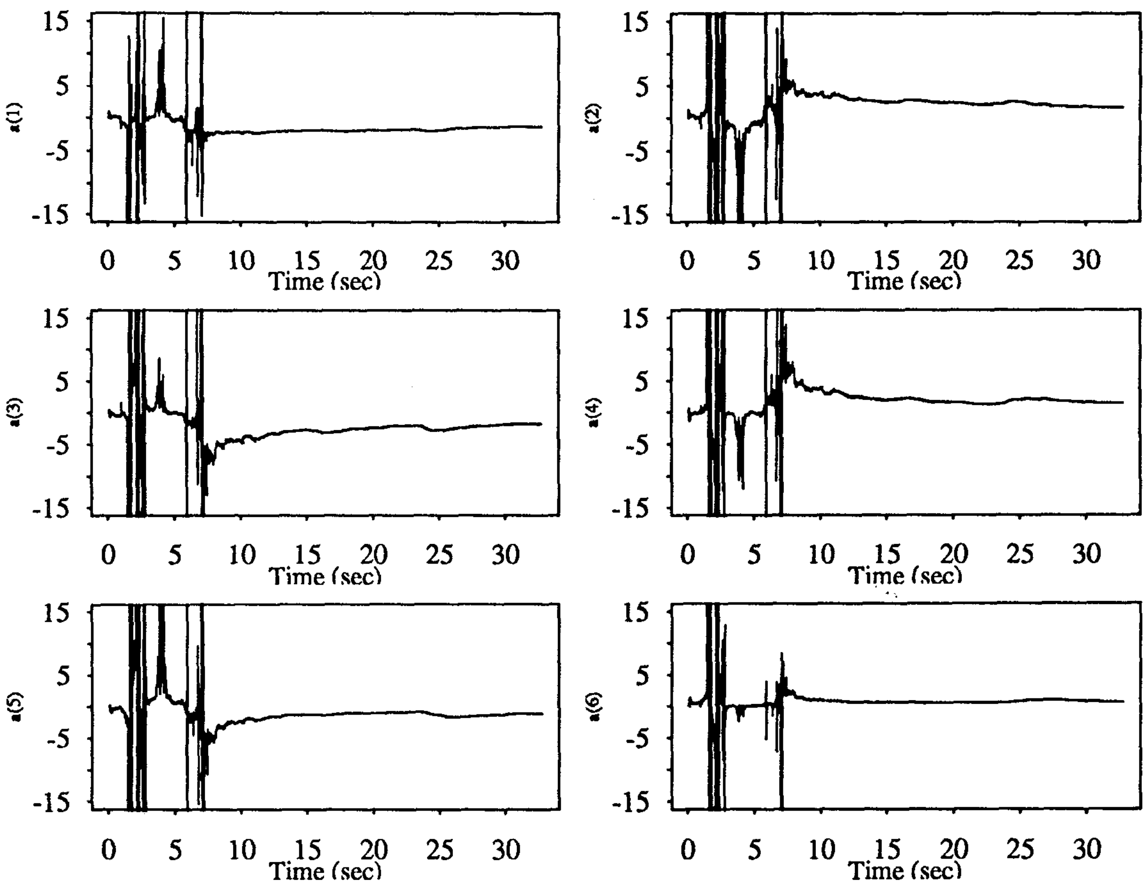


Figure 5.138

Recursive Instrumental Variable Estimation
Three Story Building Model; Sine Sweep Input
2nd Floor

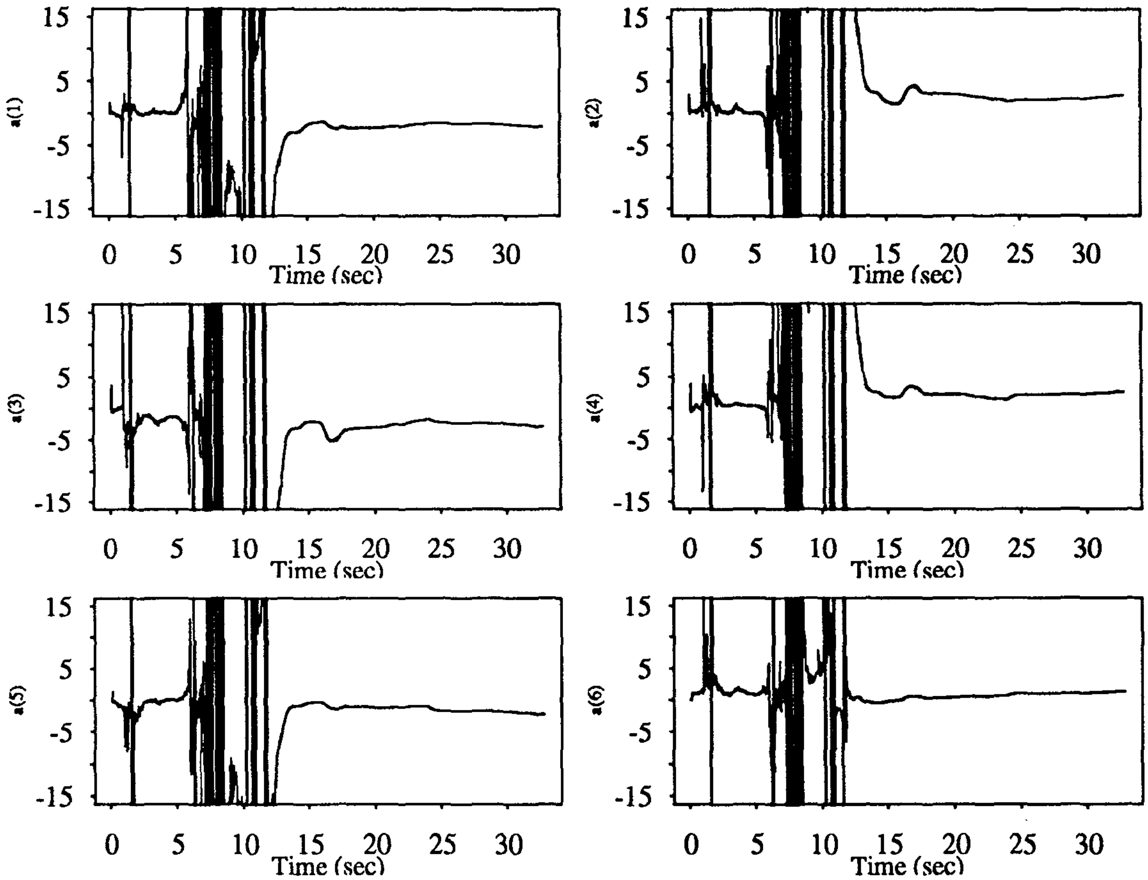


Figure 5.139

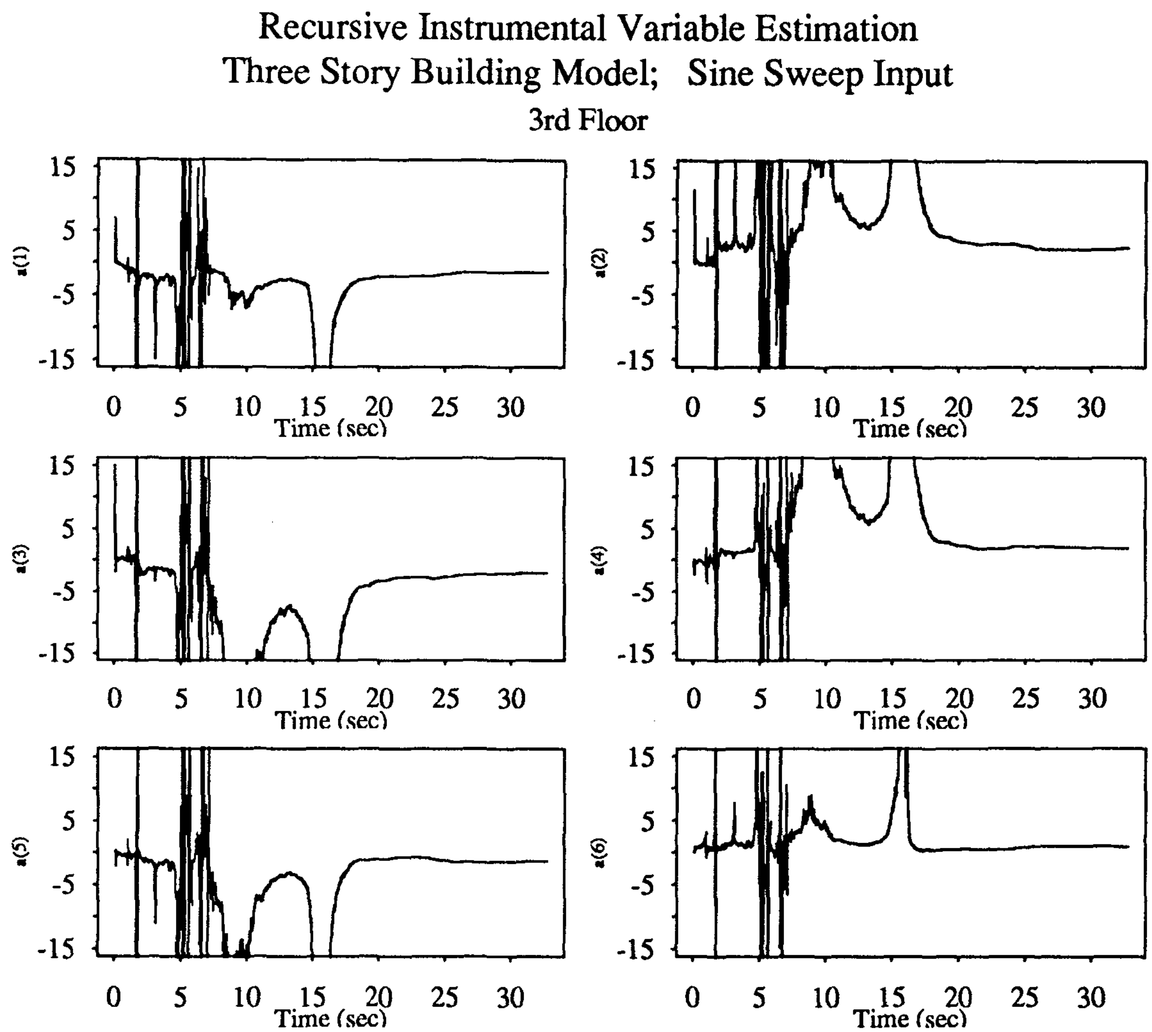
Recursive Instrumental Variable Estimation
Three Story Building Model; Sine Sweep Input
3rd Floor
a(1)
a(2)
a(3)
a(4)
a(5)
a(6)
15
5
-5
-15
0 5 10 15 20 25 30
Time (sec)

**Figure 5.140**

Recursive Instrumental Variable Estimation
Three Story Building Model; White Noise Input
1st Floor

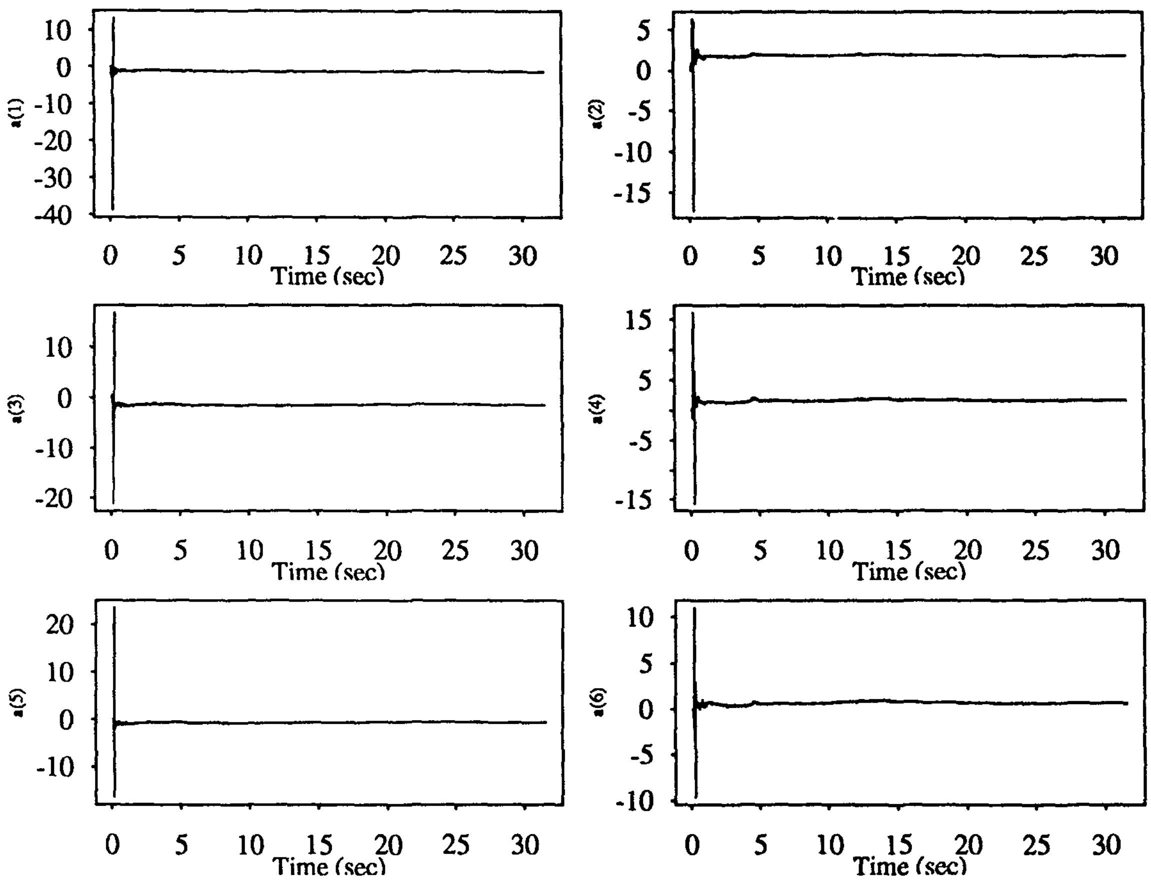


Figure 5.141

Recursive Instrumental Variable Estimation
Three Story Building Model; White Noise Input
2nd Floor

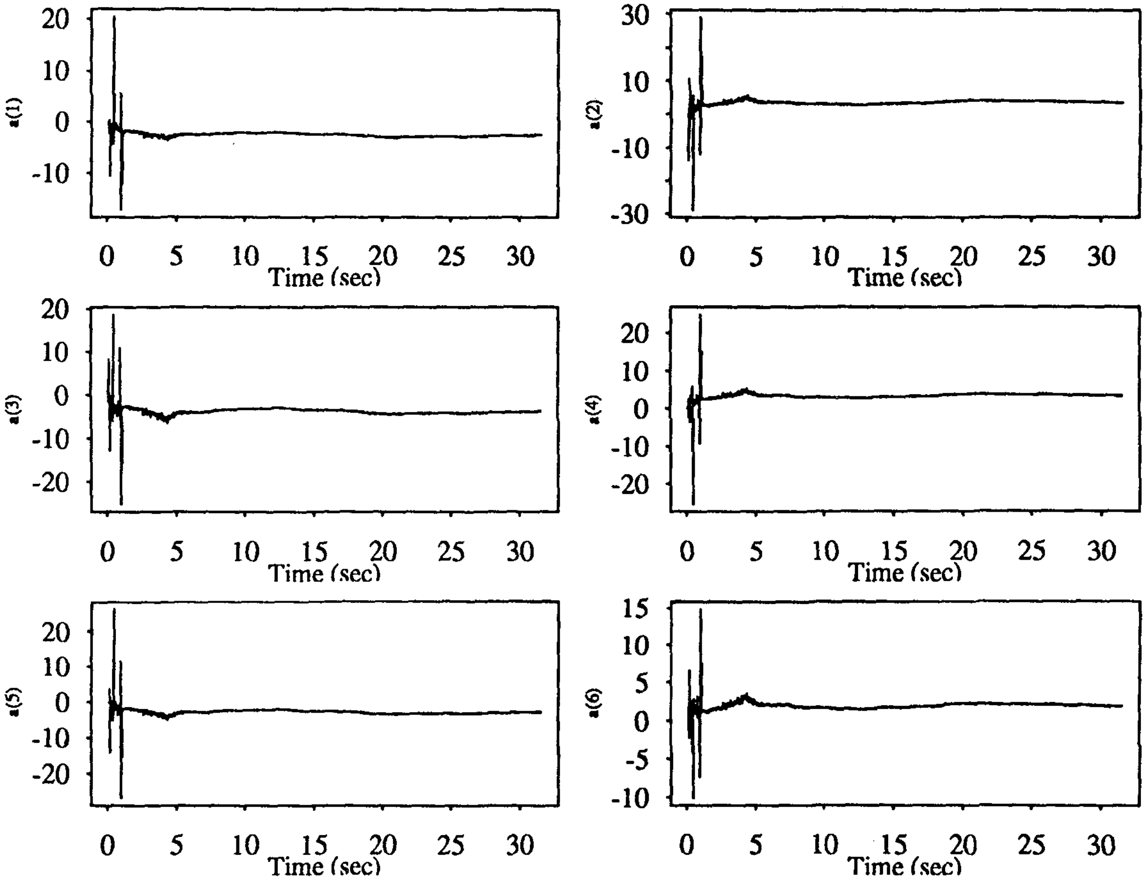


**Figure 5.142**

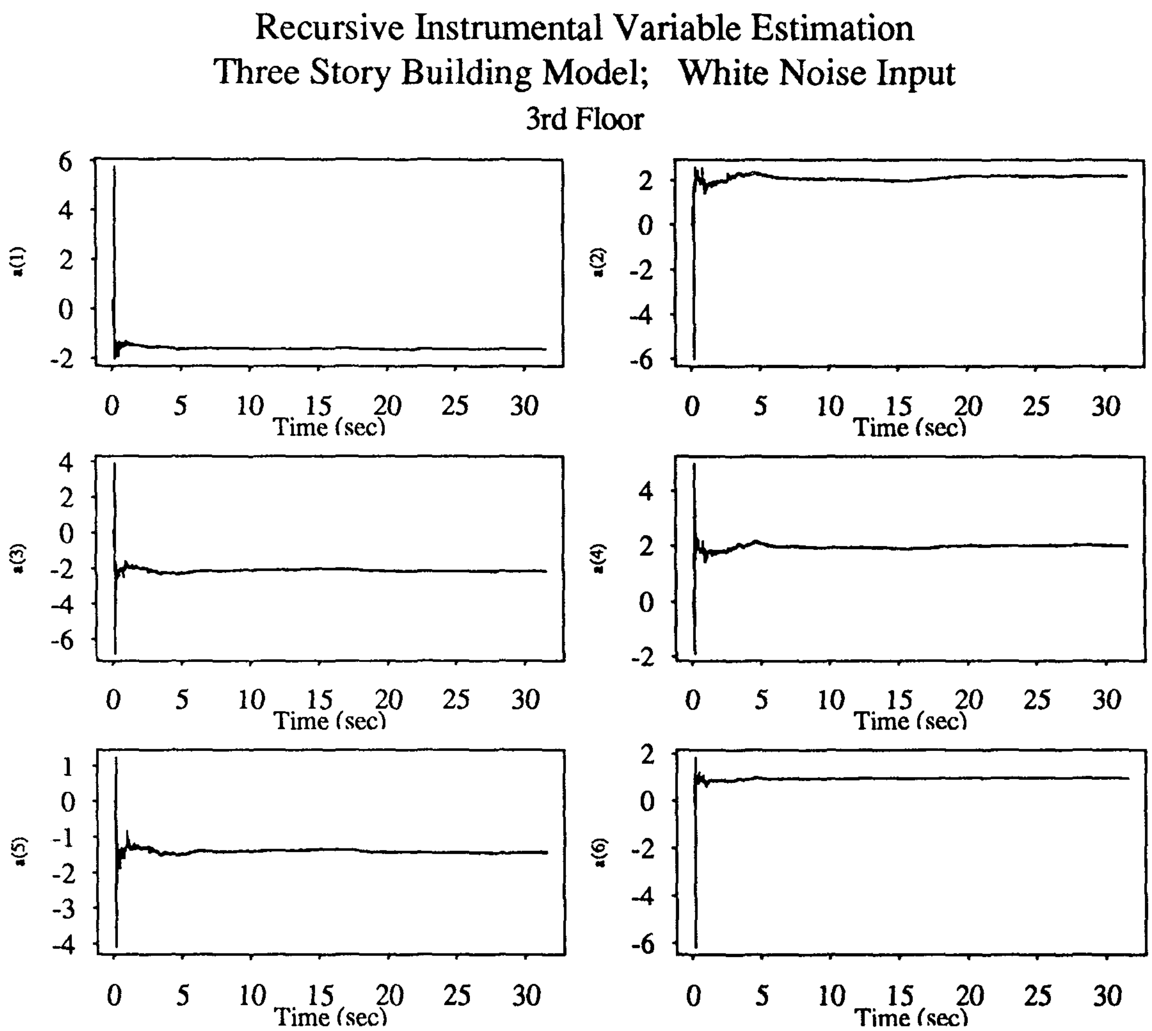
Recursive Instrumental Variable Estimation
Three Story Building Model; White Noise Input
3rd Floor
a(1)
a(2)
a(3)
a(4)
a(5)
a(6)
Time (sec)

**Figure 5.143**

Recursive Instrumental Variable Estimation
Three Story Building Model; El-Centro Input
1st Floor

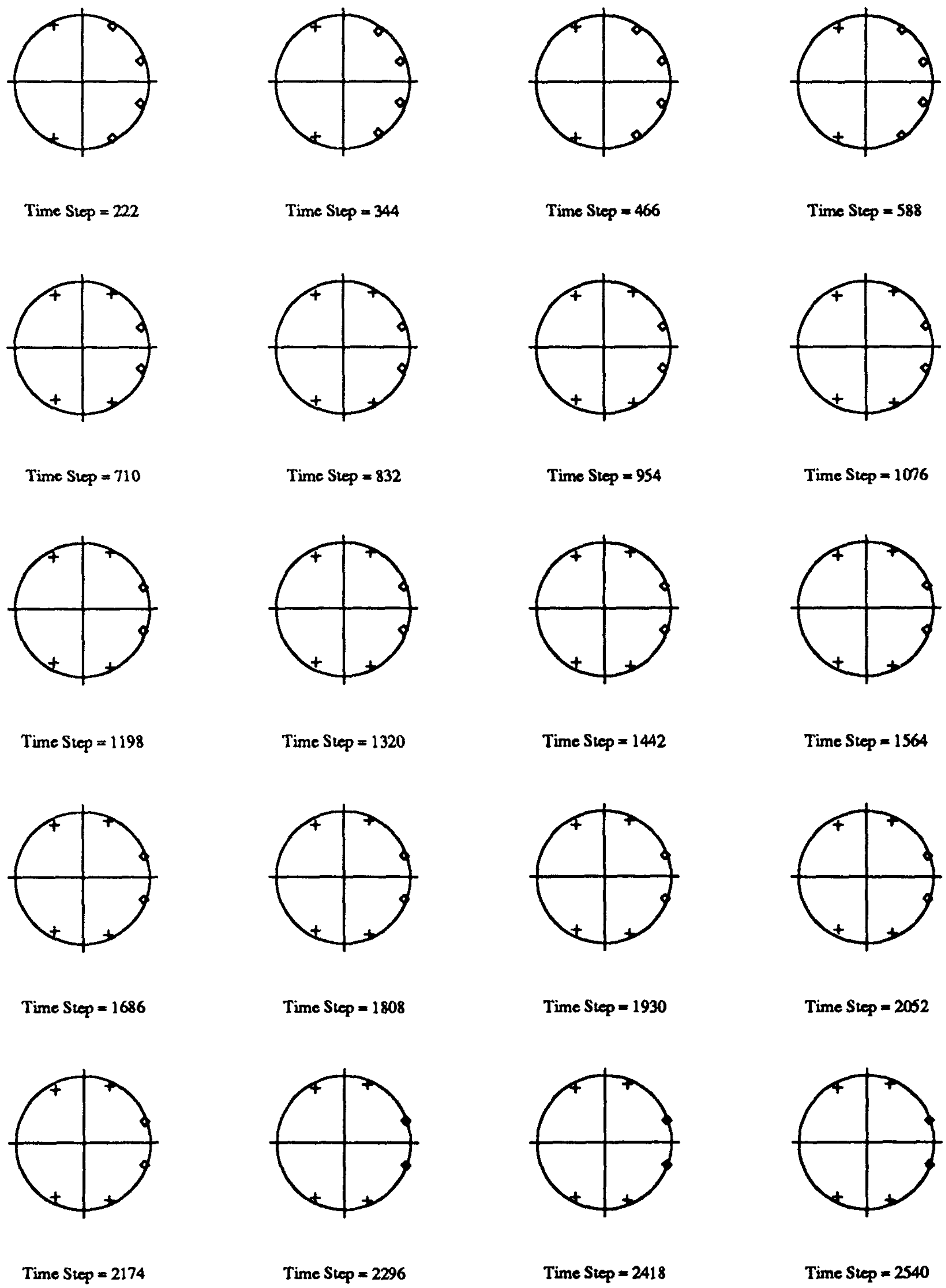


**Figure 5.144**

## Recursive Instrumental Variable Estimation
## Three Story Building Model; El-Centro Input
### 2nd Floor

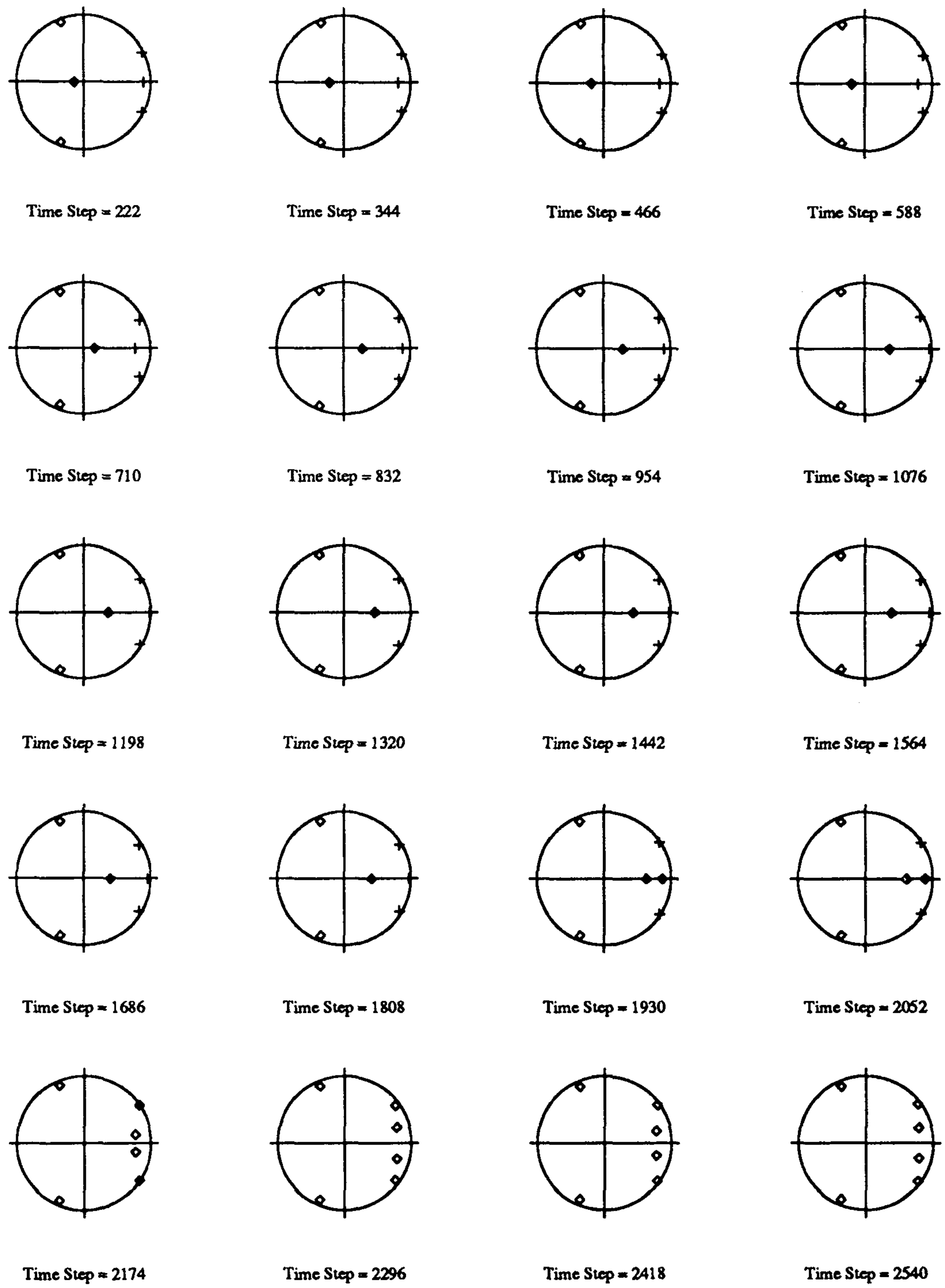


Figure 5.145

## Recursive Instrumental Variable Estimation
## Three Story Building Model; El-Centro Input
### 3rd Floor

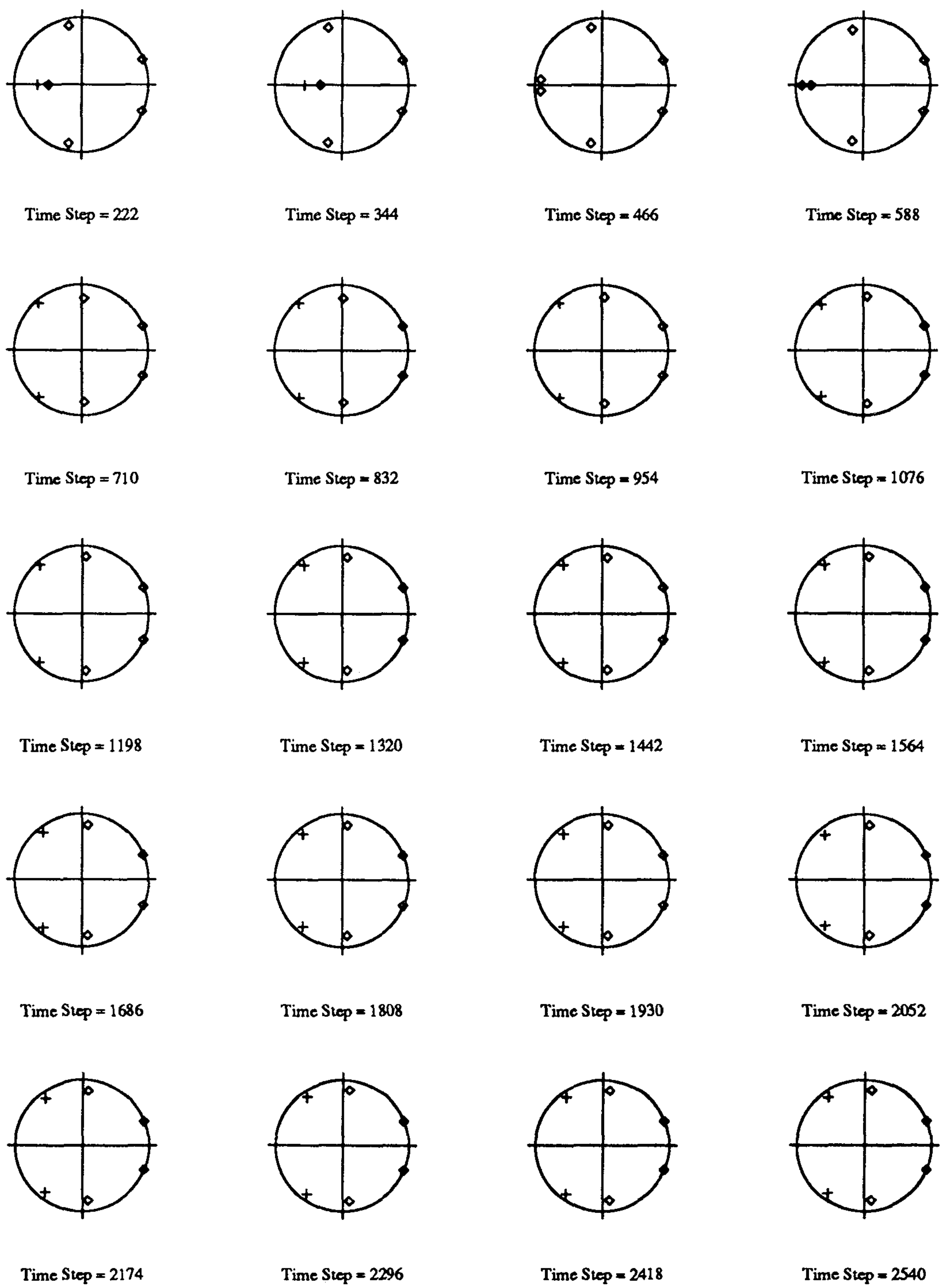


Figure 5.146

## Recursive Instrumental Variable Estimation
## Three Story Building Model; Sine Sweep Input
### 1st Floor

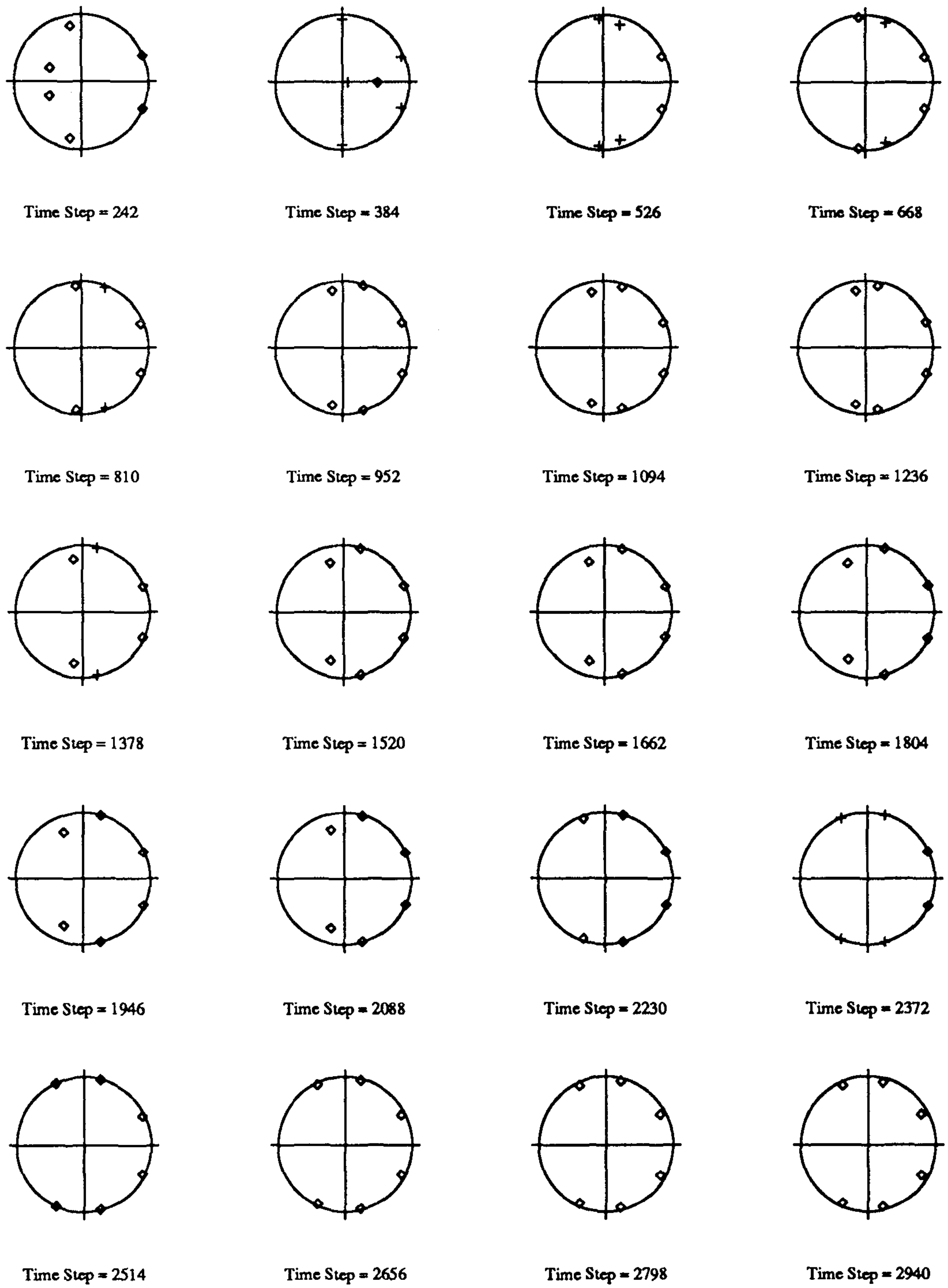


Figure 5.147

## Recursive Instrumental Variable Estimation
## Three Story Building Model; Sine Sweep Input
### 2nd Floor

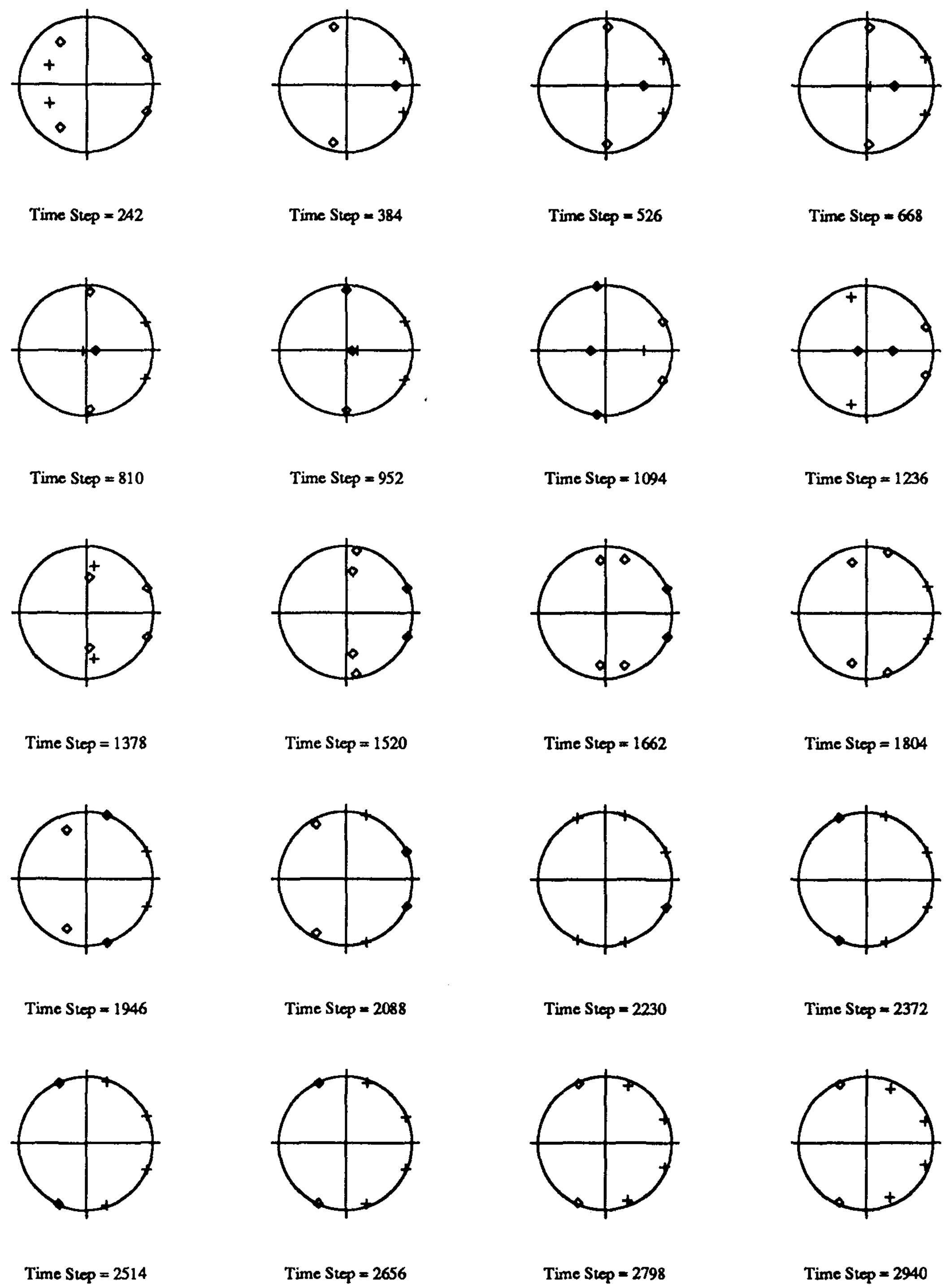


Figure 5.148

## Recursive Instrumental Variable Estimation
## Three Story Building Model; Sine Sweep Input
### 3rd Floor

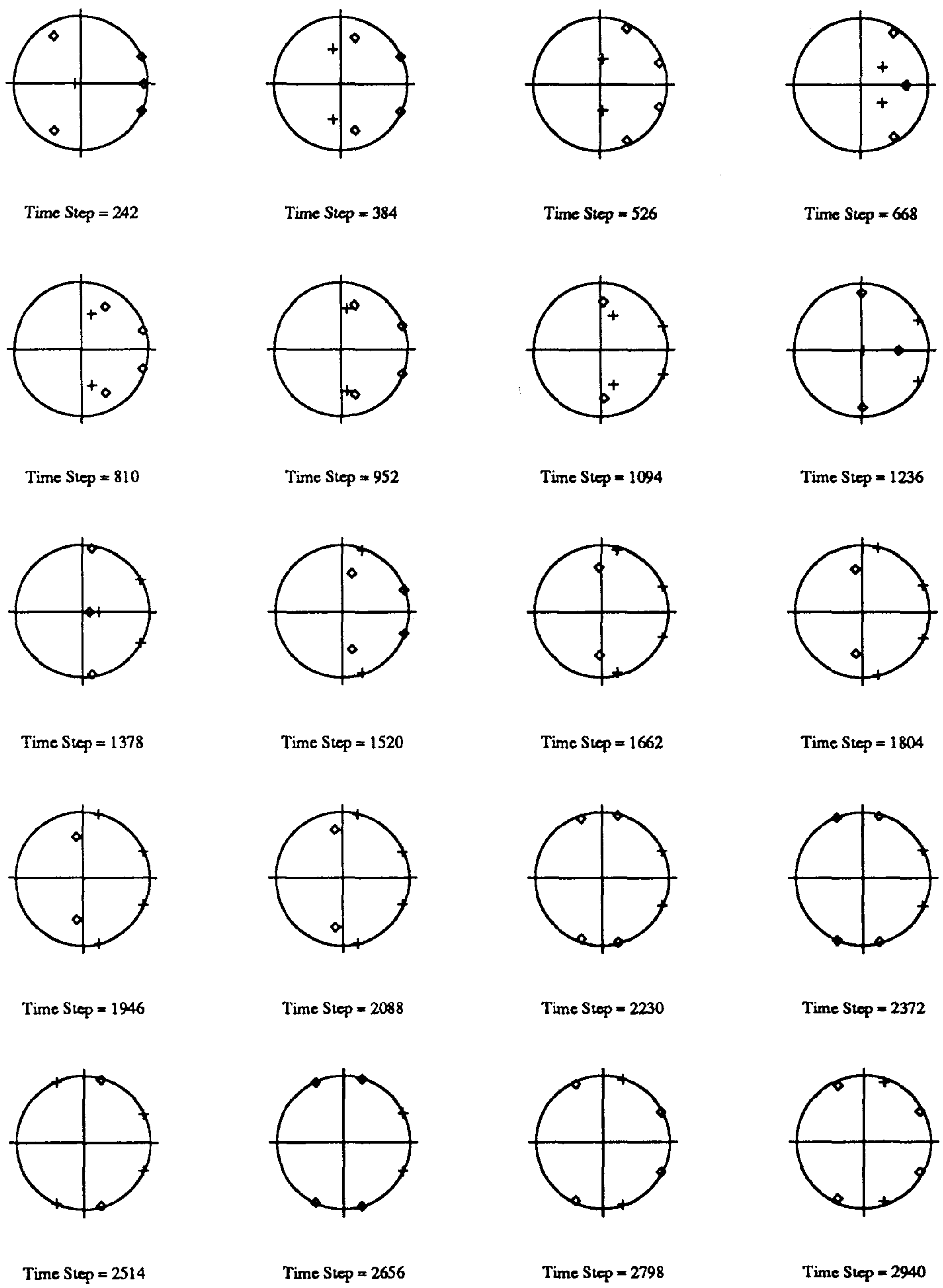


Figure 5.149

# Recursive Instrumental Variable Estimation
## Three Story Building Model; White Noise Input
### 1st Floor

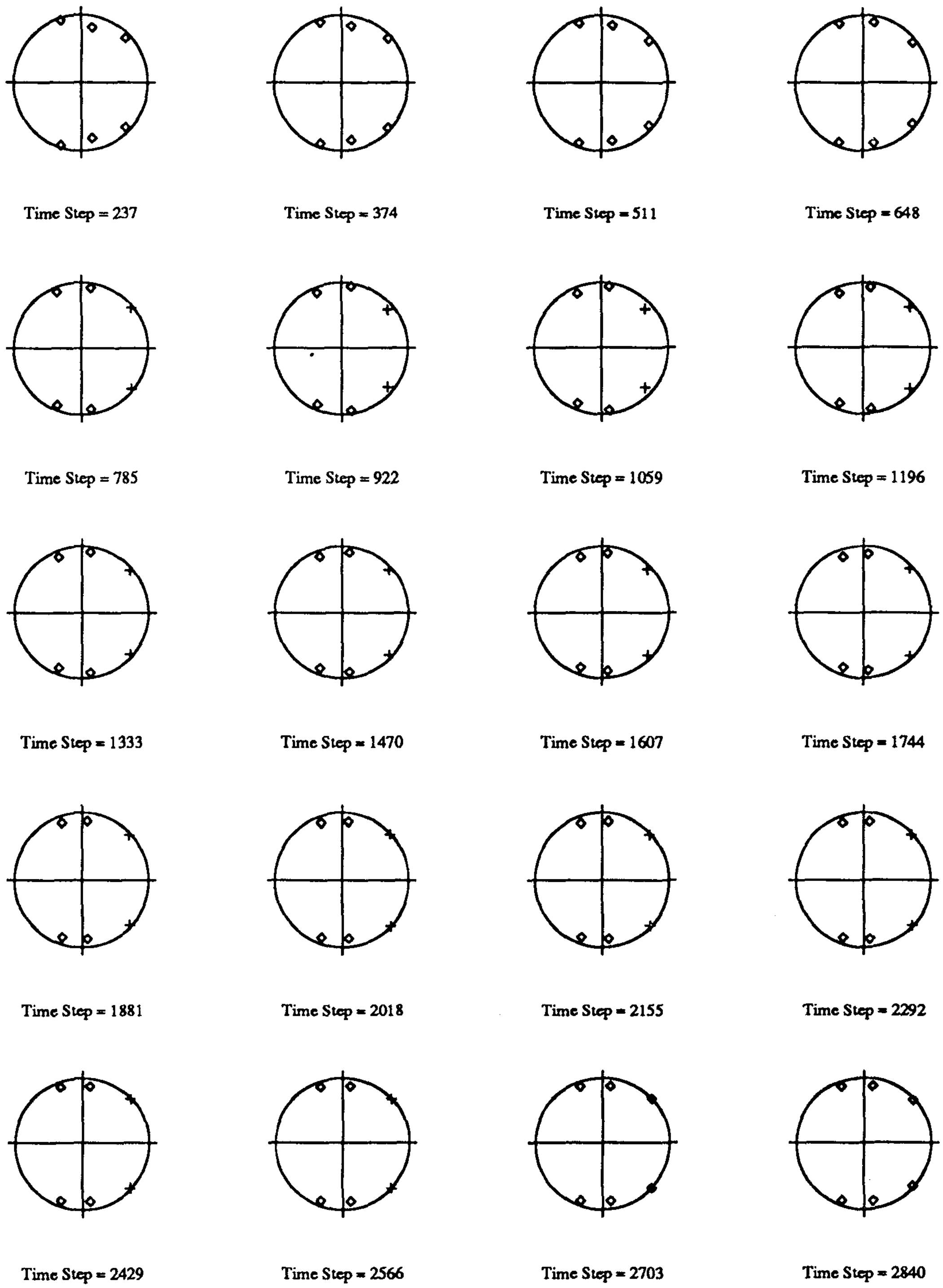


Figure 5.150

# Recursive Instrumental Variable Estimation
## Three Story Building Model; White Noise Input
### 2nd Floor

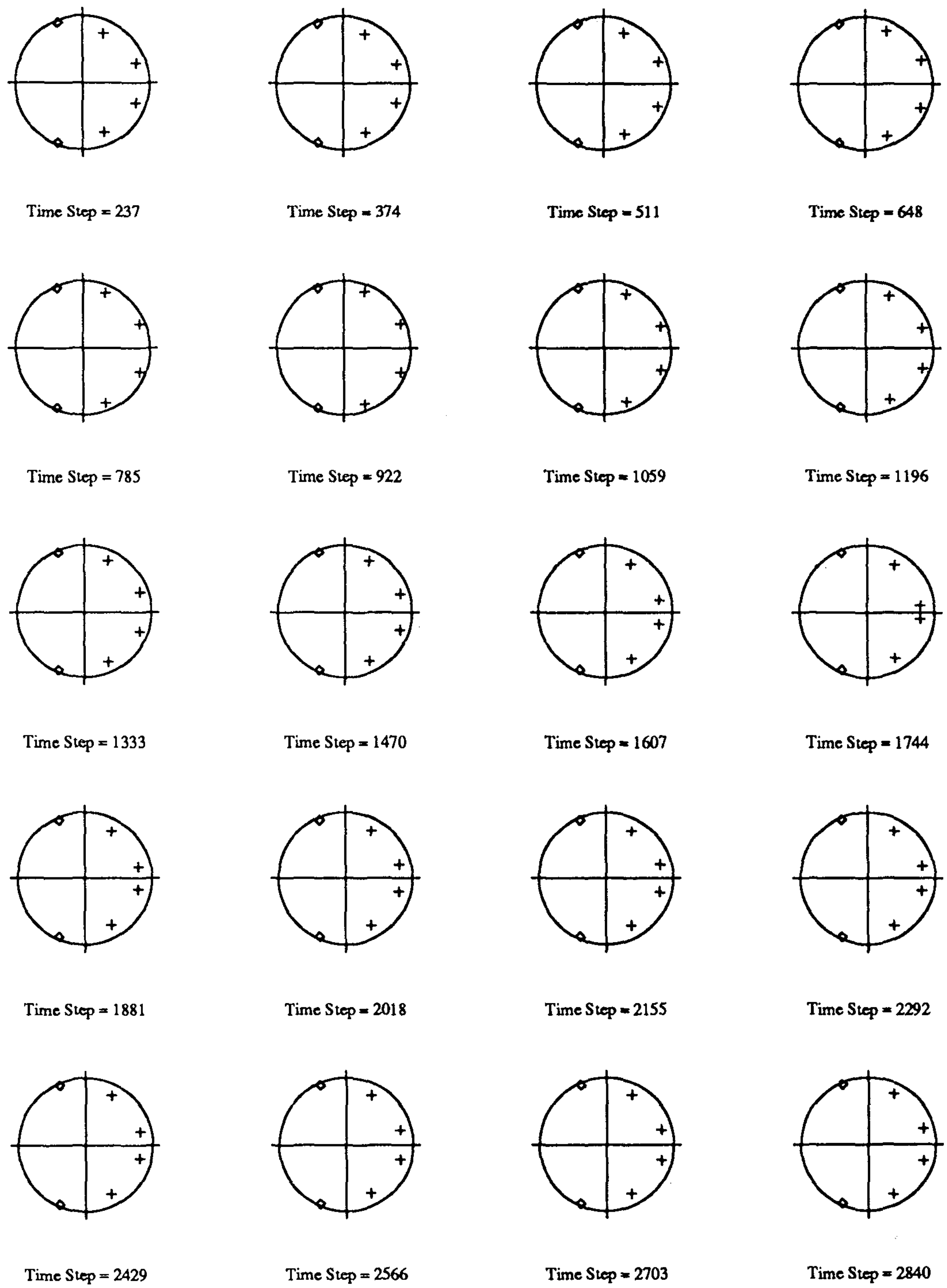


Figure 5.151

## Recursive Instrumental Variable Estimation
## Three Story Building Model;   White Noise Input
### 3rd Floor

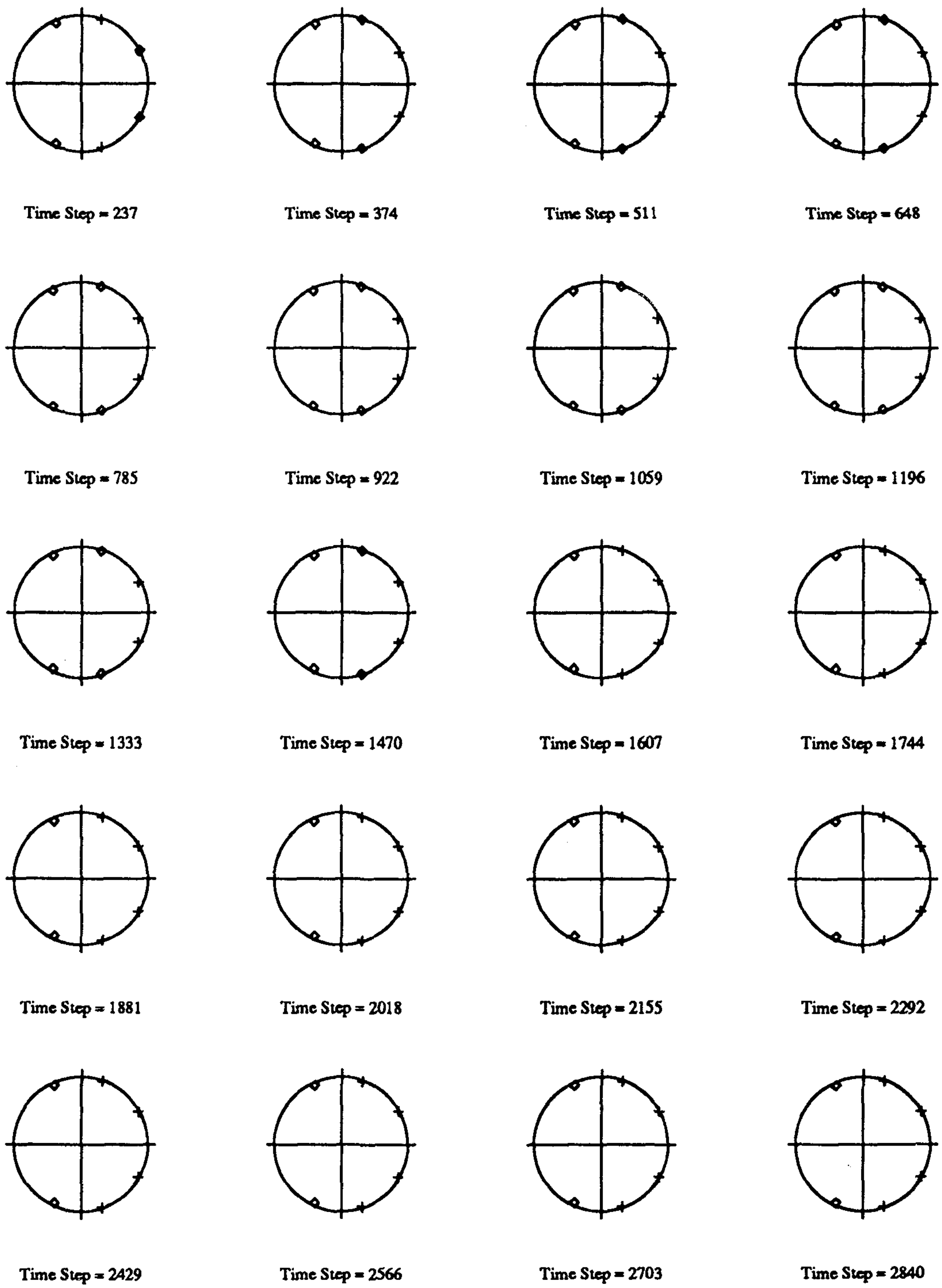


**Figure 5.152**

Recursive Instrumental Variable Estimation
Five Story Building Model; El-Centro Input
2nd Floor gamma=0.03

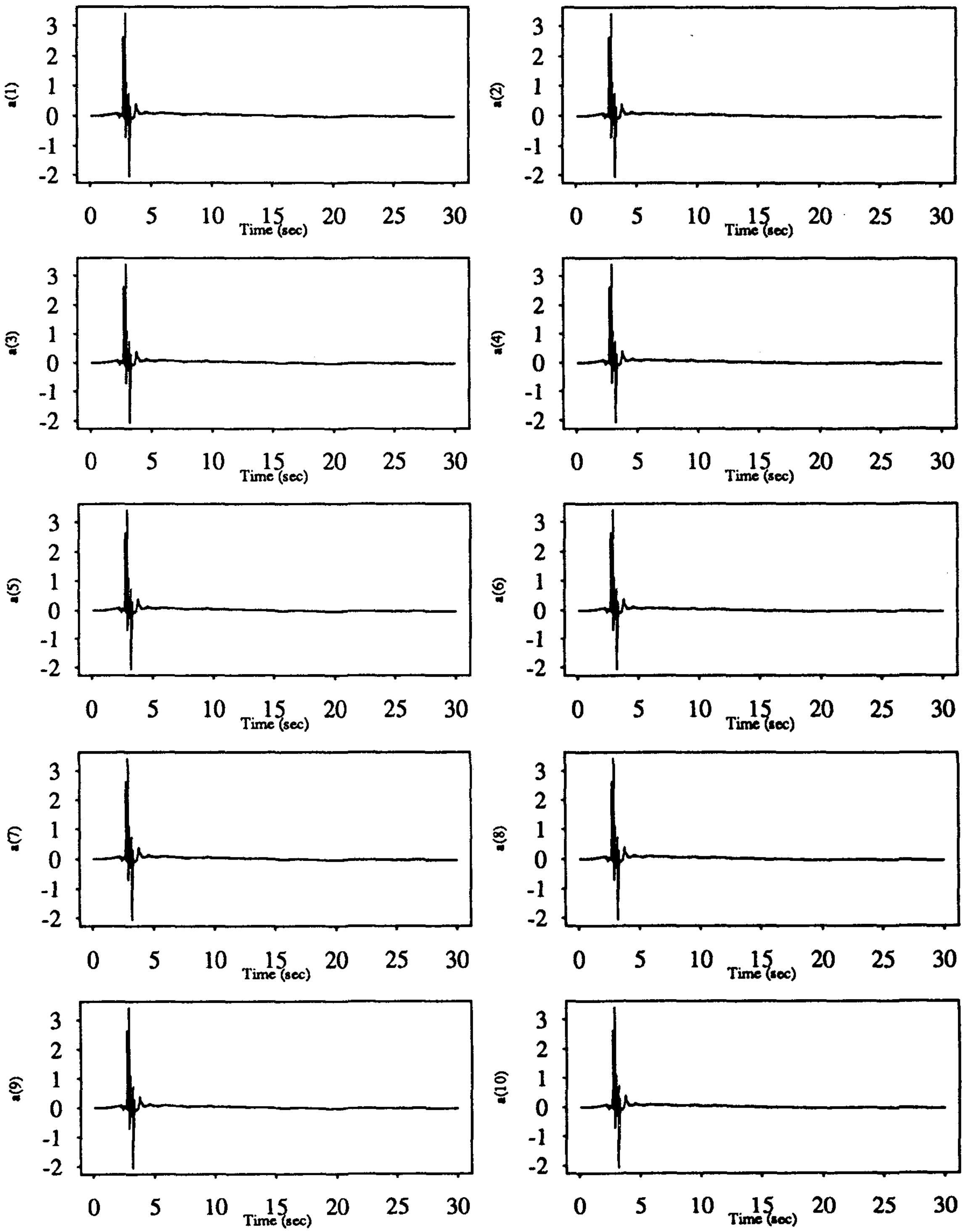


Figure 5.153

Recursive Instrumental Variable Estimation
Five Story Building Model; White Noise Input
4th Floor gamma=0.03

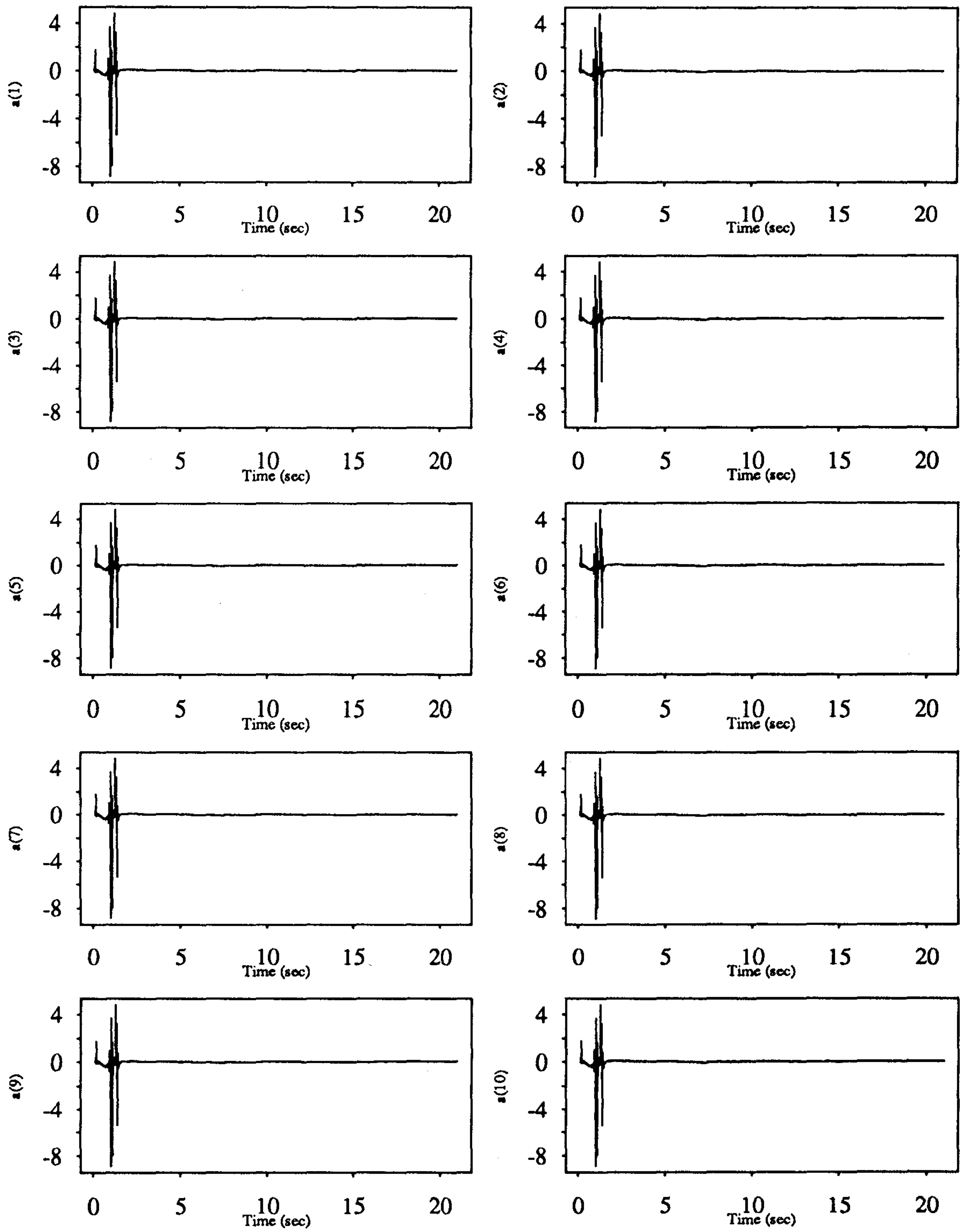


Figure 5.154

Recursive Instrumental Variable Estimation
Five Story Building Model; White Noise Input
5th Floor gamma=0.05

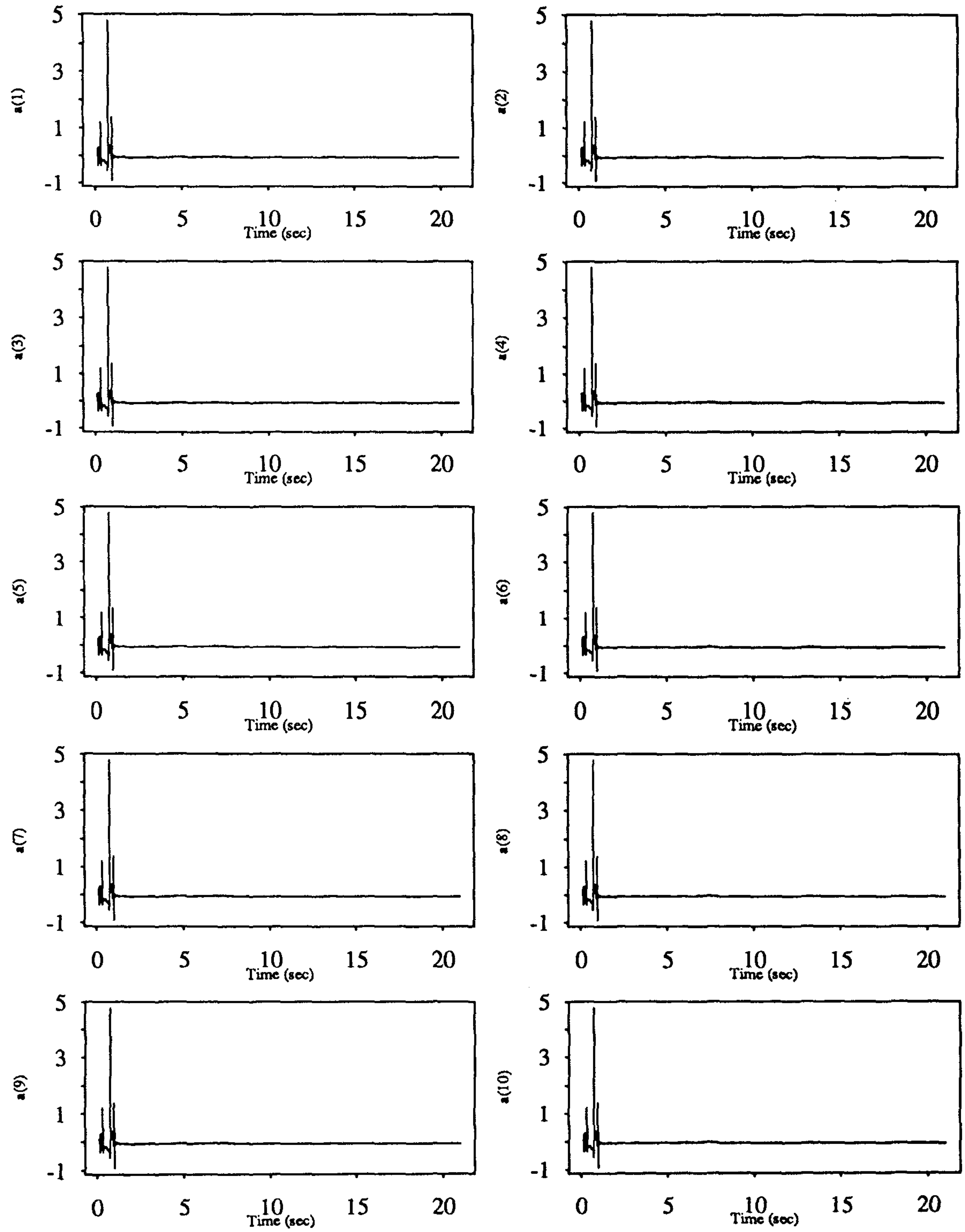


Figure 5.155

Recursive Instrumental Variable Estimation
Five Story Building Model; El-Centro Input
3rd Floor gamma=0.1

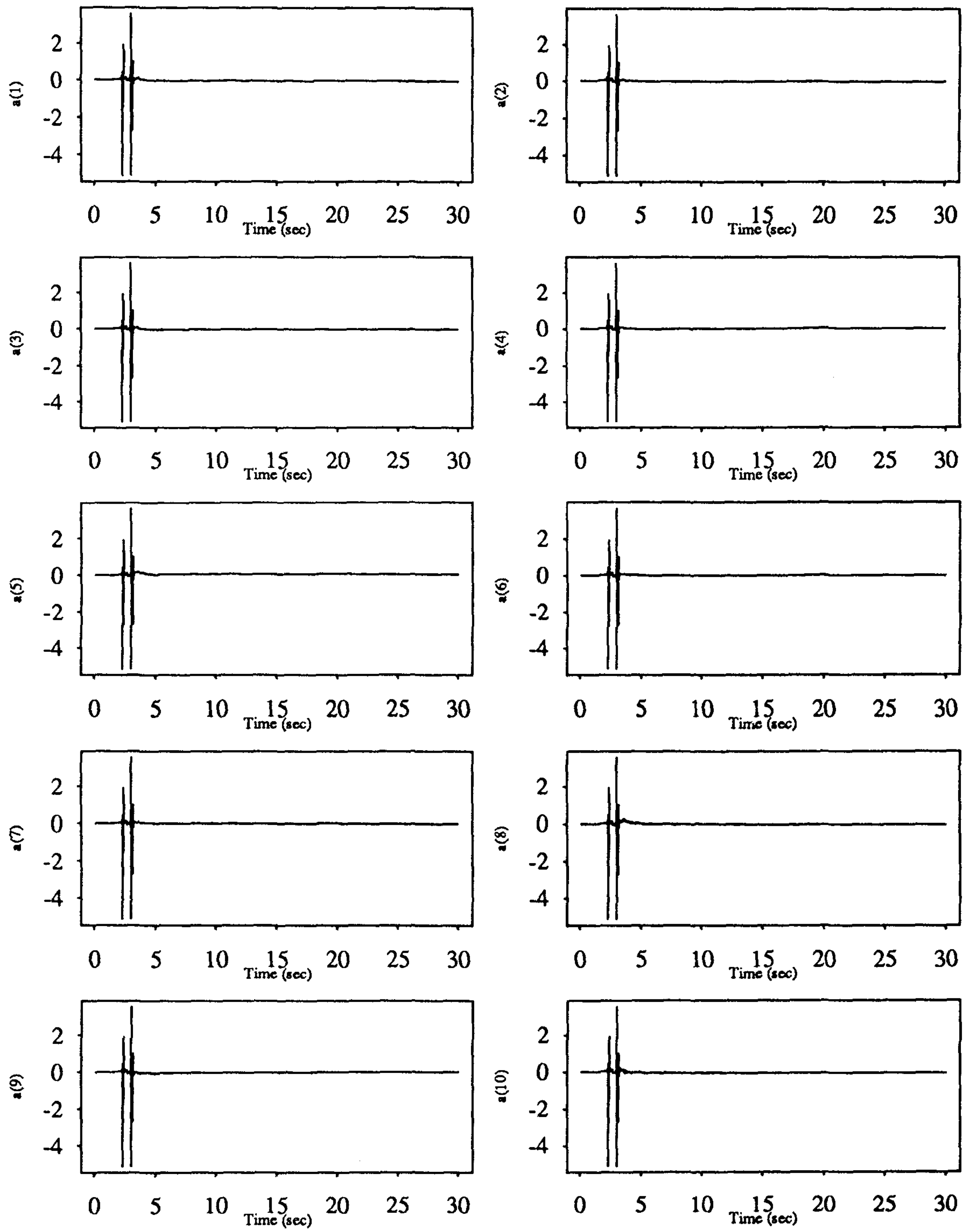


Figure 5.156

Recursive Instrumental Variable Estimation
Five Story Building Model; El-Centro Input
1st Floor gamma=0.11

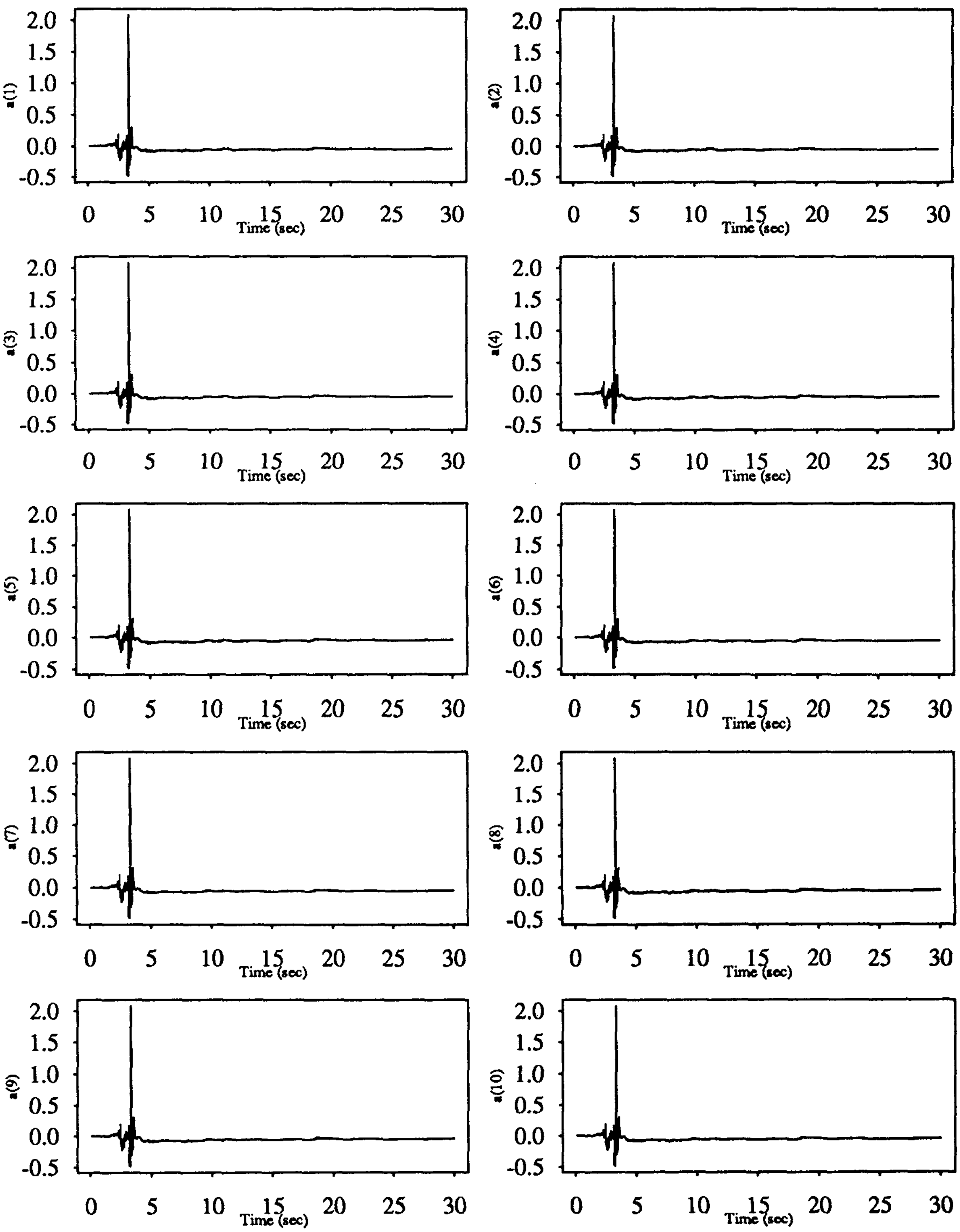


Figure 5.157

Recursive Instrumental Variable Estimation
Five Story Building Model; White Noise Input
5th Floor gamma=0.11

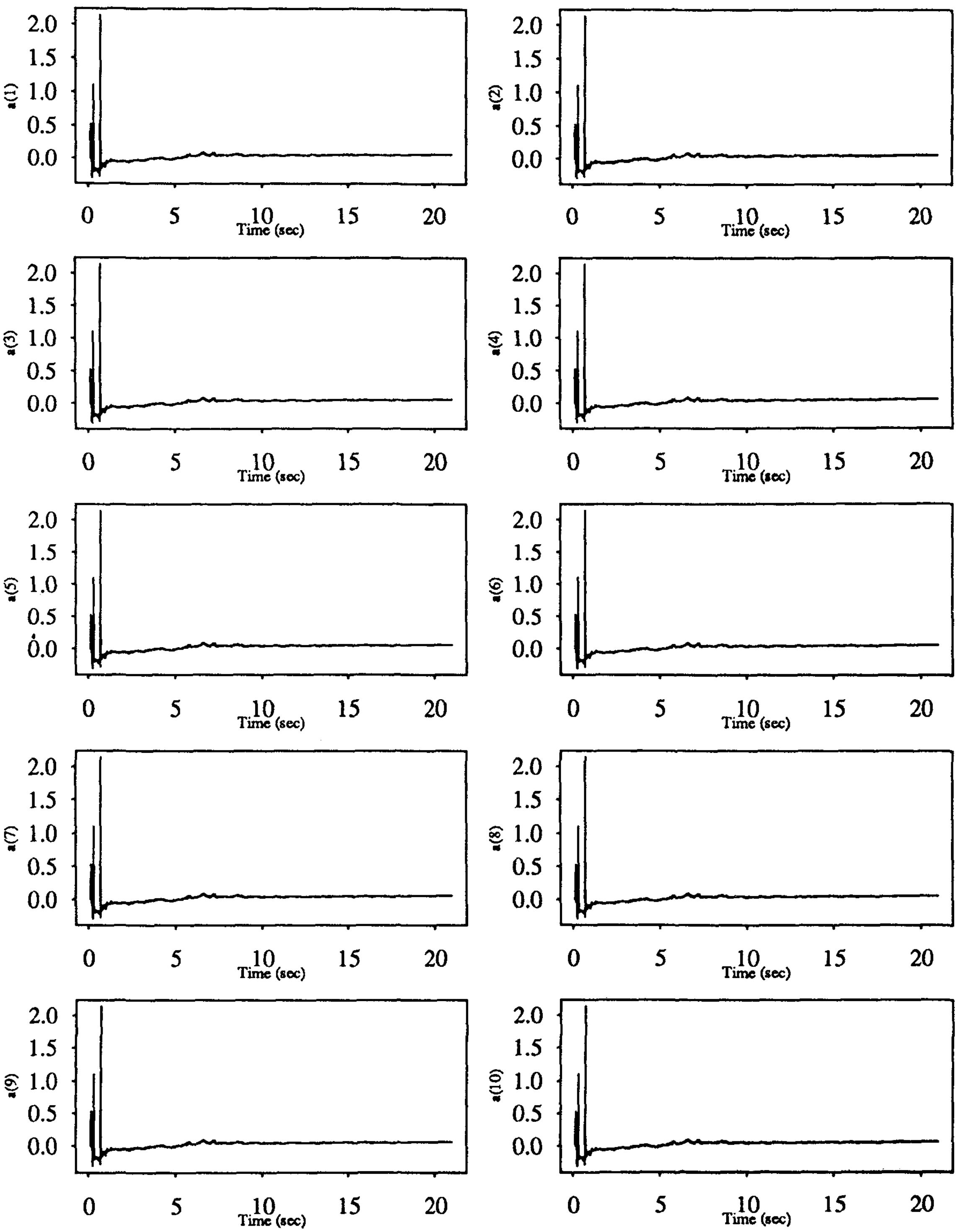


Figure 5.158

Recursive Instrumental Variable Estimation
Five Story Building Model; White Noise Input
5th Floor gamma=0.13

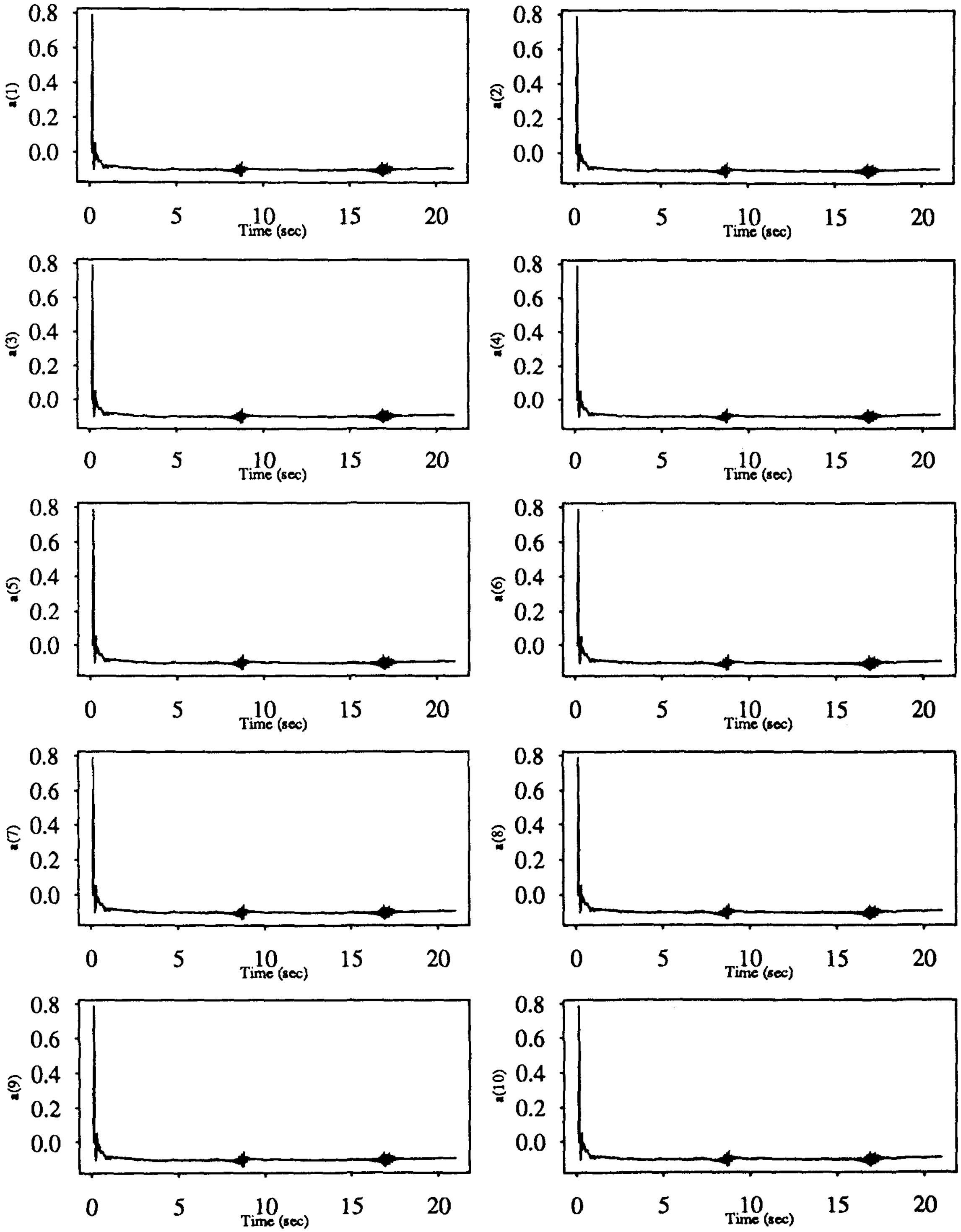


Figure 5.159

## Recursive Instrumental Variable Estimation
## Five Story Building Model; El-Centro Input

1st Floor gamma=1

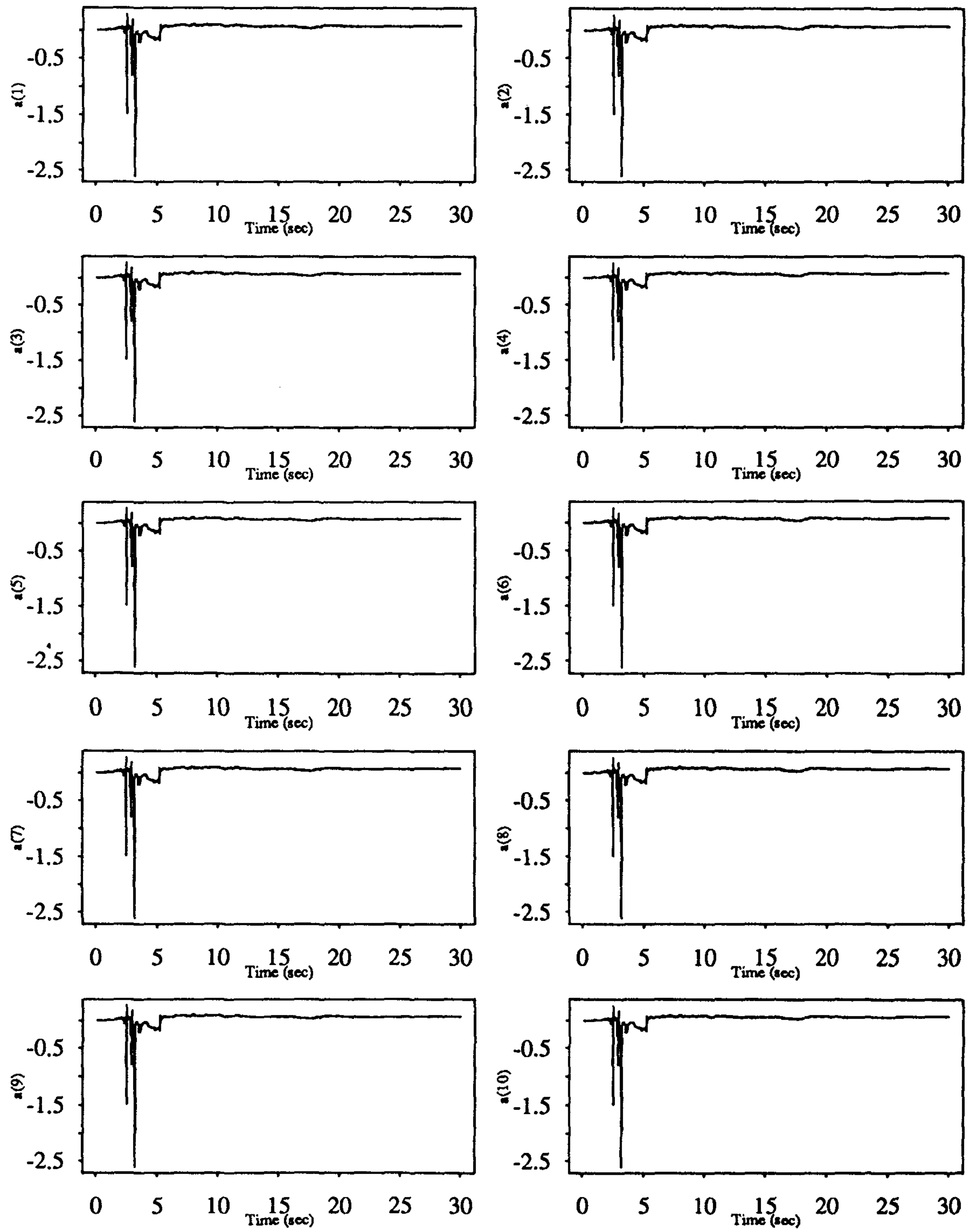


Figure 5.160

Recursive Instrumental Variable Estimation
Five Story Building Model; El-Centro Input
3rd Floor gamma=1

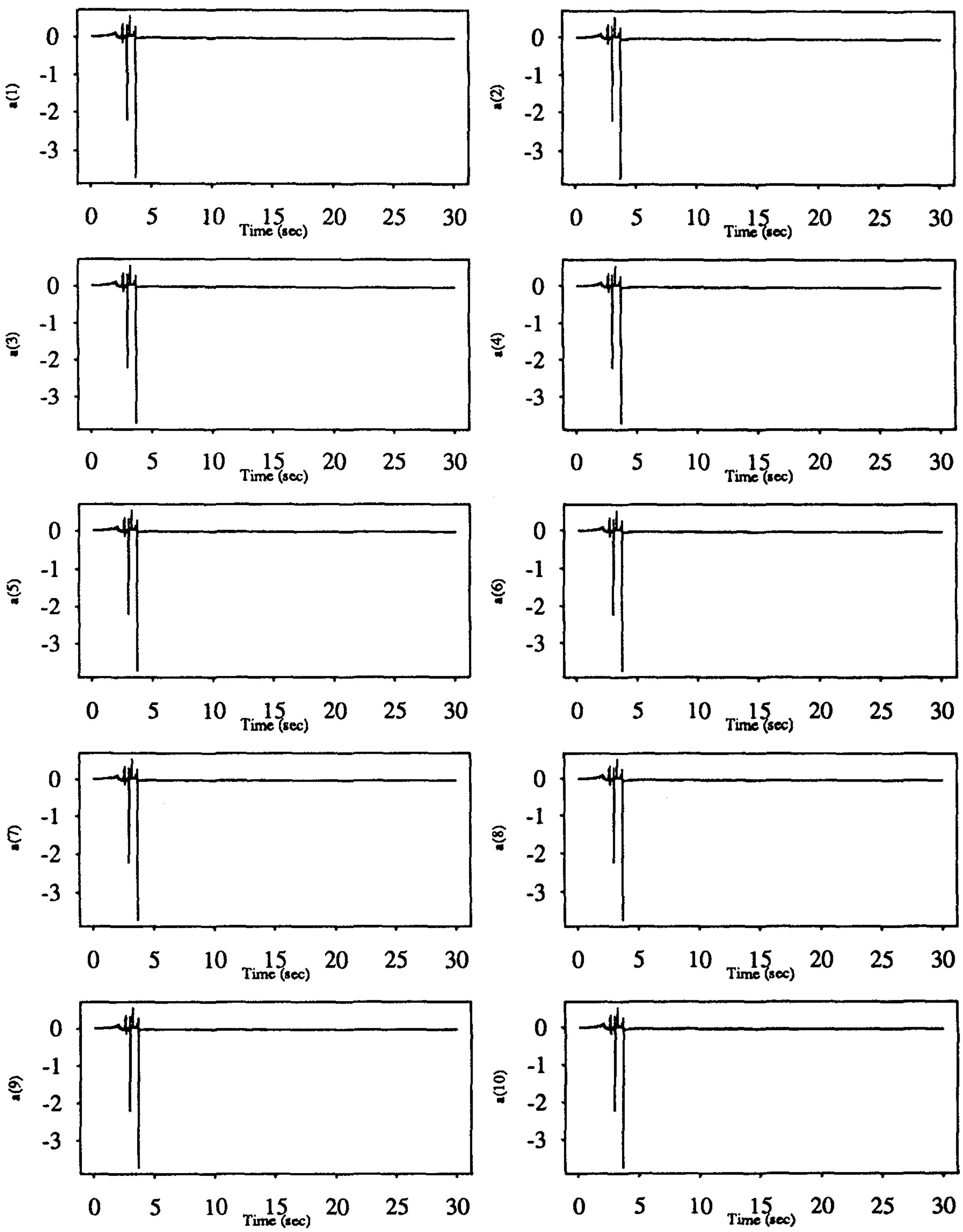


Figure 5.161

Recursive Instrumental Variable Estimation
Five Story Building Model; White Noise Input
3rd Floor gamma=1

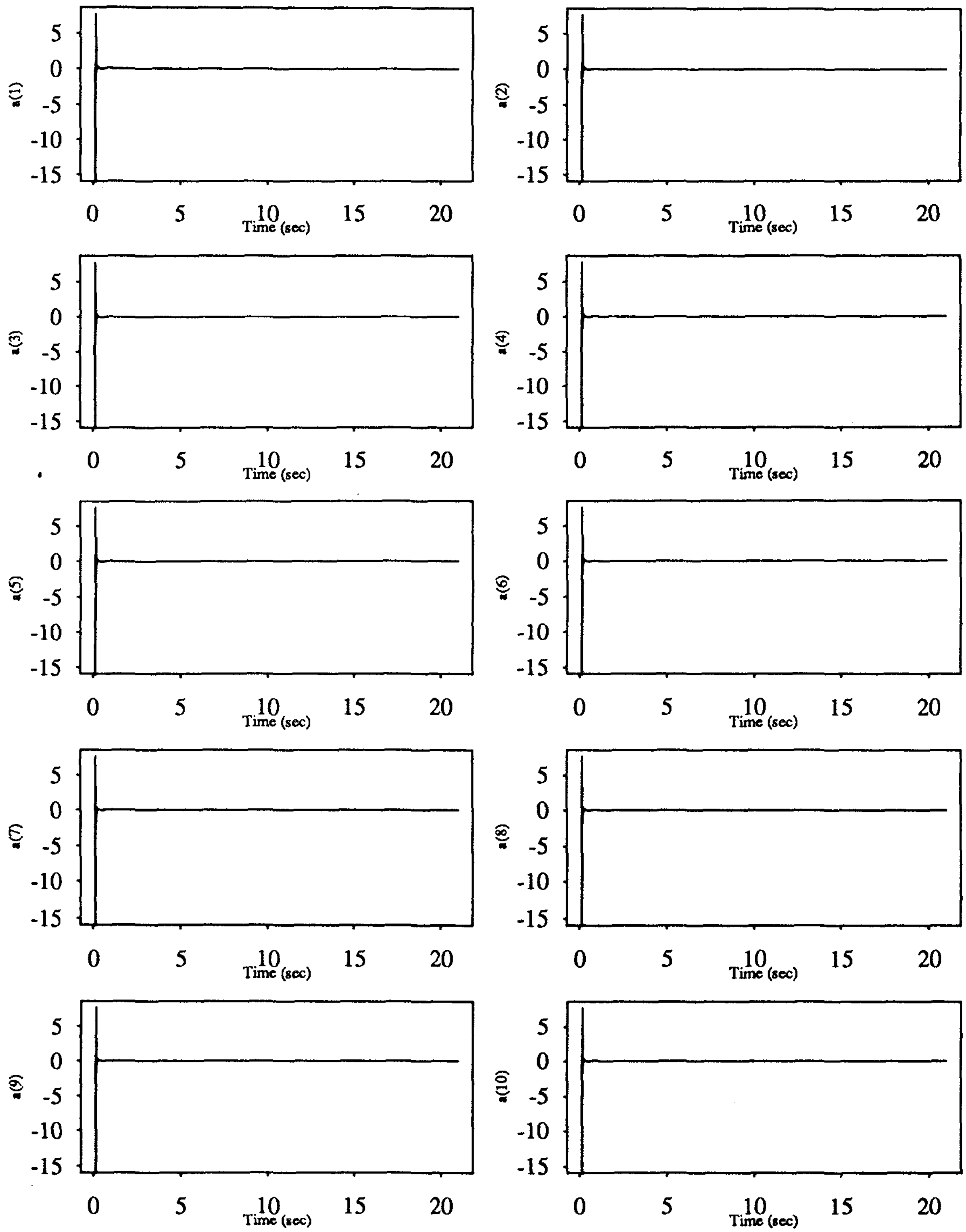


Figure 5.162

Recursive Instrumental Variable Estimation
Five Story Building Model; El-Centro Input
4th Floor gamma=1

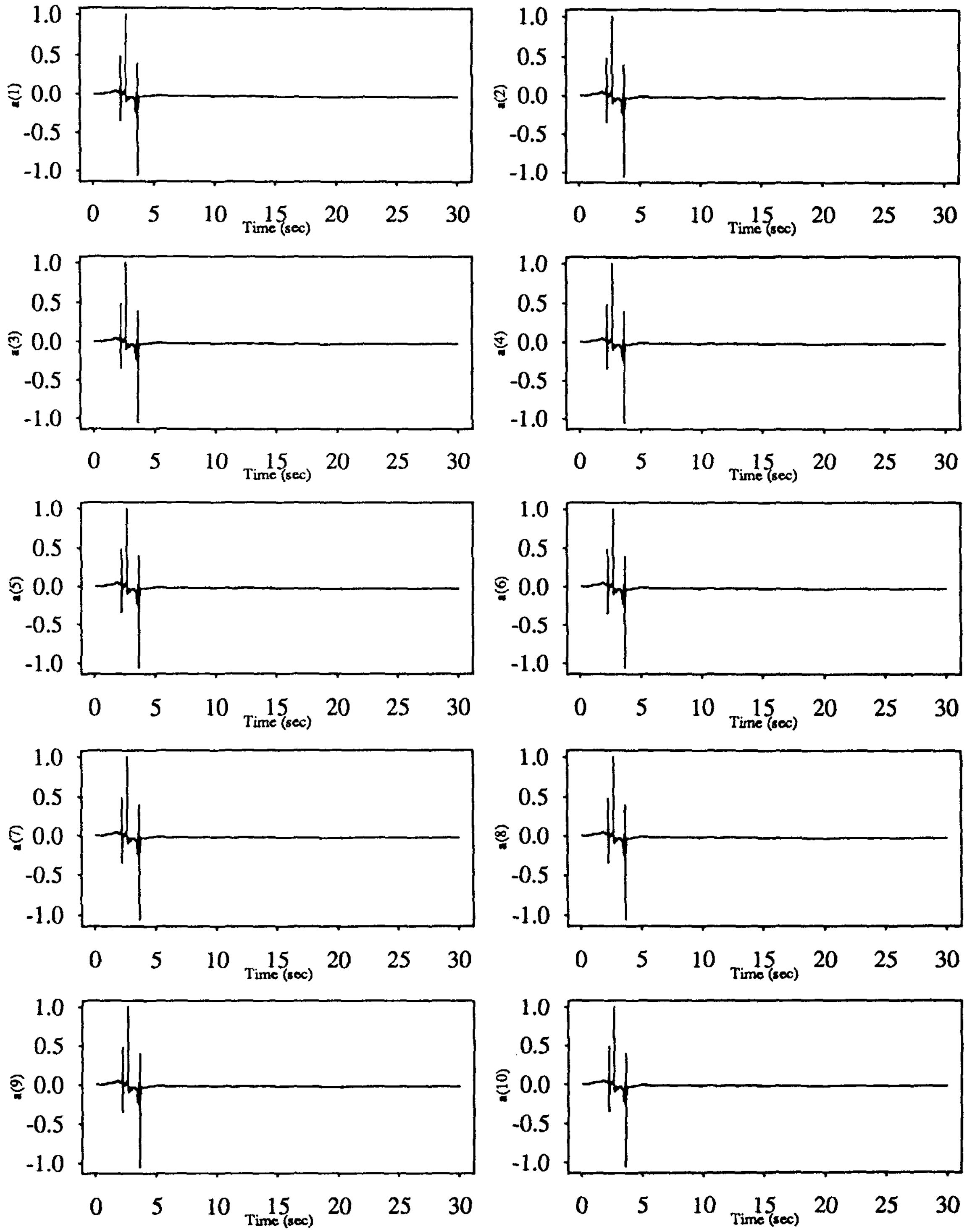


Figure 5.163

Recursive Instrumental Variable Estimation
Five Story Building Model; White Noise Input
4th Floor gamma=1

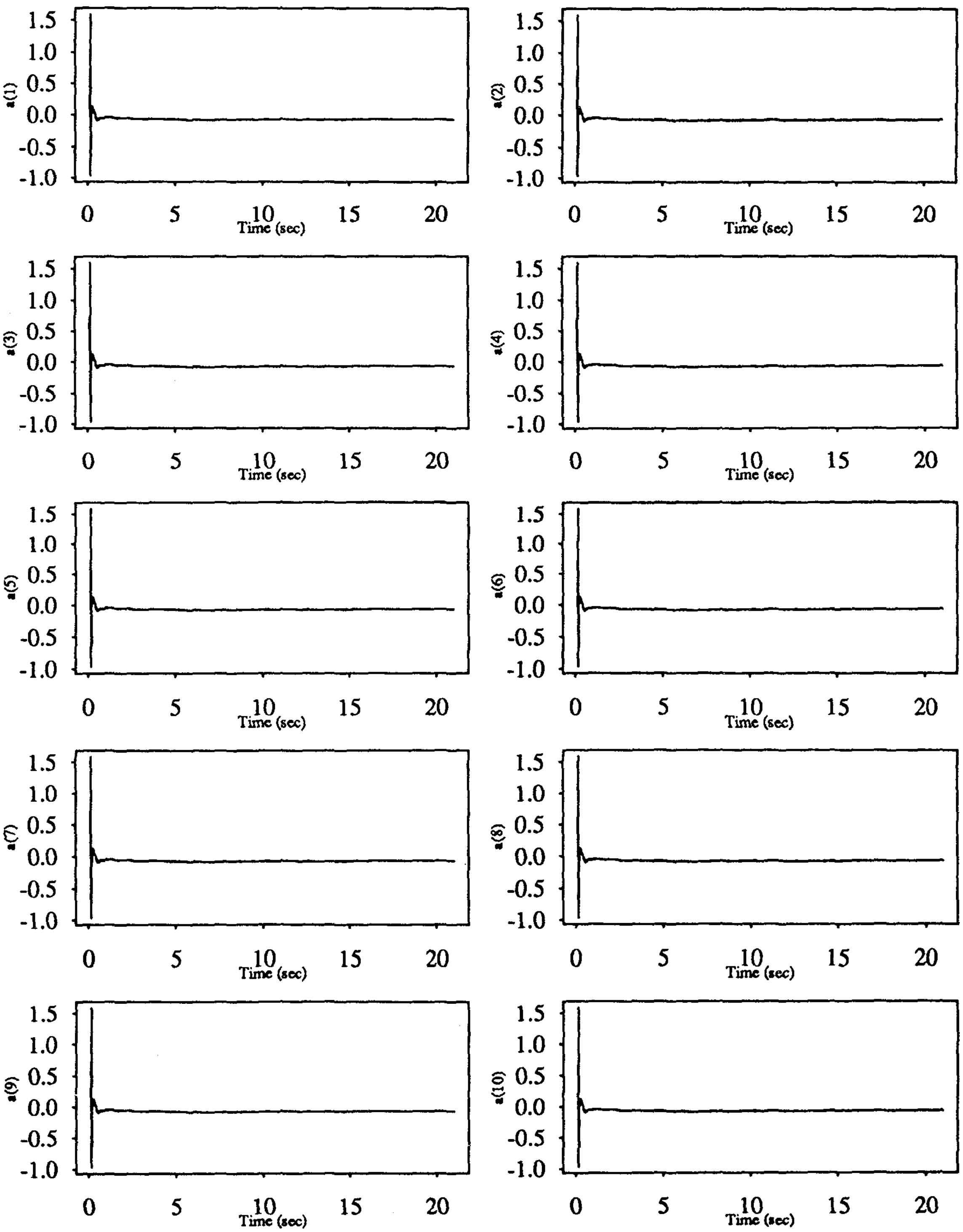


Figure 5.164

## Recursive Instrumental Variable Estimation
## Five Story Building Model; El-Centro Input
2nd Floor gamma=0.03

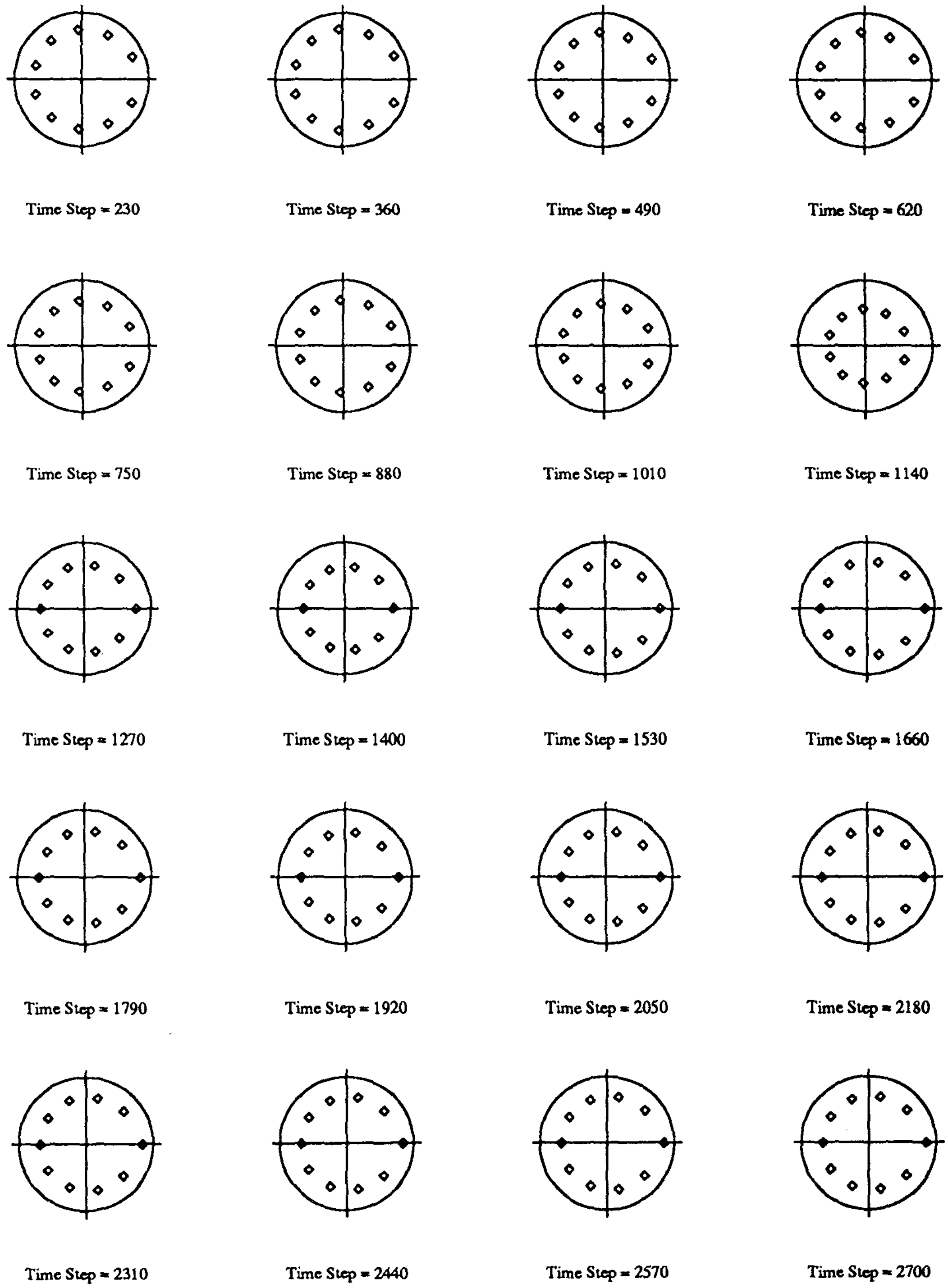


Figure 5.165

## Recursive Instrumental Variable Estimation
## Five Story Building Model; White Noise Input
4th Floor gamma=0.03

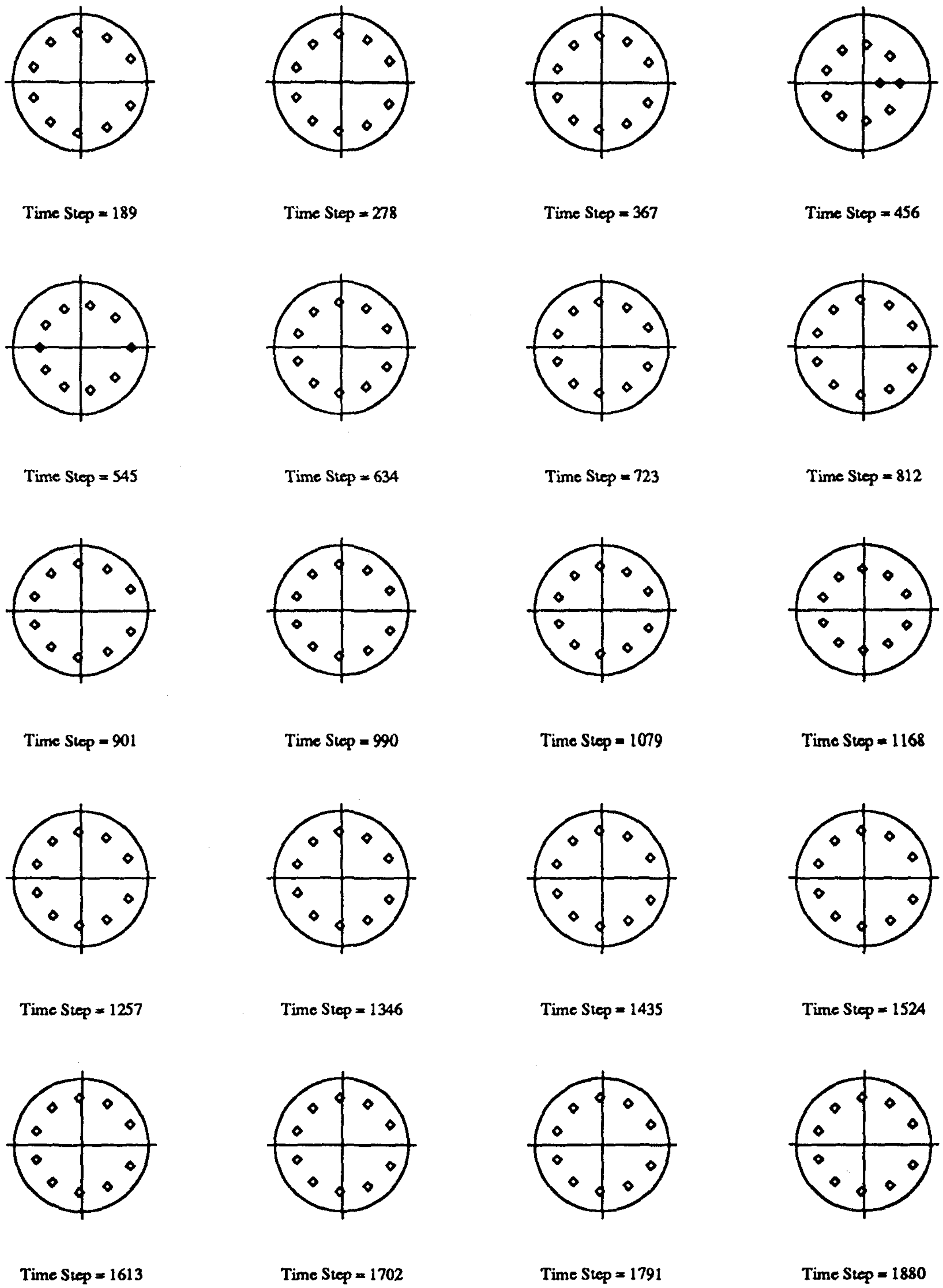


**Figure 5.166**

## Recursive Instrumental Variable Estimation
## Five Story Building Model; White Noise Input
### 5th Floor gamma=0.05

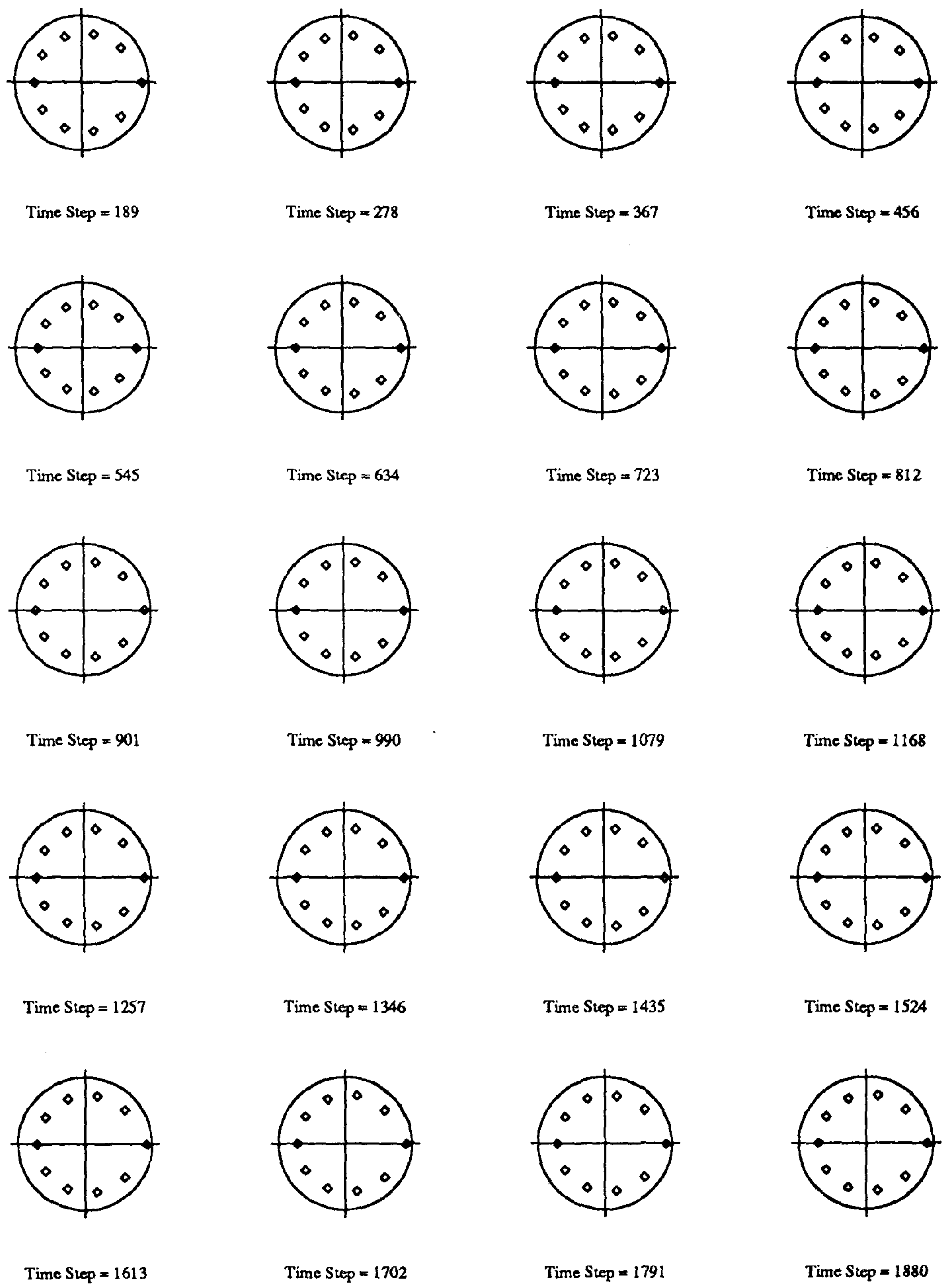


Figure 5.167

Recursive Instrumental Variable Estimation
Five Story Building Model; El-Centro Input
3rd Floor gamma=0.1

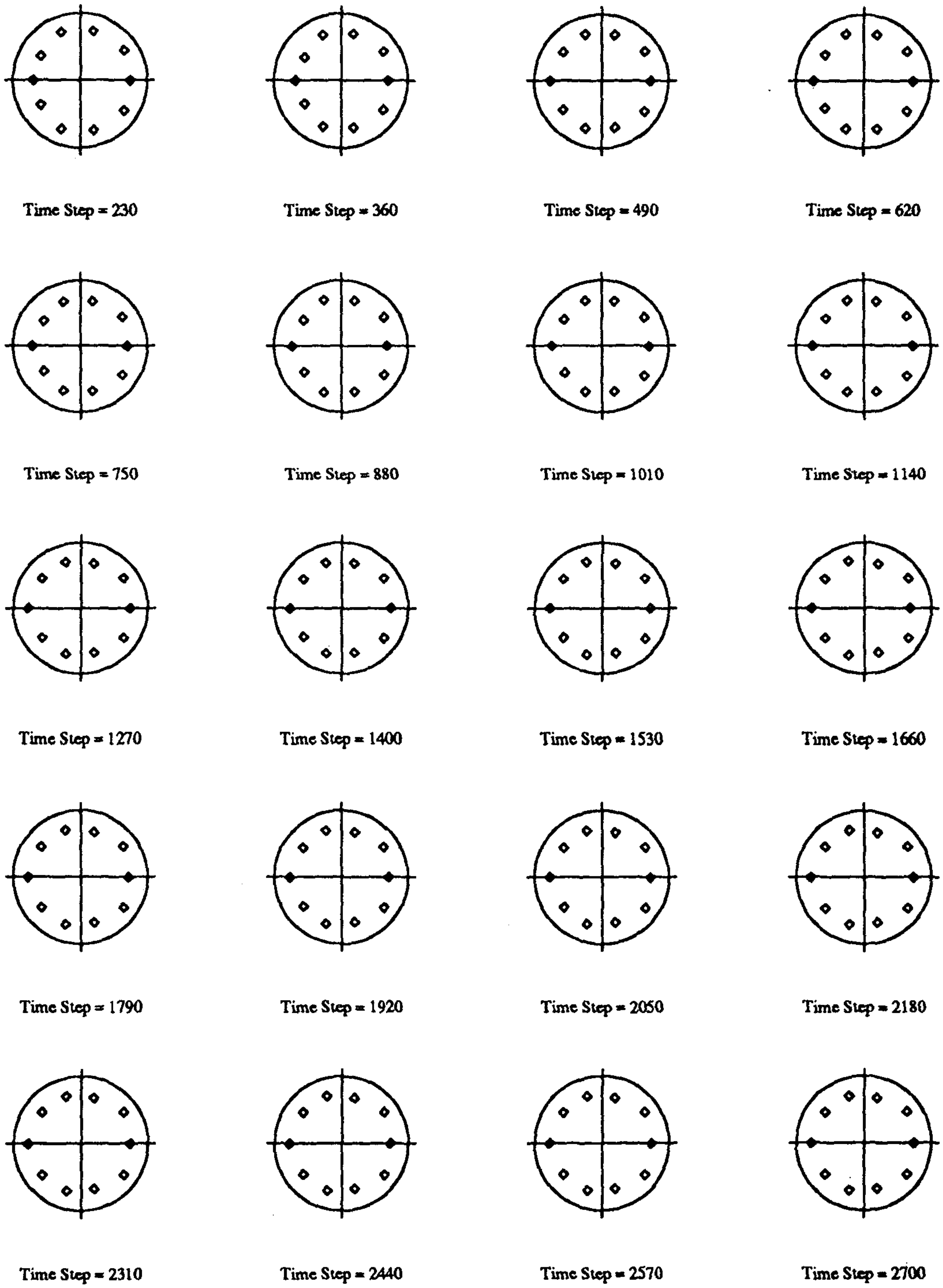


Figure 5.168

Recursive Instrumental Variable Estimation
Five Story Building Model; El-Centro Input
1st Floor gamma=0.11

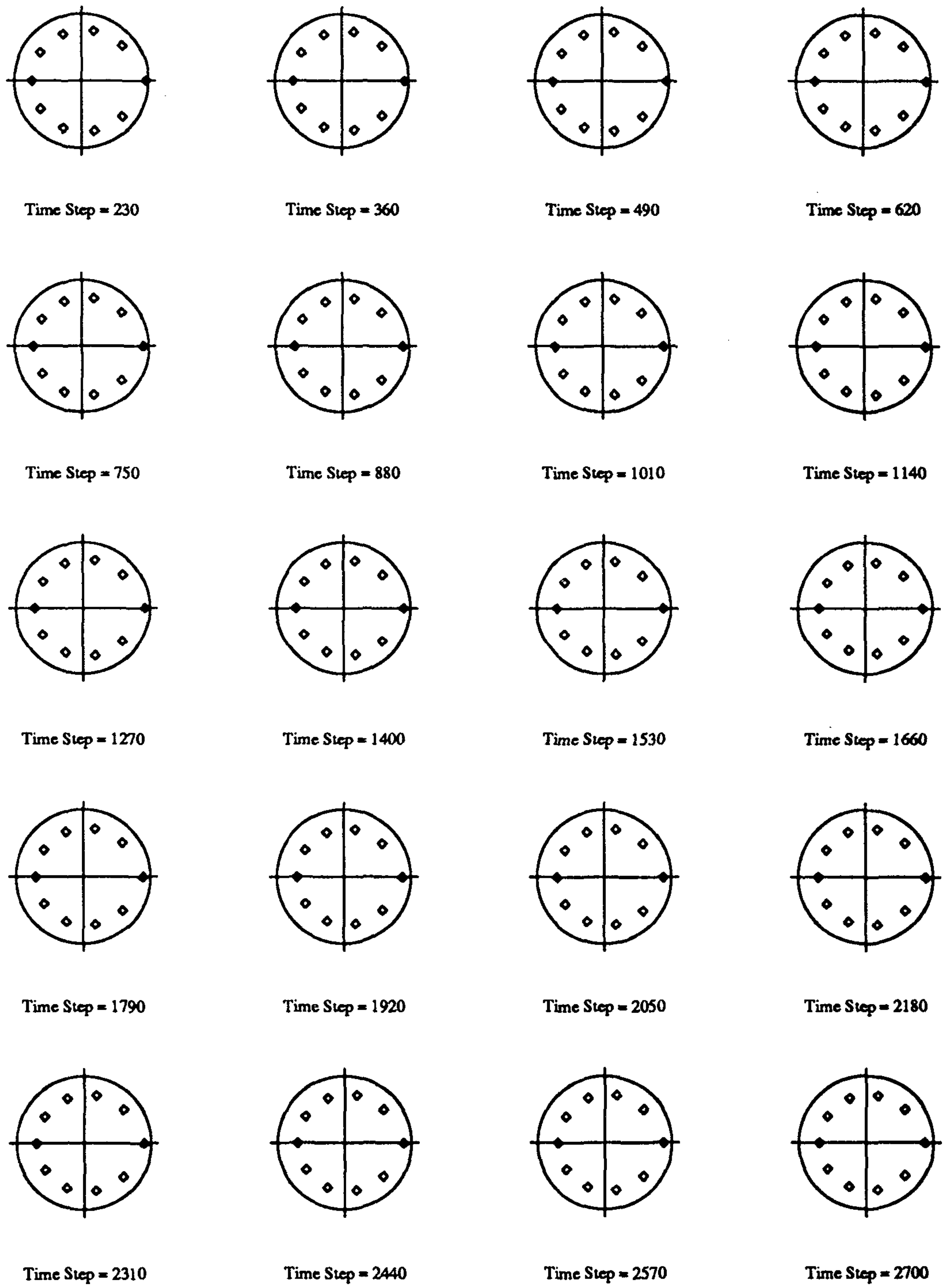


Figure 5.169

## Recursive Instrumental Variable Estimation
## Five Story Building Model; White Noise Input
### 5th Floor gamma=0.11

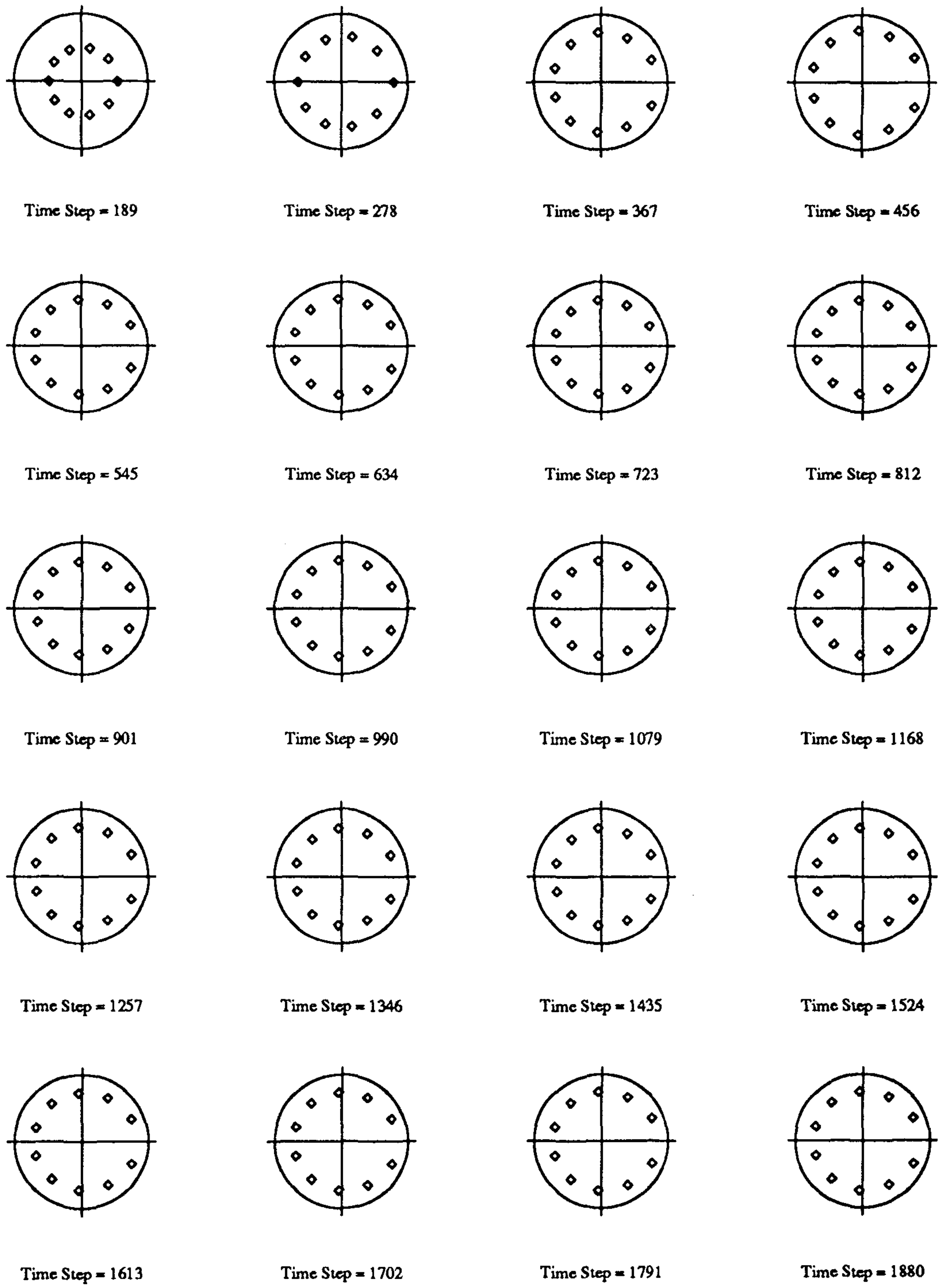


Figure 5.170

Recursive Instrumental Variable Estimation
Five Story Building Model; White Noise Input
5th Floor gamma=0.13

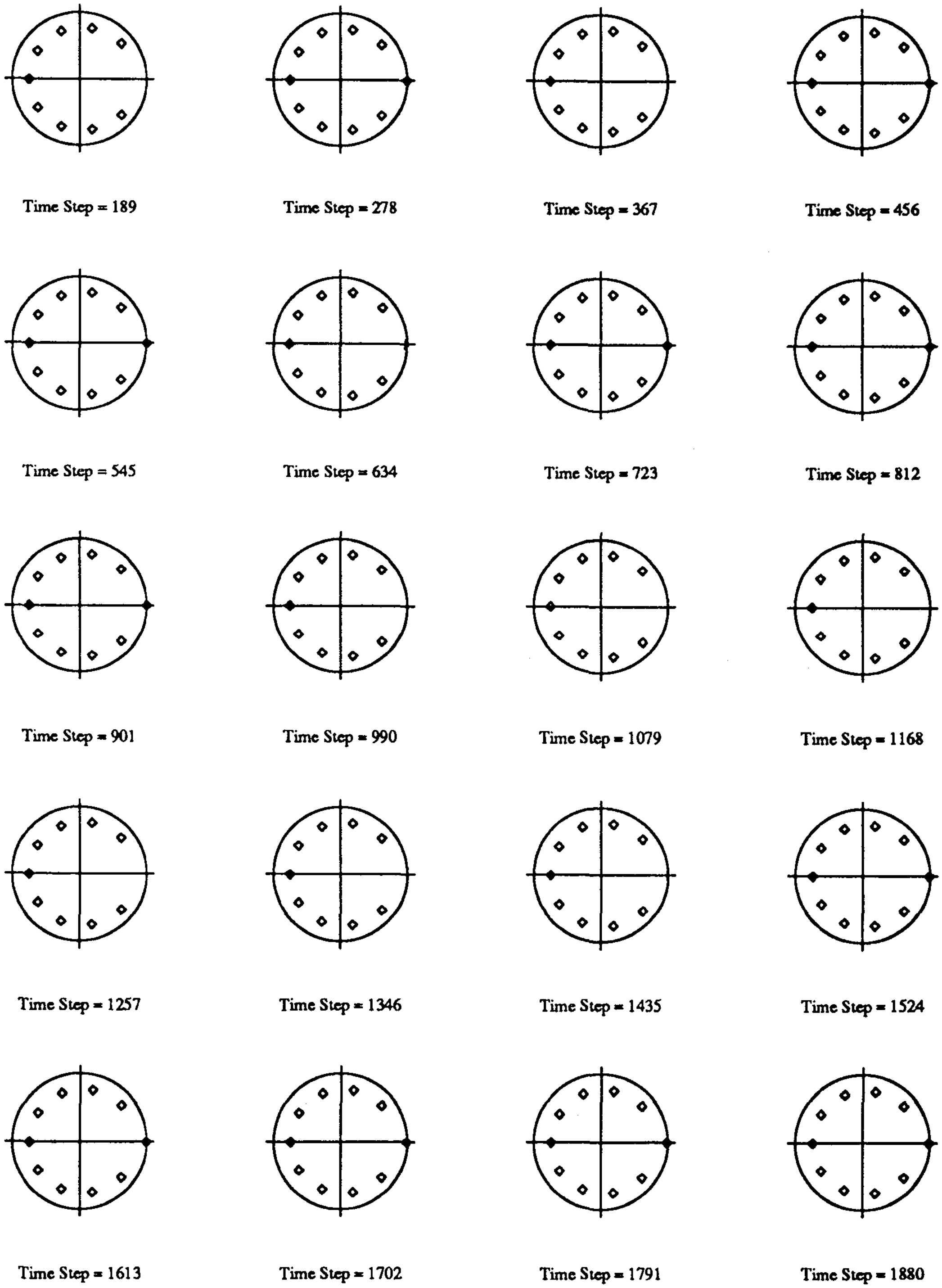


Figure 5.171

## Recursive Instrumental Variable Estimation
## Five Story Building Model; El-Centro Input
### 1st Floor gamma=1

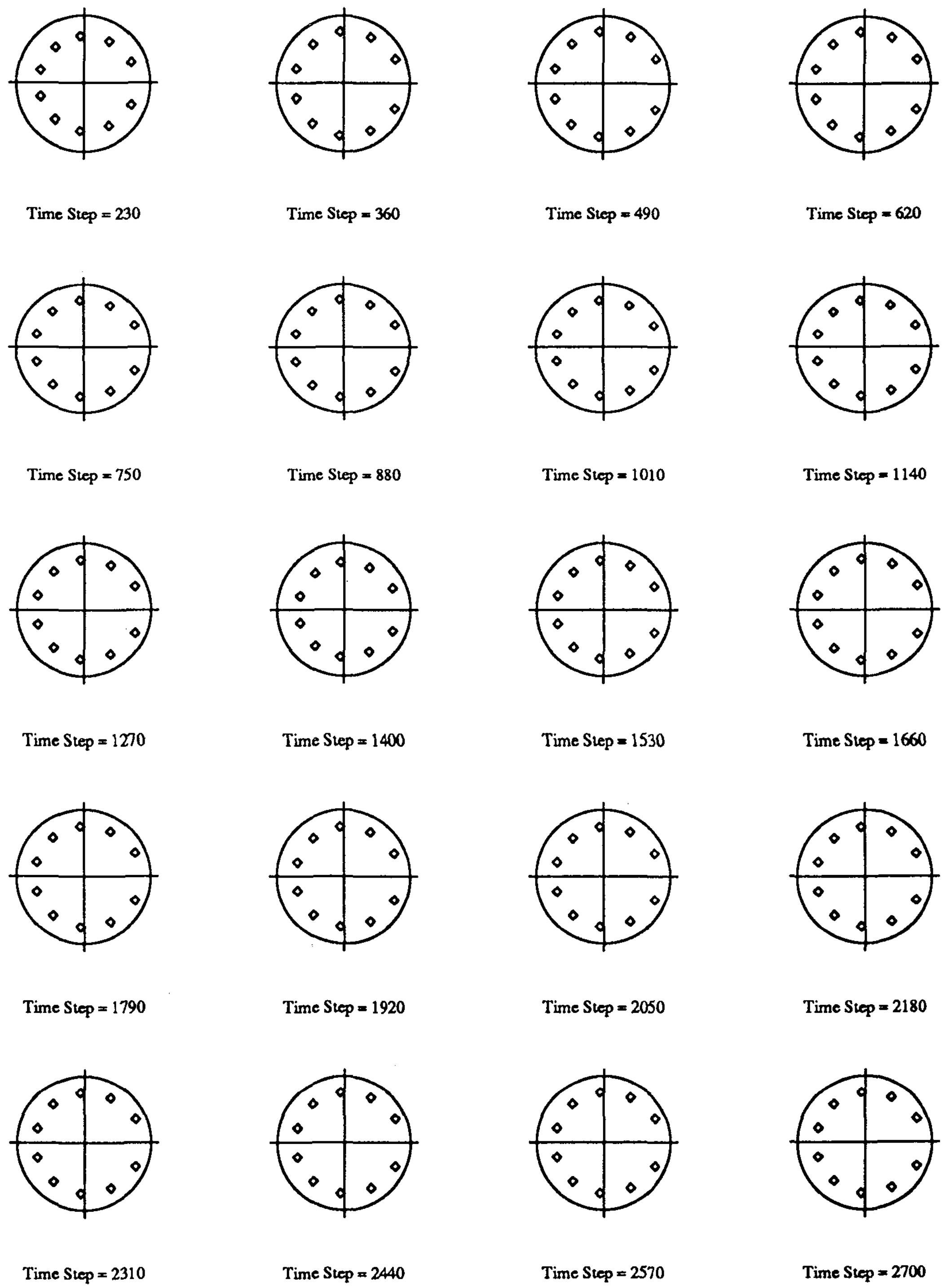


**Figure 5.172**

## Recursive Instrumental Variable Estimation
## Five Story Building Model; El-Centro Input
### 3rd Floor gamma=1

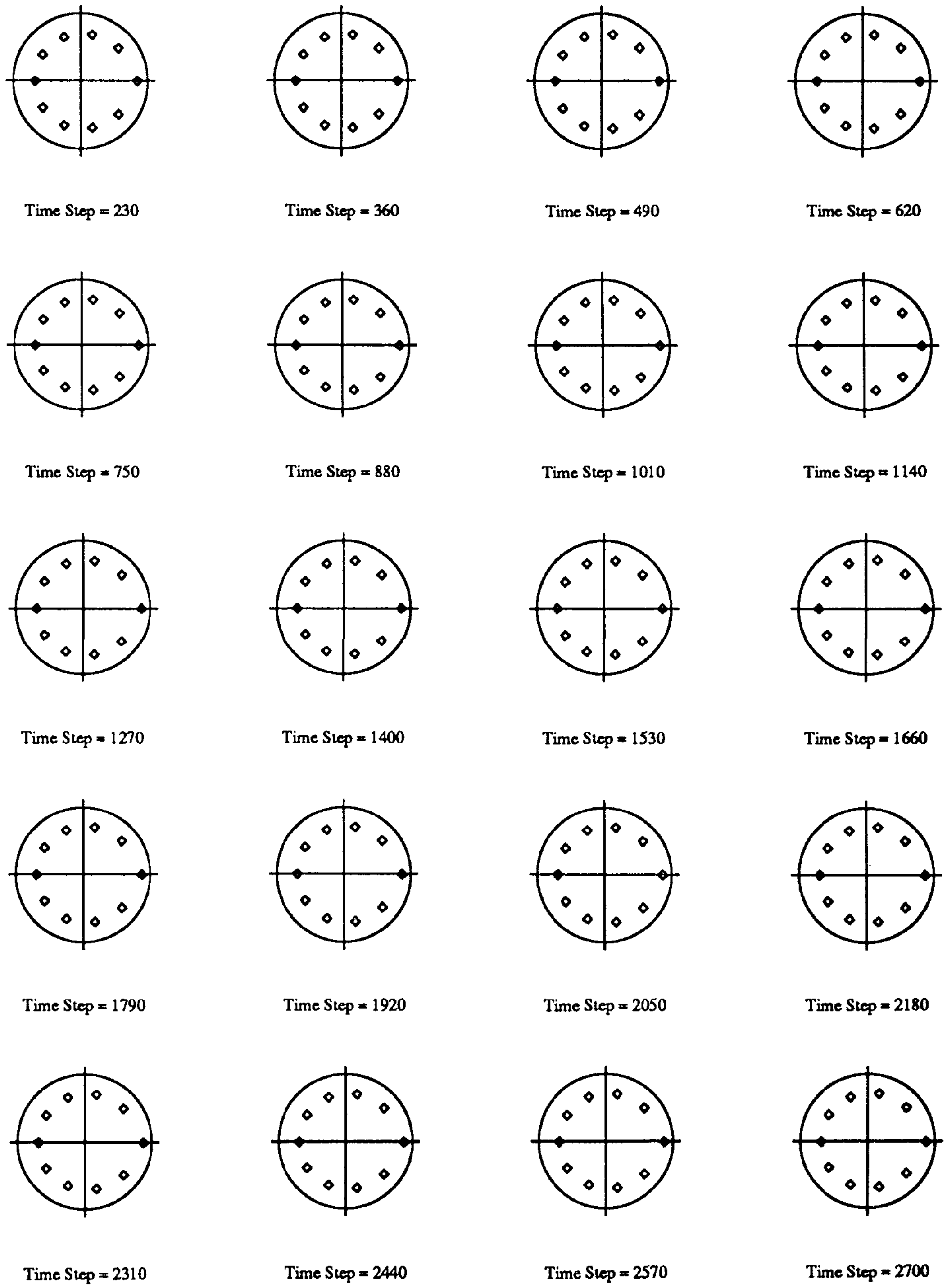


**Figure 5.173**

Recursive Instrumental Variable Estimation
Five Story Building Model; White Noise Input
3rd Floor gamma=1

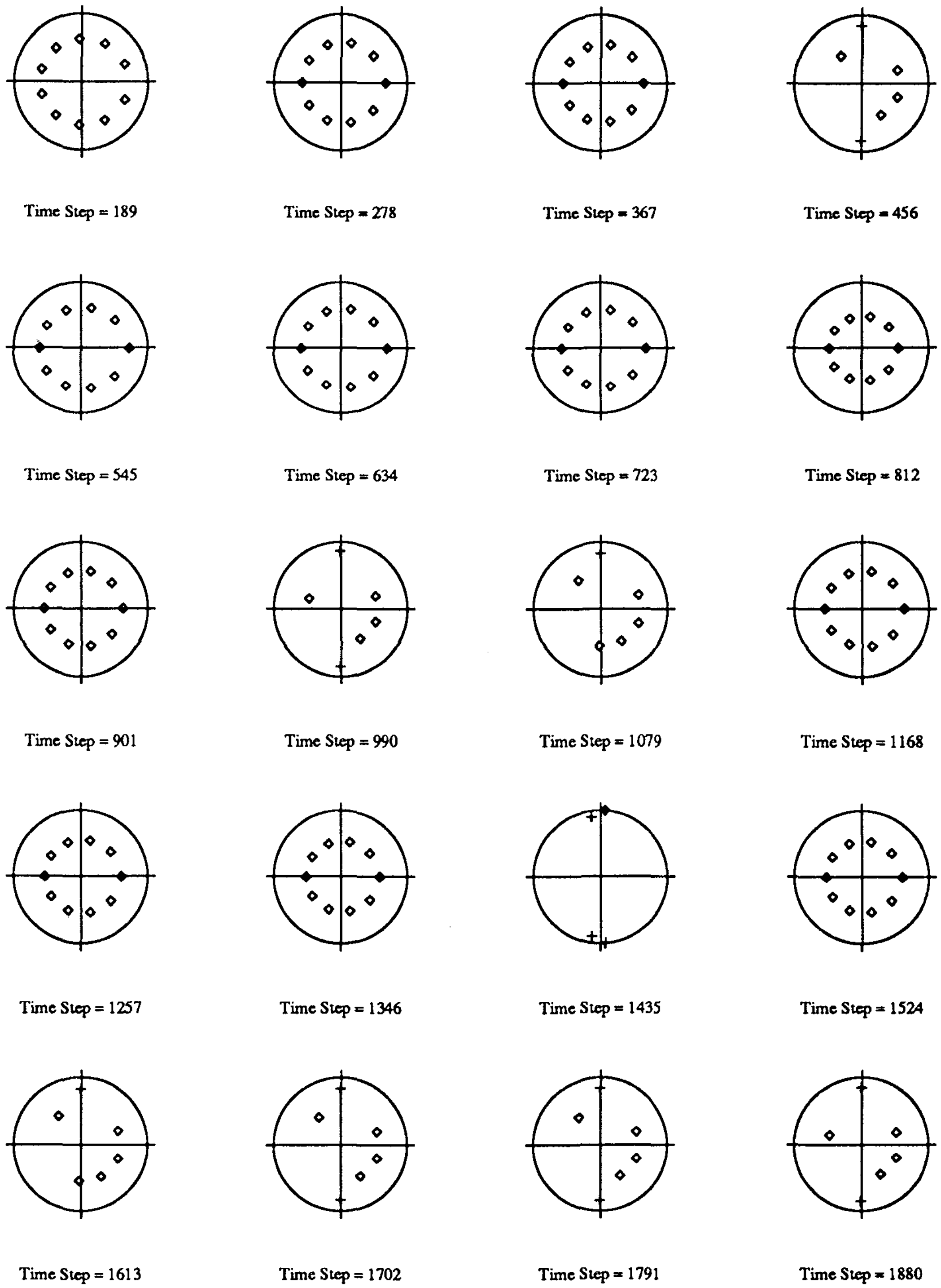


**Figure 5.174**

## Recursive Instrumental Variable Estimation
## Five Story Building Model; El-Centro Input
### 4th Floor gamma=1

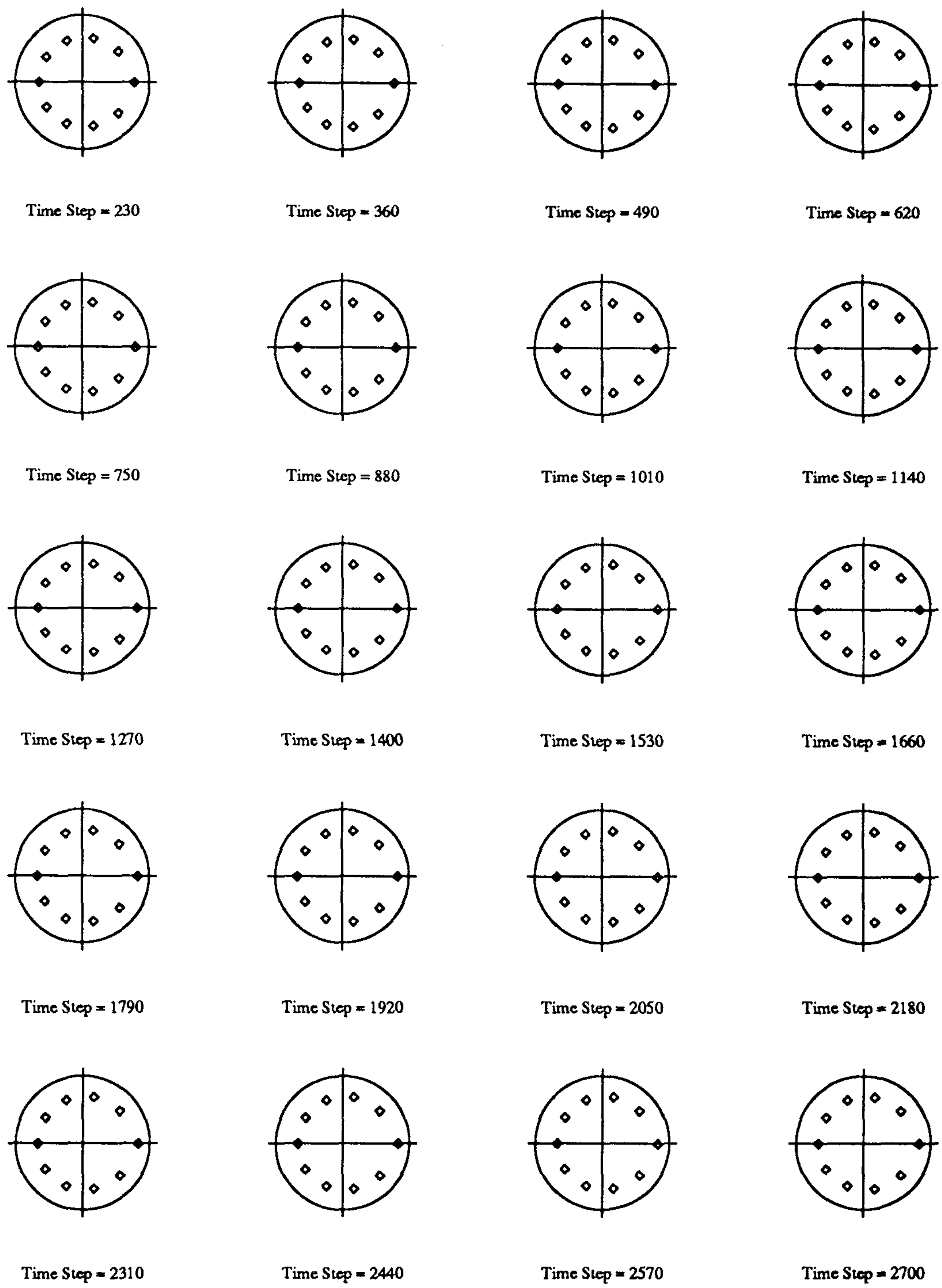


Figure 5.175

## Recursive Instrumental Variable Estimation
## Five Story Building Model; White Noise Input

4th Floor gamma=1

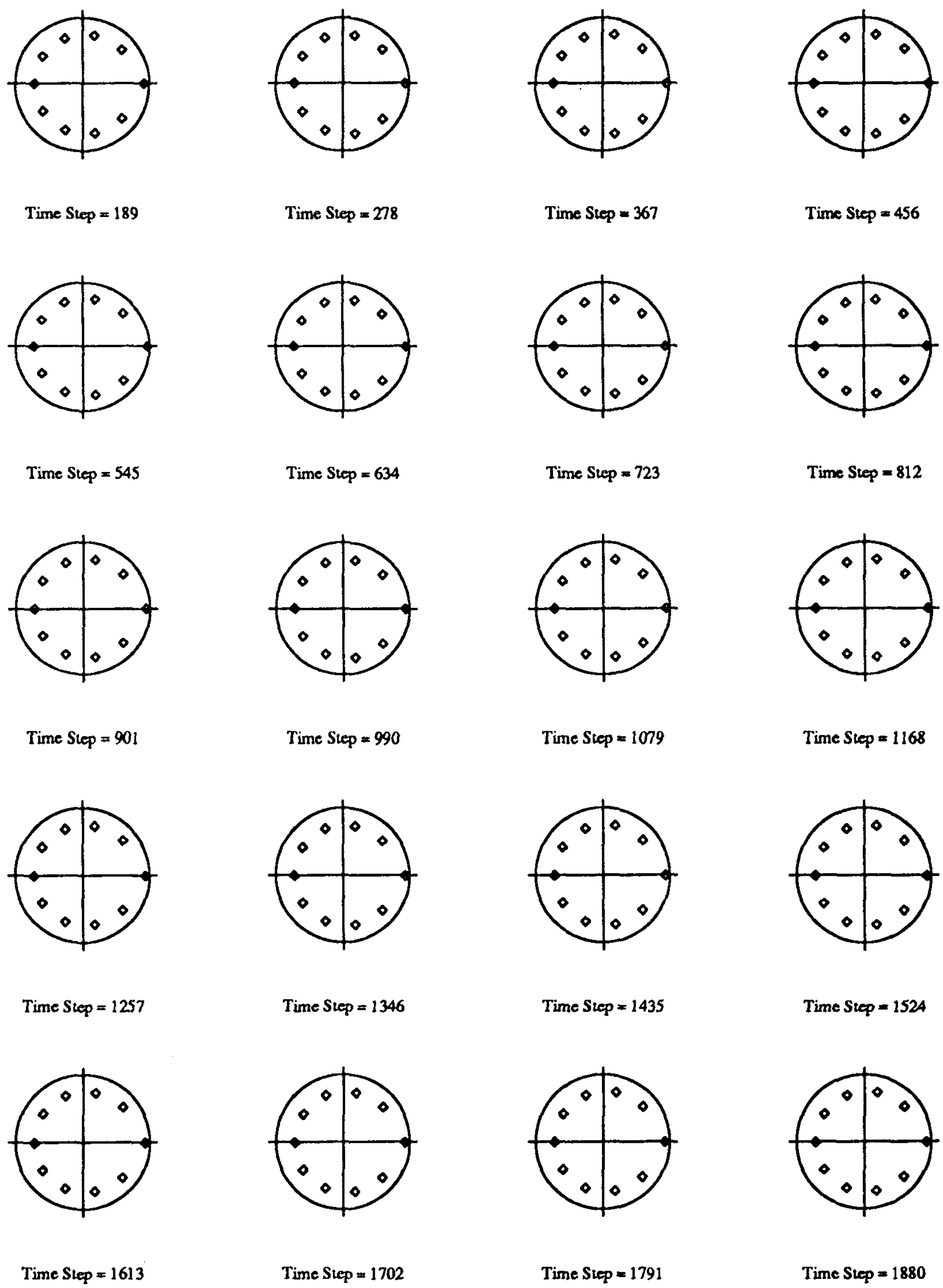


**Figure 5.176**

Recursive Instrumental Variable Estimation
Three Story Building Model; El-Centro Input
1st Floor gamma=0.03

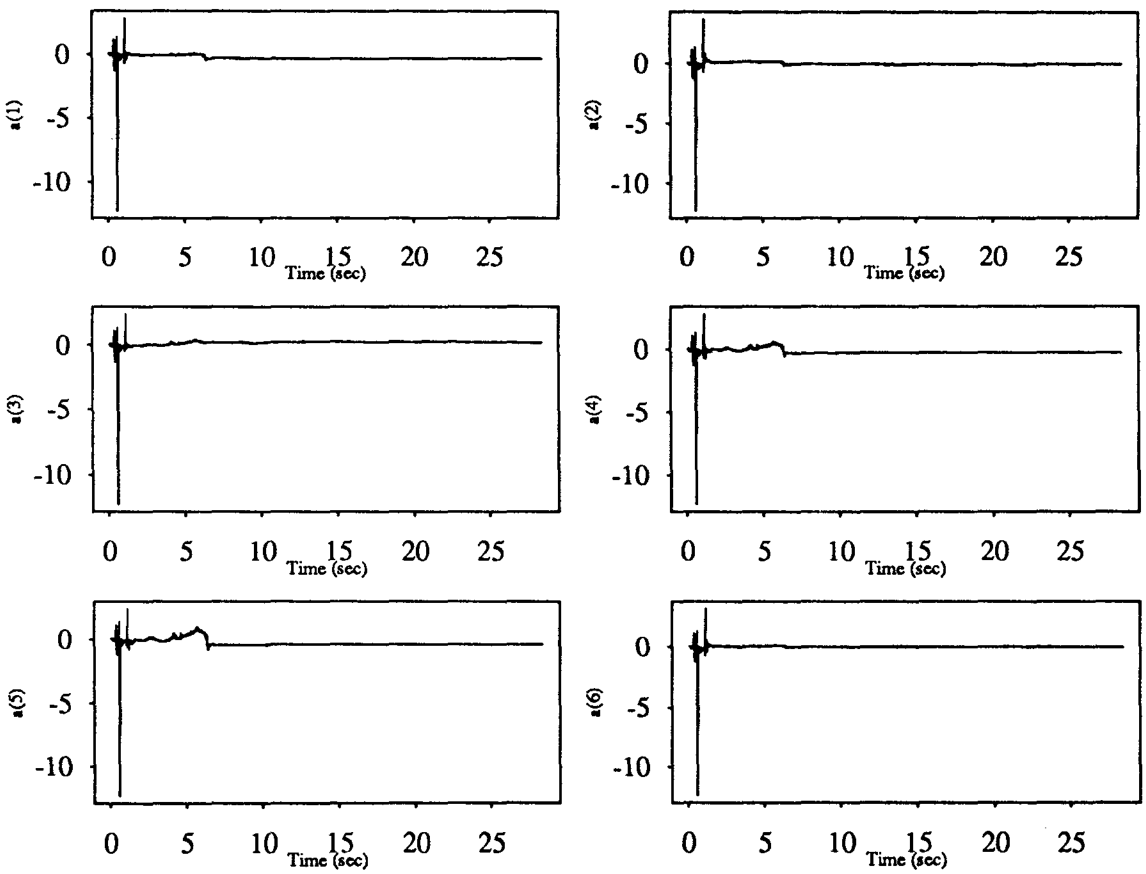


Figure 5.177

Recursive Instrumental Variable Estimation
Three Story Building Model; El-Centro Input
3rd Floor gamma=0.1

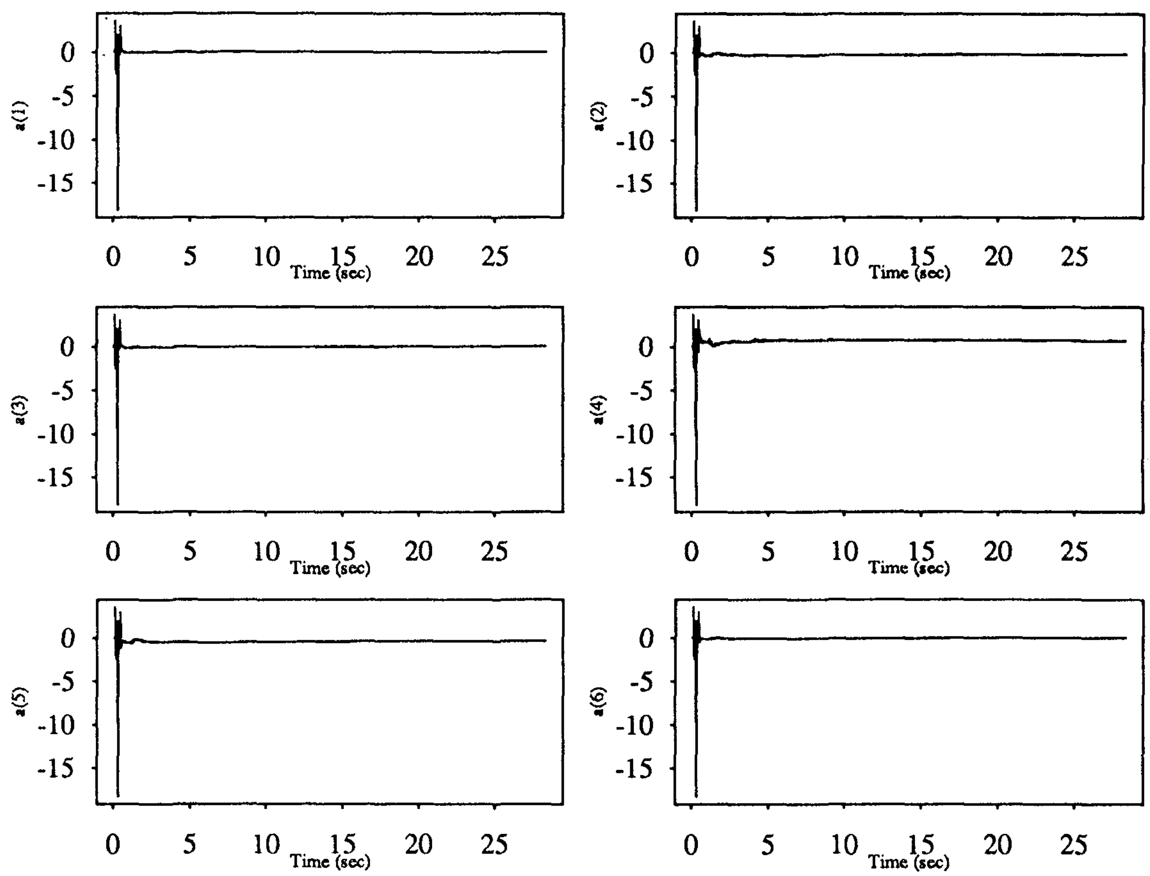


Figure 5.178

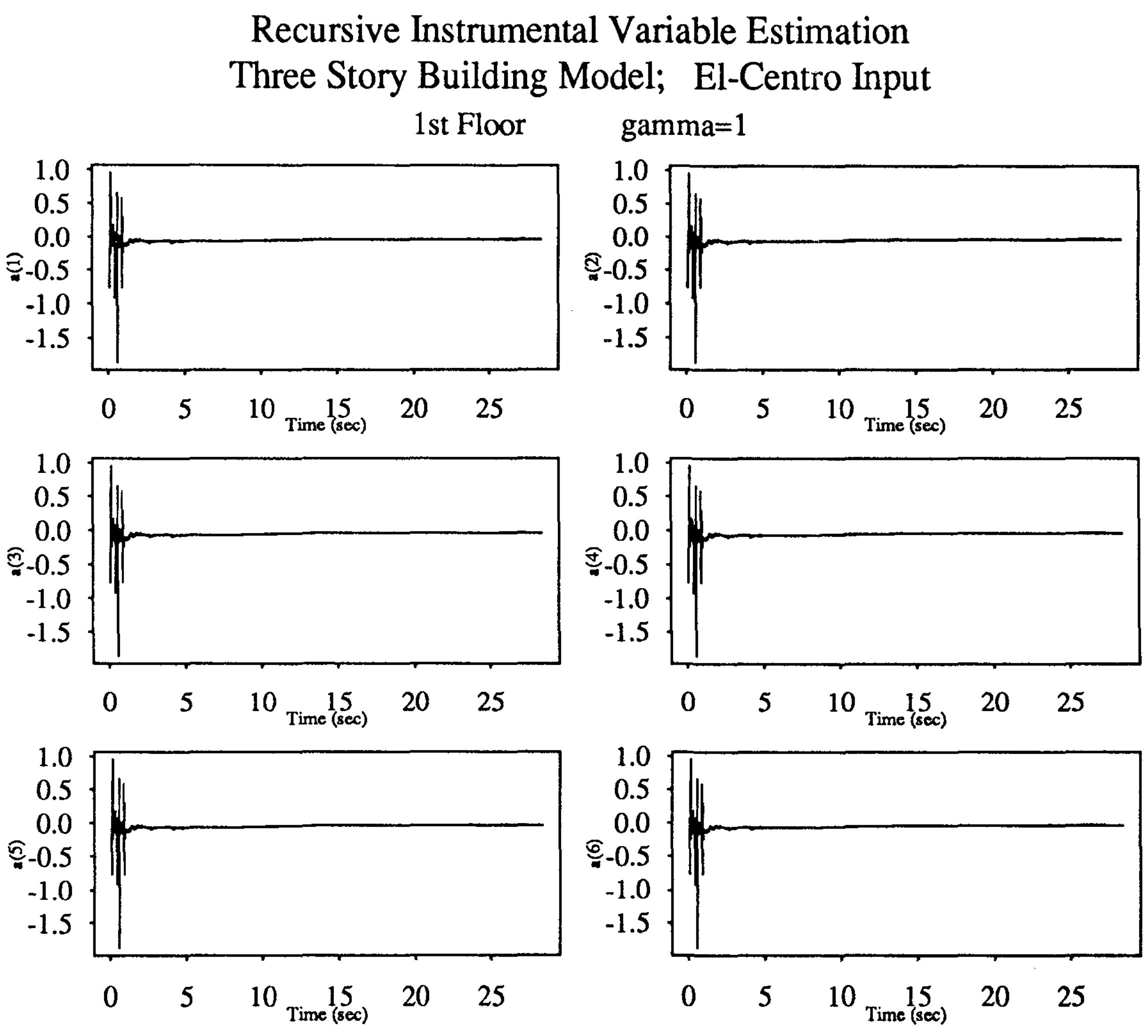

Recursive Instrumental Variable Estimation
Three Story Building Model; El-Centro Input
1st Floor gamma=1
a(1)
a(2)
a(3)
a(4)
a(5)
a(6)
1.0
0.5
0.0
-0.5
-1.0
-1.5
0
5
10
15
20
25
Time (sec)


Figure 5.179

Recursive Instrumental Variable Estimation
Three Story Building Model; El-Centro Input
3rd Floor gamma=1

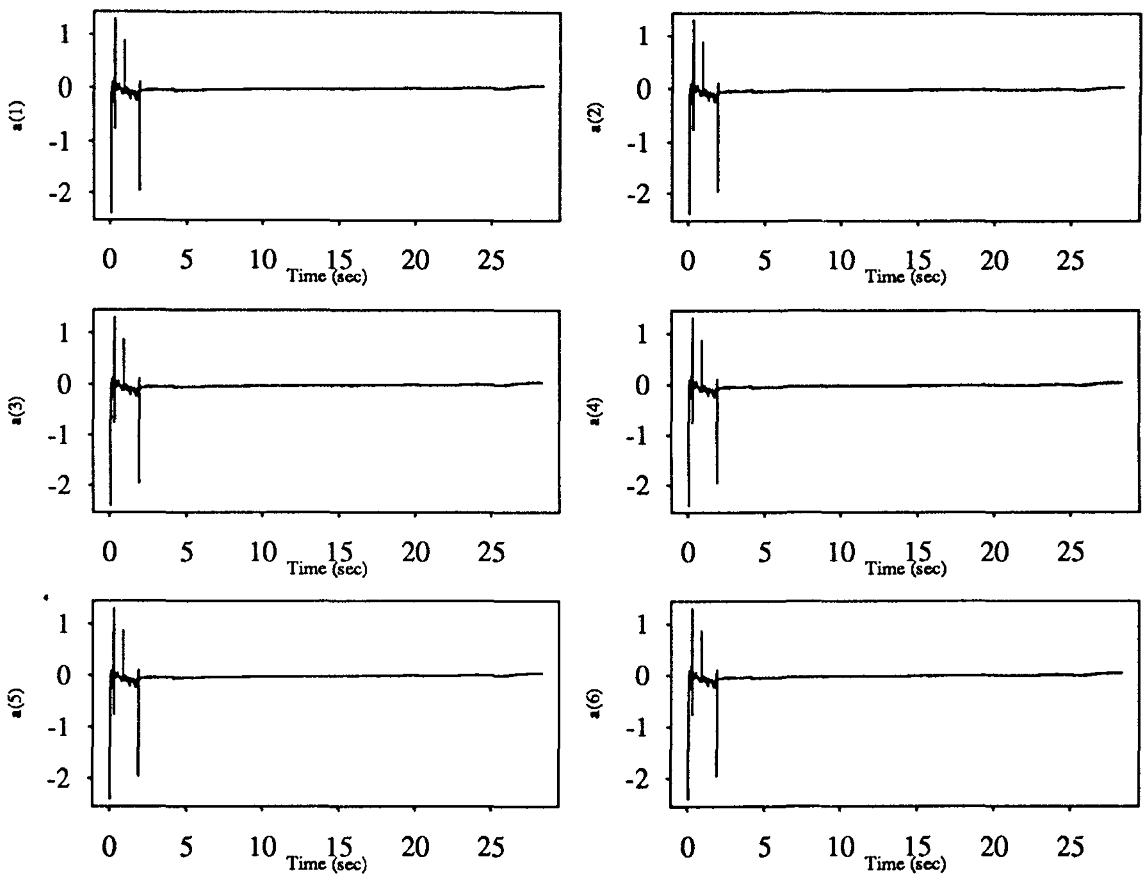


Figure 5.180

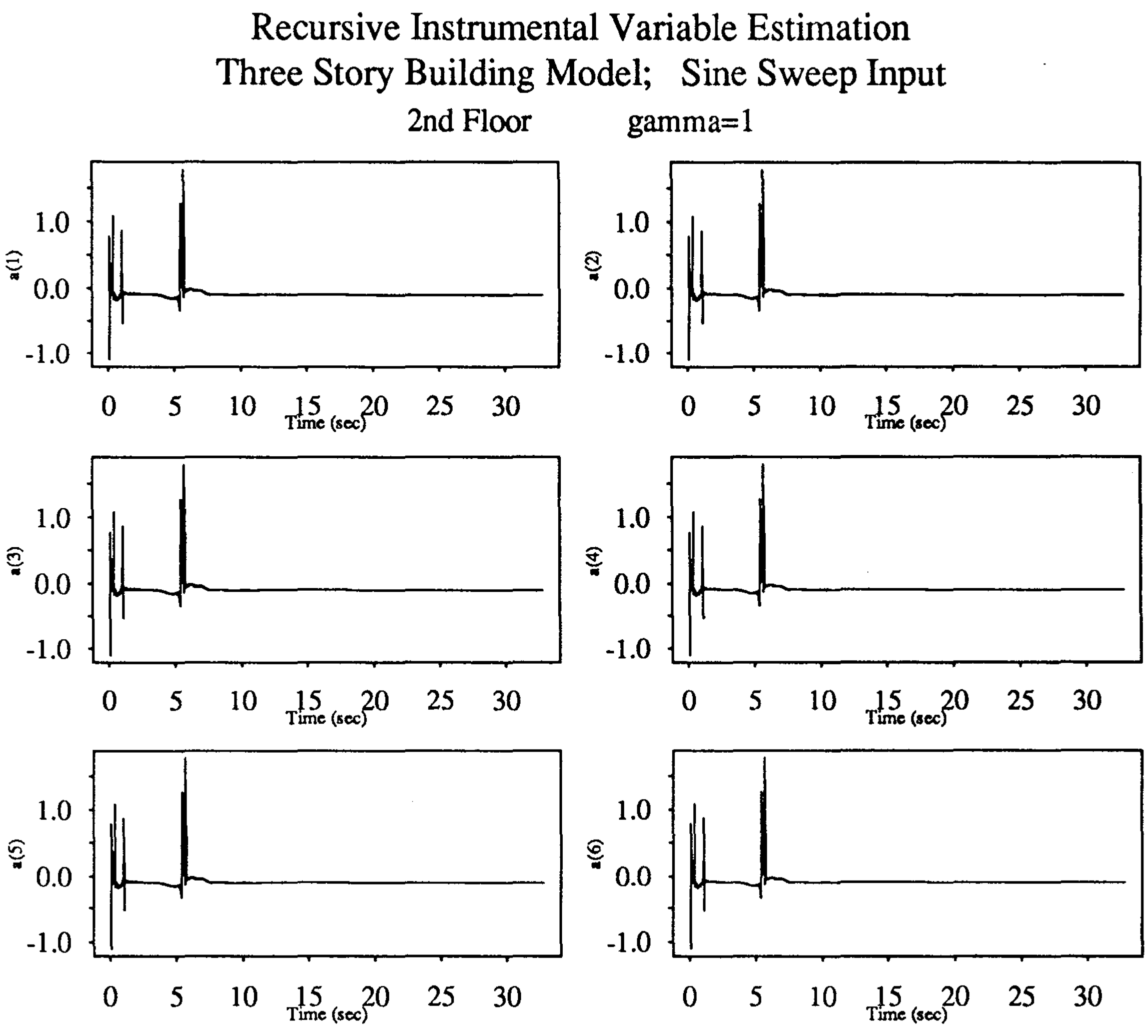
Recursive Instrumental Variable Estimation
Three Story Building Model; Sine Sweep Input
2nd Floor gamma=1
a(1)
a(2)
a(3)
a(4)
a(5)
a(6)
1.0
0.0
-1.0
0 5 10 15 20 25 30
Time (sec)

Figure 5.181

Recursive Instrumental Variable Estimation
Three Story Building Model; Sine Sweep Input
3rd Floor gamma=1

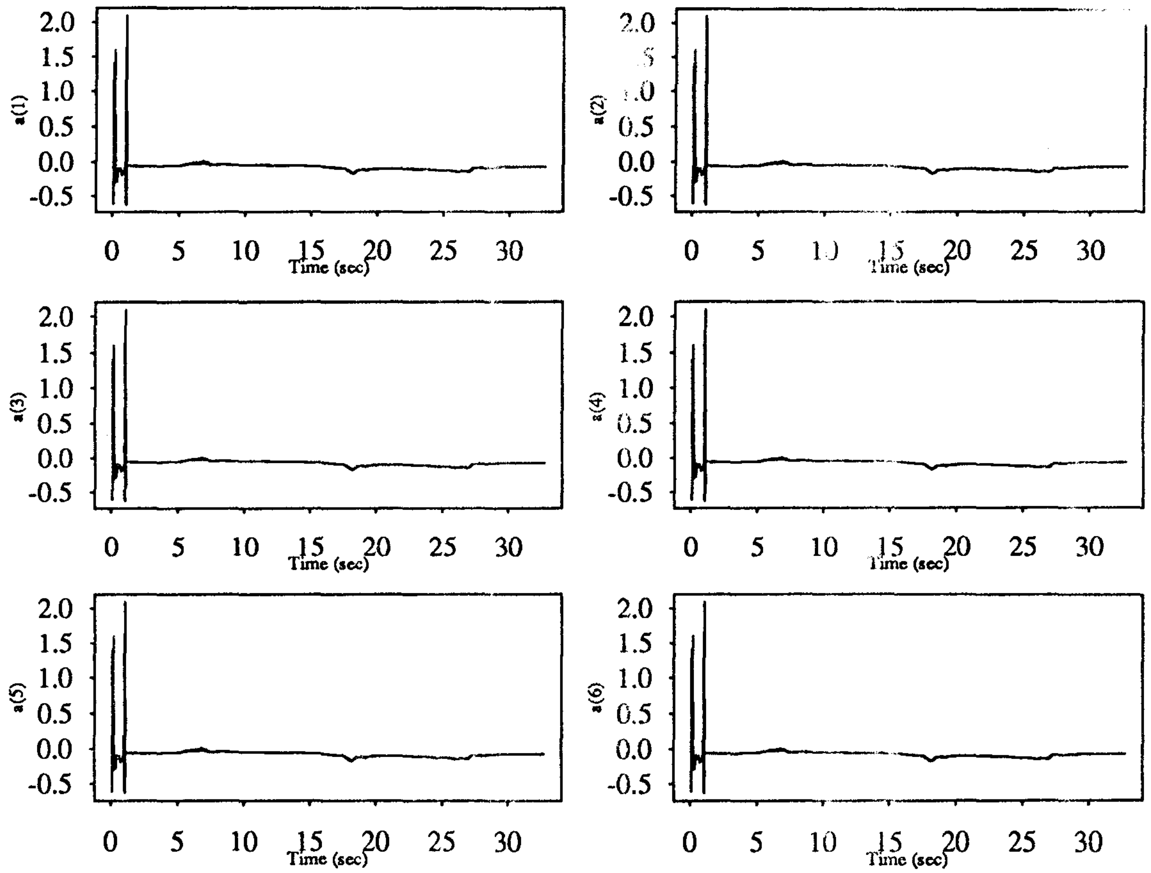


Figure 5.182

## Recursive Instrumental Variable Estimation
## Three Story Building Model; El-Centro Input
1st Floor gamma=0.03

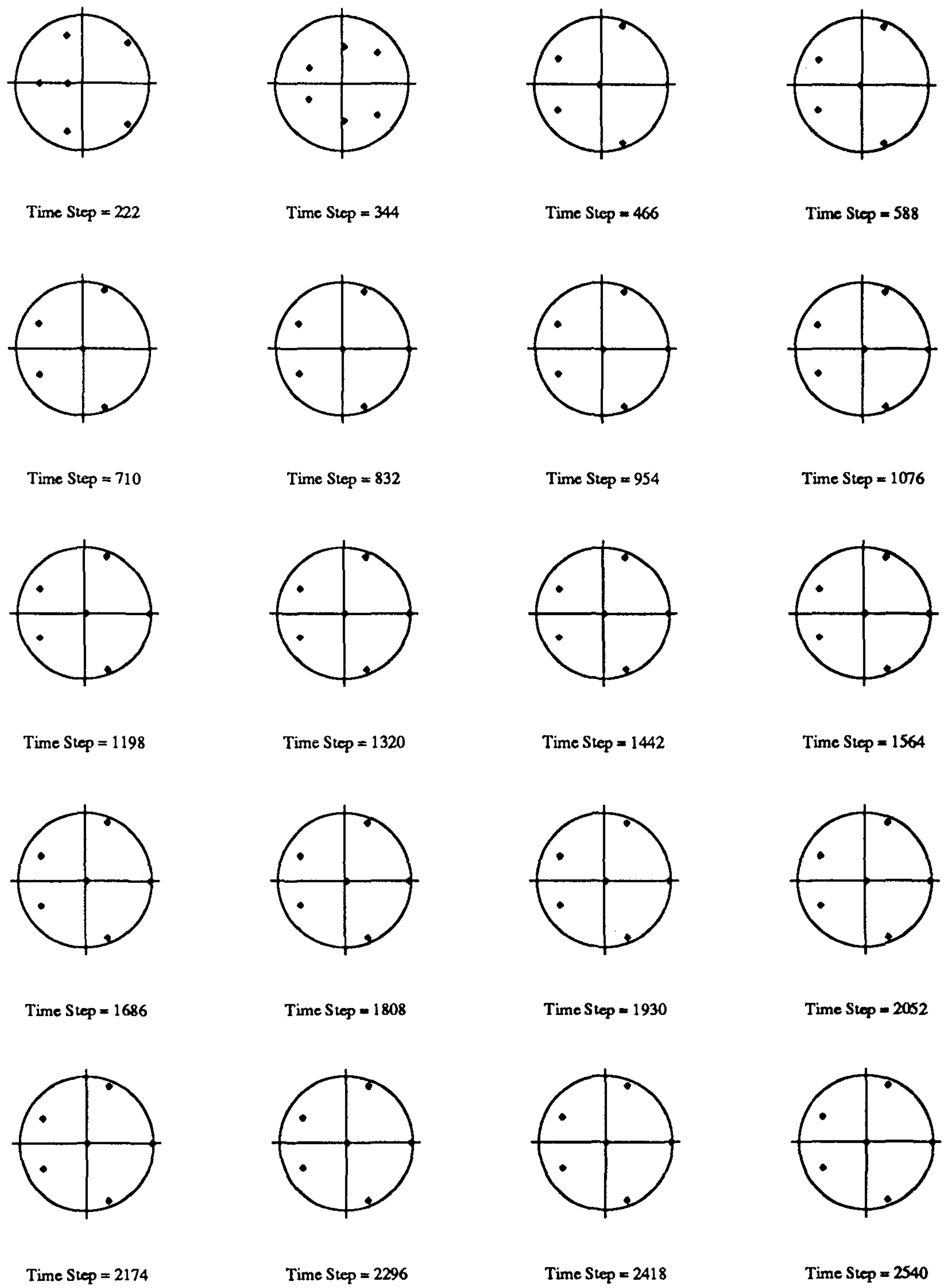


Figure 5.183

## Recursive Instrumental Variable Estimation
## Three Story Building Model; El-Centro Input
### 3rd Floor gamma=0.1

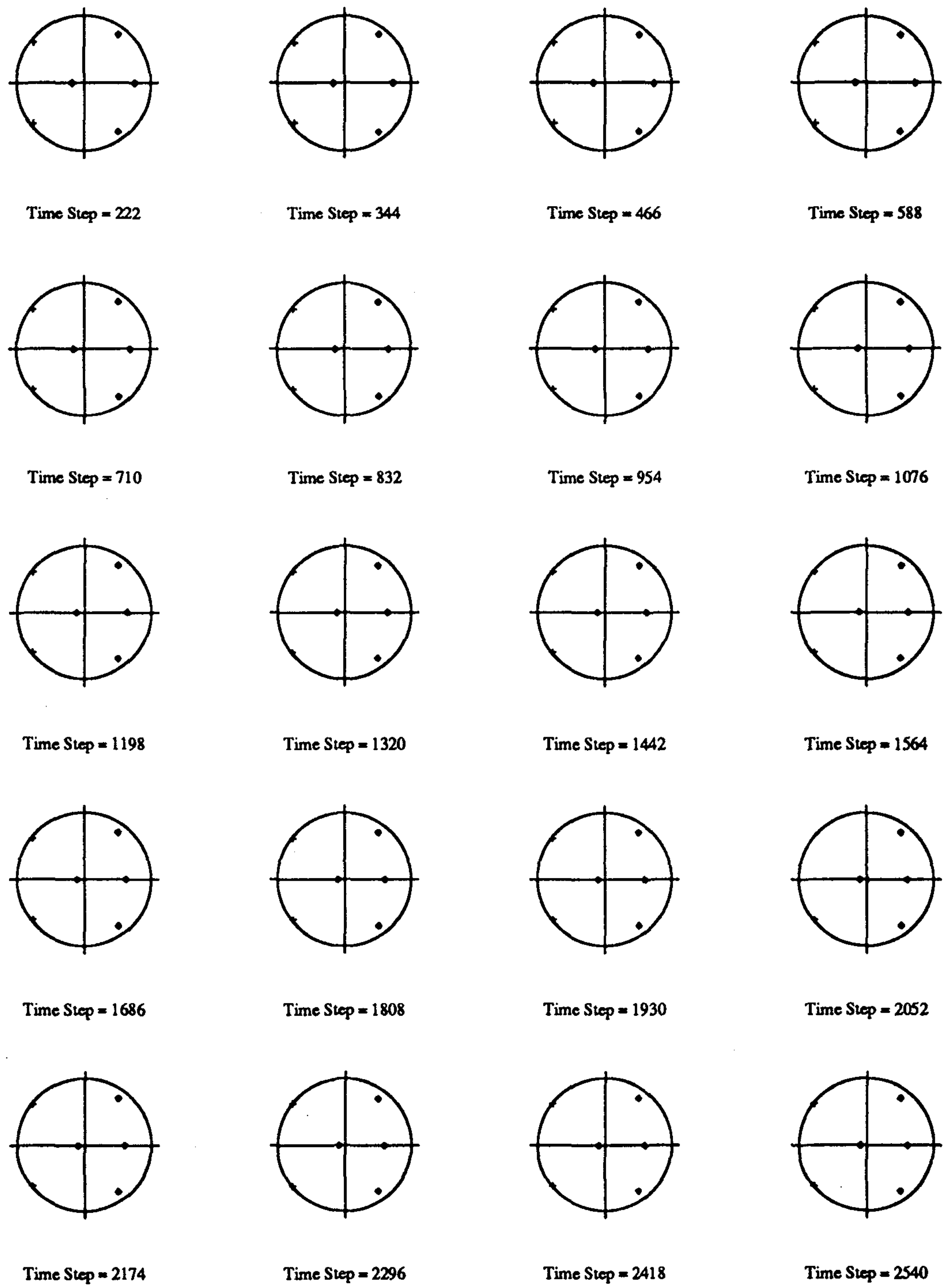


Figure 5.184

## Recursive Instrumental Variable Estimation
## Three Story Building Model; El-Centro Input

1st Floor gamma=1

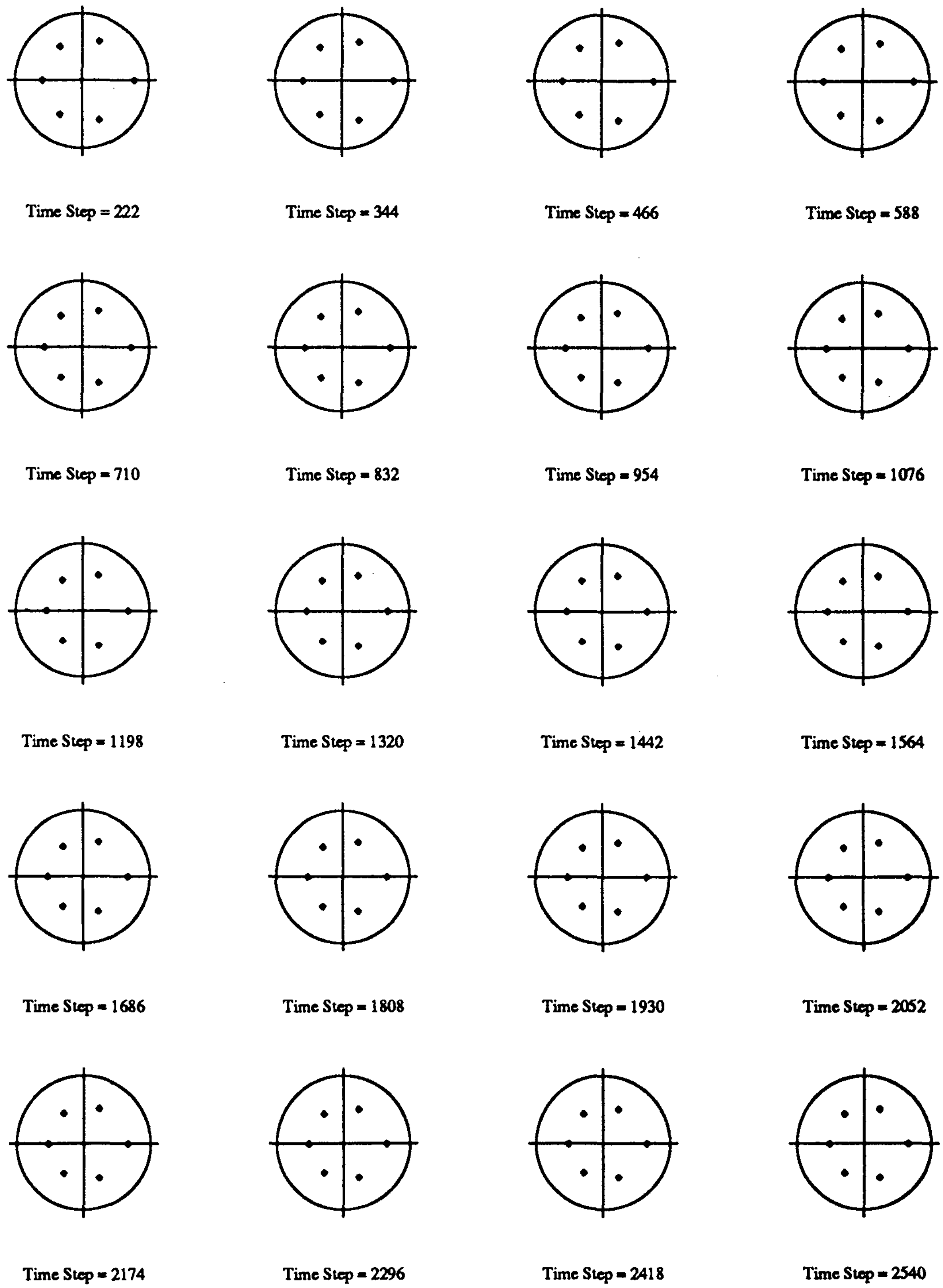


Figure 5.185

Recursive Instrumental Variable Estimation
Three Story Building Model; El-Centro Input
3rd Floor gamma=1

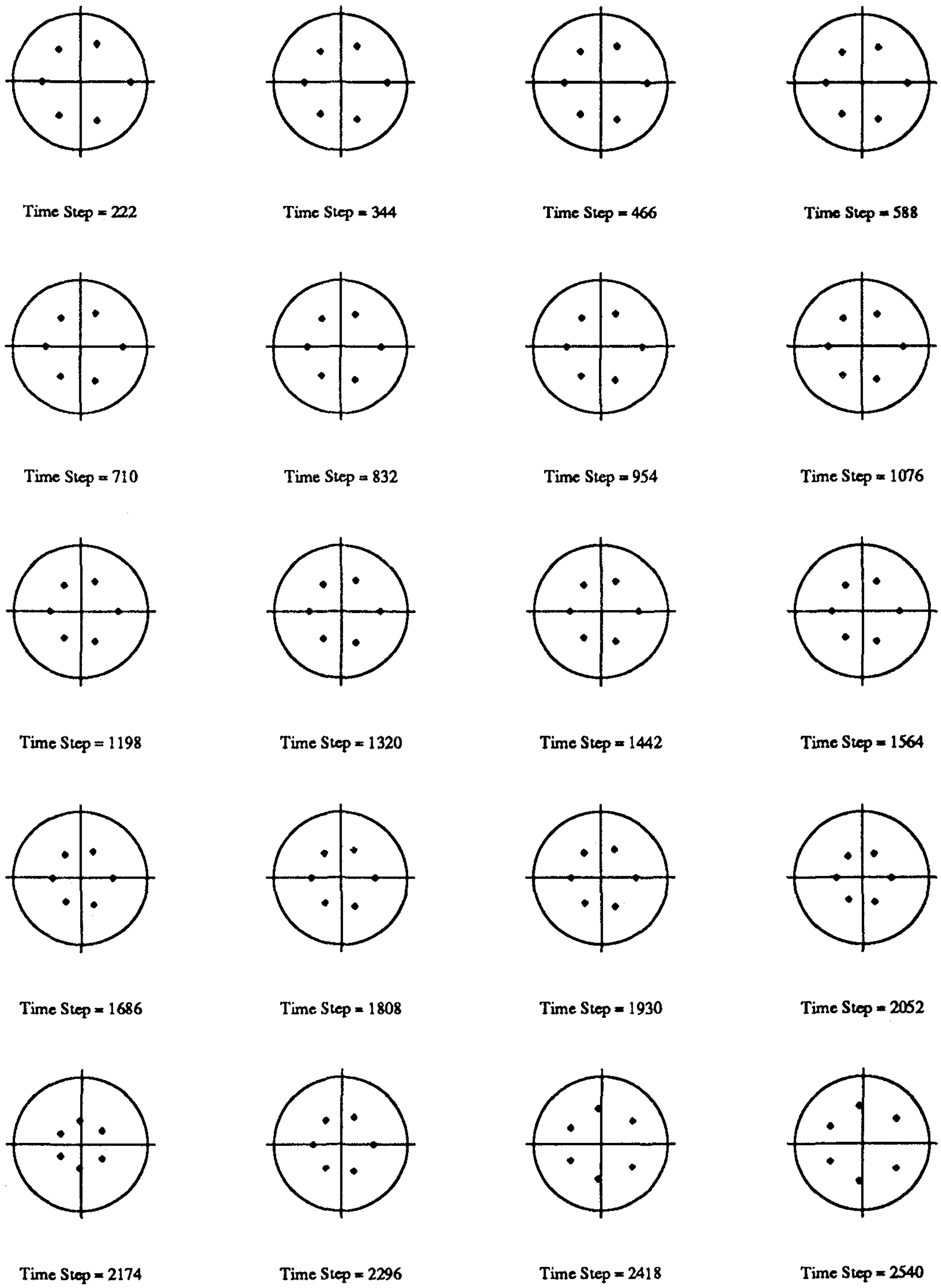


Figure 5.186

Recursive Instrumental Variable Estimation
Three Story Building Model; Sine Sweep Input
2nd Floor gamma=1

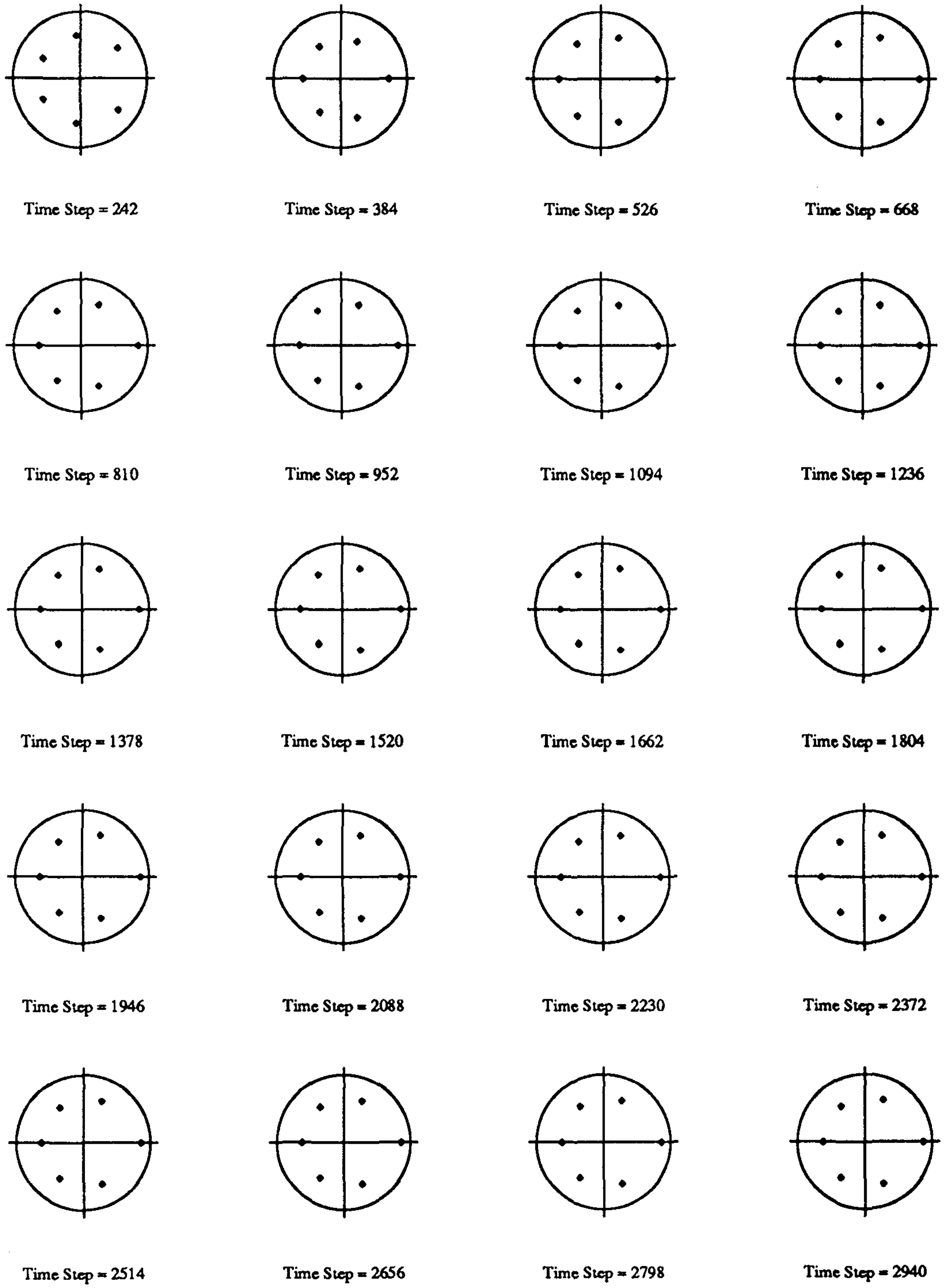


Figure 5.187

Recursive Instrumental Variable Estimation
Three Story Building Model; Sine Sweep Input
3rd Floor gamma=1

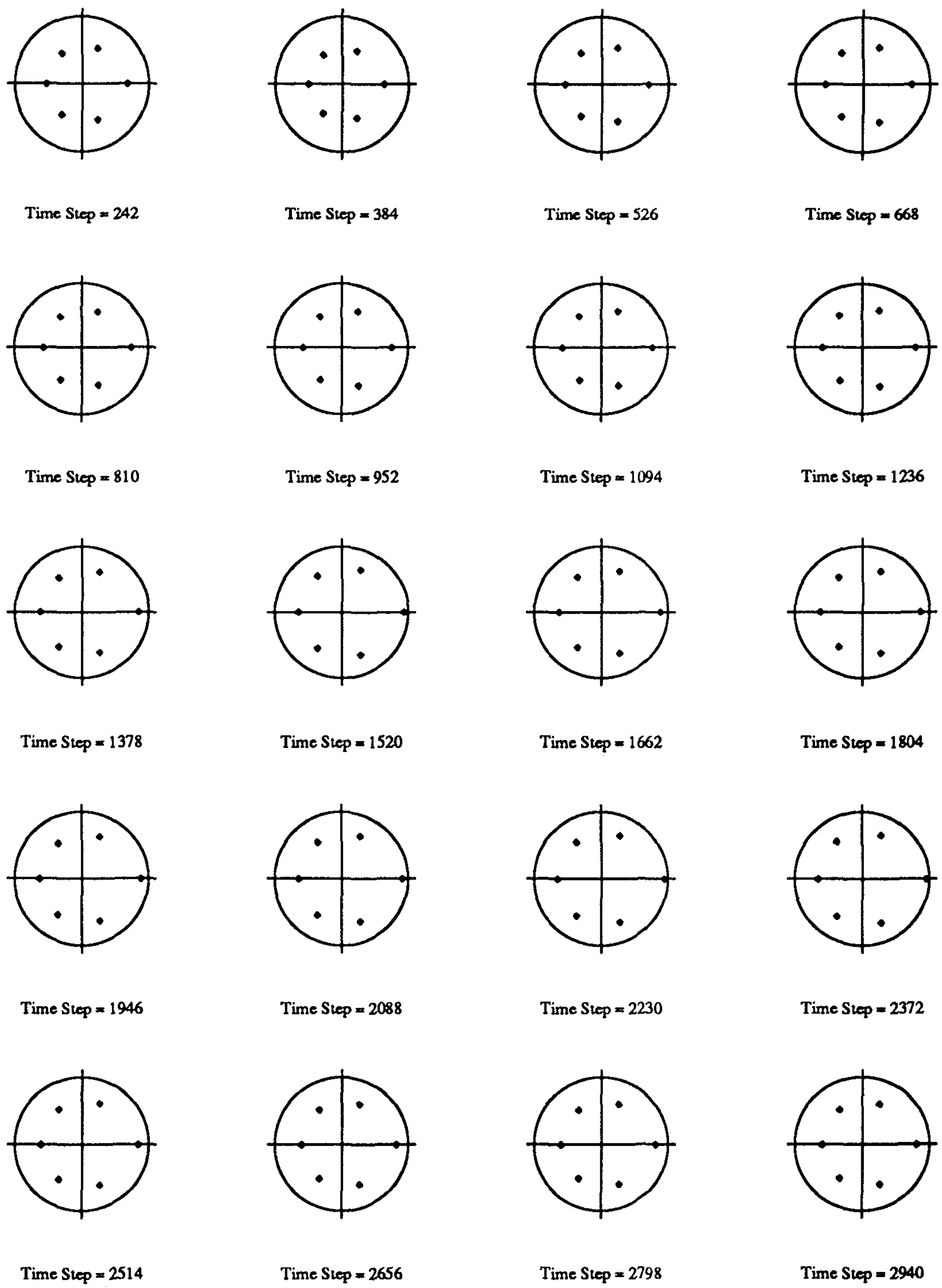


Figure 5.188

Rational Orthogonal Polynomial Curvefit
Three Story Building Model; El Centro Input
1st Floor

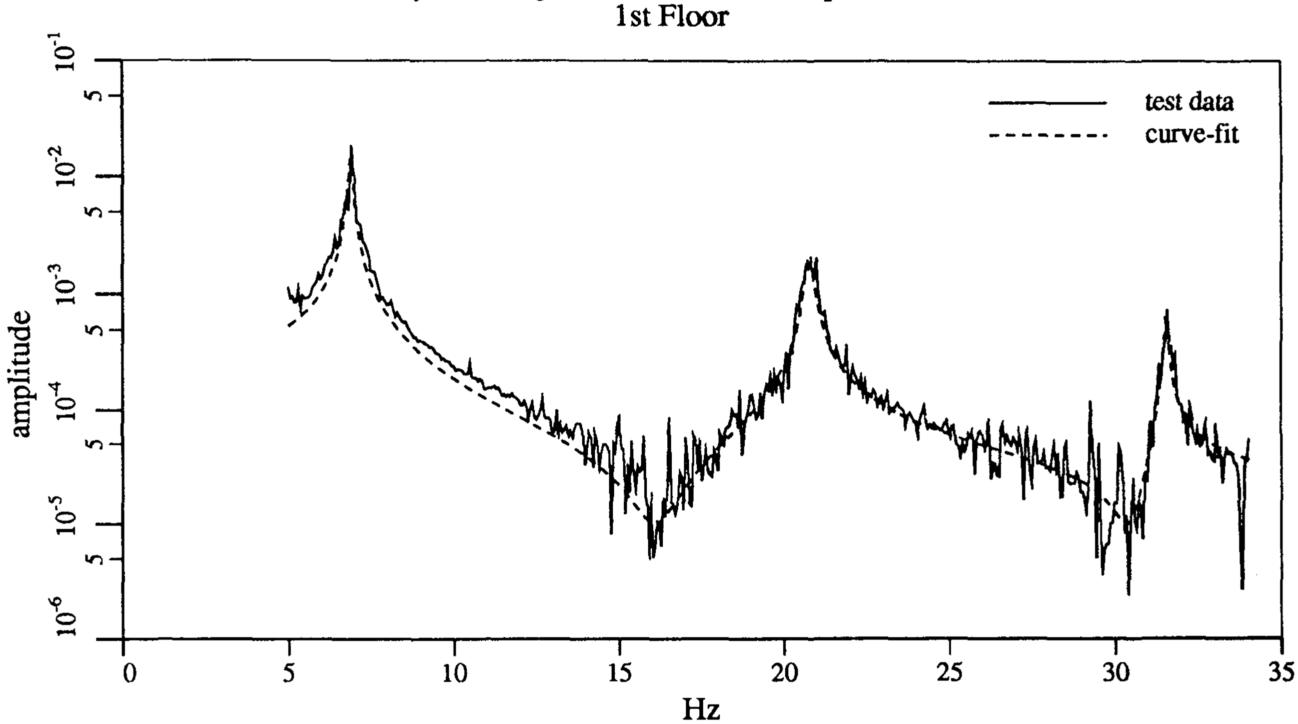


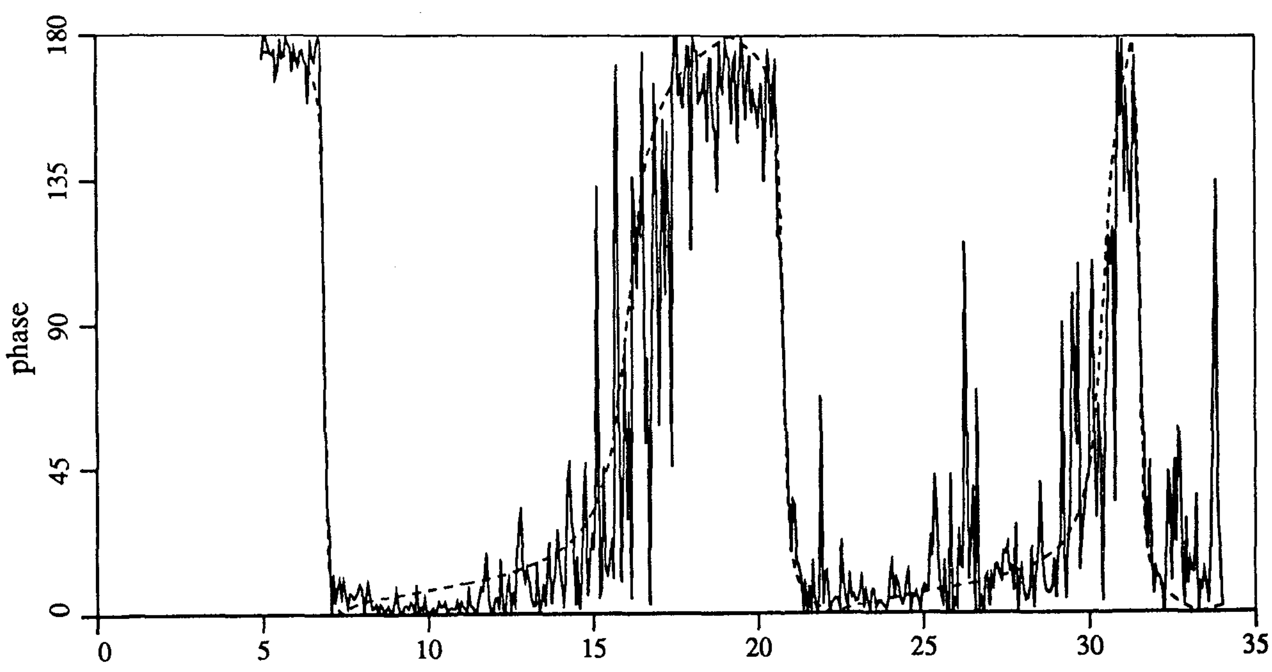


Figure 5.189

# Rational Orthogonal Polynomial Curvefit
Three Story Building Model; El Centro Input
2nd Floor

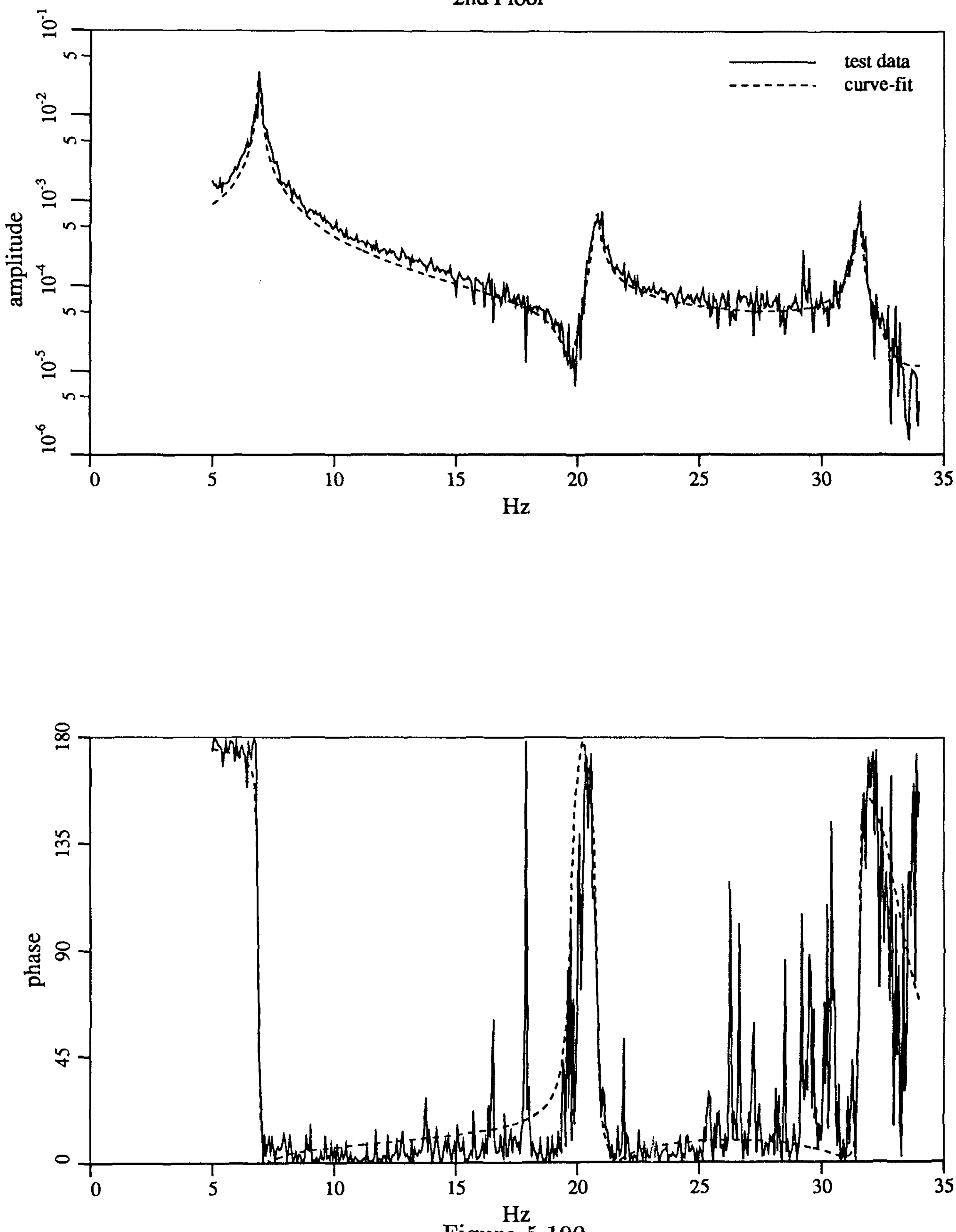


Figure 5.190

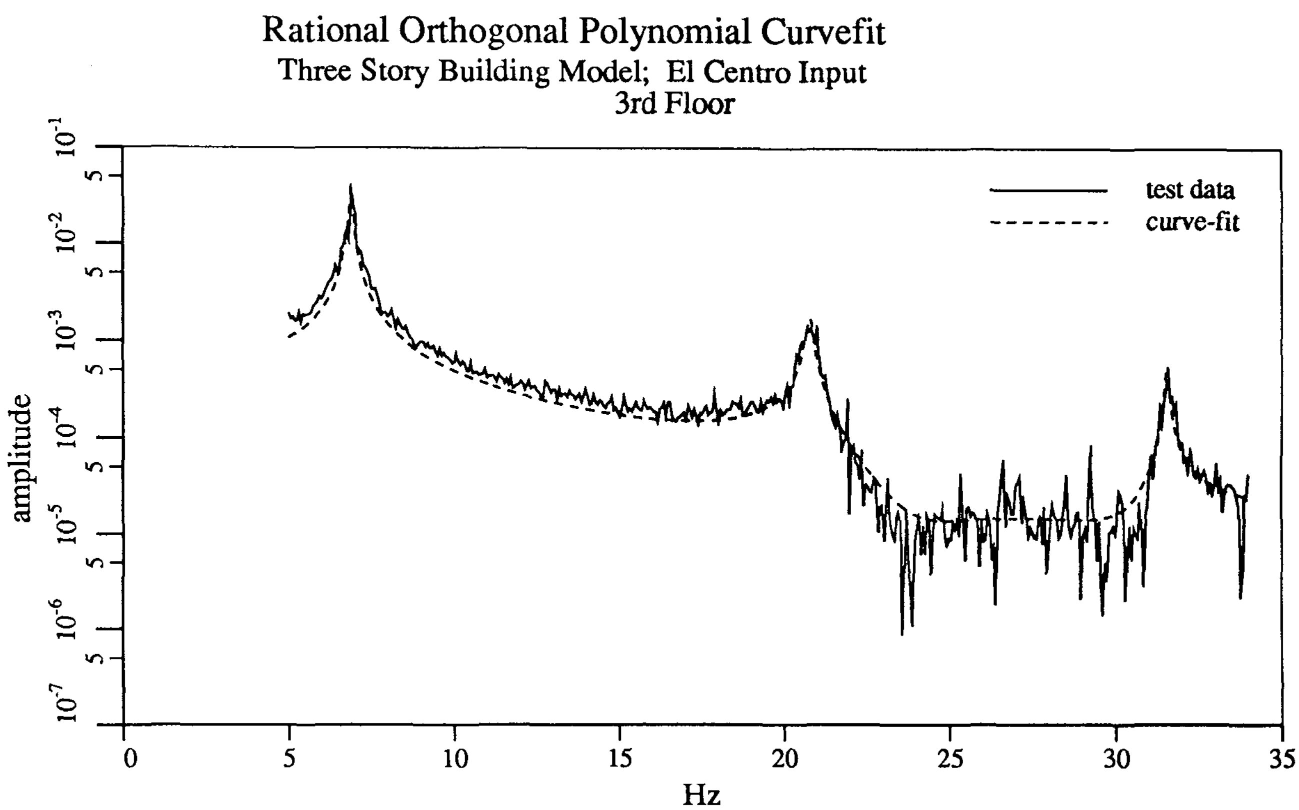

Rational Orthogonal Polynomial Curvefit
Three Story Building Model; El Centro Input
3rd Floor
amplitude
test data
curve-fit
Hz
0
5
10
15
20
25
30
35


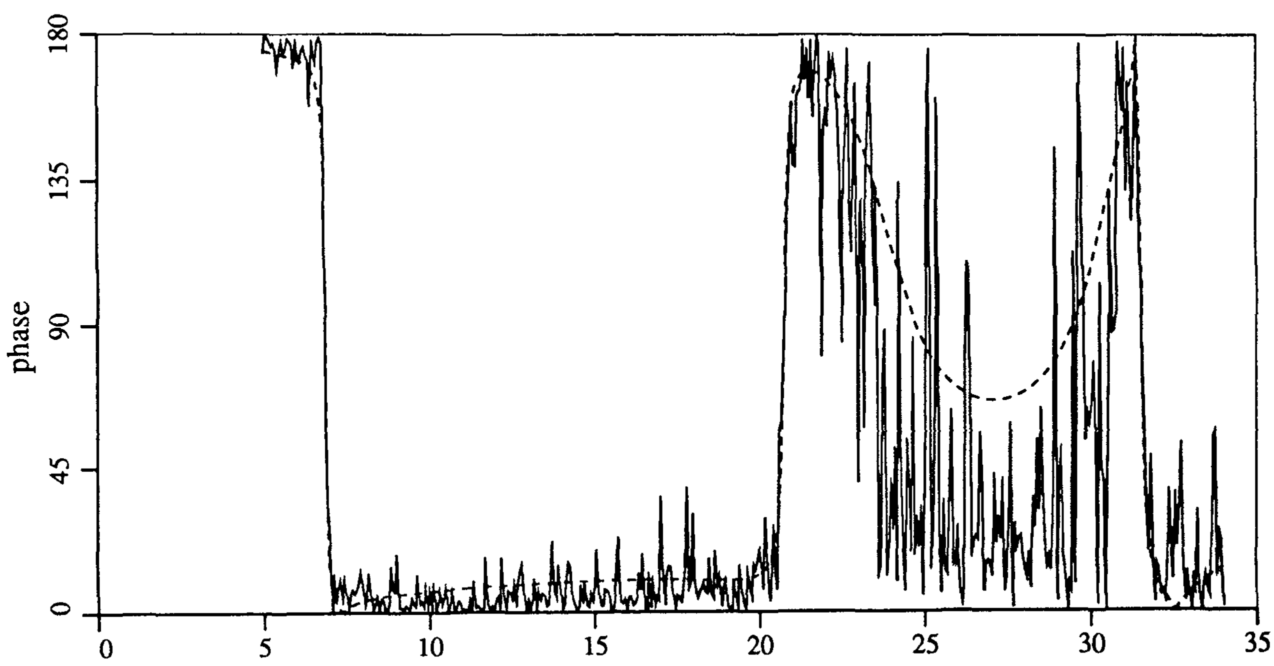

phase
180
135
90
45
0
Hz
0
5
10
15
20
25
30
35


Figure 5.191

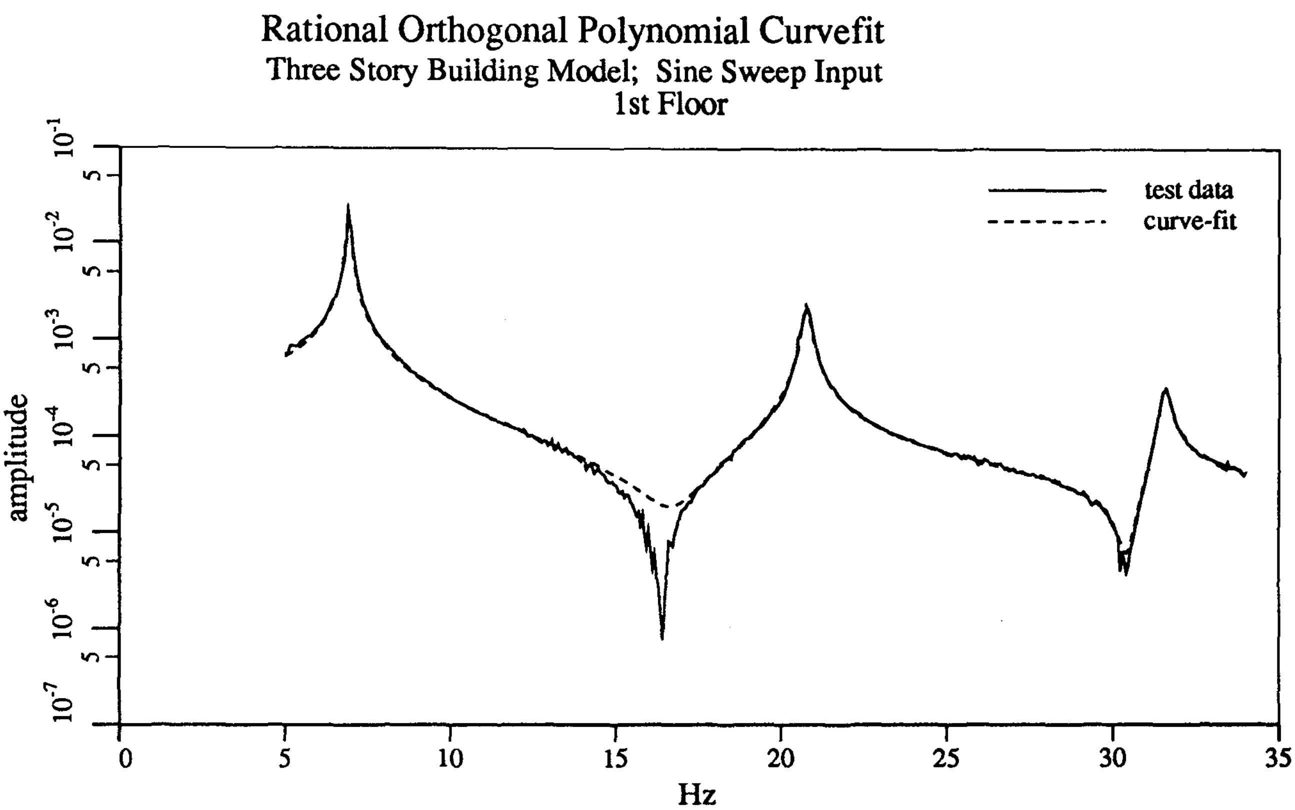

Rational Orthogonal Polynomial Curvefit
Three Story Building Model; Sine Sweep Input
1st Floor
amplitude
Hz
test data
curve-fit


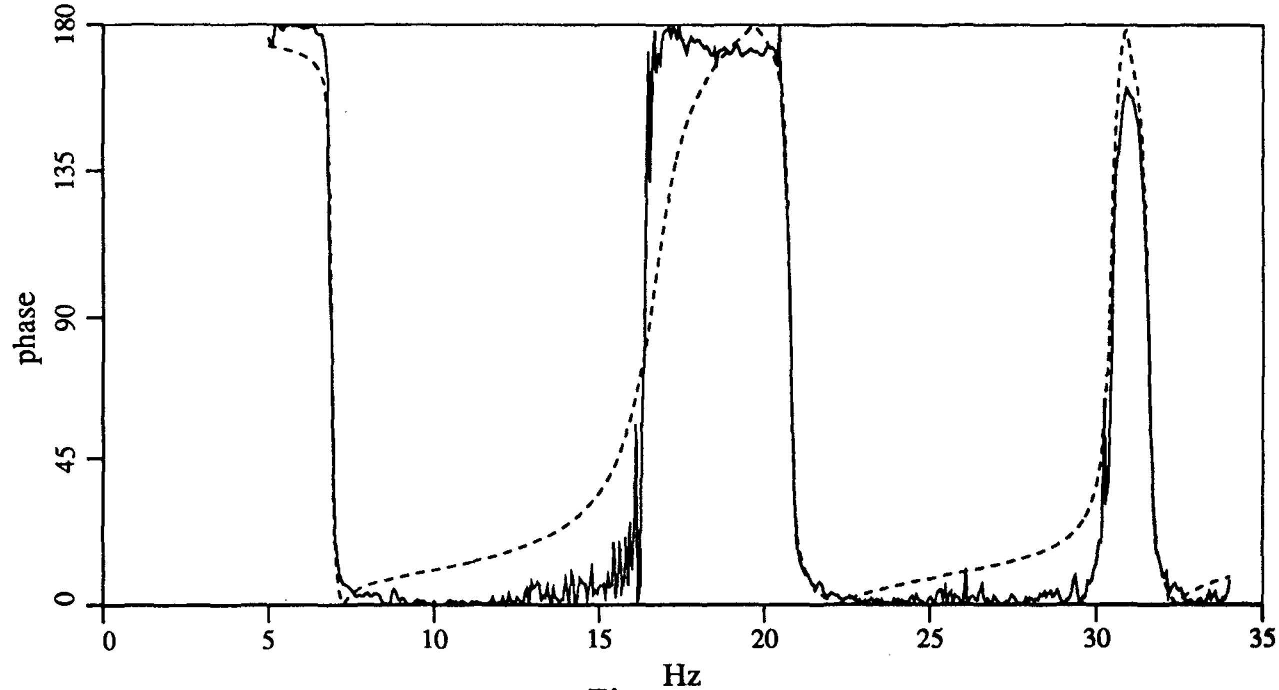

phase
Hz


Figure 5.192

# Rational Orthogonal Polynomial Curvefit

Three Story Building Model; Sine Sweep Input
2nd Floor

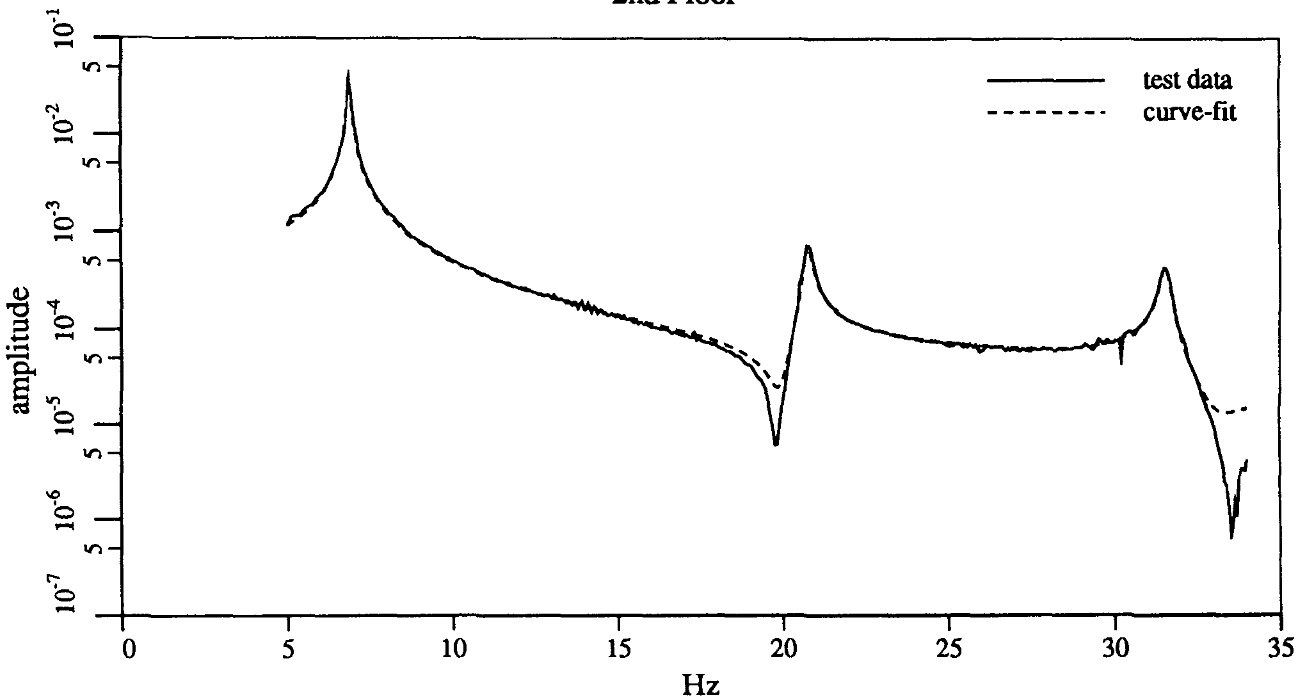


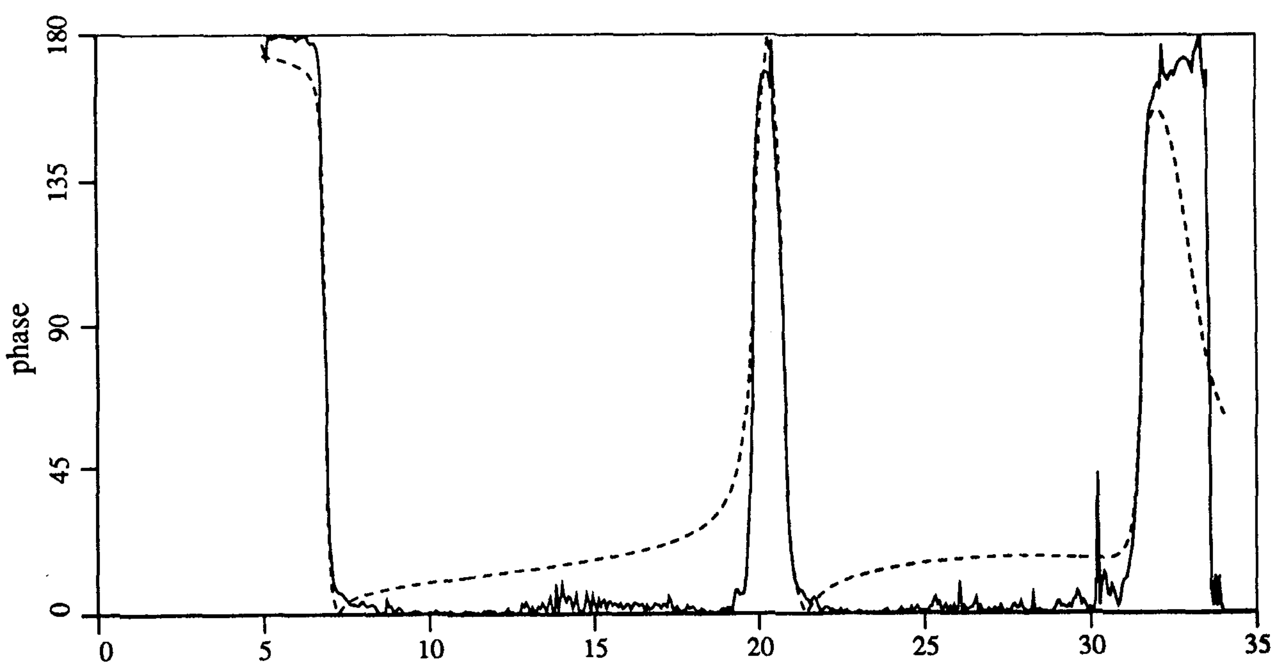


Figure 5.193

# Rational Orthogonal Polynomial Curvefit

Three Story Building Model; Sine Sweep Input
3rd Floor

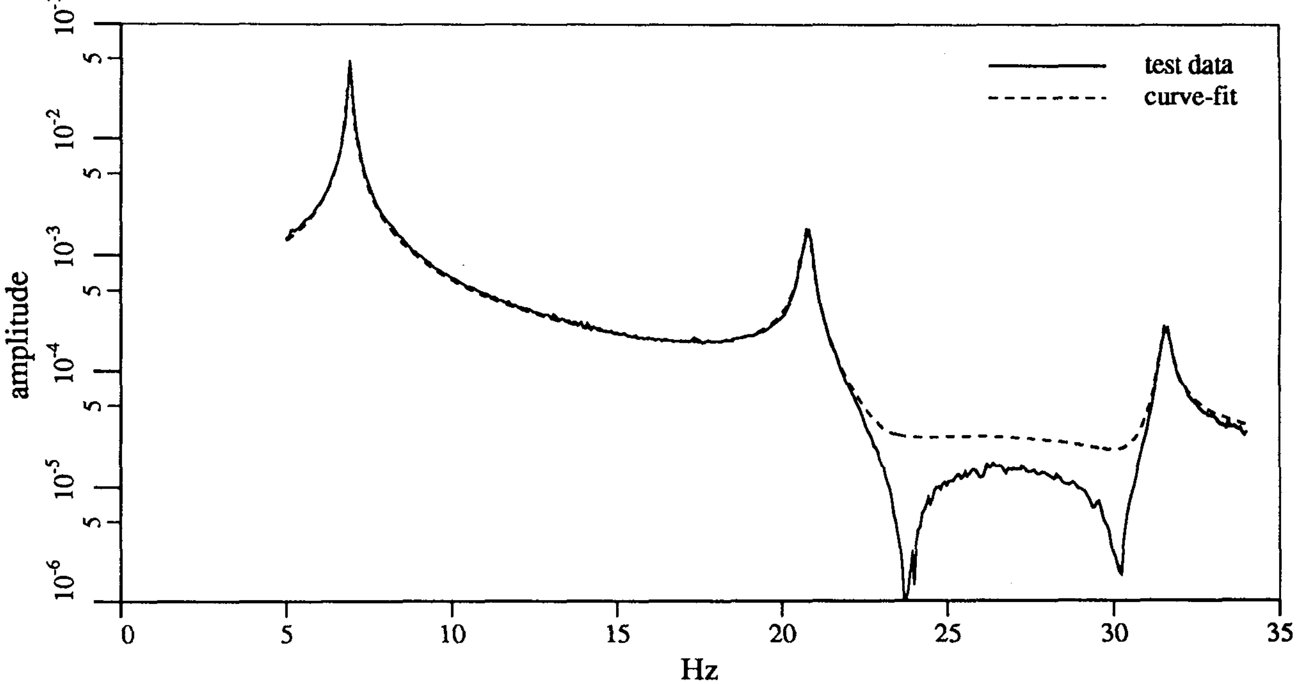


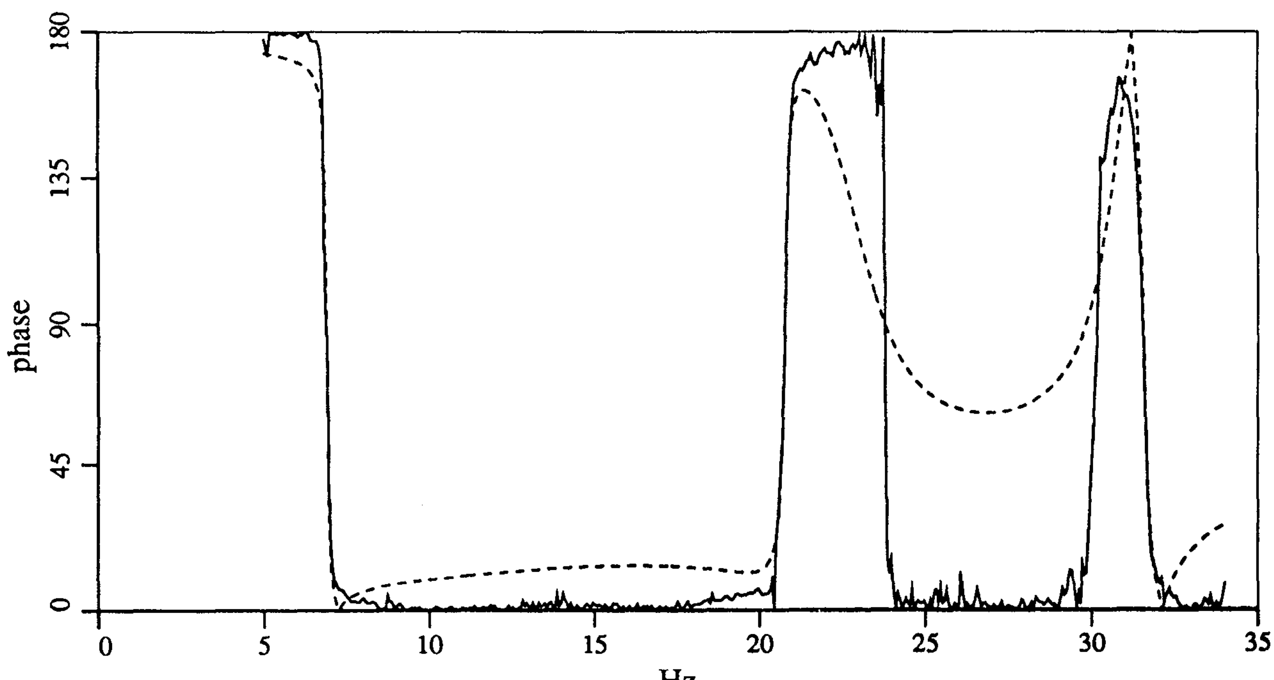


Figure 5.194

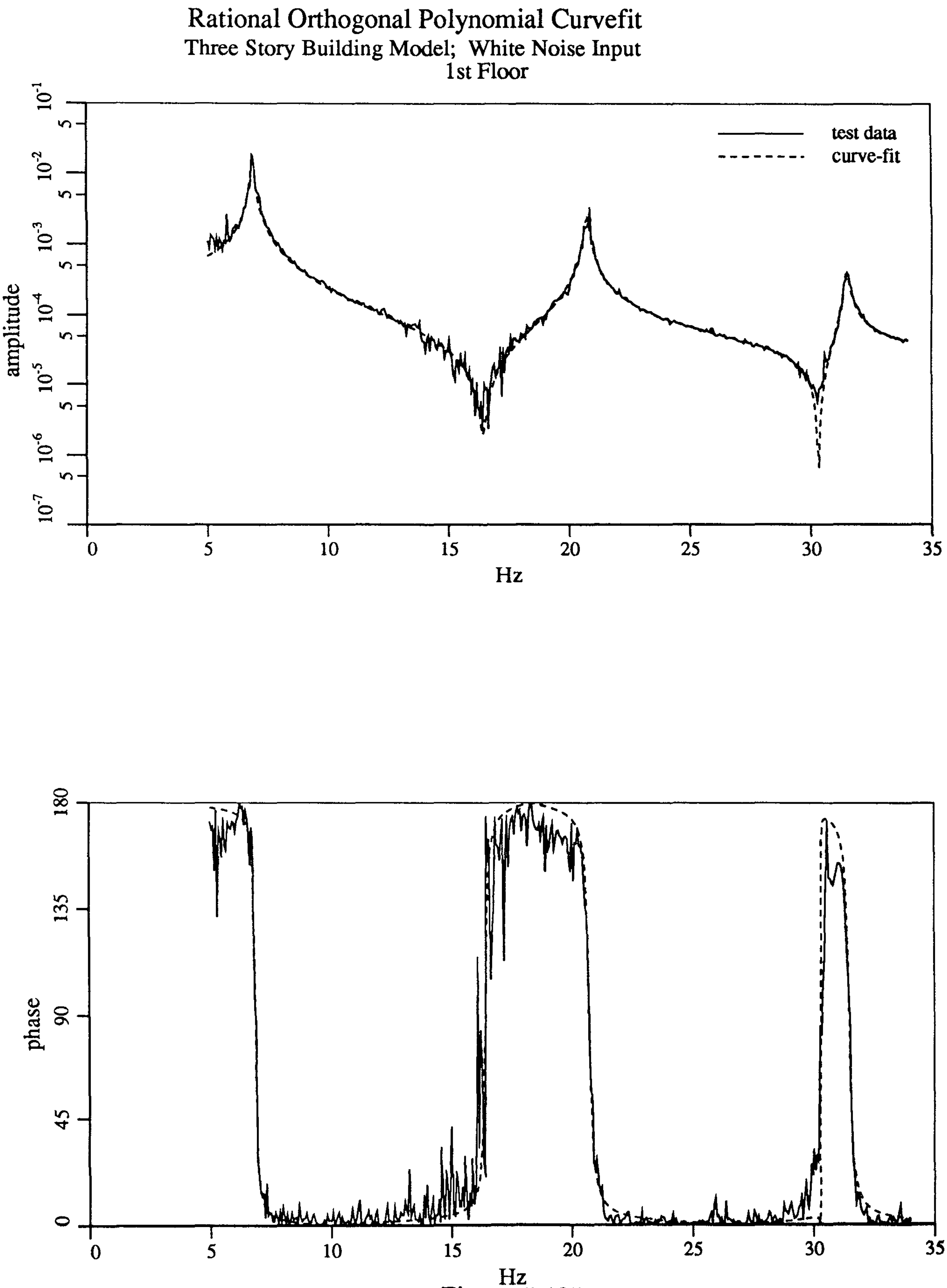

Rational Orthogonal Polynomial Curvefit
Three Story Building Model; White Noise Input
1st Floor
test data
curve-fit
amplitude
Hz
phase
Hz


Figure 5.195

Rational Orthogonal Polynomial Curvefit
Three Story Building Model; White Noise Input
2nd Floor

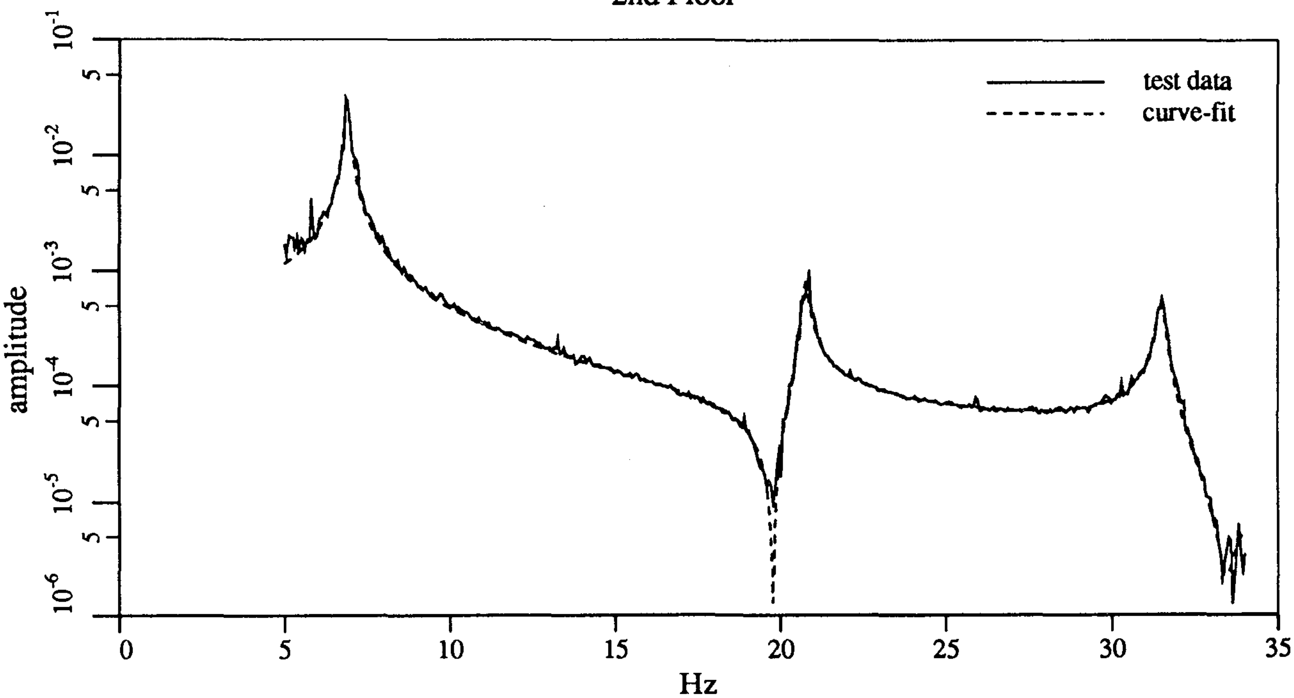


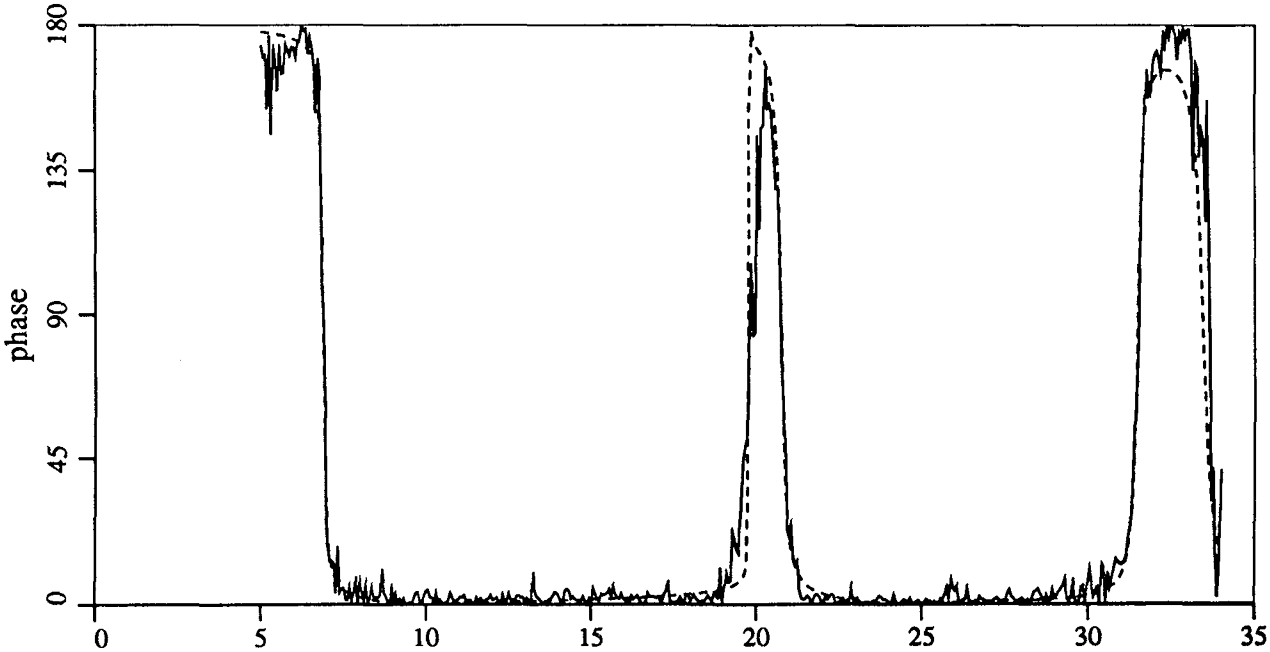


Figure 5.196

Rational Orthogonal Polynomial Curvefit
Three Story Building Model; White Noise Input
3rd Floor

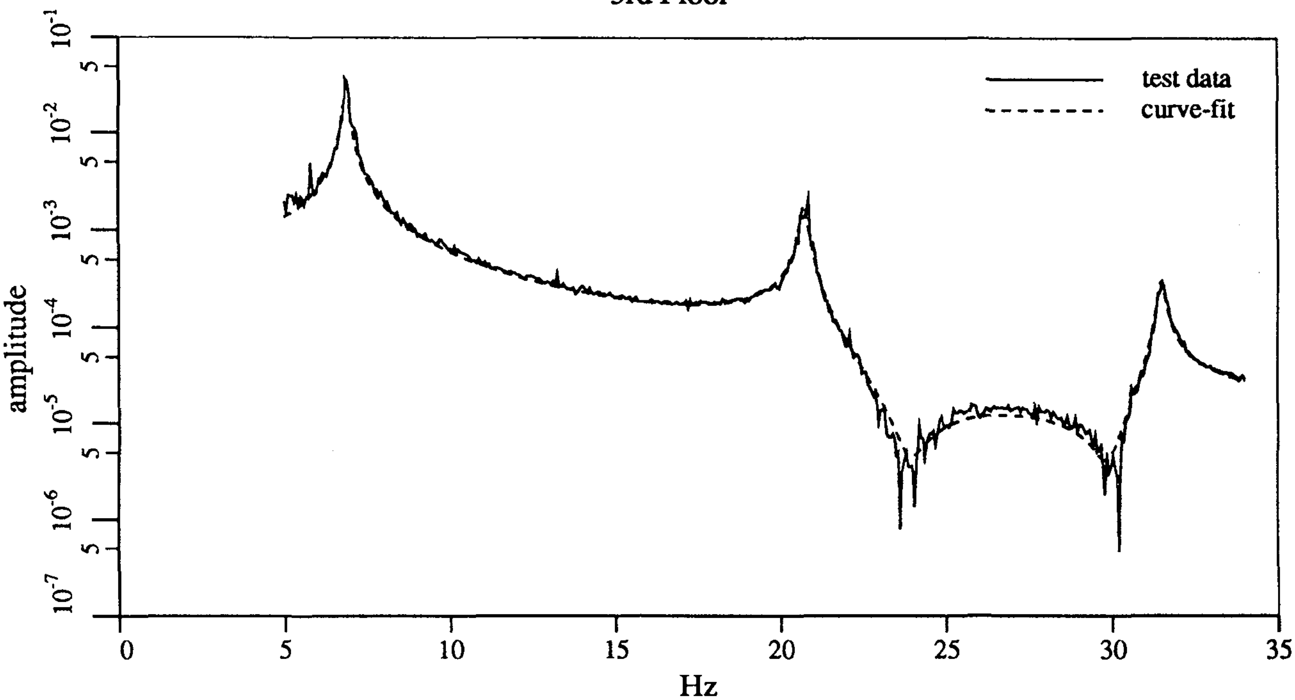


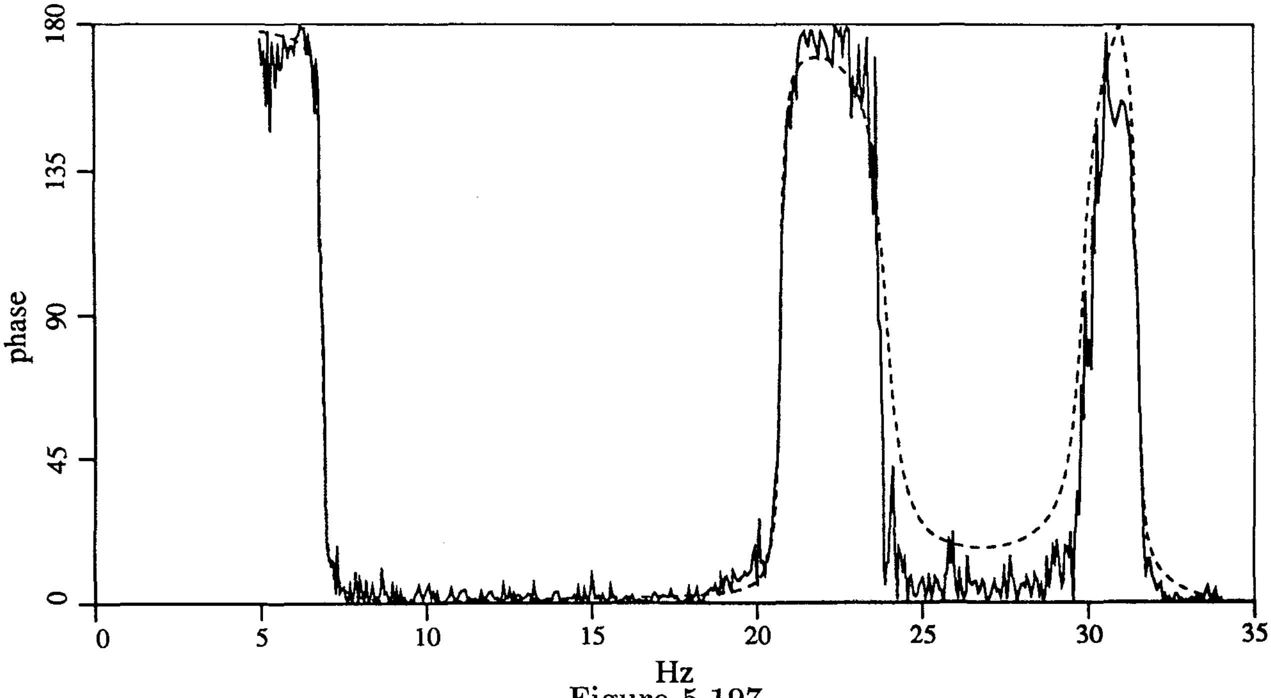


Figure 5.197

# Rational Orthogonal Polynomial Curvefit

Five Story Building Model; El Centro Input
1st Floor

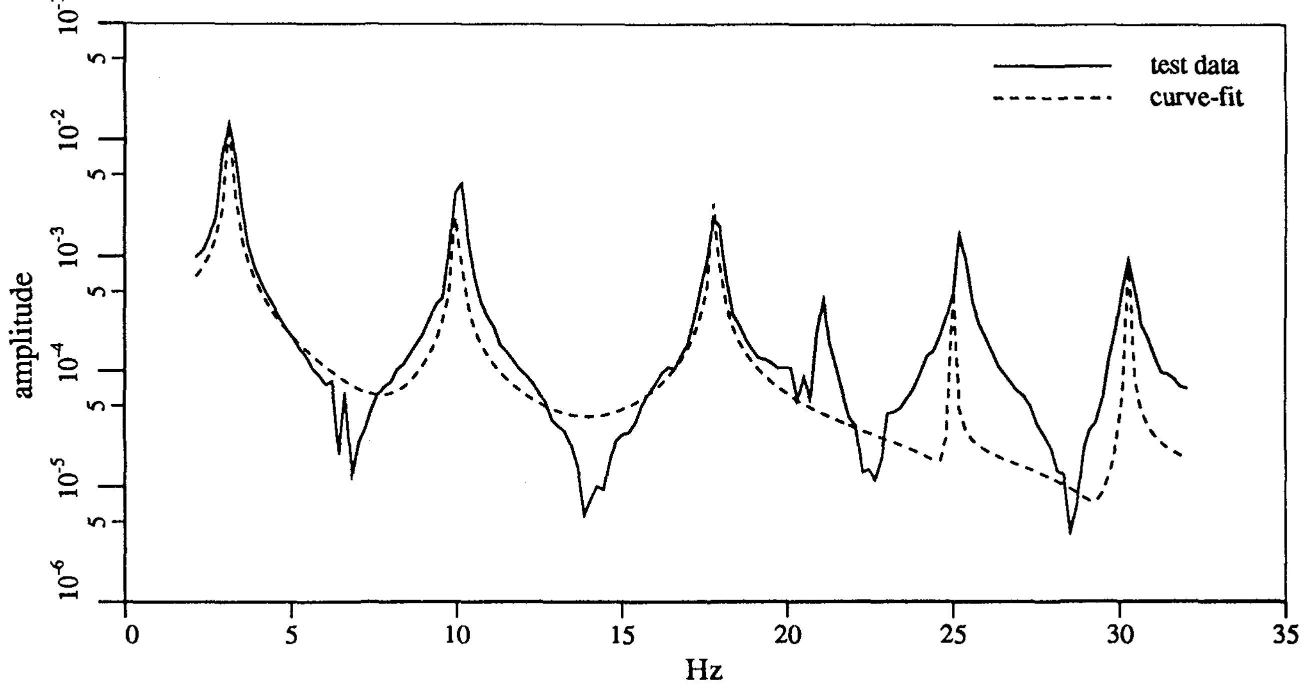


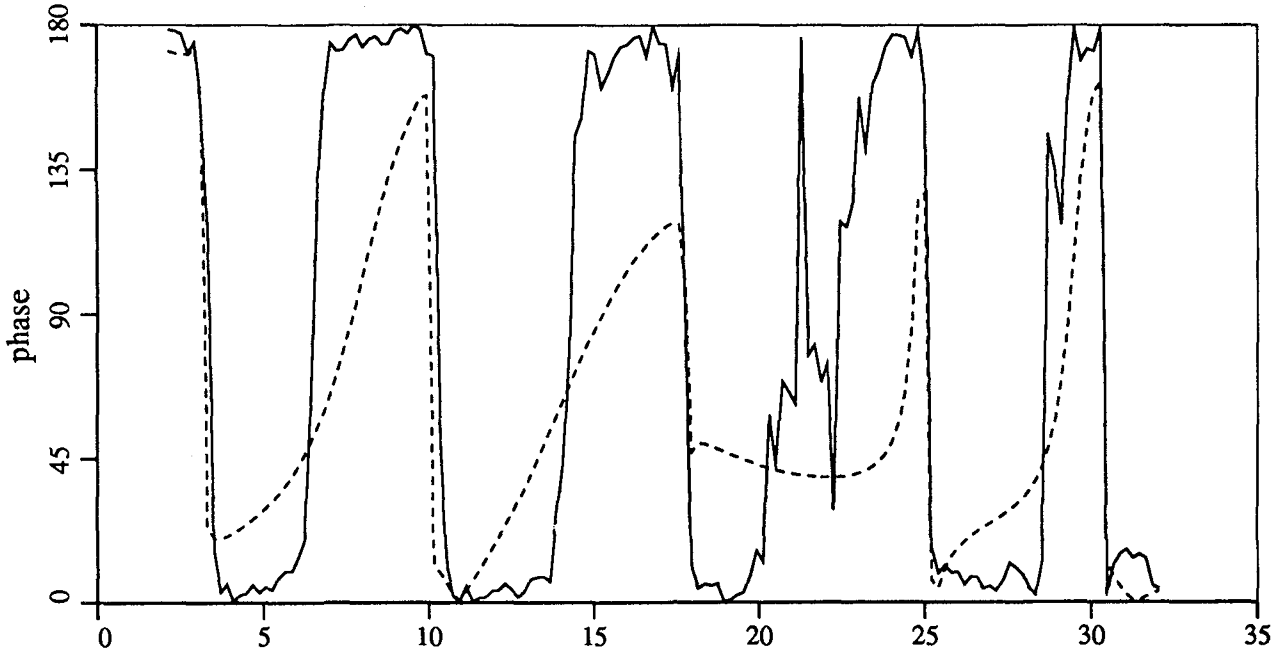


Figure 5.198

## Rational Orthogonal Polynomial Curvefit
Five Story Building Model; El Centro Input
2nd Floor

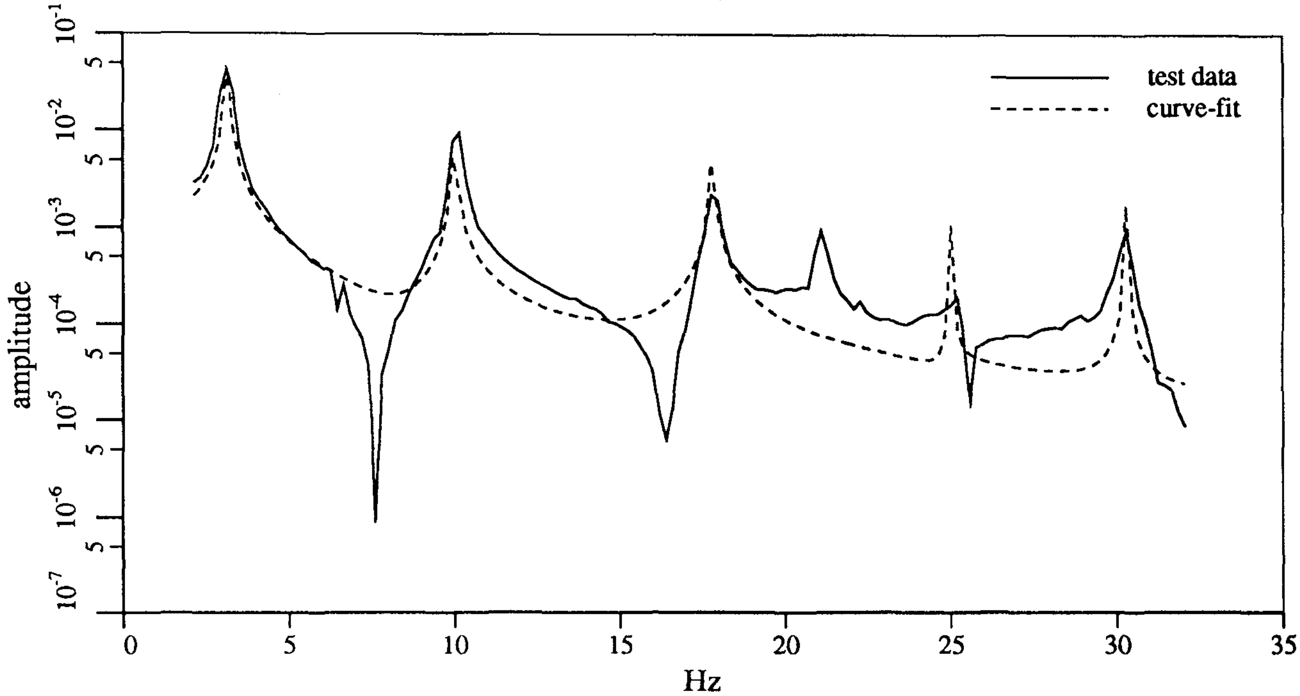


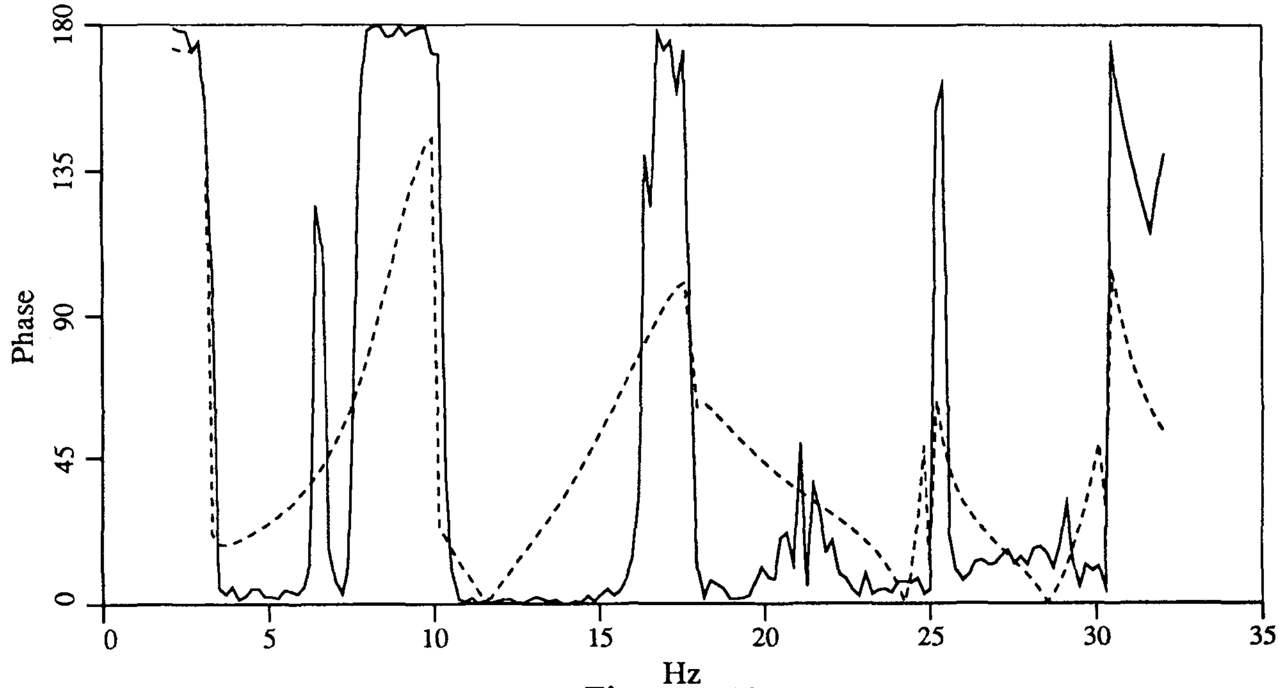


Figure 5.199

Rational Orthogonal Polynomial Curvefit
Five Story Building Model; El Centro Input
3rd Floor

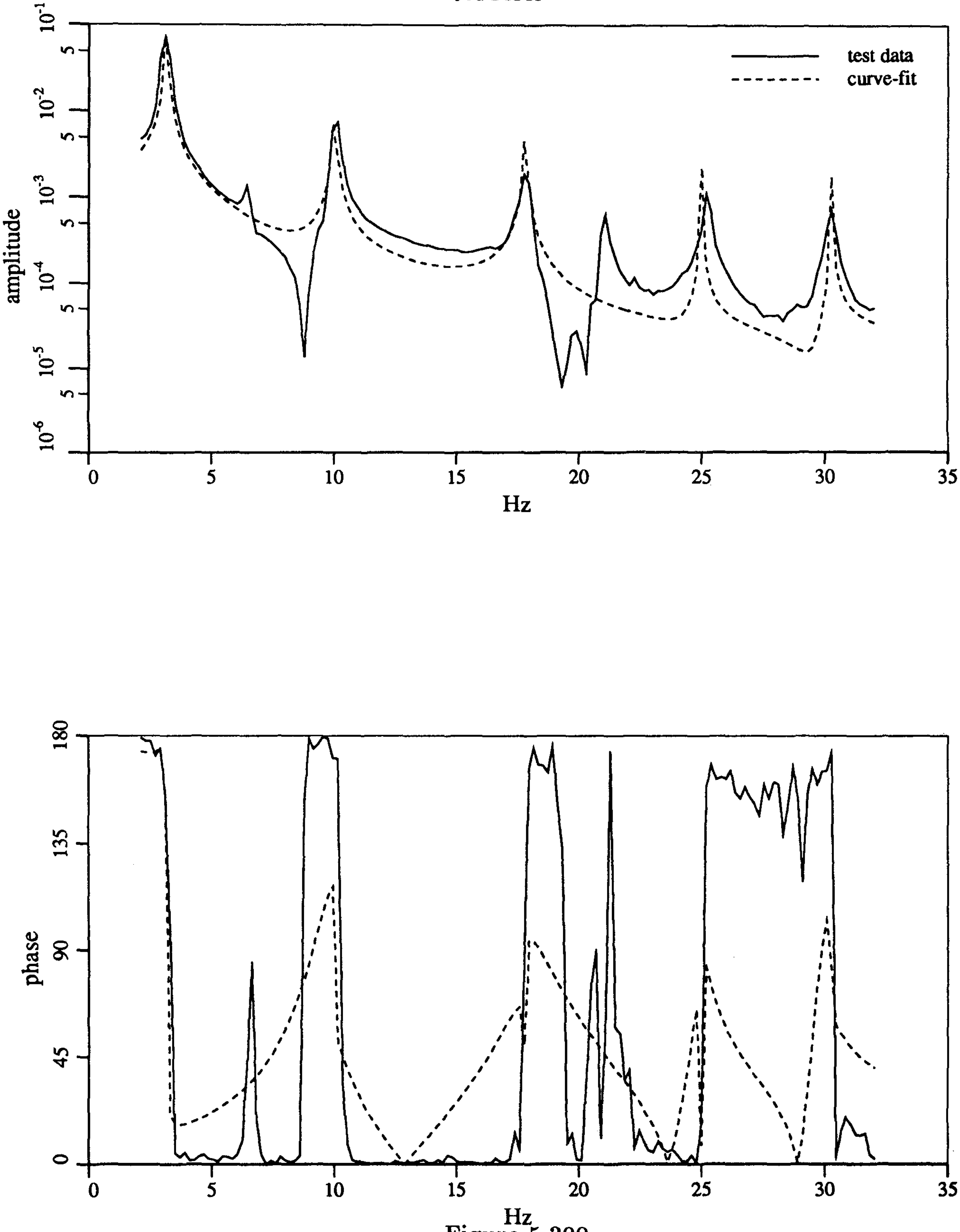


Figure 5.200

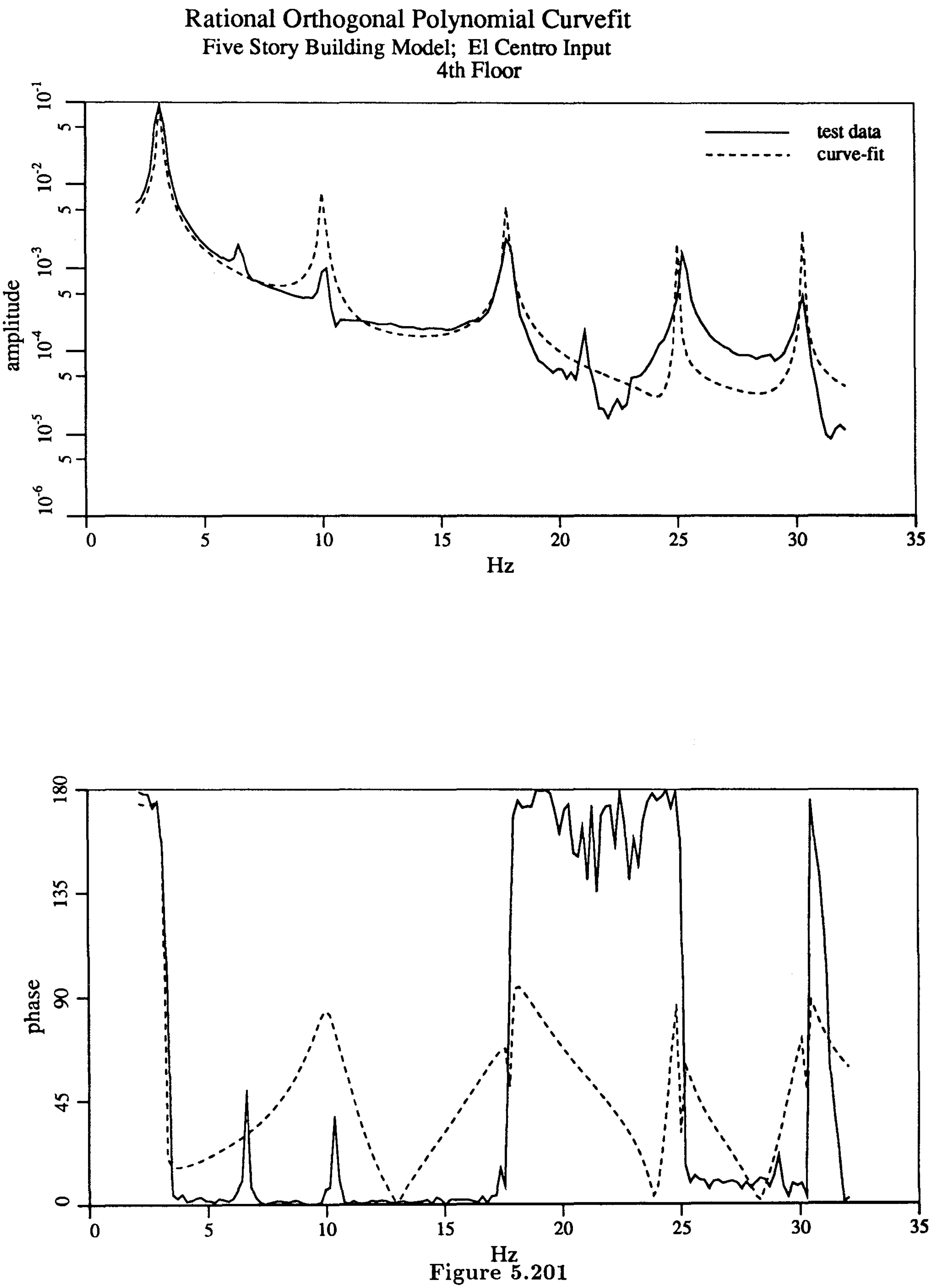
Rational Orthogonal Polynomial Curvefit
Five Story Building Model; El Centro Input
4th Floor
amplitude
test data
curve-fit
Hz
phase
Hz

Figure 5.201

# Rational Orthogonal Polynomial Curvefit

Five Story Building Model; El Centro Input
5th Floor

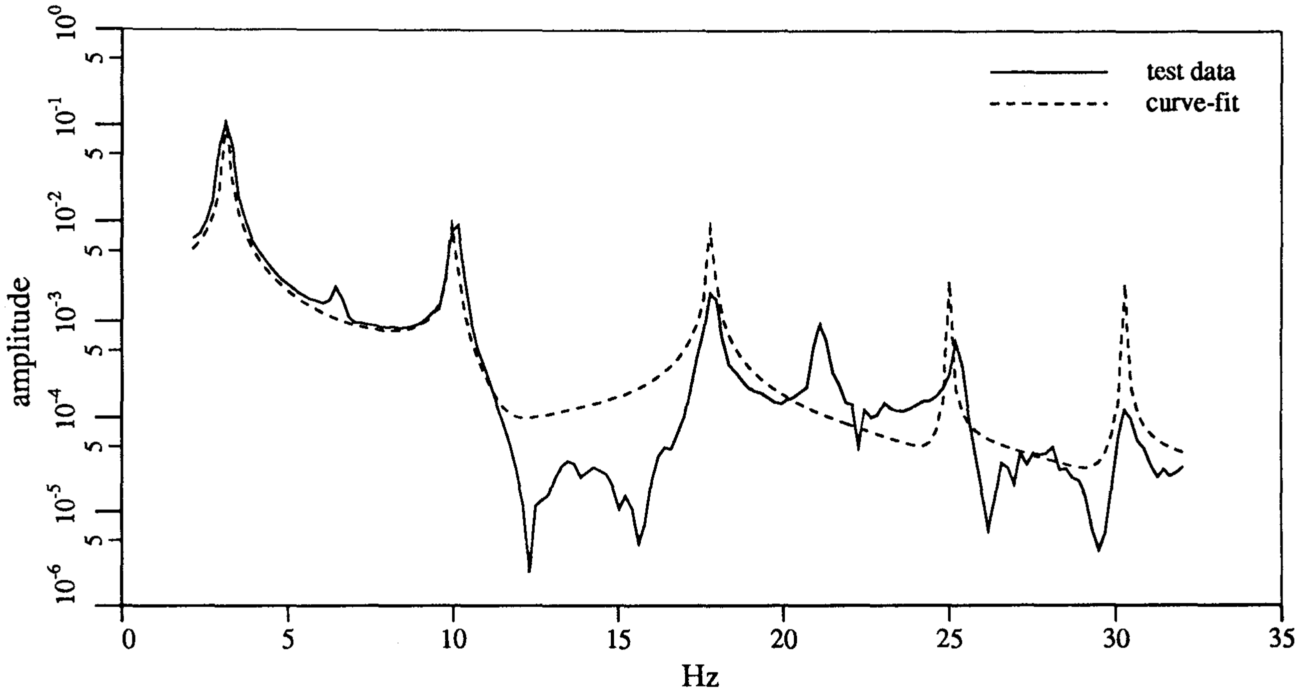


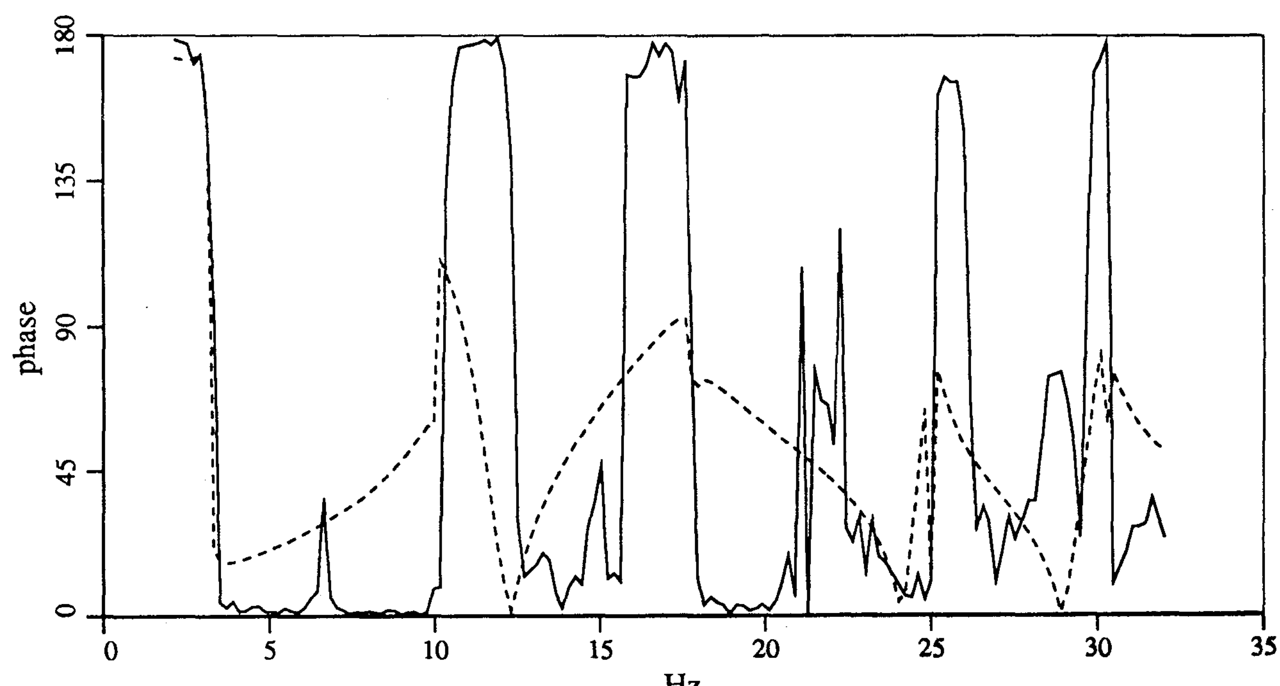


Figure 5.202

Rational Orthogonal Polynomial Curvefit
Five Story Building Model; White Noise Input
1st Floor

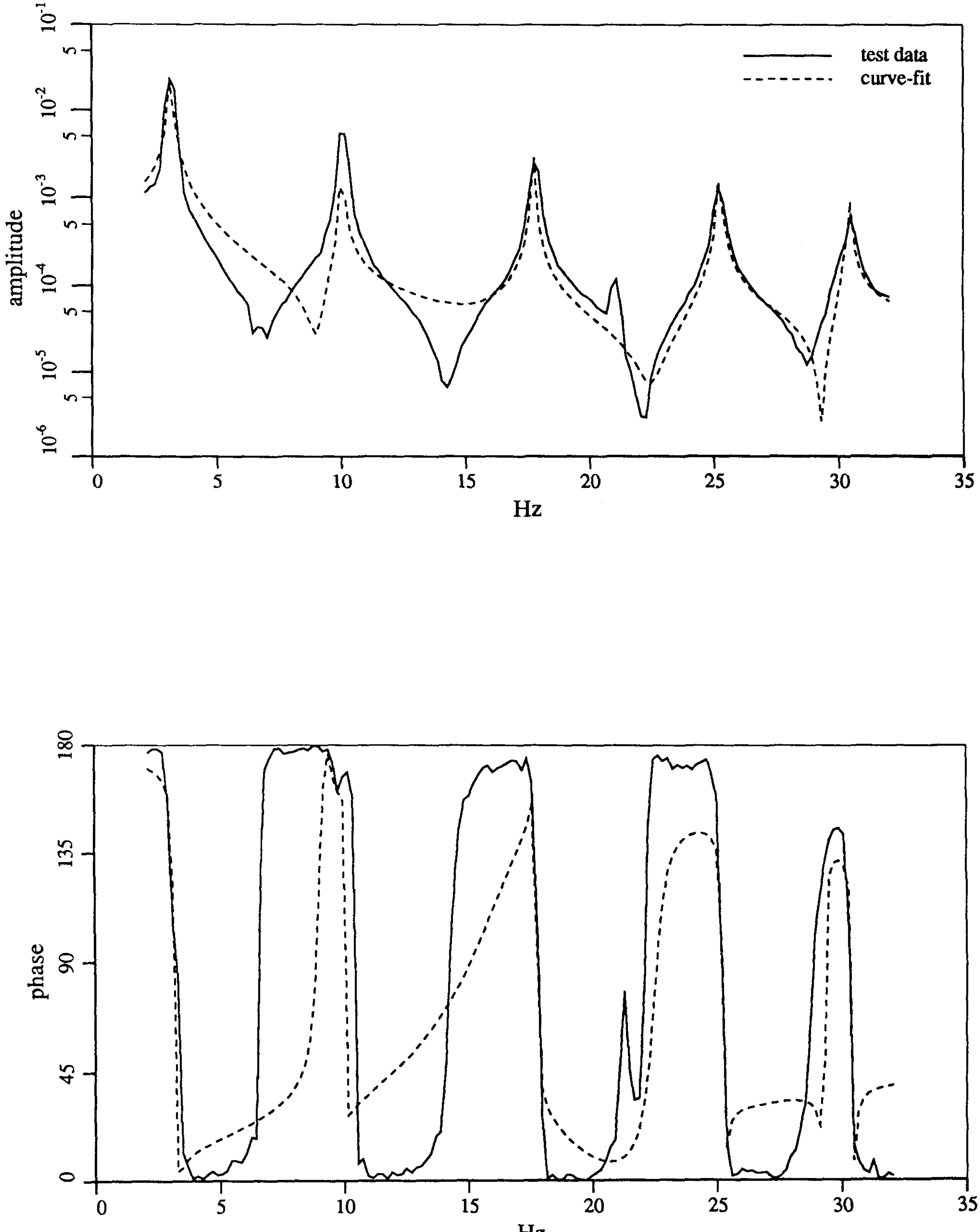


Figure 5.203

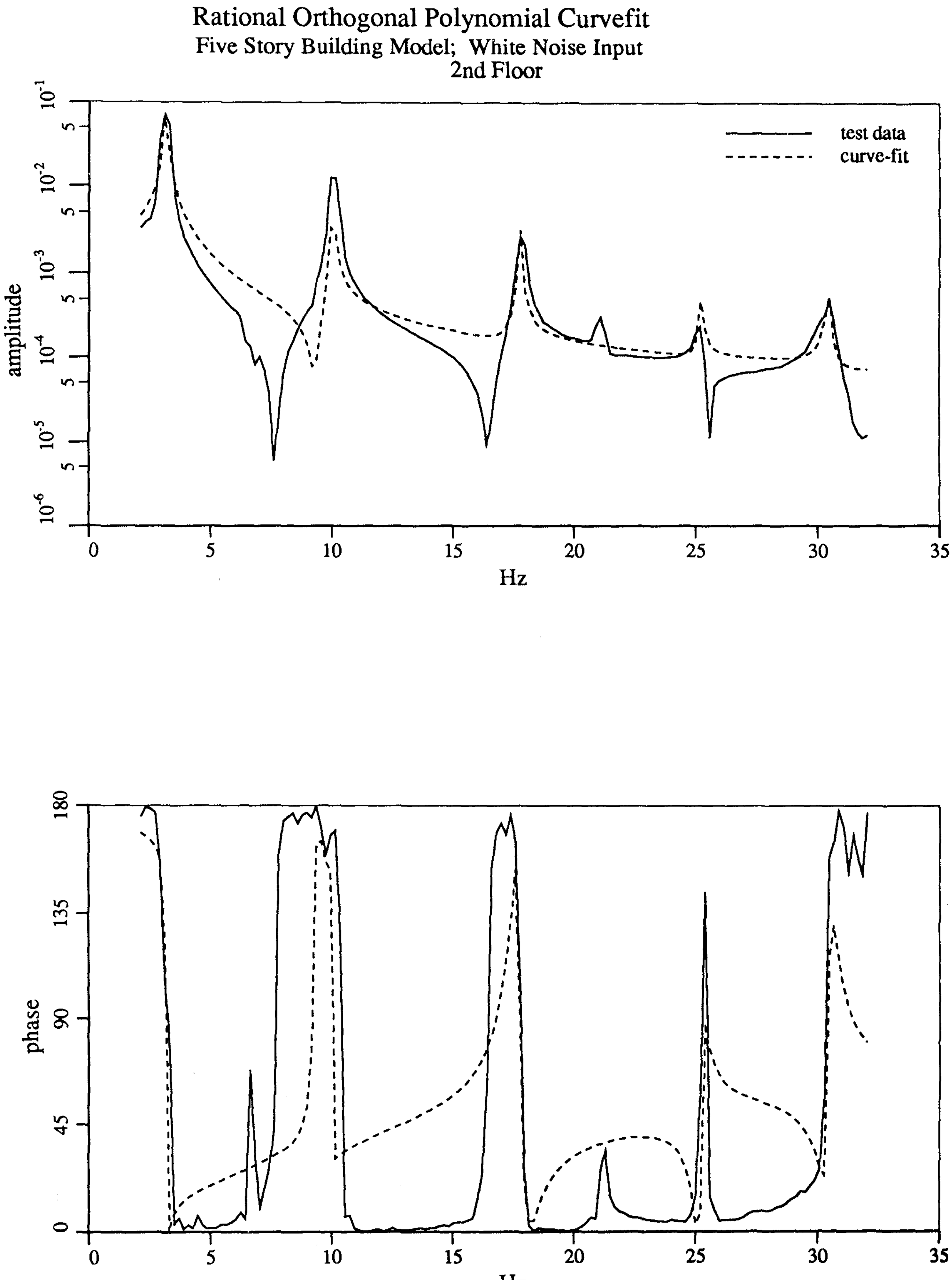

Rational Orthogonal Polynomial Curvefit
Five Story Building Model; White Noise Input
2nd Floor
test data
curve-fit
amplitude
Hz
phase
Hz


Figure 5.204

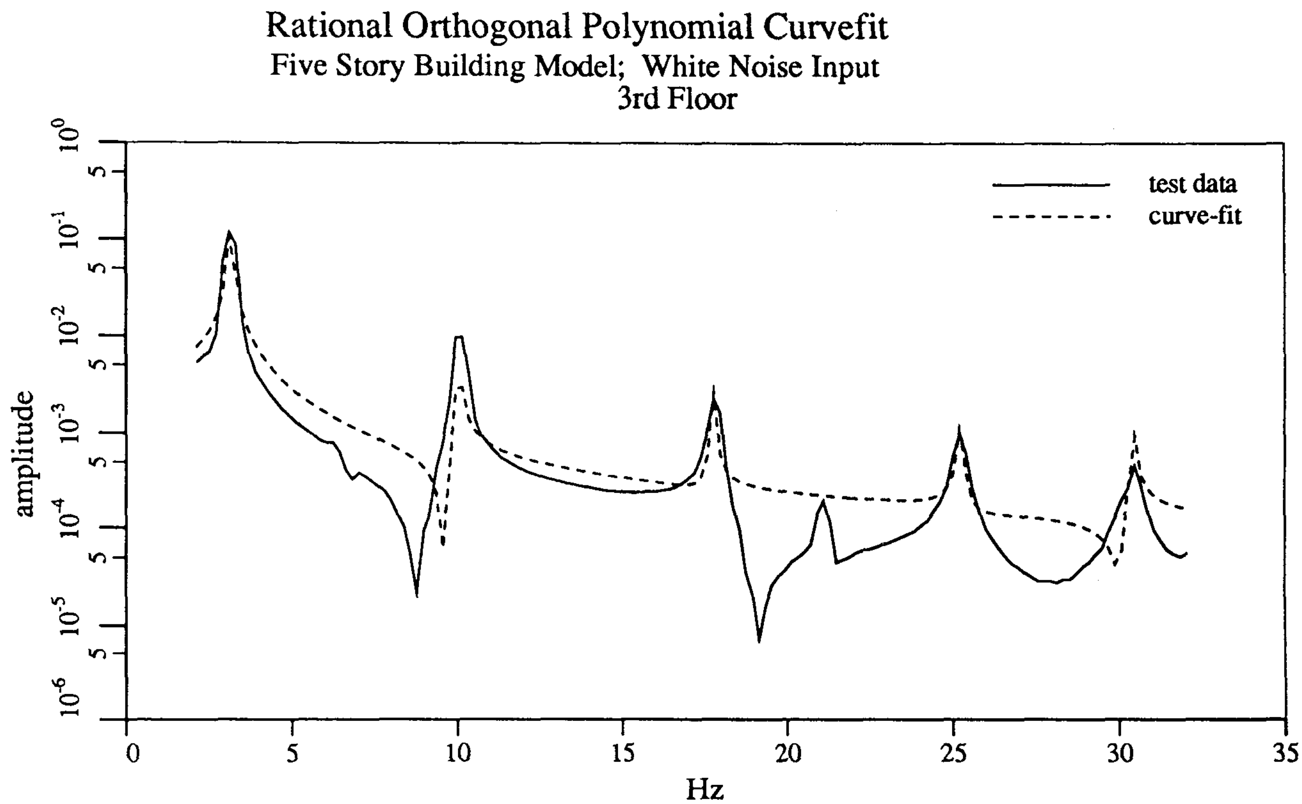

Rational Orthogonal Polynomial Curvefit
Five Story Building Model; White Noise Input
3rd Floor
test data
curve-fit
amplitude
Hz


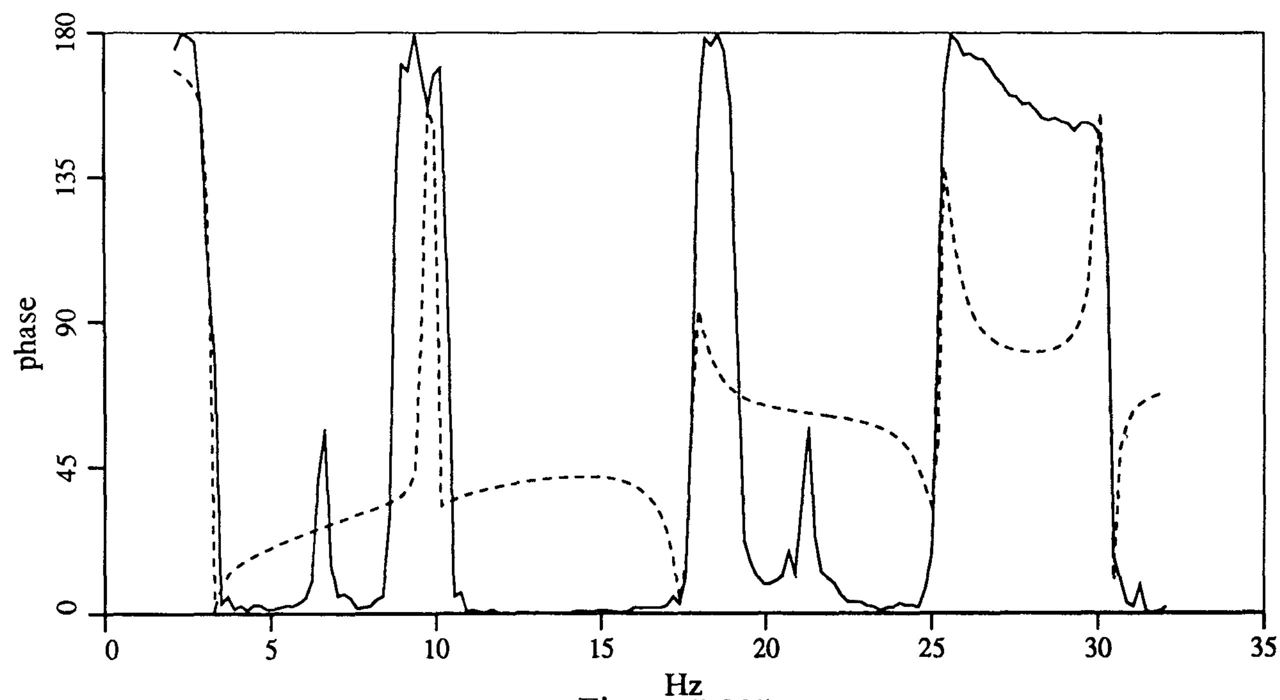

phase
Hz


Figure 5.205

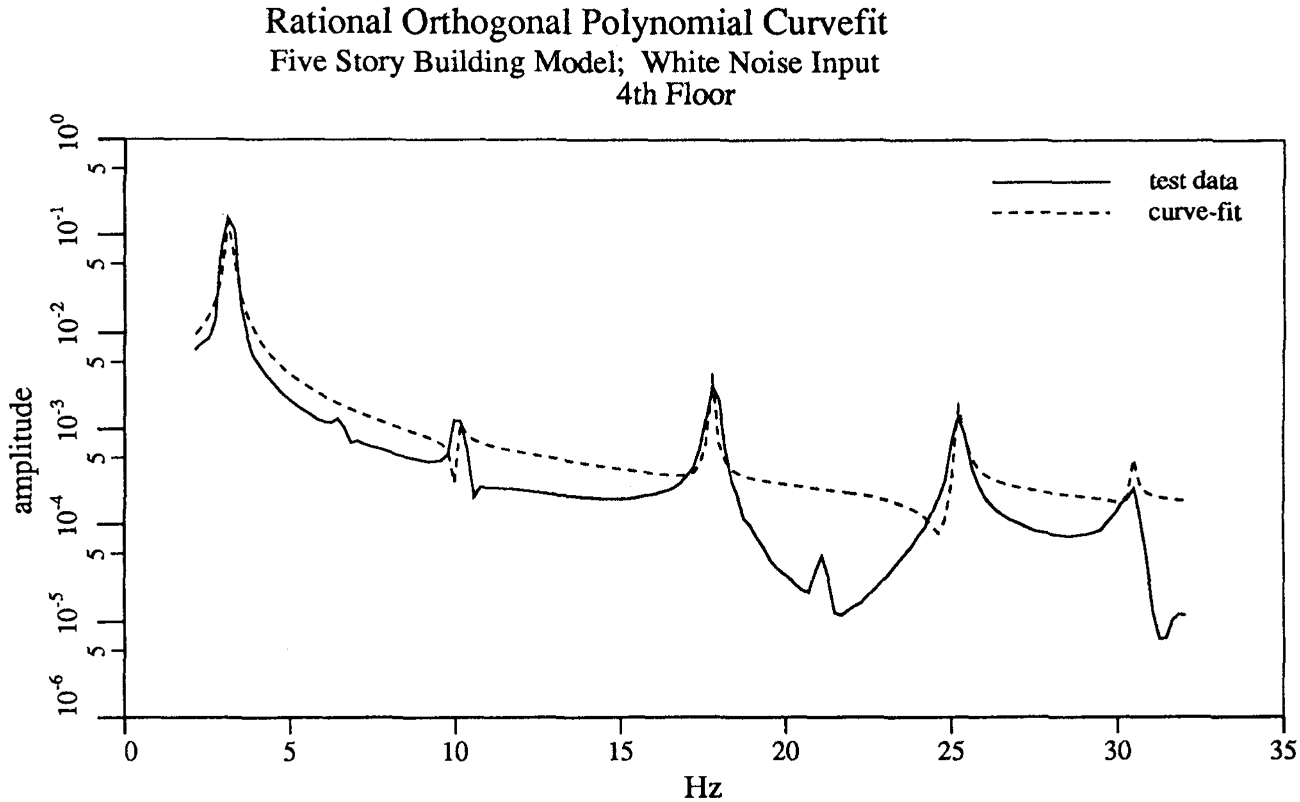
Rational Orthogonal Polynomial Curvefit
Five Story Building Model; White Noise Input
4th Floor
amplitude
test data
curve-fit
Hz

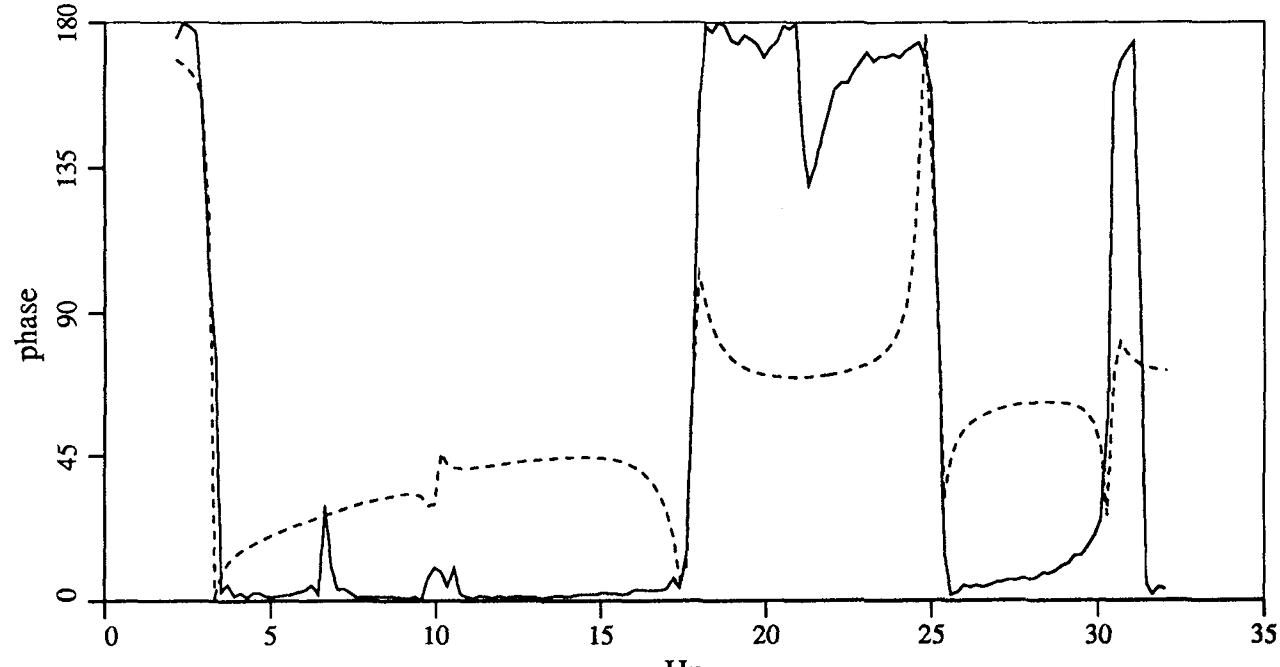
phase
180
135
90
45
0
Hz

Figure 5.206

Rational Orthogonal Polynomial Curvefit
Five Story Building Model; White Noise Input
5th Floor

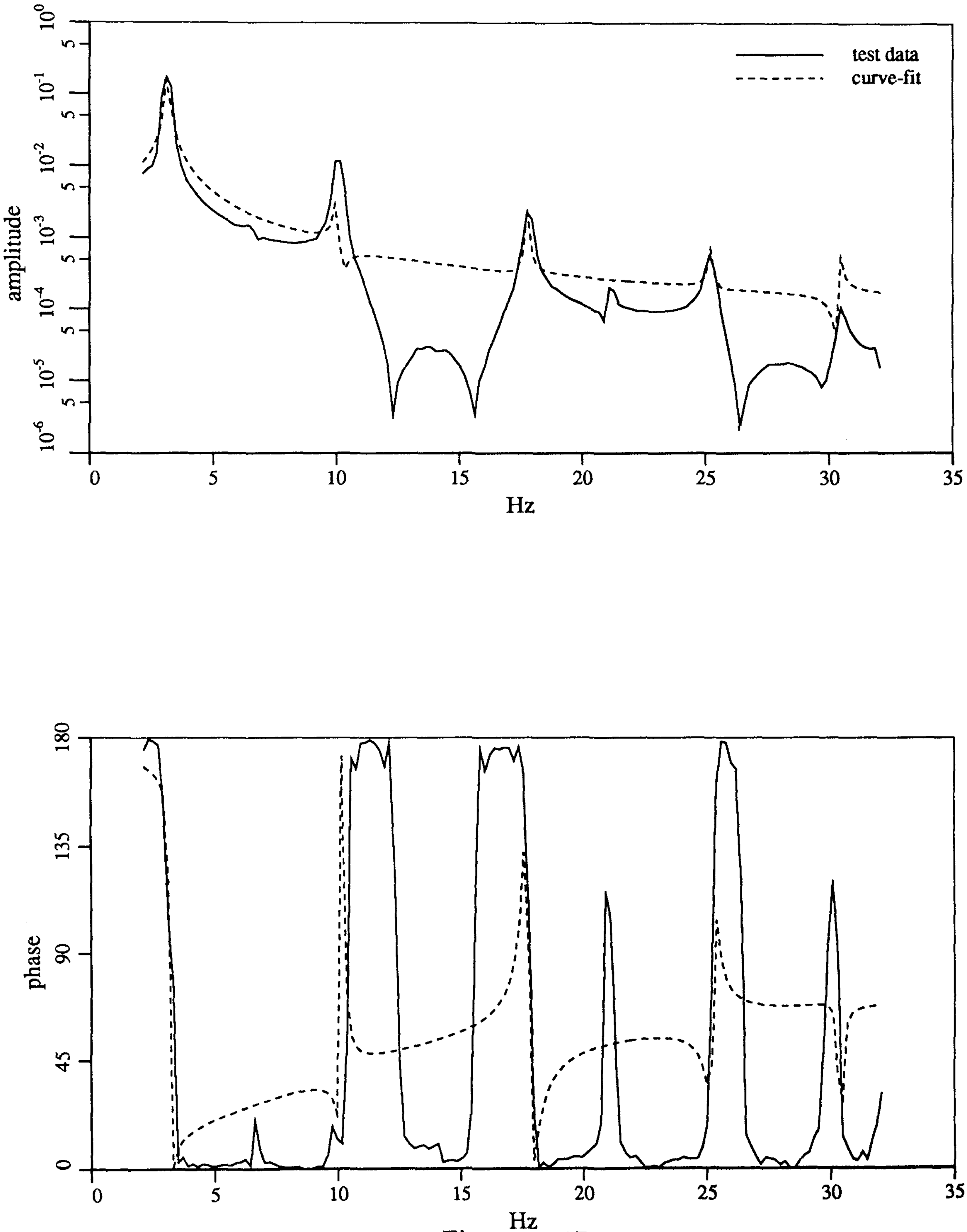


Figure 5.207

Recursive Least Squares Estimation
Five Story Building Model; Elcentro Input
1st Floor alpha=1.

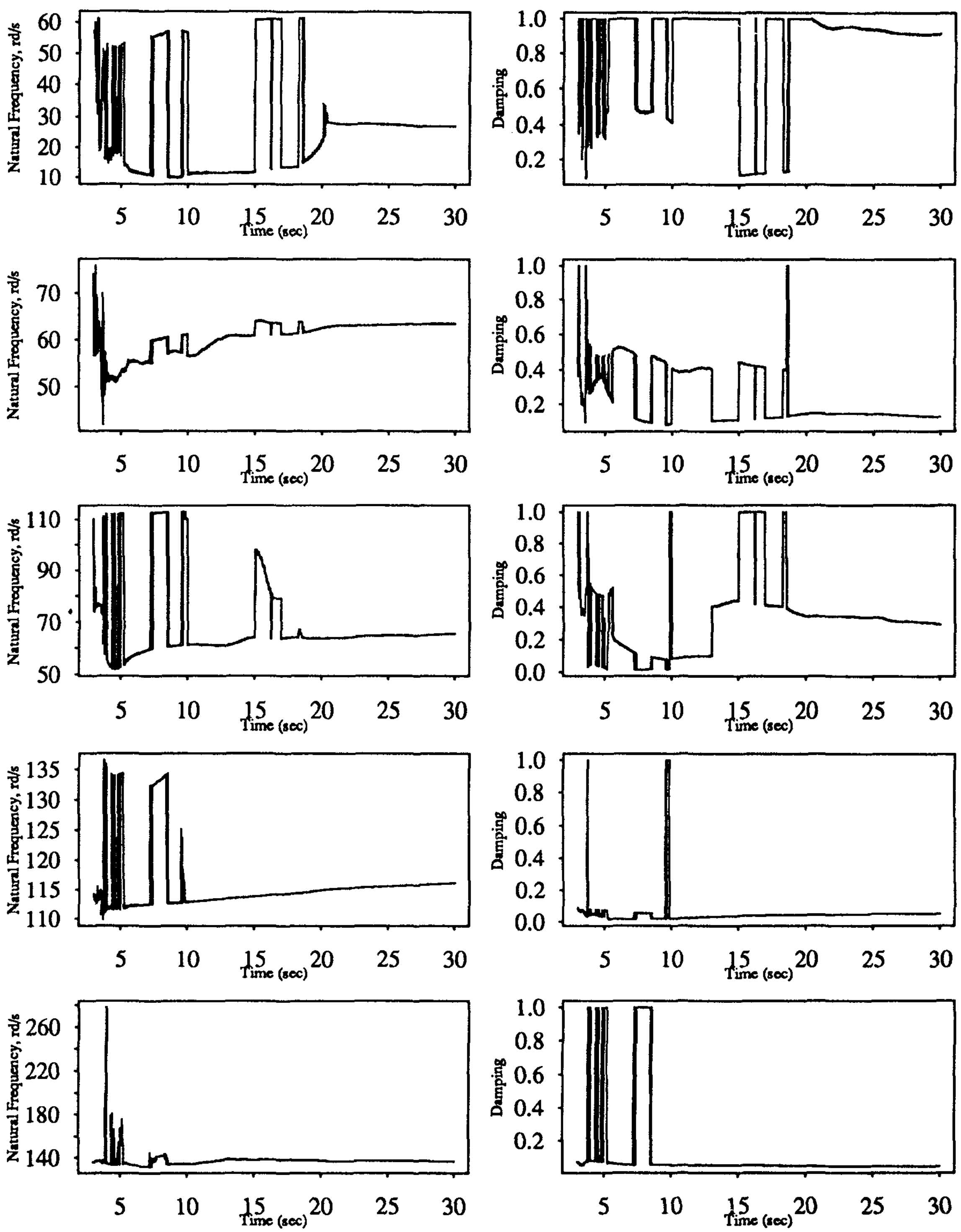


Figure 5.208

Recursive Least Squares Estimation
Five Story Building Model; Elcentro Input
2nd Floor alpha=1.

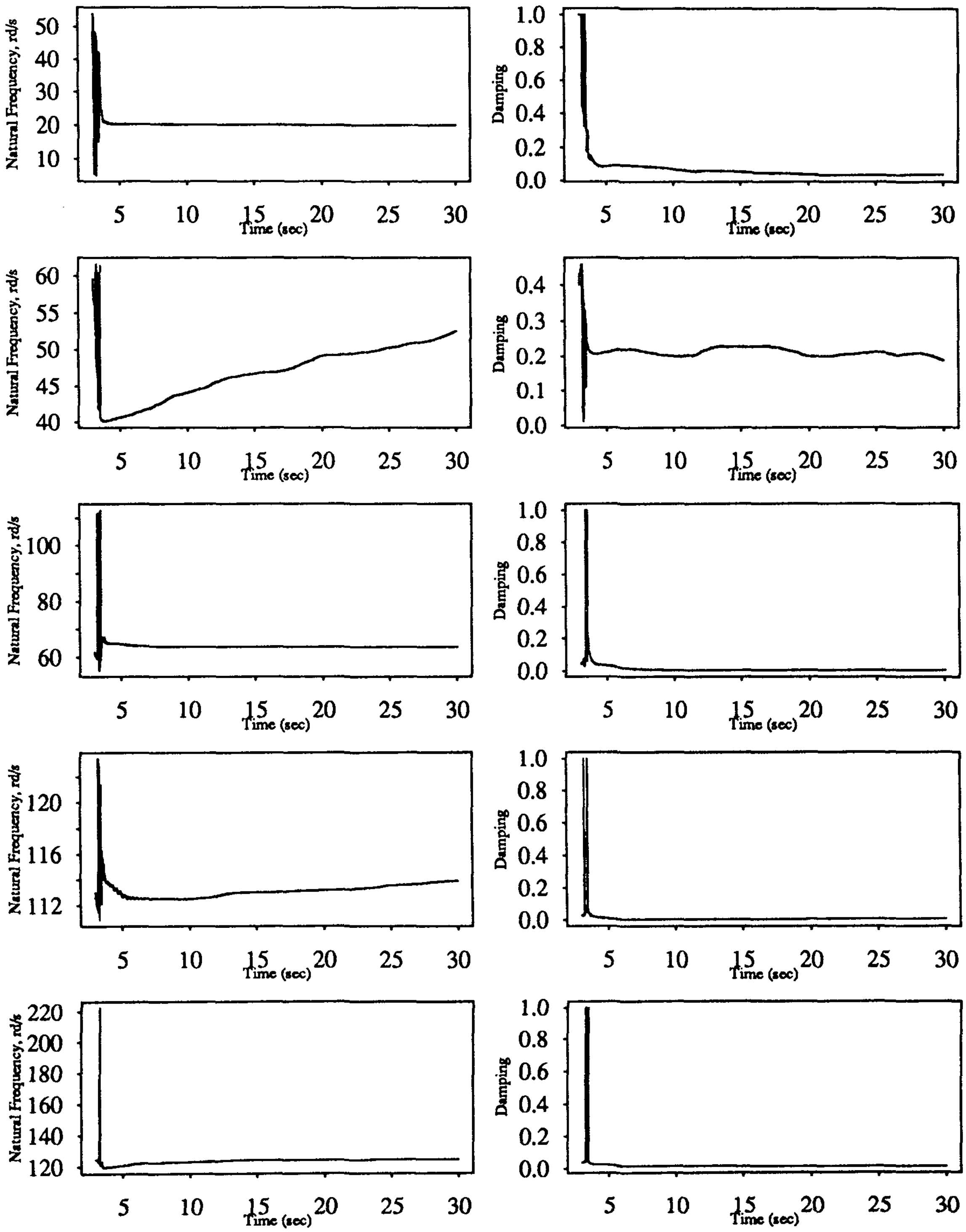


Figure 5.209

Recursive Least Squares Estimation

Five Story Building Model; Elcentro Input

3rd Floor alpha=1.

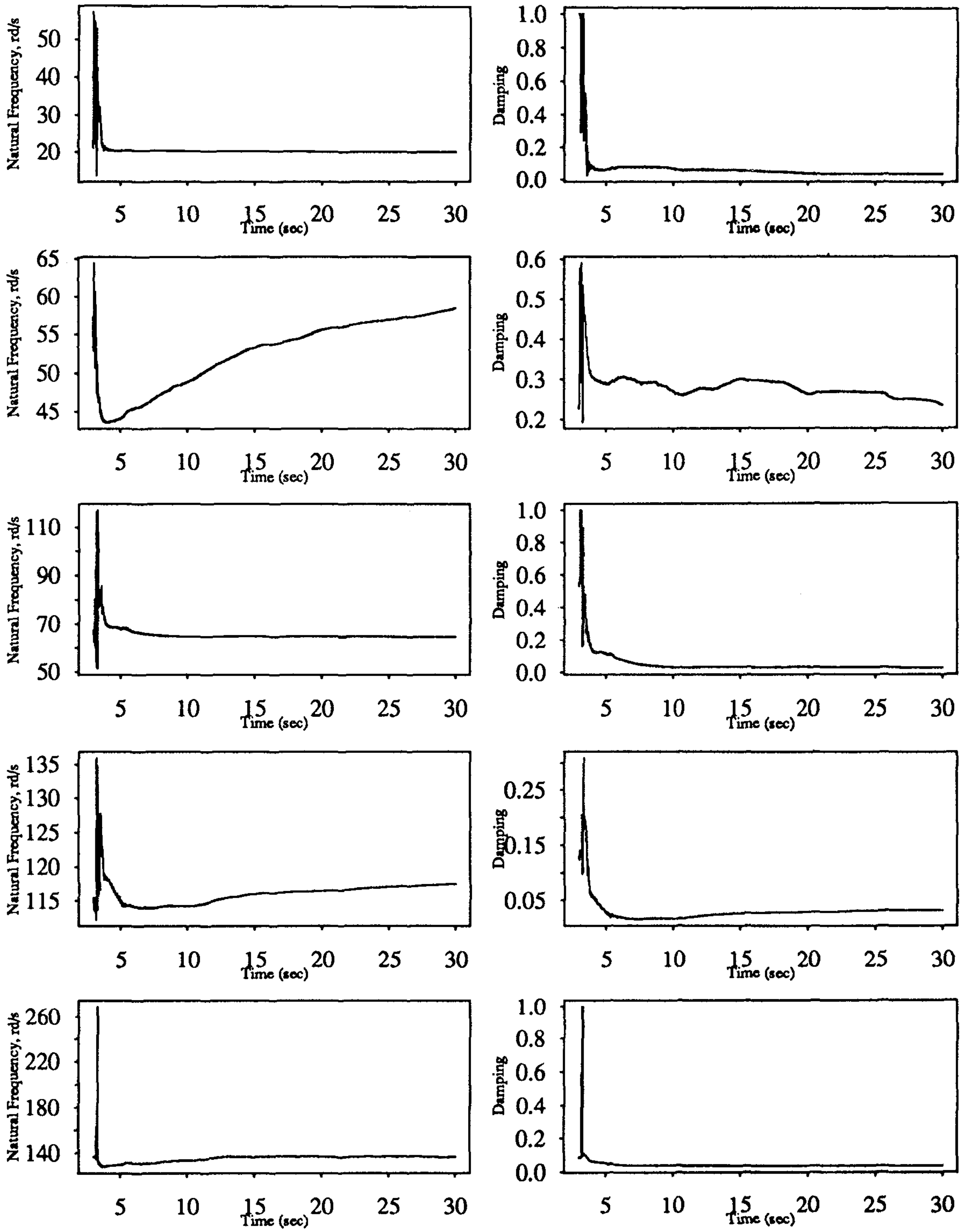


Figure 5.210

Recursive Least Squares Estimation
Five Story Building Model; Elcentro Input
4th Floor alpha=1.

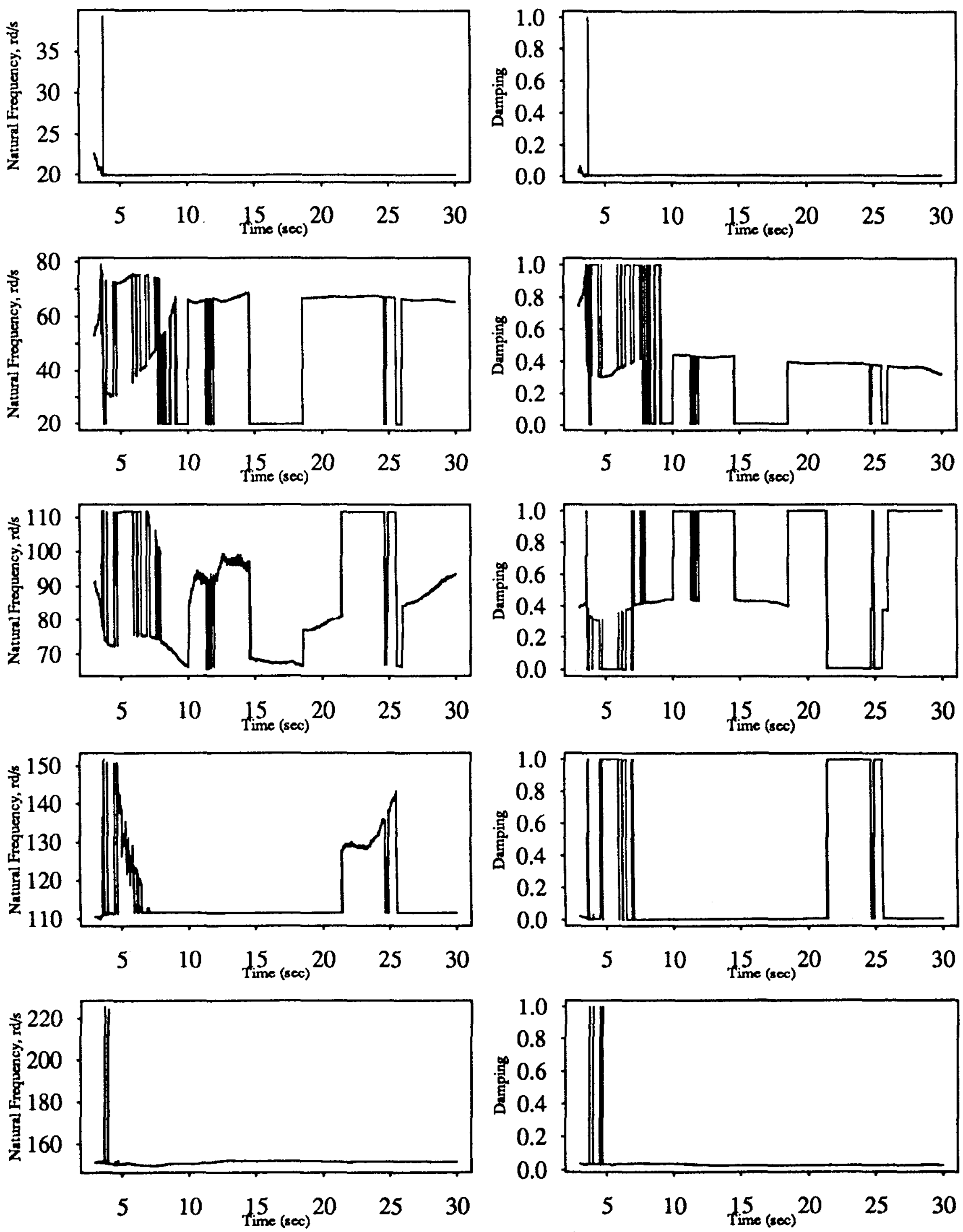


Figure 5.211

## Recursive Least Squares Estimation
## Five Story Building Model; Elcentro Input

5th Floor alpha=1.

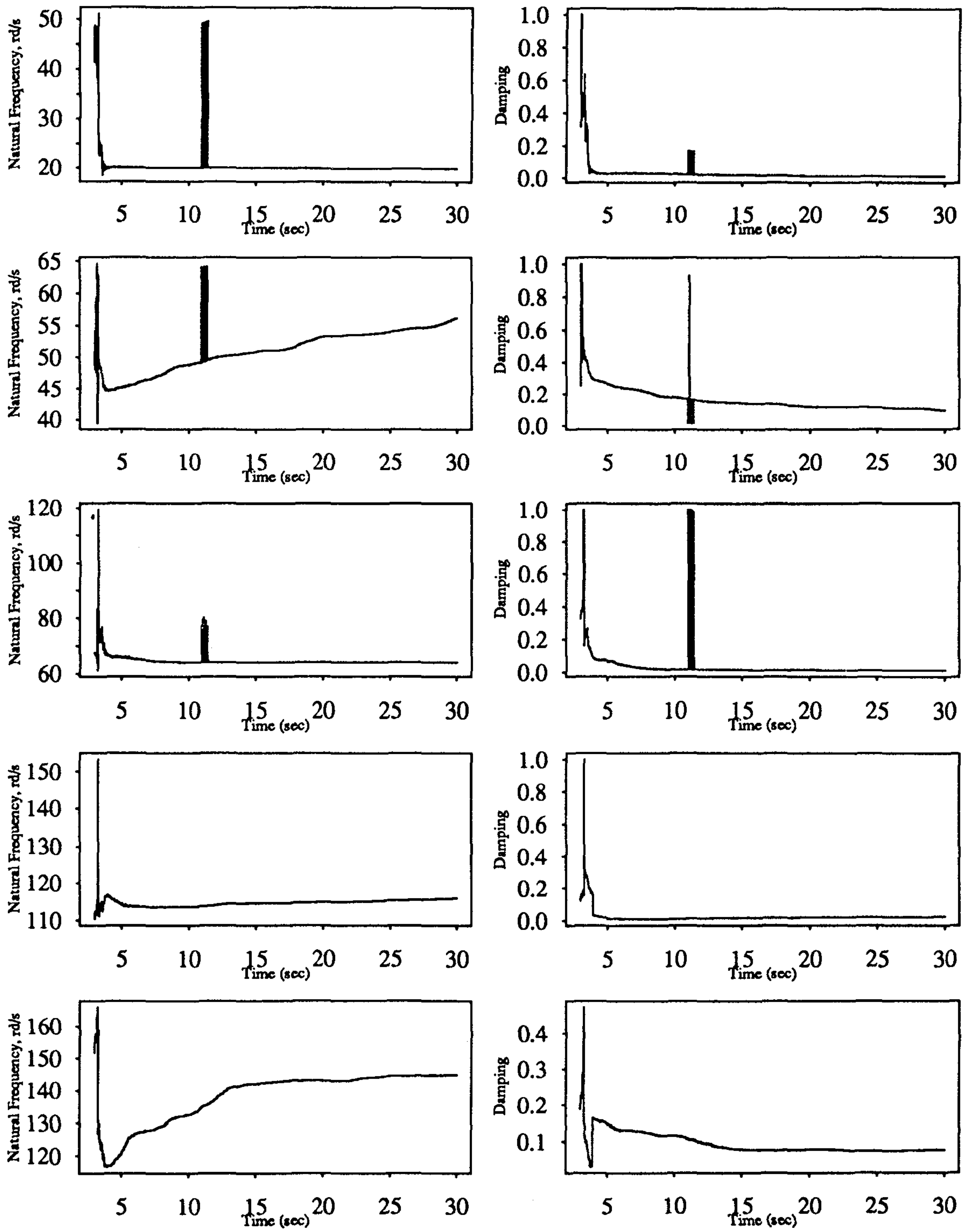


Figure 5.212

Recursive Least Squares Estimation
Five Story Building Model; White Noise Input
1st Floor alpha=1.

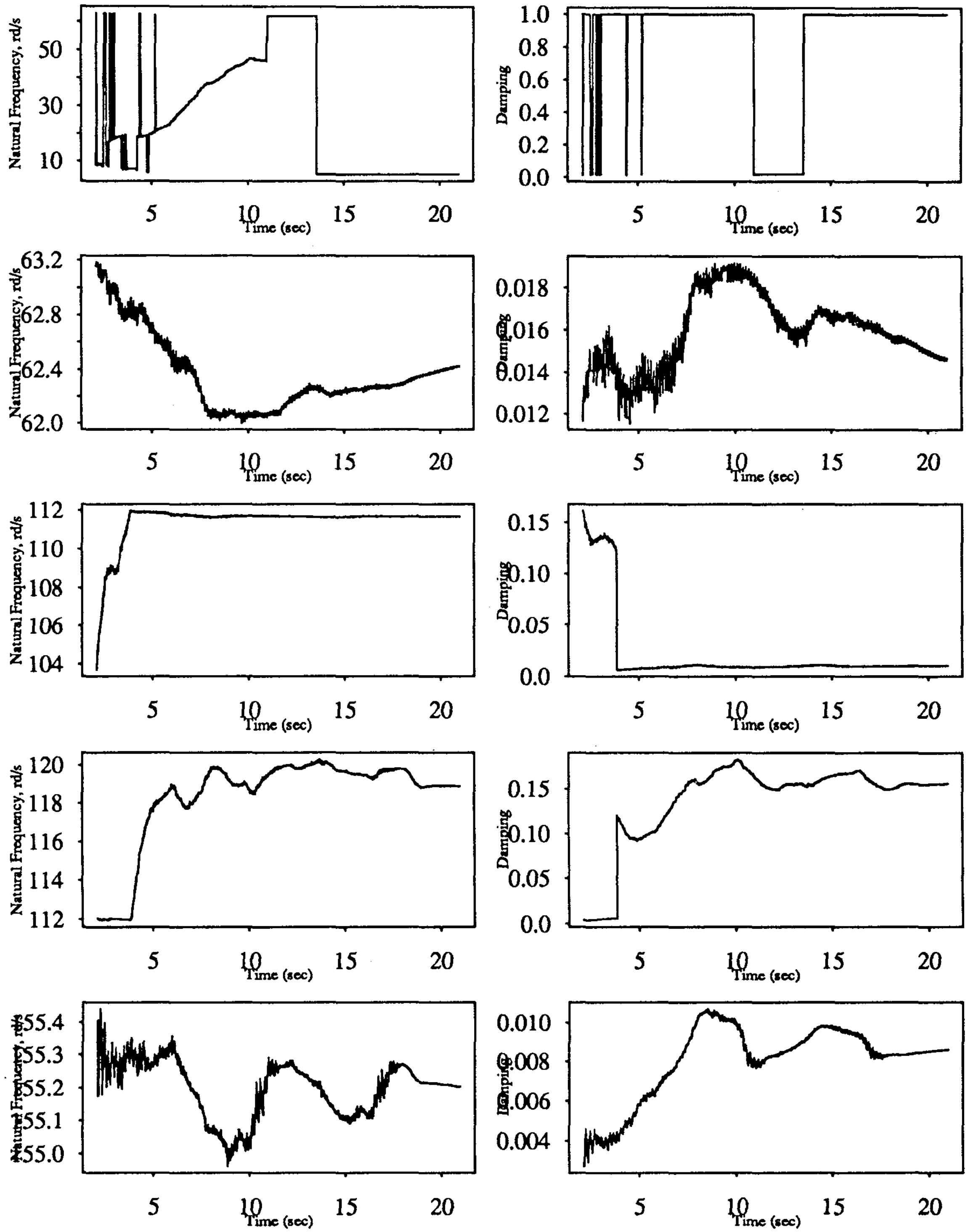


Figure 5.213

# Recursive Least Squares Estimation
## Five Story Building Model; White Noise Input
2nd Floor alpha=1.

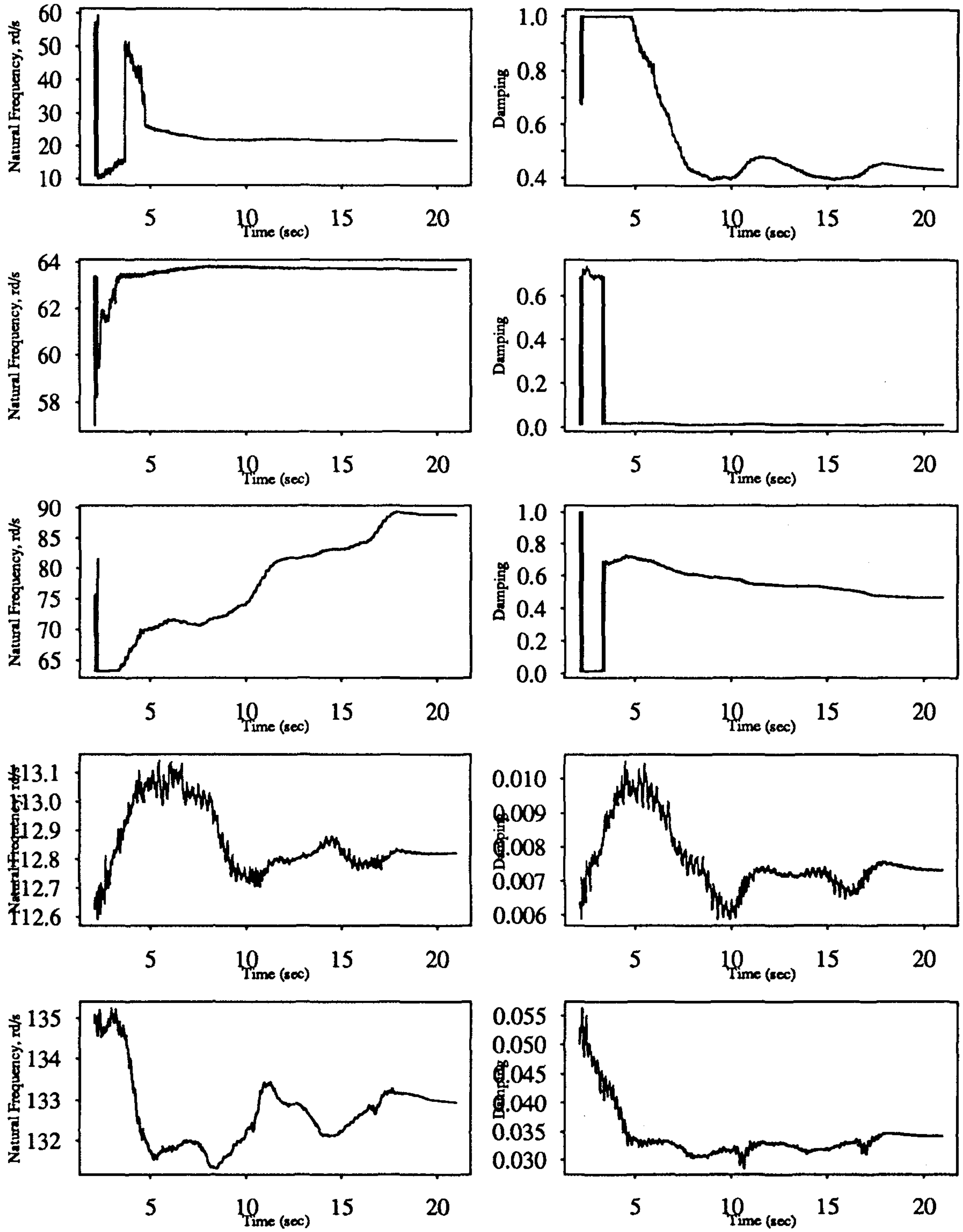


**Figure 5.214**

Recursive Least Squares Estimation
Five Story Building Model; White Noise Input
3rd Floor alpha=1.

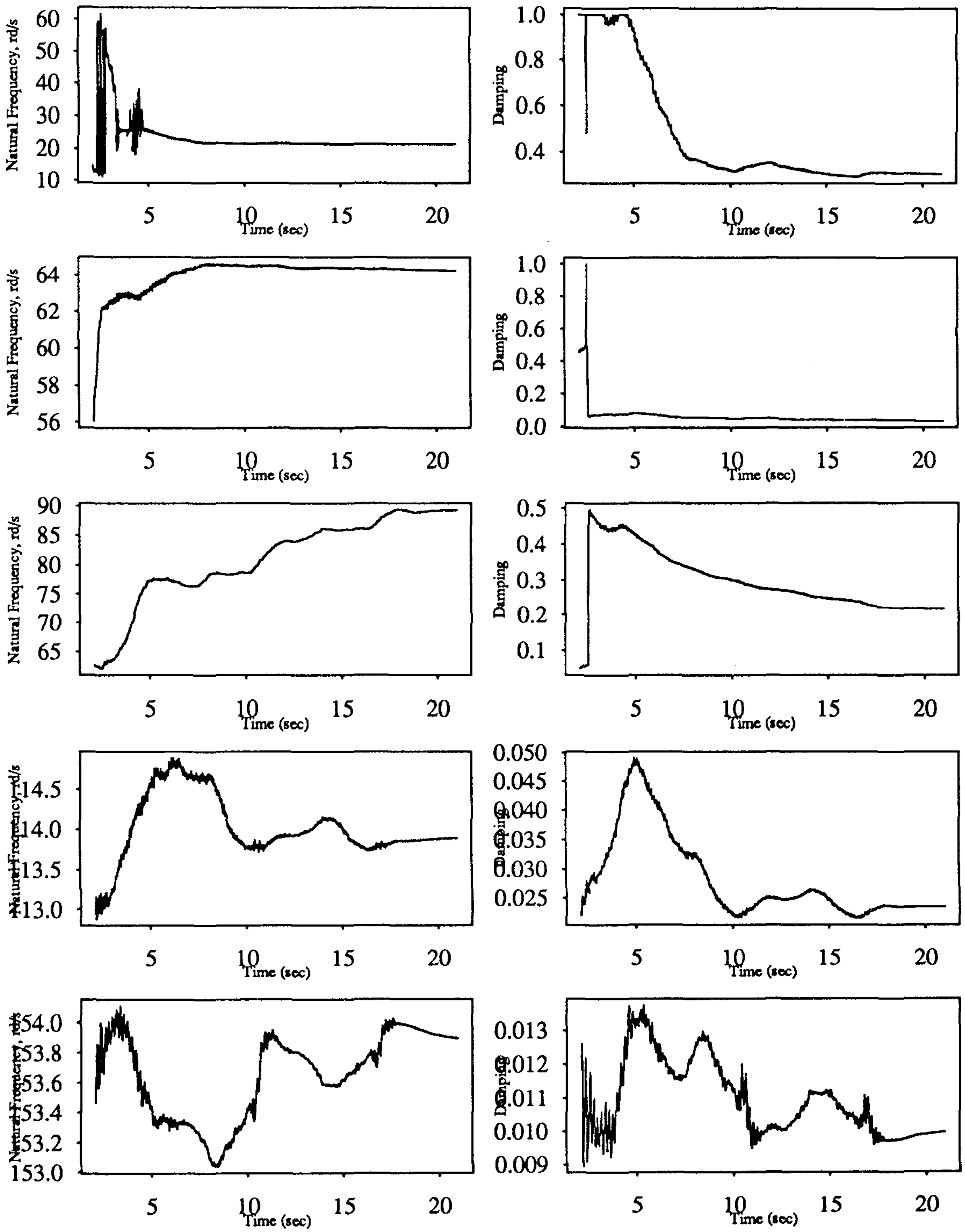


Figure 5.215

# Recursive Least Squares Estimation
## Five Story Building Model; White Noise Input
4th Floor alpha=1.

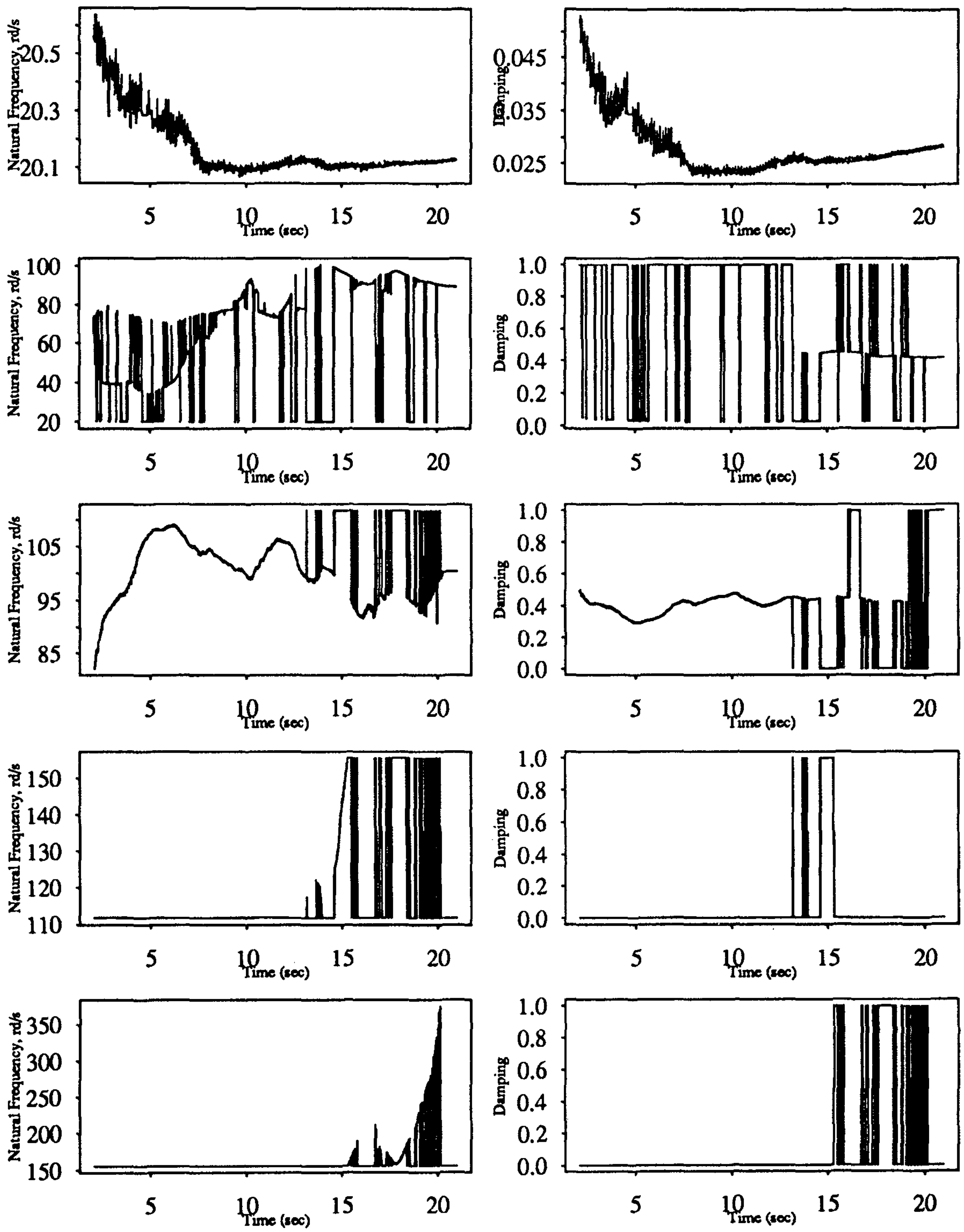


Figure 5.216

## Recursive Least Squares Estimation
## Five Story Building Model; White Noise Input
5th Floor alpha=1.

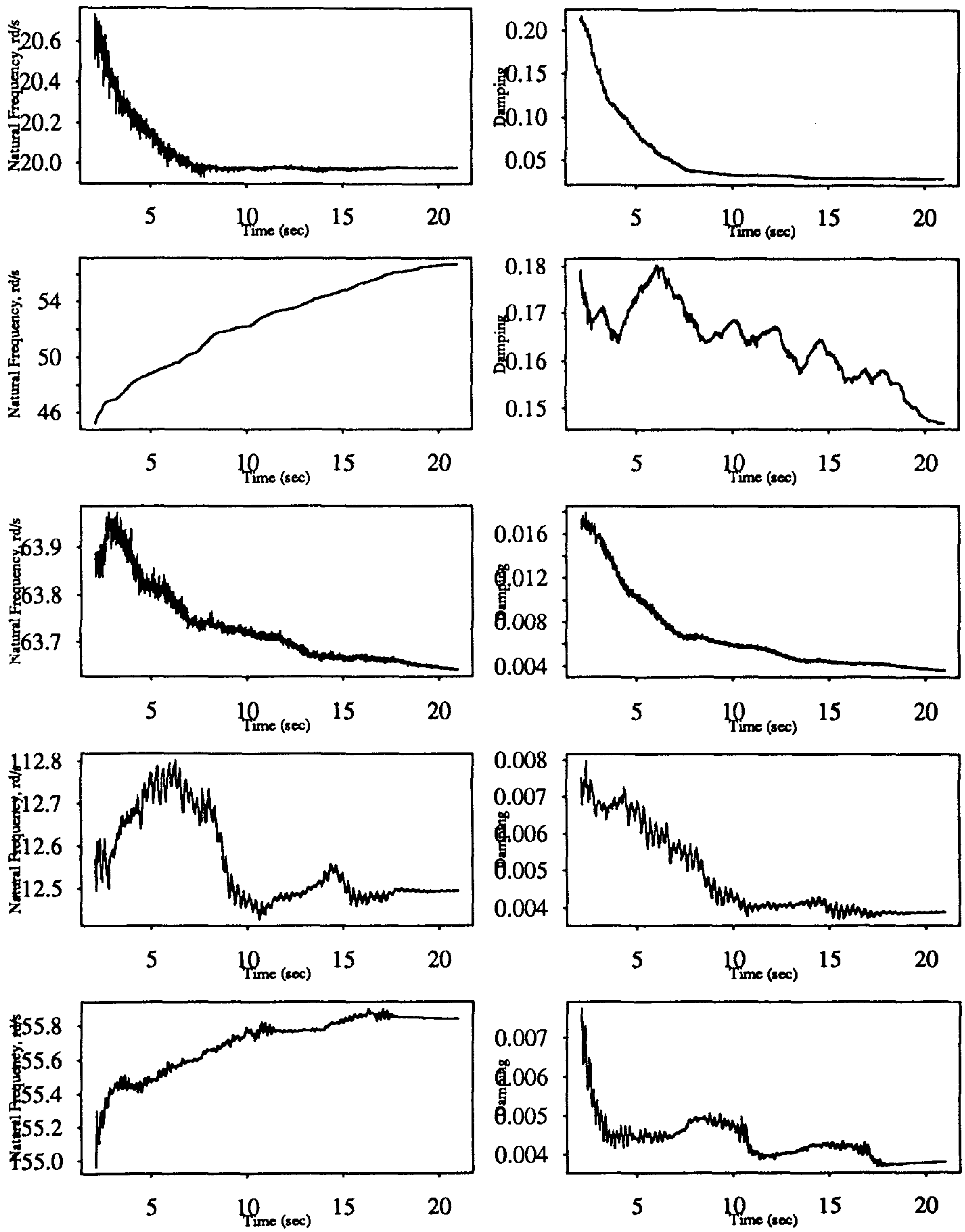


**Figure 5.217**

Recursive Least Squares Estimation
Three Story Building Model; El-Centro Input
1st Floor alpha=1.

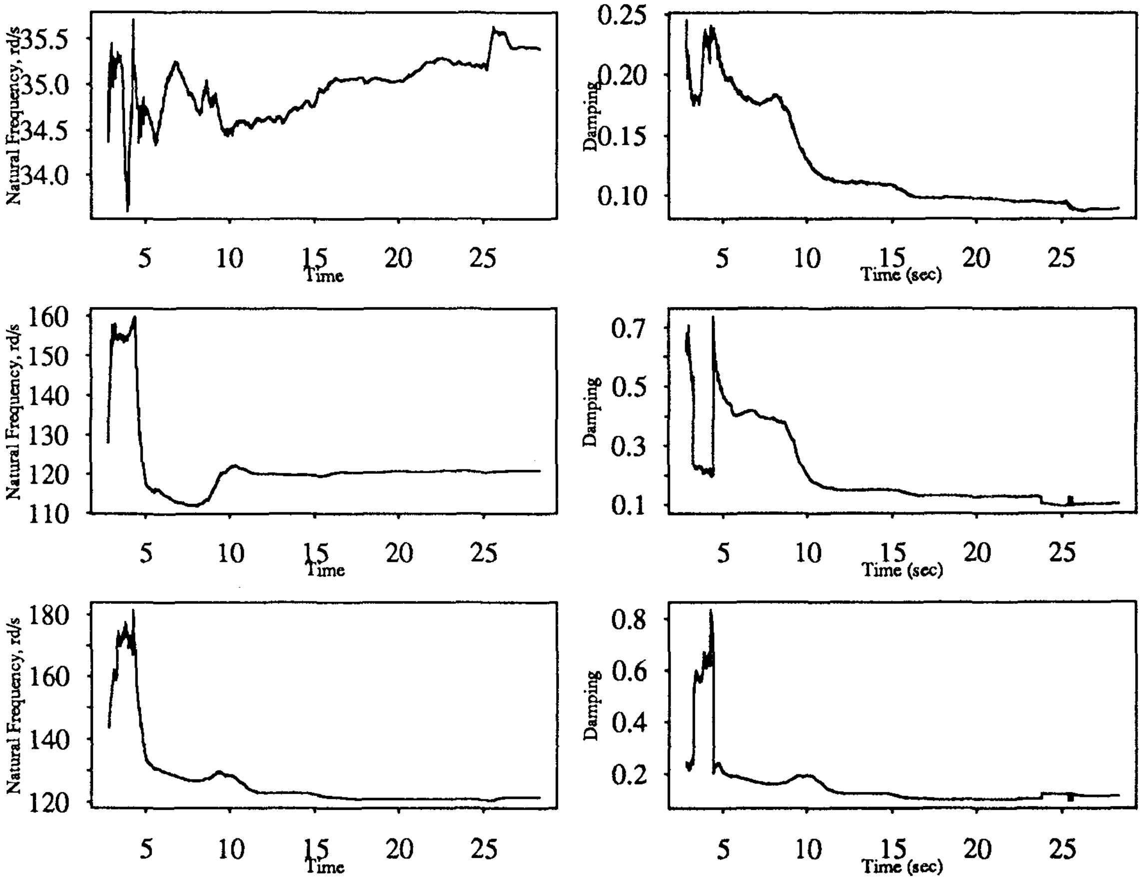


**Figure 5.218**

Recursive Least Squares Estimation
Three Story Building Model; El-Centro Input
2nd Floor alpha=1.

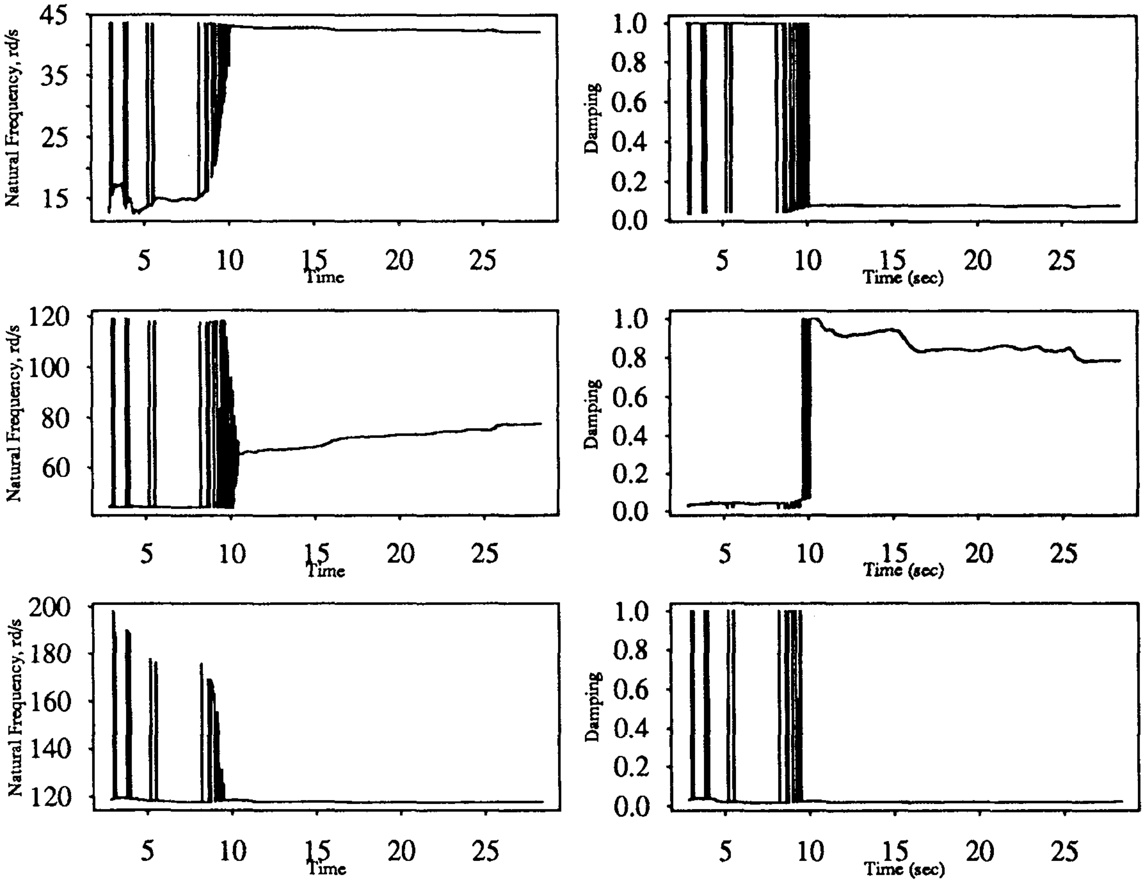


Figure 5.219

Recursive Least Squares Estimation
Three Story Building Model; El-Centro Input
3rd Floor alpha=1.

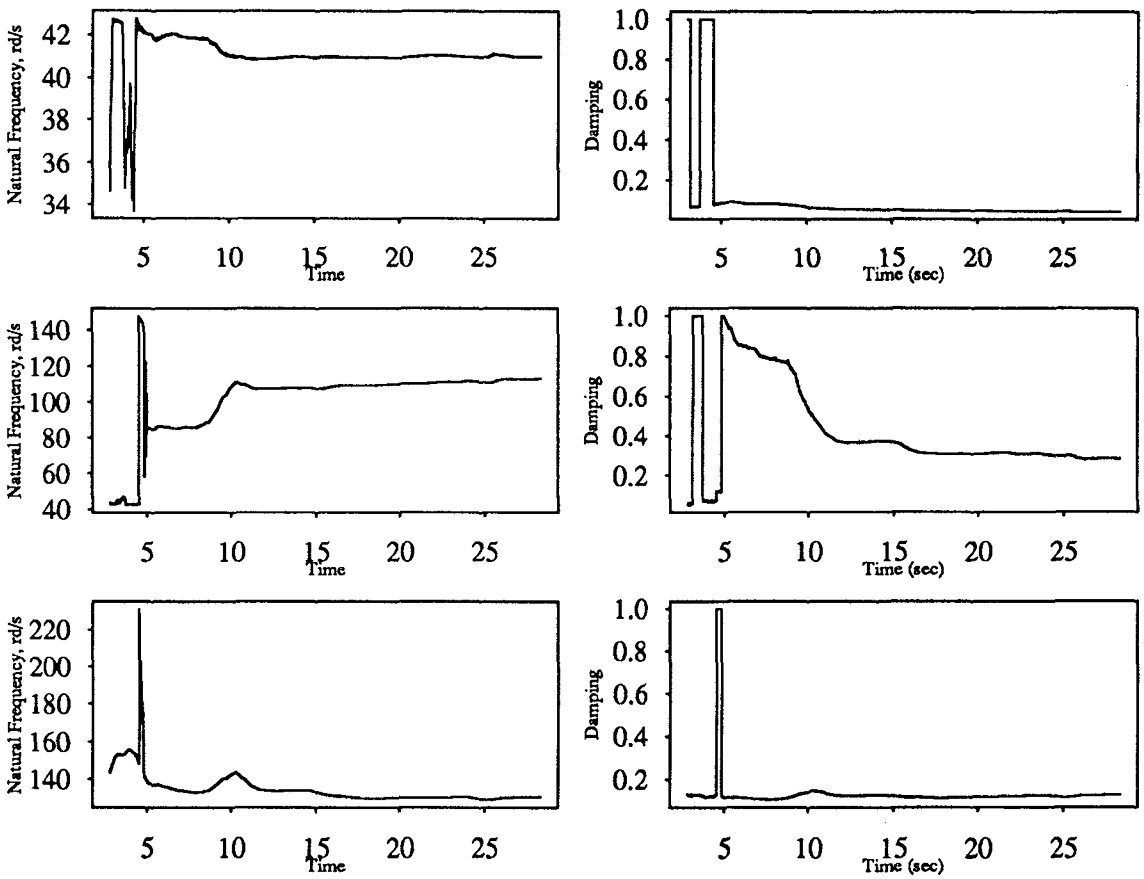


Figure 5.220

Recursive Least Squares Estimation
Three Story Building Model; Sine Sweep Input
1st Floor alpha=1.

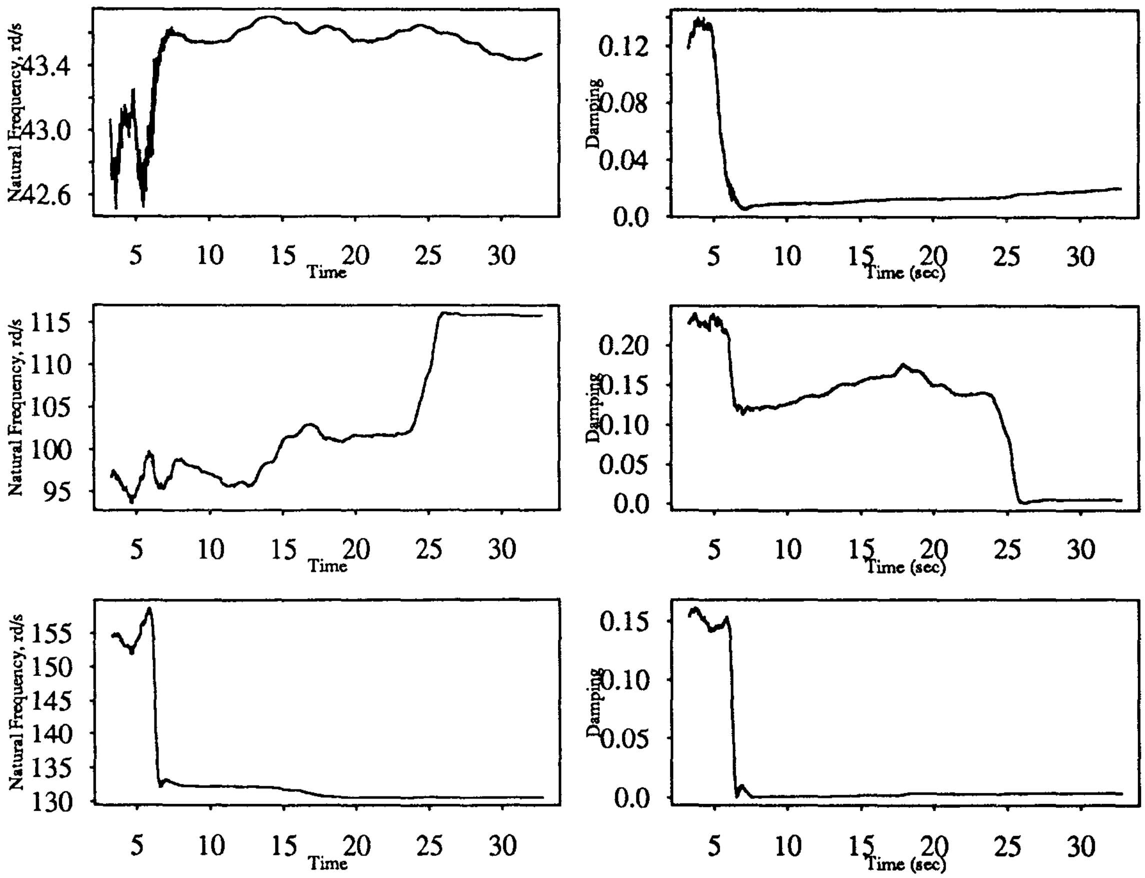


**Figure 5.221**

Recursive Least Squares Estimation
Three Story Building Model; Sine Sweep Input
2nd Floor alpha=1.

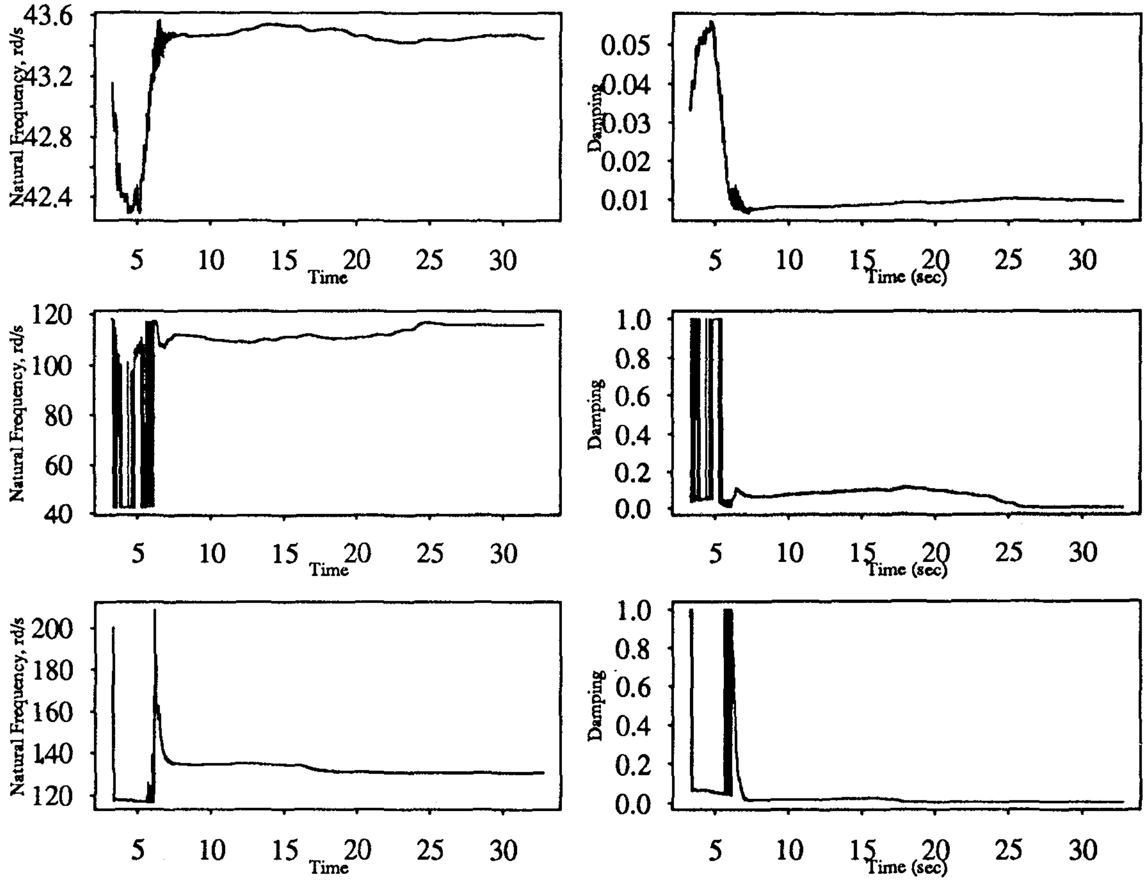


Figure 5.222

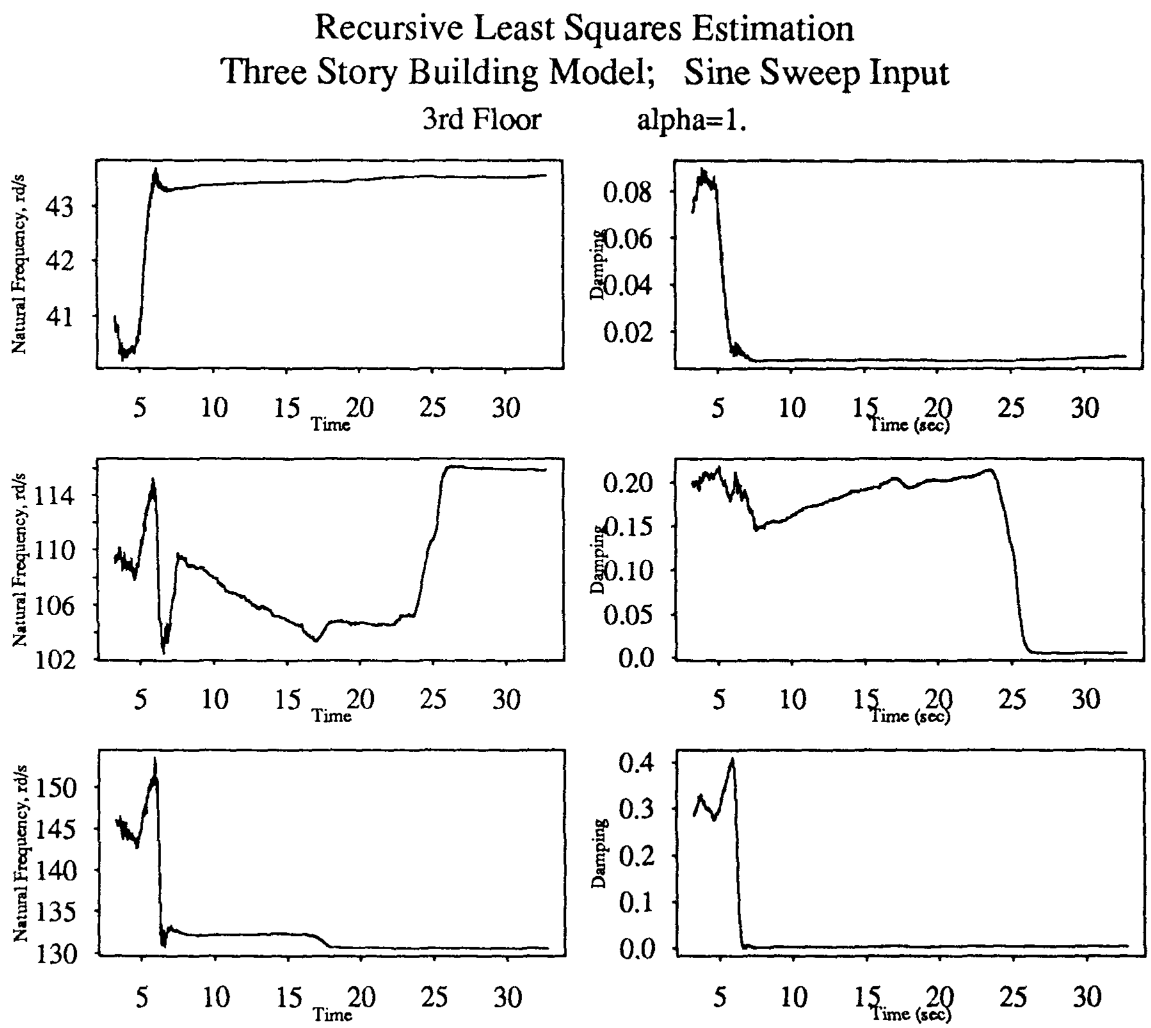
Recursive Least Squares Estimation
Three Story Building Model; Sine Sweep Input
3rd Floor alpha=1.
Natural Frequency, rd/s
Damping
Time
Time (sec)

Figure 5.223

# Recursive Least Squares Estimation
## Three Story Building Model; White Noise Input

1st Floor alpha=1.

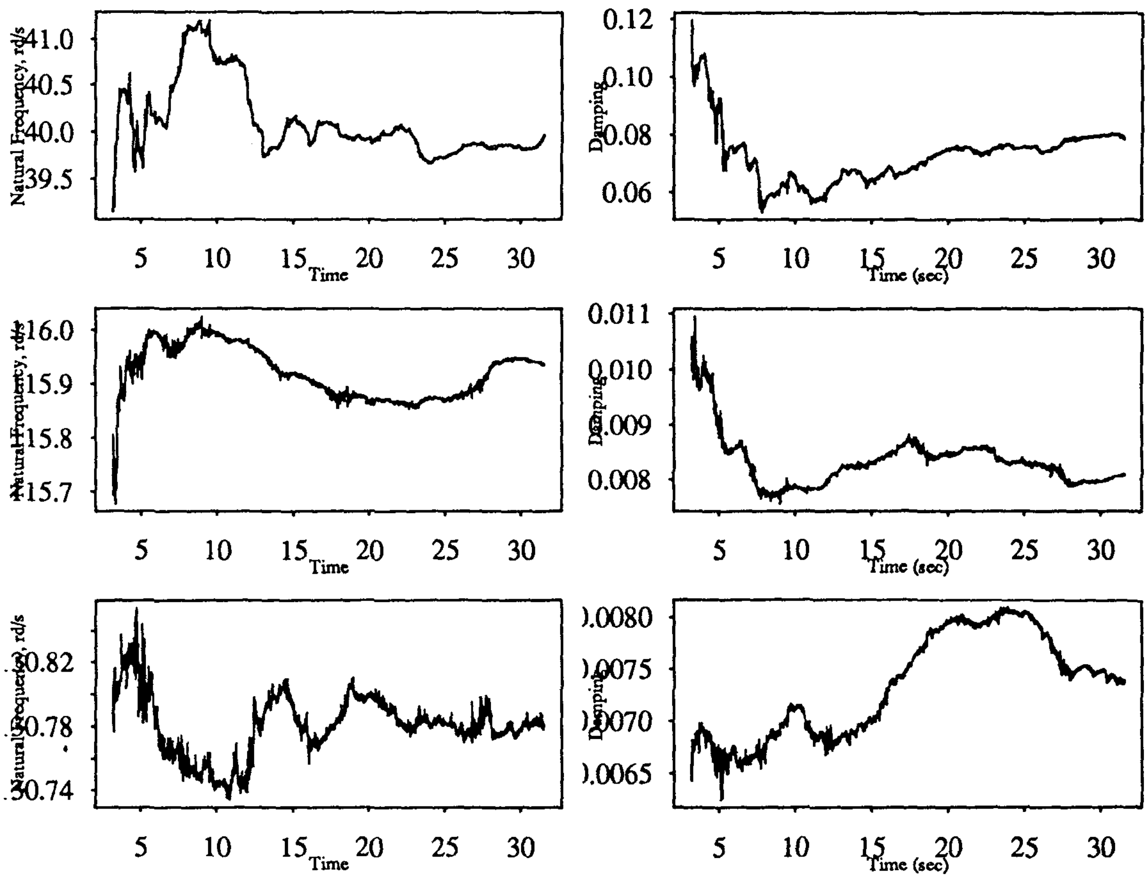


Figure 5.224

# Recursive Least Squares Estimation
## Three Story Building Model; White Noise Input

2nd Floor alpha=1.

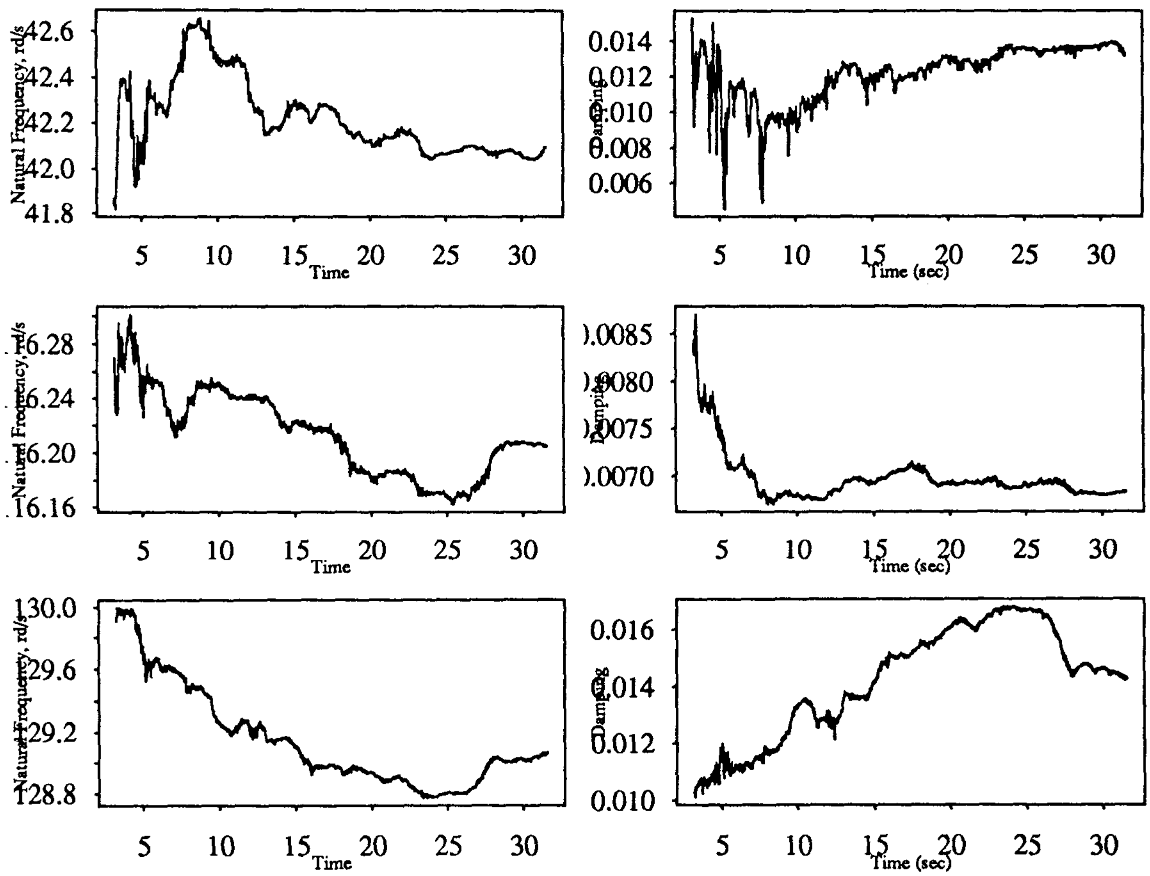


Figure 5.225

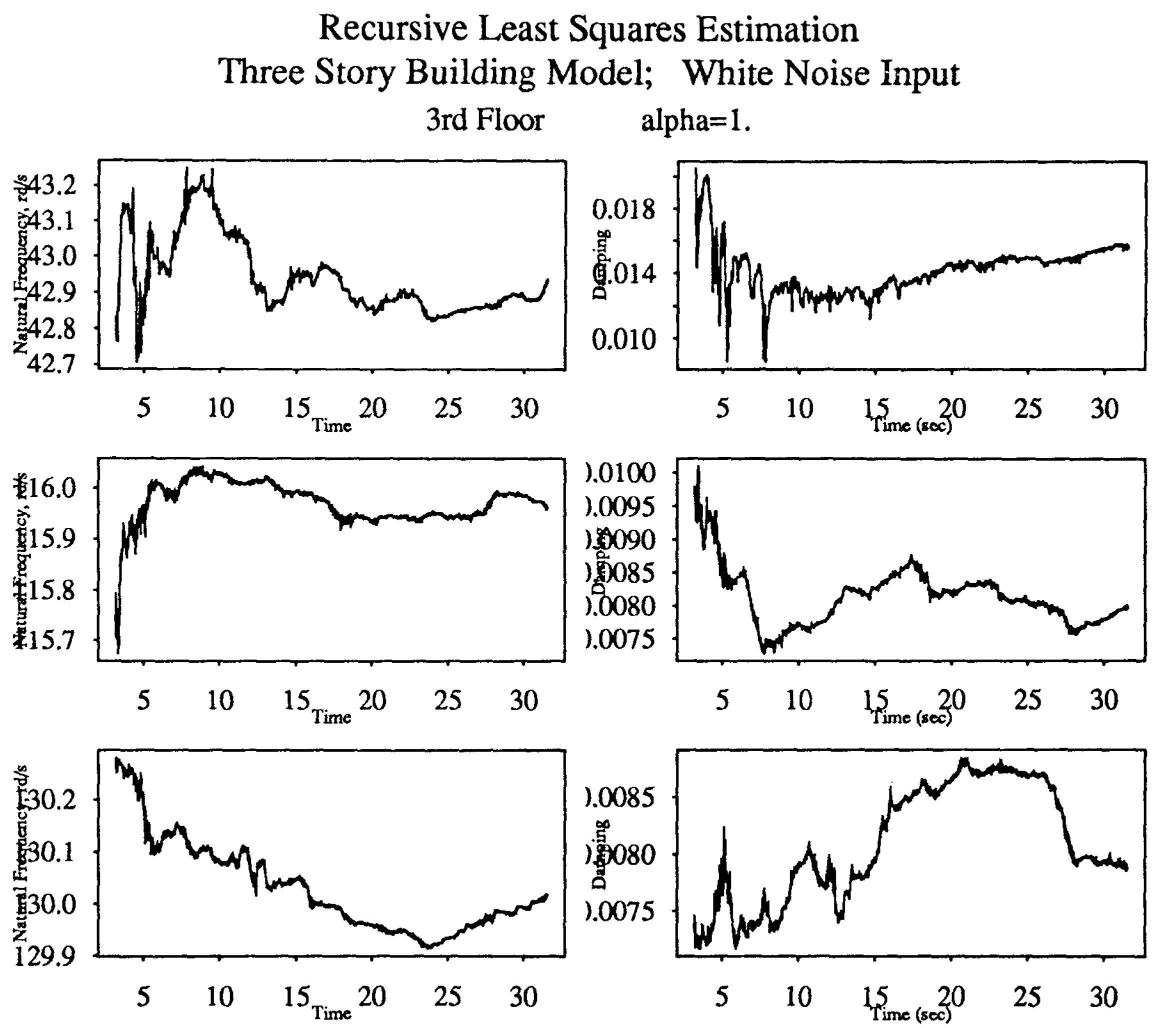
Recursive Least Squares Estimation
Three Story Building Model; White Noise Input
3rd Floor alpha=1.
Natural Frequency, rd/s
Damping
Time
Time (sec)

Figure 5.226

Recursive Least Squares Estimation
Five Story Building Model;   El-Centro Input
1st Floor   alpha=0.99

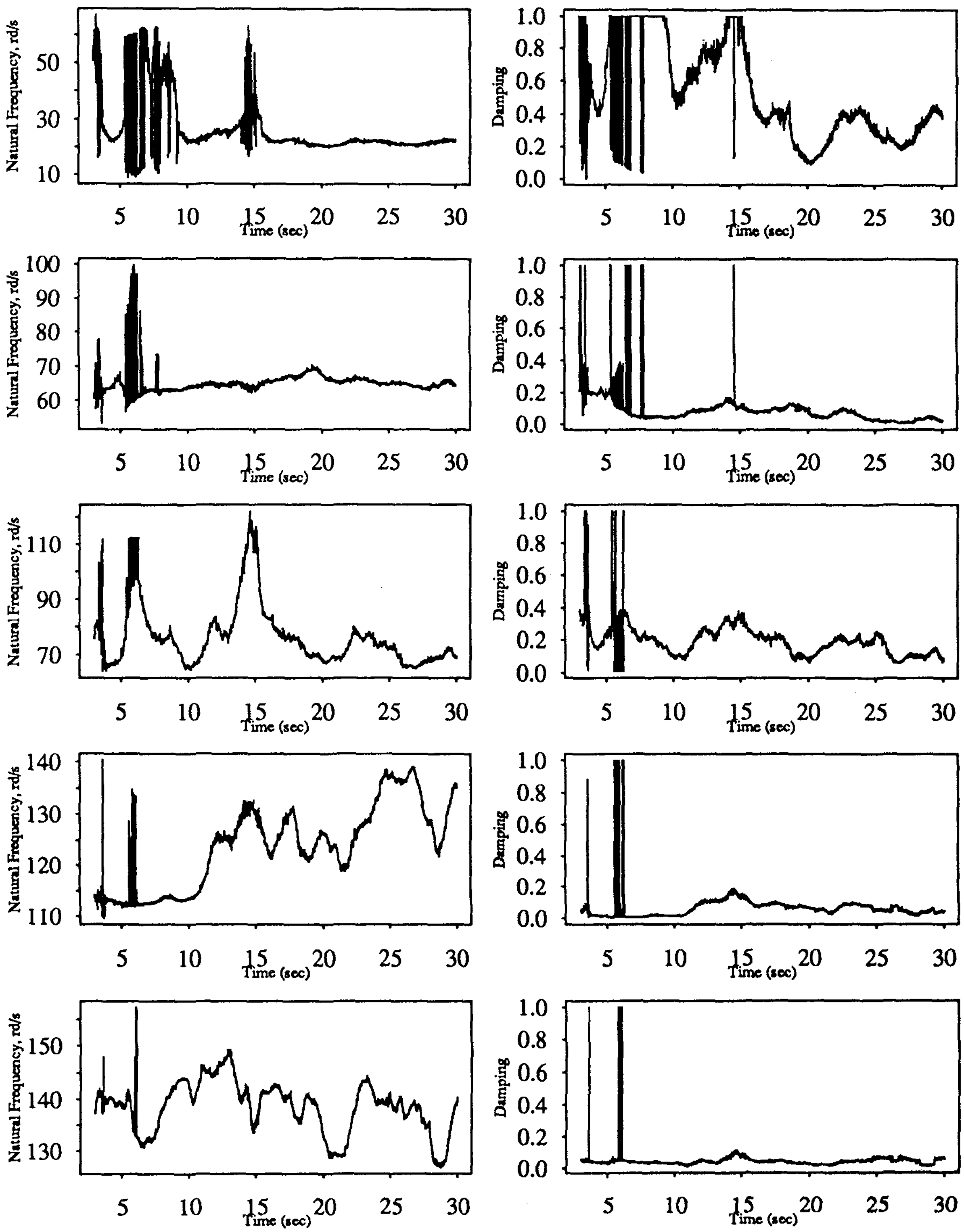


Figure 5.227

Recursive Least Squares Estimation
Five Story Building Model;  El-Centro Input
2nd Floor  alpha=0.99

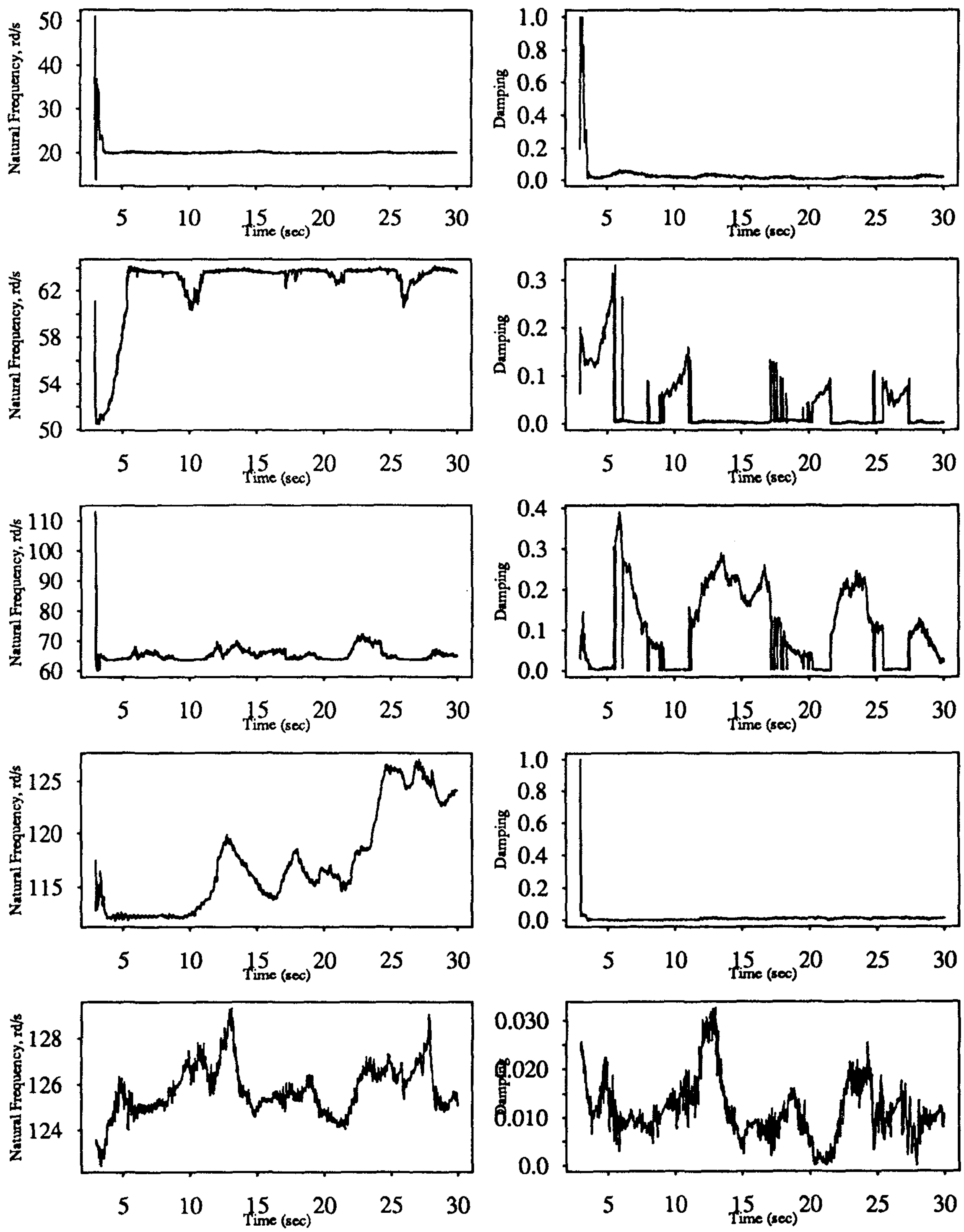


Figure 5.228

Recursive Least Squares Estimation
Five Story Building Model; El-Centro Input
3rd Floor alpha=0.99

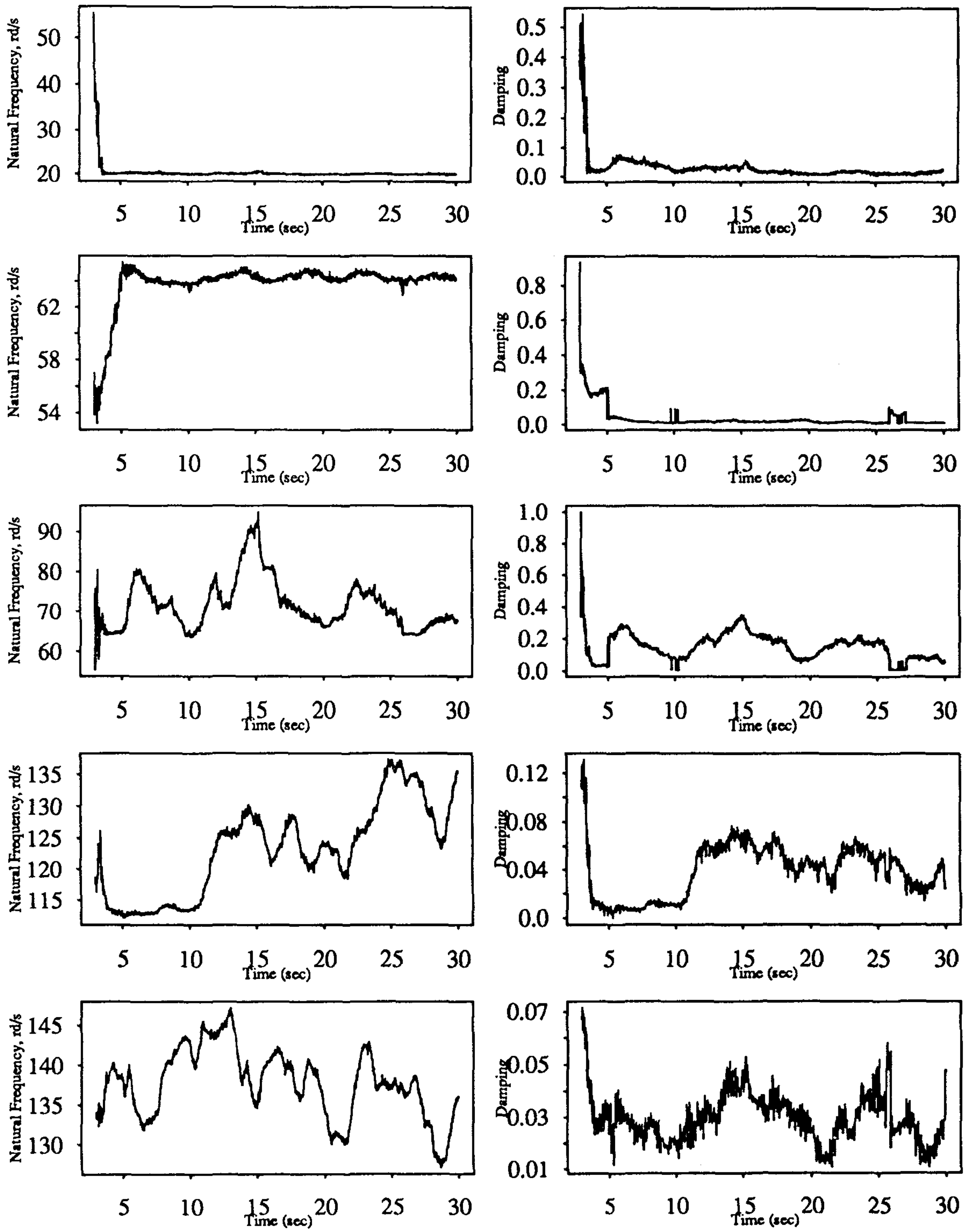


Figure 5.229

## Recursive Least Squares Estimation
## Five Story Building Model; El-Centro Input

4th Floor alpha=0.99

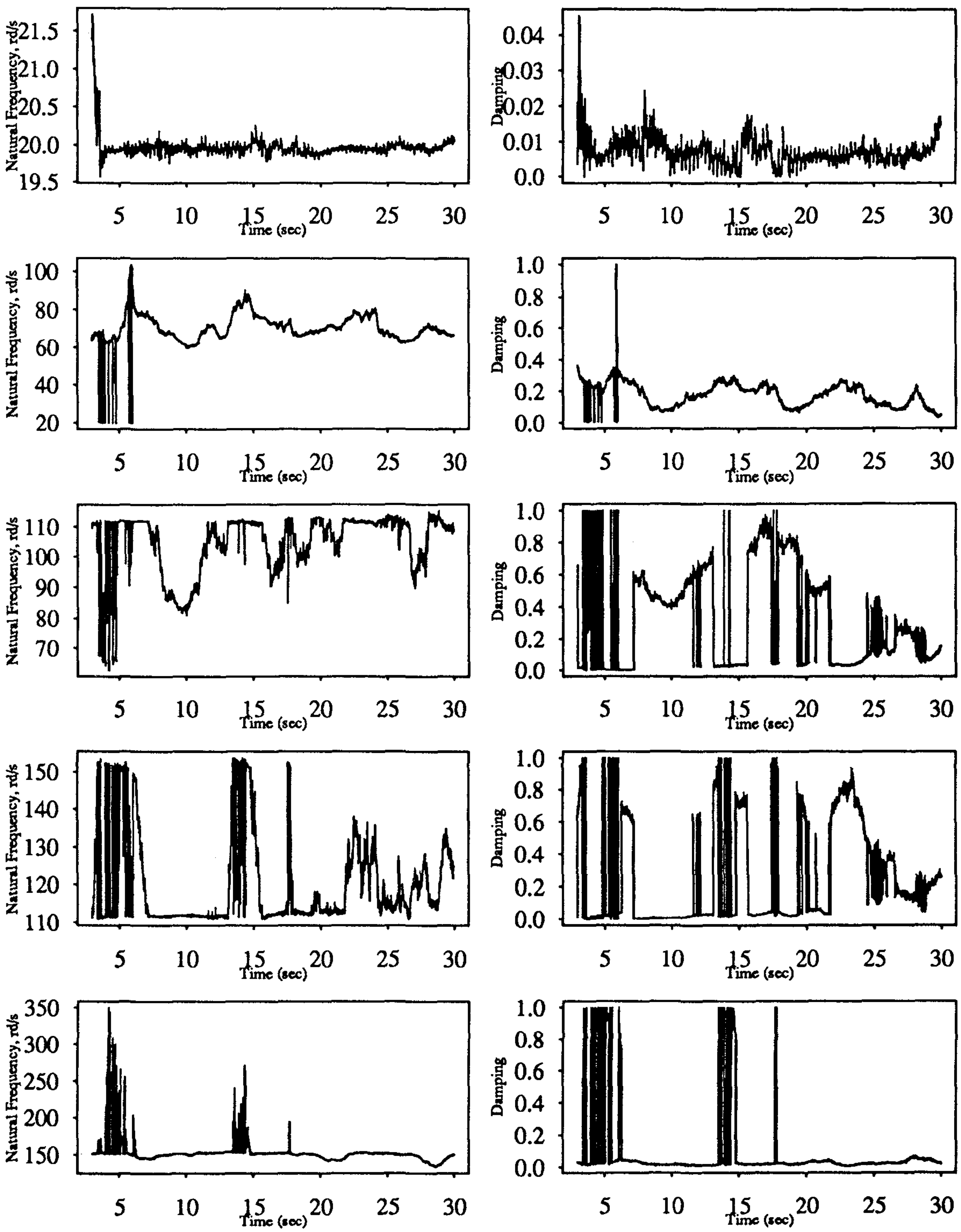


Figure 5.230

Recursive Least Squares Estimation
Five Story Building Model; El-Centro Input
5th Floor alpha=0.99

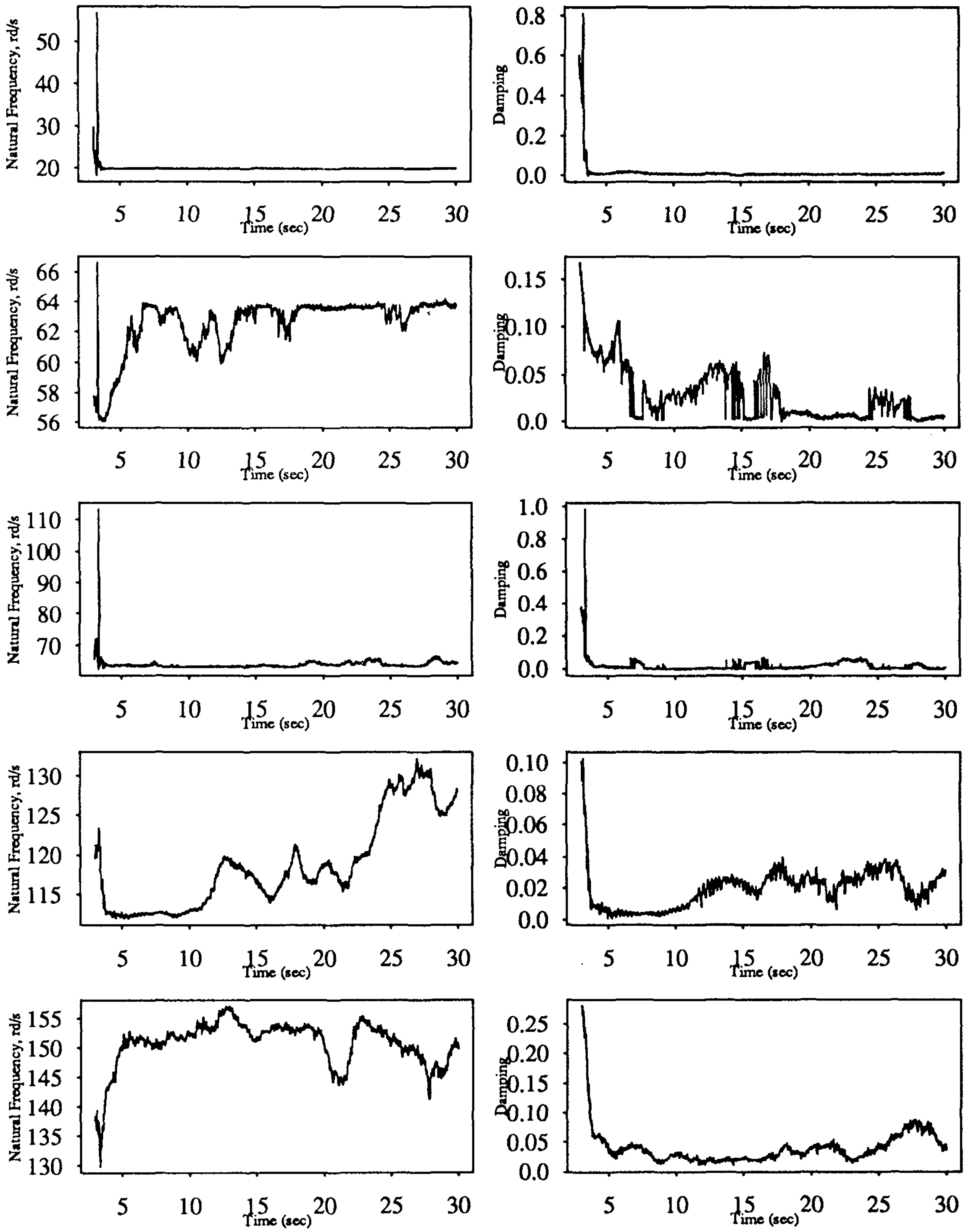


Figure 5.231

Recursive Least Squares Estimation
Five Story Building Model; White Noise Input
1st Floor alpha=0.99

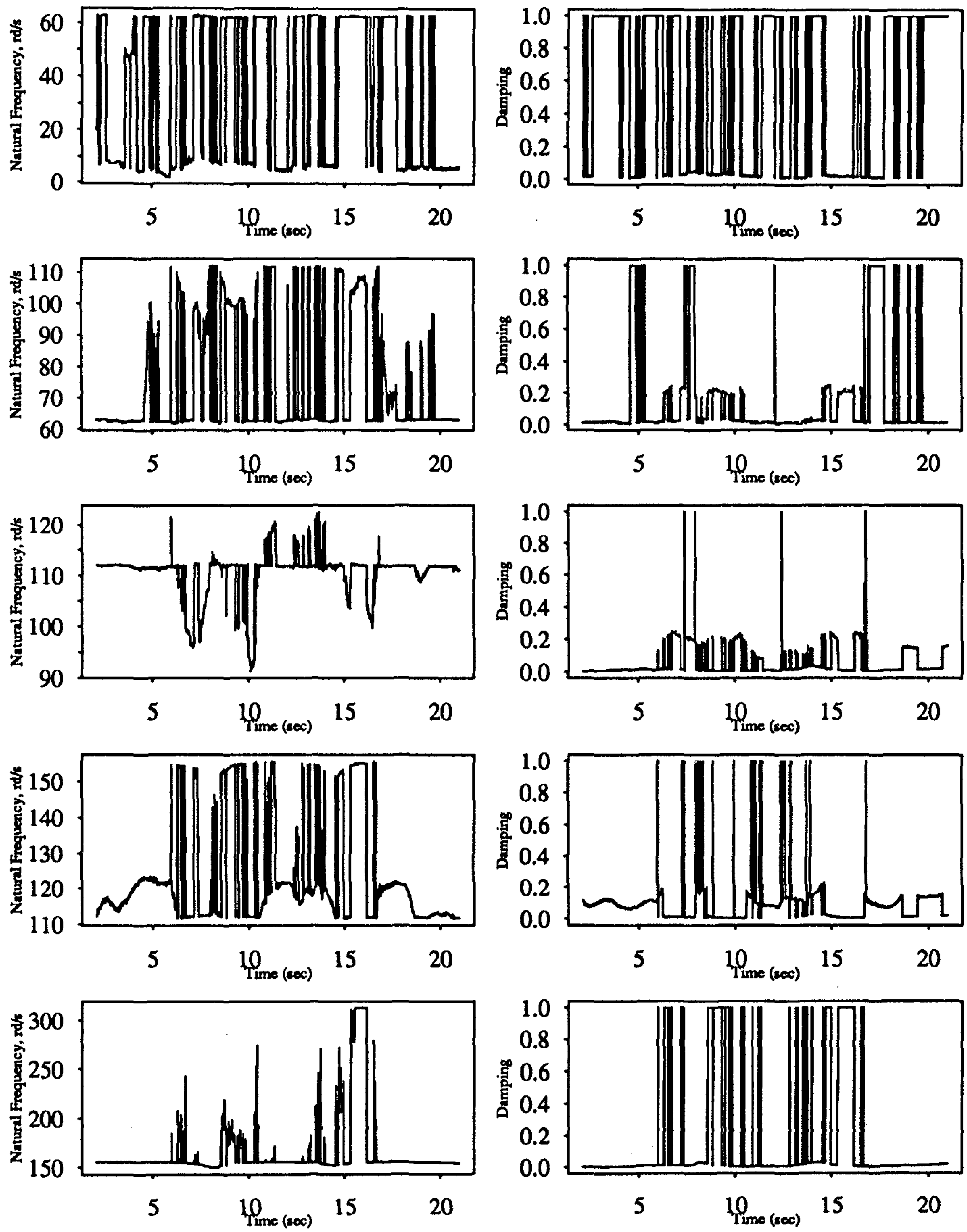


Figure 5.232

## Recursive Least Squares Estimation
## Five Story Building Model; White Noise Input
2nd Floor alpha=0.99

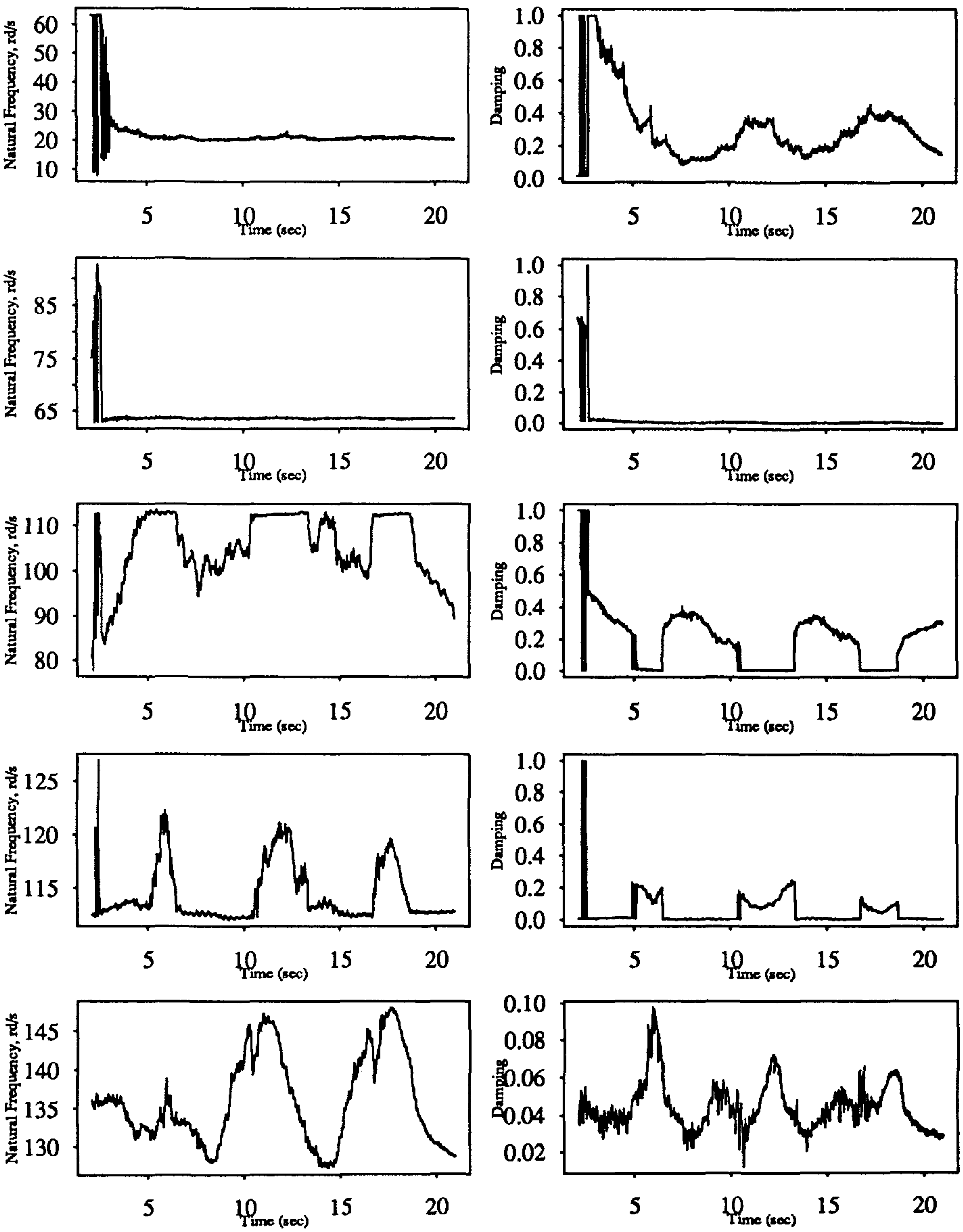


**Figure 5.233**

# Recursive Least Squares Estimation
## Five Story Building Model; White Noise Input
3rd Floor alpha=0.99

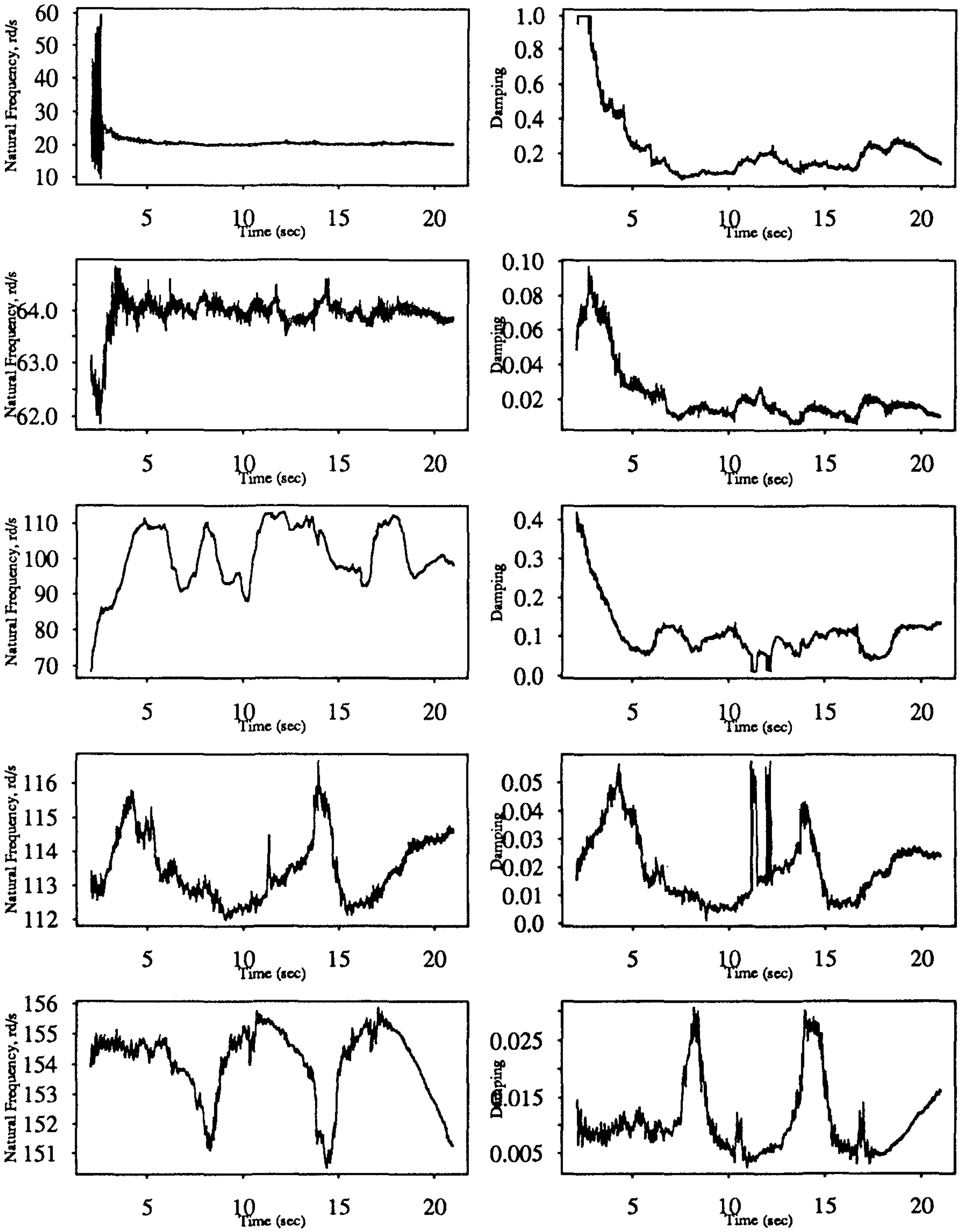


Figure 5.234

Recursive Least Squares Estimation
Five Story Building Model; White Noise Input
4th Floor alpha=0.99

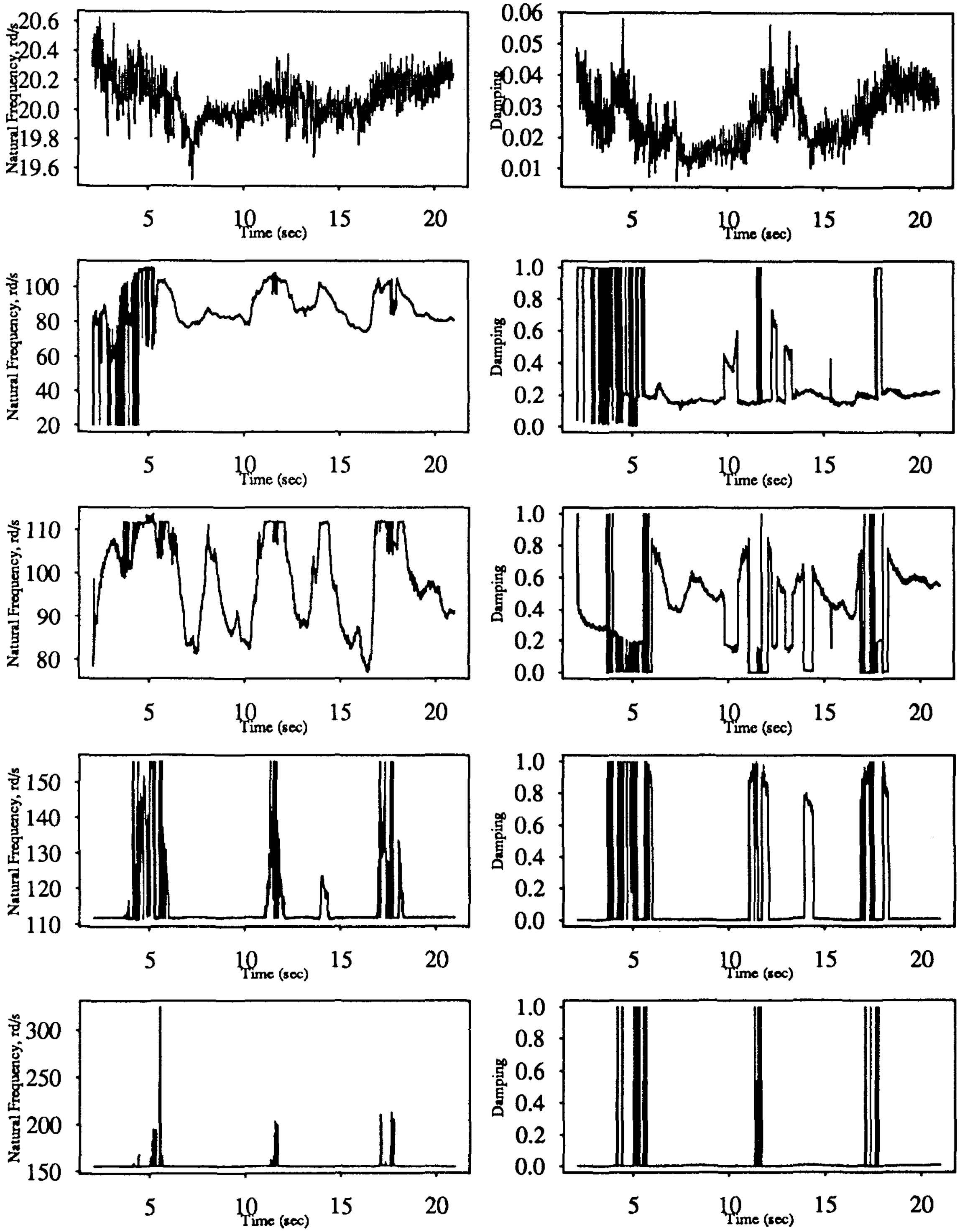


Figure 5.235

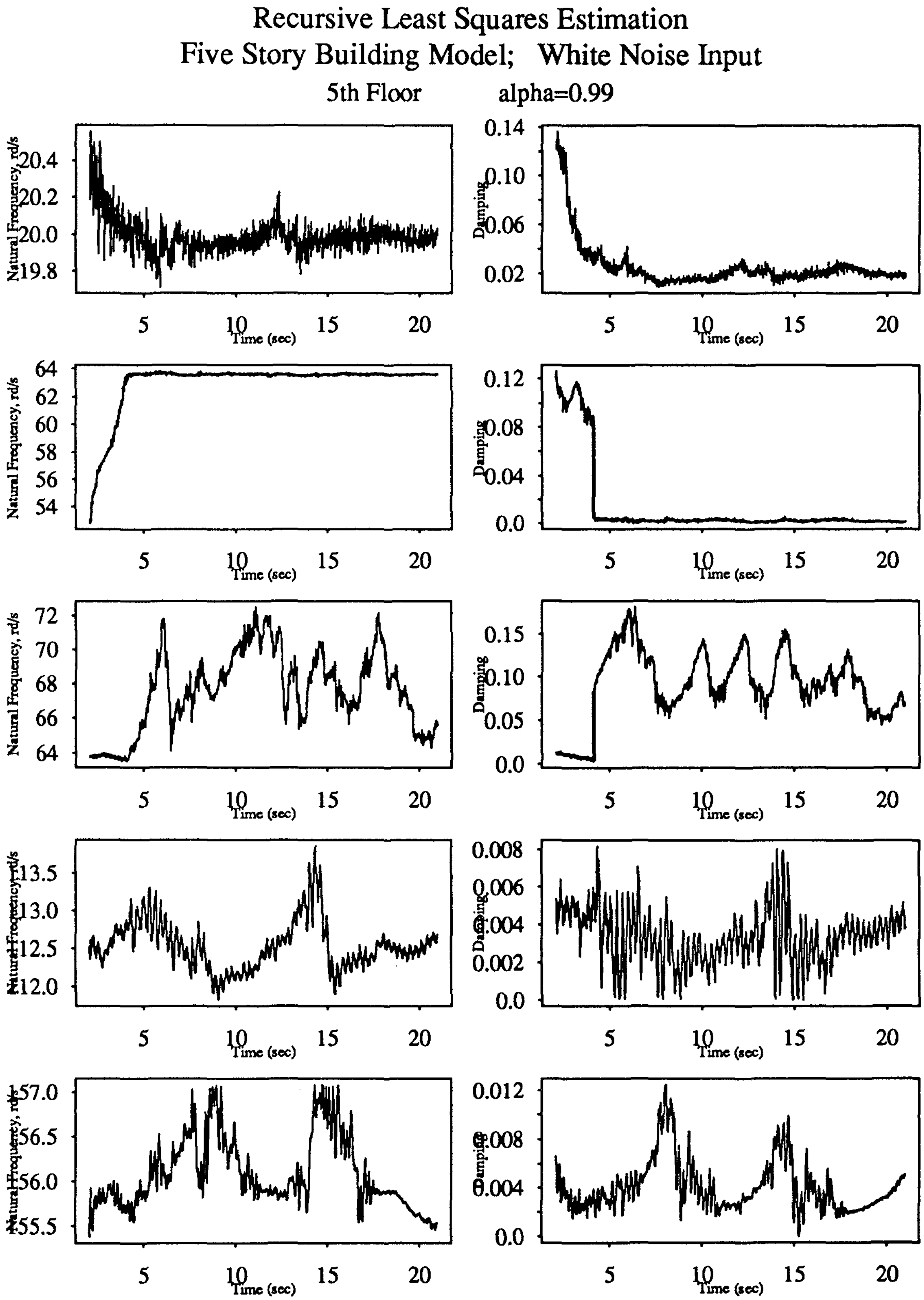
Recursive Least Squares Estimation
Five Story Building Model; White Noise Input
5th Floor alpha=0.99
Natural Frequency, rd/s
Damping
Time (sec)
5
10
15
20

Figure 5.236

# Recursive Least Squares Estimation
## Three Story Building Model; El-Centro Input

1st Floor alpha=0.99

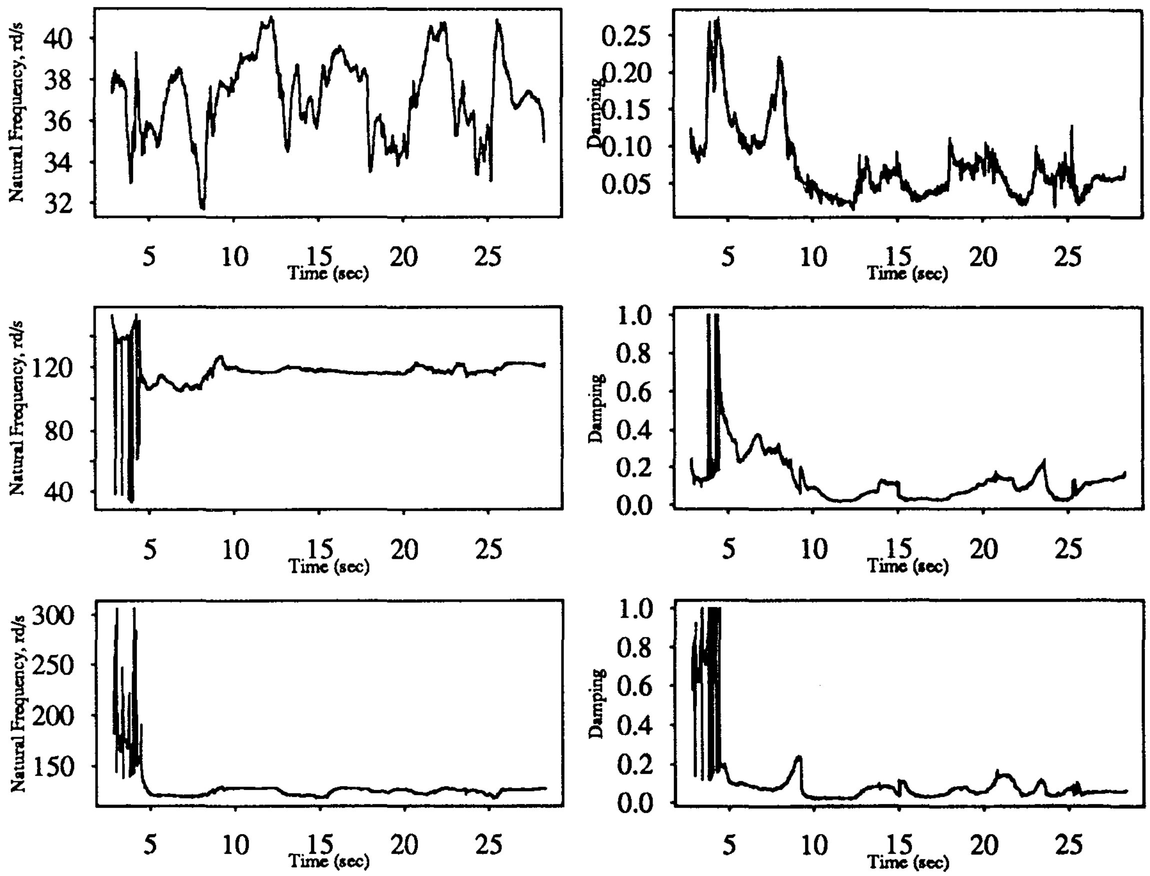


Figure 5.237

Recursive Least Squares Estimation
Three Story Building Model; El-Centro Input
2nd Floor alpha=0.99

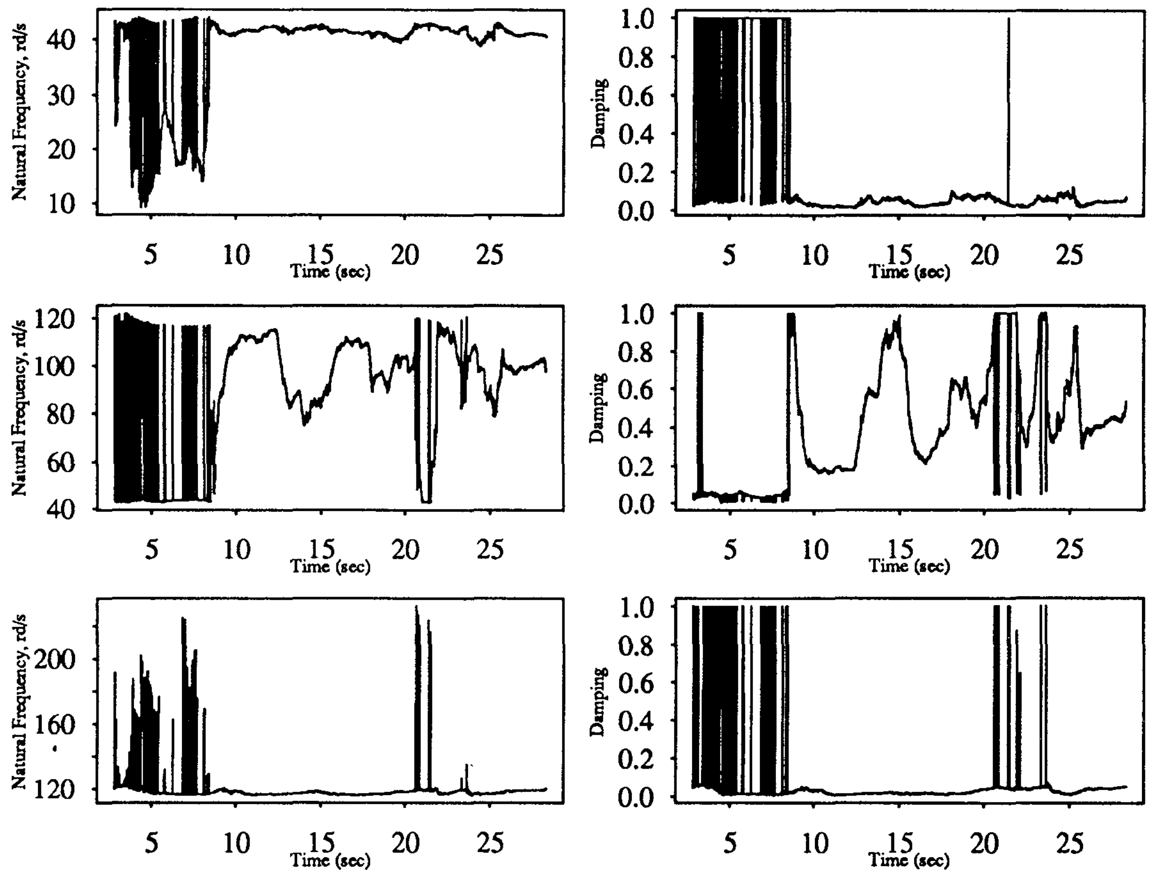


Figure 5.238

Recursive Least Squares Estimation
Three Story Building Model; El-Centro Input
3rd Floor alpha=0.99

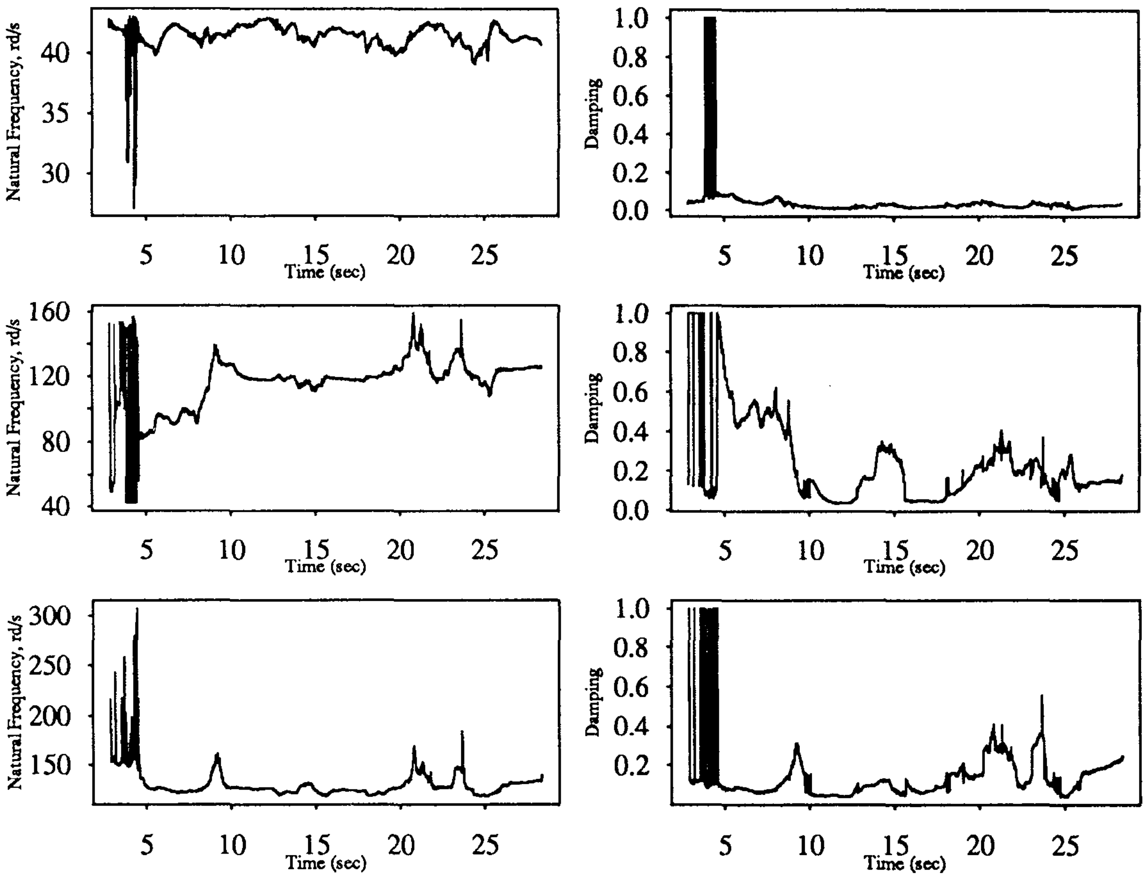


Figure 5.239

Recursive Least Squares Estimation
Three Story Building Model; Sine Sweep Input
1st Floor alpha=0.99

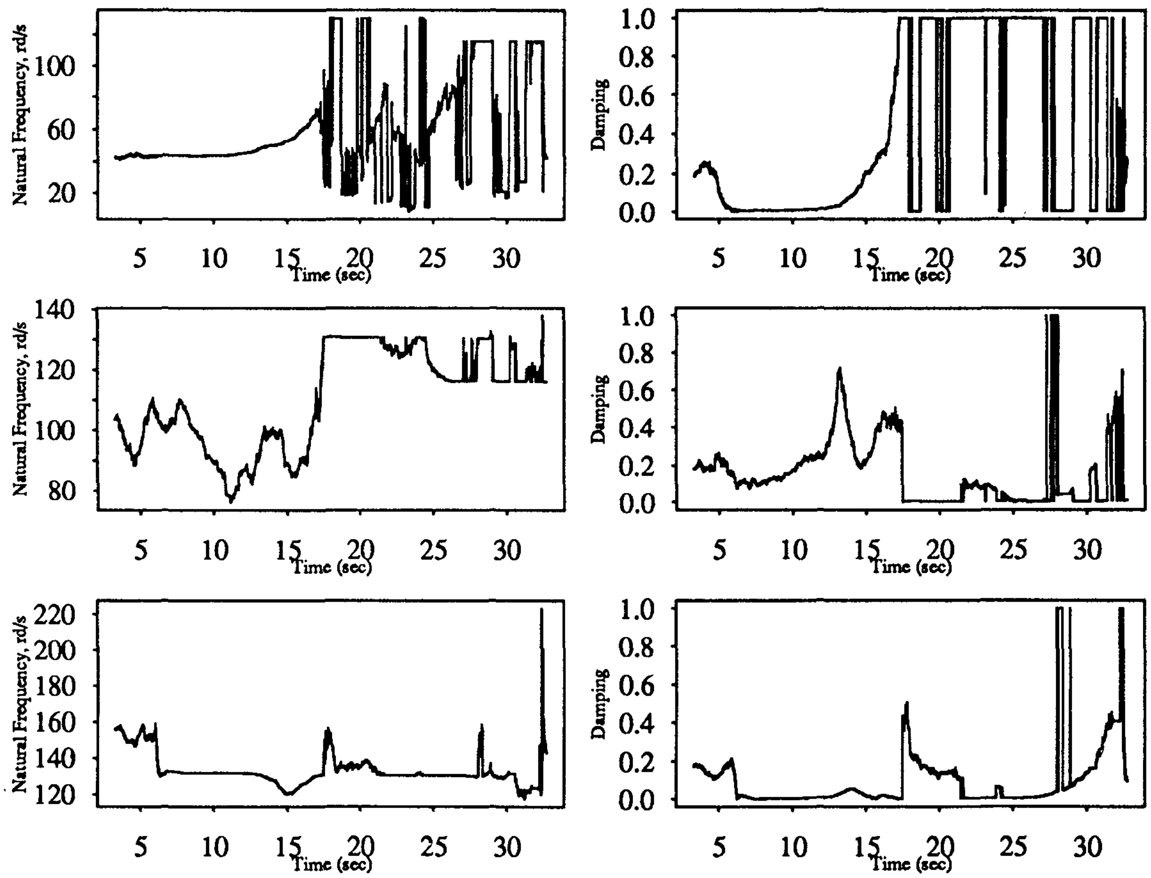


Figure 5.240

Recursive Least Squares Estimation
Three Story Building Model; Sine Sweep Input
2nd Floor alpha=0.99

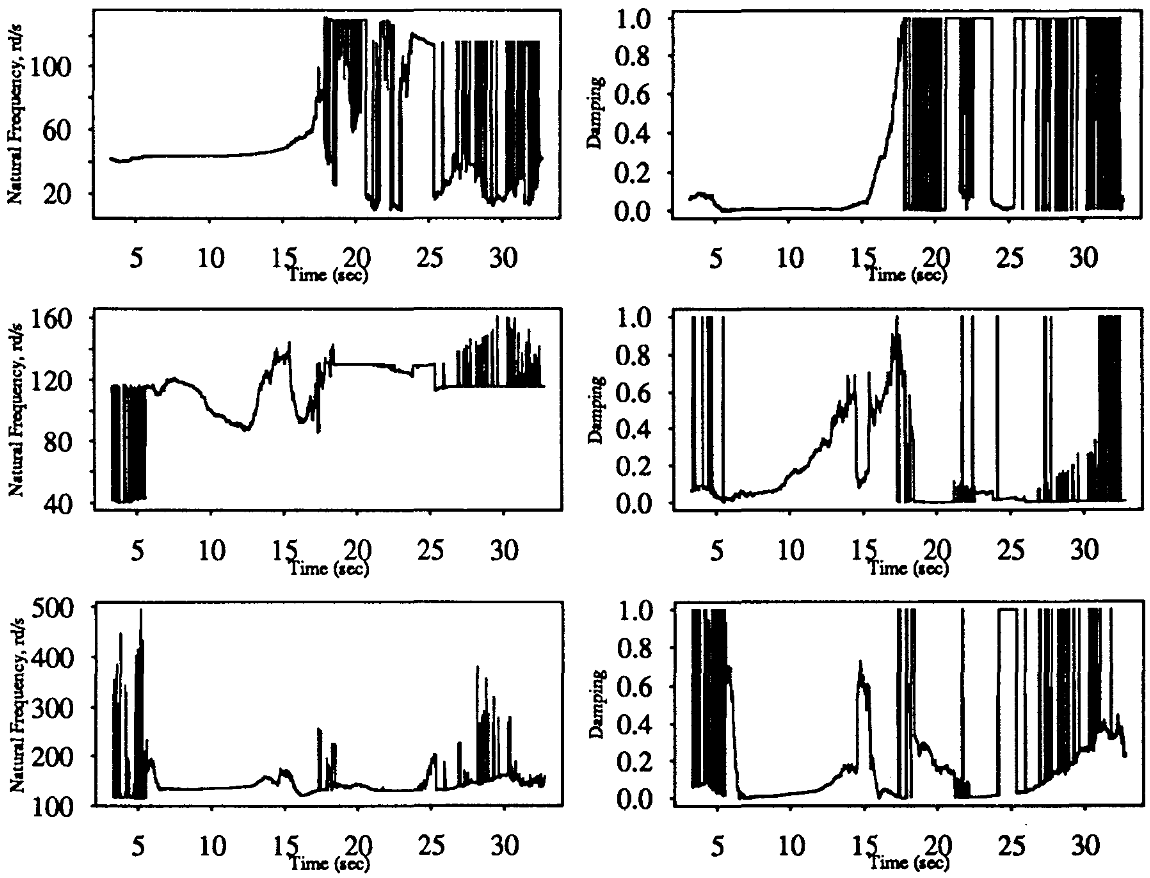


**Figure 5.241**

Recursive Least Squares Estimation
Three Story Building Model; Sine Sweep Input
3rd Floor alpha=0.99

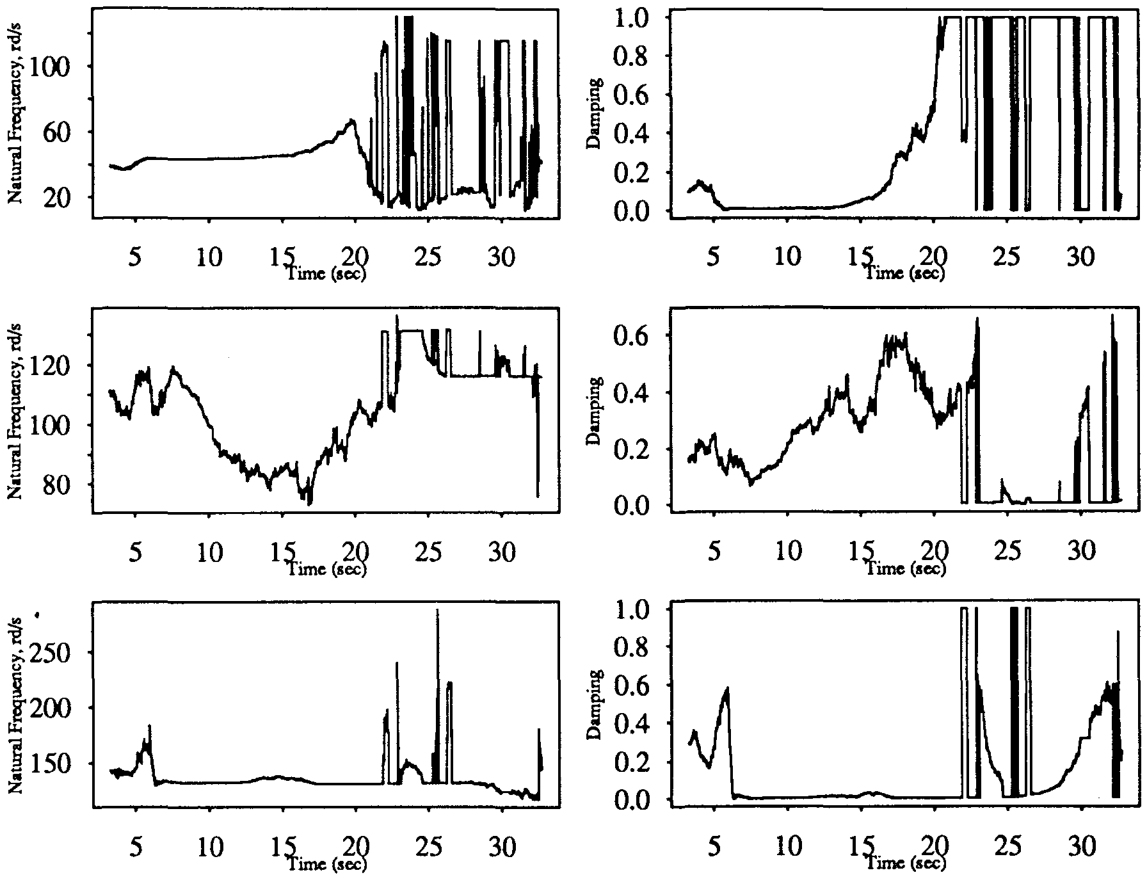


Figure 5.242

Recursive Least Squares Estimation
Three Story Building Model; White Noise Input
1st Floor alpha=0.99

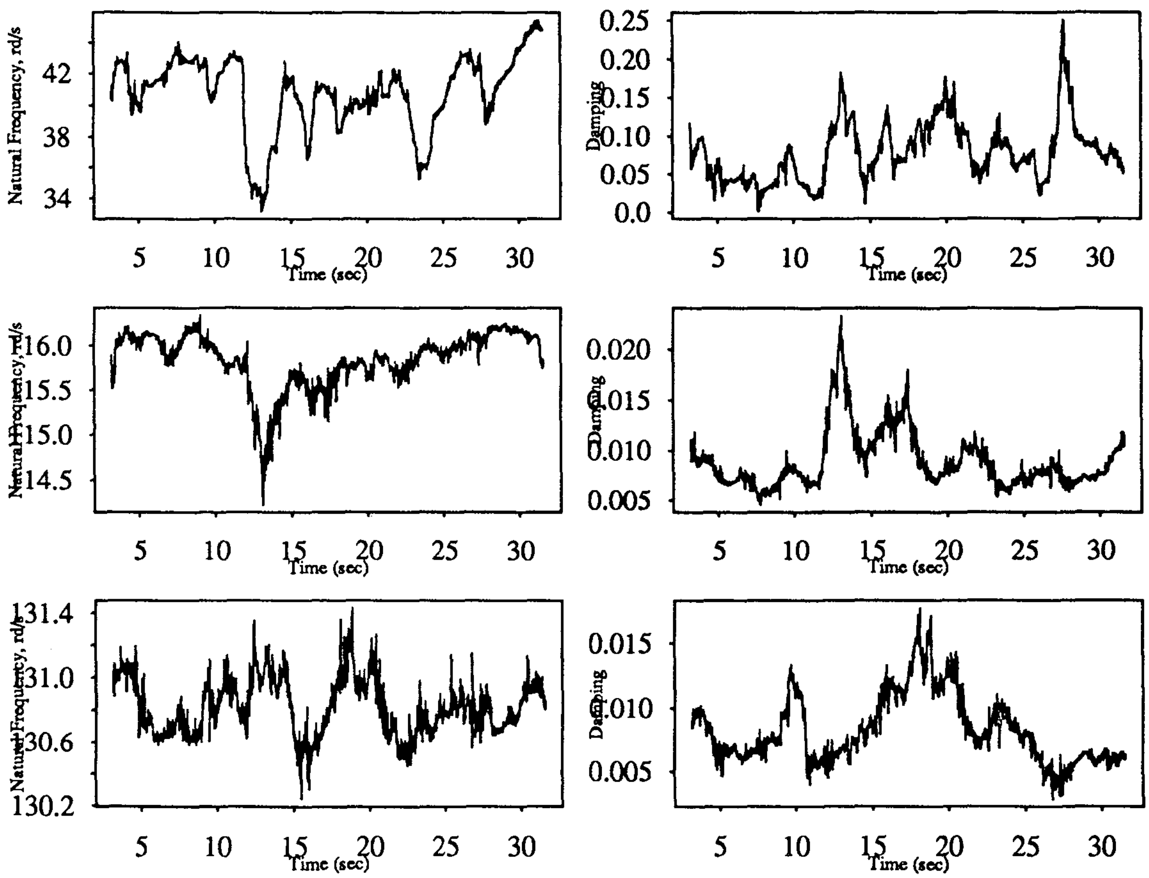


**Figure 5.243**

Recursive Least Squares Estimation

Three Story Building Model; White Noise Input

2nd Floor alpha=0.99

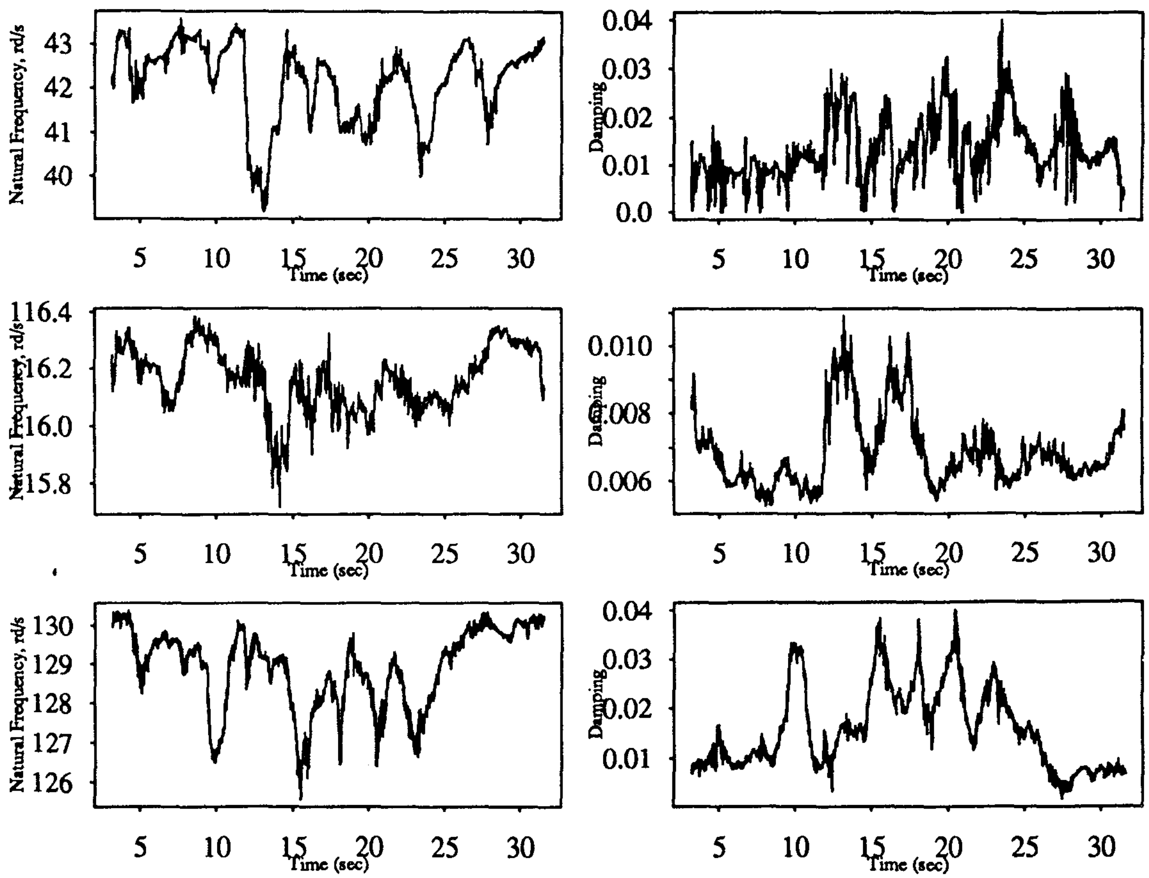


Figure 5.244

Recursive Least Squares Estimation
Three Story Building Model; White Noise Input
3rd Floor alpha=0.99

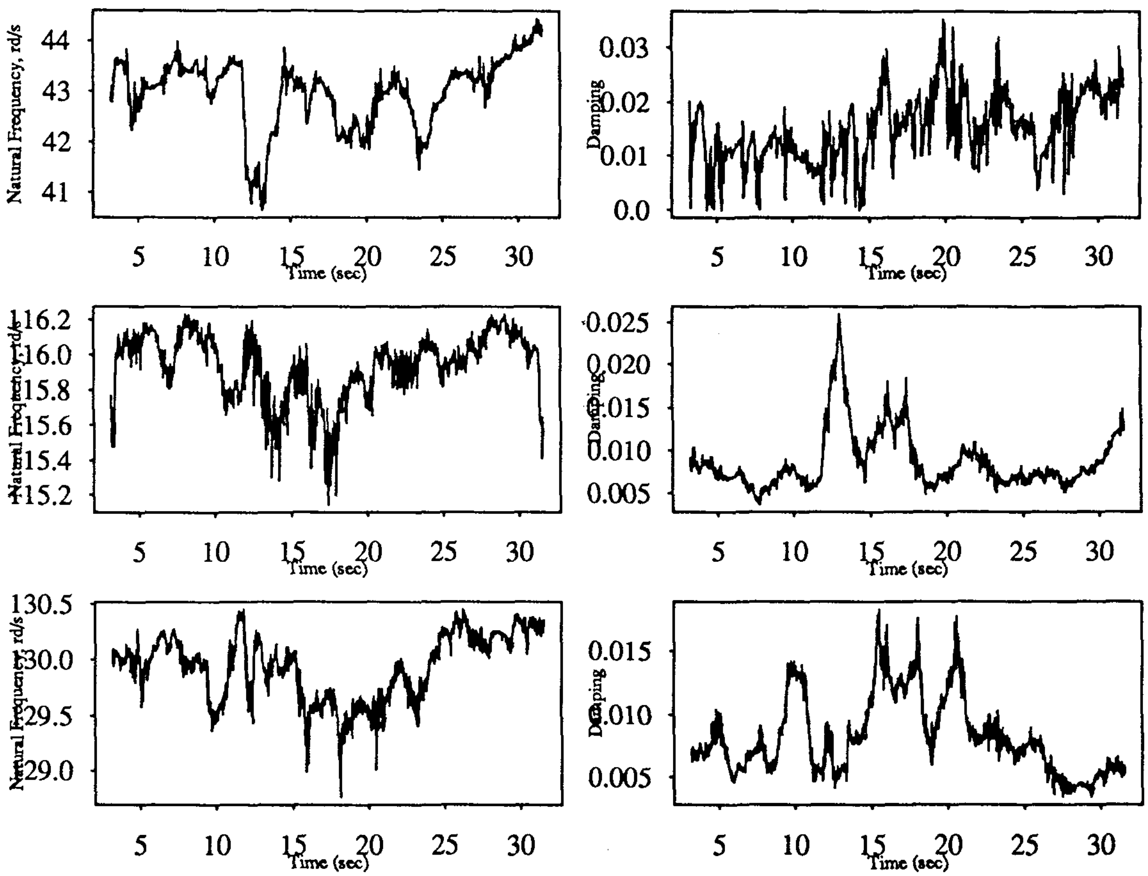


Figure 5.245

Recursive Least Squares Estimation

Five Story Building Model; El-Centro Input

1st Floor variable alpha=0.99

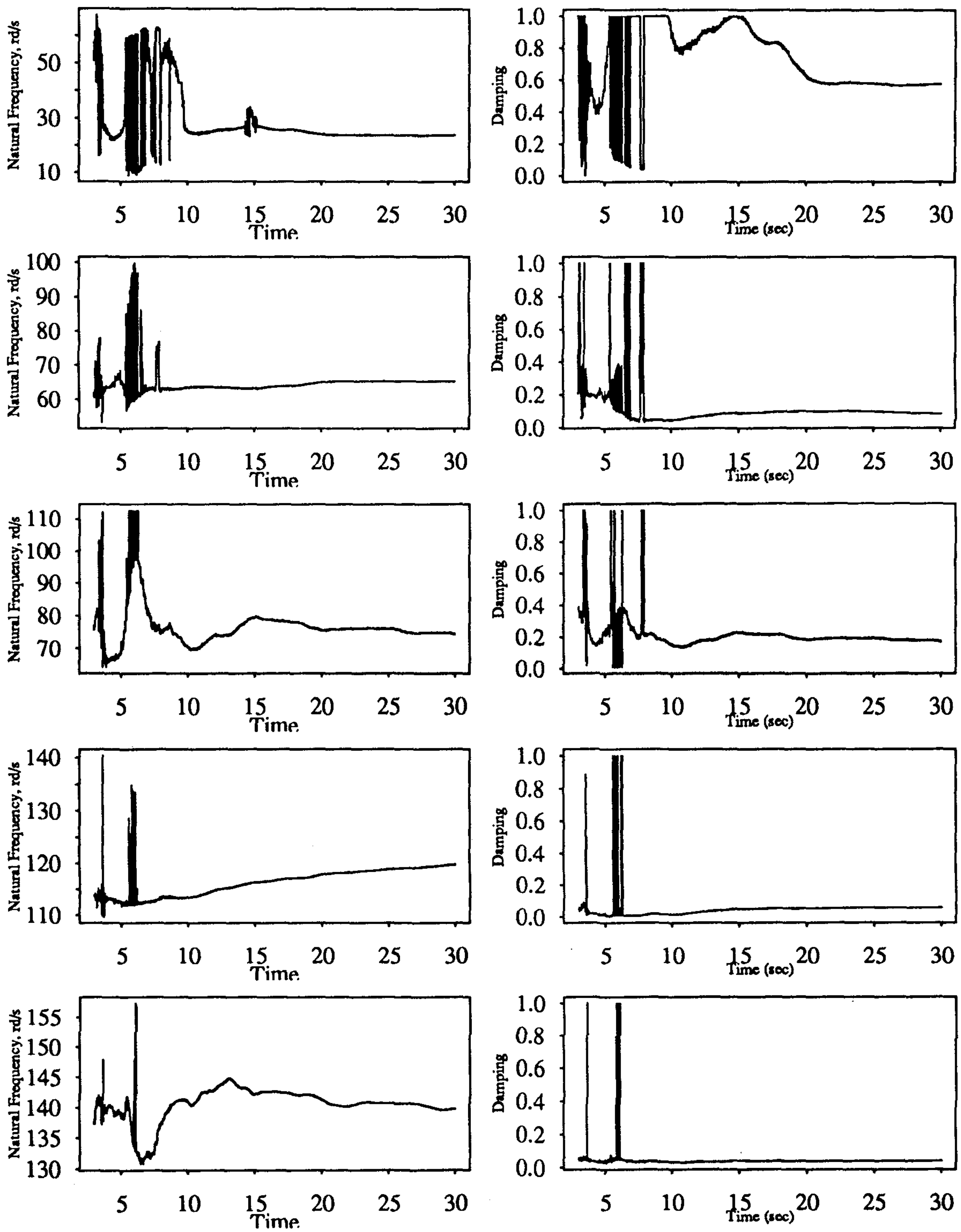


Figure 5.246

## Recursive Least Squares Estimation
### Five Story Building Model; El-Centro Input
2nd Floor variable alpha=0.99

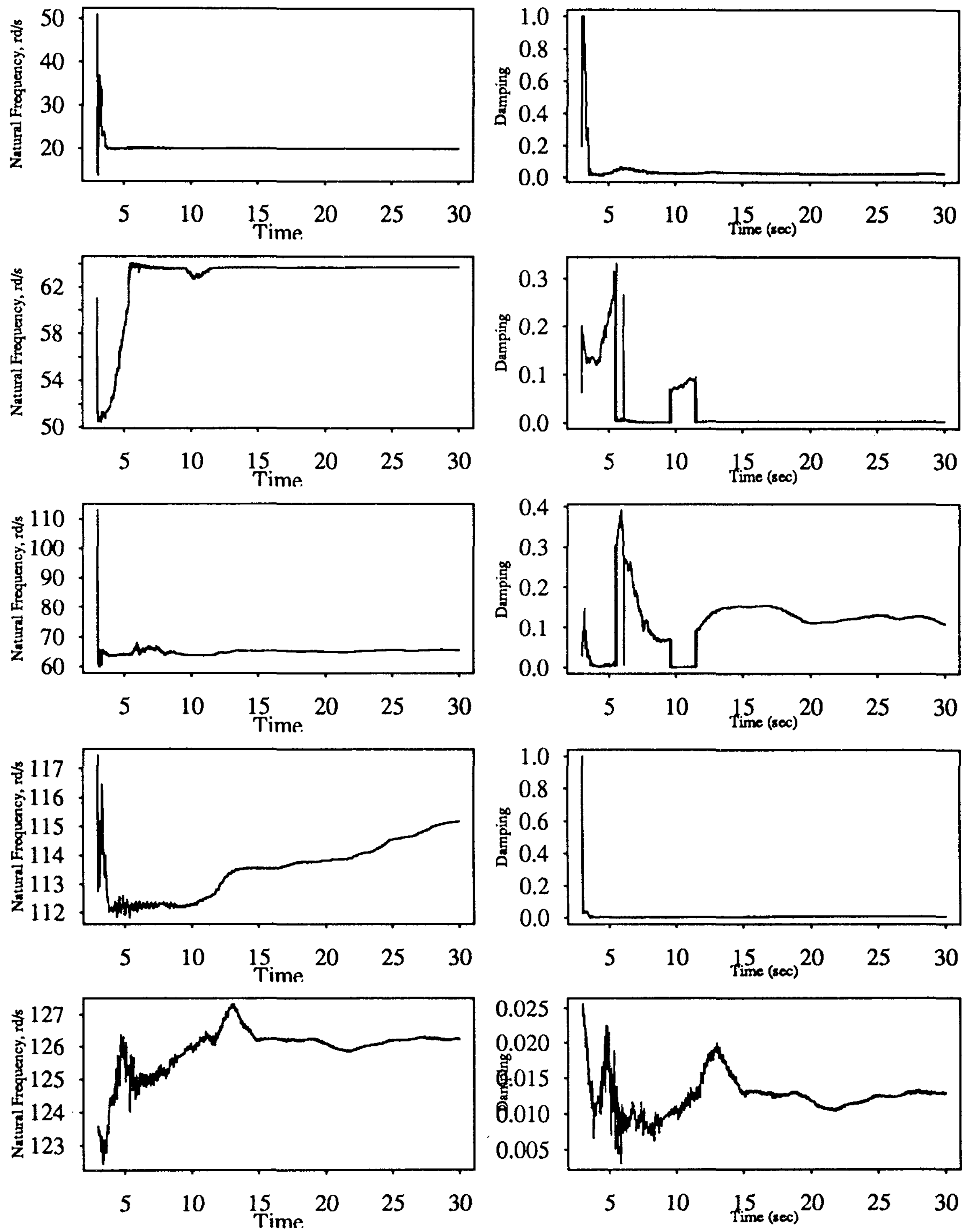


Figure 5.247

## Recursive Least Squares Estimation
## Five Story Building Model; El-Centro Input

3rd Floor variable alpha=0.99

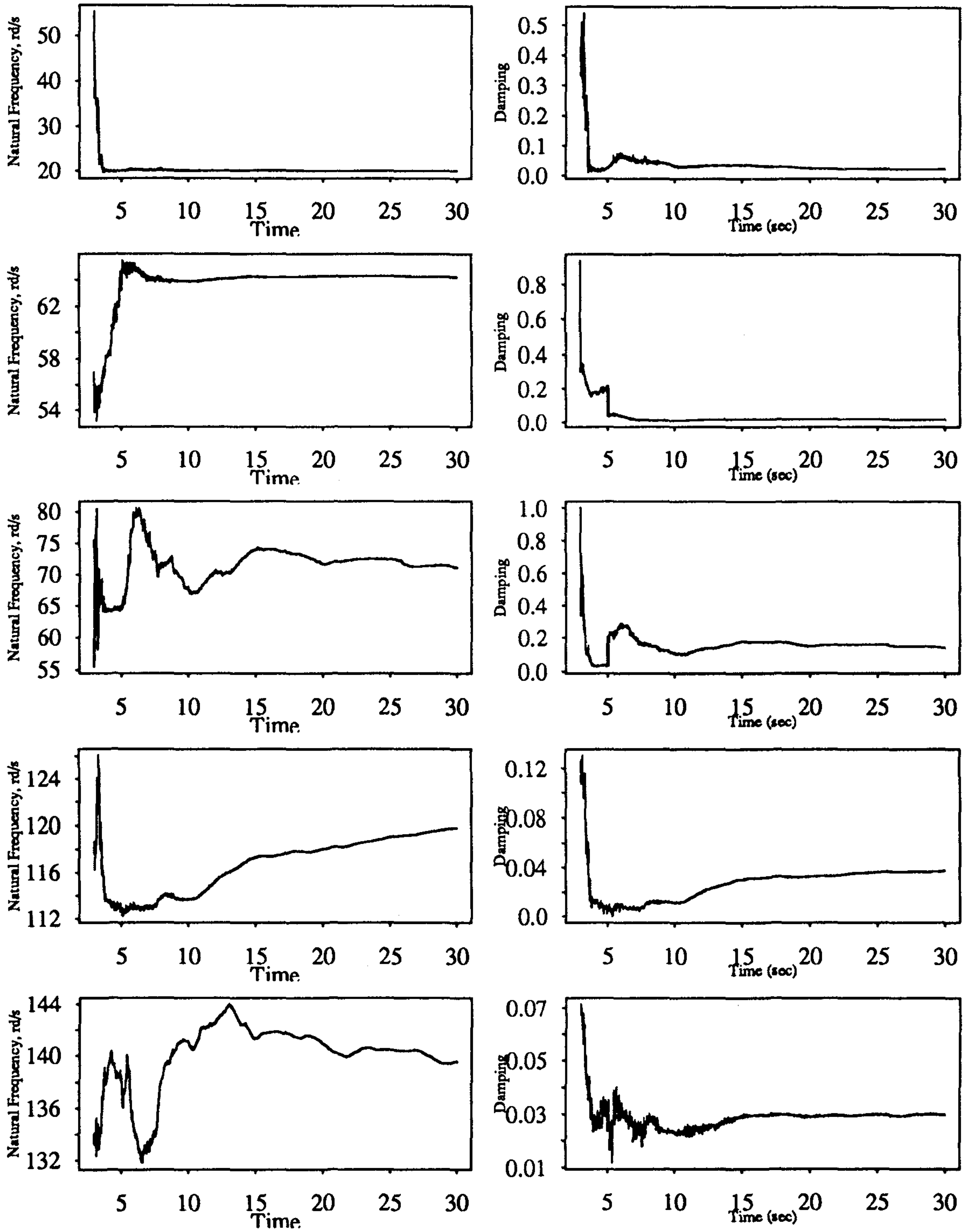


Figure 5.248

# Recursive Least Squares Estimation
## Five Story Building Model; El-Centro Input
4th Floor variable alpha=0.99

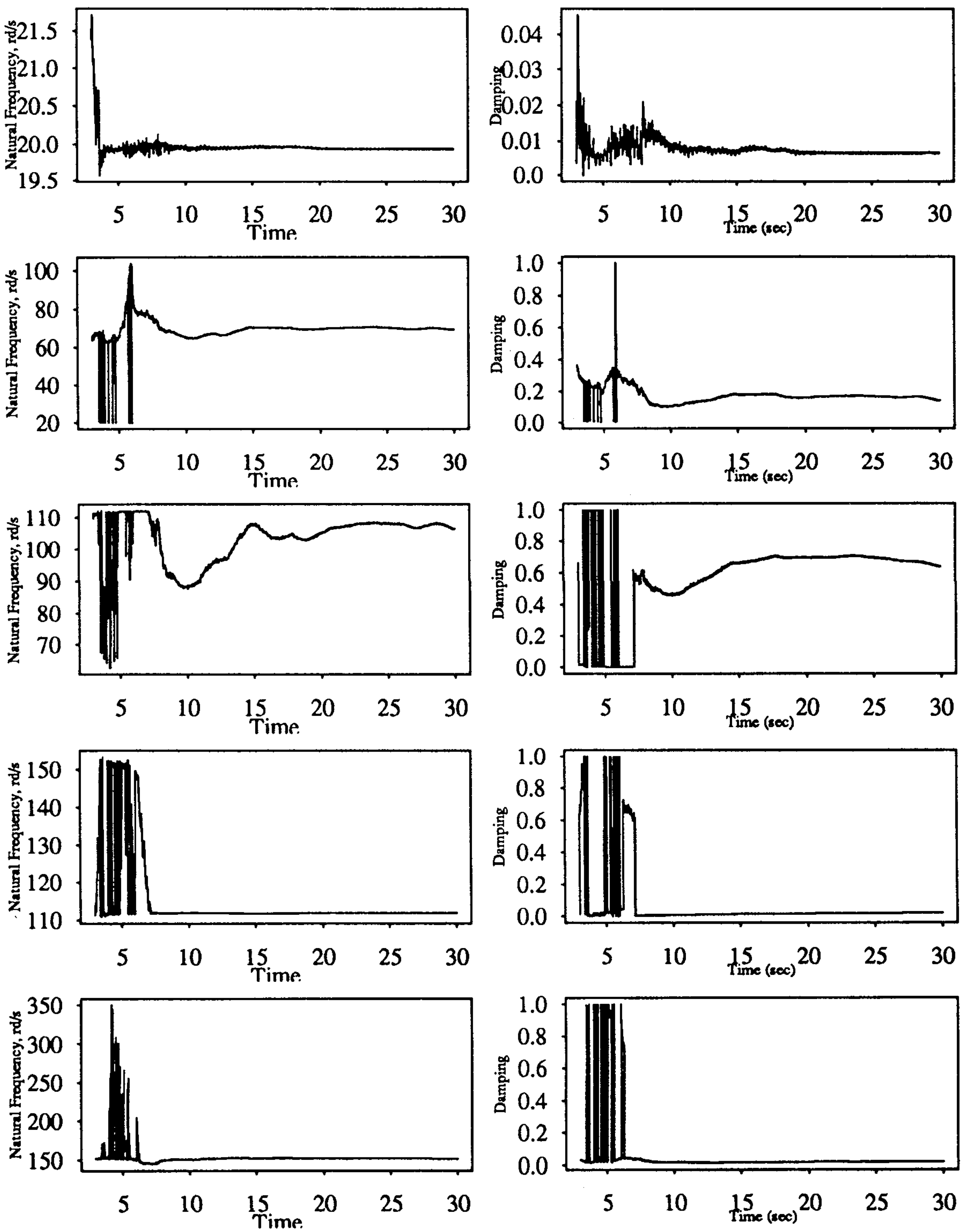


Figure 5.249

Recursive Least Squares Estimation
Five Story Building Model; El-Centro Input
5th Floor variable alpha=0.99

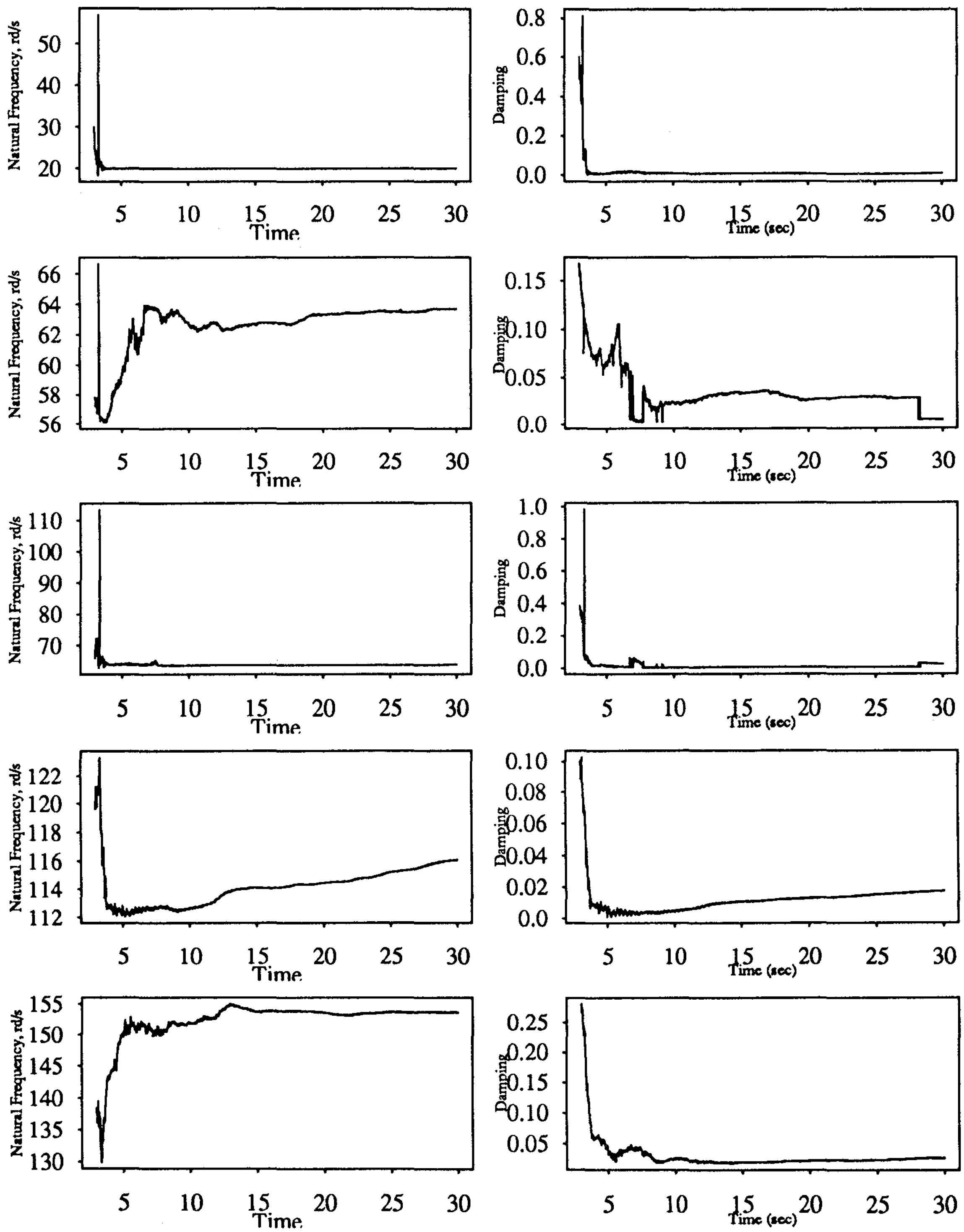


Figure 5.250

## Recursive Least Squares Estimation
## Five Story Building Model; White Noise Input

1st Floor variable alpha=0.99

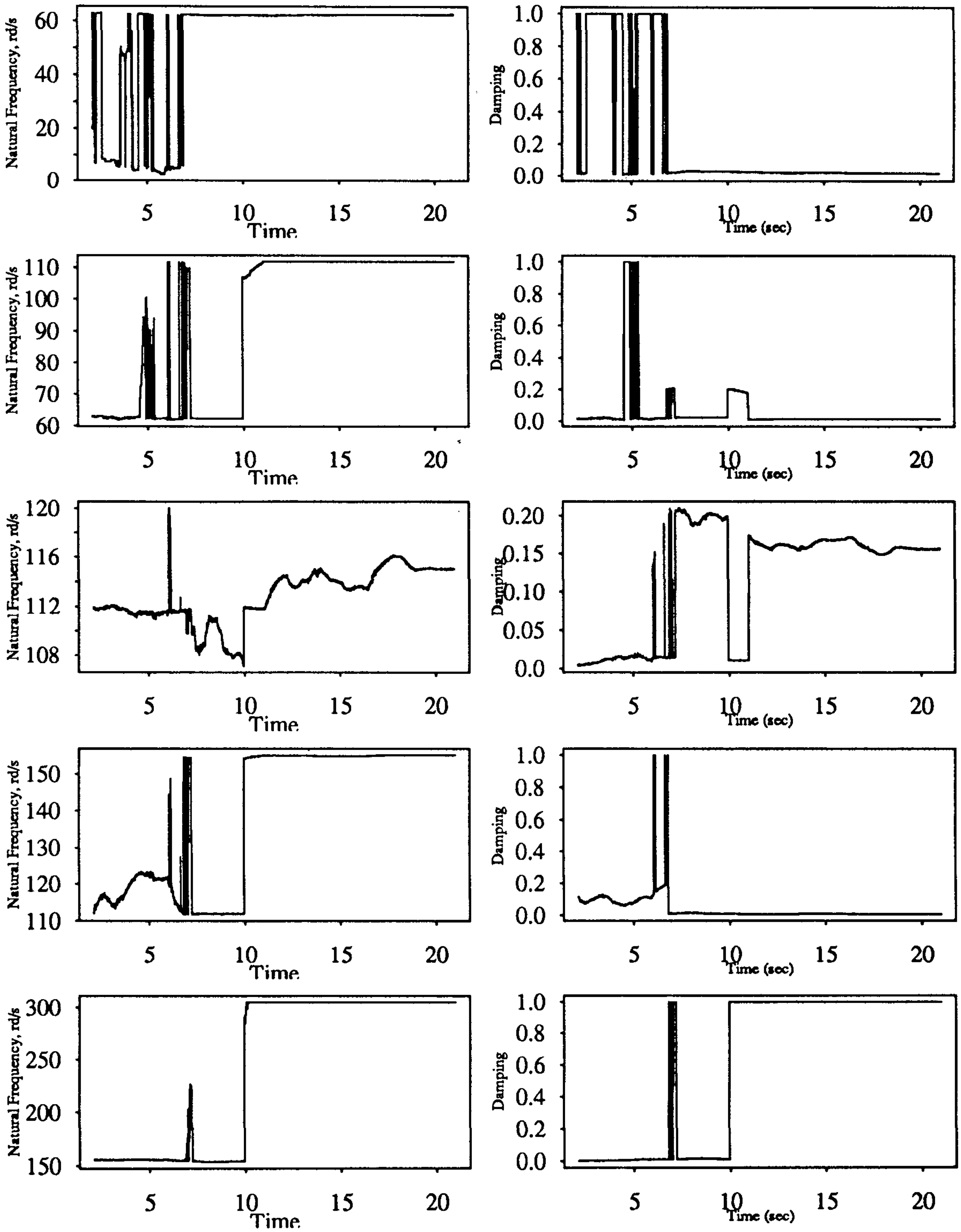


Figure 5.251

# Recursive Least Squares Estimation
## Five Story Building Model; White Noise Input
2nd Floor variable alpha=0.99

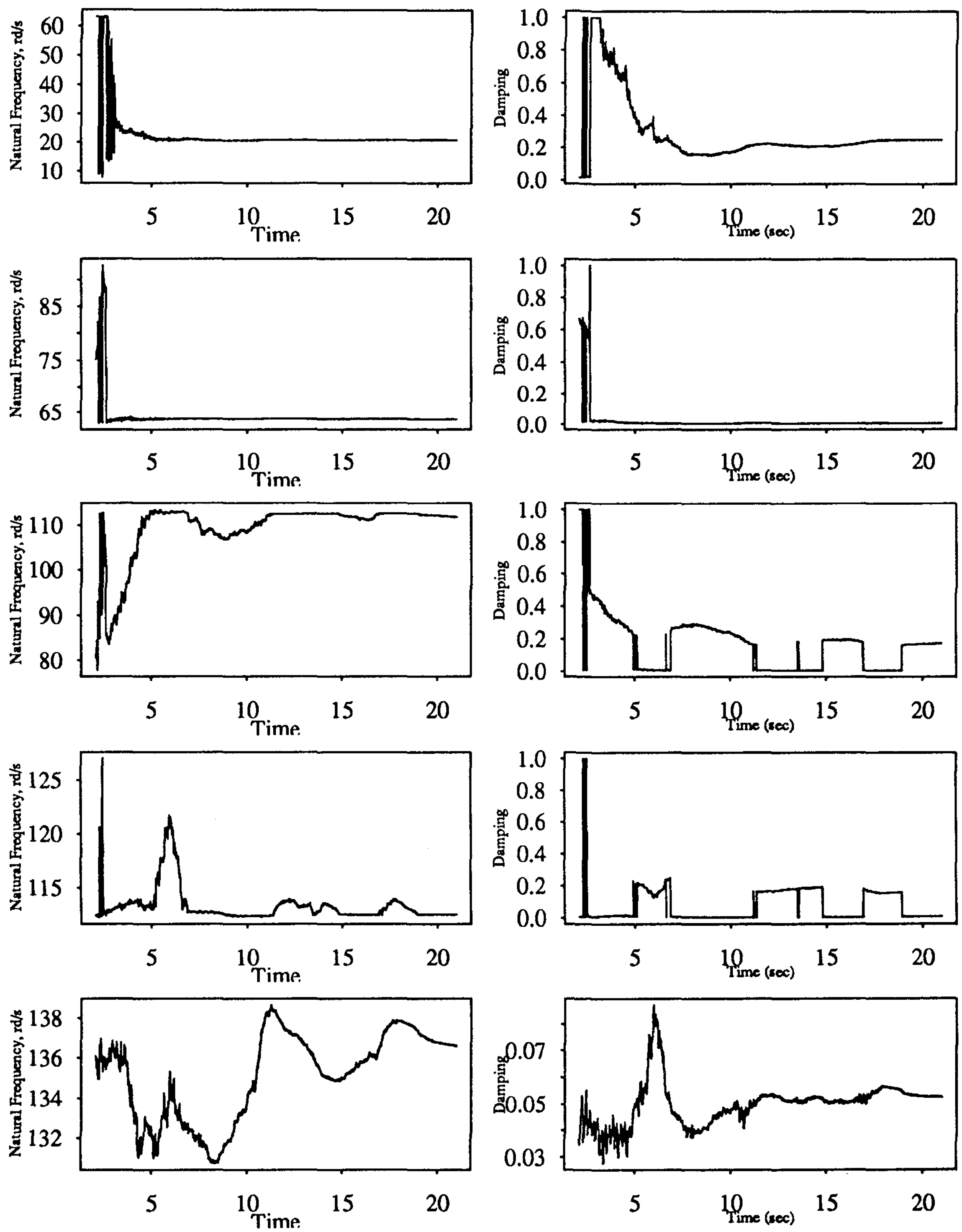


Figure 5.252

Recursive Least Squares Estimation
Five Story Building Model; White Noise Input
3rd Floor variable alpha=0.99

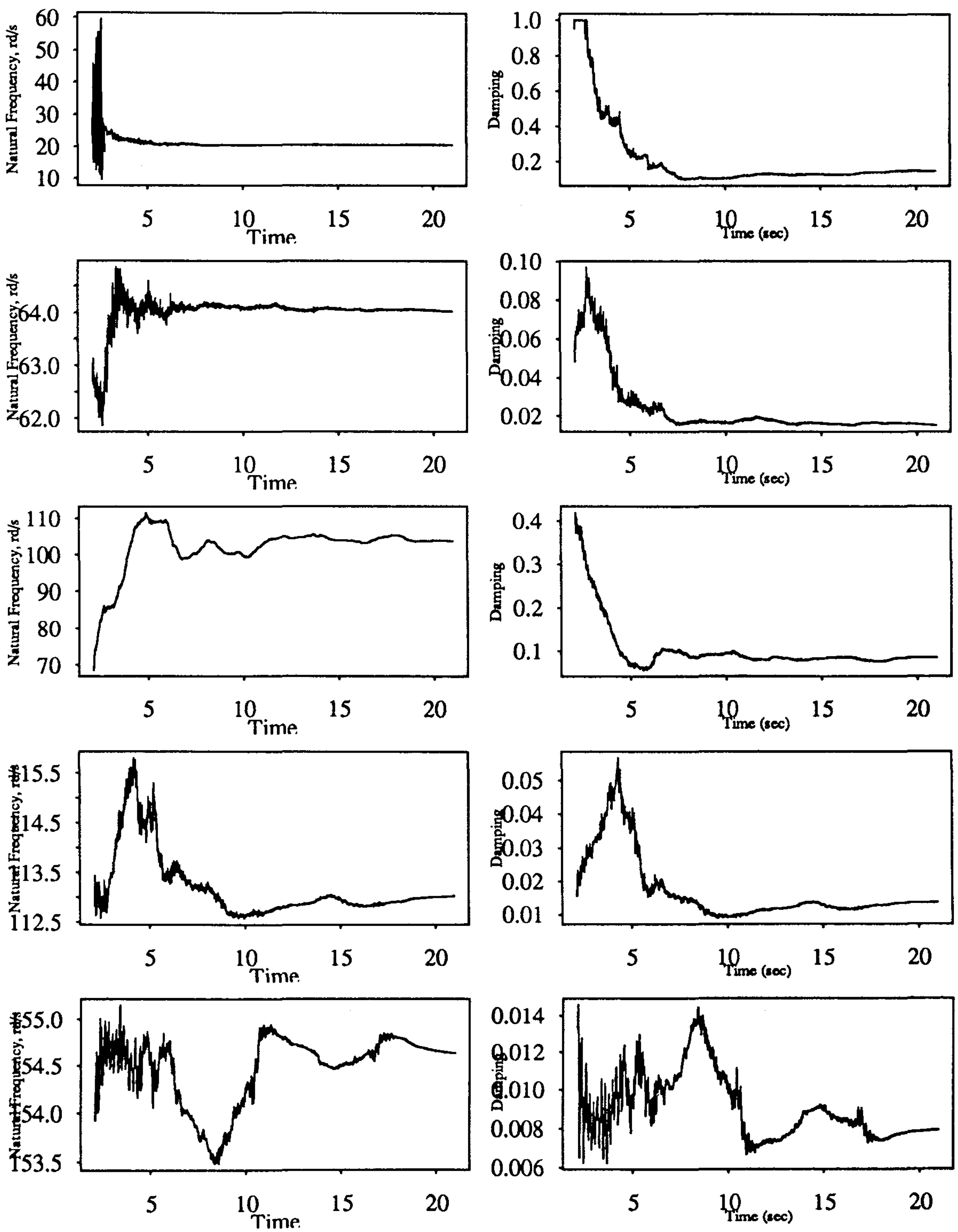


Figure 5.253

Recursive Least Squares Estimation
Five Story Building Model; White Noise Input
4th Floor variable alpha=0.99

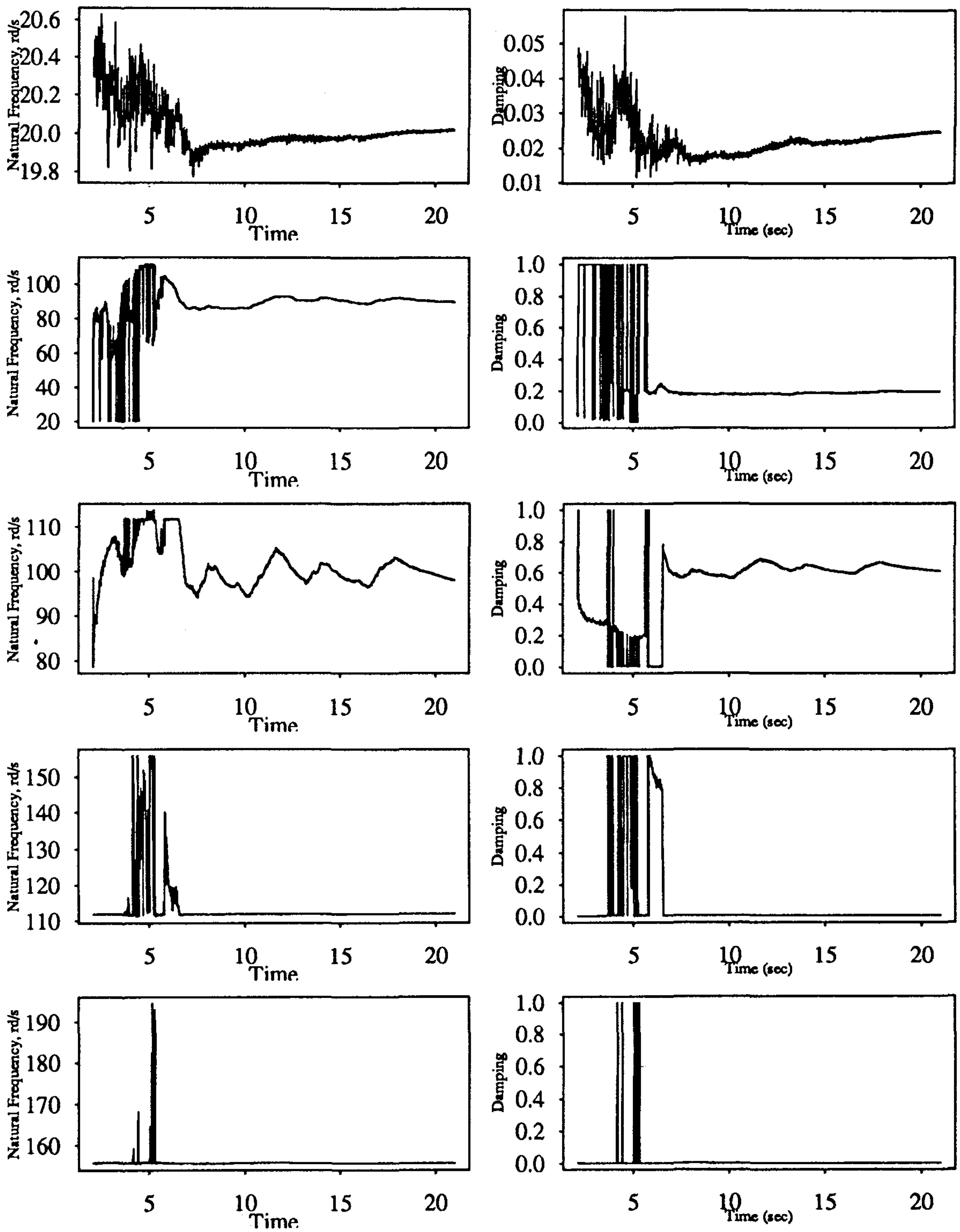


Figure 5.254

Recursive Least Squares Estimation
Five Story Building Model; White Noise Input
5th Floor variable alpha=0.99

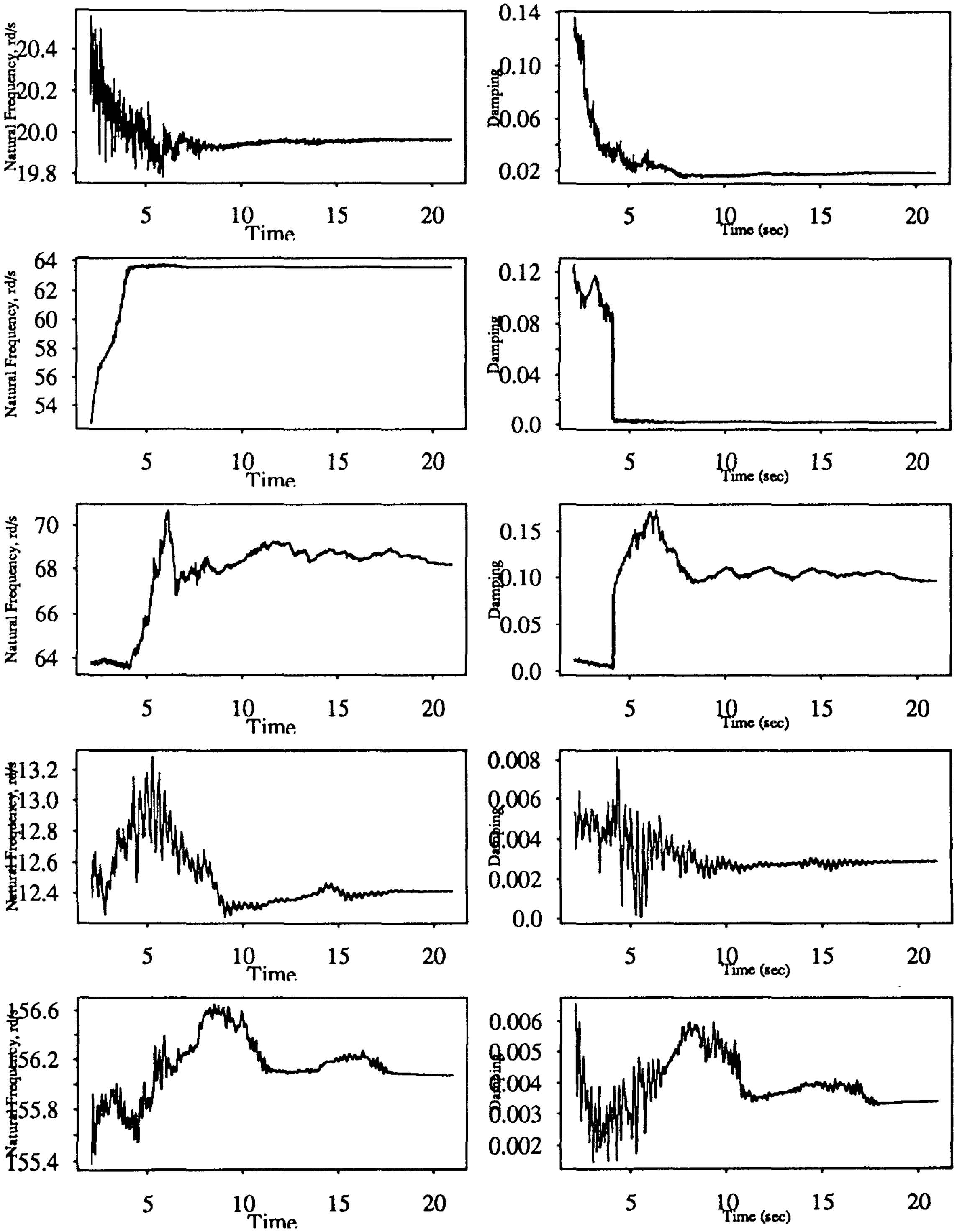


Figure 5.255

Recursive Least Squares Estimation
Three Story Building Model; El-Centro Input
1st Floor variable alpha=0.99

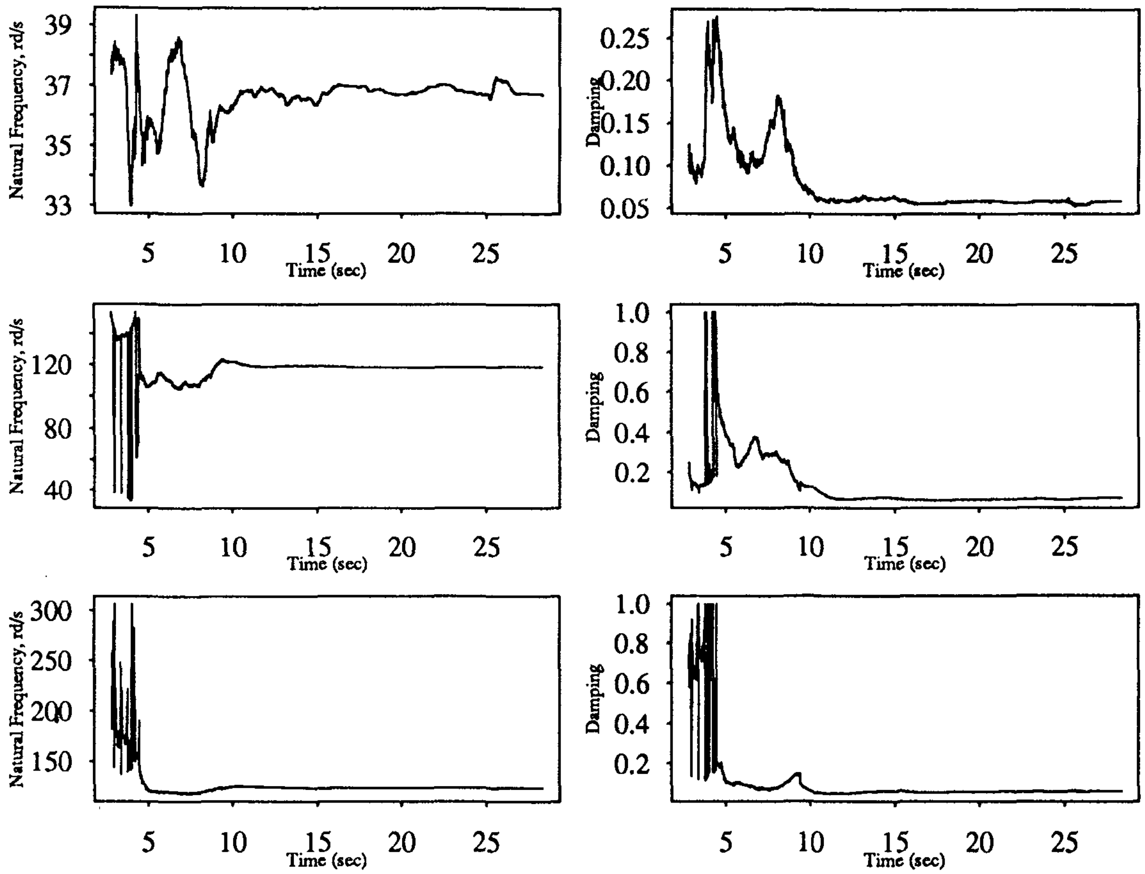


Figure 5.256

Recursive Least Squares Estimation
Three Story Building Model; El-Centro Input
2nd Floor variable alpha=0.99

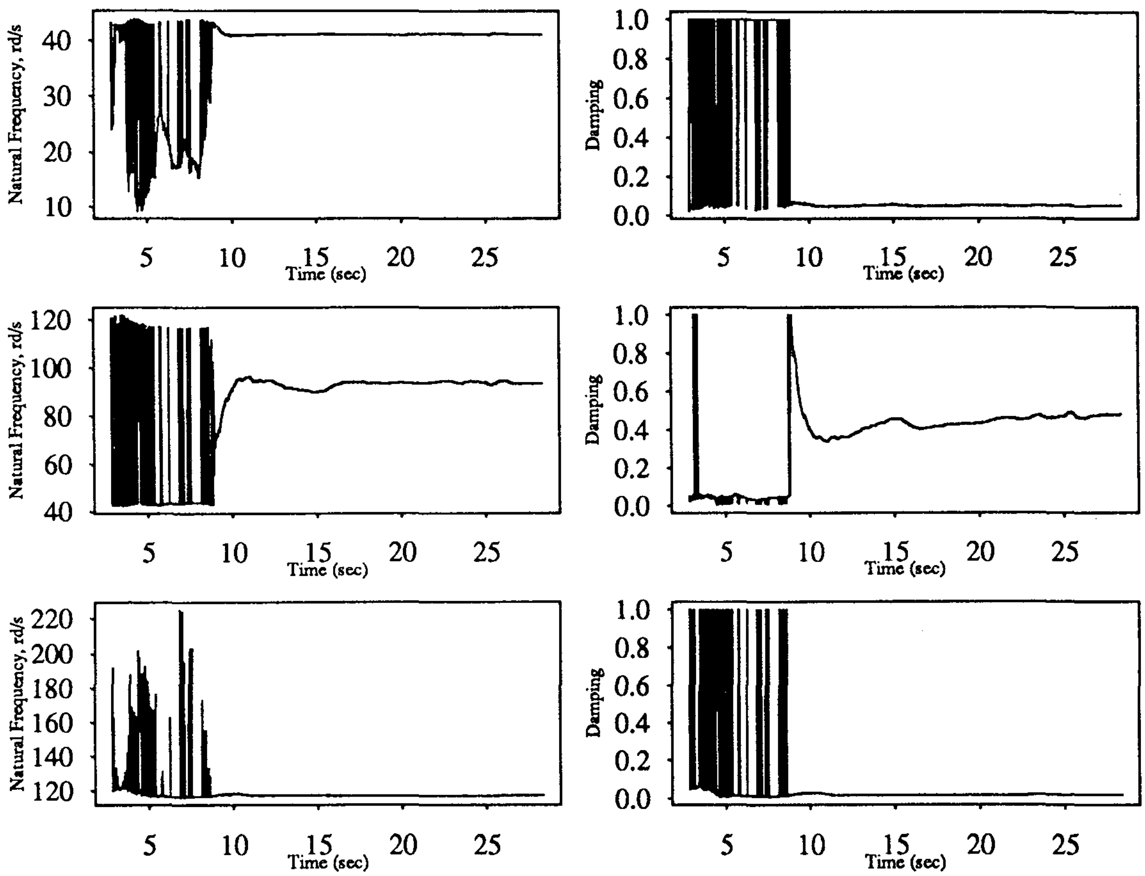


Figure 5.257

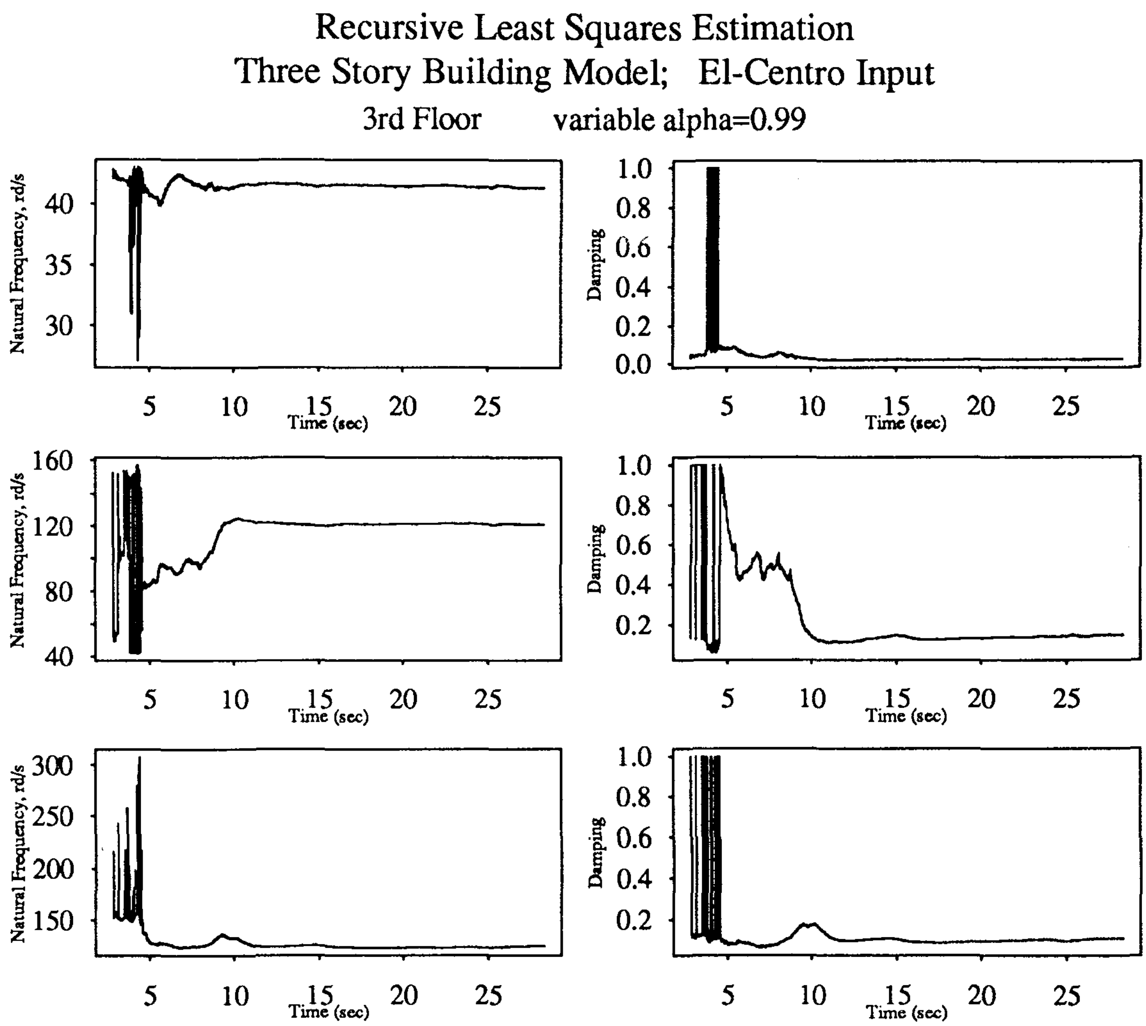
Recursive Least Squares Estimation
Three Story Building Model; El-Centro Input
3rd Floor variable alpha=0.99
Natural Frequency, rd/s
Damping
Time (sec)
5 10 15 20 25
40 35 30
160 120 80 40
300 250 200 150
1.0 0.8 0.6 0.4 0.2 0.0

Figure 5.258

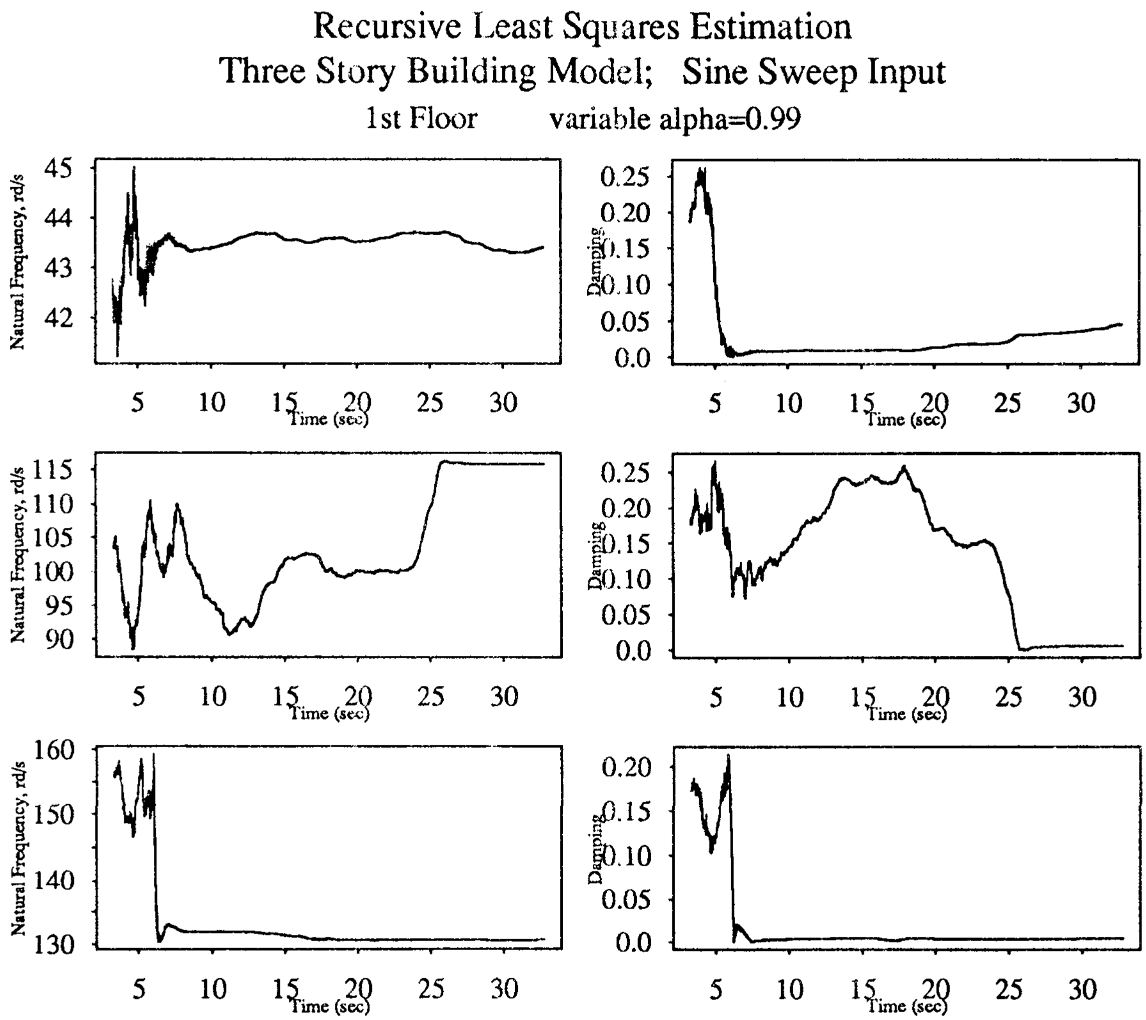

Recursive Least Squares Estimation
Three Story Building Model; Sine Sweep Input
1st Floor variable alpha=0.99
Natural Frequency, rd/s
Damping
Time (sec)
45
44
43
42
0.25
0.20
0.15
0.10
0.05
0.0
115
110
105
100
95
90
160
150
140
130
5
10
15
20
25
30


**Figure 5.259**

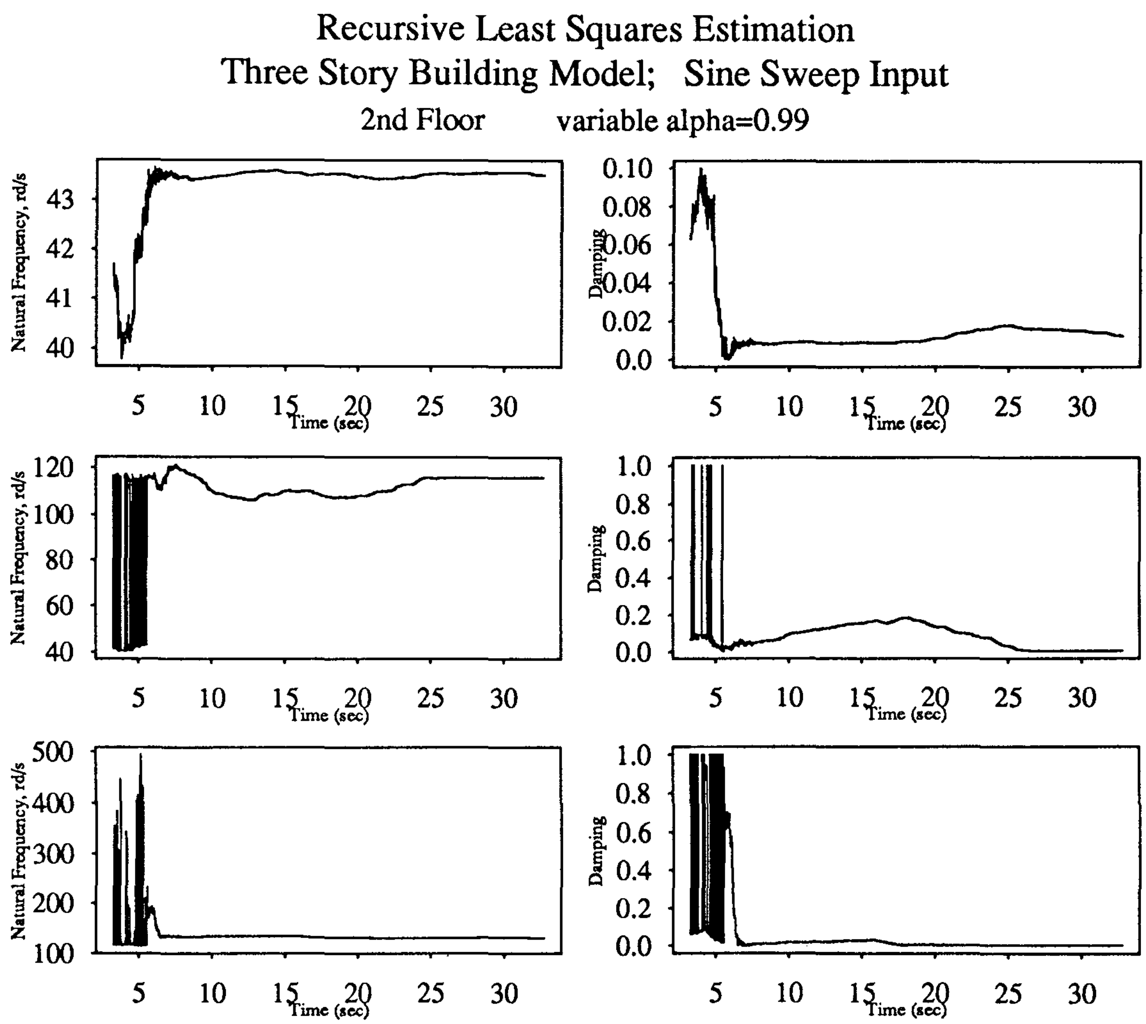
Recursive Least Squares Estimation
Three Story Building Model; Sine Sweep Input
2nd Floor variable alpha=0.99
Natural Frequency, rd/s
Damping
Time (sec)

Figure 5.260

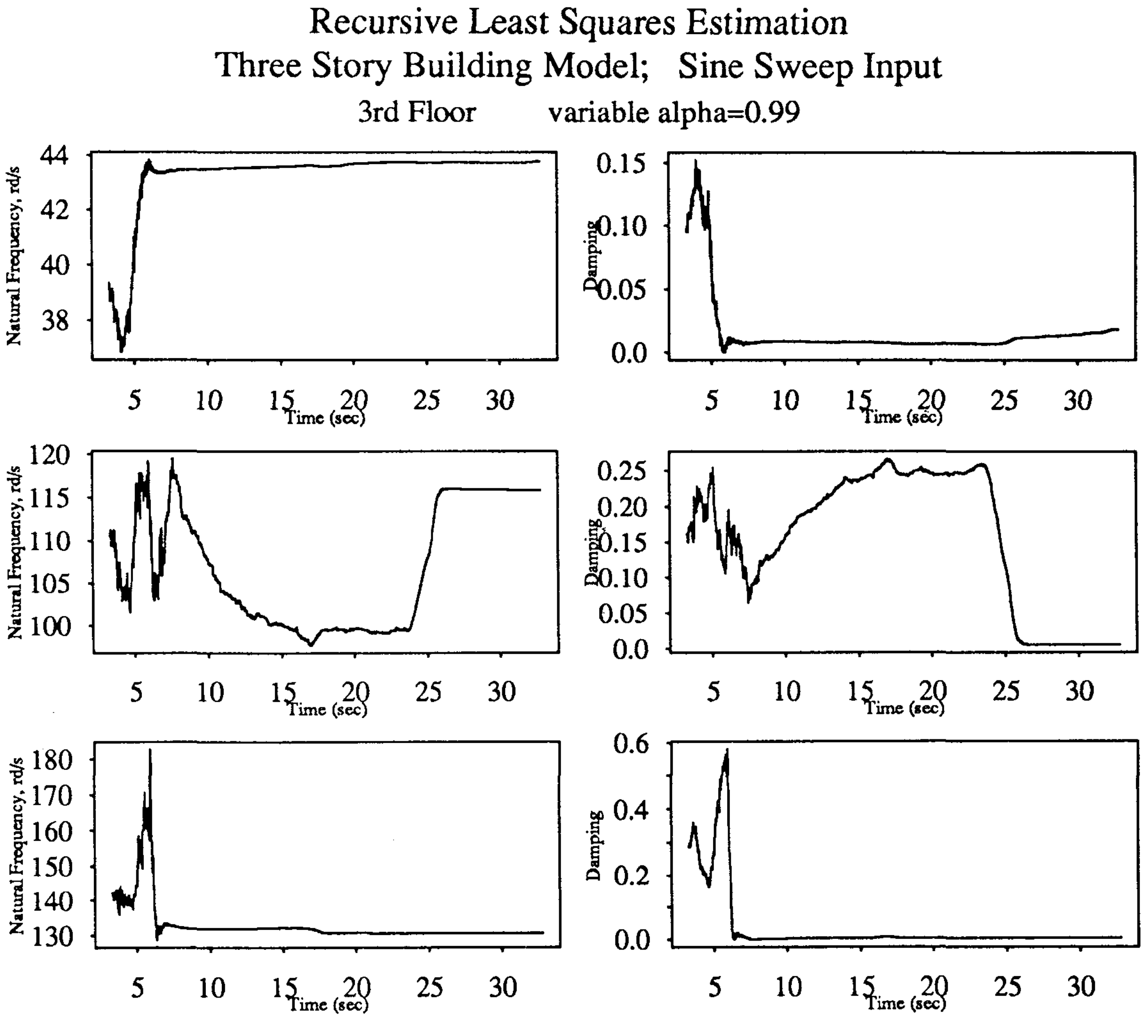
Recursive Least Squares Estimation
Three Story Building Model; Sine Sweep Input
3rd Floor variable alpha=0.99
Natural Frequency, rd/s
Damping
Time (sec)
44
42
40
38
0.15
0.10
0.05
0.0
120
115
110
105
100
0.25
0.20
0.15
0.10
0.05
180
170
160
150
140
130
0.6
0.4
0.2
5
10
15
20
25
30

Figure 5.261

Recursive Least Squares Estimation
Three Story Building Model; White Noise Input
1st Floor variable alpha=0.99

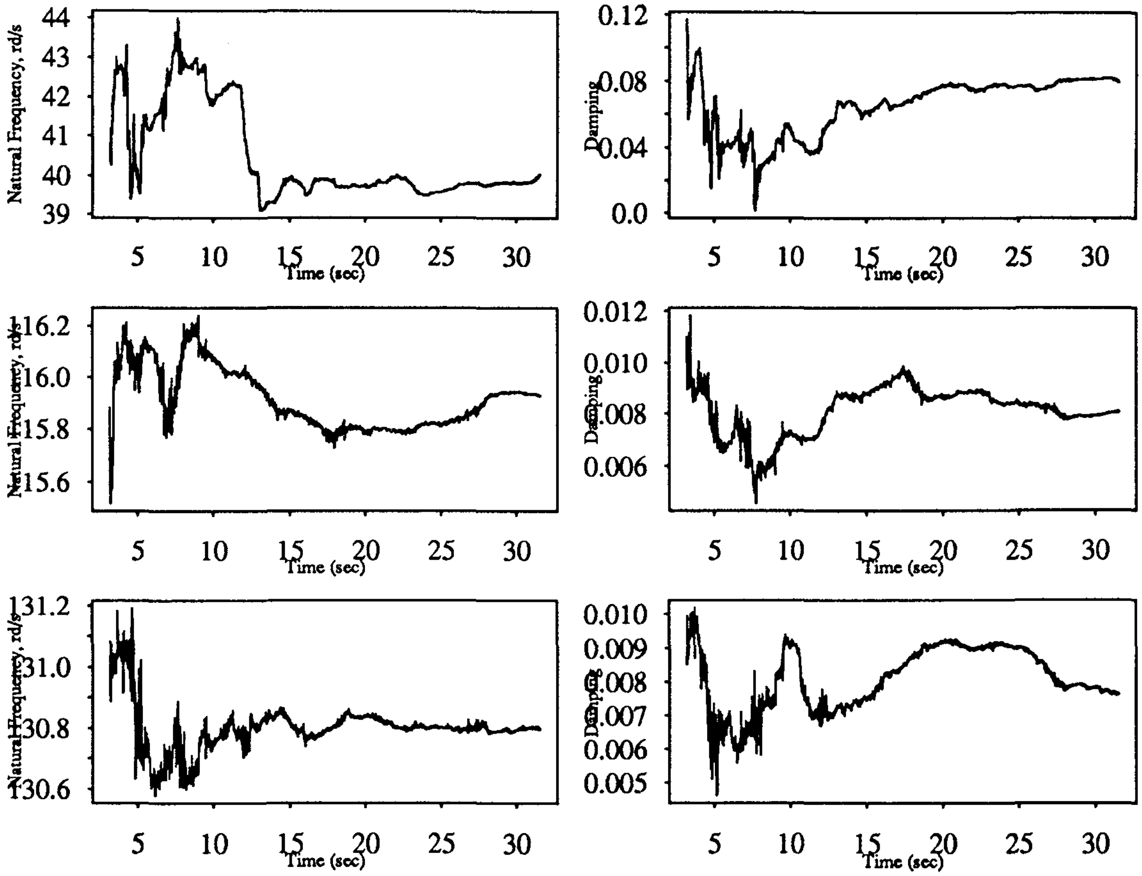


**Figure 5.262**

# Recursive Least Squares Estimation
## Three Story Building Model; White Noise Input
2nd Floor variable alpha=0.99

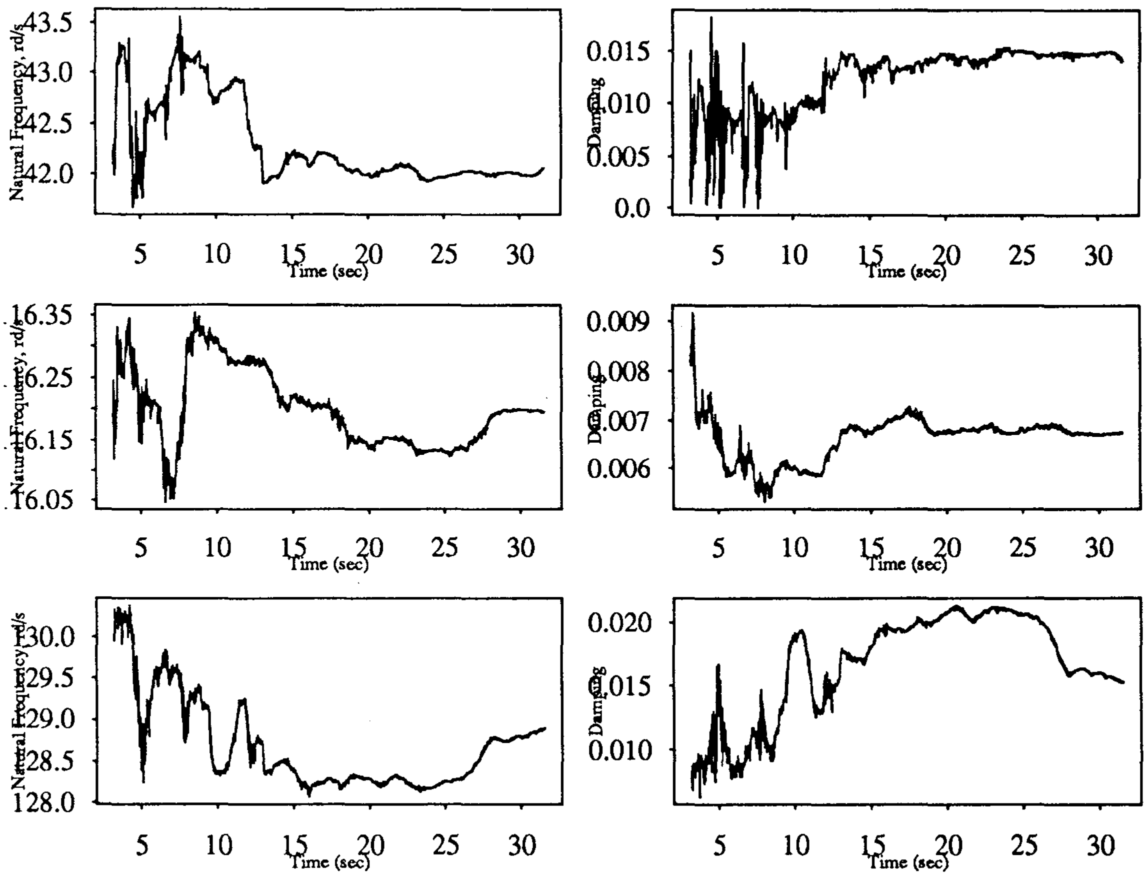


Figure 5.263

Recursive Least Squares Estimation
Three Story Building Model; White Noise Input
3rd Floor variable alpha=0.99

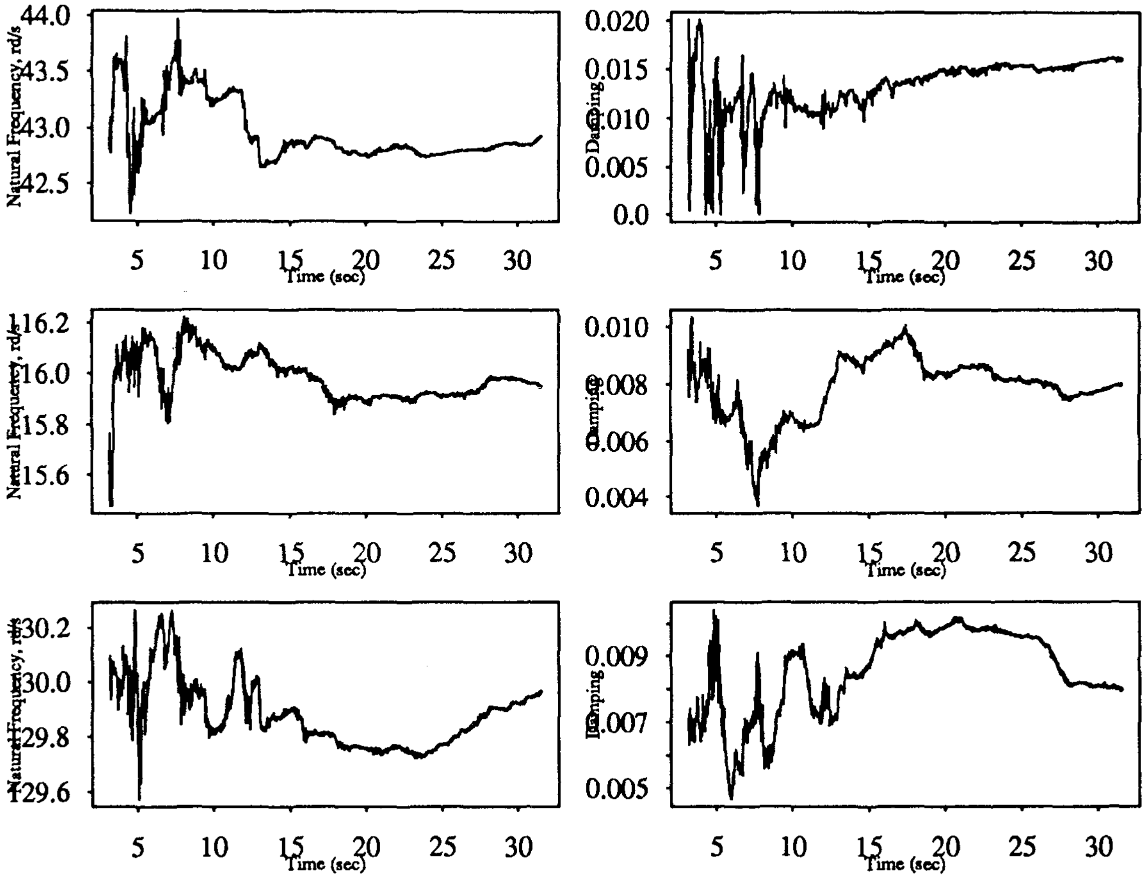


Figure 5.264

Recursive Instrumental Variable Estimation
Five Story Building Model; El-Centro Input
1st Floor

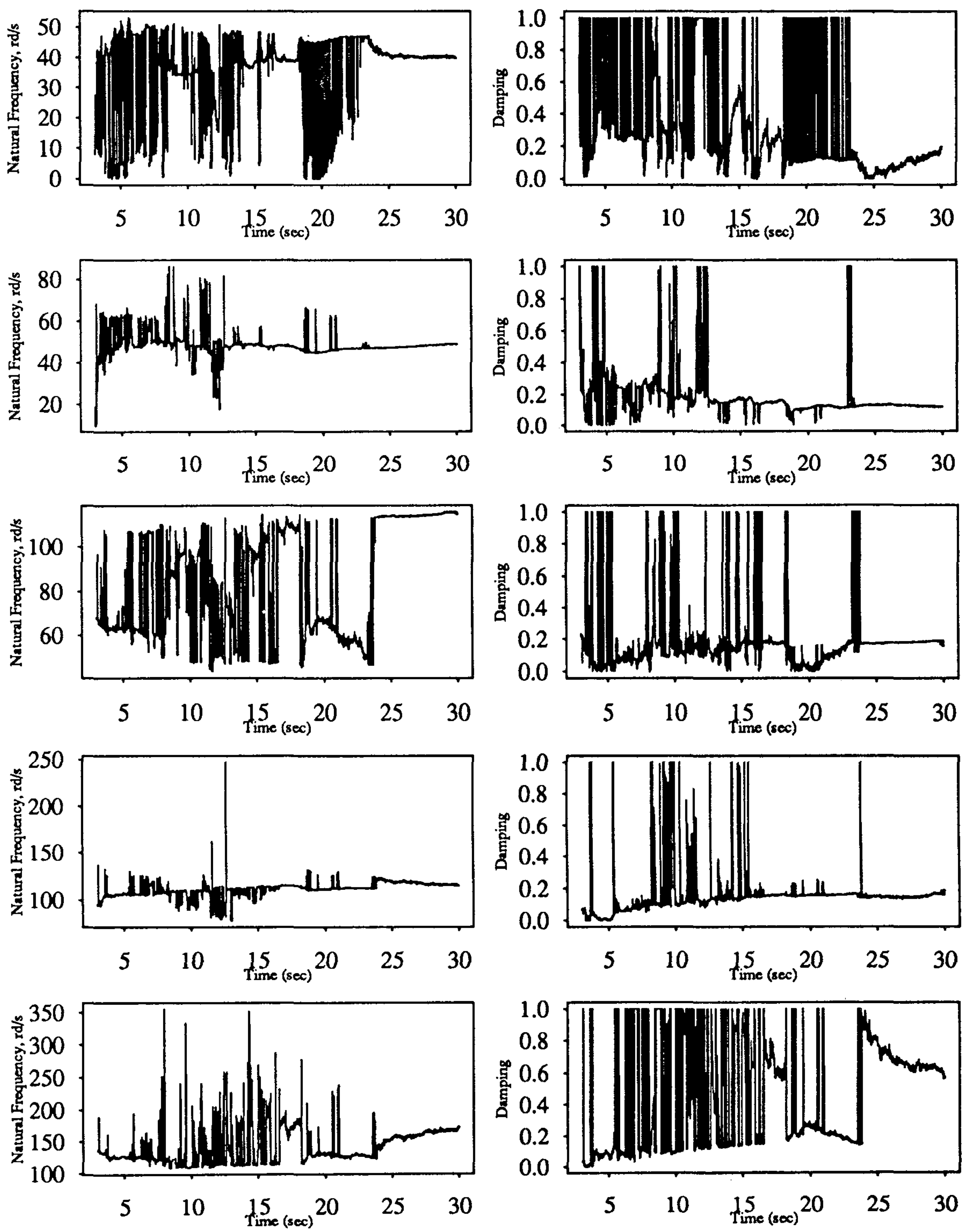


Figure 5.265

# Recursive Instrumental Variable Estimation
# Five Story Building Model; El-Centro Input

2nd Floor

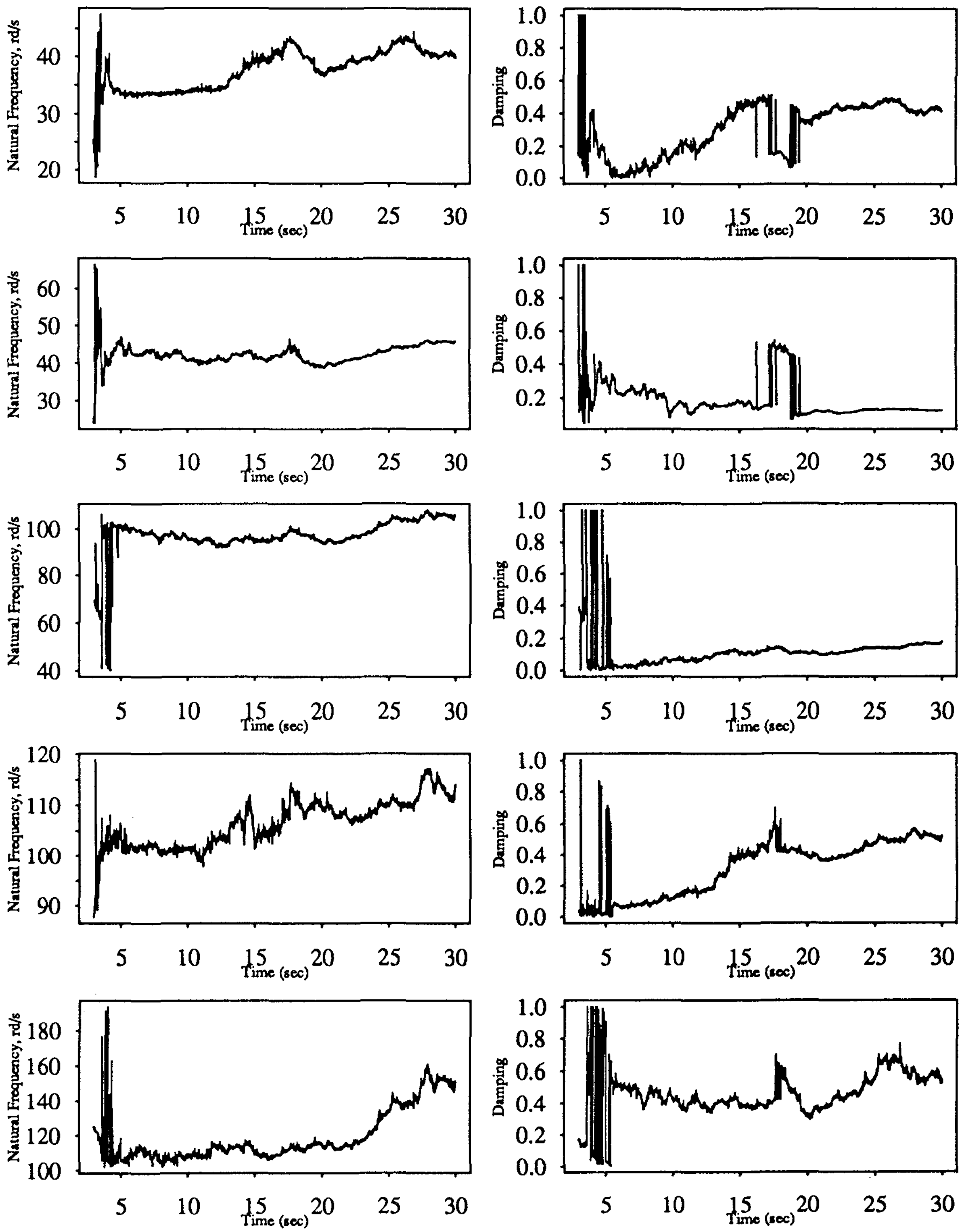


Figure 5.266

Recursive Instrumental Variable Estimation
Five Story Building Model;   El-Centro Input
3rd Floor

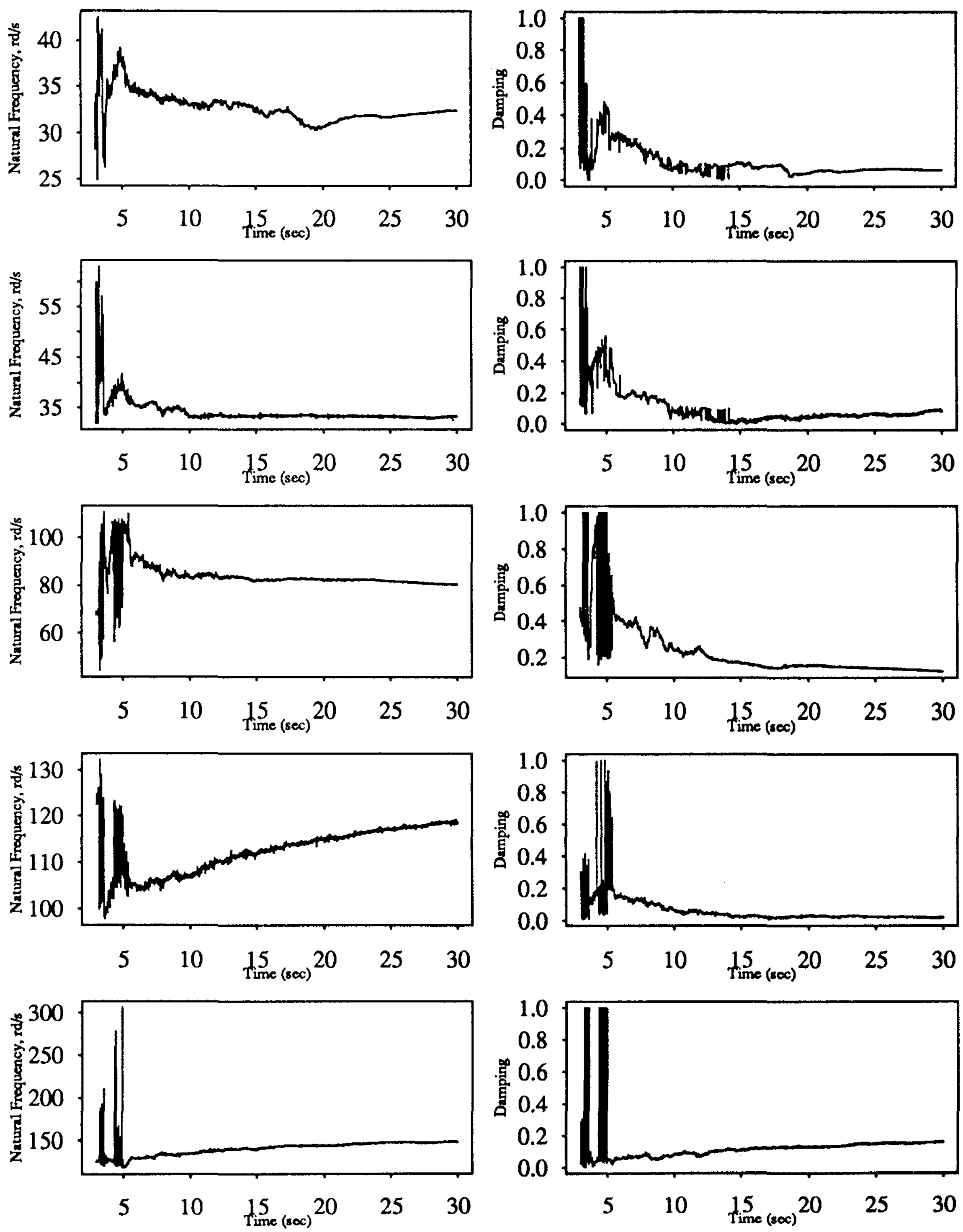


Figure 5.267

Recursive Instrumental Variable Estimation
Five Story Building Model; El-Centro Input
4th Floor

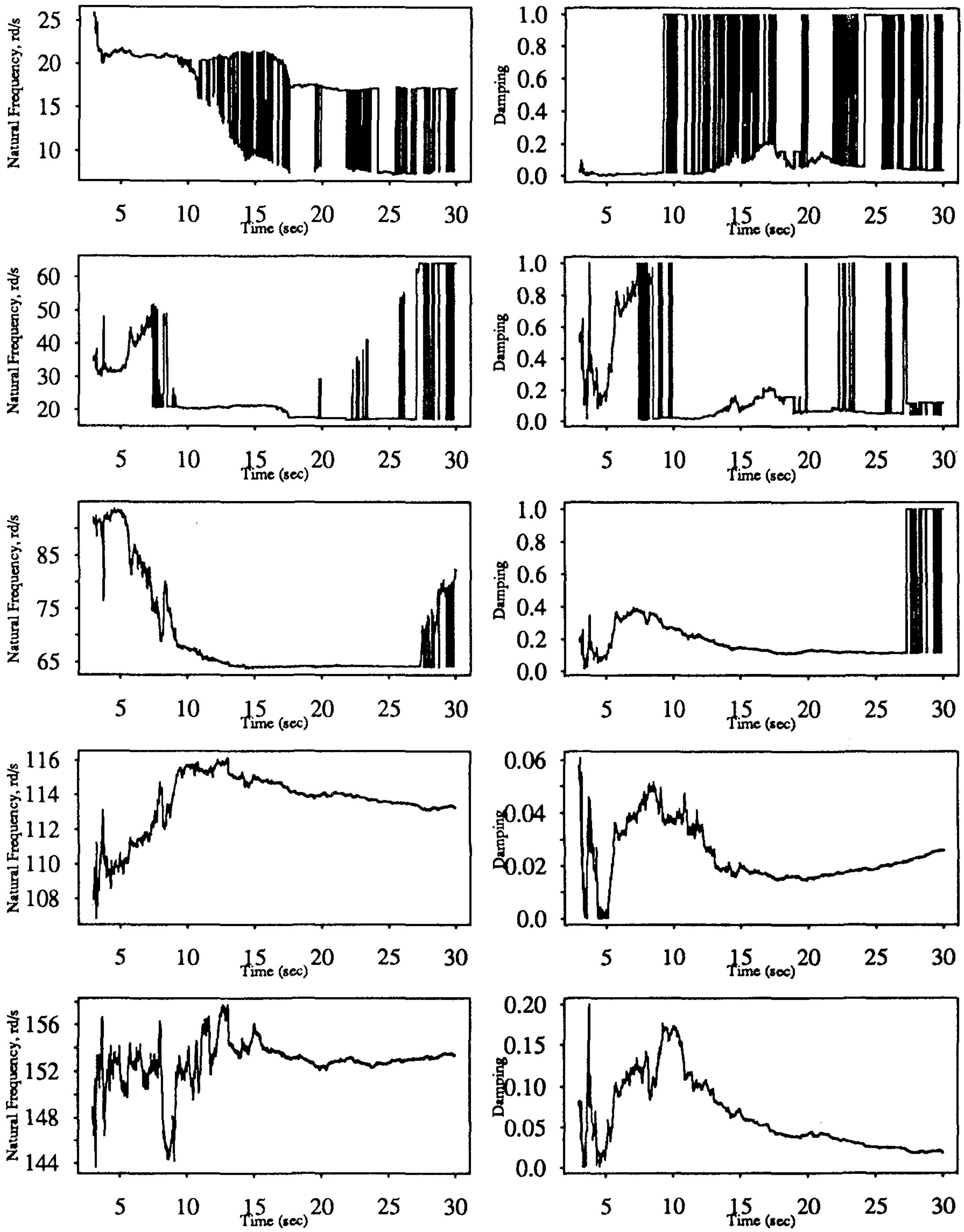


Figure 5.268

Recursive Instrumental Variable Estimation
Five Story Building Model;   El-Centro Input
5th Floor

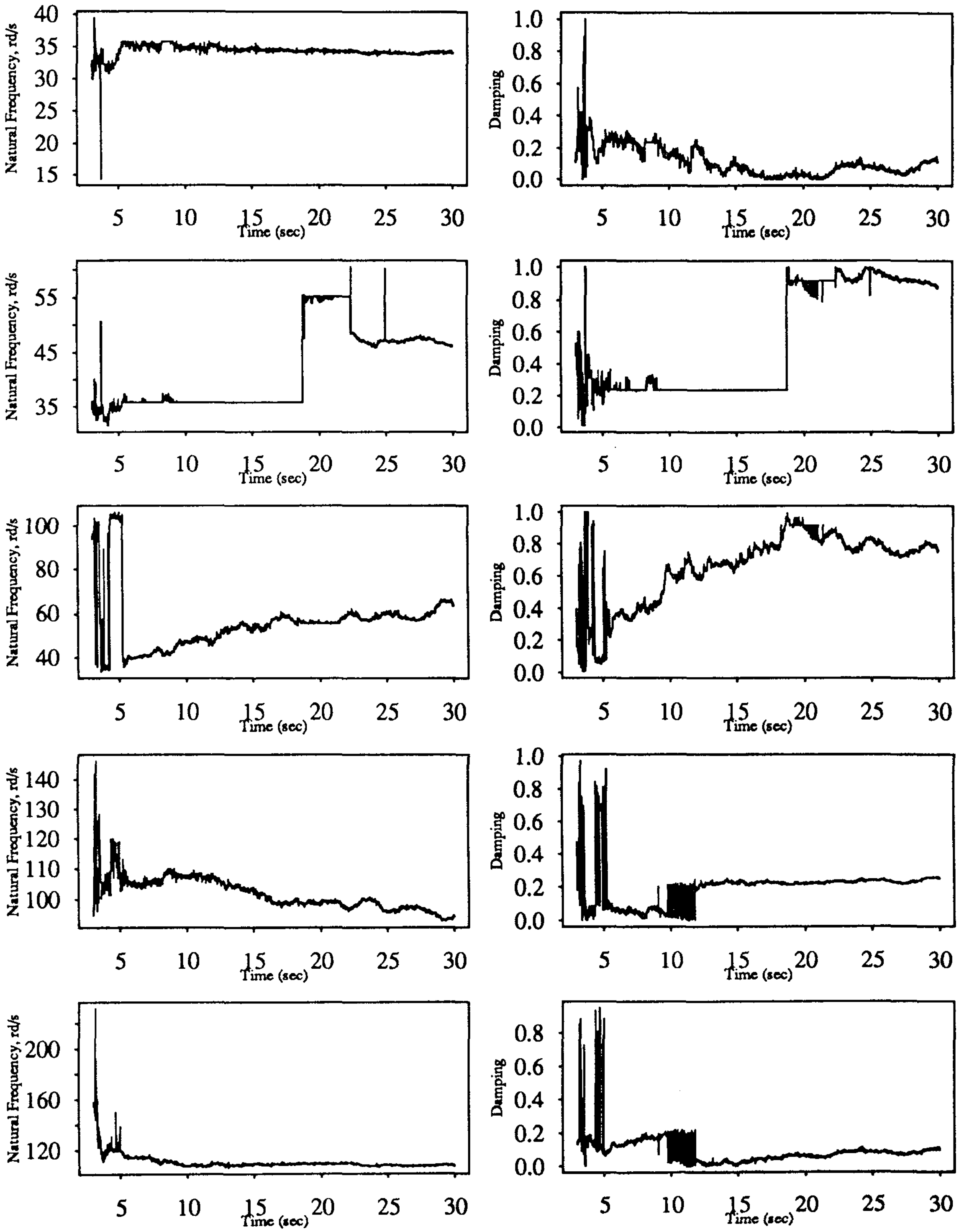


Figure 5.269

Recursive Instrumental Variable Estimation
Five Story Building Model; White Noise Input
1st Floor

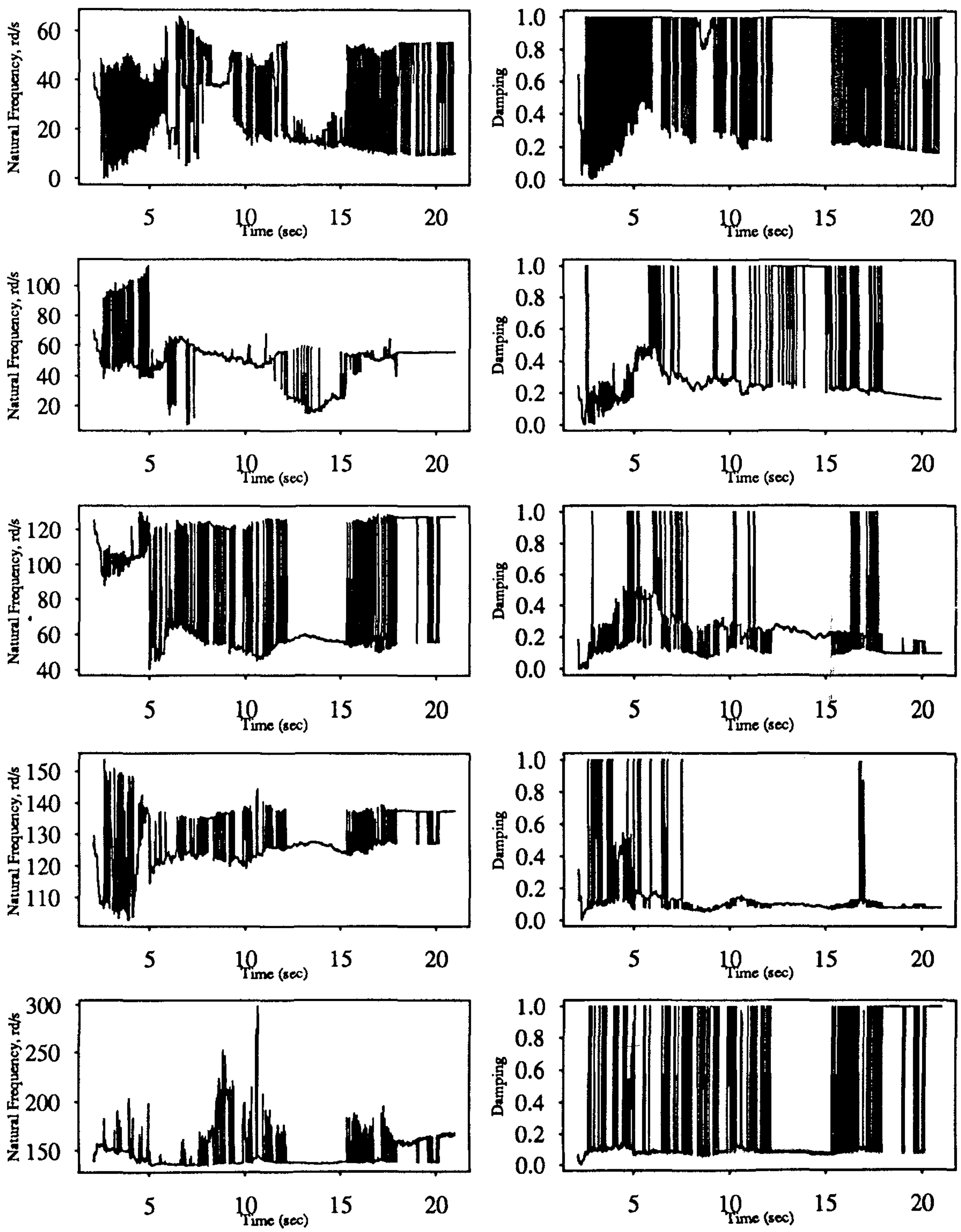


Figure 5.270

## Recursive Instrumental Variable Estimation
## Five Story Building Model; White Noise Input

2nd Floor

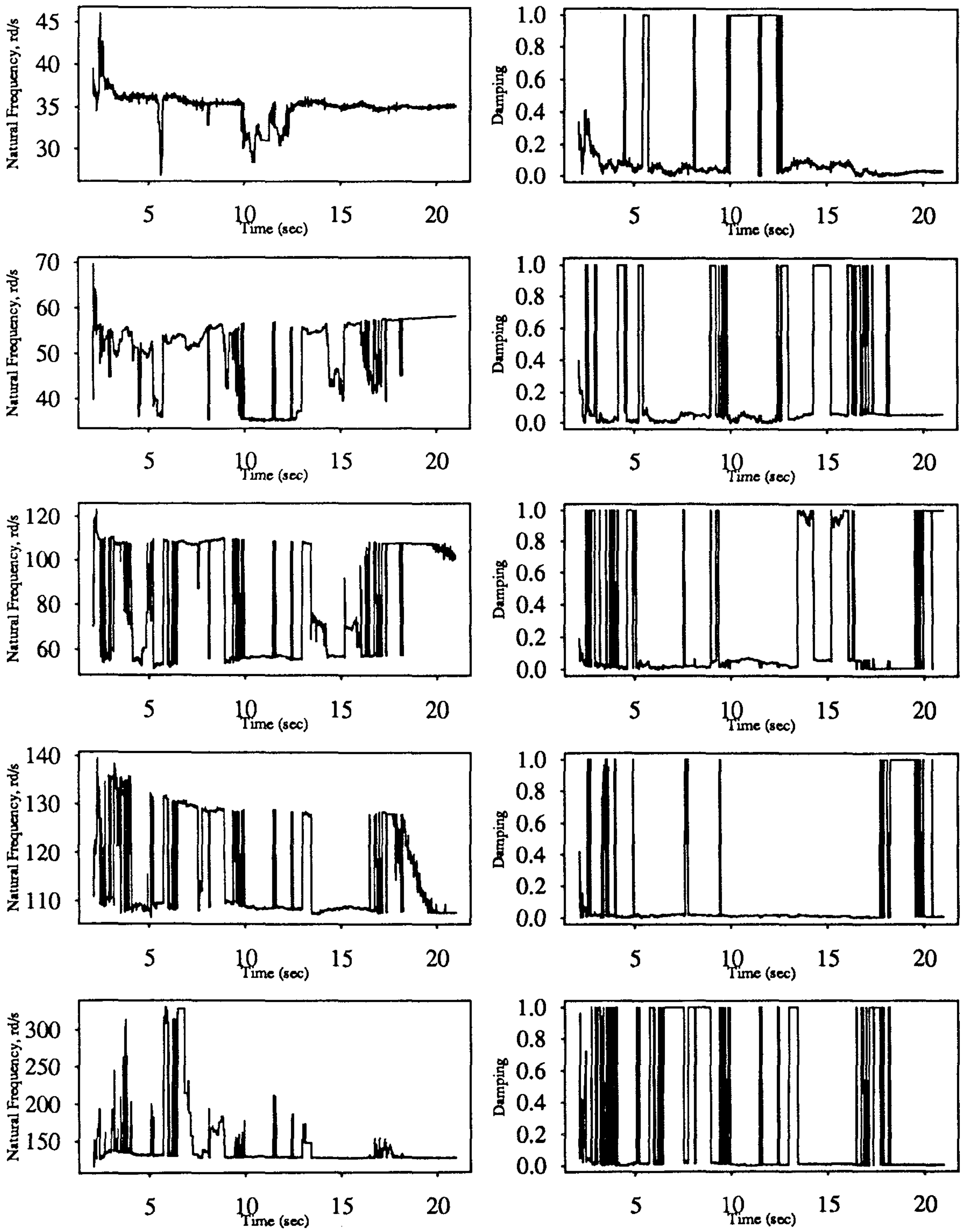


Figure 5.271

Recursive Instrumental Variable Estimation
Five Story Building Model; White Noise Input
3rd Floor

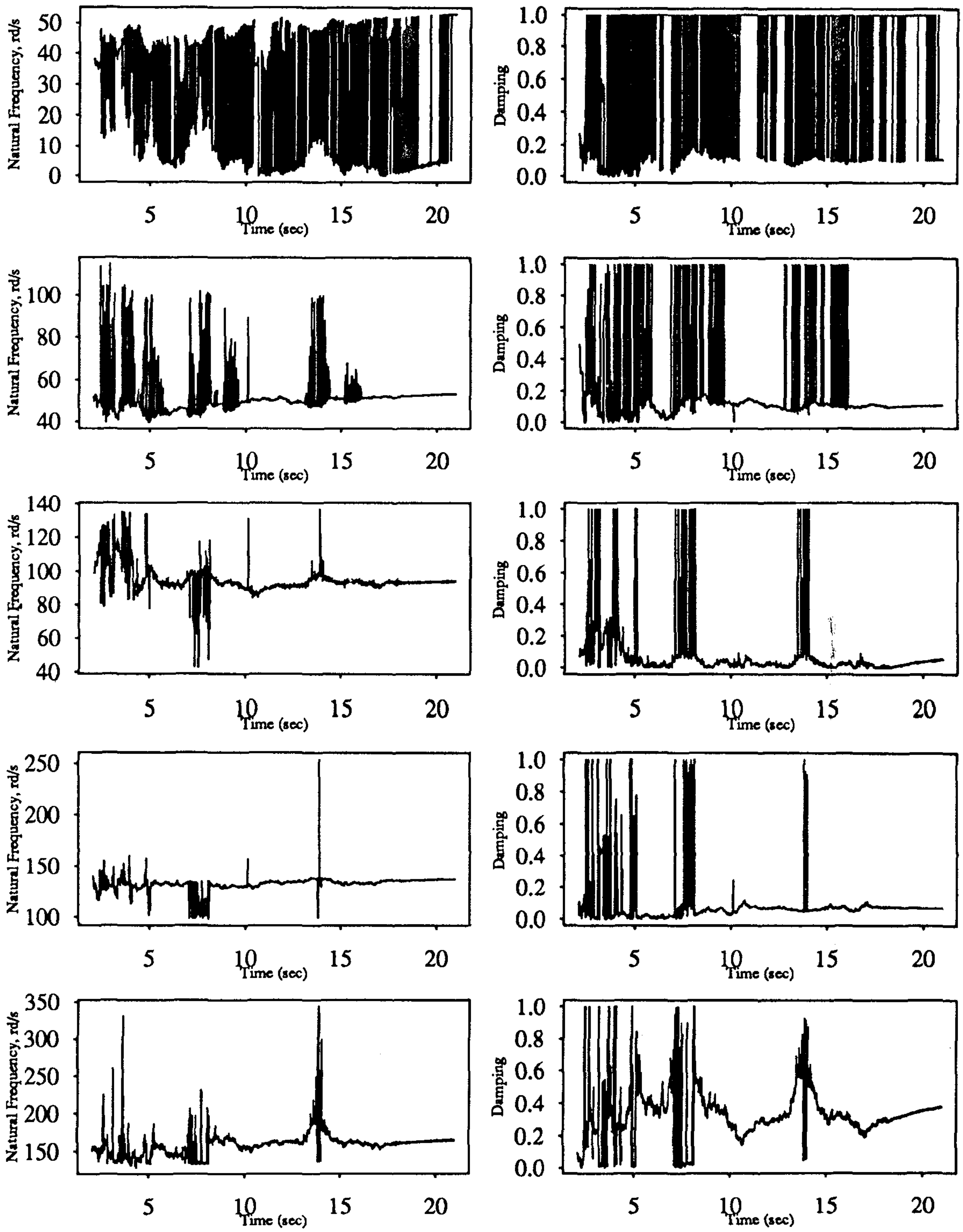


Figure 5.272

## Recursive Instrumental Variable Estimation
## Five Story Building Model; White Noise Input

4th Floor

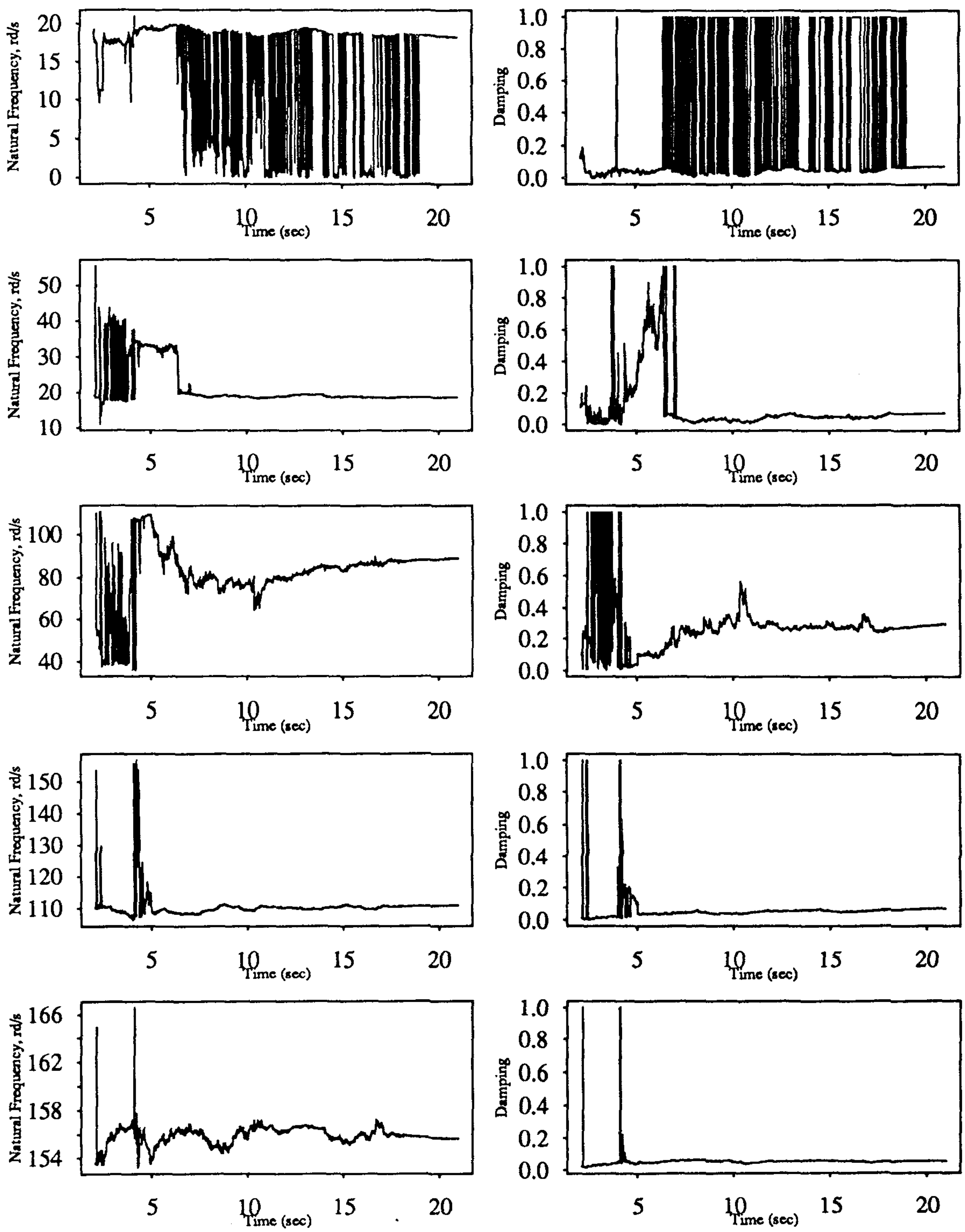


Figure 5.273

## Recursive Instrumental Variable Estimation
## Five Story Building Model; White Noise Input

5th Floor

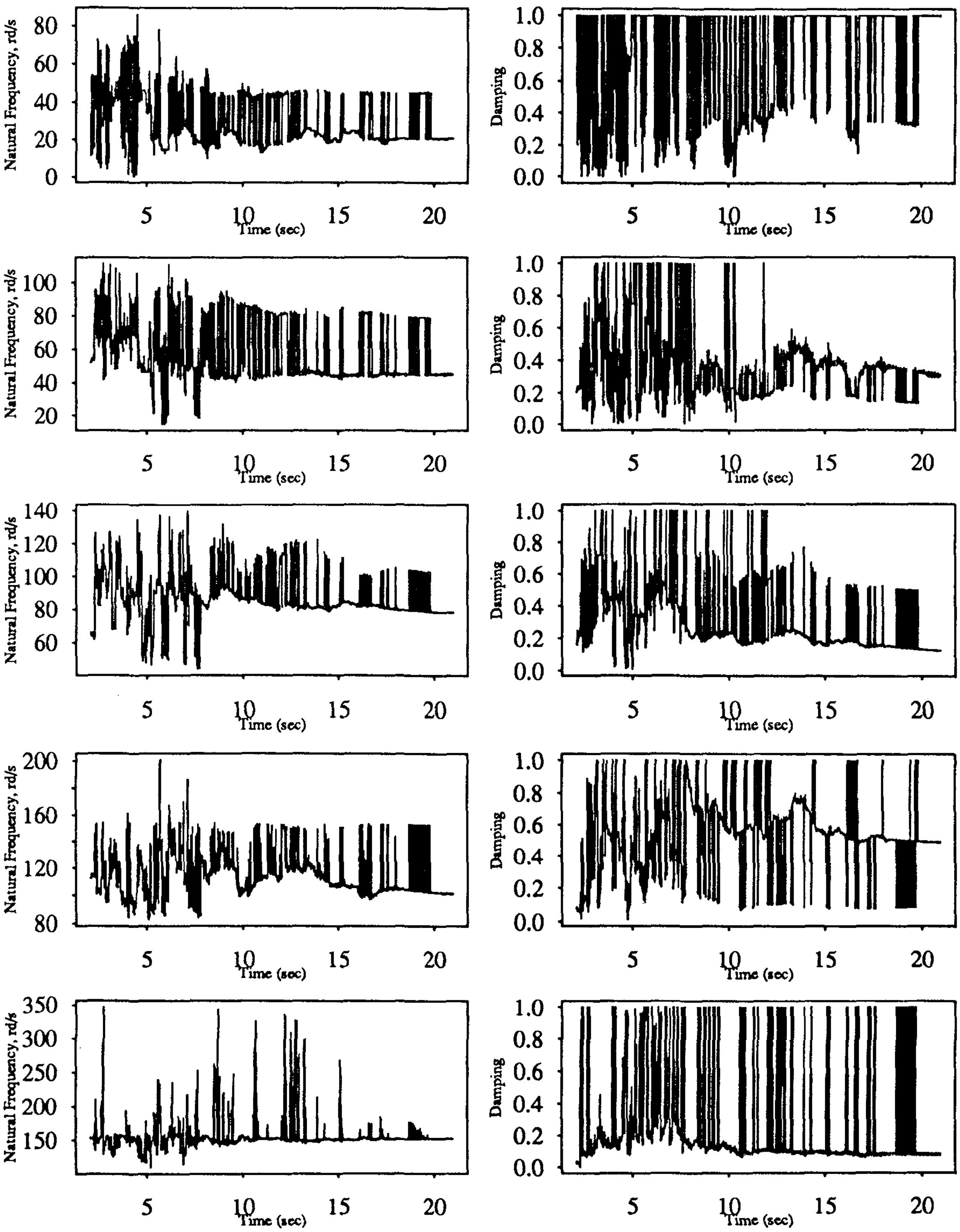


Figure 5.274

Recursive Instrumental Variable Estimation
Three Story Building Model; El-Centro Input
1st Floor

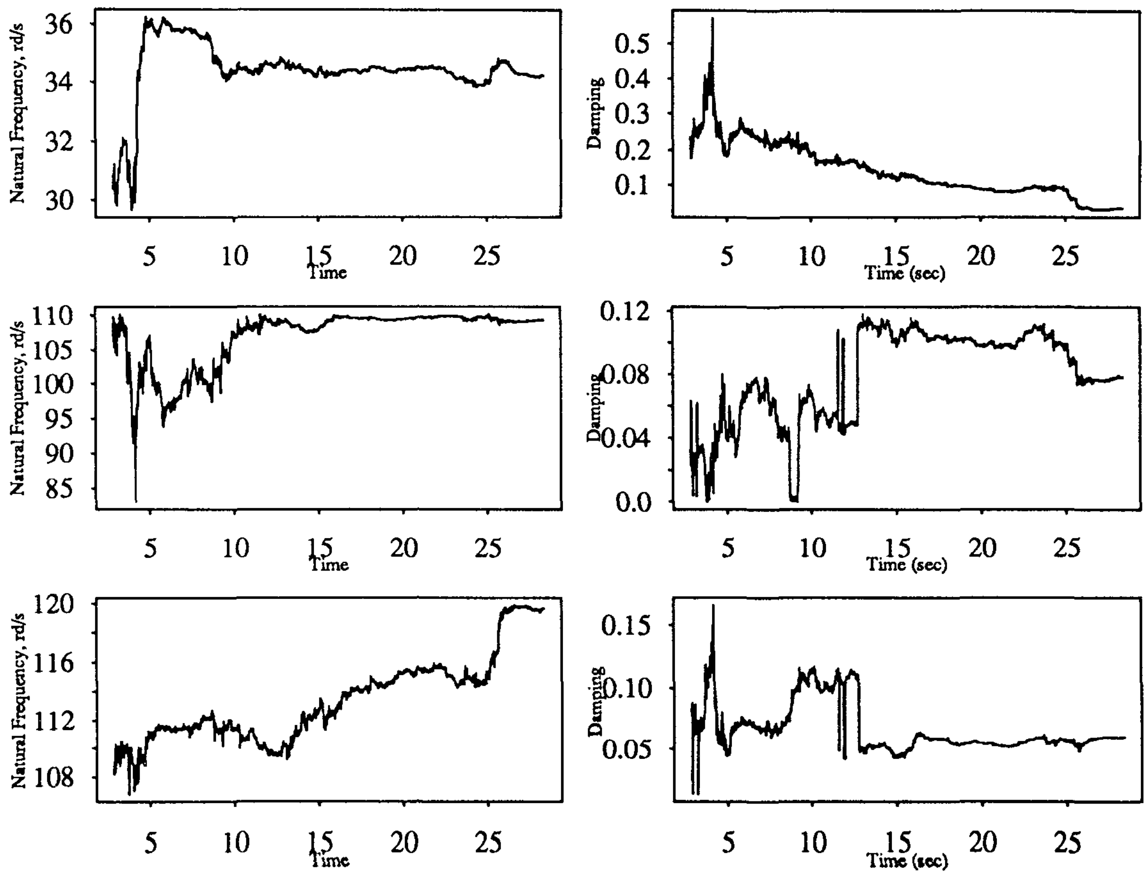


Figure 5.275

Recursive Instrumental Variable Estimation
Three Story Building Model;   El-Centro Input
2nd Floor

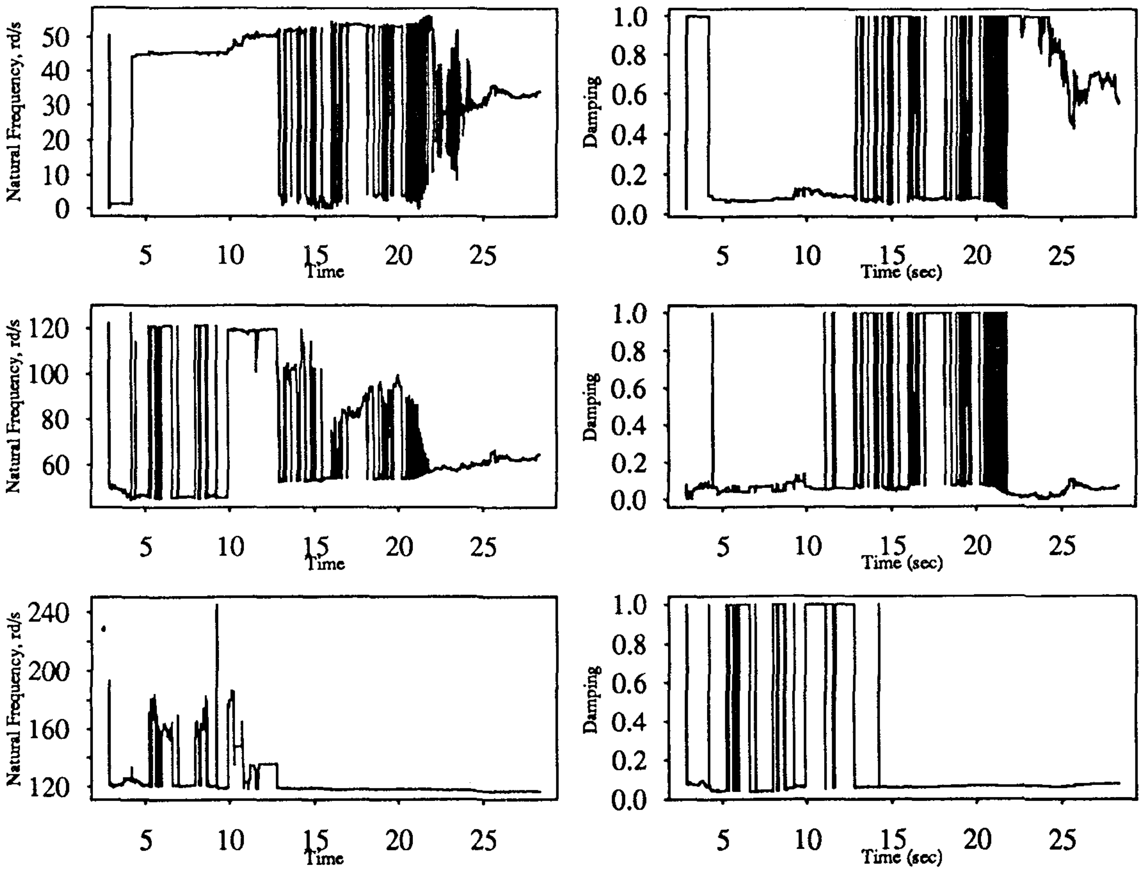


Figure 5.276

Recursive Instrumental Variable Estimation
Three Story Building Model; El-Centro Input
3rd Floor

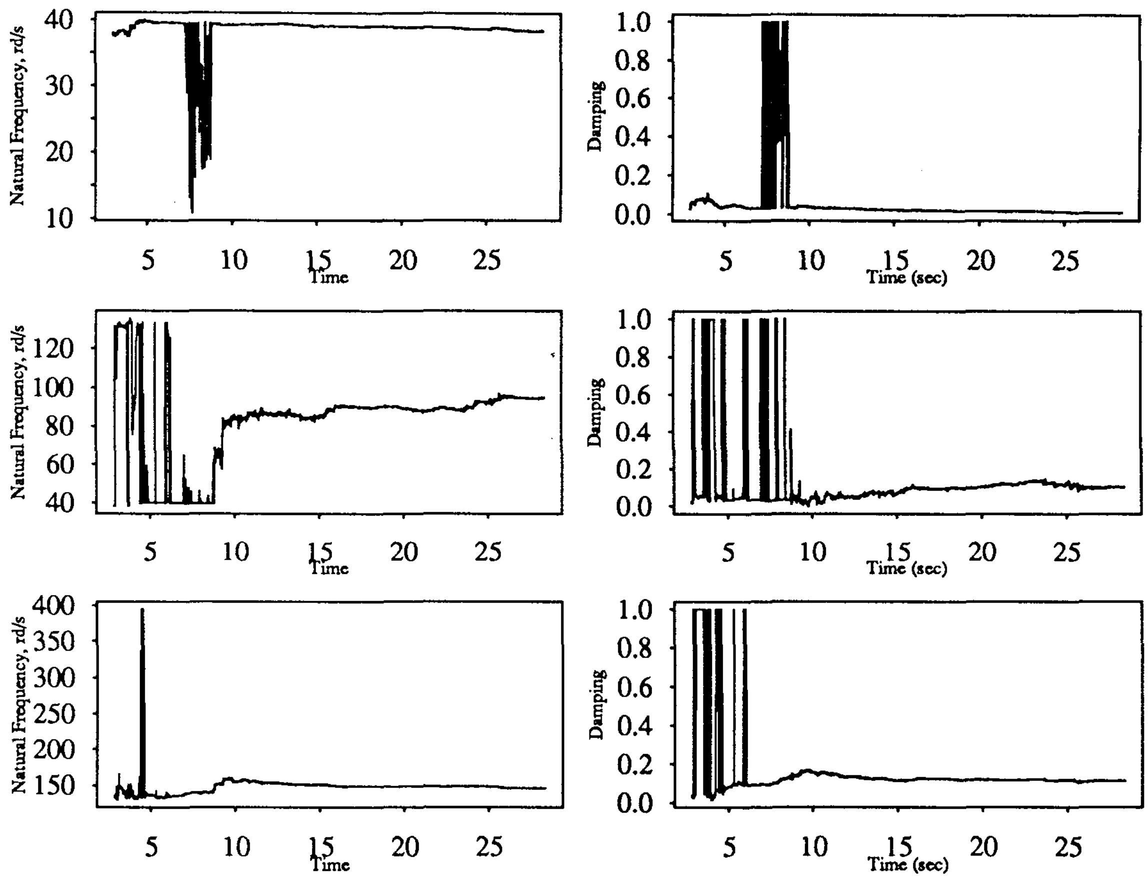


Figure 5.277

Recursive Instrumental Variable Estimation
Three Story Building Model; Sine Sweep Input
1st Floor

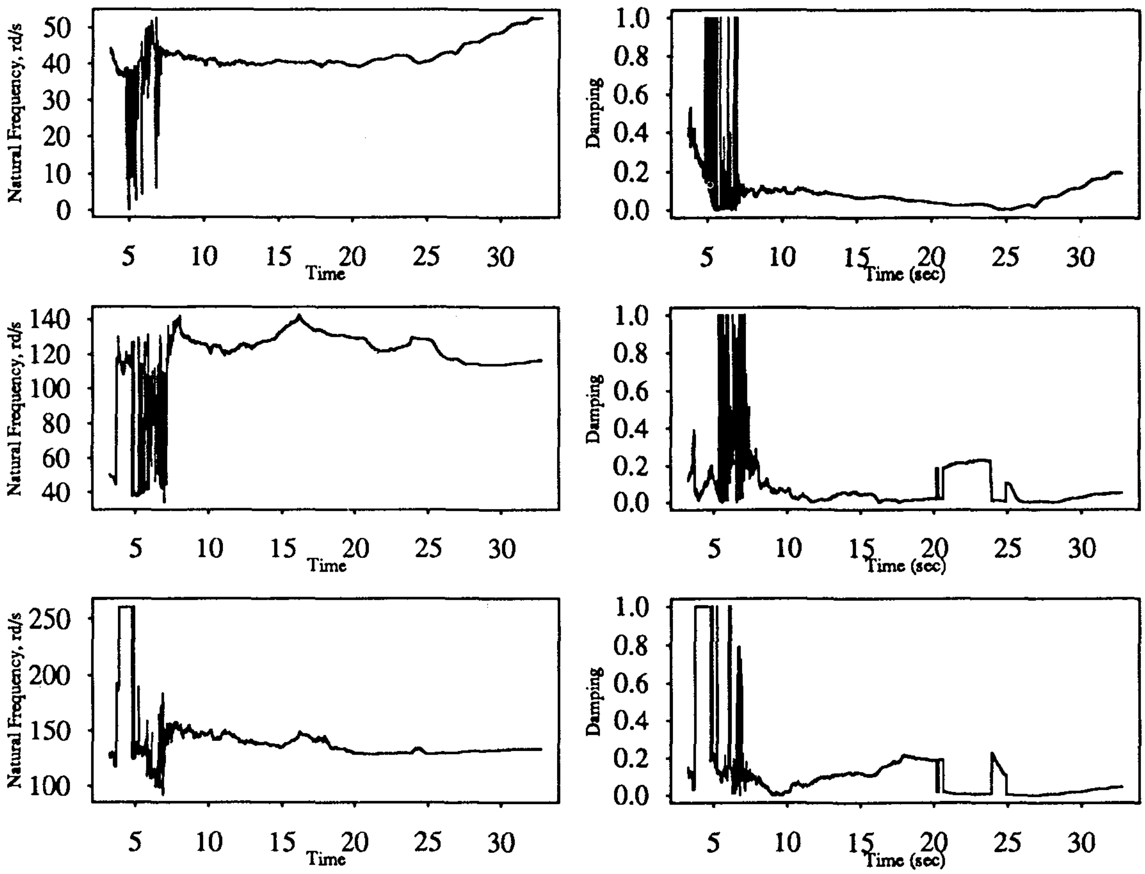


Figure 5.278

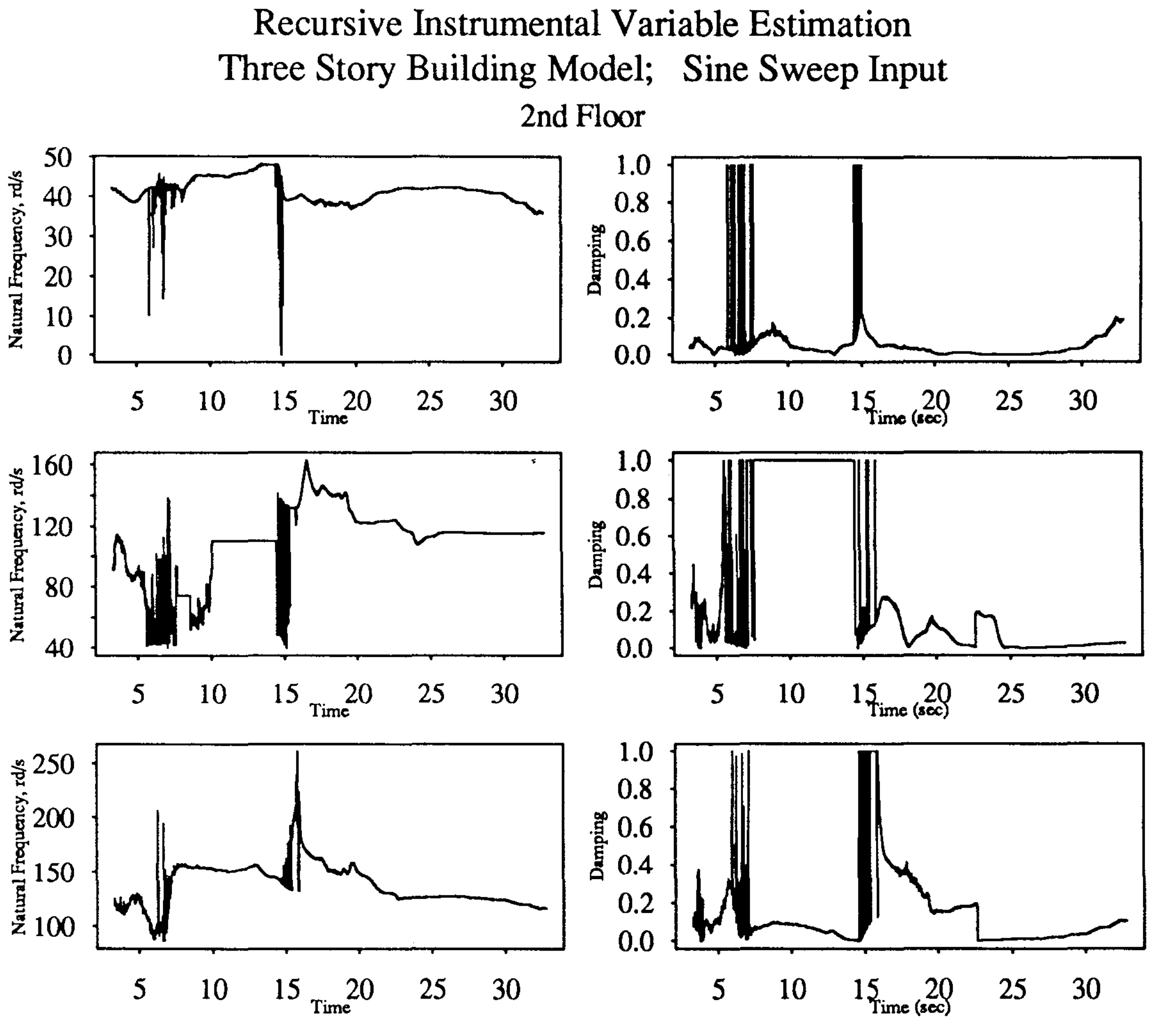

Recursive Instrumental Variable Estimation
Three Story Building Model; Sine Sweep Input
2nd Floor
Natural Frequency, rd/s
Damping
Time
Time (sec)


Figure 5.279

Recursive Instrumental Variable Estimation
Three Story Building Model; Sine Sweep Input
3rd Floor

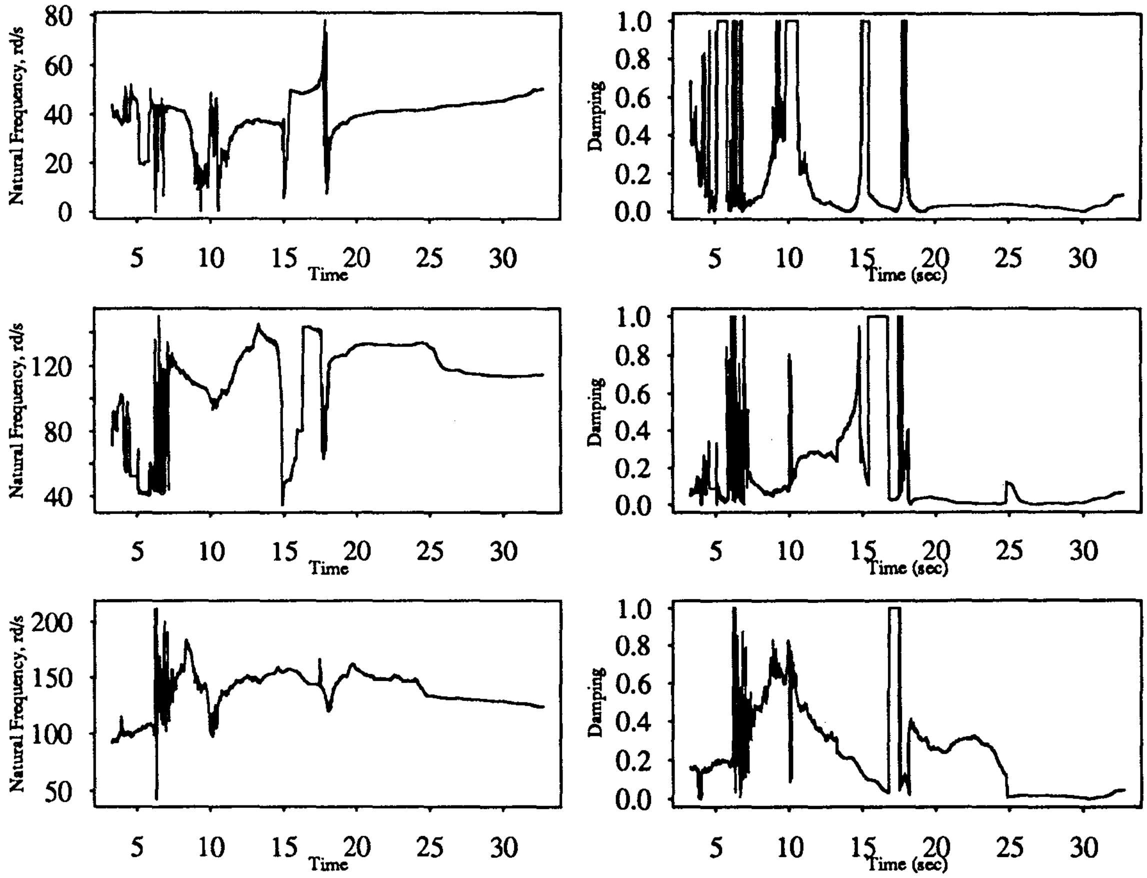


Figure 5.280

Recursive Instrumental Variable Estimation
Three Story Building Model; White Noise Input
1st Floor

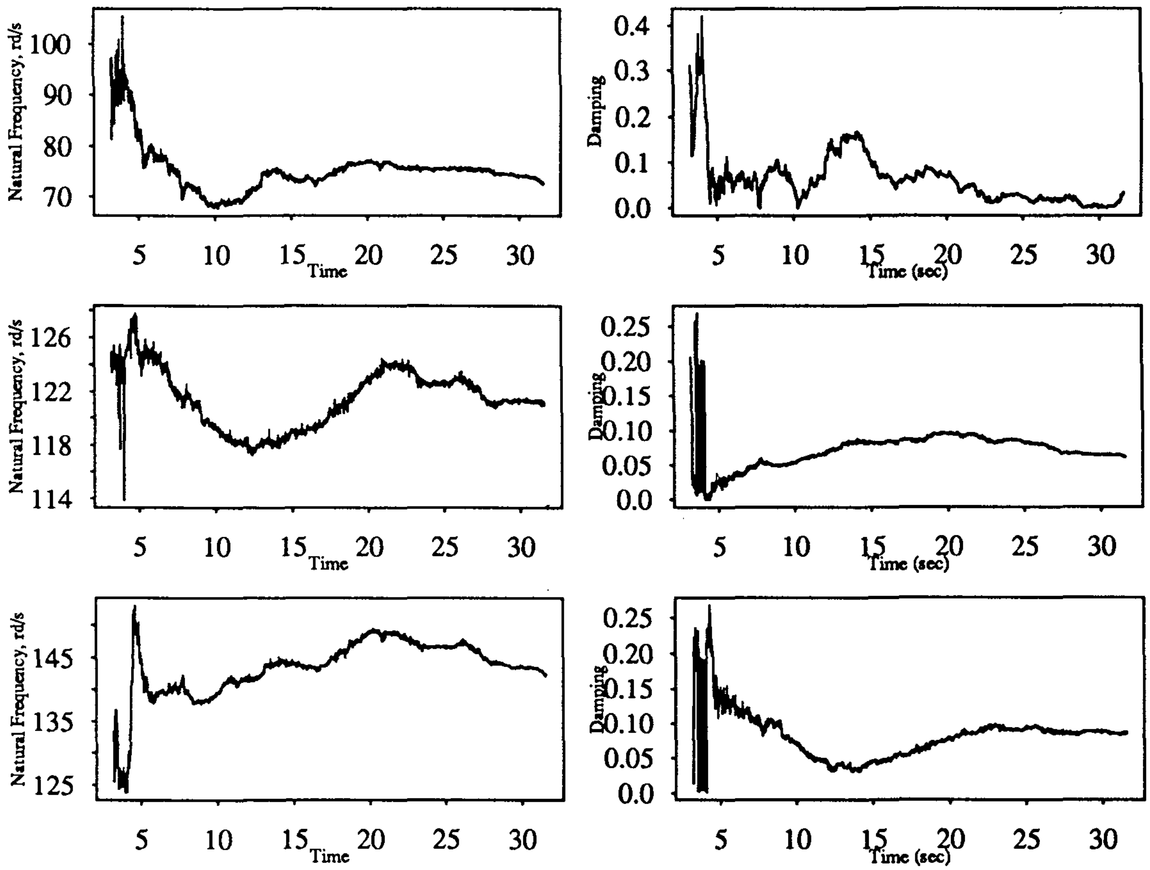


Figure 5.281

Recursive Instrumental Variable Estimation
Three Story Building Model; White Noise Input
2nd Floor

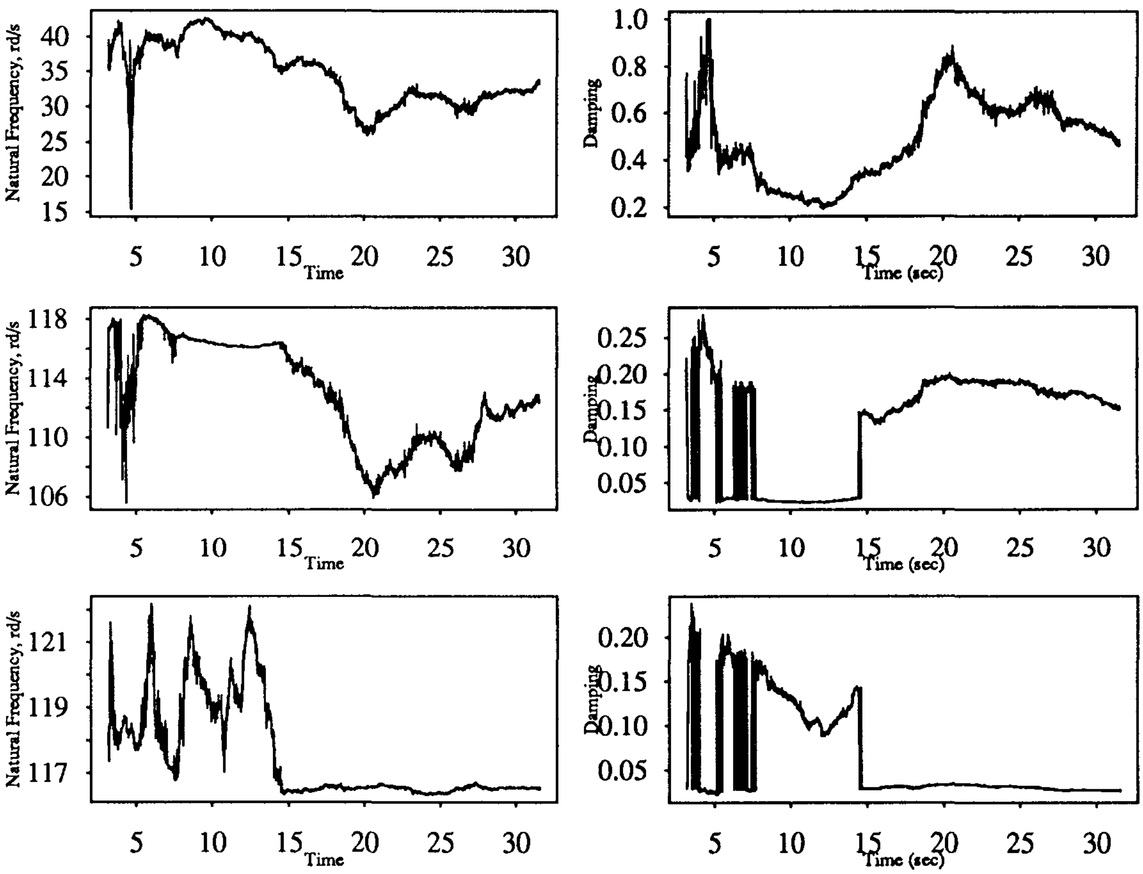


Figure 5.282

Recursive Instrumental Variable Estimation
Three Story Building Model;   White Noise Input
3rd Floor

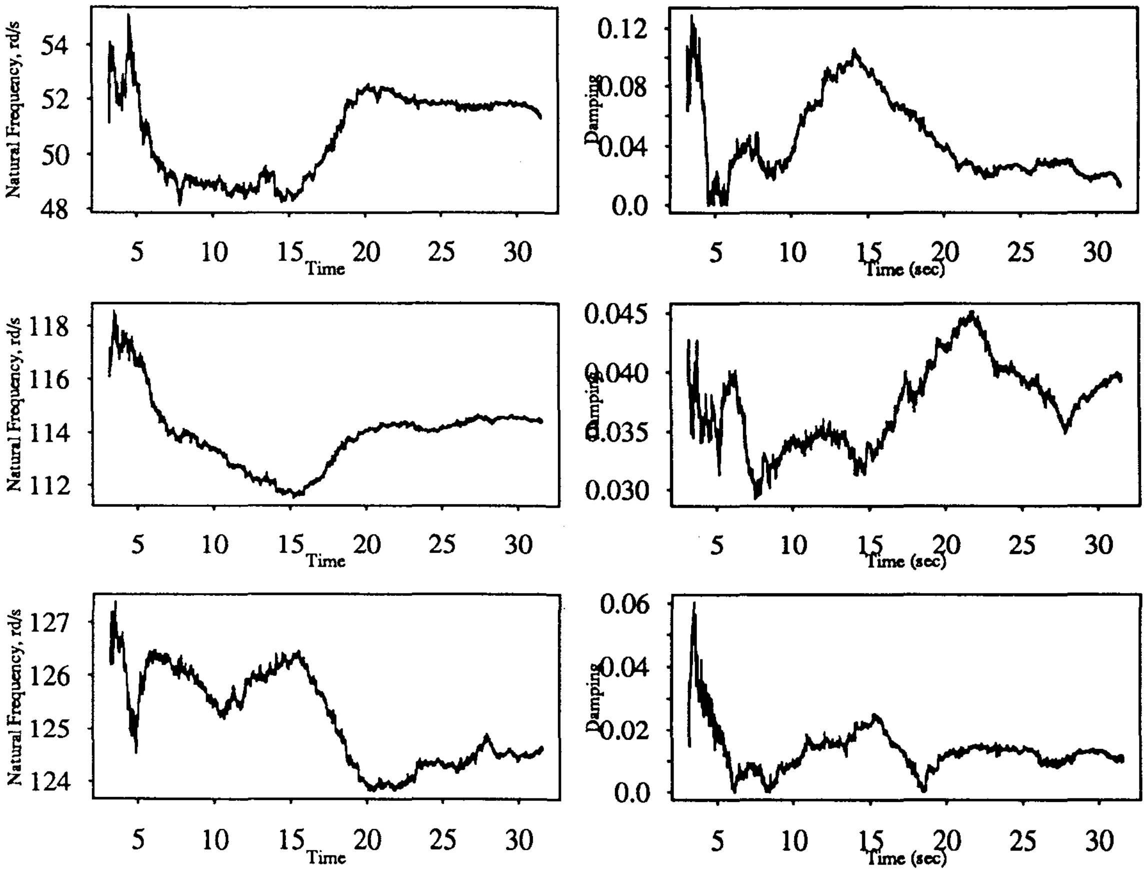


Figure 5.283

Recursive Instrumental Variable Estimation
Five Story Building Model; El-Centro Input
2nd Floor gamma=0.03

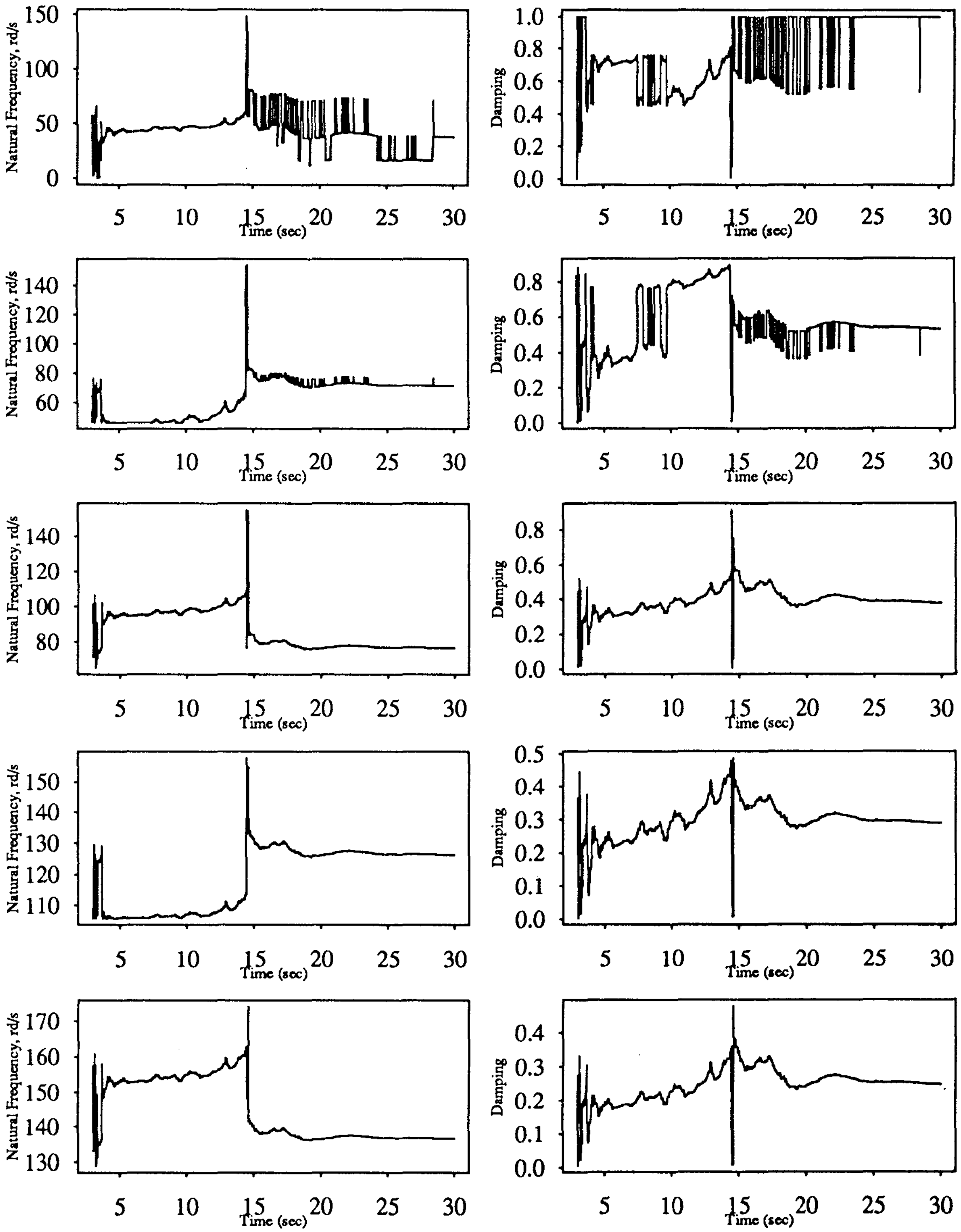


Figure 5.284

# Recursive Instrumental Variable Estimation
## Five Story Building Model; White Noise Input

4th Floor gamma=0.03

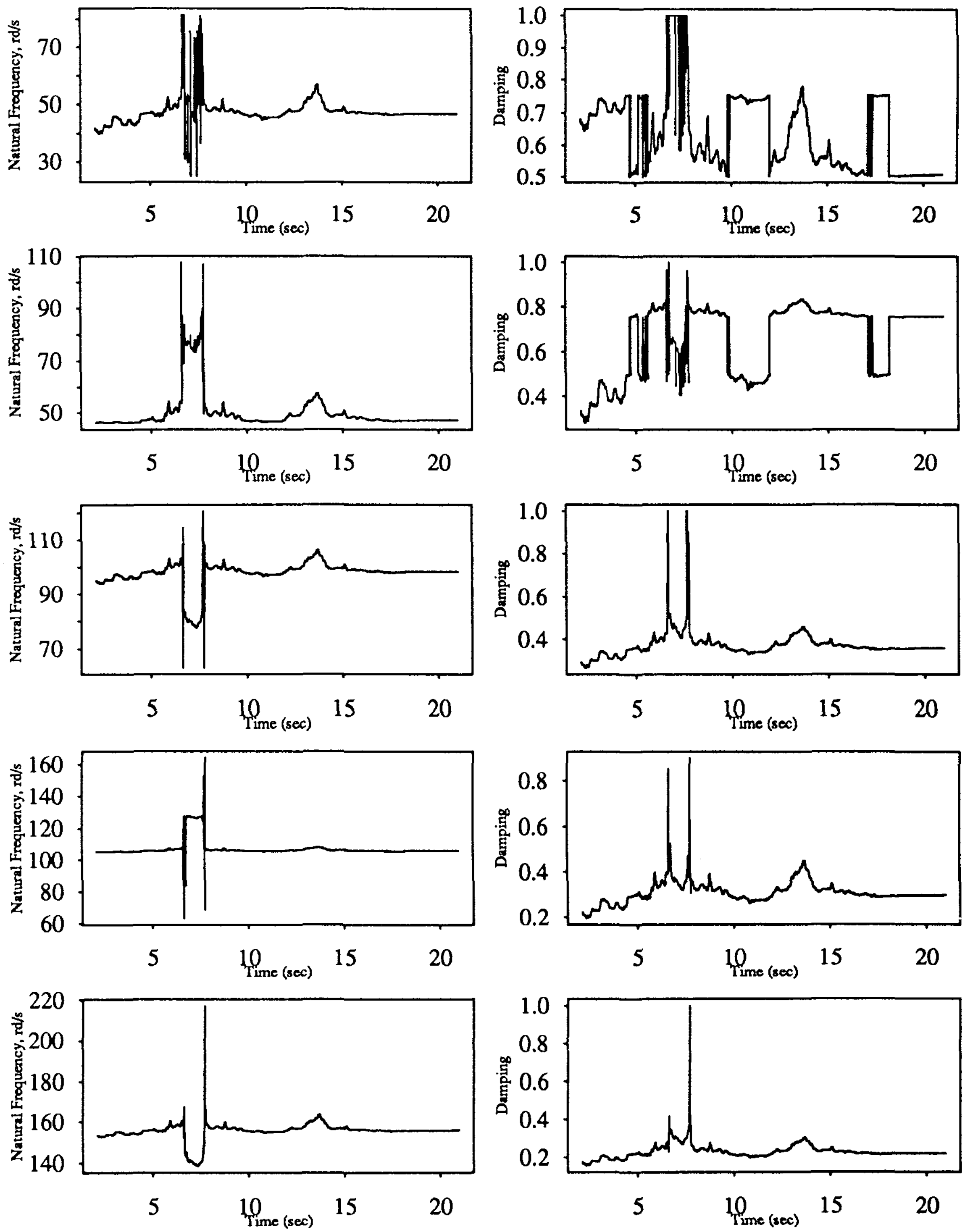


Figure 5.285

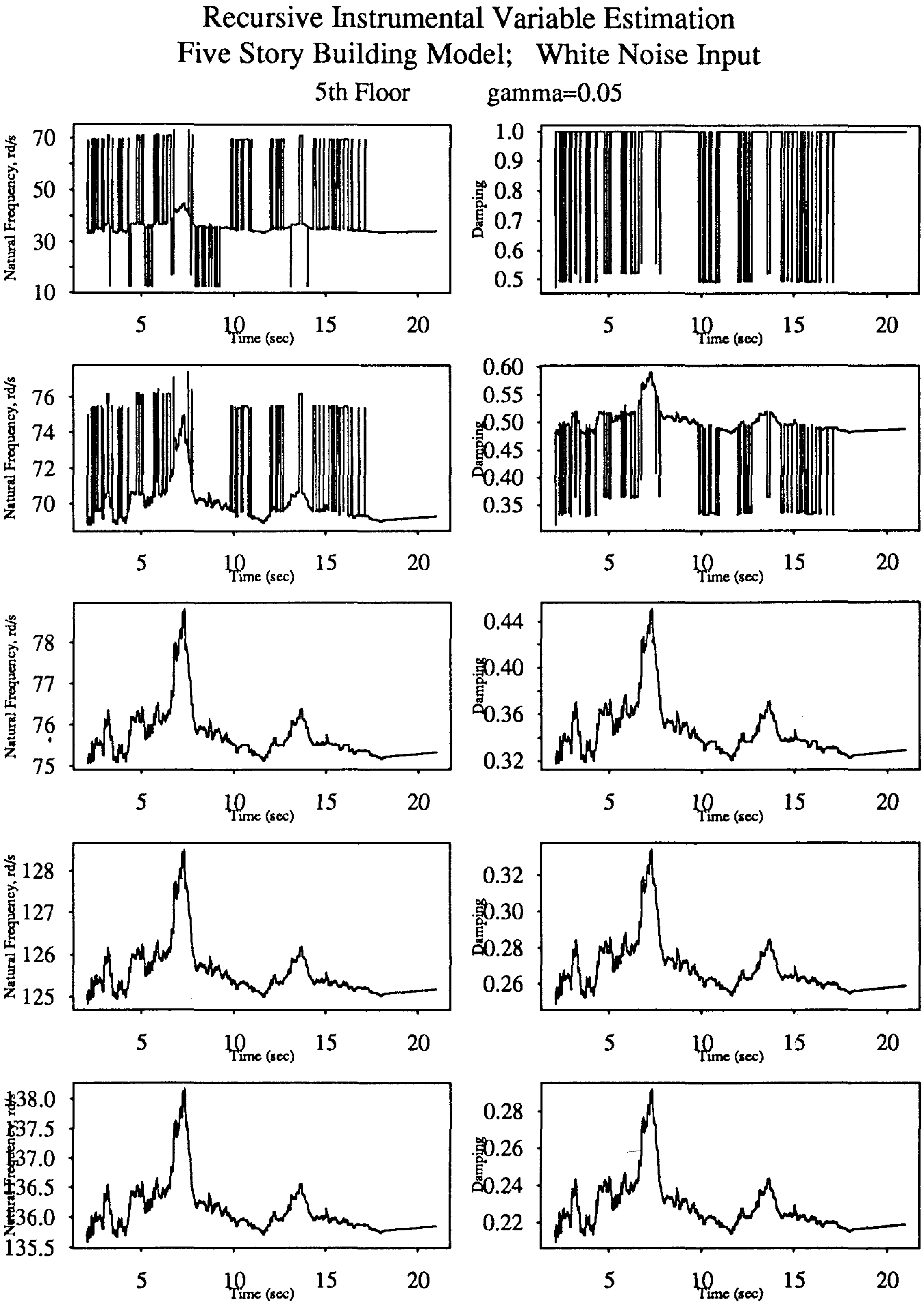
Recursive Instrumental Variable Estimation
Five Story Building Model; White Noise Input
5th Floor
gamma=0.05
Natural Frequency, rd/s
Damping
Time (sec)

Figure 5.286

Recursive Instrumental Variable Estimation
Five Story Building Model; El-Centro Input
3rd Floor gamma=0.1

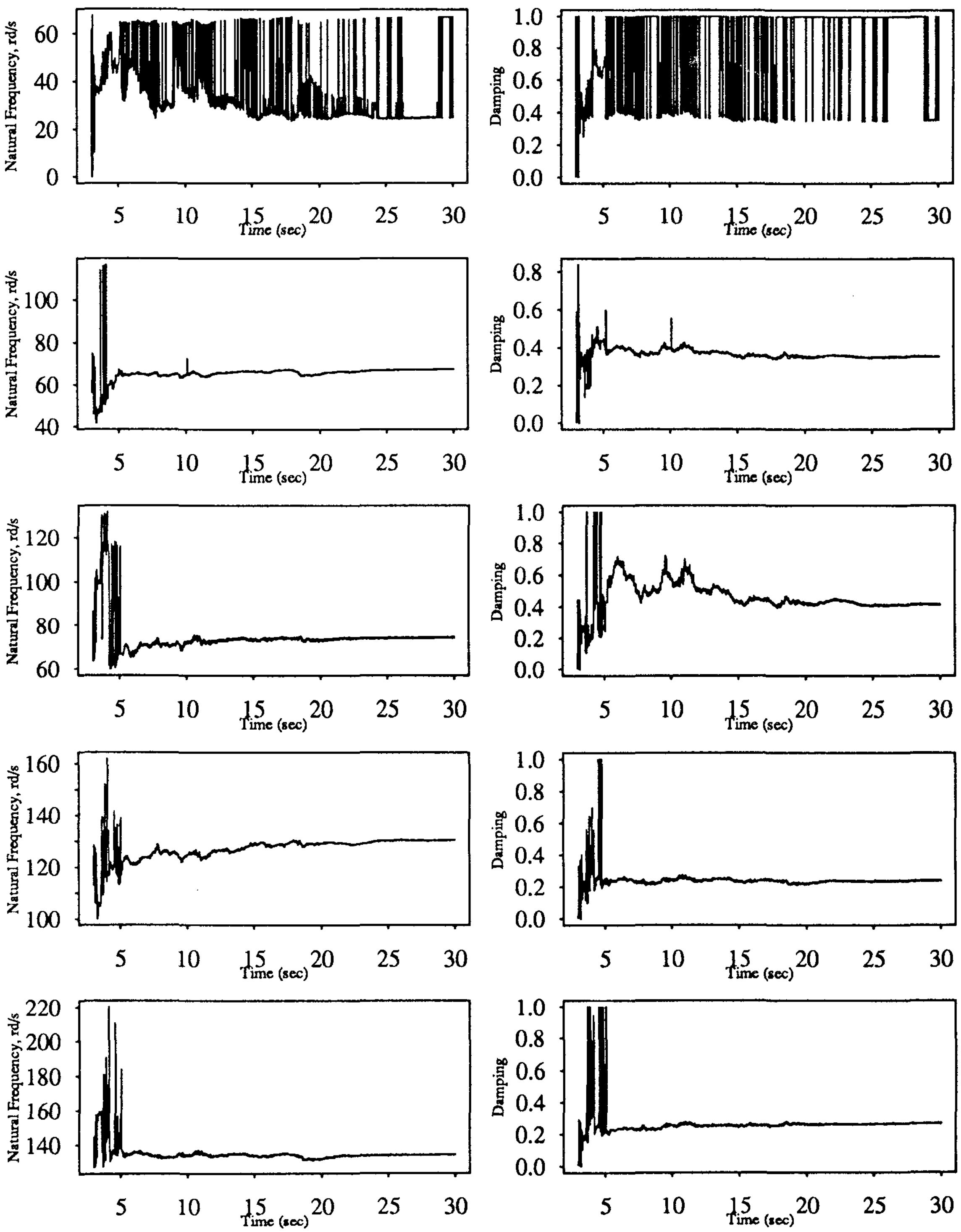


Figure 5.287

Recursive Instrumental Variable Estimation
Five Story Building Model; El-Centro Input
1st Floor gamma=0.11

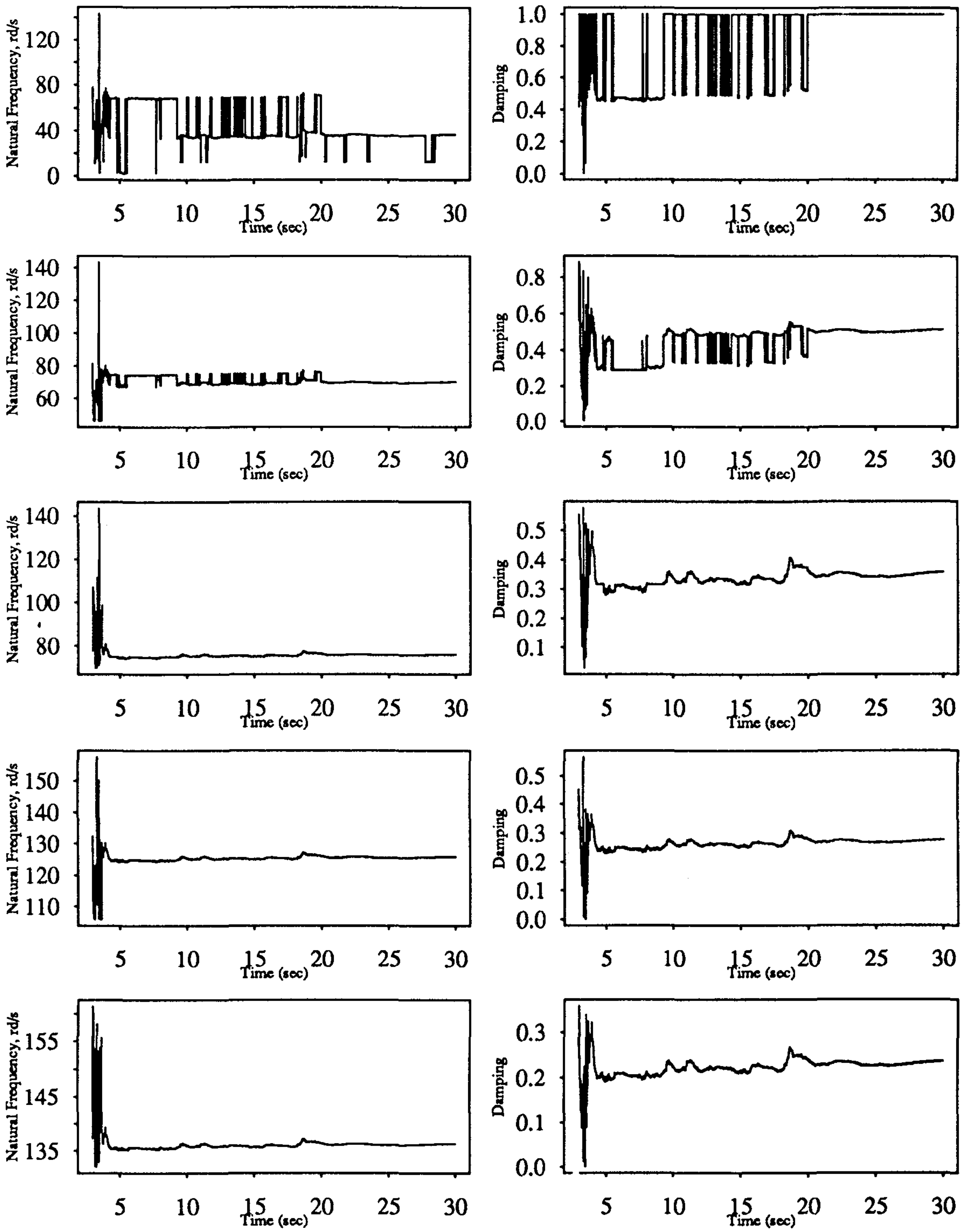


Figure 5.288

Recursive Instrumental Variable Estimation
Five Story Building Model; White Noise Input
5th Floor gamma=0.11

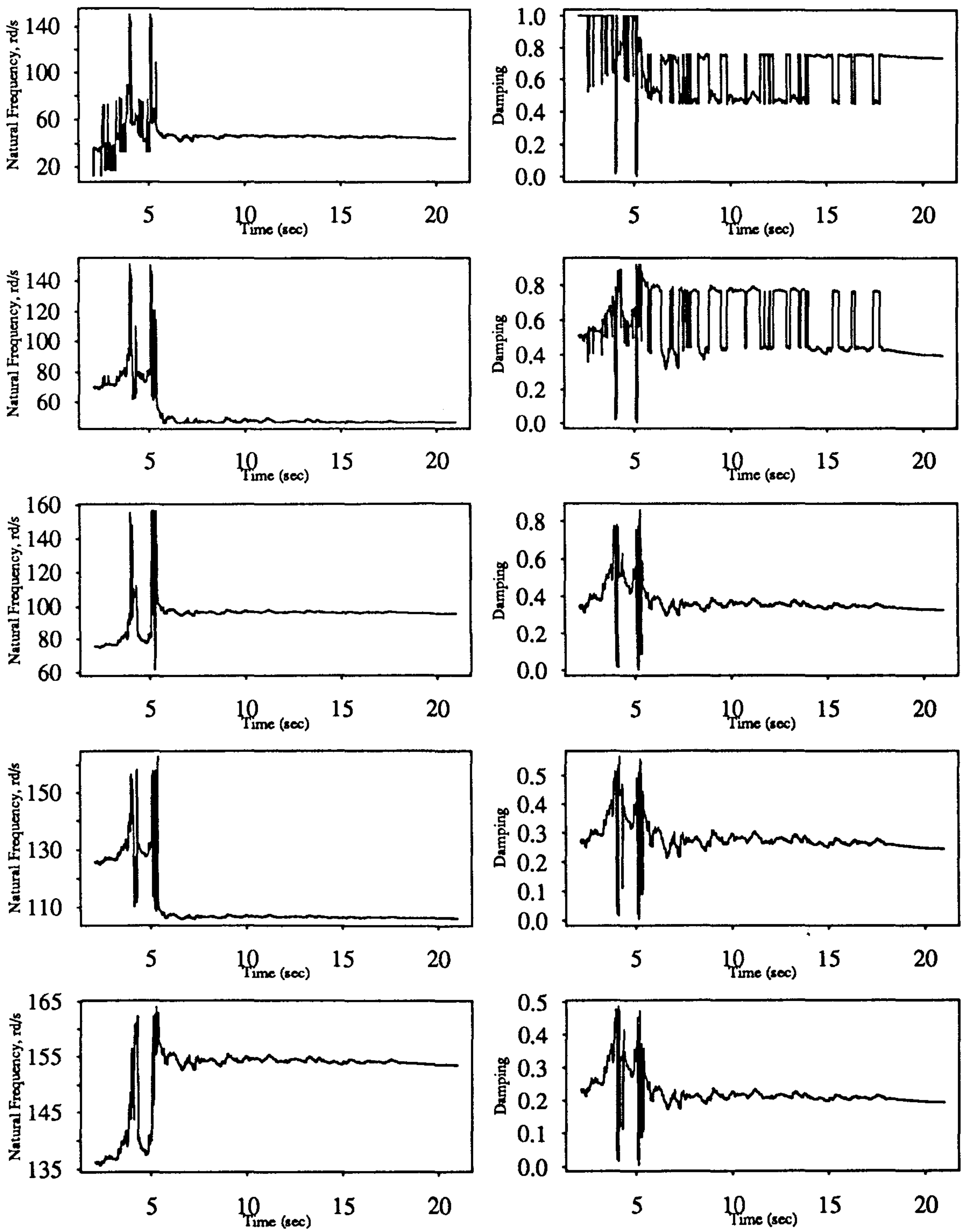


Figure 5.289

Recursive Instrumental Variable Estimation
Five Story Building Model; White Noise Input
5th Floor gamma=0.13

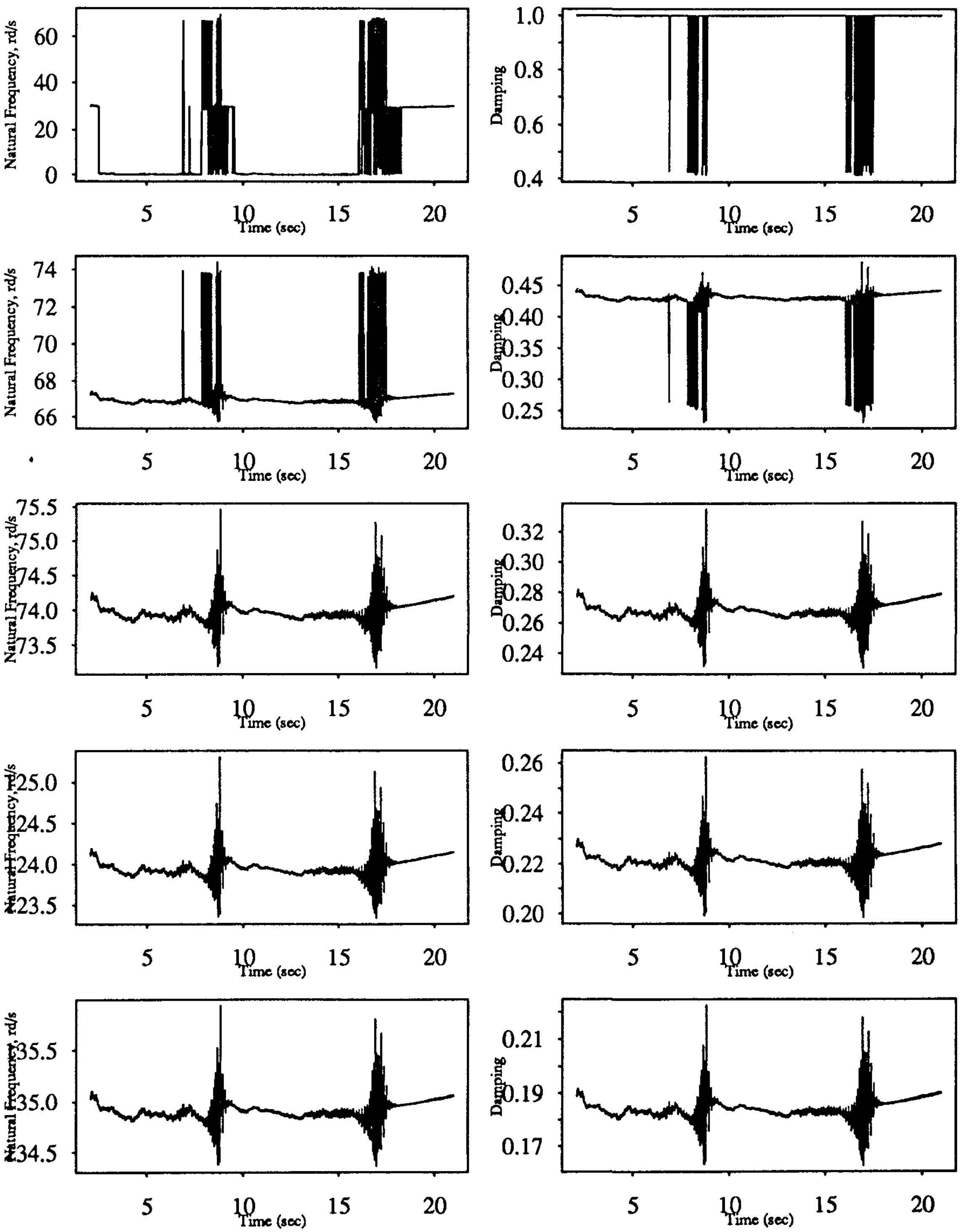


Figure 5.290

Recursive Instrumental Variable Estimation
Five Story Building Model;   El-Centro Input
1st Floor        gamma=1

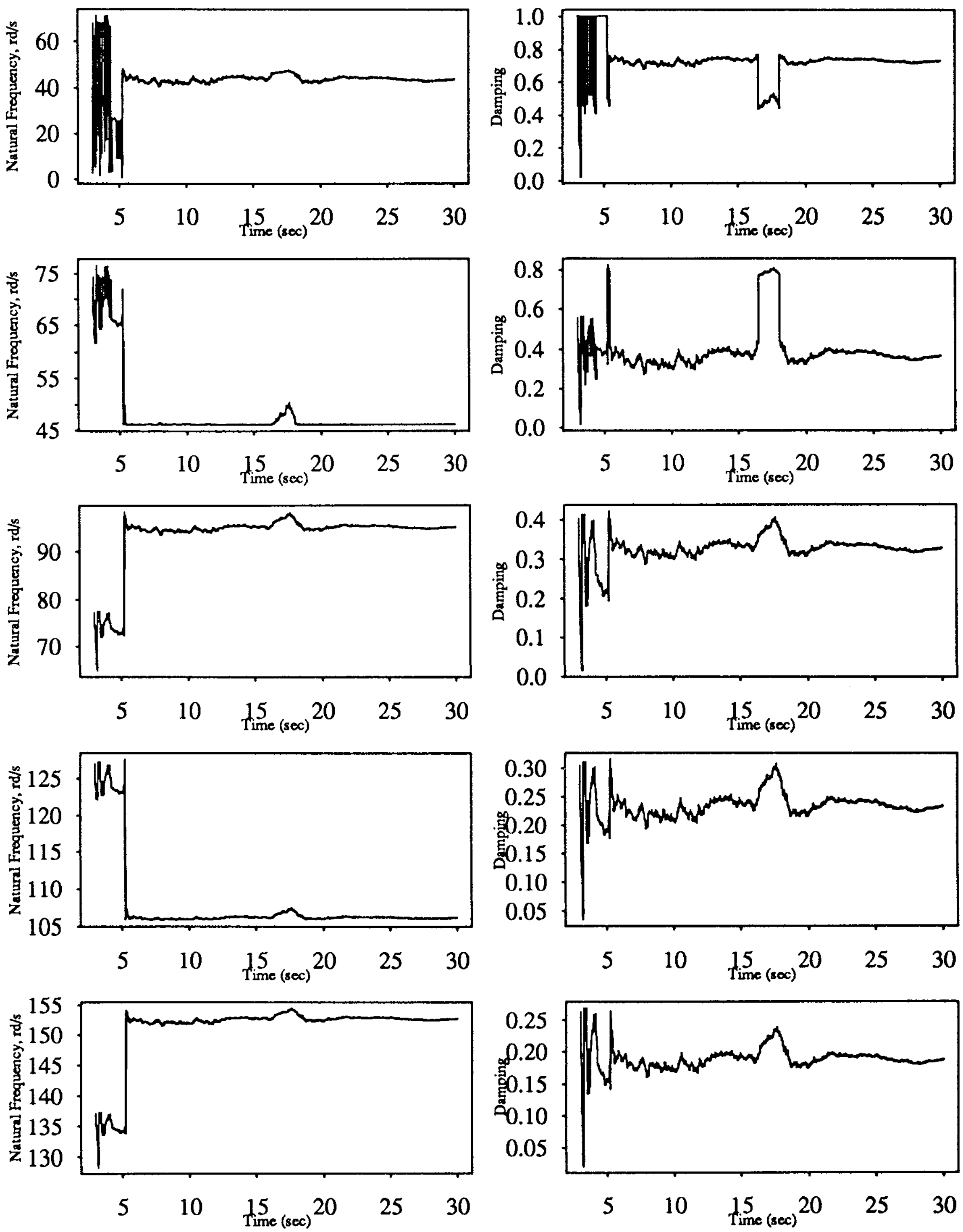


Figure 5.291

Recursive Instrumental Variable Estimation
Five Story Building Model; El-Centro Input
3rd Floor gamma=1

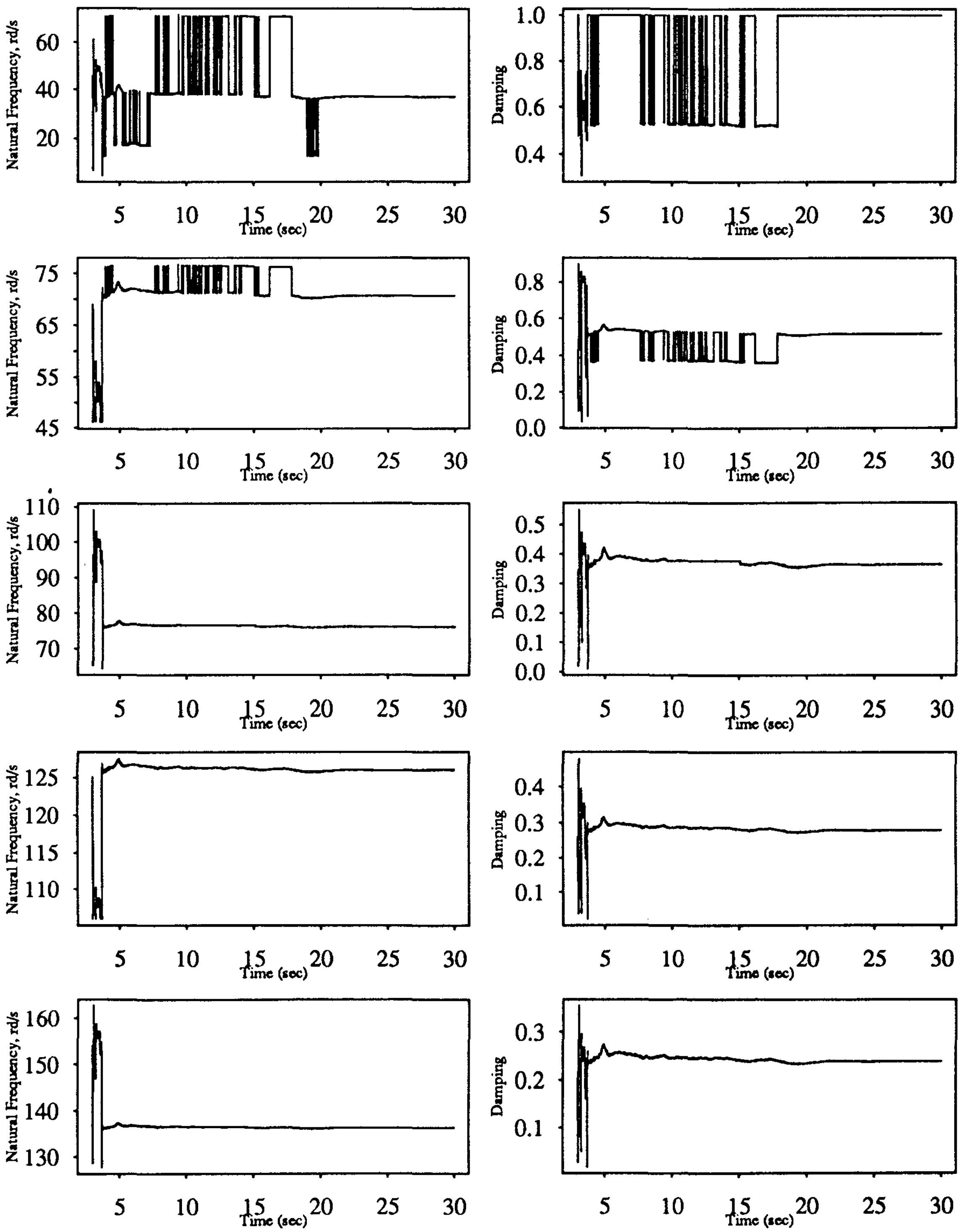


Figure 5.292

Recursive Instrumental Variable Estimation
Five Story Building Model; White Noise Input
3rd Floor gamma=1

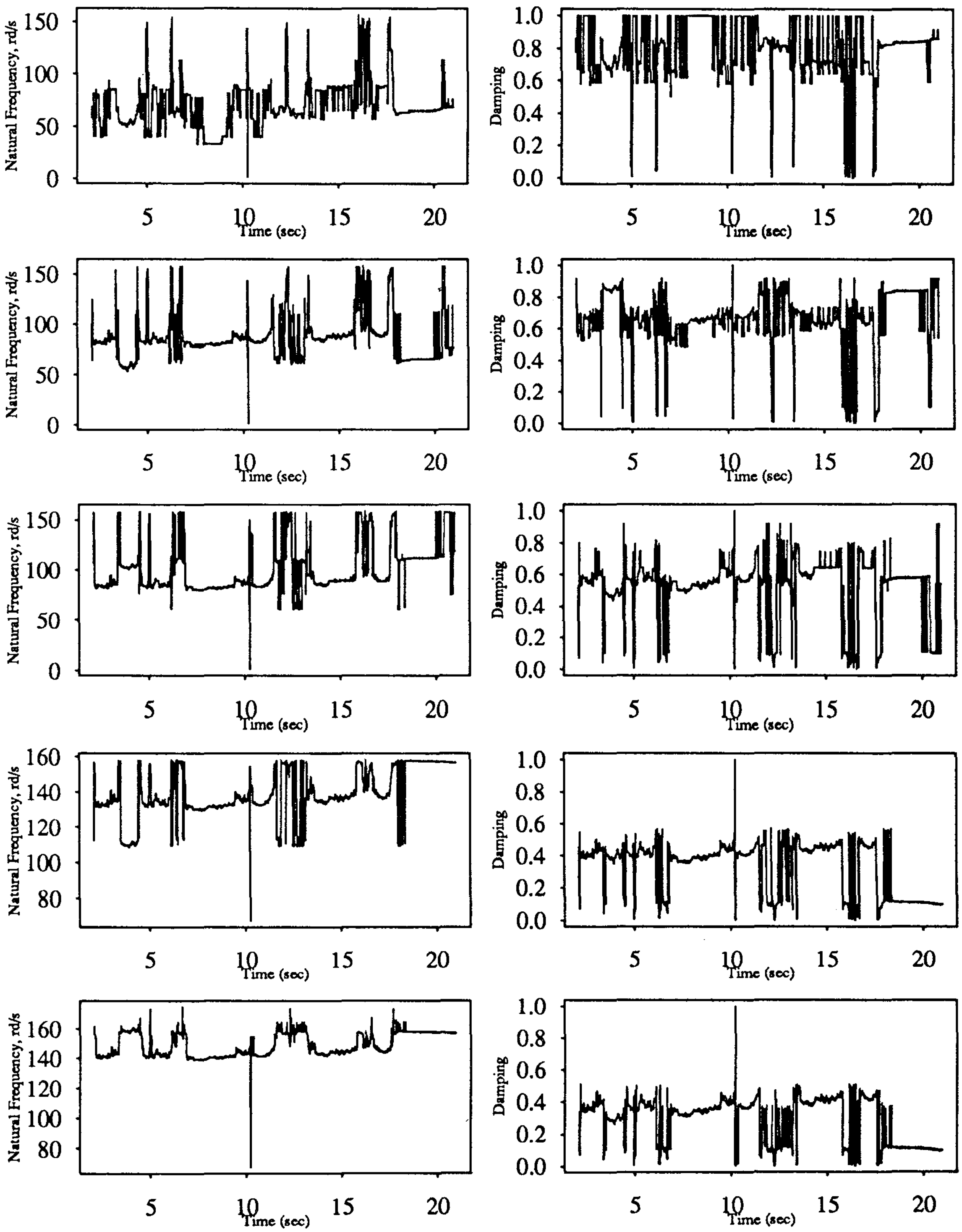


Figure 5.293

Recursive Instrumental Variable Estimation
Five Story Building Model; El-Centro Input
4th Floor gamma=1

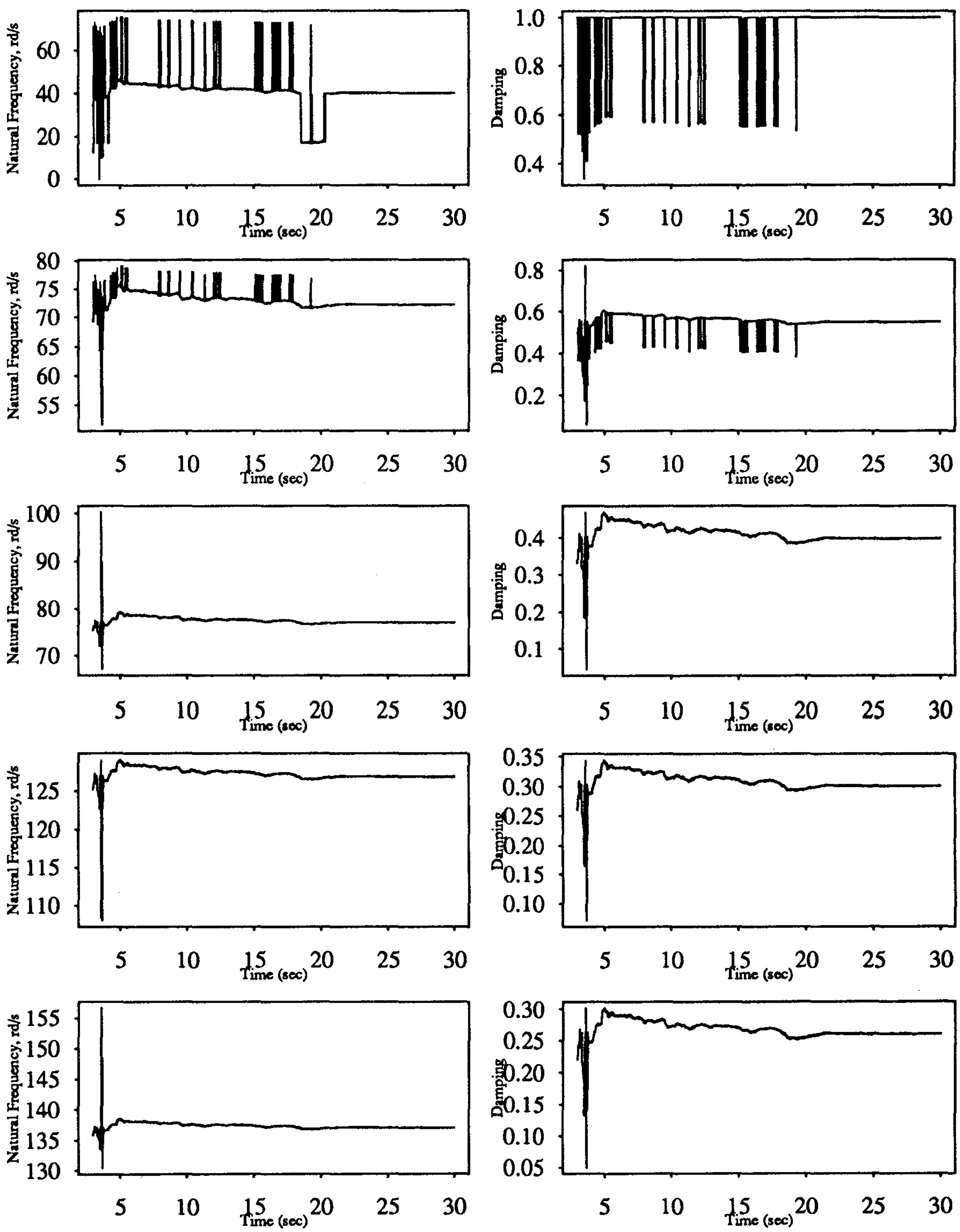


**Figure 5.294**

Recursive Instrumental Variable Estimation
Five Story Building Model; White Noise Input
4th Floor gamma=1

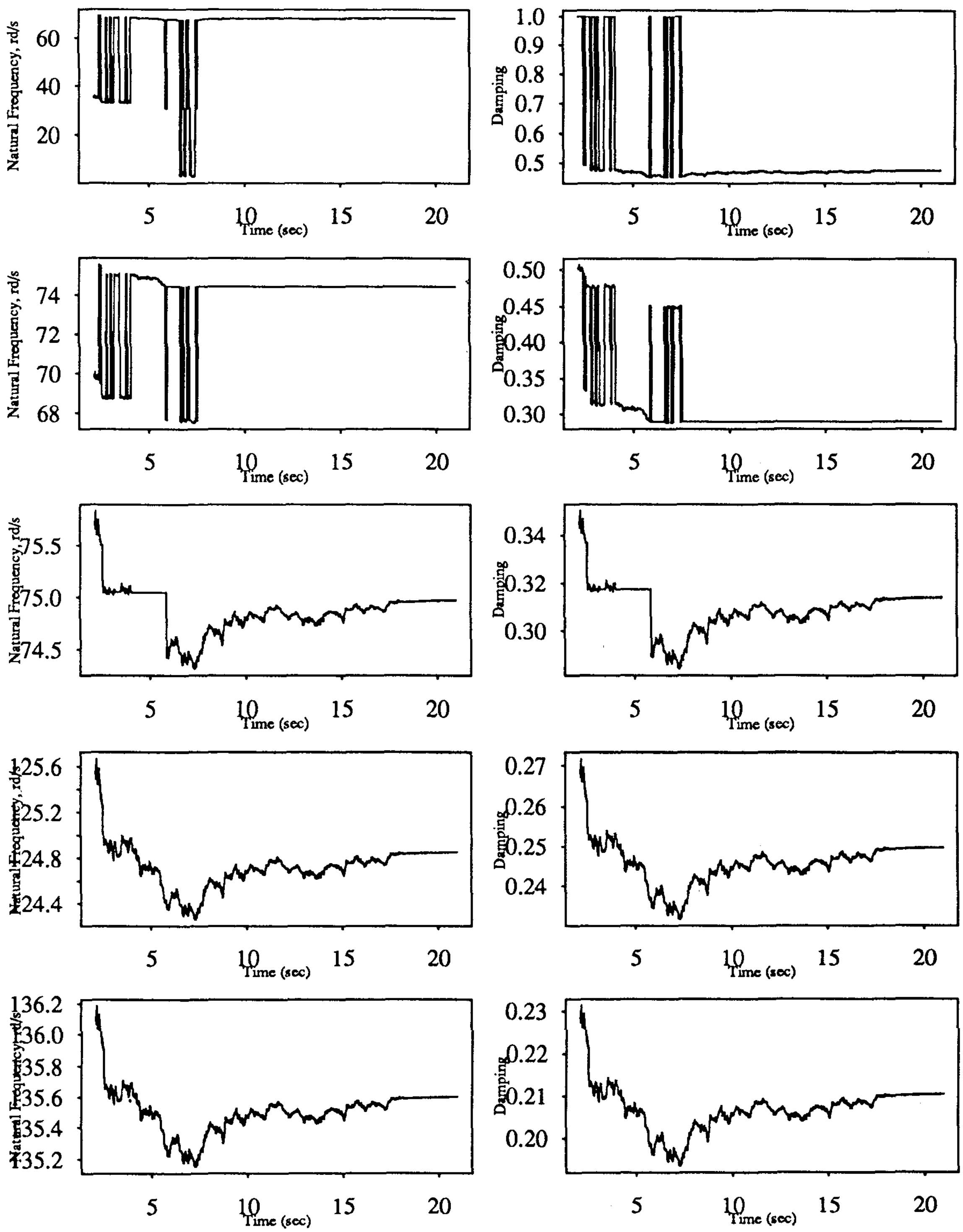


Figure 5.295

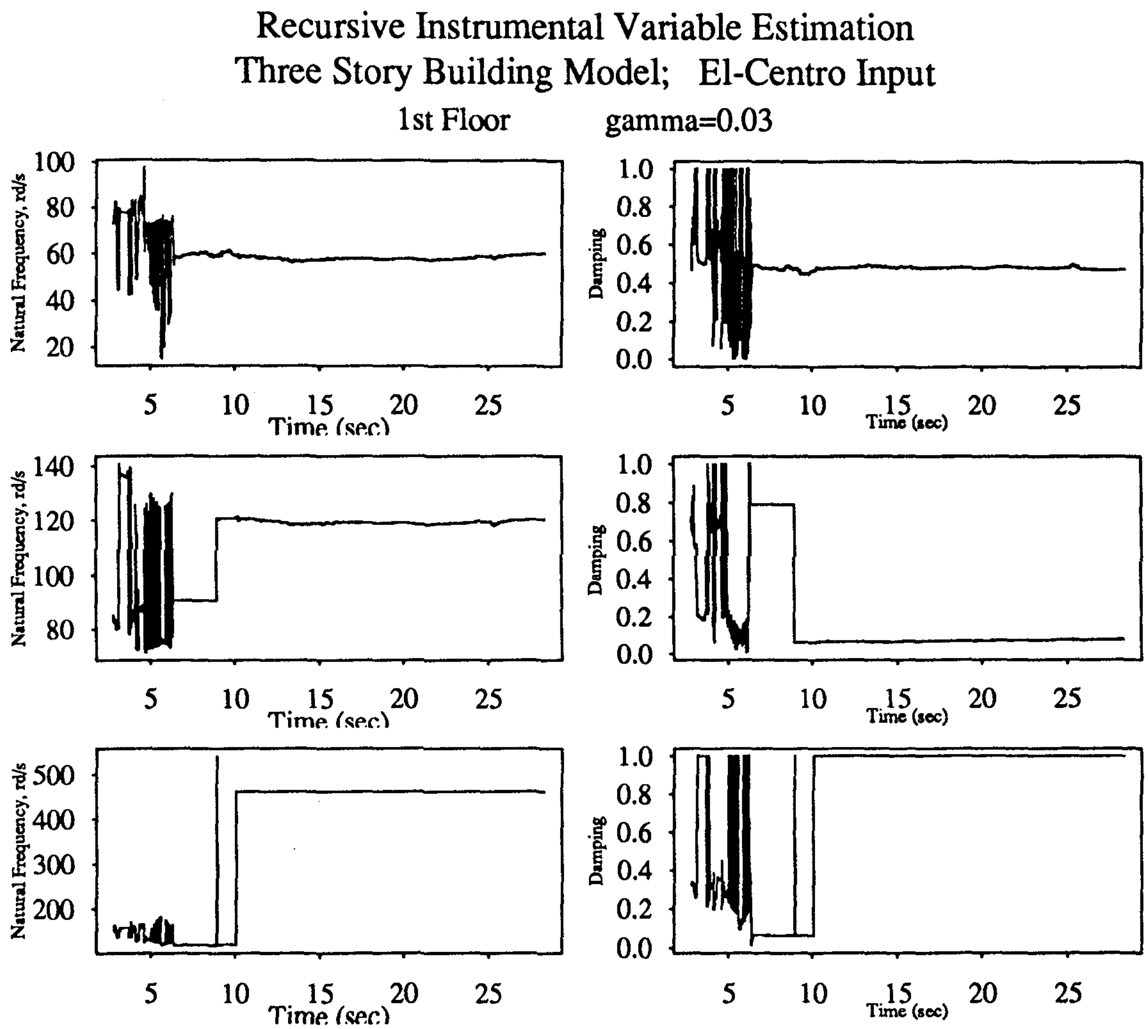
Recursive Instrumental Variable Estimation
Three Story Building Model; El-Centro Input
1st Floor gamma=0.03
Natural Frequency, rd/s
Damping
Time (sec)
100
80
60
40
20
140
120
100
80
500
400
300
200
1.0
0.8
0.6
0.4
0.2
0.0
5
10
15
20
25

**Figure 5.296**

Recursive Instrumental Variable Estimation
Three Story Building Model; White noise Input
1st Floor2 gamma=0.03

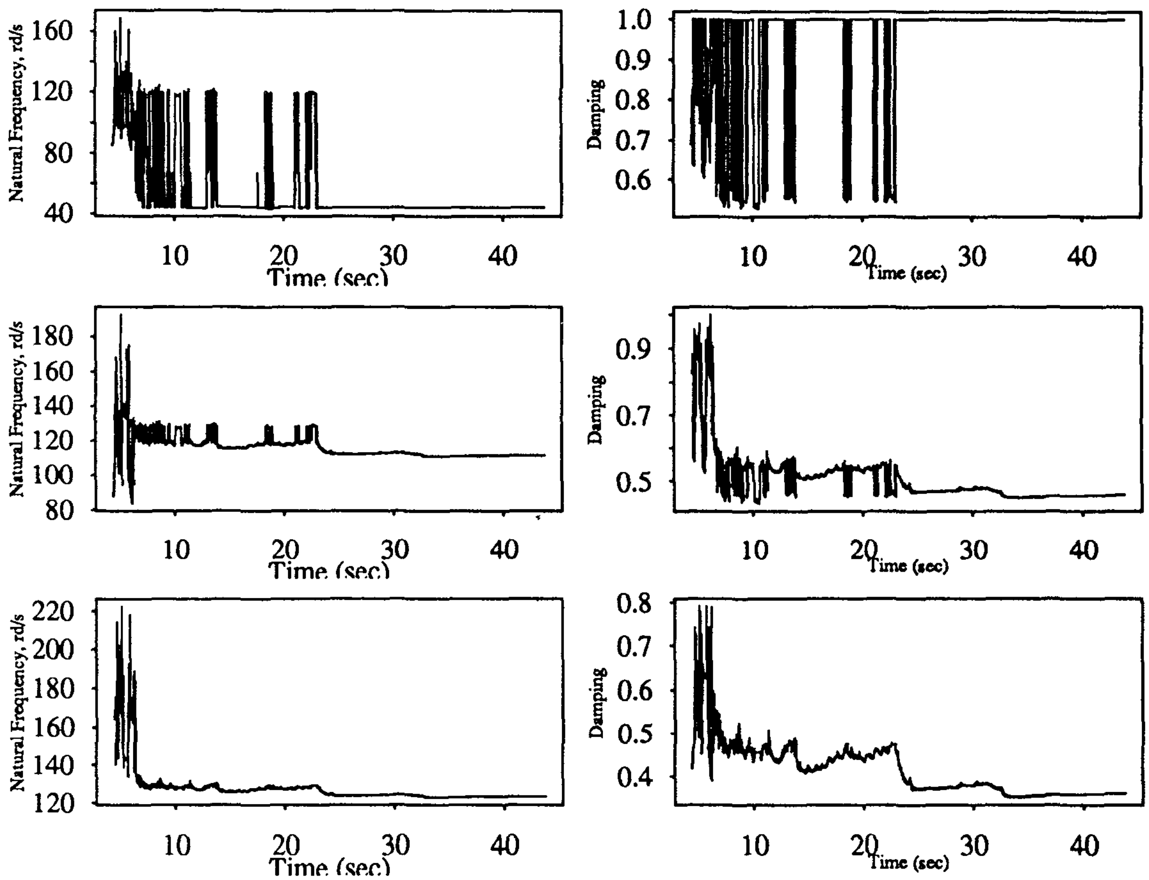


**Figure 5.297**

# Recursive Instrumental Variable Estimation
## Three Story Building Model; El-Centro Input

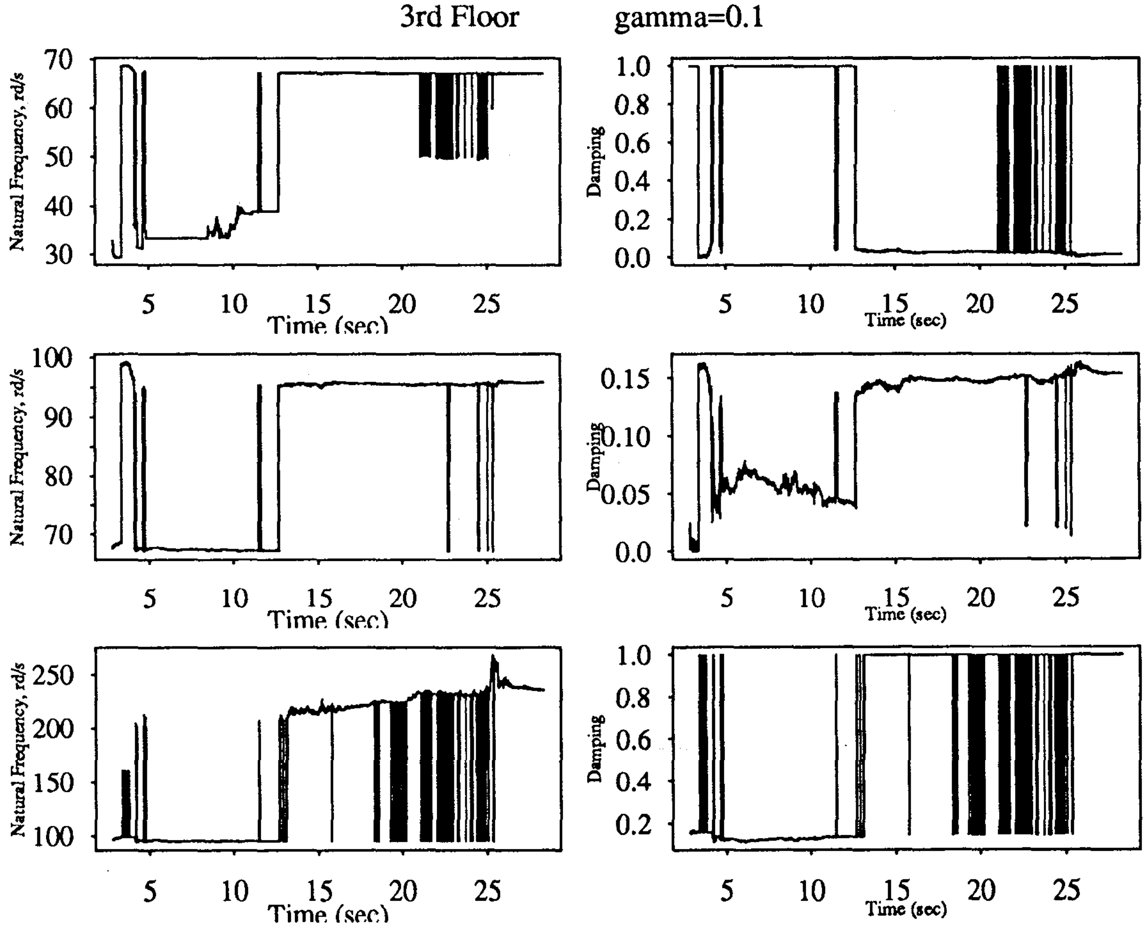


Figure 5.298

Recursive Instrumental Variable Estimation
Three Story Building Model; El-Centro Input
1st Floor gamma=1

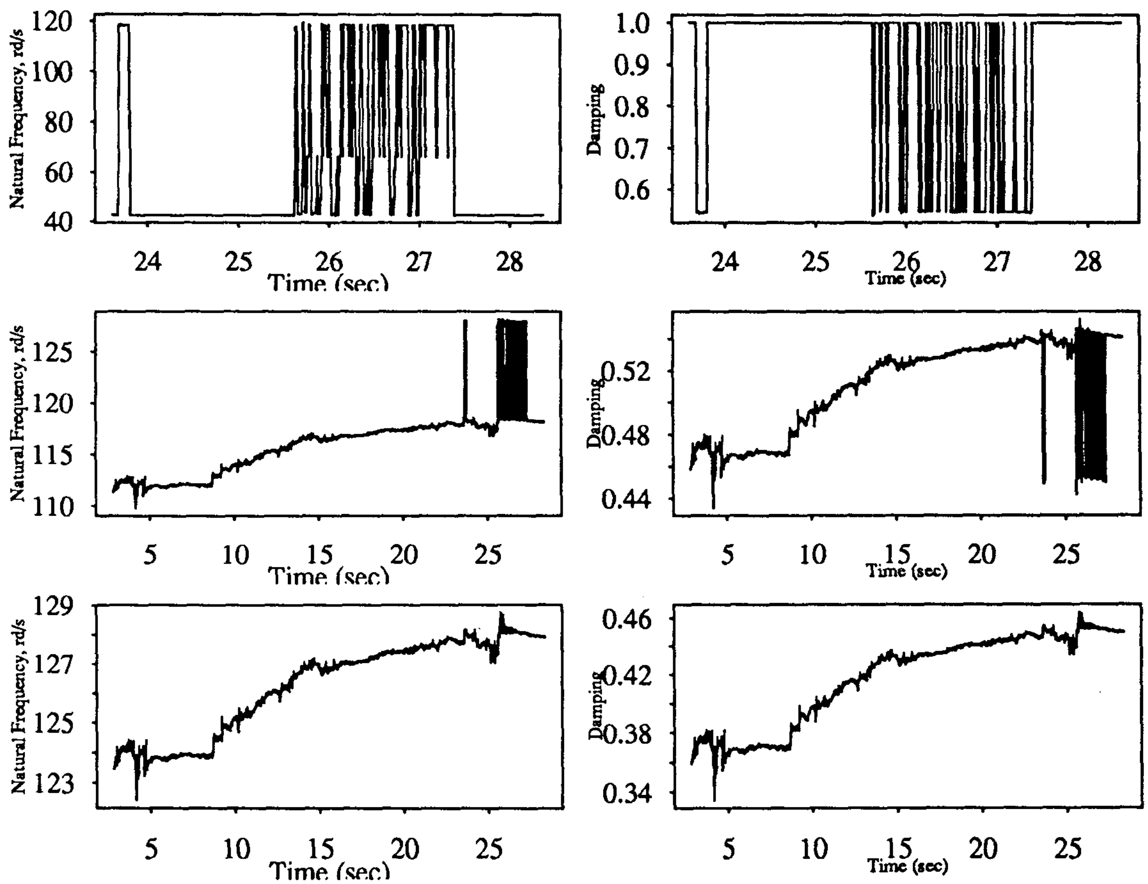


Figure 5.299

Recursive Instrumental Variable Estimation
Three Story Building Model; El-Centro Input
3rd Floor gamma=1

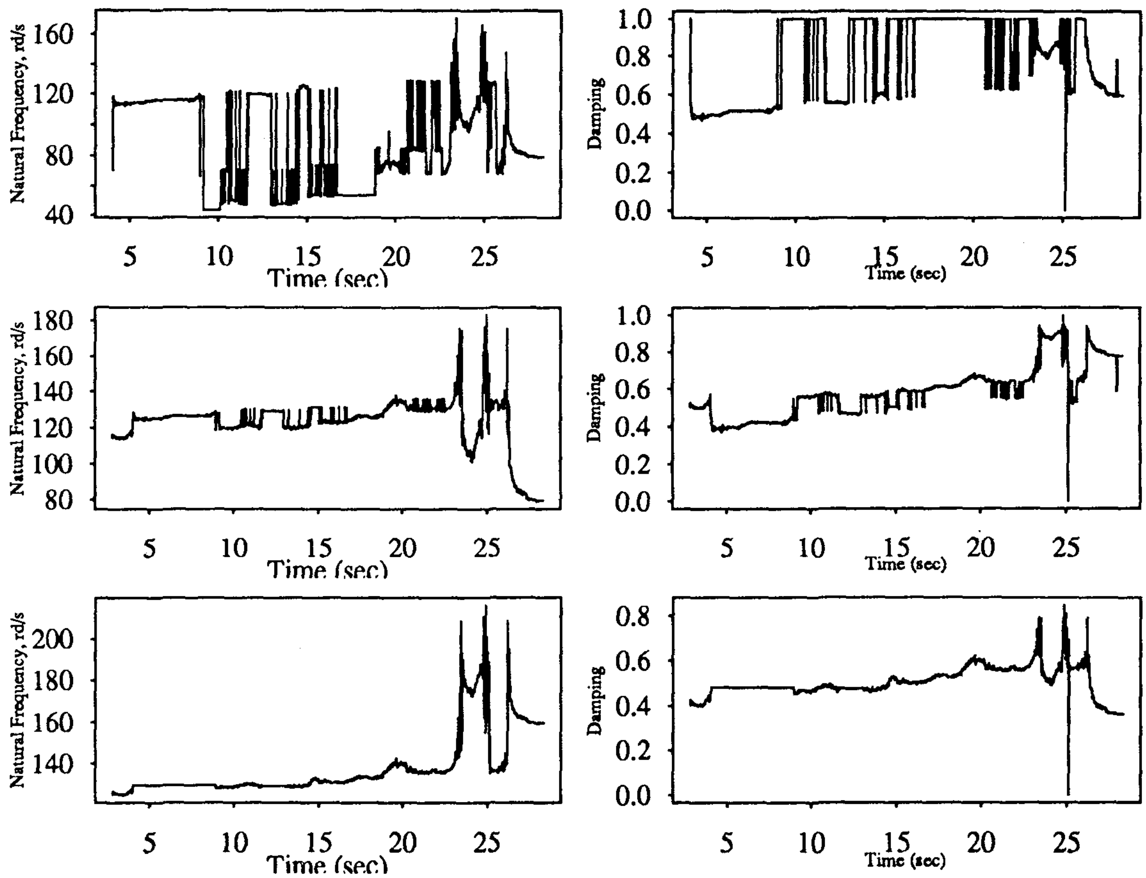


Figure 5.300

Recursive Instrumental Variable Estimation
Three Story Building Model; Sine Sweep Input
2nd Floor gamma=1

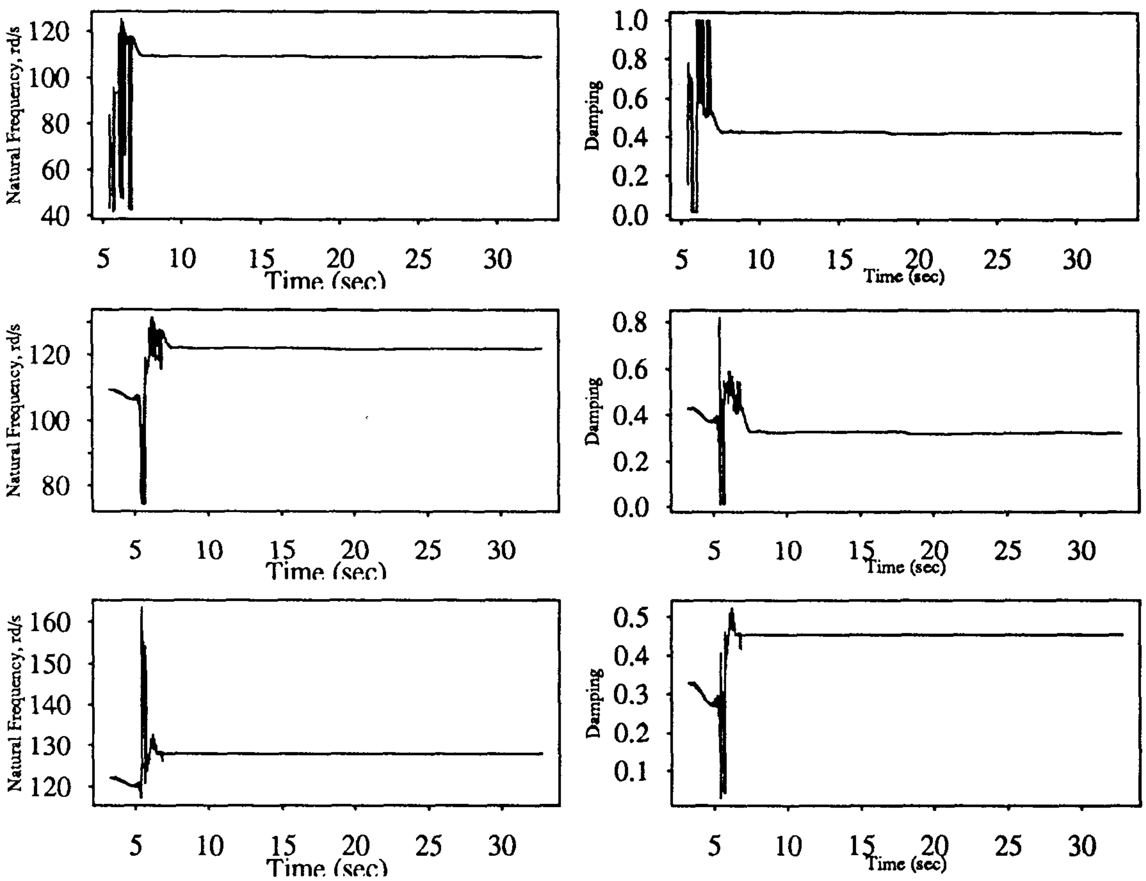


Figure 5.301

Recursive Instrumental Variable Estimation
Three Story Building Model; Sine Sweep Input
3rd Floor gamma=1

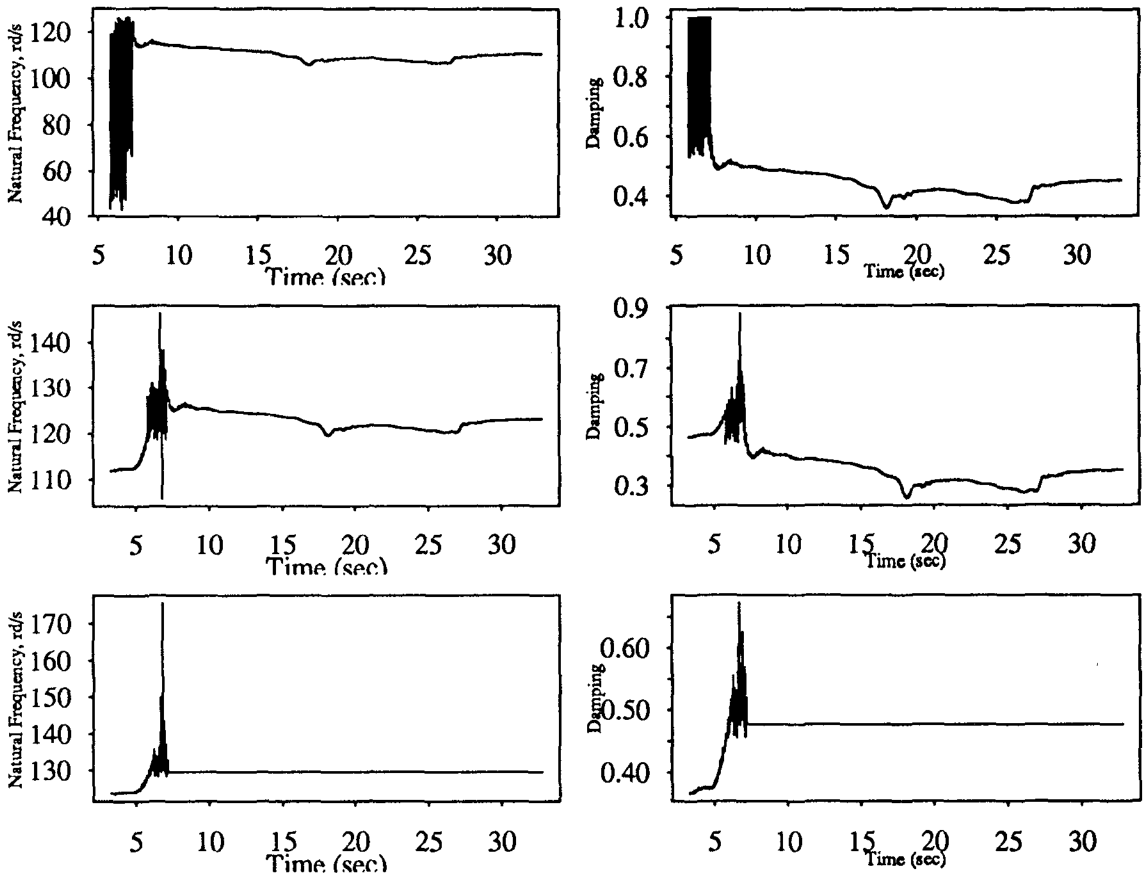


Figure 5.302

**NATIONAL CENTER FOR EARTHQUAKE ENGINEERING RESEARCH**
**LIST OF TECHNICAL REPORTS**

The National Center for Earthquake Engineering Research (NCEER) publishes technical reports on a variety of subjects related to earthquake engineering written by authors funded through NCEER. These reports are available from both NCEER's Publications Department and the National Technical Information Service (NTIS). Requests for reports should be directed to the Publications Department, National Center for Earthquake Engineering Research, State University of New York at Buffalo, Red Jacket Quadrangle, Buffalo, New York 14261. Reports can also be requested through NTIS, 5285 Port Royal Road, Springfield, Virginia 22161. NTIS accession numbers are shown in parenthesis, if available.


NCEER-87-0001 "First-Year Program in Research, Education and Technology Transfer," 3/5/87, (PB88-134275/AS).

NCEER-87-0002 "Experimental Evaluation of Instantaneous Optimal Algorithms for Structural Control," by R.C. Lin, T.T. Soong and A.M. Reinhorn, 4/20/87, (PB88-134341/AS).

NCEER-87-0003 "Experimentation Using the Earthquake Simulation Facilities at University at Buffalo," by A.M. Reinhorn and R.L. Ketter, to be published.

NCEER-87-0004 "The System Characteristics and Performance of a Shaking Table," by J.S. Hwang, K.C. Chang and G.C. Lee, 6/1/87, (PB88-134259/AS). This report is available only through NTIS (see address given above).

NCEER-87-0005 "A Finite Element Formulation for Nonlinear Viscoplastic Material Using a Q Model," by O. Gyebi and G. Dasgupta, 11/2/87, (PB88-213764/AS).

NCEER-87-0006 "Symbolic Manipulation Program (SMP) - Algebraic Codes for Two and Three Dimensional Finite Element Formulations," by X. Lee and G. Dasgupta, 11/9/87, (PB88-219522/AS).

NCEER-87-0007 "Instantaneous Optimal Control Laws for Tall Buildings Under Seismic Excitations," by J.N. Yang, A. Akbarpour and P. Ghaemmaghami, 6/10/87, (PB88-134333/AS).

NCEER-87-0008 "IDARC: Inelastic Damage Analysis of Reinforced Concrete Frame - Shear-Wall Structures," by Y.J. Park, A.M. Reinhorn and S.K. Kunnath, 7/20/87, (PB88-134325/AS).

NCEER-87-0009 "Liquefaction Potential for New York State: A Preliminary Report on Sites in Manhattan and Buffalo," by M. Budhu, V. Vijayakumar, R.F. Giese and L. Baumgras, 8/31/87, (PB88-163704/AS). This report is available only through NTIS (see address given above).

NCEER-87-0010 "Vertical and Torsional Vibration of Foundations in Inhomogeneous Media," by A.S. Veletsos and K.W. Dotson, 6/1/87, (PB88-134291/AS).

NCEER-87-0011 "Seismic Probabilistic Risk Assessment and Seismic Margins Studies for Nuclear Power Plants," by Howard H.M. Hwang, 6/15/87, (PB88-134267/AS).

NCEER-87-0012 "Parametric Studies of Frequency Response of Secondary Systems Under Ground-Acceleration Excitations," by Y. Yong and Y.K. Lin, 6/10/87, (PB88-134309/AS).

NCEER-87-0013 "Frequency Response of Secondary Systems Under Seismic Excitation," by J.A. HoLung, J. Cai and Y.K. Lin, 7/31/87, (PB88-134317/AS).

NCEER-87-0014 "Modelling Earthquake Ground Motions in Seismically Active Regions Using Parametric Time Series Methods," by G.W. Ellis and A.S. Cakmak, 8/25/87, (PB88-134283/AS).

NCEER-87-0015 "Detection and Assessment of Seismic Structural Damage," by E. DiPasquale and A.S. Cakmak, 8/25/87, (PB88-163712/AS).

NCEER-87-0016 "Pipeline Experiment at Parkfield, California," by J. Isenberg and E. Richardson, 9/15/87, (PB88-163720/AS). This report is available only through NTIS (see address given above).

NCEER-87-0017 "Digital Simulation of Seismic Ground Motion," by M. Shinozuka, G. Deodatis and T. Harada, 8/31/87, (PB88-155197/AS). This report is available only through NTIS (see address given above).

NCEER-87-0018 "Practical Considerations for Structural Control: System Uncertainty, System Time Delay and Truncation of Small Control Forces," J.N. Yang and A. Akbarpour, 8/10/87, (PB88-163738/AS).

NCEER-87-0019 "Modal Analysis of Nonclassically Damped Structural Systems Using Canonical Transformation," by J.N. Yang, S. Sarkani and F.X. Long, 9/27/87, (PB88-187851/AS).

NCEER-87-0020 "A Nonstationary Solution in Random Vibration Theory," by J.R. Red-Horse and P.D. Spanos, 11/3/87, (PB88-163746/AS).

NCEER-87-0021 "Horizontal Impedances for Radially Inhomogeneous Viscoelastic Soil Layers," by A.S. Veletsos and K.W. Dotson, 10/15/87, (PB88-150859/AS).

NCEER-87-0022 "Seismic Damage Assessment of Reinforced Concrete Members," by Y.S. Chung, C. Meyer and M. Shinozuka, 10/9/87, (PB88-150867/AS). This report is available only through NTIS (see address given above).

NCEER-87-0023 "Active Structural Control in Civil Engineering," by T.T. Soong, 11/11/87, (PB88-187778/AS).

NCEER-87-0024 Vertical and Torsional Impedances for Radially Inhomogeneous Viscoelastic Soil Layers," by K.W. Dotson and A.S. Veletsos, 12/87, (PB88-187786/AS).

NCEER-87-0025 "Proceedings from the Symposium on Seismic Hazards, Ground Motions, Soil-Liquefaction and Engineering Practice in Eastern North America," October 20-22, 1987, edited by K.H. Jacob, 12/87, (PB88-188115/AS).

NCEER-87-0026 "Report on the Whittier-Narrows, California, Earthquake of October 1, 1987," by J. Pantelic and A. Reinhorn, 11/87, (PB88-187752/AS). This report is available only through NTIS (see address given above).

NCEER-87-0027 "Design of a Modular Program for Transient Nonlinear Analysis of Large 3-D Building Structures," by S. Srivastav and J.F. Abel, 12/30/87, (PB88-187950/AS).

NCEER-87-0028 "Second-Year Program in Research, Education and Technology Transfer," 3/8/88, (PB88-219480/AS).

NCEER-88-0001 "Workshop on Seismic Computer Analysis and Design of Buildings With Interactive Graphics," by W. McGuire, J.F. Abel and C.H. Conley, 1/18/88, (PB88-187760/AS).

NCEER-88-0002 "Optimal Control of Nonlinear Flexible Structures," by J.N. Yang, F.X. Long and D. Wong, 1/22/88, (PB88-213772/AS).

NCEER-88-0003 "Substructuring Techniques in the Time Domain for Primary-Secondary Structural Systems," by G.D. Manolis and G. Juhn, 2/10/88, (PB88-213780/AS).

NCEER-88-0004 "Iterative Seismic Analysis of Primary-Secondary Systems," by A. Singhal, L.D. Lutes and P.D. Spanos, 2/23/88, (PB88-213798/AS).

NCEER-88-0005 "Stochastic Finite Element Expansion for Random Media," by P.D. Spanos and R. Ghanem, 3/14/88, (PB88-213806/AS).

NCEER-88-0006 "Combining Structural Optimization and Structural Control," by F.Y. Cheng and C.P. Pantelides, 1/10/88, (PB88-213814/AS).

NCEER-88-0007 "Seismic Performance Assessment of Code-Designed Structures," by H.H-M. Hwang, J-W. Jaw and H-J. Shau, 3/20/88, (PB88-219423/AS).

NCEER-88-0008 "Reliability Analysis of Code-Designed Structures Under Natural Hazards," by H.H-M. Hwang, H. Ushiba and M. Shinozuka, 2/29/88, (PB88-229471/AS).

NCEER-88-0009 "Seismic Fragility Analysis of Shear Wall Structures," by J-W Jaw and H.H-M. Hwang, 4/30/88, (PB89-102867/AS).

NCEER-88-0010 "Base Isolation of a Multi-Story Building Under a Harmonic Ground Motion - A Comparison of Performances of Various Systems," by F-G Fan, G. Ahmadi and I.G. Tadjbakhsh, 5/18/88, (PB89-122238/AS).

NCEER-88-0011 "Seismic Floor Response Spectra for a Combined System by Green's Functions," by F.M. Lavelle, L.A. Bergman and P.D. Spanos, 5/1/88, (PB89-102875/AS).

NCEER-88-0012 "A New Solution Technique for Randomly Excited Hysteretic Structures," by G.Q. Cai and Y.K. Lin, 5/16/88, (PB89-102883/AS).

NCEER-88-0013 "A Study of Radiation Damping and Soil-Structure Interaction Effects in the Centrifuge," by K. Weissman, supervised by J.H. Prevost, 5/24/88, (PB89-144703/AS).

NCEER-88-0014 "Parameter Identification and Implementation of a Kinematic Plasticity Model for Frictional Soils," by J.H. Prevost and D.V. Griffiths, to be published.

NCEER-88-0015 "Two- and Three- Dimensional Dynamic Finite Element Analyses of the Long Valley Dam," by D.V. Griffiths and J.H. Prevost, 6/17/88, (PB89-144711/AS).

NCEER-88-0016 "Damage Assessment of Reinforced Concrete Structures in Eastern United States," by A.M. Reinhorn, M.J. Seidel, S.K. Kunnath and Y.J. Park, 6/15/88, (PB89-122220/AS).

NCEER-88-0017 "Dynamic Compliance of Vertically Loaded Strip Foundations in Multilayered Viscoelastic Soils," by S. Ahmad and A.S.M. Israil, 6/17/88, (PB89-102891/AS).

NCEER-88-0018 "An Experimental Study of Seismic Structural Response With Added Viscoelastic Dampers," by R.C. Lin, Z. Liang, T.T. Soong and R.H. Zhang, 6/30/88, (PB89-122212/AS).

NCEER-88-0019 "Experimental Investigation of Primary - Secondary System Interaction," by G.D. Manolis, G. Juhn and A.M. Reinhorn, 5/27/88, (PB89-122204/AS).

NCEER-88-0020 "A Response Spectrum Approach For Analysis of Nonclassically Damped Structures," by J.N. Yang, S. Sarkani and F.X. Long, 4/22/88, (PB89-102909/AS).

NCEER-88-0021 "Seismic Interaction of Structures and Soils: Stochastic Approach," by A.S. Veletsos and A.M. Prasad, 7/21/88, (PB89-122196/AS).

NCEER-88-0022 "Identification of the Serviceability Limit State and Detection of Seismic Structural Damage," by E. DiPasquale and A.S. Cakmak, 6/15/88, (PB89-122188/AS).

NCEER-88-0023 "Multi-Hazard Risk Analysis: Case of a Simple Offshore Structure," by B.K. Bhartia and E.H. Vanmarcke, 7/21/88, (PB89-145213/AS).

NCEER-88-0024 "Automated Seismic Design of Reinforced Concrete Buildings," by Y.S. Chung, C. Meyer and M. Shinozuka, 7/5/88, (PB89-122170/AS).

NCEER-88-0025 "Experimental Study of Active Control of MDOF Structures Under Seismic Excitations," by L.L. Chung, R.C. Lin, T.T. Soong and A.M. Reinhorn, 7/10/88, (PB89-122600/AS).

NCEER-88-0026 "Earthquake Simulation Tests of a Low-Rise Metal Structure," by J.S. Hwang, K.C. Chang, G.C. Lee and R.L. Ketter, 8/1/88, (PB89-102917/AS).

NCEER-88-0027 "Systems Study of Urban Response and Reconstruction Due to Catastrophic Earthquakes," by F. Kozin and H.K. Zhou, 9/22/88, (PB90-162348/AS).

NCEER-88-0028 "Seismic Fragility Analysis of Plane Frame Structures," by H.H-M. Hwang and Y.K. Low, 7/31/88, (PB89-131445/AS).

NCEER-88-0029 "Response Analysis of Stochastic Structures," by A. Kardara, C. Bucher and M. Shinozuka, 9/22/88, (PB89-174429/AS).

NCEER-88-0030 "Nonnormal Accelerations Due to Yielding in a Primary Structure," by D.C.K. Chen and L.D. Lutes, 9/19/88, (PB89-131437/AS).

NCEER-88-0031 "Design Approaches for Soil-Structure Interaction," by A.S. Veletsos, A.M. Prasad and Y. Tang, 12/30/88, (PB89-174437/AS).

NCEER-88-0032 "A Re-evaluation of Design Spectra for Seismic Damage Control," by C.J. Turkstra and A.G. Tallin, 11/7/88, (PB89-145221/AS).

NCEER-88-0033 "The Behavior and Design of Noncontact Lap Splices Subjected to Repeated Inelastic Tensile Loading," by V.E. Sagan, P. Gergely and R.N. White, 12/8/88, (PB89-163737/AS).

NCEER-88-0034 "Seismic Response of Pile Foundations," by S.M. Mamoon, P.K. Banerjee and S. Ahmad, 11/1/88, (PB89-145239/AS).

NCEER-88-0035 "Modeling of R/C Building Structures With Flexible Floor Diaphragms (IDARC2)," by A.M. Reinhorn, S.K. Kunnath and N. Panahshahi, 9/7/88, (PB89-207153/AS).

NCEER-88-0036 "Solution of the Dam-Reservoir Interaction Problem Using a Combination of FEM, BEM with Particular Integrals, Modal Analysis, and Substructuring," by C-S. Tsai, G.C. Lee and R.L. Ketter, 12/31/88, (PB89-207146/AS).

NCEER-88-0037 "Optimal Placement of Actuators for Structural Control," by F.Y. Cheng and C.P. Pantelides, 8/15/88, (PB89-162846/AS).

NCEER-88-0038 "Teflon Bearings in Aseismic Base Isolation: Experimental Studies and Mathematical Modeling," by A. Mokha, M.C. Constantinou and A.M. Reinhorn, 12/5/88, (PB89-218457/AS).

NCEER-88-0039 "Seismic Behavior of Flat Slab High-Rise Buildings in the New York City Area," by P. Weidlinger and M. Ettouney, 10/15/88, (PB90-145681/AS).

NCEER-88-0040 "Evaluation of the Earthquake Resistance of Existing Buildings in New York City," by P. Weidlinger and M. Ettouney, 10/15/88, to be published.

NCEER-88-0041 "Small-Scale Modeling Techniques for Reinforced Concrete Structures Subjected to Seismic Loads," by W. Kim, A. El-Attar and R.N. White, 11/22/88, (PB89-189625/AS).

NCEER-88-0042 "Modeling Strong Ground Motion from Multiple Event Earthquakes," by G.W. Ellis and A.S. Cakmak, 10/15/88, (PB89-174445/AS).

NCEER-88-0043 "Nonstationary Models of Seismic Ground Acceleration," by M. Grigoriu, S.E. Ruiz and E. Rosenblueth, 7/15/88, (PB89-189617/AS).

NCEER-88-0044 "SARCF User's Guide: Seismic Analysis of Reinforced Concrete Frames," by Y.S. Chung, C. Meyer and M. Shinozuka, 11/9/88, (PB89-174452/AS).

NCEER-88-0045 "First Expert Panel Meeting on Disaster Research and Planning," edited by J. Pantelic and J. Stoyle, 9/15/88, (PB89-174460/AS).

NCEER-88-0046 "Preliminary Studies of the Effect of Degrading Infill Walls on the Nonlinear Seismic Response of Steel Frames," by C.Z. Chrysostomou, P. Gergely and J.F. Abel, 12/19/88, (PB89-208383/AS).

| | |
|---|---|
| NCEER-88-0047 | "Reinforced Concrete Frame Component Testing Facility - Design, Construction, Instrumentation and Operation," by S.P. Pessiki, C. Conley, T. Bond, P. Gergely and R.N. White, 12/16/88, (PB89-174478/AS). |
| NCEER-89-0001 | "Effects of Protective Cushion and Soil Compliancy on the Response of Equipment Within a Seismically Excited Building," by J.A. HoLung, 2/16/89, (PB89-207179/AS). |
| NCEER-89-0002 | "Statistical Evaluation of Response Modification Factors for Reinforced Concrete Structures," by H.H-M. Hwang and J-W. Jaw, 2/17/89, (PB89-207187/AS). |
| NCEER-89-0003 | "Hysteretic Columns Under Random Excitation," by G-Q. Cai and Y.K. Lin, 1/9/89, (PB89-196513/AS). |
| NCEER-89-0004 | "Experimental Study of 'Elephant Foot Bulge' Instability of Thin-Walled Metal Tanks," by Z-H. Jia and R.L. Ketter, 2/22/89, (PB89-207195/AS). |
| NCEER-89-0005 | "Experiment on Performance of Buried Pipelines Across San Andreas Fault," by J. Isenberg, E. Richardson and T.D. O'Rourke, 3/10/89, (PB89-218440/AS). |
| NCEER-89-0006 | "A Knowledge-Based Approach to Structural Design of Earthquake-Resistant Buildings," by M. Subramani, P. Gergely, C.H. Conley, J.F. Abel and A.H. Zaghw, 1/15/89, (PB89-218465/AS). |
| NCEER-89-0007 | "Liquefaction Hazards and Their Effects on Buried Pipelines," by T.D. O'Rourke and P.A. Lane, 2/1/89, (PB89-218481). |
| NCEER-89-0008 | "Fundamentals of System Identification in Structural Dynamics," by H. Imai, C-B. Yun, O. Maruyama and M. Shinozuka, 1/26/89, (PB89-207211/AS). |
| NCEER-89-0009 | "Effects of the 1985 Michoacan Earthquake on Water Systems and Other Buried Lifelines in Mexico," by A.G. Ayala and M.J. O'Rourke, 3/8/89, (PB89-207229/AS). |
| NCEER-89-R010 | "NCEER Bibliography of Earthquake Education Materials," by K.E.K. Ross, Second Revision, 9/1/89, (PB90-125352/AS). |
| NCEER-89-0011 | "Inelastic Three-Dimensional Response Analysis of Reinforced Concrete Building Structures (IDARC-3D), Part I - Modeling," by S.K. Kunnath and A.M. Reinhorn, 4/17/89, (PB90-114612/AS). |
| NCEER-89-0012 | "Recommended Modifications to ATC-14," by C.D. Poland and J.O. Malley, 4/12/89, (PB90-108648/AS). |
| NCEER-89-0013 | "Repair and Strengthening of Beam-to-Column Connections Subjected to Earthquake Loading," by M. Corazao and A.J. Durrani, 2/28/89, (PB90-109885/AS). |
| NCEER-89-0014 | "Program EXKAL2 for Identification of Structural Dynamic Systems," by O. Maruyama, C-B. Yun, M. Hoshiya and M. Shinozuka, 5/19/89, (PB90-109877/AS). |
| NCEER-89-0015 | "Response of Frames With Bolted Semi-Rigid Connections, Part I - Experimental Study and Analytical Predictions," by P.J. DiCorso, A.M. Reinhorn, J.R. Dickerson, J.B. Radziminski and W.L. Harper, 6/1/89, to be published. |
| NCEER-89-0016 | "ARMA Monte Carlo Simulation in Probabilistic Structural Analysis," by P.D. Spanos and M.P. Mignolet, 7/10/89, (PB90-109893/AS). |
| NCEER-89-P017 | "Preliminary Proceedings from the Conference on Disaster Preparedness - The Place of Earthquake Education in Our Schools," Edited by K.E.K. Ross, 6/23/89. |
| NCEER-89-0017 | "Proceedings from the Conference on Disaster Preparedness - The Place of Earthquake Education in Our Schools," Edited by K.E.K. Ross, 12/31/89, (PB90-207895). |

NCEER-89-0018 "Multidimensional Models of Hysteretic Material Behavior for Vibration Analysis of Shape Memory Energy Absorbing Devices, by E.J. Graesser and F.A. Cozzarelli, 6/7/89, (PB90-164146/AS).

NCEER-89-0019 "Nonlinear Dynamic Analysis of Three-Dimensional Base Isolated Structures (3D-BASIS)," by S. Nagarajaiah, A.M. Reinhorn and M.C. Constantinou, 8/3/89, (PB90-161936/AS).

NCEER-89-0020 "Structural Control Considering Time-Rate of Control Forces and Control Rate Constraints," by F.Y. Cheng and C.P. Pantelides, 8/3/89, (PB90-120445/AS).

NCEER-89-0021 "Subsurface Conditions of Memphis and Shelby County," by K.W. Ng, T-S. Chang and H-H.M. Hwang, 7/26/89, (PB90-120437/AS).

NCEER-89-0022 "Seismic Wave Propagation Effects on Straight Jointed Buried Pipelines," by K. Elhmadi and M.J. O'Rourke, 8/24/89, (PB90-162322/AS).

NCEER-89-0023 "Workshop on Serviceability Analysis of Water Delivery Systems," edited by M. Grigoriu, 3/6/89, (PB90-127424/AS).

NCEER-89-0024 "Shaking Table Study of a 1/5 Scale Steel Frame Composed of Tapered Members," by K.C. Chang, J.S. Hwang and G.C. Lee, 9/18/89, (PB90-160169/AS).

NCEER-89-0025 "DYNA1D: A Computer Program for Nonlinear Seismic Site Response Analysis - Technical Documentation," by Jean H. Prevost, 9/14/89, (PB90-161944/AS).

NCEER-89-0026 "1:4 Scale Model Studies of Active Tendon Systems and Active Mass Dampers for Aseismic Protection," by A.M. Reinhorn, T.T. Soong, R.C. Lin, Y.P. Yang, Y. Fukao, H. Abe and M. Nakai, 9/15/89, (PB90-173246/AS).

NCEER-89-0027 "Scattering of Waves by Inclusions in a Nonhomogeneous Elastic Half Space Solved by Boundary Element Methods," by P.K. Hadley, A. Askar and A.S. Cakmak, 6/15/89, (PB90-145699/AS).

NCEER-89-0028 "Statistical Evaluation of Deflection Amplification Factors for Reinforced Concrete Structures," by H.H.M. Hwang, J-W. Jaw and A.L. Ch'ng, 8/31/89, (PB90-164633/AS).

NCEER-89-0029 "Bedrock Accelerations in Memphis Area Due to Large New Madrid Earthquakes," by H.H.M. Hwang, C.H.S. Chen and G. Yu, 11/7/89, (PB90-162330/AS).

NCEER-89-0030 "Seismic Behavior and Response Sensitivity of Secondary Structural Systems," by Y.Q. Chen and T.T. Soong, 10/23/89, (PB90-164658/AS).

NCEER-89-0031 "Random Vibration and Reliability Analysis of Primary-Secondary Structural Systems," by Y. Ibrahim, M. Grigoriu and T.T. Soong, 11/10/89, (PB90-161951/AS).

NCEER-89-0032 "Proceedings from the Second U.S. - Japan Workshop on Liquefaction, Large Ground Deformation and Their Effects on Lifelines, September 26-29, 1989," Edited by T.D. O'Rourke and M. Hamada, 12/1/89, (PB90-209388/AS).

NCEER-89-0033 "Deterministic Model for Seismic Damage Evaluation of Reinforced Concrete Structures," by J.M. Bracci, A.M. Reinhorn, J.B. Mander and S.K. Kunnath, 9/27/89.

NCEER-89-0034 "On the Relation Between Local and Global Damage Indices," by E. DiPasquale and A.S. Cakmak, 8/15/89, (PB90-173865).

NCEER-89-0035 "Cyclic Undrained Behavior of Nonplastic and Low Plasticity Silts," by A.J. Walker and H.E. Stewart, 7/26/89, (PB90-183518/AS).

NCEER-89-0036 "Liquefaction Potential of Surficial Deposits in the City of Buffalo, New York," by M. Budhu, R. Giese and L. Baumgrass, 1/17/89, (PB90-208455/AS).

NCEER-89-0037 "A Determinstic Assessment of Effects of Ground Motion Incoherence," by A.S. Veletsos and Y. Tang, 7/15/89, (PB90-164294/AS).

NCEER-89-0038 "Workshop on Ground Motion Parameters for Seismic Hazard Mapping," July 17-18, 1989, edited by R.V. Whitman, 12/1/89, (PB90-173923/AS).

NCEER-89-0039 "Seismic Effects on Elevated Transit Lines of the New York City Transit Authority," by C.J. Costantino, C.A. Miller and E. Heymsfield, 12/26/89, (PB90-207887/AS).

NCEER-89-0040 "Centrifugal Modeling of Dynamic Soil-Structure Interaction," by K. Weissman, Supervised by J.H. Prevost, 5/10/89, (PB90-207879/AS).

NCEER-89-0041 "Linearized Identification of Buildings With Cores for Seismic Vulnerability Assessment," by I-K. Ho and A.E. Aktan, 11/1/89, (PB90-251943/AS).

NCEER-90-0001 "Geotechnical and Lifeline Aspects of the October 17, 1989 Loma Prieta Earthquake in San Francisco," by T.D. O'Rourke, H.E. Stewart, F.T. Blackburn and T.S. Dickerman, 1/90, (PB90-208596/AS).

NCEER-90-0002 "Nonnormal Secondary Response Due to Yielding in a Primary Structure," by D.C.K. Chen and L.D. Lutes, 2/28/90, (PB90-251976/AS).

NCEER-90-0003 "Earthquake Education Materials for Grades K-12," by K.E.K. Ross, 4/16/90, (PB91-113415/AS).

NCEER-90-0004 "Catalog of Strong Motion Stations in Eastern North America," by R.W. Busby, 4/3/90, (PB90-251984)/AS.

NCEER-90-0005 "NCEER Strong-Motion Data Base: A User Manuel for the GeoBase Release (Version 1.0 for the Sun3)," by P. Friberg and K. Jacob, 3/31/90 (PB90-258062/AS).

NCEER-90-0006 "Seismic Hazard Along a Crude Oil Pipeline in the Event of an 1811-1812 Type New Madrid Earthquake," by H.H.M. Hwang and C-H.S. Chen, 4/16/90(PB90-258054).

NCEER-90-0007 "Site-Specific Response Spectra for Memphis Sheahan Pumping Station," by H.H.M. Hwang and C.S. Lee, 5/15/90, (PB91-108811/AS).

NCEER-90-0008 "Pilot Study on Seismic Vulnerability of Crude Oil Transmission Systems," by T. Ariman, R. Dobry, M. Grigoriu, F. Kozin, M. O'Rourke, T. O'Rourke and M. Shinozuka, 5/25/90, (PB91-108837/AS).

NCEER-90-0009 "A Program to Generate Site Dependent Time Histories: EQGEN," by G.W. Ellis, M. Srinivasan and A.S. Cakmak, 1/30/90, (PB91-108829/AS).

NCEER-90-0010 "Active Isolation for Seismic Protection of Operating Rooms," by M.E. Talbott, Supervised by M. Shinozuka, 6/8/9, (PB91-110205/AS).

NCEER-90-0011 "Program LINEARID for Identification of Linear Structural Dynamic Systems," by C-B. Yun and M. Shinozuka, 6/25/90, (PB91-110312/AS).

NCEER-90-0012 "Two-Dimensional Two-Phase Elasto-Plastic Seismic Response of Earth Dams," by A.N. Yiagos, Supervised by J.H. Prevost, 6/20/90, (PB91-110197/AS).

NCEER-90-0013 "Secondary Systems in Base-Isolated Structures: Experimental Investigation, Stochastic Response and Stochastic Sensitivity," by G.D. Manolis, G. Juhn, M.C. Constantinou and A.M. Reinhorn, 7/1/90, (PB91-110320/AS).

NCEER-90-0014 "Seismic Behavior of Lightly-Reinforced Concrete Column and Beam-Column Joint Details," by S.P. Pessiki, C.H. Conley, P. Gergely and R.N. White, 8/22/90, (PB91-108795/AS).

NCEER-90-0015 "Two Hybrid Control Systems for Building Structures Under Strong Earthquakes," by J.N. Yang and A. Danielians, 6/29/90, (PB91-125393/AS).

NCEER-90-0016 "Instantaneous Optimal Control with Acceleration and Velocity Feedback," by J.N. Yang and Z. Li, 6/29/90, (PB91-125401/AS).

NCEER-90-0017 "Reconnaissance Report on the Northern Iran Earthquake of June 21, 1990," by M. Mehrain, 10/4/90, (PB91-125377/AS).

NCEER-90-0018 "Evaluation of Liquefaction Potential in Memphis and Shelby County," by T.S. Chang, P.S. Tang, C.S. Lee and H. Hwang, 8/10/90, (PB91-125427/AS).

NCEER-90-0019 "Experimental and Analytical Study of a Combined Sliding Disc Bearing and Helical Steel Spring Isolation System," by M.C. Constantinou, A.S. Mokha and A.M. Reinhorn, 10/4/90, (PB91-125385/AS).

NCEER-90-0020 "Experimental Study and Analytical Prediction of Earthquake Response of a Sliding Isolation System with a Spherical Surface," by A.S. Mokha, M.C. Constantinou and A.M. Reinhorn, 10/11/90, (PB91-125419/AS).

NCEER-90-0021 "Dynamic Interaction Factors for Floating Pile Groups," by G. Gazetas, K. Fan, A. Kaynia and E. Kausel, 9/10/90, (PB91-170381/AS).

NCEER-90-0022 "Evaluation of Seismic Damage Indices for Reinforced Concrete Structures," by S. Rodríguez-Gómez and A.S. Cakmak, 9/30/90, PB91-171322/AS).

NCEER-90-0023 "Study of Site Response at a Selected Memphis Site," by H. Desai, S. Ahmad, E.S. Gazetas and M.R. Oh, 10/11/90, (PB91-196857/AS).

NCEER-90-0024 "A User's Guide to Strongmo: Version 1.0 of NCEER's Strong-Motion Data Access Tool for PCs and Terminals," by P.A. Friberg and C.A.T. Susch, 11/15/90, (PB91-171272/AS).

NCEER-90-0025 "A Three-Dimensional Analytical Study of Spatial Variability of Seismic Ground Motions," by L-L. Hong and A.H.-S. Ang, 10/30/90, (PB91-170399/AS).

NCEER-90-0026 "MUMOID User's Guide - A Program for the Identification of Modal Parameters," by S. Rodríguez-Gómez and E. DiPasquale, 9/30/90, (PB91-171298/AS).

NCEER-90-0027 "SARCF-II User's Guide - Seismic Analysis of Reinforced Concrete Frames," by S. Rodríguez-Gómez, Y.S. Chung and C. Meyer, 9/30/90, (PB91-171280/AS).

NCEER-90-0028 "Viscous Dampers: Testing, Modeling and Application in Vibration and Seismic Isolation," by N. Makris and M.C. Constantinou, 12/20/90 (PB91-190561/AS).

NCEER-90-0029 "Soil Effects on Earthquake Ground Motions in the Memphis Area," by H. Hwang, C.S. Lee, K.W. Ng and T.S. Chang, 8/2/90, (PB91-190751/AS).

NCEER-91-0001 "Proceedings from the Third Japan-U.S. Workshop on Earthquake Resistant Design of Lifeline Facilities and Countermeasures for Soil Liquefaction, December 17-19, 1990," edited by T.D. O'Rourke and M. Hamada, 2/1/91, (PB91-179259/AS).

NCEER-91-0002 "Physical Space Solutions of Non-Proportionally Damped Systems," by M. Tong, Z. Liang and G.C. Lee, 1/15/91, (PB91-179242/AS).

NCEER-91-0003 "Kinematic Seismic Response of Single Piles and Pile Groups," by K. Fan, G. Gazetas, A. Kaynia, E. Kausel and S. Ahmad, 1/10/91, to be published.

NCEER-91-0004 "Theory of Complex Damping," by Z. Liang and G. Lee, to be published.

NCEER-91-0005 "3D-BASIS - Nonlinear Dynamic Analysis of Three Dimensional Base Isolated Structures: Part II," by S. Nagarajaiah, A.M. Reinhorn and M.C. Constantinou, 2/28/91, (PB91-190553/AS).

NCEER-91-0006 "A Multidimensional Hysteretic Model for Plasticity Deforming Metals in Energy Absorbing Devices," by E.J. Graesser and F.A. Cozzarelli, 4/9/91.

NCEER-91-0007 "A Framework for Customizable Knowledge-Based Expert Systems with an Application to a KBES for Evaluating the Seismic Resistance of Existing Buildings," by E.G. Ibarra-Anaya and S.J. Fenves, 4/9/91, (PB91-210930/AS).

NCEER-91-0008 "Nonlinear Analysis of Steel Frames with Semi-Rigid Connections Using the Capacity Spectrum Method," by G.G. Deierlein, S-H. Hsieh, Y-J. Shen and J.F. Abel, 7/2/91, (PB92-113828/AS).

NCEER-91-0009 "Earthquake Education Materials for Grades K-12," by K.E.K. Ross, 4/30/91, (PB91-212142/AS).

NCEER-91-0010 "Phase Wave Velocities and Displacement Phase Differences in a Harmonically Oscillating Pile," by N. Makris and G. Gazetas, 7/8/91, (PB92-108356/AS).

NCEER-91-0011 "Dynamic Characteristics of a Full-Sized Five-Story Steel Structure and a 2/5 Model," by K.C. Chang, G.C. Yao, G.C. Lee, D.S. Hao and Y.C. Yeh," to be published.

NCEER-91-0012 "Seismic Response of a 2/5 Scale Steel Structure with Added Viscoelastic Dampers," by K.C. Chang, T.T. Soong, S-T. Oh and M.L. Lai, 5/17/91 (PB92-110816/AS).

NCEER-91-0013 "Earthquake Response of Retaining Walls; Full-Scale Testing and Computational Modeling," by S. Alampalli and A-W.M. Elgamal, 6/20/91, to be published.

NCEER-91-0014 "3D-BASIS-M: Nonlinear Dynamic Analysis of Multiple Building Base Isolated Structures," by P.C. Tsopelas, S. Nagarajaiah, M.C. Constantinou and A.M. Reinhorn, 5/28/91, (PB92-113885/AS).

NCEER-91-0015 "Evaluation of SEAOC Design Requirements for Sliding Isolated Structures," by D. Theodossiou and M.C. Constantinou, 6/10/91, (PB92-114602/AS).

NCEER-91-0016 "Closed-Loop Modal Testing of a 27-Story Reinforced Concrete Flat Plate-Core Building," by H.R. Somaprasad, T. Toksoy, H. Yoshiyuki and A.E. Aktan, 7/15/91.

NCEER-91-0017 "Shake Table Test of a 1/6 Scale Two-Story Lightly Reinforced Concrete Building," by A.G. El-Attar, R.N. White and P. Gergely, 2/28/91, to be published.

NCEER-91-0018 "Shake Table Test of a 1/8 Scale Three-Story Lightly Reinforced Concrete Building," by A.G. El-Attar, R.N. White and P. Gergely, 2/28/91, to be published.

NCEER-91-0019 "Transfer Functions for Rigid Rectangular Foundations," by A.S. Veletsos, A.M. Prasad and W.H. Wu, 7/31/91, to be published.

NCEER-91-0020 "Hybrid Control of Seismic-Excited Nonlinear and Inelastic Structural Systems," by J.N. Yang, Z. Li and A. Danielians, 8/1/91.

NCEER-91-0021 "The NCEER-91 Earthquake Catalog: Improved Intensity-Based Magnitudes and Recurrence Relations for U.S. Earthquakes East of New Madrid," by L. Seeber and J.G. Armbruster, 8/28/91.

NCEER-91-0022 "Proceedings from the Implementation of Earthquake Planning and Education in Schools: The Need for Change - The Roles of the Changemakers," by K.E.K. Ross and F. Winslow, 7/23/91.

NCEER-91-0023 "A Study of Reliability-Based Criteria for Seismic Design of Reinforced Concrete Frame Buildings," by H.H.M. Hwang and H-M. Hsu, 8/10/91.

NCEER-91-0024 "Experimental Verification of a Number of Structural System Identification Algorithms," by R.G. Ghanem, H. Gavin and M. Shinozuka, 9/18/91.